Copy No. _____

NCHRP Project 17-10(2)

Structural Supports for Highway Signs, Luminaires and Traffic Signals

Draft Final Report

Appendix A: Project Surveys and Results
Appendix B: Wind Loads Report
Appendix C: Fatigue Resistant Design of Noncantilevered Sign Support Structures
Appendix D: Sample Calculation for Proposed Drag Coefficient Transition Equation for Tapered Multi-Sided Sections
Appendix E: Proposed Combined Stress Ratio Equation for Square and Rectangular Tubes Bent about a Diagonal Axis
Appendix F: Proposed Performance Specification for FRP Poles
Appendix G: Retrofitting and Rehabilitating Fatigue-Damaged Support Structures

Prepared for
National Cooperative Highway Research Program
Transportation Research Board
National Research Council

Fouad H. Fouad, Principal Investigator
James S. Davidson, Co-PI
Norbert Delatte, Co-PI
Elizabeth A. Calvert, Co-PI
Shen-en Chen, Investigator
Edgar Nunez, Graduate Research Assistant
Ramy Abdalla, Graduate Research Assistant

The University of Alabama at Birmingham
Department of Civil and Environmental Engineering
Birmingham, Alabama

May 2002

Appendix A

Project Surveys and Results

TABLE OF CONTENTS

State Departments of Transportation Survey

NCHRP Project 17-10(2)
Standard Specifications for Structural Supports for Highway Signs, Luminaires, and Traffic Signals

Please return this survey to us by 30 August 1999

The main objective of NCHRP Project 17-10(2) is to enhance the recently adopted *Standard Specifications for Structural Supports for Highway Signs, Luminaires, and Traffic Signals* developed under Project 17-10 and to provide a strategic plan for future development of the specification.

The purpose of this survey is to obtain input from the state DOTs on the specific topics that are to be addressed by NCHRP Project 17-10(2). The specific topics include fatigue and vibration of noncantilevered support structures, foundations, drag coefficients for round and multi-sided sections, structure-specific connection plate and base plate flatness tolerances for erection, bending about the diagonal axis of rectangular sections, fiber-reinforced composite support structures, design examples, and retrofit/rehabilitation for fatigue damaged support structures.

Your response to this survey is very important to the Research Team. To facilitate your response, you may obtain this survey as a word document, fill it in, and return it to us by electronic mail. To obtain the survey as a word document, email a request to ndelatte@eng.uab.edu. If you mail the survey, please use the enclosed envelope or send it to the address on the last page.

If you would prefer to discuss these issues over the phone rather than fill out this survey, please call Professor Norbert Delatte at (205) 934-8436.

Please provide the name and contact information for the main contact person filling out this survey:

Organization: _____
Name: _____
Position: _____
Mailing address: _____
_____
_____
_____
Telephone: _____
Fax: _____
Electronic mail address: _____

In addition, if there are other individuals within your organization who can provide additional information concerning the technical issues addressed below, please provide contact information at the end of the survey.

Topic #1 – Field Performance of Support Structures
Topic Objective: The Research Team will review relevant practice, performance data, research findings, and other information related to sign, signal, and luminaire structures. This information will be assembled from foreign and domestic technical literature and from unpublished experiences of engineers, owners, material suppliers, fabricators, and others. Information on actual field performance is of particular interest.

Questions:

1. Has your agency observed any wind damage failures of structural supports designed using current guidelines? To what type of loading or event (wind, truck vibration, etc.) was the failure attributed?

   Yes ____ No ____
   Loading type:
   Wind less than 50 mph_____ Wind more than 50 mph_____
   Truck vibration _____ Vehicle impact _____ Other (please specify):

Topic #2 – Fatigue and Vibration in Noncantilevered Support Structures
Topic Objective: The Research Team will develop a report for consideration by the AASHTO SCOBS that addresses fatigue and vibration in noncantilevered support structures, specifically the overhead bridge-type sign and traffic signal supports.

Questions:

2. Has your agency observed any fatigue-related failures of structural supports designed using 1994 or earlier guidelines? If so, what types of structures?

   Yes ____ No ____
   Structure type: Overhead cantilever ____Overhead bridge ____Roadside sign ____
   Street lighting poles ____ High-level lighting poles____Traffic sign supports ____
   Span wire supports ____
   Other (please specify):

3. Has your agency investigated or used any vibration mitigation measures (devices or practices) for support structures? Please send information about any devices used to the address on the last page of the survey.

   Yes ____ No ____

4. Do you have any special details for fatigue resistant designs? If so, please send detail drawings to the address on the last page of the survey.

   Yes ____ No ____

Topic #3 – Retrofit and Rehabilitation of Fatigue-Damaged Structures
Topic Objective: The Research Team will prepare a manual for retrofitting and rehabilitating fatigue damaged support structures. It is anticipated that this manual can be developed based on the experience of the states and fabricators. Guidance on repair/replacement decisions shall also be provided.

Questions:

1. For the typical support structures listed in the table below, please check those that your agency inspects and the frequency of inspection.

Structure Type	Not Inspected	Inspected Semi-Annually	Inspected Annually	Other (Specify)
Overhead cantilever				
Overhead bridge				
Roadside sign				
Street lighting poles				
High-level lighting poles				
Traffic signal supports				
Span wire supports				

Structure type definitions:
Overhead cantilever (also balanced and unbalanced) – top left three illustrations, Figure 1-1
Overhead bridge – top right illustration, plus middle left two illustrations, Figure 1-1
Roadside sign – middle right illustration, Figure 1-1
Street lighting poles – middle two illustrations, Figure 1-2
High-level lighting– left and right illustrations, Figure 1-2
Traffic signal/span wire supports – all, Figure 1-3

5. Do you repair fatigue-damaged structures? If so, what methods do you typically use?

   Yes ____ No ____
   Methods:

6. Have you developed a maintenance plan, set of procedures, or manual for the retrofit and rehabilitation of fatigue-damaged structures? If so, please send a copy to the address on the last page of the survey.

   Yes ____ No ____

7. If there is a person or persons in your agency who can provide additional information on retrofit and rehabilitation of fatigue-damaged support structures, please provide contact information at the end of the survey.

Topic #4 – Plate Flatness Tolerances
Topic Objective: The Research Team will review current practice to identify the need for structure-specific connection plate and base plate flatness tolerances for erection and recommend tolerances based on the findings.

Questions:
1. Do you have specifications or practices for connection plate and base plate flatness tolerances? Do certain types of structures have specific tolerances? If so, please indicate what structures.

   Yes____ No ____
   Structure type: Overhead cantilever ____ Overhead bridge ____
   Roadside sign ____ Street lighting poles ____
   High-level lighting____ Traffic sign supports ____
   Span wire supports ____
   Other (please specify):

8. What manufacturers do you commonly use to supply your structures?

   Ameron_____ Hapco ____ Valmont ____ Union Metal ____
   Newmark_____ P&K Pole Products ____ Wal-Par ____Whatley ____
   Shakespeare ____
   Other (please specify):

Topic #5 – Fiber-Reinforced Composite Support Structures
Topic Objective: The Research Team will develop performance specifications and acceptance testing procedures for fiber-reinforced composite support structures.

Questions:
1. For what types of support structures do you use fiber-reinforced composites? Do you have performance specifications and/or acceptance testing procedures for them?

Structure Type	Use FRC (Y/N)	Have performance specifications	Have acceptance testing procedures
Roadside sign			
Street lighting poles			
Other			

2. Do you rely on data provided by the manufacturer? Which manufacturer? If so, has the data proven to be reliable?

   Yes ____ No ____

Newmark_____ Valmont ____ P&K Pole Products ____ Whatley ____
Shakespeare ____ Strongwell_____
Other (please specify):
Yes ____ No ____

3. If you have a specification or acceptance testing procedures for fiber-reinforced composite support structures, please send a copy to the address at the end of the survey.

Topic #6 - Foundations

Topic Objective: The Research Team will provide selection criteria and design guidance for support-structure foundations including reinforced and unreinforced cast-in-drilled-hole piles, steel screw-in foundations, and spread footings. The team will also include design details for anchor bolts. At a minimum, the team will address anchorage types (hooked or straight), embedment length, and pretensioning.

Questions:

1. What failures of foundations or anchor bolts have you observed?

   None ____ Foundation (please state type) ____ Anchor bolts ____

2. What types of foundation (by percentage) do you use for these respective types of structures?

Structure type	Reinforced cast-in-drilled-hole piles	Unreinforced cast-in-drilled-hole piles	Steel screw-in foundations	Spread footings	Directly embedded pole	Other – please specify in remarks
Overhead cantilever						
Overhead bridge						
Roadside sign						
Street lighting poles						
High-level lighting poles						
Traffic signal supports						
Span wire supports						

3. What type of anchor bolts do you use for these respective types of structures?

Structure type	Grade of steel[1]	Bolt diameter (typical, inches)[2]	Embedment length (typical, inches)[3]	Hooked or straight (h, s, or both)	Pretensioned bolts (yes/no)
Overhead cantilever					
Overhead bridge					
Roadside sign					
Street lighting poles					
High-level lighting poles					
Traffic signal supports					
Span wire supports					

Notes:
a. Grade of steel – please write in A307, A325, A490, or other (specify other):
b. To the nearest 1/8" or ¼"
c. To the nearest 1"

4. What design criteria and design guidelines for foundations do you use?

   Broms____ Commercial software_____ FHWA manuals_____
   Other (please specify):

5. What design criteria and design guidelines for anchor bolts do you use?

Topic #7 – Bending About the Diagonal Axis of Rectangular Sections
Topic Objective: The Research Team will establish strength and failure criteria for bending about the diagonal axis of rectangular sections and recommend design guidelines.

Questions:

6. Do you have strength and failure criteria and/or design guidelines for bending of rectangular sections about a diagonal axis? If so, please send a copy to the address at the end of the survey.

   Yes ____ No ____

Topic #8 – Design Examples

Topic Objective: The Research Team will prepare complete design examples that show good design practice for support structures while illustrating key features of the specification.

Questions:

1. Please provide copies or drawings and design calculations for support structures to the Research Team at the address at the end of this survey.

2. Do you use software to design support structures? What software?

   Yes ____ No ____ Software ____

3. Do you do your own designs? If not, please provide a contact who does your designs at the end of the survey.

   Yes ____ No ____

Please provide additional contacts if available:

Topic	Name	Telephone number

Return survey to: Dr. Norbert Delatte; Assistant Professor
Telephone: (205) 934-8436, Fax: (205) 934-9855; Internet: ndelatte@eng.uab.edu
Department of Civil and Environmental Engineering
The University of Alabama at Birmingham
1075 13th Street South (Hoehn Building), Suite 120
Birmingham, AL 35294-4440

State Departments of Transportation Survey Results

The following are the results for the state departments of transportation (DOTs) survey. The results are presented in the same format as the questions submitted to the DOTs with comments on the results following each topic.

Topic #1 – Field Performance of Support Structures
Topic Objective: The Research Team will review relevant practice, performance data, research findings, and other information related to sign, signal, and luminaire structures. This information will be assembled from foreign and domestic technical literature and from unpublished experiences of engineers, owners, material suppliers, fabricators, and others. Information on actual field performance is of particular interest.

Questions:
1. Has your agency observed any wind damage failures of structural supports designed using current guidelines? To what type of loading or event (wind, truck vibration, etc.) was the failure attributed?

Table 1. Wind Damage Failure Results

Wind Damage Failures			Type of Wind Damage Failure (Number of States)				
Yes	No	DNA	Wind Speed <50mph	Wind Speed >50mph	Truck	Vehicle	Other
59.57%	40.43%	0.00%	11	16	5	10	Fatigue (2)
ID - Had failure on aluminum truss - thought to be wind related, but could have been accident related.							

Comment
The majority of states have had wind damage failures of structural supports. Most incidents related to high speed winds (greater than 50 mph).

Topic #2 – Fatigue and Vibration in Noncantilevered Support Structures
Topic Objective: The Research Team will develop a report for consideration by the AASHTO SCOBS that addresses fatigue and vibration in noncantilevered support structures, specifically the overhead bridge-type sign and traffic signal supports.

Questions:
1. Has your agency observed any fatigue-related failures of structural supports designed using 1994 or earlier guidelines? If so, what types of structures?

Table 2. Fatigue Related Failures

Fatigue Related Failures per State	%
Yes	52.08
No	47.92
Fatigue Related Failures per State	%
Overhead Cantilevered	25.00
Overhead Bridges	16.67
Roadside Sign	0.00
Structure Lighting Poles	8.33
High Level Lighting Poles	8.33
Traffic Sign Supports	8.33
Span Wire Supports	2.08

2. Has your agency investigated or used any vibration mitigation measures (devices or practices) for support structures? Please send information about any devices used to the address on the last page of the survey.

Table 3. Vibration/Mitigation Measures

	%
Yes	41.67
No	56.25
DNA	2.08

3. Do you have any special details for fatigue resistant designs? If so, please send detail drawings to the address on the last page of the survey.

Table 4. Special Fatigue Details

	%
Yes	16.67
No	83.33

Comment
From the results presented in Tables 2 thru 4, it is apparent that the majority of states have had fatigue related failures of structural supports. Most of the incidents reported can be correlated to either overhead cantilever or overhead bridge type of structures. Despite fatigue problems experienced, only 41.6% of states have used and/or investigated vibration/mitigation measures, and only 16.7% of states have any special details for fatigue resistant designs.

Topic #3 – Retrofit and Rehabilitation of Fatigue-Damaged Structures
Topic Objective: The Research Team will prepare a manual for retrofitting and rehabilitating fatigue damaged support structures. It is anticipated that this manual can be developed based on the experience of the states and fabricators. Guidance on repair/replacement decisions shall also be provided.

Questions:
1. For the typical support structures listed in the table below, please check those that your agency inspects and the frequency of inspection.

Table 5. Inspection of Support Structures

Inspections by State	%
Perform Inspection	66.67
Don't Perform Inspection	29.17
DNA	4.17
Inspections by Structure Type	**%**
Overhead Cantilevered	60.42
Overhead Bridges	58.33
Roadside Sign	12.50
Structure Lighting Poles	10.42
High Level Lighting Poles	43.75
Traffic Sign Supports	14.58
Span Wire Supports	14.58

Comment
From the results presented in Table 5, it is apparent that the majority of states perform inspections (66.67%), however, a relative high number (29.17%) do not perform inspections. The inspections seem to be focused mostly on overhead cantilever, overhead bridge, and high level lighting (poles) type of structures. This fact appears to be consistent with the fatigue-related failures reported.

4. Do you repair fatigue-damaged structures? If so, what methods do you typically use?

Table 6. Repair Fatigue-Damaged Structures

	%
Yes	27.08
No	56.25
DNA	16.67

Comment
It is remarkable that despite the high percentage of states conducting inspections, only a minority (27.08%) of states repairs fatigue-damaged structures. A possible explanation may be that it is not simple or easy to characterize structural damage as fatigue-related.

5. Have you developed a maintenance plan, set of procedures, or manual for the retrofit and rehabilitation of fatigue-damaged structures? If so, please send a copy to the address on the last page of the survey.

Table 7. Maintenance Plan and Retrofit Manual

	%
Yes	2.08
No	83.33
DNA	14.58

Comment
The results shown in Table 7 indicate a low incidence of fatigue-related damage or a lack of expertise in dealing with fatigue induced structural problems.

6. If there is a person or persons in your agency who can provide additional information on retrofit and rehabilitation of fatigue-damaged support structures, please provide contact information at the end of the survey.

Topic #4 – Plate Flatness Tolerances
Topic Objective: The Research Team will review current practice to identify the need for structure-specific connection plate and base plate flatness tolerances for erection and recommend tolerances based on the findings.

Question:
1. Do you have specifications or practices for connection plate and base plate flatness tolerances? Do certain types of structures have specific tolerances? If so, please indicate what structures.

Table 8. Specifications for Connection Plate and Base Plate Flatness Tolerances

By State	No. of States
Yes	10
No	37
DNA	1
By Structure Type	**No. of States**
Overhead Cantilever	9
Overhead Bridge	10
Roadside sign	4
Street Light Poles	6
High-Level Lighting Poles	6
Traffic Signal Supports	6
Span Wire Supports	4

Comment
Only 10 states responded yes to this question. Overhead cantilever or overhead bridge type of structures seem to be the target of most specific tolerances.

7. What manufacturers do you commonly use to supply your structures?

Table 9. Manufacturers

Manufacturers	No. of States
Valmont	37
Union Metal	36
Ameron	16
Hapco	14
Walla	11
P&K Pole Products	10
Brookfield	7
Millerbernd	5
Hurtt	4
L. B. Foster	4
Summit	4
Commercial Fabricators, Inc.	3
Shakespeare	3
Value Structures	3
Wascot	3
JEM	2
Northwest Signal Supply, Inc.	2
Sigma	2
American - High Mass	1
American Pole Structures	1
Colombia Metal Fabricators	1
Di - Highway	1
Engineering Design International	1
Falcon Steel	1
Hogan, Inc.	1
Lexington Standard	1
Newmark	1
Remington Steel & Sign Corp.	1
Steve Johnson Co.	1
Stonybrook	1
Thomas & Betts	1
Universal Industrial Sales and Syro Steel	1
White Oak Metals	1
Wichita Steel Fab, Inc.	1
Ziese Manufacturing	1
Whatley	0

Comment
This table reflects the fact that the most commonly used manufacturers are producers of steel or aluminum structures, which in turn are the most common structures used for structural supports.

Topic #5 – Fiber-Reinforced Composite Support Structures
Topic Objective: The Research Team will develop performance specifications and acceptance testing procedures for fiber-reinforced composite support structures.

Questions:
1. For what types of support structures do you use fiber-reinforced composites? Do you have performance specifications and/or acceptance testing procedures for them?

Table 10. Use of FRC

By State	%
Use FRC	18.75
Don't Use	68.75
NA	12.50
By Structure Type	
Roadside sign	2.08
Street lighting	12.50
Others	4.17

2. Do you rely on data provided by the manufacturer? Which manufacturer? If so, has the data proven to be reliable?

Table 11. Data Provided by the Manufacturer

Rely on Manufacturer Data	%
Yes	22.92
No	14.58
NA	62.50
Which Manufacturer	%
Newmark	2.08
Valmont	2.08
P&K Pole Products	0.00
Whatley	0.00
Shakespeare	6.25
Strongwell	0.00
Others	12.50

3. If you have a specification or acceptance testing procedures for fiber-reinforced composite support structures, please send a copy to the address at the end of the survey.

Table 12. Specifications for FRC

	%
Yes	2.08
No	2.08
NA	95.83

Comment
From the results presented in Tables 10 thru 12, it is apparent that 18.75% of the states use or have used FRC structures, 68.75% of the states do not use or have not used FRC structures, and for 12.50% of the state, FRC is not applicable. When the state DOTs were asked whether they have specifications or acceptance testing procedures for FRC structures, 2.08% responded yes, 2.08% responded no, while 95.83% responded not applicable.

Considering the states that use or have used FRC, the major applications are: street lighting 67%, roadside signs 11%, and other structures 22%. In summary, the results of the survey indicate that FRP is mainly used for lighting poles and roadside supports. The results also revealed that very few states have specifications for FRP structures.

Topic #6 - Foundations
Topic Objective: The Research Team will provide selection criteria and design guidance for support-structure foundations including reinforced and unreinforced cast-in-drilled-hole piles, steel screw-in foundations, and spread footings. The team will also include design details for anchor bolts. At a minimum, the team will address anchorage types (hooked or straight), embedment length, and pretensioning.

Questions:
1. What failures of foundations or anchor bolts have you observed?

Table 13. Types of Failures

	%
Foundation	10.53
Anchor Bolt	42.11
None	76.32
Notes: Some states may have more than one type of failure. ID – cast – in –place shaft, reinforced – settlement & tilting	

Comment
The results presented in Table 13 indicate that in general foundation/anchor bolt failures are not very common. 76.32% states report none of these failures. However, when these failures occur, they can be linked most of the time to an anchor bolt failure (42.11% vs. 10.53 %).

4. What types of foundation (by percentage) do you use for these respective types of structures?

Table 14. Foundation Types

Structure Type (Percentage)	Reinforced Cast-In Drilled Hole Piles	Unreinforced Cast-In Drilled Hole Piles	Steel Screw-In Foundations	Spread Footings	Directly Embedded Poles	Other
Overhead Cantilever	65	0	0	42	0	3
Overhead Bridge	58	0	0	45	0	3
Roadside sign	37	22	0	6	29	2
Street Light Poles	63	3	10	11	3	5
High-Level Lighting Poles	75	0	0	14	0	3
Traffic Signal Supports	84	0	0	9	2	3
Span Wire Supports	55	2	0	5	20	2
Number of States Reported		48				

5. What type of anchor bolts do you use for these respective types of structures?

Table 15. Type of Anchor Bolts

Type of Bolts	Overhead Cantilever %	Overhead Bridge %	Road-side Sign %	Street Light Poles %	High-Level Lighting Poles %	Traffic Signal Supports %	Span Wire Supports %
A36	14.9	17.0	8.5	10.6	6.4	10.6	6.4
A36M	2.1	2.1	2.1	2.1	0.0	0.0	0.0
A193	2.1	2.1	0.0	0.0	0.0	0.0	0.0
A307	17.0	14.9	10.6	19.1	14.9	19.1	14.9
A320	2.1	2.1	0.0	0.0	0.0	0.0	0.0
A325	14.9	12.8	14.9	14.9	12.8	10.6	12.8
A449	10.6	8.5	2.1	4.3	2.1	12.8	6.4
A490	6.4	8.5	2.1	2.1	2.1	2.1	0.0
A499	2.1	2.1	2.1	2.1	2.1	2.1	2.1
A572	0.0	0.0	0.0	0.0	0.0	2.1	0.0
A576	2.1	2.1	0.0	6.4	2.1	4.3	2.1
A588	0.0	0.0	0.0	0.0	0.0	2.1	0.0
A615	0.0	0.0	0.0	0.0	4.3	2.1	0.0
A687	2.1	2.1	2.1	6.4	2.1	8.5	4.3
F1554 (Gr.36)	4.3	2.1	0.0	2.1	2.1	4.3	2.1
F1554 (Gr.55)	8.5	8.5	6.4	8.5	10.6	10.6	6.4
F1554 (Gr.105)	0.0	0.0	0.0	0.0	4.3	2.1	0.0
AASHTO M314 Gr.36	0.0	2.1	0.0	2.1	0.0	0.0	0.0
AASHTO M314 Gr.55	8.5	6.4	4.3	8.5	6.4	8.5	2.1
AASHTO M314 Gr.105	2.1	2.1	2.1	2.1	2.1	2.1	2.1
M31 Gr75	0.0	0.0	0.0	0.0	2.1	0.0	0.0
M103 Gr65-35	0.0	0.0	0.0	0.0	0.0	2.1	0.0
Manufacturer	2.1	2.1	2.1	4.3	2.1	4.3	4.3
50	2.1	2.1	0.0	2.1	2.1	2.1	2.1
55 ksi	4.3	2.1	0.0	6.4	6.4	4.3	2.1
85 ksi	4.3	4.3	0.0	6.4	6.4	4.3	2.1
Did not answer	4.3	10.6	53.2	17.0	29.8	12.8	44.7

Comment
From the results presented in Table 15, it is apparent that low strength A307 anchor bolts are very commonly used, followed closely by high strength A325 anchor bolts. This may be explained by the fact that the structural demands of most support structures are

not very large, therefore combination of low strength/low cost, makes A307 anchor bolts appealing for most designers/states.

Table 16. Anchor Bolt Diameter

Structure Type	Bolt Diameter (in)			Number of States That Did Not Answer
	Minimum	Maximum	Average	
Overhead Cantilever	0.50	3.25	1.88	7
Overhead Bridge	0.88	3.00	1.74	9
Roadside sign	0.50	2.25	1.14	31
Street Light Poles	0.50	2.50	1.09	15
High-Level Lighting Poles	0.50	2.75	1.80	22
Traffic Signal Supports	0.50	2.75	1.54	14
Span Wire Supports	0.50	2.75	1.59	28

Comment
From the results presented in Table 16, it is clear that for overhead cantilever, overhead bridge, and high level lighting pole structures the average anchor bolt diameter is slightly larger than 1-3/4 inches. For traffic signal and span wire supports, the average anchor bolt diameter is slightly larger than 1-1/2 inches, whereas for street light poles, the average anchor bolt diameter is slightly larger than 1 inch.

Table 17. Anchor Bolt Embedment Length

Structure Type	Embedment Length (inches)			Number of States That Did Not Answer
	Minimum	Maximum	Average	
Overhead Cantilever	30	180	58.36	14
Overhead Bridge	22	180	51.84	15
Roadside sign	15	144	45.88	36
Street Light Poles	12	90	40.26	15
High-Level Lighting Poles	25	104	65.67	23
Traffic Signal Supports	18	110	58.48	18
Span Wire Supports	20	114	57.88	31

Comment
From the results presented in Table 17, it is apparent that average embedment length ranges from 40 inches for street light poles to 66 inches for high level lighting poles. It is interesting that despite a larger average embedment length for high level lighting poles, some exceptional overhead cantilever or overhead bridge supports have longer anchor bolt embedment lengths (up to 180 inches) than the larger high level lighting pole embedment length (104 inches). This fact shows that the range of anchor bolt embedment lengths is larger for overhead cantilever or overhead bridge supports than for high level lighting poles.

Table 18. Number of States That Reported on Shape of Anchor Bolt

Structure Type	Answered	DNA
Overhead Cantilever	44	4
Overhead Bridge	41	7
Roadside Sign	16	32
Street Light Poles	37	11
High-Level Lighting Poles	31	17
Traffic Signal Supports	40	8
Span Wire Supports	27	21

Table 19. Shape of Anchor Bolt

Structure Type	Hooked %	Straight %	Both %	Plate %	DNA %
Overhead Cantilever	31.8	59.1	9.1	0.0	6.3
Overhead Bridge	26.8	63.4	9.8	0.0	12.5
Roadside Sign	43.8	50.0	6.3	0.0	64.6
Street Light Poles	70.3	16.2	13.5	0.0	20.8
High-Level Lighting Poles	32.3	41.9	22.6	3.2	33.3
Traffic Signal Supports	60.0	22.5	15.0	2.5	14.6
Span Wire Supports	48.1	29.6	14.8	3.7	43.8

Comment
From the results presented in Table 19, it is apparent that hooked anchor bolts are still very commonly used, despite some disadvantages reported by several researchers. Also, the data presented in Table 19 shows that hooked anchor bolts are preferred for street light poles and traffic signal supports, whereas straight anchor bolts are preferred for overhead cantilever supports, overhead bridge supports, roadside signs, and high level lighting poles.

Table 20. Number of States That Reported on Use of Pretensioned Bolts

Structure Type	Num. of States that Answered	DNA
Overhead Cantilever	42	5
Overhead Bridge	39	8
Roadside Sign	20	27
Street Light Poles	35	12
High-Level Lighting Poles	31	16
Traffic Signal Supports	38	9
Span Wire Supports	25	22

Table 21. Use of Pretensioned Bolts

Structure Type	Yes %	No %	DNA %
Overhead Cantilever	7.14	92.86	10.64
Overhead Bridge	7.69	92.31	17.02
Roadside Sign	5.00	95.00	57.45
Street Light Poles	8.57	91.43	25.53
High-Level Lighting Poles	6.45	93.55	34.04
Traffic Signal Supports	10.53	89.47	19.15
Span Wire Supports	8.00	92.00	46.81

Comment
From the results presented in Table 21, it is apparent that the use of pretensioned bolts is very marginal with percentages of use not exceeding 11%.

6. What design criteria and design guidelines for foundations and anchor bolts do you use?

Table 22. Design Criteria and Design Guidelines for Foundations

Design Criteria and Guidelines for Foundations	Number of States
FHWA manuals	15
AASHTO	12
Broms	11
COM624	5
Commercial	4
LPILE	4
Rutledge Method	2
Geotechnical Engineers Designed Foundations	1
LT BASE Program Dr. Roy Bordon NCSU	1
NAVFAC	1
Reese - PY Curves	1
Uniform Building Code	1
Note: Some states may use more than one design method.	

Comment
From Table 22, it is apparent that the majority of states use for foundation design either the FHWA manuals, AASHTO, or Broms.

Table 23. Design Criteria and Design Guidelines for Foundations and Anchor Bolts

Design Criteria and Guidelines for Anchor Bolts	
AASHTO	27
AISC	5
55 ksi is Sufficient	2
ASTM	2
ACI	1
Brass Analysis	1
Concrete International Design and Construction 7/81 Vol. 3 #7	1
FHWA Manuals	1
Manufacturer's Design	1
MIDOT Guidelines	1
NCHRP412	1
NH Standards	1
NJ/PA Standards	1
Old Concrete Fundamentals	1
TTl105-3	1
Uses Ring Plate	1
DNA	4
Note: Some states may use more than one design method.	

Comment
From Table 23, it is apparent that the majority of states use for anchor bolt design AASHTO with a few states using AISC or other methods.

Topic #7 – Bending About the Diagonal Axis of Rectangular Sections
Topic Objective: The Research Team will establish strength and failure criteria for bending about the diagonal axis of rectangular sections and recommend design guidelines.

Questions:
1. Do you have strength and failure criteria and/or design guidelines for bending of rectangular sections about a diagonal axis? If so, please send a copy to the address at the end of the survey.

Table 24. Design Guidelines for Bending about the Diagonal

YES	NO	DNA
0%	97.92%	2.08%

Comment
The results show an impressive response highlighting the importance of research on this topic.

Topic #8 – Design Examples
Topic Objective: The Research Team will prepare complete design examples that show good design practice for support structures while illustrating key features of the specification.

Questions:
1. Please provide copies or drawings and design calculations for support structures to the Research Team at the address at the end of this survey.

2. Do you use software to design support structures? What software? Do you do your own designs?

Table 25. Software to Design Support Structures

Yes	No	DNA
52.08%	43.75%	4.17%

Table 26. Types of Software Used

Type	Num. Of States
In House Program	15
Brass Pole	6
STRUDL	5
SABRE	2
STAAD	2
COM624	1

Table 27. Own Designs

Yes	No	DNA
62.50%	37.50%	4.17%
Some states do some of their own designs.		

Comment
From the results presented in Tables 23 thru 25, it is apparent that the majority of states use software for design of structural supports. Most states use in-house programs and commercially available software packages. A majority of states do their own designs.

Manufacturers' Survey

NCHRP Project 17-10(2)
Standard Specifications for Structural Supports for Highway Signs, Luminaires, and Traffic Signals

We will be contacting you by 30 August 1999 concerning the topics of this survey

The main objective of NCHRP Project 17-10(2) is to enhance the recently adopted *Standard Specifications for Structural Supports for Highway Signs, Luminaires, and Traffic Signals* developed under Project 17-10 and to provide a strategic plan for future development of the specification.

The purpose of this survey will be to obtain input from support structure manufacturers on the specific topics that are to be addressed by NCHRP Project 17-10(2). The specific topics include fatigue and vibration of noncantilevered support structures, foundations, drag coefficients for round and multi-sided sections, structure-specific connection plate and base plate flatness tolerances for erection, bending about the diagonal axis of rectangular sections, fiber-reinforced composite support structures, design examples, and retrofit/rehabilitation for fatigue damaged support structures.

We plan to contact you shortly by telephone concerning the topics of this survey. We are providing this advance copy to you so that you will have some warning of this phone call.

We would appreciate it if you could send a copy of your latest catalog to the address at the back of the survey.

Please provide the name and contact information for the main contact person filling out this survey:

Organization: _____
Name: _____
Position: _____
Mailing address: _____
_____
_____
_____
Telephone: _____
Fax: _____
Electronic mail address: _____

In addition, if there are other individuals within your organization who can provide additional information concerning the technical issues addressed below, please provide contact information at the end of the survey.

1. What types of materials and structure types do you provide for state transportation agencies (DOT's, etc)?

Materials	Structure types	Other
Steel ___	Street lighting poles ____	Anchor bolts ___
Aluminum ____	High-mast lighting poles ____	Prefab foundations ___
Concrete ____	Overhead sign structure (truss span type) ____	Other ____
Wood ____	Overhead sign structure (cantilever truss) ____	
Fiberglass ____	Overhead sign structure (monotube span type) _____	
Other ____	Roadside sign ____	
	Cantilevered traffic signal structure (tubular) ____	
	Span-type traffic signal structure (tubular) ____	
	Traffic signal poles ____	
	Other ___	

Please describe other:

2. Is the design done "in-house" or as a standard provided by the state transportation agency (DOT)?

   In-house ____ Agency provided ____

3. Do you currently use the AASHTO *Standard Specifications for Structural Supports for Highway Signs, Luminaires, and Traffic Signals*?

   Yes ___ No ___ Edition, if used:

4. Who is responsible for detailing connections for structures you sell?

   Agency ___ Manufacturer ___ Other (please specify):

Topic #1 – Field Performance of Support Structures

Topic Objective: The Research Team will review relevant practice, performance data, research findings, and other information related to sign, signal, and luminaire structures. This information will be assembled from foreign and domestic technical literature and from unpublished experiences of engineers, owners, material suppliers, fabricators, and others. Information on actual field performance is of particular interest.

Questions:

1. Do you have knowledge of any failures of structural supports designed using current guidelines (1994 or earlier)? To what type of loading or event (wind, truck vibration, etc.) was the failure attributed?

   Yes ____ No ____
   Loading type: Wind less than 50 mph ____ Wind more than 50 mph ____
   Truck vibration ____ Vehicle impact ____
   Other (please specify):

Topic #2 – Fatigue and Vibration in Noncantilevered Support Structures
Topic Objective: The Research Team will develop a report for consideration by the AASHTO SCOBS that addresses fatigue and vibration in noncantilevered support structures, specifically overhead bridge type sign supports.

Questions:

1. Have you investigated or used any vibration mitigation measures (devices or practices) for support structures? Please send information about any devices used to the address on the last page of the survey.

   Yes ____ No ____

2. Do you have any special details for fatigue resistant designs? If so, please send detail drawings to the address on the last page of the survey. Indicate why the detail should be used.

   Yes ____ No ____

3. Have you found any details that are particularly susceptible to fatigue damage? If so, please send drawings to the address on the last page of the survey. Indicate why the detail should not be used.

   Yes ____ No ____

4. Are you calculating a fatigue load? If so, what method are you using? Indicate structure type.

   Yes ____ No ____
   Structure type: Cantilevered overhead sign ____ Overhead sign (span type) ____
   Roadside sign ____ Street lighting poles ____ High-level lighting poles____
   Traffic sign supports ____ Span wire supports ____
   Other (please specify):

Topic #3 – Retrofit and Rehabilitation of Fatigue-Damaged Structures
Topic Objective: The Research Team will prepare a manual for retrofitting and rehabilitating fatigue damaged support structures. It is anticipated that this manual can be developed based on the experience of the states and fabricators. Guidance on repair/replacement decisions shall also be provided.

Questions:

1. Have you been involved in the repair of fatigue-damaged structures? If so, what methods do you typically use?

   Yes ____ No ____
   Methods:

2. Have you developed a maintenance plan, set of procedures, or manual for the retrofit and rehabilitation of fatigue-damaged structures? If so, please send a copy to the address on the last page of the survey.

   Yes ____ No ____

3. If there is a person or persons in your company who can provide additional information on retrofit and rehabilitation of fatigue-damaged support structures, please provide contact information at the end of the survey.

Topic #4 – Plate Flatness Tolerances

Topic Objective: The Research Team will review current practice to identify the need for structure-specific connection plate and base plate flatness tolerances for erection, and recommend tolerances based on the findings.

Questions:

1. Do you have specifications or practices for connection plate and base plate flatness tolerances? Do certain types of structures have specific tolerances? If so, please indicate what structures. Do any agencies that order structures from you have specified tolerances?

   Yes ____ No ____
   Structure type: Cantilevered overhead sign ____ Overhead sign (span type) ____
   Roadside sign ____ Street lighting poles ____ High-level lighting poles____
   Traffic sign supports ____ Span wire supports ____
   Other (please specify):

Topic #5 – Fiber-Reinforced Composite Support Structures

Topic Objective: The Research Team will develop performance specifications and acceptance testing procedures for fiber-reinforced composite support structures. This question is only for manufacturers of fiber-reinforced composite support structures.

Questions:

1. What types of support structures do you sell made of fiber-reinforced composites? Do you or the state transportation agency have performance specifications and/or acceptance testing procedures for them?

2. If you have a specification or acceptance testing procedures for fiber-reinforced composite support structures, please send a copy to the address at the end of the survey.

3. Do you provide design or performance information to transportation agencies that purchase fiber reinforced composite structures? If so, please send a copy to the address at the end of the survey.

Topic #6 - Foundations

Topic Objective: The Research Team will provide selection criteria and design guidance for support-structure foundations including reinforced and unreinforced cast-in-drilled-hole piles, steel screw-in foundations, and spread footings. The team will also include design details for anchor bolts. At a minimum, the team will address anchorage types (hooked or straight), embedment length, and pretensioning.

Questions:

1. Are you involved in design or construction of foundations or anchor bolts for any structures you supply?

   Yes ____ No ____

Topic #7 – Bending About the Diagonal Axis of Rectangular Sections

Topic Objective: The Research Team will establish strength and failure criteria for bending about the diagonal axis of rectangular sections and recommend design guidelines.

Questions:

1. Do you have strength and failure criteria and/or design guidelines for bending of rectangular sections about a diagonal axis? If so, please send a copy to the address at the end of the survey.

   Yes ____ No ____

Topic #8 – Drag Coefficients

Topic Objective: The Research Team will use existing research findings to develop drag coefficients for tapered poles that transition from multisided shapes to round shapes.

Questions:

1. Are you aware of any research conducted on drag coefficients for poles that transition from multisided to round? If so, please provide a contact or reference.

   Yes ____ No ____ Contact/reference ____

Topic #9 – Design Examples
Topic Objective: The Research Team will prepare complete design examples that show good design practice for support structures while illustrating key features of the specification.

Questions:

1. The Research Team is interested in any sample drawings and design calculations that may be available. Please send any information to the address at the end of this survey.

2. Do you use software to design support structures? What software?

   Yes ____ No ____ Software ____

3. Do you do your own designs? If not, please provide a contact who does your designs at the end of the survey.

   Yes ____ No ____

Return survey to:
Dr. Norbert Delatte
Assistant Professor
Telephone: (205) 934-8436, Fax: (205) 934-9855
Internet: ndelatte@eng.uab.edu
Department of Civil and Environmental Engineering
The University of Alabama at Birmingham
1075 13th Street South (Hoehn Building), Suite 120
Birmingham, AL 35294-4440

Comments:

Manufacturers' Survey Results

1. What types of materials and structure types do you provide for state transportation agencies (DOT's, etc)?

Materials	Structure types	Other
Steel _4_	Street lighting poles _5__	Anchor bolts _6_
Aluminum _4_	High-mast lighting poles __4__	Prefab foundations _1_
Concrete __1__	Overhead sign structure (truss span type) __4__	Other ____
Wood __0__	Overhead sign structure (cantilever truss) _4___	
Fiberglass __1_	Overhead sign structure (monotube span type) __4___	
Other __0__	Roadside sign _1___	
	Cantilevered traffic signal structure (tubular) _4___	
	Span-type traffic signal structure (tubular) _4___	
	Traffic signal poles __6__	
	Other ___	

Please describe other:

Floodlight Antenna	Prefab – Screw – In Type
Bridge Mounted Structures	
Fluted Poles	
Cityscape Structures	
Sport Lighting Poles	

2. Is the design done "in-house" or as a standard provided by the state transportation agency (DOT)?

In-house _6___ Agency provided __4__ N/A __1__

3. Do you currently use the AASHTO *Standard Specifications for Structural Supports for Highway Signs, Luminaires, and Traffic Signals*?

Yes _6__ No _0__ N/A __1__ Edition, if used: 1994

4. Who is responsible for detailing connections for structures you sell?

Agency _3__ Manufacturer __3_ N/A __1__

Topic #1 – Field Performance of Support Structures
Topic Objective: The Research Team will review relevant practice, performance data, research findings, and other information related to sign, signal, and luminaire structures. This information will be assembled from foreign and domestic technical literature and

from unpublished experiences of engineers, owners, material suppliers, fabricators, and others. Information on actual field performance is of particular interest.

Questions:

1. Do you have knowledge of any failures of structural supports designed using current guidelines (1994 or earlier)? To what type of loading or event (wind, truck vibration, etc.) was the failure attributed?

   Yes _5___ No __1__ N/A __1__
   Loading type: Wind less than 50 mph __3__Wind more than 50 mph __2__
   Truck vibration _2___ Vehicle impact __1__
   Other (please specify): Material Problems
   Fraction of A Percent

Topic #2 – Fatigue and Vibration in Noncantilevered Support Structures

Topic Objective: The Research Team will develop a report for consideration by the AASHTO SCOBS that addresses fatigue and vibration in noncantilevered support structures, specifically overhead bridge type sign supports.

Questions:

1. Have you investigated or used any vibration mitigation measures (devices or practices) for support structures? Please send information about any devices used to the address on the last page of the survey.

   Yes _2___ No __2__ N/A __3__
   Use Some Dampers
   Use Loads to Change Frequency

2. Do you have any special details for fatigue resistant designs? If so, please send detail drawings to the address on the last page of the survey. Indicate why the detail should be used.

   Yes __1__ No __3__ N/A __3__

3. Have you found any details that are particularly susceptible to fatigue damage? If so, please send drawings to the address on the last page of the survey. Indicate why the detail should not be used.

   Yes __1__ No __3__ N/A __3__

4. Are you calculating a fatigue load? If so, what method are you using? Indicate structure type.

   Yes __2__ No __2__ N/A __3__
   Structure type: Cantilevered overhead sign ____ Overhead sign (span type) __1__

Roadside sign ____ Street lighting poles _1___ High-level lighting poles__1__

Traffic sign supports __1__ Span wire supports ____

Other (please specify):

Problems with Airports
Aluminum More Susceptible Than Steel
Variable Message Sign

Topic #3 – Retrofit and Rehabilitation of Fatigue-Damaged Structures

Topic Objective: The Research Team will prepare a manual for retrofitting and rehabilitating fatigue damaged support structures. It is anticipated that this manual can be developed based on the experience of the states and fabricators. Guidance on repair/replacement decisions shall also be provided.

Questions:

1. Have you been involved in the repair of fatigue-damaged structures? If so, what methods do you typically use?

   Yes _2___ No _3___ N/A __2__

   Methods:

2. Have you developed a maintenance plan, set of procedures, or manual for the retrofit and rehabilitation of fatigue-damaged structures? If so, please send a copy to the address on the last page of the survey.

   Yes __0__ No __5__ N/A __2__

3. If there is a person or persons in your company who can provide additional information on retrofit and rehabilitation of fatigue-damaged support structures, please provide contact information at the end of the survey.

Topic #4 – Plate Flatness Tolerances

Topic Objective: The Research Team will review current practice to identify the need for structure-specific connection plate and base plate flatness tolerances for erection, and recommend tolerances based on the findings.

Questions:

1. Do you have specifications or practices for connection plate and base plate flatness tolerances? Do certain types of structures have specific tolerances? If so, please indicate what structures. Do any agencies that order structures from you have specified tolerances?

   Yes _3___ No __2__ N/A __2__

   Structure type: Cantilevered overhead sign __1_ Overhead sign (span type) __1__

Roadside sign ____ Street lighting poles ____ High-level lighting poles____
Traffic sign supports _1___ Span wire supports ____
Other (please specify):

CalTrans
Street Lighting Poles

Topic #5 – Fiber-Reinforced Composite Support Structures
Topic Objective: The Research Team will develop performance specifications and acceptance testing procedures for fiber-reinforced composite support structures. This question is only for manufacturers of fiber-reinforced composite support structures.

DNA: 5
Number of Responses: 1

Questions:
1. What types of support structures do you sell made of fiber-reinforced composites? Do you or the state transportation agency have performance specifications and/or acceptance testing procedures for them?

   EXTREN Structural Shapes and Plates
   Duragrid Fiberglass Grating
   SAFRAIL FRP Handrail
   Custom Designed Pultruded Shapes

2. If you have a specification or acceptance testing procedures for fiber-reinforced composite support structures, please send a copy to the address at the end of the survey.

   Information was provided.

3. Do you provide design or performance information to transportation agencies that purchase fiber reinforced composite structures? If so, please send a copy to the address at the end of the survey.

   Information was provided.

Topic #6 - Foundations
Topic Objective: The Research Team will provide selection criteria and design guidance for support-structure foundations including reinforced and unreinforced cast-in-drilled-hole piles, steel screw-in foundations, and spread footings. The team will also include design details for anchor bolts. At a minimum, the team will address anchorage types (hooked or straight), embedment length, and pretensioning.

Questions:

1. Are you involved in design or construction of foundations or anchor bolts for any structures you supply?

   Yes __3__ Anchor Bolts Only No __3__ N/A __1__

Topic #7 – Bending About the Diagonal Axis of Rectangular Sections

Topic Objective: The Research Team will establish strength and failure criteria for bending about the diagonal axis of rectangular sections and recommend design guidelines.

Questions:

1. Do you have strength and failure criteria and/or design guidelines for bending of rectangular sections about a diagonal axis? If so, please send a copy to the address at the end of the survey.

   Yes __1__ No __5__ N/A __1__

Topic #8 – Drag Coefficients

Topic Objective: The Research Team will use existing research findings to develop drag coefficients for tapered poles that transition from multisided shapes to round shapes.

Questions:

1. Are you aware of any research conducted on drag coefficients for poles that transition from multisided to round? If so, please provide a contact or reference.

   Yes __0__ No __6__ N/A __1__

Topic #9 – Design Examples

Topic Objective: The Research Team will prepare complete design examples that show good design practice for support structures while illustrating key features of the specification.

Questions:

1. The Research Team is interested in any sample drawings and design calculations that may be available. Please send any information to the address at the end of this survey.

2. Do you use software to design support structures? What software?

   Yes _5___ No __1__ N/A __1__
   Software:

MathCad, AutoCad, Basic, Old Basic Programs Written for AASHTO Manuals, 3-D Design Software, Excel – In House

3. Do you do your own designs? If not, please provide a contact who does your designs at the end of the survey.

   Yes __5__ No __0__ N/A __2__

Appendix B

Wind Loads Report

Table of Contents

List of Tables

List of Figures

WIND LOADS REPORT

1 Introduction

An examination of the current *Supports Specifications* (1994) reveals that the wind loading criteria are based primarily on information and procedures that were first advanced in the early 1960's and 1970's. Through the work of NCHRP Project 17-10, significant changes have been introduced in the proposed *Supports Specifications* (1999), which affect the presentation, terminology, and calculated wind loads. The major changes in the proposed *Supports Specifications* are primarily due to an updated wind map. These changes may result in increase or decrease in the magnitude of calculated wind pressure depending on site location.

Wind load calculations in the proposed *Supports Specifications* have been revised to be based on a 3-second gust wind speed, rather than a fastest-mile wind speed. The number of maps, representing 10-, 25-, and 50-year mean recurrence intervals, have been reduced to one 50-year mean recurrence interval map with importance factors used to adjust the intervals. Height factors have also been adjusted for the 3-second-gust wind speed. The coefficients of drag have been modified slightly. The increase or reduction in calculated wind pressures, which result from the use of the updated wind map, are primarily due to the differences in the current and revised wind speed maps.

The proposed *Supports Specifications* has been updated to reflect currently accepted design procedures to calculate wind loads. The wind loads portion of the proposed specification is based on the 1995 version of ASCE 7, and modified specifically for structural supports for highway signs, luminaries, and traffic signals. *ASCE 7 Minimum Design Loads for Buildings and Other Structures* is considered the most authoritative standard on wind loading in the United States, and most design codes and specifications have generally adopted or referenced ASCE 7.

The main goal of this report is to provide an in-depth explanation of the new wind map (3 second gust) and its impact on the calculated design wind pressures on structural supports. In addition, the flexibility of the structural support as it affects the gust effect factors is considered, and methods for incorporating the flexibility of the structure in the wind loading computation are evaluated. More specifically, this report addresses the following:

- the basis for wind pressure calculations in the current and proposed specifications
- wind load comparisons between the current (1994) and proposed (1999) specifications
- recommendations for gust effect factors for flexible structures
- suggested research needs pertaining to wind loads for structural supports

2 Historical Perspective

2.1 Introduction

The first wind load standard published in the United States was the American Standards Association (ASA) Standard in 1955 (ASA, 1955). The ASA Standards gave wind pressures to be used for designing buildings and other structures. The wind pressures varied geographically and increased with height above ground. Wind speed maps were not given in this standard.

The first wind load standard containing wind speed maps was published by the American National Standards Institute (ANSI, formerly ASA), Standard A58.1, in 1972 (ANSI, 1972). Along with wind speed maps, this standard included the sophistication of gust response factors and pressures for parts and portion to obtain wind loads. The design basis wind speed was given as the fastest-mile wind speed.

A revision to the wind load standard was published in 1982 (ANSI, 1982). The ANSI A58.1-1982 Standard separated loads for the main wind-force resisting system and the components and cladding of buildings. In addition, it used one wind speed map for 50-year mean recurrence interval (MRI) and introduced the importance factor to obtain wind speeds for other MRIs. More details for wind speed maps and their evolvement are given in the subsequent section.

In the mid-1980s, the American Society of Civil Engineers (ASCE) assumed responsibility for the committee, which establishes design loads for buildings and other structures. The ASCE Committee 7 made minor changes to the ANSI A58.1-1982 provisions and published the revised version as ASCE 7-88 (ASCE, 1990). A revised version of ASCE 7-88 was published as ASCE 7-93 (ASCE, 1994) with no changes in wind load provisions.

Major changes were made to wind load provisions that are contained in ANSI/ASCE 7-95 (ASCE, 1996). Adopting the use of 3-second gust design wind speed instead of fastest-mile wind speed required modification of exposure (height and terrain) coefficients, gust effect factors, importance factors, and some pressure coefficients. The ANSI/ASCE consensus, which is in process, demands that every negative vote be resolved through written responses and that 75% of the returned ballots be affirmative. The ANSI/ASCE 7-95 is the basis for the newly approved AASHTO 1999 wind load provisions.

ASCE has published a new revision to wind load provisions; ASCE 7-98 was published in July 1999. There are some changes in the new version of ASCE 7, such as refinement in wind speed contours in hurricane regions and the addition of directionality factor; however, these changes are not as drastic as the one in ASCE 7-95.

The following sections describe the history and/or background for design wind speeds and maps, formula used for obtaining design pressures, gust effect factors for non-wind sensitive structures, height/terrain coefficients, and drag coefficients.

2.2 Design Pressure Formulation

Physics-based equations were specified in ANSI A58.1-1982 to delineate important parameters as well as to provide an understanding of wind load calculations. Prior to this standard, design wind pressures were either given in a table or important parameters were combined in tabular form. The velocity pressure equation in ANSI A58.1-1982 is as follows:

$$q_z = 0.00256\, K_z\, (I\, V)^2$$

where q_z is velocity pressure in psf,
V is wind speed in mph,
I is importance factor, and
K_z is coefficient for height and terrain.

This equation strictly modifies wind speed and converts wind speed to pressure; it is independent of structure type and shape. The generic design pressure equation is:

$$p_z = q_z\, G\, C$$

where p_z is design pressure in psf,
q_z is velocity pressure in psf,
G is gust response factor (not gust factor), and
C is pressure or force (drag) coefficient.

These same equations are used in ASCE 7-88 and ASCE 7-93. In ASCE 7-95, minor changes are made to the equations. In ASCE 7-95, a new topographic factor K_{zt} is added for wind speed-up on hills and escarpments; this factor is used in special cases. Also, importance factor I is placed outside of the parentheses and its values are adjusted accordingly.

The newly adopted AASHTO 1999 provisions use the same equations as ANSI A58.1-1982 or ASCE 7-95, but they are combined into one equation for simplicity. The AASHTO 1999 equation is:

$$p_z = 0.00256\, K_z\, G\, V^2\, I_r\, C_d$$

where p_z is design pressure in psf,
K_z is coefficient for height and terrain,
G is gust effect factor,
V is wind speed (3-second gust) in mph,
I_r is importance factor, and
C_d is drag coefficient.

The values of each of the parameters have to be adjusted in these equations to reflect averaging time for wind speeds (e.g., fastest-mile or 3-second gust) and updated data. But, the basic design pressure formulation has remained the same since ANSI A58.1-1982.

One important scientific difference between the AASHTO 1999 equation and the ANSI/ASCE 7-95 equation is the gust effect factor. In ANSI/ASCE 7-95, the gust effect factor incorporates wind-structure interaction characteristics, while the gust effect factor in AASHTO 1999 considers only the characteristics of wind. More explanation on this is given in Section 2.6 on Gust Effect Factor.

2.3 Design Wind Speeds

2.3.1 Introduction

Design wind speed is the most critical parameter in the wind pressure equation because the wind speed value is squared to obtain design pressure. A 10% change in wind speed changes the design pressure by 21%. On the other hand, assessment of design wind speed is difficult because it depends heavily on historical records and statistical analysis.

The development of wind speed maps involves the historical record of maximum annual wind speed value, statistical analysis of the wind speed data, and current assessment of wind speed contours (isotachs). For consistency purposes, wind speed values are normalized to a specific height above ground (30 ft or 10 m), specific exposure (Exposure C: flat, open terrain of airports), and a specified averaging time (fastest-mile or 3-second gust speed). Wind speed maps are developed for various probabilities of exceeding specified wind speeds. It is important to recognize that statistical analysis provides expected value with an error-band; this error-band strongly depends on the length of record. If the length of record in short, the error-band is large; the error-band gets smaller as the length of record gets longer.

Averaging time of wind speed (fastest-mile or 3-second gust) is important because it affects height and exposure factor and gust effect factor. These factors are discussed in subsequent sections. Sections 2.3 and 2.4 discuss the evolution of wind speed maps and the probabilities of exceeding design wind speeds, respectively.

2.3.2 Wind Speed Maps

History and background of the wind speed maps that are used in national wind load standards and used in AASHTO standards are given here.

2.3.2.1 ANSI A58.1-1972 and AASHTO 1995 Maps

H.C.S. Thom, a senior research fellow with the Environmental Science Service Administration, organized the wind speed data collected at the 138 National Weather Service (NWS) stations in the late 1960s. The NWS recorded maximum fastest-mile wind speed at each of its stations. Thom subjected maximum annual wind speed values

at each station to statistical analysis using Fisher-Tippett Type II extreme value distribution (Thom, 1968). Using the results of the statistical analysis, he produced five maps for different annual probability of exceeding wind speed: (1) 0.01 (100-year MRI), (2) 0.02 (50-year MRI), (3) 0.04 (25-year MRI), (4) 0.10 (10-year MRI), and (5) 0.50 (2-year MRI). These were the first wind speed maps produced in the United States on a probabilistic basis. The maps are shown in Figures 2.1 through 2.5.

The ANSI A58.1 committee adopted three maps for its 1972 wind load provision standard: 100-year, 50-year, and 25-year MRIs. The AASHTO standard also adopted three maps in its 1985 specifications: 50-year, 25-year, and 10-year MRIs. The AASHTO 1994 specifications continued to use the maps that H.C.S. Thom produced in the late 1960s.

Since the length of record at each NWS station in the 1960s was relatively short, the error-band was fairly large. Thom discussed error-bands in his research paper (Thom, 1968), which was published in the ASCE journal in 1968.

2.3.2.2 ANSI A58.1-1982 Map

During the period of 1977-79, Emil Simiu from the National Bureau of Standards (NBS) and M. Changery from the National Climatic Data Center (NCDC) worked together to review historical records of wind speed data for the United States. Even though the NCDC archives wind speed data from approximately two thousand stations around the country (Changery, 1979), data from only 129 stations were found to be consistent and of good quality. Only NWS stations collected and archived fastest-mile wind speed values; the locations of these sites are shown in Figure 2.6 (Mehta, 1984). The data of these stations were subjected to statistical analysis by Simiu using Fisher-Tippett Type I (Gumbel) extreme value distribution (Simiu et al., 1979). The statistical analysis provided wind speed values associated with different MRIs at each of the stations.

The wind load subcommittee of the ANSI A58.1 committee on loads had the difficult task of developing wind speed maps using Simiu's results. After several iterations, the subcommittee developed a map for 0.02 annual probability of exceeding wind speed (50-year MRI); this map is shown in Figure 2.7. It became apparent that the subcommittee was not able to develop maps for other MRIs because paucity of data did not permit consistent wind speed contours (isotachs). To circumvent the problem of producing maps for other MRIs, the importance factor I was introduced.

The importance factor I provides basic wind speeds associated with MRI of 100 and 25 years (annual probability of 0.01 and 0.04, respectively). The importance factors were determined using the ratios of wind speeds associated with desired MRI to 50 year MRI. The ratios for all 129 NWS stations were obtained to assess mean and standard deviations of the values. The importance factor value was established as mean plus one standard deviation of the ratios; these values were 1.07 for 100-year MRI and 0.95 for 25-year MRI. Thus, the wind speed for 100-year MRI can be obtained by multiplying the wind speed value from the map (Figure 2.7) with the importance factor of 1.07.

As can be seen in Figure 2.6, very few NWS stations are located in the hurricane-prone areas of the Atlantic and Gulf Coast regions. There is not sufficient recorded wind speed data available for landfalling hurricanes. A numerical simulation procedure was used by researchers at NBS to generate hurricane wind speed data (Batts et al., 1980). Monte Carlo simulation permitted matching historically recorded characteristics of hurricane storms. The hurricane wind speed data (generated by numerical simulation) was subjected to statistical analysis. The analysis provided wind speed values for 50-year MRI at stations every 50 nautical miles along the coast. The ANSI A58.1 subcommittee on wind loads developed the wind speed contours for hurricane-prone regions. The final map adopted for ANSI A58.1-1982 is shown in Figure 2.7.

The probability distribution of hurricane winds determined by Batts et al. (1980) is different from that of wind speeds of inland stations (Simiu et al., 1979). Higher values of importance factor for the hurricane ocean line were specified in ANSI A58.1-1982 to account for the same probability of overload as that for inland areas. The importance factor values, which permit determination of wind speeds for 100-year and 25-year MRI, are shown in Table 2.1.

It is recognized that certain geographic regions, such as mountainous and valley terrains, may have characteristics that cause significant variation of wind speeds. Lack of data as well as potential of high winds (e.g., Boulder, Colorado) suggested that these are special cases. The special wind regions are shaded in the map (Figure 2.7) and local designers or officials are encouraged to investigate wind history, analyze the available data, and consult a meteorologist if there is a reason to believe that winds in special wind regions are significantly different from the wind speeds obtained from the map. A minimum basic wind speed of 70 mph was recommended in ANSI A58.1-1982.

The wind speed map (Figure 2.7) developed for ANSI A58.1-1982 was used in ANSI/ASCE 7-88 (ASCE, 1990) and ANSI/ASCE 7-93 (ASCE, 1994). The wind speed values given in the map are fastest-mile speed at 30 ft above ground in flat, open terrain (Exposure C) associated with 50-year MRI (0.02 annual probability).

2.3.2.3 ANSI/ASCE 7-95 Map

In the early 1990s, it seemed appropriate that the design wind speed map of ANSI A58.1-1982 (also used in ANSI/ASCE 7-88 and 7-93) should be updated since there was additional historical data of 10 years or more. In addition, it was found that the NWS stations had stopped collecting and archiving fastest-mile wind speed values in mid-1980s. The ASCE 7 Subcommittee on Wind Loads, after an 18-month deliberation, agreed to adopt the 3-second gust speed as the basic design wind speed. The reasons for adopting the gust speed value are: (1) historical records for fastest-mile wind speed will not be available for future years, (2) more data for gust speed are available since military and Department of Energy installations, in addition to NWS stations, collect and archive maximum annual gust speed values, and (3) media always report maximum annual gust speed in storms and it is easy for the public to understand the value. Jon Peterka at Colorado State University (currently at CPP, Inc.) conducted the research to update the wind speed map.

Historical wind speed data archived at NCDC was reviewed to assess consistency and homogeneity of data. It was found that 485 stations around the country had at least five years (most of them 20 to 50 years) of good quality maximum annual gust wind speed data. Instead of using data of individual stations, the researchers combined data from several adjoining stations, thus creating a record of 200 to 300 years in length, rather than 10 to 50 year in length (Peterka, 1992; Peterka and Shahid, 1993). Care was taken to ensure that the data of adjoining stations were independent and that the maximum wind speed values recorded were not from the same storm. The long series of values were subjected to statistical analysis using a Fisher-Tippett Type I extreme value distribution. The long length of record significantly reduced error-band in the statistical results. This procedure gave the same speed as did area-averaged 50-year MRI speed from a set of combined stations. The results of the statistical analysis showed that variation in 50-year MRI wind speeds over the eastern three-quarters of the contiguous United States was insufficient to justify wind speed contours (for non-hurricane winds). The results gave wind speed value of 90 mph for 50-year MRI in this area. In the western one-quarter of the country, wind speeds for 50-year MRI were a little less, closer to 85 mph. There was no statistical justification to provide a division line between 85 mph and 90 mph other than the political boundaries. Thus, the non-hurricane design wind speeds in the contiguous United States have only two values, 85 mph and 90 mph, as shown in Figure 2.8.

The wind speed contours in hurricane-prone regions (Figure 2.8) were determined using numerical simulation of hurricane storms. Three independent studies were reviewed (Batts et al., 1980; Georgiou et al., 1983; Vickery and Twisdale, 1993). Speeds in the three studies were converted from specified averaging time to peak gust values. The results of the studies provided wind speed contours at the coastline. Additional wind speed contours were fit between the coastline and the 90 mph contour (see Figure 2.8) by assuming that hurricane winds diminish in approximately 100 miles from the coastline.

The wind speed values on the map are for 50-year MRI. Importance factor I was determined to convert 50-year wind speeds to 100-year or 25-year MRI wind speeds in a similar manner as described for ANSI A58.1-1982. However, the importance factor values in ANSI/ASCE 7-95 are different from the ANSI A58.1-1982 standard because I is placed outside the parentheses, and thus is square of the wind speed ratios (the ANSI/ASCE 7-95 formula reflects this). Separate importance factor values for hurricane wind speeds are not given because they are included by adjusting wind speed contour values and shifting contour locations.

Special wind regions are indicated in the wind speed map (Figure 2.8) to reflect mountain ranges, river valleys, and other unusual local geography. Winds in some local areas of special regions have been known to be substantially higher than the ones indicated in the map. When selecting basic wind speeds in these special regions, use of regional climatic data and consultation with a wind engineer or a meteorologist is recommended.

ANSI/ASCE 7-95 permits assessment of 50-year design wind speed from regional climatic data provided extreme value statistical analysis procedures are used in reducing the data and factors, such as length of record, error-band, averaging time, anemometer height, quality of data, and terrain exposure, are taken into account. Limited length of record can have a large error-band and leads to a large uncertainty in

50-year wind speed. It is possible to have a 20 mph error in wind speed at an individual station with a record length of 30 years. Whenever possible, it is desirable to combine records at several stations to make a longer length of record.

The wind speed map developed for ANSI/ASCE 7-95 is used in AASHTO 1999. The map wind speed is 3-second gust speed at 10 m (33 ft) above ground in flat, open terrain (Exposure C) associated with 50-year MRI (0.02 annual probability).

2.4 Probability of Exceeding Wind Speeds

Annual probability (reciprocal of MRI) of exceeding wind speed relates to any one year. For example, annual probability of 0.02 means that there is a 2% chance of exceeding 50-year MRI wind speed in any one year. However, the probability of exceeding wind speed for a structure depends on the life of the structure. The probability that the design wind speed will be exceeded during the life of the structure is given by the equation:

$$P = 1 - (1 - P_a)^n$$

where P is the probability of exceeding wind speed,
P_a is the annual probability of exceeding (reciprocal of MRI), and
n is the life of the structure.

The probability that design wind speed will be exceeded increases or decreases with the MRI used and with the life of the structure. Values of probability of exceeding design wind speed for different MRI and different life of structure are given in Table 2.2. As an example, if a design wind speed is based on an annual probability of P_a = 0.02 (50-year MRI), there exists a probability of 0.64 (64%) that the design wind speed will be exceeded during the 50-year life of the structure. If the life of structure is 25 years and the design wind speed is for 50-year MRI, the probability is 40% that the design wind speed will be exceeded during the life of the structure. Since the wind pressures are related to allowable stress design, buildings or structures are not expected to collapse if wind speed exceeds design wind speed by a small amount.

2.5 Variation of Wind Speed with Height

2.5.1 Introduction

Wind is movement of air in the atmosphere. When air is moving because of atmospheric conditions or low and high pressures, it encounters friction of the earth's surface. This friction retards the movement of air; wind is reduced closer to the earth's surface. This zone close to earth's surface where friction has influence on wind is about 1,000 ft deep and is called the atmospheric boundary layer. Most buildings and structures are situated in this atmospheric boundary layer. The top of the atmospheric

boundary layer is called gradient height, above which friction of earth's surface has no influence on wind. In the atmospheric boundary layer, wind speed increases with height above ground up to the gradient height.

2.5.2 Terrain Exposure

In the United States, terrain exposures representing ground roughness are divided into four groups. The roughness categories or exposures considered in the United States standards ANSI A58.1-1982 through ANSI/ASCE 7-95 are as follows:

Exposure A: Large city centers with at least 50% of the buildings having a height in excess of 70 ft.

Exposure B: Urban and suburban areas, wooded areas, or other terrains with numerous closely spaced obstructions having the size of single-family dwellings or larger.

Exposure C: Open terrain with scattered obstructions having heights generally less than 30 ft; flat, open country and grasslands are part of this category.

Exposure D: Flat, unobstructed areas exposed to wind flowing over open water for a distance of at least one mile.

Airports where most of the wind speed data are recorded fit in Exposure C category. Wind speed values given in the map are associated with Exposure C category. In addition, Exposure C category is generally used as a default terrain.

Depending on the roughness categories, the wind speeds decrease as the atmosphere approaches the ground, which is the same concept as saying that wind speed increases with increasing height above ground. The gradient heights at which ground friction no longer affects wind speed also depend on exposure categories. The gradient heights for four exposure categories are: Exposure A, 1500 ft; Exposure B, 1200 ft; Exposure C, 900 ft; and Exposure D, 700 ft. Wind speed variations with height over these exposure categories are illustrated in Figure 2.9.

2.5.3 Height and Exposure Factor K_z

The wind speed variations with height and exposure are determined by the following power-law equation:

$$\frac{V_{z_1}}{V_{z_2}} = \left(\frac{z_1}{z_2}\right)^{1/\alpha}$$

Where V_{z1}, V_{z2} are wind speeds at height of z_1 and z_2,

z_1, z_2 are height above ground, and
α is the power-law coefficient.

The power-law coefficient α depends on exposure category and on averaging time of wind speed. For example, for Exposure C category α = 7.0 for fastest-mile wind speed, while α = 9.5 for 3-second gust speed.

Wind speeds obtained from the map are referenced to Exposure C category and 33 ft above ground. It is possible to calculate gradient height wind speed using power-law coefficient α and gradient height for Exposure C category. This allows determination wind speed of any height in any exposure category with appropriate use of the power-law coefficient α and gradient height value.

For simplicity, height and exposure factor K_z is determined as a ratio of square of the wind speed (or height). For fastest-mile wind speed (used in ANSI A58.1-1982 through ANSI/ASCE 7-93), the height and exposure factor is determined by the equation:

$$K_z = 2.58\left(\frac{z}{z_g}\right)^{2/\alpha}$$

$$15 \text{ ft} \le z \le z_g$$

where K_z is height and exposure factor,
z is height above ground,
z_g is gradient height for exposure of interest, and
α is the power-law coefficient for exposure of interest.

Values of gradient height z_g and power-law coefficient α are given in Table 2.3. The equation is valid for any height less than gradient height; wind speed is constant above gradient height. The value of height and exposure factor below 15 feet is assumed to be constant; high turbulence near the ground gives uncertainty in use of the equation.

For 3-second gust wind speed (used in ANSI/ASCE 7-95 and AASHTO 1999), the height and exposure factor is determined by the equation:

$$K_z = 2.01\left(\frac{z}{z_g}\right)^{2/\alpha}$$

$$15 \text{ ft} \le z \le z_g$$

where K_z is height and exposure factor,
z is height above ground,
z_g is gradient height for exposure of interest, and
α is the power-law coefficient for exposure of interest.

Values of power-law coefficient α for 3-second gust speed are given in Table 2.3.

2.6 Gust Effect Factor for Non-Wind Sensitive Structures

2.6.1 Introduction

Gust effect factor (GEF) or gust response factor (GRF) represent equivalent static load on a structure because of the gustiness in wind. In contrast, gust factor (GF) is the ratio of peak gust to design mean wind speed value. The ANSI A58.1 and ASCE 7 wind load provisions have used GEF (GRF is another name for it) while AASHTO wind load provisions have utilized GF.

Gustiness of wind has three characteristics of interest: (1) intensity of gust above mean wind speed, (2) size of the gust, and (3) frequency of gusts. If frequency of gust matches frequency of vibration of structure, that structure would be considered wind-sensitive. Generally, gust frequencies greater than 1 Hz (one cycle per second) are negligible. Thus, structures with fundamental frequency greater than 1 Hz (period of vibration less than 1 second) are considered to be non-wind sensitive structures. Flexible structures with fundamental frequency less than 1 Hz (period of vibration greater than 1 second) can have resonance response in wind; GEF for these wind-sensitive structures is discussed in Section 4 of this report.

2.6.2 GRF in ANSI A58.1-1982

The gust response factor (GRF) accounts for additional loading effects due to wind gustiness over the fastest-mile speed. For non-wind sensitive structures, GRF takes into consideration randomness of gust loading over surfaces of the structure; gust frequency effect is negligible. The formulation of GRF was developed by Vellozzi and Cohen (1968) using the initial work of Davenport (1961). The GRF, G_z, at height z is given by the equation:

$$G_z = 1 + \frac{3\sigma}{P_z}$$

where G_z is GRF at height z,
P_z is mean wind pressure at height z, and
σ is standard deviation of wind pressure.

If fluctuating pressure is assumed to be Gaussian distribution, 3σ represents the peak value with 99% coverage. By utilizing input power spectrum of the wind gusts and output power spectrum of response, Vellozzi and Cohen (1968) developed the equation for GRF as:

$$G_z = 1 + 5.1 T_z R$$

where T_z is turbulence intensity at height z, and
R is response factor.

The above equation is based on mean hourly wind speed. For shorter averaging time of fastest-mile wind speed, the equation becomes:

$$G_z = 0.65 + 3.31 T_z R$$

where T_z is turbulence intensity at height z, and
R is response factor.

For non-wind sensitive structures, the response factor R is assumed to have a constant value of 1.10. Thus, the GRF becomes:

$$G_z = 0.65 + 3.65 T_z$$

where T_z is turbulence intensity at height z.

Turbulence intensity T_z depends on exposure surface roughness and height above ground. The value of T_z decreases as height above ground increases; its value increases as exposure category in rougher (e.g., suburban vs. open) terrain. By using a simple equation for T_z, values of G_z are determined and tabulated for all four exposures and for various heights above ground.

The GRF values developed for ANSI A58.1-1982 continued to be used through ANSI/ASCE 7-93.

2.6.3 GEF in ANSI/ASCE 7-95

With the use of 3-second gust speed as design wind speed in ANSI/ASCE 7-95, gust effect factor (GEF) should be close to unity for non-wind sensitive structures. The GEF is controlled by turbulence intensity and by random nature of wind pressures over the surface area of the structure. The equations for GEF are:

$$G = 0.9\left(\frac{1 + 7 I_z Q}{1 + 7 I_z}\right) \qquad (2\text{-}1)$$

$$Q^2 = \frac{1}{1 + 0.63\left(\frac{b + h}{L_z}\right)^{0.63}}$$

where G is gust effect factor,
I_z is turbulence intensity at equivalent height z, as defined in ASCE 7-95
Q is representation of background response,
L_z is longitudinal integral scale at equivalent height z, as defined in ASCE 7-95
b is structure width, and
h is structure height.

Examination of these ominous looking equations reveals that GEF is dependent on turbulence intensity and size of the structure facing wind. An artificial factor of 0.9 was added in the ANSI/ASCE 7-95 equation to make wind loads similar in magnitude to the previous standard.

In most cases, the value of GEF from these equations is between 0.8 and 0.9. The ANSI/ASCE 7-95 permits use of G = 0.85 for non-wind sensitive structures in Exposure C category.

The equations for GEF shown above were developed by A. Kareem working with G. Solari (Kareem, 1992; Solari, 1993). They used a unified approach to structures that are wind sensitive and non-wind sensitive. Resonance response for wind sensitive structures is added to background response to develop GEF for wind sensitive structures. Wind sensitive structure GEF is discussed in Section 4 of this report with simplification of equations for highway structures. GEF for non-wind sensitive highway structures can be taken as in the range of 0.8 to 1.0, but until additional research is done, should be taken as 1.14, as provided by the proposed AASHTO (1999) specification.

2.6.4 GF in AASHTO 1994

The wind load provisions of AASHTO 1994 used a gust factor (GF) of 1.3; it was not the gust response factor. The value of 1.3 was multiplied to the fastest-mile wind speed. This multiplication in effect represented an increase in wind speed to reflect peak gust. The structure's size or dynamic characteristics or variation of gustiness with roughness of exposure category and with height above ground were not considered. The gust factor gave safe structures, but perhaps was conservative.

2.6.5 GEF in AASHTO 1999

The gust effect factor (GEF) in the AASHTO 1999 wind load provisions is in effect the gust factor. It is recognized that wind load provisions of AASHTO 1994 have been in use for a long time, and these provisions provided reasonably satisfactory structures. Since the gust factor is directly related to wind speed, it changes proportionally to a change in wind speed value (associated with averaging time).

AASHTO 1999 uses the wind speed map that was advanced in ANSI/ASCE 7-95. The wind speeds in this map are 3-second gust speeds. The Durst (1960) curve presented in ANSI/ASCE 7-95 suggest that the ratio of the fastest-mile speed to 3-second gust speed is approximately equal to 0.82. The ratio of the fastest-mile wind speed to the 3-second gust wind speed is determined using the ratio of probable maximum wind speed averaged over t seconds to an hourly mean speed in Figure 2.10. Thus, gust duration for fastest-mile wind speed is the time it takes a column of air at a given velocity to travel one mile. The gust duration for the 3-second gust wind speed is 3 seconds. From Figure 2.9, the ratio V(t) to an hourly speed V_{3600} is determined for the

fastest-mile wind speeds and the 3-second gust wind speeds. These ratios are used to calculate the ratio of the fastest-mile wind speed to the 3-second gust wind speed as follows:

$$\frac{V_{fm}(t) \,/\, V_{3600}}{V_3 \,/\, V_{3600}} = \frac{V_{fm}(t)}{V_3} \approx 0.82$$

where V_{fm} is fastest-mile wind speed,
V_{3600} is mean hourly wind speed, and
V_3 is 3-second gust wind speed.

Table 2.4 provides values for ratios of V_{fm}/V_{3600} and V_3/V_{3600} for various wind speeds, which were determined from Figure 2.10. With V_{fm}/V_{3600} and V_3/V_{3600} known, the ratio V_{fm}/V_3 can be determined and is provided in Table 2.4. The values determined graphically in Table 2.4 for V_{fm}/V_3 are approximately equal to the selected value of 0.82.

The relationship between the fastest-mile wind speeds and the 3-second gust wind speeds may be represented by the following equation:

$$\left(G_{fm} V_{fm}\right)^2 = G_3 V_3^{\,2}$$

where G_{fm} is gust effect factor associated with fastest-mile wind speed,
G_3 is gust effect factor associated with 3-second gust speed,
V_{fm} is fastest-mile wind speed, and
V_3 is 3-second gust wind speed.

The 3-second gust can be determined as follows:

$$G_3 = \left(G_{fm} \frac{V_{fm}}{V_3} \right)^2 = (1.3 * 0.82)^2 = (1.066)^2 = 1.14$$

2.7 Drag Coefficient

Drag coefficients for supports structures are provided in Table 3-5 of the proposed (1999) *Supports Specifications.* The values were revised to account for the use of SI units, the 3-second gust wind velocity, and the mean recurrence intervals. New drag coefficient values for square and diamond tubes have been added. The drag coefficient for the square shape is revised to reflect the influence from the ratio of the corner radius to depth of the member. The drag coefficient for the diamond shape is significantly higher than the value given in the 1994 edition of the specification.

Table 2.1. Importance Factor, I

Annual Probability	MRI (Years)	ANSI A58.1-1982		ASCE 7-95
		Inland	Hurricane	
0.02	50	1.00	1.05	1.00
0.01	100	1.07	1.11	1.15
0.04	25	0.95	1.00	0.87

Notes:

1. Values of I in ASCE 7-95 are square of the values of I in ANSI A58.1-1982 because of formulation.
2. Wind speed contours for hurricanes in ASCE 7-95 incorporates different probability distribution of hurricane wind; I values are same for inland and hurricane winds.

Table 2.2. Probability of Exceeding Design Wind Speed During Life of a Structure

Annual Probability P_a	MRI Years	Life of Structure n years				
		1	5	10	25	50
0.10	10	0.10	0.40	0.65	0.93	0.99
0.04	25	0.04	0.18	0.34	0.64	0.87
0.02	50	0.02	0.10	0.18	0.40	0.64
0.01	100	0.01	0.05	0.10	0.22	0.40

Table 2.3. Values of Gradient Height z_g and Power-Law Coefficient α

Exposure Category	Gradient Height, z_g, ft	Power-Law Coefficient α	
		ANSI A58.1-1982	ASCE 7-95
A: Urban	1500	3.0	5.0
B: Suburban	1200	4.5	7.0
C: Open	900	7.0	9.5
D: Water	700	10.0	11.5

Table 2.4. Ratio of Fastest-Mile Wind Speed to 3-Second Gust Wind Speed

Location	Fastest-Mile Wind Speed	Gust Duration for Fastest-Mile Wind Speed	Ratio of Probable Maximum Speed Averaged Over t Seconds To Hourly Mean Speed	Ratio of Probable Maximum Speed Averaged Over t Seconds To Hourly Mean Speed	V_{fm}/V_3
	V_{fm} (mph)	t (sec)	$V_{fm}(t)/V_{3600}$	V_3/V_{3600}	
Non-Hurricane	70	51.4	1.265	1.525	0.83
Non-Hurricane	80	45	1.285	1.525	0.842
Non-Hurricane	90	40	1.295	1.525	0.849
Hurricane	90	40	1.375	1.67	0.823
Hurricane	100	36	1.39	1.67	0.832
Hurricane	110	32.7	1.40	1.67	0.838
Selected Value					0.82

ISOTACH 0.01 QUANTILES, IN MILES PER HOUR: ANNUAL EXTREME-MILE 30 FT ABOVE GROUND, 100-YR MEAN RE-
RRENCE INTERVAL

Figure 2.1. Wind Map: 100-Year Mean Recurrence Interval (Thom, 1968)

ISOTACH 0.02 QUANTILES, IN MILES PER HOUR: ANNUAL EXTREME-MILE 30 FT ABOVE GROUND, 50-YR MEAN RE-
CURRENCE INTERVAL

Figure 2.2. Wind Map: 50-Year Mean Recurrence Interval (Thom, 1968)

ISOTACH 0.04 QUANTILES, IN MILES PER HOUR: ANNUAL EXTREME-MILE 30 FT ABOVE GROUND, 25-YR MEAN RECURRENCE INTERVAL

Figure 2.3. Wind Map: 25-Year Mean Recurrence Interval (Thom, 1968)

ISOTACH 0.10 QUANTILES, IN MILES PER HOUR: ANNUAL EXTREME-MILE 30 FT ABOVE GROUND, 10-YR MEAN RECURRENCE INTERVAL

Figure 2.4. Wind Map: 10-Year Mean Recurrence Interval (Thom, 1968)

ISOTACH 0.50 QUANTILES, IN MILES PER HOUR: ANNUAL EXTREME-MILE 30 FT ABOVE GROUND, 2-YR MEAN
CURRENCE INTERVAL

Figure 2.5. Wind Map: 2-Year Mean Recurrence Interval (Thom, 1968)

Figure 2.6. Locations of 129 U.S. Weather Stations (Mehta, 1984)

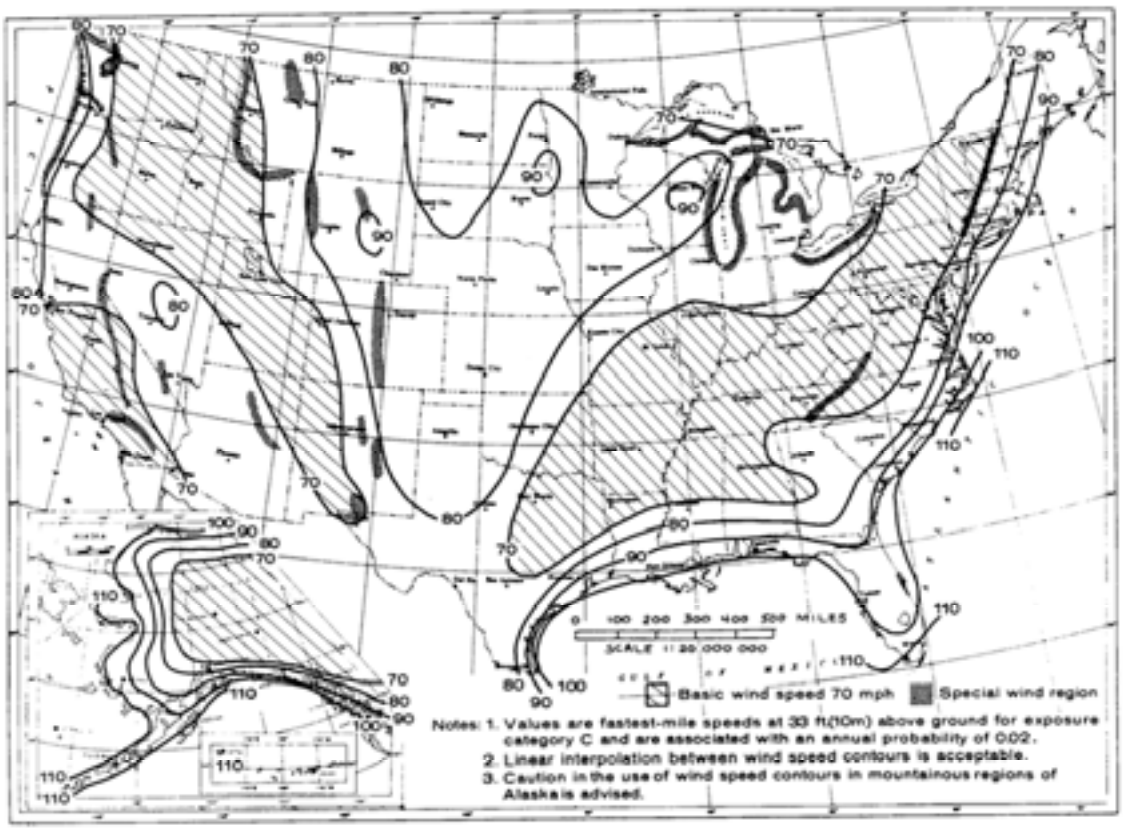

Figure 2.7. Basic Wind Speed Map (ANSI A58.1-1982)

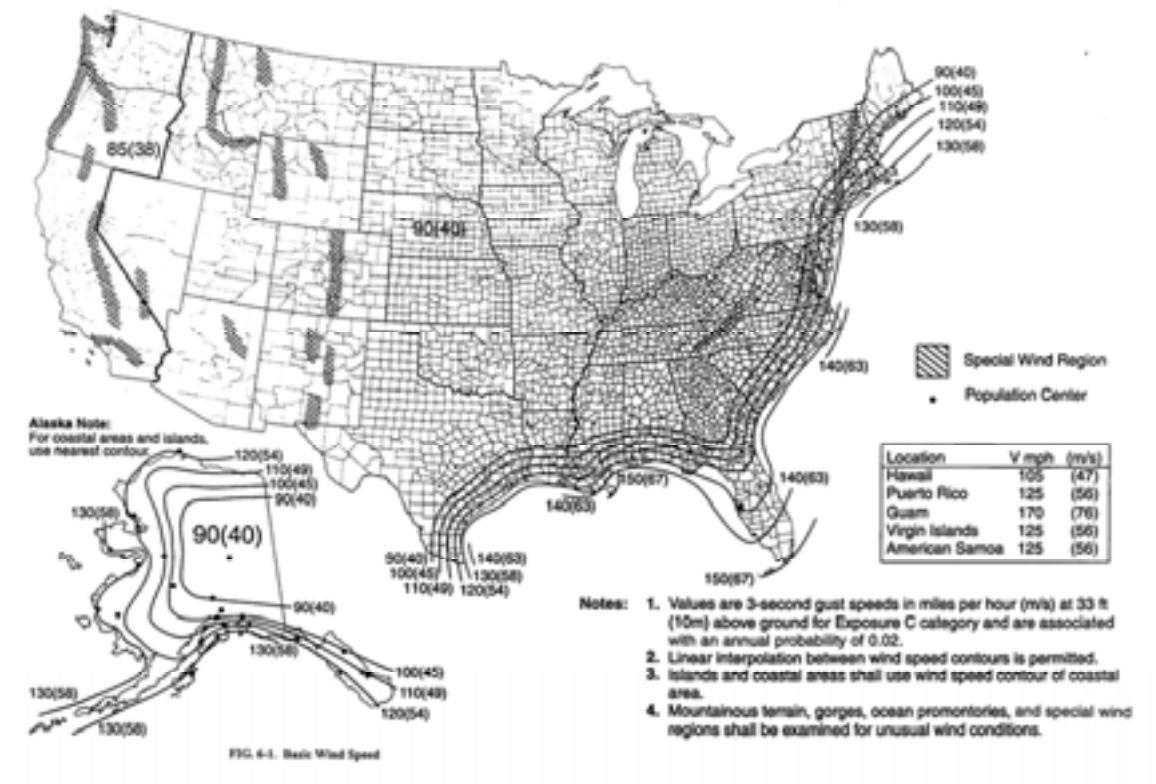

Figure 2.8. Basic Wind Speed Map (ANSI/ASCE 7-95)

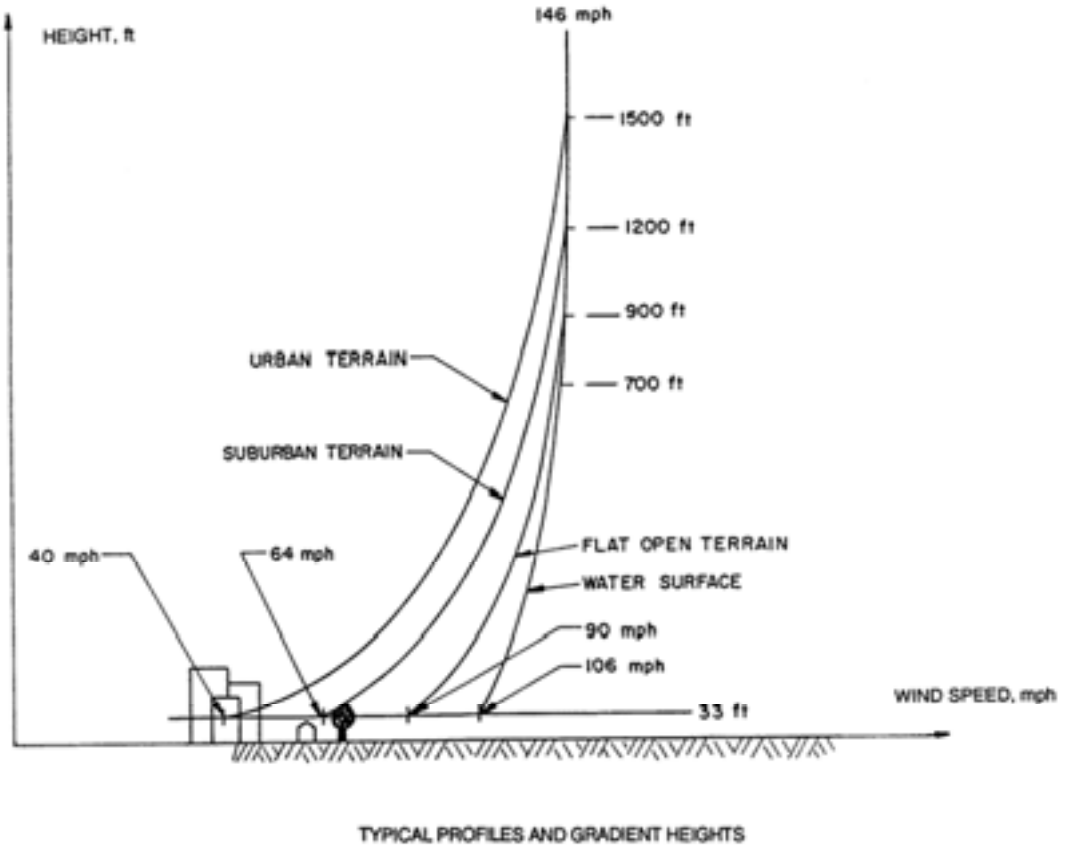

Figure 2.9. Wind Speed Variations with Height

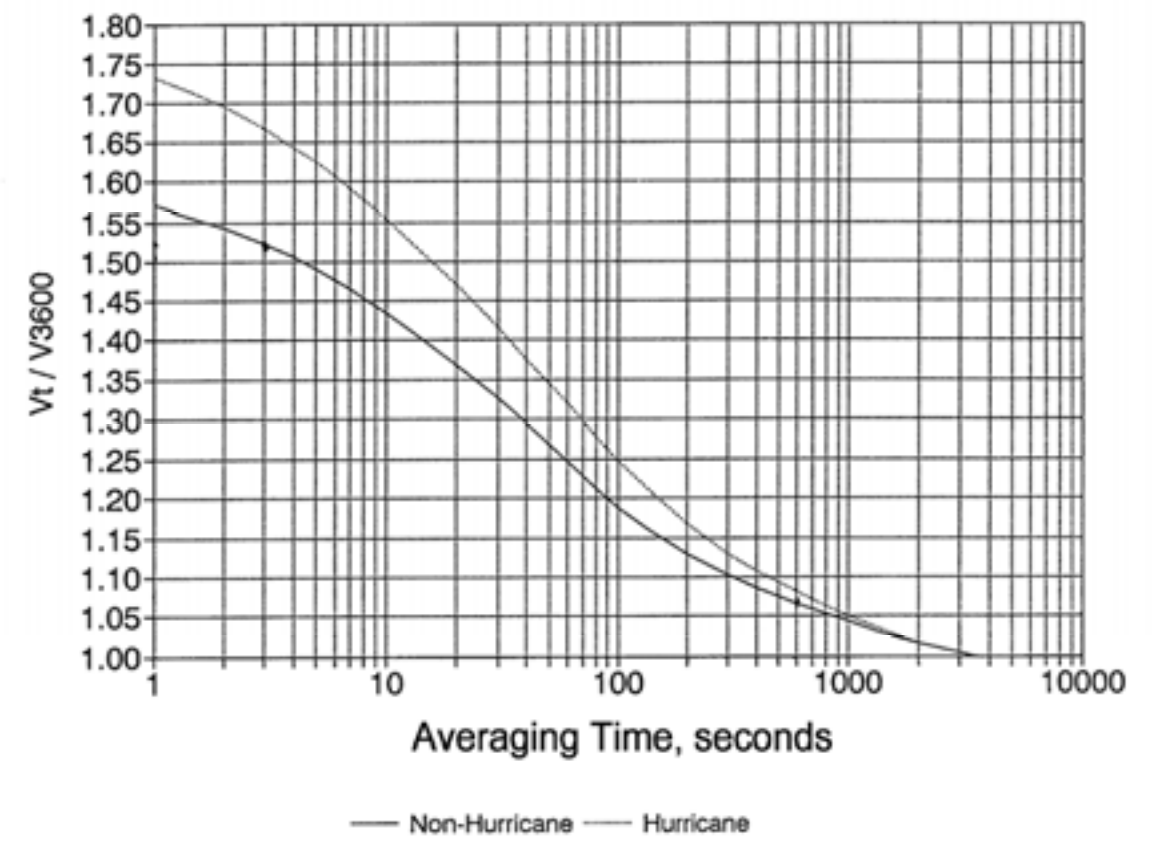

Figure 2.10. Ratio of Wind Speed Averaged Over t Seconds to Hourly Mean Speed (ANSI/ASCE 7-95)

3 Wind Load Comparisons for Current (1994) vs. Proposed (1999) *Supports Specifications*

The changes in the wind loading criteria provided by the proposed specification represent a major and fundamental update to the wind loading criteria of current (1994) *Supports Specifications*. These changes, representing over 20 years of progress in the wind technology, update the *Supports Specifications* to the most current wind methodology. The effects of changing the wind loading criteria and wind map are reviewed in this section of the report. Differences in design wind loads as a result of using different wind speed maps and calculation method were compared for the proposed specification and the current specification for a large number of cities across the United States in an effort to ascertain the effect of the new wind provisions on the design of structural supports.

A comprehensive list of 145 cities was selected for evaluation in this study. The list was representative of urban and rural areas and included Alaska and Hawaii. Comparisons were made between the proposed and current specifications by city, region, and nation-wide. For each site, comparisons were made between the proposed and current specifications by calculating wind pressures for the 10, 25, and 50-year mean recurrence intervals. For the current specification, wind pressures were calculated per Section 1.2.5(A) with a drag coefficient of 1.0. For the proposed specification, wind pressures were calculated per Section 3.8.1 with a drag coefficient of 1.0. To evaluate the effect of structure type and configuration, comparisons were also made by calculating base shears for six support structures.

3.1 Selection of Cities

A list of 145 cities selected for study is shown in Table A-1, sorted by state. This list provides wind sites that include population centers, as well as the rural parts of the United States. The 145 cities include all the cities shown on the 1994 AASHTO wind map, as well as the 75 largest cities in the United States with population greater than 500,000 people.

3.2 Site Groupings

The list of 145 cities was divided into six basic groups (wind regions), based on wind speeds and importance factors given by the proposed specification. The six groups, which cover the contiguous United States, Alaska, and Hawaii, may be listed as follows:

1. Interior Wind Region: 87 cities, 90 mph
2. West Coast Wind Region: 14 cities, 85 mph

3. East Coast Wind Region: 25 cities, based on the hurricane wind region (hurricane contours) on the Atlantic and Gulf Coast areas with winds of 100 mph to 150 mph
4. Alaska: 16 cities, 90 mph to 130 mph
5. Hawaii: 3 cities, 105 mph
6. Special Wind Region: 4 cities, based on the shaded areas on the wind map of the proposed specification

The basic wind speed and importance factors for the 50, 25, and 10-year mean recurrence intervals for the proposed specification, as well as the 50, 25, and 10-year wind speeds from the current AASHTO specification, were determined for each of the 145 cities. The 145 cities were sorted by 3-second gust wind speed for the proposed specification, and by the 50, 25, and 10-year wind speeds for the current AASHTO specification. The 145 cities can be grouped into 44 site-specific locations, which have the same 3-second gust wind speed, as well as the same 50, 25, and 10-year wind speeds from the current AASHTO specification. Table A-2 provides the list of 145 cities as sorted by site, which includes the basic wind speed and importance factors from the proposed specification and the 50, 25, and 10-year wind speeds from the current specification.

The wind regions are noted as follows:

Wind Region	No. of Site-Specific Locations	No. of Cities	Cities with Population > 500,000	Cities with Population < 500,000
Interior Wind Region	8	85	46	39
West Coast Wind Region	6	12	7	5
East Coast Wind Region	17	25	18	7
Alaska	8	16	0	16
Hawaii	1	3	1	2
Special Wind Region	4	4	3	1
Total	44	145	75	70

3.3 Special Wind Regions

Four cities out of the 145 cities were located in the shaded areas on the proposed AASHTO wind map. The cities were Los Angeles, California; Denver, Colorado; Great Falls, Montana; and Portland, Oregon. Two of the cities are located in the interior wind region, and the other two cities are located in the west coast wind region. These shaded areas on the proposed AASHTO wind map include mountainous terrain, gorges, ocean promontories, and special wind regions (SWR) that need to be examined for unusual wind conditions. These four cities are provided in the list of wind sites, but are not included in the wind pressure or base shear comparisons, since more specific wind information is required for these areas that is not provided by the proposed AASHTO wind map.

3.4 Wind Pressure Comparison

For each of the 40 site-specific locations, except those sites in special wind regions, wind pressure was calculated for heights from ground line to 200 feet above ground line for the proposed and current specifications. Figures B-1 through B-80 show the effective wind pressure for 50, 25, and 10-year mean recurrence intervals for the proposed and current specifications, as well as the ratio of wind pressures for the proposed to current specification. The ratio of wind pressures for the proposed to current specification is also provided in Table A-3 for the 50-year mean recurrence interval, Table A-4 for the 25-year mean recurrence interval, and Table A-5 for the 10-year mean recurrence interval. The numbers in parentheses are the number of cities out of 145 that are represented by the data.

As shown in the figures, the wind pressure distribution according to the current specification exhibits a step function, whereas the proposed specification has a gradual change of wind pressure with height. The ratio of wind pressures varies with height, but can be divided into two sets of data, those with heights above 15 feet and those with heights less than 15 feet. All graphs show a higher wind pressure ratio for heights less than 15 feet than for heights greater than 15 feet. The graphs for heights less than 15 feet would be applicable for small and medium roadside signs. The roadside signs would have a 10-year mean recurrence interval. The graphs also indicate that the wind pressure ratios for the proposed to current specification vary with the mean recurrence interval, which implies that changes in wind pressures, when upgrading from the current to proposed specification, will vary for different structure types at a specific site.

Figures B-81 through B-95 show the range of ratios of wind pressures for the proposed to current specification for the 50, 25, and 10-year mean recurrence intervals for the interior wind region, the west coast wind region, the east coast wind region, Alaska, and Hawaii. For each wind region, the figures show all sites in that region, the average ratio of wind pressures for the proposed to current specification, and the range of ratios of wind pressures for the proposed to current specification.

The figures show that the average of the wind pressure ratios for the proposed to current specification varies with site. It is interesting to note that for all sites the range of wind pressure ratios varies by –10% to +13% from the average.

Figures B-96 through B-105 show the average ratio of wind pressures for the proposed to current specification at each site-specific location for the 50, 25, and 10-year mean recurrence intervals. The figures are divided into the interior wind region, the west coast wind region, the east coast wind region, Alaska, and Hawaii. Figures are provided for heights greater than 15 feet and for heights less than 15 feet. These figures depict the variation of the average of the wind pressure ratios as a function of site and mean recurrence interval.

Figures B-106 and B-107 show the average ratio of wind pressures for the proposed to current specification for the mean recurrence intervals of 50, 25, and 10 years. The average wind pressure ratios for each wind region (i.e., interior wind region, west coast wind region, east coast wind region, Alaska, and Hawaii) are also included. The greatest increase in wind pressure occurs in the east coast wind region, while the greatest decrease in wind pressure occurs in Hawaii.

In summary, Figure B-108 shows the average ratio of wind pressures for the proposed to current specification for the mean recurrence intervals of 50, 25, and 10 years for all 141 cities. The averages are provided for heights above 15 feet and heights below 15 feet. The averages above 15 feet are approximately 0.98, while the ratio below 15 feet is approximately 1.11.

3.5 Base Shear Comparison

Six support structures were selected so that base shears could be compared between the proposed and current specifications. Sketches for the non-cantilevered overhead sign, the cantilevered overhead sign, the high mast lighting pole, the cantilevered traffic signal structure, the streetlighting pole, and the roadside sign are provided in Figures B-109 through B-114. Base shears for the proposed and current specifications were calculated for each site.

Base shears and ratios for the proposed and current specifications are provided in Table A-6 for the non-cantilevered overhead sign (50-year MRI), in Table A-7 for the cantilevered overhead sign (50-year MRI), in Table A-8 for the high mast lighting pole (50-year MRI), Table A-9 for the cantilevered traffic signal structure (25-year MRI), in Table A-10 for the streetlighting pole (25-year MRI), and in Table A-11 for the roadside sign (10-year MRI).

Figures B-115 through B-144 provide base shear comparisons for the six support structures. The figures are divided by wind region and include the interior wind region, the west coast wind region, the east coast wind region, Alaska, and Hawaii. Base shears are provided for each site-specific location.

Figures B-145 through B-149 provide the ratio of base shears for the proposed to current specification for the six support structures. The figures are presents for the interior wind region, the west coast wind region, the east coast wind region, Alaska, and Hawaii. The ratios vary with site, as well as structure type.

Figure B-150 provides the average base shear ratios for each wind region as well as the average base shear ratio for all 141 cities. Values are provided for each of the six support structures. An increase in the average wind pressure is occurring in the east coast wind region and a decrease in the average wind pressure is occurring in Hawaii.

Figure B-151 provides the average base shear ratios for all 141 cities for each of the six support structures. The average wind pressure ratio over all 141 cities decreases by about 3% for all structure types, except for the roadside sign structure, which increases by 13%.

3.6 Summary

In comparing the current versus the wind provisions proposed by NCHRP 17-10, it is apparent that changes in wind pressure, either decreasing or increasing, are highly site-specific. However, when looking at the average ratio of wind pressures for the proposed to current specification, the average ratio for 141 cities is only 0.98 for heights greater than 15 feet and 1.13 for heights less than 15 feet.

For the six support structures selected in this study, the changes in base shears are consistent with those provided for the wind pressure ratios. The average base shear ratio is 0.97 for all supports structures, except for the roadside sign structures, which has a base shear ratio of 1.13.

Thus, it can be said that **on the average** wind loads on support structures, except for roadside signs, computed in accordance to the new wind provisions are comparable to the loads computed using the current *Supports Specifications* (1994). However, the differences could vary considerably depending on the specific location on the map. Tables 3.1, 3.2, and 3.3 provides a summary of the differences in wind pressure for the 5 wind regions across the United States for each of the mean recurrence intervals.

In Tables 3.1, 3.2, and 3.3 the total number of cities of 145 has been grouped according to the percent increase or decrease in wind pressure for the proposed versus current specification. Table 3.1 for the 50-year MRI would be applicable for overhead sign structures and high mast lighting poles; 73% of the cities are within the range of 20% decrease to 10% increase in wind pressure; 45% of the cities are within 10% increase/decrease in wind pressure. Table 3.2 for the 25-year MRI is applicable for cantilevered traffic signal structures and streetlighting poles; 70% of the cities are within the range of 30% decrease to 10% increase in pressure; 58% of the cities are within 10% increase/decrease in wind pressure. Table 3.3 for the 10-year MRI is applicable for roadside sign structures; 72% of the cities are within a 20% decrease to a 20% increase in wind pressure; 45% of the cities will have a 10% to 20% increase in wind pressure.

Insert Tables 3.1, 3.2, 3.3

4 GEF for Wind Sensitive Structures

4.1 Introduction

The proposed (1999) AASHTO specification currently includes a gust factor, but not a gust effect factor for wind sensitive structures. A review was done on methods for incorporating the flexibility of structural supports in the wind loading computation. A comparison has been made with the procedure for wind sensitive structures in the latest version of the national standard of ASCE 7-98 that was developed for flexible buildings. Simplified equations for wind sensitive structures have been proposed. However, insufficient research is available on gust effect factors for flexible support structures.

4.2 Background

Wind flow around a structure induces fluid-structure interaction since wind is fluid. In classical fluid mechanics (air, water, or other fluid), fluid-structure interaction is a very complex problem. Fluid flow acts or interacts with a structure to cause vibrations. These vibrations are divided into three separate phenomena for simplicity: 1) Resonance response in the direction of flow, 2) Vortex shedding response across the flow, and 3) Galloping or fluttering. Wind being fluid, it also causes wind-induced vibrations in highway structures, which are slender and flexible or wind sensitive.

Section 2.6 discusses wind sensitive and non-wind sensitive structures. Structures are generally considered wind sensitive if their fundamental frequency is less than 1 Hz (period of vibration greater than 1 second). Wind sensitive structures will have resonance response in the direction of wind; it is called along-wind response. The resonance response causes loads in addition to what is described in Section 2 for non-wind sensitive structures. These additional loads are taken care of by the gust effect factor (GEF) for wind-sensitive structures in the wind load standards. Formulation of GEF in ASCE 7-98 and its simplification for highway structures are presented in Sections 4.3 through 4.5.

Across-wind vibration due to vortex shedding and violent vibrations of galloping or fluttering due to instability are considered special cases and require advice from wind engineers and/or wind tunnel or full-scale testing. These phenomena are not covered in ASCE 7-98 or other U.S. standards. The phenomena are briefly described in Section 4.6.

4.3 GEF for Along-Wind Response

Gust effect factor (GEF) for non-wind sensitive structures is presented in Section 2.6. Structures with fundamental frequency greater than 1 Hz (period of vibration less than 1 second) are considered non-wind sensitive structures. Flexible structures with fundamental frequency less than 1 Hz (period of vibration greater than 1 second) are

considered wind-sensitive structures because they can have resonance response in addition to response due to turbulence in wind.

As discussed in Section 2.6, the procedure to determine GEF (also called gust response factor) has evolved from the work by Davenport in 1961 (Davenport, 1961). Graphical and analytical procedures are included in the national standards ANSI A58.1-1982, ASCE 7-88, ASCE 7-95 and the latest ASCE 7-98. It is our goal to develop a simplified procedure specifically applicable to highway wind-sensitive structures such as traffic signal structures, sign structures, and lighting poles. Naturally, this simplification has restrictions, but it covers most of the common structures in current use. The simplification is based on the latest analytical procedure given in ASCE 7-98.

4.4 GEF Procedure of ASCE 7-98

For wind-sensitive structures, GEF in ASCE 7-98 is calculated using the following equation:

$$GEF = 0.925\left[\frac{1+1.7I_Z\sqrt{g_Q^2Q^2+g_R^2R^2}}{1+1.7g_vI_Z}\right] \tag{4-1}$$

Parameters in the above equation are determined using a series of equations. Peak factors g_V and g_Q are given as a constant value of 3.4. Peak factor g_R is determined as:

$$g_R = \sqrt{2\ln(3600\,n)} + \frac{0.577}{\sqrt{2\ln(3600\,n)}} \tag{4-2}$$

where n is the natural frequency of structure in the along wind direction, Hz
ln is the natural logarithm.

Turbulence intensity I_z is determined as:

$$I_z = c\left(\frac{33}{z}\right)^{1/6} \tag{4-3}$$

where z is the height at which turbulence intensity is assessed; in ASCE 7-98, it is taken as 0.6 times the height of the structure with minimum value shown in Table 4.1
c is a constant (values shown in Table 4.1).

Background response factor Q is determined using the following equation:

$$Q^2 = \frac{1}{1 + 0.63\left(\frac{B+h}{L_z}\right)^{0.63}} \tag{4-4}$$

where B is the width of the structure
h is the height of the structure.

Integral length scale L_z is determined as:

$$L_z = \ell\left(\frac{z}{33}\right)^{\epsilon} \tag{4-5}$$

where ℓ and ϵ are constants given in Table 4.1
z is the height above ground used in equation 4-3.

Resonance response factor R is determined using the following equation:

$$R^2 = \frac{1}{\beta} R_n R_h R_B \left(0.53 + 0.47 R_L\right) \tag{4-6}$$

where β is the critical damping ratio.

Other parameters are determined using the following series of equations:

$$R_n = \frac{7.47N}{\left(1 + 10.3N\right)^{5/3}} \tag{4-7}$$

$$N = \frac{nL_z}{\overline{V}} \tag{4-8}$$

$$\overline{V} = b\left(\frac{z}{33}\right)^{\overline{\alpha}} V\sqrt{I}\left(\frac{88}{60}\right) \tag{4-9}$$

where V is the basic design wind speed, mph
I is the importance factor
z is the height above ground used in equation 4-3
$\overline{\alpha}$ and b are constants given in Table 4.1
n is the natural frequency of structure in the along wind direction, Hz, and
L_z is from equation 4-5.

$$R_h = \frac{1}{\eta} - \frac{1}{2\eta^2}\left(1 - e^{-2\eta}\right) \geq 1.0 \tag{4-10}$$

using $\eta = 4.6\frac{nh}{\overline{V}}$

where n is the natural frequency of structure in the along wind direction, Hz

$\overline{V}$ is from equation 4-9
h is the height of the structure.

$$R_B = \frac{1}{\eta} - \frac{1}{2\eta^2}\left(1 - e^{-2\eta}\right) \geq 1.0 \qquad (4\text{-}11)$$

using $\eta = 4.6\frac{nB}{\overline{V}}$

where n is the natural frequency of structure in the along wind direction, Hz
$\overline{V}$ is from equation 4-9
B is the width of the structure across wind.

$$R_L = \frac{1}{\eta} - \frac{1}{2\eta^2}\left(1 - e^{-2\eta}\right) \geq 1.0 \qquad (4\text{-}12)$$

using $\eta = 15.4\frac{nL}{\overline{V}}$

where n is the natural frequency of structure in the along wind direction, Hz
$\overline{V}$ is from equation 4-9
L is the length of the structure in the direction of wind.

Highway structures have limited dimensions. For example, length in the direction of wind is generally small compared to other dimensions. Also, for high-level lighting poles, the dimensions across and along wind are small compared to the height. These specific geometrical characteristics permit simplification of the calculations for GEF. Parametric studies and simplified equations are presented in the subsequent sections.

4.5 Simplified GEF Equation

4.5.1 Parametric Studies of GEF

To assess what are the most critical parameters for GEF, a parametric study is conducted for the ASCE 7-98 equations. According to the detailed procedure of the ASCE, the variables involved in the equations could be divided into three groups:

- *Geometric Variables*: These variables include the height and width of the structure. It should be noted that for the high-level lighting posts the width is quite small compared to the height.

- *Wind Characteristics Variables*: These variables include turbulence intensity I_z, design wind speed V, longitudinal integral scale L_z, and correlation of gusts.

- *Structure Related Variable*s: These variables are structure's natural frequency of vibration n, and critical damping ratio β. There is no analytical procedure to determine critical damping ratio β; it can only be determined from full-scale testing.

For this parametric study two high-level lighting poles are chosen since they represent the most slender and flexible highway structures. Their dimensions and structural characteristics are shown in Table 4.2. The three parameters that have a significant effect on GEF are found to be wind speed V, structure's frequency of vibration n, and critical damping ratio β.

For the two poles, GEFs are determined using the equations of ASCE 7-98 for various wind speeds. The calculated GEFs versus wind speed V are shown in Figure 4.1. It is found that when design wind speed increases from 90 mph to 150 mph, the GEF for the same pole increases by about 16%.

To assess the effects of structure's natural frequency on GEF, the natural frequencies of the poles is varied from 0.1 to 0.9 Hz. For these calculations, design wind speed was kept constant at 100 mph and critical damping ratio is assumed to be 0.02. As can be seen in Figure 4.2, the GEF values vary significantly with natural frequency of vibration. When natural frequency increased from 0.1 to 0.9 Hz, the GEF value decreased by almost 40%.

Damping is made up of two components, 1) structural (mechanical) damping and 2) aerodynamic damping. The structural damping depends on the material, type of connection, flexibility of structure and rigidity of foundation. Structural damping is not a constant number since it depends on the amplitude of vibration and the participation of different modes of vibration. As a rule, higher modes of vibration will have higher damping. Consequently, the more there is participation of the higher modes, the more the structural damping. For welded steel structures, structural (mechanical) damping may be as low as 0.5% or as high as 2.0% depending on the amplitude of vibration, higher modes of vibration and flexibility of foundation. The aerodynamic damping depends on the amplitude of vibration, the shape of the structure and the wind speed. Therefore, aerodynamic damping can be significant in the case of tall flexible structure with large deflection. There is no theoretical procedure for obtaining damping ratios. Precise damping values could only be determined through full-scale experiments. More information on damping can be obtained from Kareem (1996) and Watanabe (1995). Figure 4.3 shows GEFs calculated using damping range of 0.5% to 3.5%. GEF values vary significantly with the value of the damping ratio. When the damping ratio decreases from 0.02 to 0.01 the GEF increases by about 20%.

Based on the parametric study, it can be concluded that the significant parameters involved in the calculation of GEF are the structure natural frequency, the design wind speed, and the critical damping ratio.

Other parameters such as width and space correlation are taken into account for rigid structures (non-wind sensitive), but are not significant for wind sensitive structures.

4.5.2 Simplified Equation for High-Level Lighting Poles

The rational procedure for obtaining GEF for flexible structures given in ASCE 7-98 has been studied thoroughly for the following characteristics of high-level lighting poles:

- Poles are located in exposure “C”.
- Pole height range from 70 to 200 feet with a practical average of 125 feet.
- Natural frequency of structures range from 0.2 Hz to 1.0 Hz.
- Design wind speed range from 90 mph to 150 mph.

The rational procedure of the ASCE 7-98 is modified with series expansion, assumptions, and simplification to yield the following simplified equation:

$$GEF = \left[0.8 + C\left(\frac{V\sqrt{I}}{n} \right)^{0.64} \left(\frac{1}{\beta} \right) \right] \times \left[0.68 + 16\,\beta \right] \qquad (4\text{-}13)$$

where V is design wind speed, mph
I is the importance factor
n is the natural frequency of structure in along wind direction, Hz
β is the damping ratio
C is a constant = 2.75×10^{-4} ($C = 4.6 \times 10^{-4}$ SI)

Assumptions:

- Pole width is negligible compared to pole height.
- Turbulence intensity I_z is taken as 0.20.
- Since the pole has very small width and depth (in direction of wind), it is assumed that gust space components are perfectly correlated.

In equation 4-13, the second bracketed term becomes 1.0 for damping ratio of $\beta = 0.02$. The correlation of the proposed equation with the ASCE 7-98 rational procedure is studied. It is found that the proposed equation is well correlated for $\frac{V\sqrt{I}}{n}$ in the range of 200 up to 700 where V is expressed in mph. In case $\frac{V\sqrt{I}}{n}$ exceeds the limiting value, it is recommended to use the ASCE 7-98 rational procedure.

In equation 4-13, as well as in the ASCE 7-98 rational procedure, all the terms are well established except for the damping ratio β. As mentioned previously, there is no theoretical or analytical procedure to determine a specific value of damping ratio. However, based on engineering judgment, a damping ratio of 0.02 is quite acceptable for welded steel high-level lighting poles. It is felt that this value is reasonable, and perhaps conservative, because high mast poles are likely to have some aerodynamic damping value in addition to mechanical damping.

Figure 4.4 shows how the proposed equation correlates with the rational procedure of the ASCE 7-98.

4.5.3 Simplified Equation for Signal and Sign Structures

Traffic signal and sign structures are different from high-level lighting poles in two

aspects: 1) they are shorter in height and 2) the width of the fixtures is significant compared to the height. This makes the background response component larger than that of the high-level lighting post. Additionally, the resonant response component in the GEF becomes less significant compared to the background one.

In signal light structures, the structures might have cantilever arms with fixtures of significant width, i.e., the B dimension is significant. To perform calculations using the rational procedure of the ASCE 7-98, some assumptions are made, these are:

- B dimension (width of signal fixtures) is 8 feet, equivalent to two signal fixtures.
- For short lighting poles (h = 25 feet), the B dimension is 7 feet for the arm length.
- For structures supporting signs, the width of the sign B can be 20 feet.
- The damping ratio is taken as 0.01 and 0.02; results for both values are reported.
- Wind speeds are considered to be 90 and 150 mph to establish upper and lower bound values of wind speeds.

It is expected that the highest wind speed (150-mph) together with the lowest damping ratio (0.01) will yield the highest GEF. Conversely, the lowest wind speed (90-mph) together with the highest damping expected will yield the lowest GEF. Both combinations of values are used within the ASCE 7-98 procedure to demonstrate the complete range of GEF.

A simplified equation for GEF for such structures is developed. It is similar to that of the high-level lighting posts. The equation is in the following form:

$$GEF = \left[0.95 + C \left(\frac{V\sqrt{I}}{n} \right)^{0.64} \left(\frac{1}{\beta} \right) \right] \qquad (4\text{-}14)$$

where V is design wind speed, mph
I is the importance factor
n is the natural frequency of structure in the along wind direction, Hz
β is the damping ratio
$C = 2.75 \times 10^{-4}$ ($C = 4.6 \times 10^{-4}$ SI)

Assumptions:

- Turbulence intensity I_z is taken as 0.20.
- Since the dimensions are relatively small, gust space components are correlated.

It should be noted that the constant term in the equation is larger in value compared to that of the high-level lighting posts. This is due to the fact that the height is not large (i.e., the wind forces are well-correlated over the structure). Moreover, the equation does not need the correction factor [0.68 + 16 β] that appeared in equation 4-13 since resonance response is not dominating.

Attention should be given to the variable n since it is not the across (perpendicular to) wind natural frequency of vibration, but it is the along (in the direction of) wind one.

The damping ratio for such structures is recommended to be taken as 0.015 as they are not supposed to have as large amplitudes as the high mast poles; therefore, the aerodynamic damping will be low.

Equation 4-14 gives well-correlated results for $\frac{V\sqrt{I}}{n}$ values up to 400 where V is expressed in mph. Table 4.3 shows GEF values obtained using the ASCE 7-98 rational procedure with the mentioned assumptions and the corresponding GEF values obtained by the simplified equation for different cases.

4.6 Vortex Shedding and Galloping

4.6.1 Vortex Shedding Vibrations

Vortex shedding is a well-investigated phenomenon in fluid mechanics. When wind flow separates from the structure, vortices are formed in the flow. These vortices go downstream along with the flow. Von Karman showed that, at some flow speed, the vortices are formed alternatively on each side of the structure; a vortex trail is shown in Figure 4.5.

When wind is passing around a structure, such as a pole, vortices are shed on each side at some frequency (see Figure 4.5). Each vortex applies a small force normal to wind flow on the structure. Thus, the vortex shedding forces are applied alternatively on each side of the structure. If the frequency of application of these forces match the natural frequency of the structure, vortex shedding response of the structure in the across wind direction (normal to wind flow) becomes large.

Vortex shedding frequency n_V is described by the following equation:

$$n_V = \frac{S\,V}{D} \tag{4-15}$$

where V is steady wind speed, fps
D is the dimension of the structure normal to flow, feet
S is the Strouhal number.

The Strouhal number is a characteristic constant for each structure shape. It can only be determined experimentally. Strouhal numbers for most common shapes are given in fluid mechanics books; one source is by Simiu and Scanlan (1996).

For the vortex shedding problem to become significant, two items are necessary: 1) the structure is fairly flexible, and 2) the wind is steady and persistent. Since the vortex shedding forces are small, they have to act over a period of time to cause the across wind resonance response. Vortex shedding at high wind speeds such as 90 to 150 mph is not a major problem because high wind speeds do not last for a long time. Steady wind causing vortex shedding can result in fatigue cracking. None of the United States standards or codes addresses the vortex shedding problem. It is recommended

that a wind engineer be consulted if a vortex shedding problem occurs.

4.6.2 Galloping and Fluttering Vibrations

In fluid mechanics, the fluid-structure interaction can cause violent vibrations of the structure or its components. Certain structural shapes can become unstable in wind flow, causing galloping. The oscillations during galloping are of large amplitude in the direction normal to wind flow; the amplitude can be as much as 10 times the dimension of the structure. An example of galloping is power line conductors that have received a coating of ice under the condition of freezing rain. The coating of ices changes the shape of the conductor for it to become unstable and cause it to gallop. McDonald et al (1995) assessed that traffic signal structures galloped when wind blew from behind the signal light fixture. This galloping depended on the shape of the combined cantilever arm and signal light fixture. The problem was solved by providing aerodynamic damping with a horizontal plate.

Fluttering is aeroelastic oscillations of flexible structures or panels. It is a very rapid oscillation where a structure's deflection induces unstable oscillations. Other examples are the flutter of the taut fabric of tents and flags.

Galloping and fluttering vibrations are special cases of vibrations. They are complex phenomena and, most often, require wind tunnel or full-scale testing to mitigate them.

4.7 Summary

1. Gust effect factor for non-wind sensitive highway structures, which have an along-wind natural frequency greater than 1 Hertz, will usually be in the range of 0.8 to 1.0. However, for simplicity, and in order to account for the flexibility of support structures in general, a unified gust effect factor (GEF) of 1.14 could be used, as provided by the proposed AASHTO (1999) specification.

2. In general, for wind sensitive highway support structures, which have an along-wind natural frequency less than 1 Hertz, the GEF that is provided by ASCE 7-98 (equation 4-1) may be used.

3. The GEF for wind sensitive structures has been simplified for certain support structures. For tubular steel high mast lighting structures with heights greater than 70 feet, equation 4-13 may be used, where $\frac{V\sqrt{I}}{n}$ is in the range of 200 up to 700.

4. For traffic signal structures, overhead sign structures, and streetlighting poles, equation 4-14 may be used and is valid for $\frac{V\sqrt{I}}{n}$ values up to 400.

5. GEF for wind sensitive highway structures provided by the equations in items 2, 3,

and 4 will probably be in the range of 1.0 to 2.0. A minimum value for the gust effect factor of 1.14 could be used, as provided by the proposed AASHTO (1999) specification.

6. Roadside signs are not anticipated to be wind-sensitive. Since most of these structures will have an along wind natural frequency greater than 1 Hertz, the gust factor of 1.14 can be applied to these structure types.

7. A proposed specification and commentary for the GEF for wind sensitive structural supports is provided in Appendix C.

8. Until further research is performed to verify the GEF for wind sensitive and non-wind sensitive structural supports, it is recommended to use the GEF of 1.14 for all structure types as provided in the proposed *Supports Specifications*. While this factor is greater than the GEF for non-wind sensitive structures, it is smaller than the GEF for wind sensitive structures. Additionally, the use of the GEF of 1.14 will result in wind pressures that are on the average comparable to the wind pressures computed using the current (1994) *Supports Specifications*, for which satisfactory structural performance has been demonstrated.

Table 4.1. Constants for GEF (ASCE 7-98)

Exposure	b	c	ℓ (ft)	$\in$	$\bar{\alpha}$	z_{min} (ft)
Suburban B	0.45	0.30	320	1/3	1/4.0	30
Open C	0.65	0.20	500	1/5	1/6.5	15
Water D	0.80	0.15	650	1/8	1/9.0	7

Table 4.2. Characteristics of Poles A and B

	Pole Height (ft)	Top Diameter (in)	Bottom Diameter (in)	Natural Frequency (Hz)
Pole A	150	7.75	28.375	0.247
Pole B	150	28.375	28.375	0.294

Table 4.3. Comparison of GEF for ASCE 7-98 and Simplified Equation.

Configuration	n* (Hz)	W. Speed	β	G_f (ASCE)	G_f (Simp.)	G_f (Simp.)/ G_f (ASCE)
Cantilever mast arm, 18-ft high, 48-ft span supporting two signals.	0.80	90	0.02	1.206	1.230	1.02
	0.80	150	0.01	1.572	1.730	1.10
Monotube span-type sign, 20-ft high,100-ft span, supporting two signals.	0.50	90	0.02	1.367	1.330	0.97
	0.50	150	0.01	2.034	2.000	0.98
Cantilever Highway sign, 20-ft high, 40-ft span, sign is assumed to be 20-ft width.	0.78	90	0.02	1.205	1.231	1.02
	0.78	150	0.01	1.749	1.740	0.99
Lighting pole, 25-ft high, 7-ft span.	0.72	90	0.02	1.214	1.250	1.03
	0.72	150	0.01	1.776	1.780	1.00

* n is the along (in direction of) wind natural frequency and not the across (perpendicular to) wind one.

Figure 4.1. Effect of Design Wind Speed on Gust Effect Factor. For Poles A and B, $\beta = 0.02$, I = 1.0

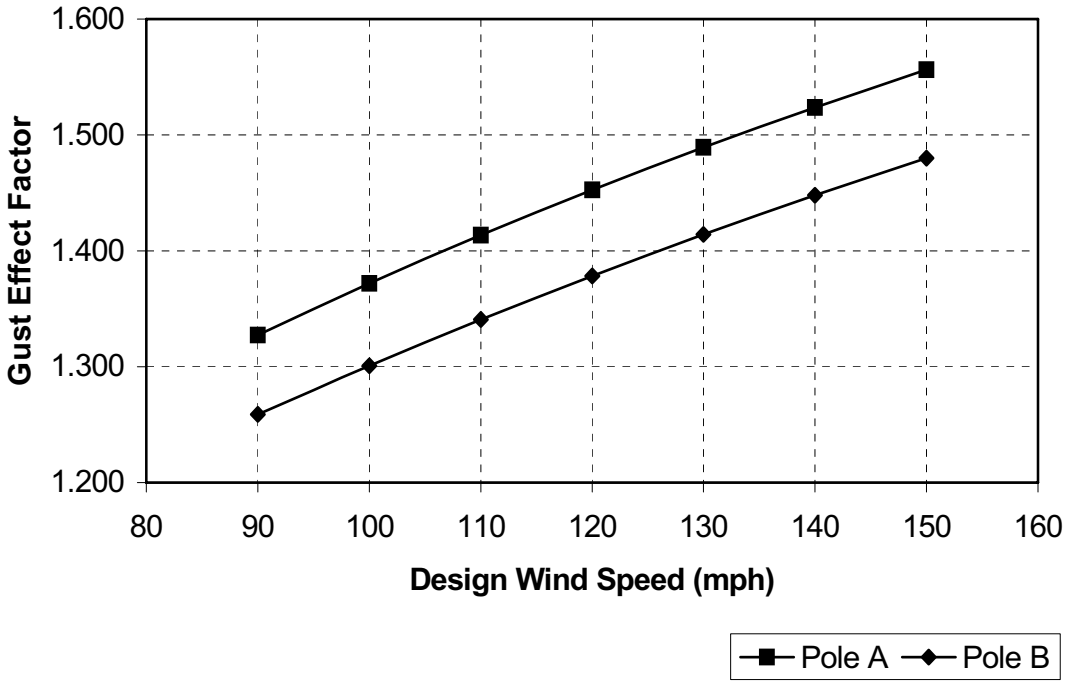

Figure 4.2. Effect of Natural Frequency on Gust Effect Factor. For Poles A and B, Design Wind Speed V = 100 mph, $\beta = 0.02$, I = 1.0.

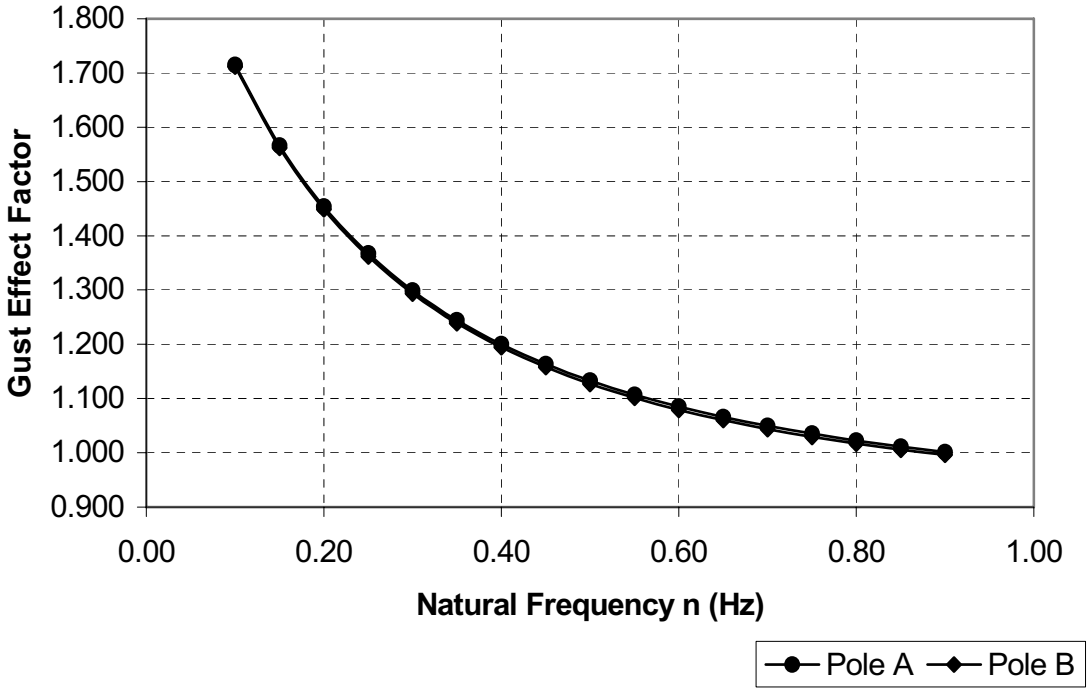

Figure 4.3. Effect of Damping Ratio (β) on Gust Effect Factor. For Poles A and B, Design Wind Speed V = 100 mph, I = 1.0.

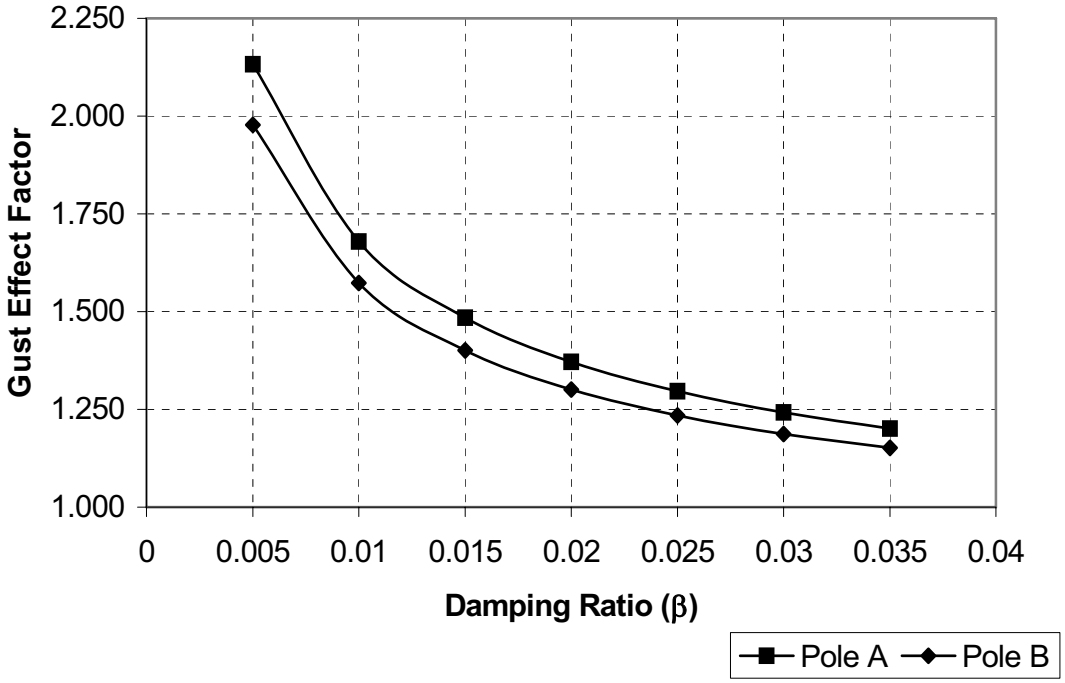

Figure 4.4. GEF Correlation Between ASCE 7-98 Rational Procedure and Proposed Simplified Equation. β = 0.02, I = 1.0.

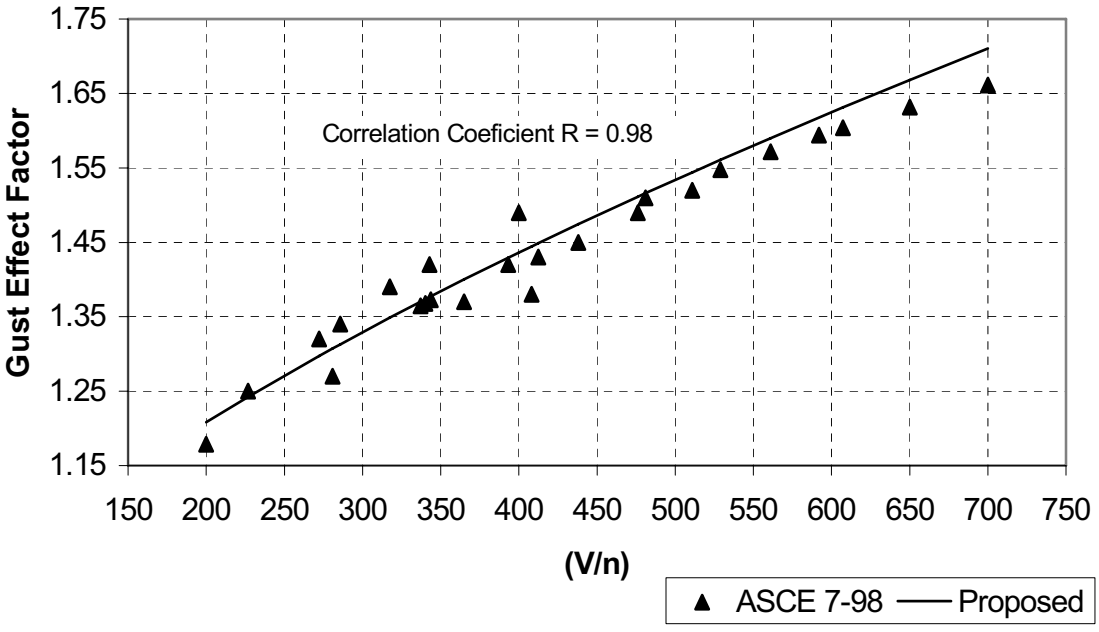

Figure 4.5. Von Karman Vortex Trail.

5 Summary and Recommendations

5.1 Summary

On the average, wind loads on support structures computed in accordance to the new wind provisions are comparable to the loads computed using the current *Supports Specifications* (1994). However, the differences could vary considerably depending on the specific location on the map.

The proposed (1999) *Supports Specifications* has incorporated a single value for the gust effect factor of 1.14. It is recommended that this value be used for wind sensitive as well as non-wind sensitive structures. This value will produce about the same wind pressure on the average as that computed using the current (1994) *Supports Specifications*. Structures with a natural frequency in the along wind direction less than 1 Hertz are considered wind-sensitive; GEF equations for such structures are provided in this report and result in values in the range of 1.0 to 2.0. At this time, however, it is recommended to use the GEF of 1.14, until further research can verify the accuracy of the proposed GEF equations for flexible structural supports.

5.2 Recommended Future Work

Recommendations for future work include the following:

1. Evaluation of ASCE 7-98

   The proposed *Supports Specifications* is based on information in ASCE 7-95. ASCE 7-98 *Minimum Design Loads for Buildings and Other Structures* has just been published. The ASCE 7-98 Standard should be reviewed for updates that could be applicable to the *Supports Specifications* wind loading criteria. Important considerations in the newly published ASCE 7-98 document include the load factor for wind, a wind directionality factor, and changes in the hurricane contours on the wind map.

2. Gust effect factors for support structures

   The gust effect factors for wind sensitive and non-wind sensitive structures provided in Sections 2.6.3, 4.4, 4.5.2, and 4.5.3 should be verified by physical wind tunnel testing on typical support structures. Insufficient research is available on gust effect factors for flexible support structures, and the only published information was developed primarily for buildings.

References

AASHTO, 1994: "Standard Specifications for Structural Supports for Highway Signs, Luminaires and Traffic Signals," American Association of State Highway and Transportation Officials.

AASHTO, 1999: "Standard Specifications for Structural Supports for Highway Signs, Luminaires and Traffic Signals," *Third Draft*, American Association of State Highway and Transportation Officials.

ANSI, 1972: "Building Code Requirements for Minimum Design Loads in Buildings and Other Structures," ANSI A58.1-1972, American National Standards Institute, New York, NY.

ANSI, 1982: "Minimum Design Loads for Buildings and Other Structures," A58.1-1982, American National Standards Institute, New York, NY.

ASA, 1955: "Minimum Design Loads in Buildings and Other Structures," A58.1-1955, American Standards Association (currently ANSI), New York, NY.

ASCE 7-88, 1990: "Minimum Design Loads for Buildings and Other Structures," American Society of Civil Engineers, 347 East 47th St., New York, NY, pp. 92.

ASCE, 1994: "Minimum Design Loads for Buildings and Other Structures," ASCE 7-93, American Society of Civil Engineers, New York, New York, 1993.

ASCE, 1996: "Minimum Design Loads for Buildings and Other Structures," ASCE 7-95, American Society of Civil Engineers, New York, NY.

ASCE 1999: "Minimum Design loads for Buildings and Other Structures," ASCE 7-98 Public Ballot Copy, American Society of Civil Engineers, New York, NY.

Batts, M.E., Cordes, M.R., Russell, L.R., Shaver, J.R. and Simiu, E., 1980: "Hurricane Wind Speeds in the United States," NBS Building Science Series 124, National Bureau of Standards, Washington, DC, pp. 41.

Changery, M., 1979: "Data Collection and Storage," *Proceedings of the Workshop on Wind Climate* (November 1979, Ashville, NC), Ed. K. Mehta, Institute for Disaster Research, Texas Tech University, Lubbock, TX.

Davenport, A.G., 1961: "The Application of Statistical Concepts to the Wind Loading of Structures," *Proceedings*, Institution of Civil Engineers, Vol. 19, Paper 6480.

Durst, C.S., 1960: "Wind Speeds Over Short Periods of Time," *Meteorological Magazine*, Vol. 89, London, England, pp. 181-186.

Georgiou, P.N., Davenport, A.G., and Vickery, B.J., 1983: "Design Wind Speeds in Regions Dominated by Tropical Cyclones," *Journal of Wind Engineering and Industrial Aerodynamics*, Vol. 13, pp. 139-152.

Kareem, A., 1992: "Dynamic Response of High-Rise Buildings to Stochastic Wind Loads," *Journal of Wind Engineering and Industrial Aerodynamics*, pp. 41-44.

Kareem, A., and Gurley, K., 1996, "Damping in Structures: Its Evaluation and Treatment of Uncertainty," *Journal of Wind Engineering and Industrial Aerodynamics*, 59, pp. 131-157.

McDonald, J.R., Mehta, K.C., Oler, W.W., and Pulipaka, N., 1995, "Wind Load Effects on Signs, Luminaries, and Traffic Signal Structures," Report 1303-1F, Wind Engineering Research Center, Texas Tech University, submitted to Texas Department of Transportation, Austin, Texas, 182 p.

Mehta, K.C., 1984: "Wind Load Provisions of ANSI A58.1-1982," *Journal of Structural Engineering*, ASCE, Vol. 110, No. 4, pp. 769-784.

Peterka, J.A., 1992: "Improved Extreme Wind Prediction in the United States," *Journal of Wind Engineering and Industrial Aerodynamics*, Vol. 41, pp. 533-541.

Peterka, J.A. and Shahid, S., 1993: "Extreme Gust Wind Speeds in the U.S.," *Proceedings*, 7th U.S. National Conference on Wind Engineering, UCLA, Los Angeles, CA, Vol. 2, pp. 503-512.

Simiu, E., Changery, M.J., and Filliben, J.J., 1979: "Extreme Wind Speeds at 129 Stations in the Contiguous United States," Building Science Series Report 118, National Bureau of Standards, Washington, DC.

Simiu, E., and Scanlan, R.H., 1996, *Wind Effects on Structures*, John Wiley and Sons, Inc., 3rd Edition.

Solari, G., 1993: "Gust Buffeting II: Dynamic Along-Wind Response," *Journal of Structural Engineering*, ASCE, 119(2).

Thom, H.C.S., 1968: "New Distributions of Extreme Winds in the United States," *Journal of the Structural Division*, Proceedings, ASCE, Vol. 94, No. ST7, pp. 1787-1801.

Vellozzi, J.W. and Cohen E., 1968: "Gust Response Factors," *Journal of Structural Engineering*, Proceedings, ASCE, Vol. 94, No. ST6, pp. 1295-1313.

Vickery, P.J. and Twisdale, L.A., 1993: "Hurricane Wind Speeds at Inland Locations," *Proceedings*, ASCE Structures Congress (Atlanta, GA), ASCE, New York, NY, April, pp. 473-478.

Watanabe, Y., Isyumov, N., and Davenport, A.G., 1995, "Empirical Aerodynamic Damping Function for Tall Buildings," *Proceedings* of the Ninth International Conference on Wind Engineering (New Delhi, India, Jan. 1995), Wiley Eastern Ltd., publisher, pp. 1362-1371.

Appendix A

Tables for Wind Load Comparison

List of Tables

				Proposed AASHTO Specifications (1999)				Current AASHTO Specifications (1994)		
State	City	Pop. Ranking	Site	Wind Speed (mph)	Imp. Factor (50-yr)	Imp. Factor (25-yr)	Imp. Factor (10-yr)	Wind Speed, 50-year (mph)	Wind Speed, 25-year (mph)	Wind Speed, 10-year (mph)
AK	Anchorage		A-2	100	1.00	0.89	0.76	90	80	70
AK	Annette		A-3	110	1.00	0.89	0.76	90	80	70
AK	Barrow		A-5	120	1.00	0.89	0.76	90	90	80
AK	Barter Is.		A-4	110	1.00	0.89	0.76	100	90	80
AK	Bethel		A-7	130	1.00	0.89	0.76	100	90	80
AK	Cold Bay		A-7	130	1.00	0.89	0.76	100	90	80
AK	Fairbanks		A-1	90	1.00	0.89	0.76	70	70	60
AK	Ft. Yukon		A-1	90	1.00	0.89	0.76	70	70	60
AK	Juneau		A-2	100	1.00	0.89	0.76	90	80	70
AK	Kodiak		A-7	130	1.00	0.89	0.76	100	90	80
AK	Nome		A-8	130	1.00	0.89	0.76	110	100	90
AK	Northway		A-1	90	1.00	0.89	0.76	70	70	60
AK	Seward		A-7	130	1.00	0.89	0.76	100	90	80
AK	Sitka		A-6	120	1.00	0.89	0.76	100	90	80
AK	St. Paul Is.		A-8	130	1.00	0.89	0.76	110	100	90
AK	Yakutat		A-6	120	1.00	0.89	0.76	100	90	80
AL	Birmingham	53	I-2	90	1.00	0.87	0.71	70	70	60
AL	Mobile	75	E-11	130	1.00	0.80	0.54	90	70	60
AR	Little Rock	72	I-2	90	1.00	0.87	0.71	70	70	60
AZ	Phoenix	16	I-2	90	1.00	0.87	0.71	70	70	60
AZ	Tucson	57	I-2	90	1.00	0.87	0.71	70	70	60
AZ	Yuma		I-1	90	1.00	0.87	0.71	70	60	60
CA	Bakersfield	65	W-1	85	1.00	0.87	0.71	60	50	50
CA	Eureka		W-3	85	1.00	0.87	0.71	70	60	60
CA	Fresno	56	W-1	85	1.00	0.87	0.71	60	50	50
CA	Los Angeles	2	W-7	SWR	N/A	N/A	N/A	60	50	50
CA	Sacramento	26	W-2	85	1.00	0.87	0.71	70	60	50
CA	San Diego	17	W-1	85	1.00	0.87	0.71	60	50	50
CA	San Francisco	5	W-2	85	1.00	0.87	0.71	70	60	50
CA	Stockton	73	W-1	85	1.00	0.87	0.71	60	50	50
CO	Denver	20	I-9	SWR	N/A	N/A	N/A	80	80	70
CO	Grand Junction		I-7	90	1.00	0.87	0.71	80	80	70
CT	Hartford	37	E-4	110	1.00	0.80	0.58	70	70	60
DC	Washington	4	I-2	90	1.00	0.87	0.71	70	70	60
FL	Jacksonville	47	E-8	120	1.00	0.80	0.54	80	70	60
FL	Miami	12	E-17	150	1.00	0.80	0.54	110	100	80
FL	Orlando	31	E-11	130	1.00	0.80	0.54	90	70	60
FL	Pensacola		E-12	130	1.00	0.80	0.54	90	80	60
FL	Sarasota	74	E-13	130	1.00	0.80	0.54	90	80	70
FL	Tampa	21	E-13	130	1.00	0.80	0.54	90	80	70
FL	West Palm Beach	48	E-15	140	1.00	0.80	0.54	100	90	80

Table A—1. List of Cities, Sorted by State.

				Proposed AASHTO Specifications (1999)				Current AASHTO Specifications (1994)		
State	City	Pop. Ranking	Site	Wind Speed (mph)	Imp. Factor (50-yr)	Imp. Factor (25-yr)	Imp. Factor (10-yr)	Wind Speed, 50-year (mph)	Wind Speed, 25-year (mph)	Wind Speed, 10-year (mph)
GA	Atlanta	11	I-4	90	1.00	0.87	0.71	80	70	60
HI	Adak		H-1	105	1.00	0.80	0.64	105	98	90
HI	Honolulu	55	H-1	105	1.00	0.80	0.64	105	98	90
HI	Shemya		H-1	105	1.00	0.80	0.64	105	98	90
ID	Boise		I-4	90	1.00	0.87	0.71	80	70	60
ID	Pocatello		I-7	90	1.00	0.87	0.71	80	80	70
IL	Chicago	3	I-2	90	1.00	0.87	0.71	70	70	60
IL	Springfield		I-2	90	1.00	0.87	0.71	70	70	60
IN	Indianapolis	28	I-8	90	1.00	0.87	0.71	90	80	70
IO	Des Moines		I-5	90	1.00	0.87	0.71	80	70	70
IO	Dubuque		I-7	90	1.00	0.87	0.71	80	80	70
KS	Dodge City		I-7	90	1.00	0.87	0.71	80	80	70
KY	Lexington		I-2	90	1.00	0.87	0.71	70	70	60
KY	Louisville	49	I-4	90	1.00	0.87	0.71	80	70	60
LA	Baton Rouge	71	E-6	110	1.00	0.80	0.58	90	70	70
LA	New Orleans	33	E-13	130	1.00	0.80	0.54	90	80	70
LA	Shreveport		I-2	90	1.00	0.87	0.71	70	70	60
MA	Boston	7	E-7	110	1.00	0.80	0.58	90	80	70
MA	Springfield	70	E-1	100	1.00	0.87	0.71	70	70	60
ME	Caribou		I-2	90	1.00	0.87	0.71	70	70	60
ME	Portland		E-3	100	1.00	0.87	0.71	80	80	70
MI	Detroit	8	I-4	90	1.00	0.87	0.71	80	70	60
MI	Grand Rapids	46	I-4	90	1.00	0.87	0.71	80	70	60
MI	Lansing		I-4	90	1.00	0.87	0.71	80	70	60
MI	Sault Ste. Marie		I-2	90	1.00	0.87	0.71	70	70	60
MN	Duluth		I-2	90	1.00	0.87	0.71	70	70	60
MN	International Falls		I-2	90	1.00	0.87	0.71	70	70	60
MN	Minneapolis	15	I-5	90	1.00	0.87	0.71	80	70	70
MO	Kansas City	24	I-3	90	1.00	0.87	0.71	70	70	70
MO	St. Louis	18	I-2	90	1.00	0.87	0.71	70	70	60
MS	Jackson		I-2	90	1.00	0.87	0.71	70	70	60
MT	Billings		I-7	90	1.00	0.87	0.71	80	80	70
MT	Great Falls		I-10	SWR	N/A	N/A	N/A	80	70	70
MT	Havre		I-2	90	1.00	0.87	0.71	70	70	60
MT	Missoula		I-4	90	1.00	0.87	0.71	80	70	60
NC	Charlotte	32	I-2	90	1.00	0.87	0.71	70	70	60
NC	Greensboro	38	I-2	90	1.00	0.87	0.71	70	70	60
NC	Hatteras		E-16	140	1.00	0.80	0.54	110	100	80
NC	Raleigh	45	I-4	90	1.00	0.87	0.71	80	70	60
NC	Wilmington		E-14	130	1.00	0.80	0.54	100	100	80
ND	Bimarck		I-3	90	1.00	0.87	0.71	70	70	70

Table A—1. List of Cities, Sorted by State. (Continued)

				Proposed AASHTO Specifications (1999)				Current AASHTO Specifications (1994)		
State	City	Pop. Ranking	Site	Wind Speed (mph)	Imp. Factor (50-yr)	Imp. Factor (25-yr)	Imp. Factor (10-yr)	Wind Speed, 50-year (mph)	Wind Speed, 25-year (mph)	Wind Speed, 10-year (mph)
ND	Fargo		I-5	90	1.00	0.87	0.71	80	70	70
ND	Williston		I-2	90	1.00	0.87	0.71	70	70	60
NE	Lincoln		I-5	90	1.00	0.87	0.71	80	70	70
NE	North Platte		I-7	90	1.00	0.87	0.71	80	80	70
NE	Omaha	61	I-5	90	1.00	0.87	0.71	80	70	70
NH	Concord		E-1	100	1.00	0.87	0.71	70	70	60
NM	Albuquerque	62	I-5	90	1.00	0.87	0.71	80	70	70
NV	Las Vegas	35	I-2	90	1.00	0.87	0.71	70	70	60
NV	Reno		I-4	90	1.00	0.87	0.71	80	70	60
NV	Tonopah		I-2	90	1.00	0.87	0.71	70	70	60
NV	Winnemucca		I-4	90	1.00	0.87	0.71	80	70	60
NY	Albany	54	I-2	90	1.00	0.87	0.71	70	70	60
NY	Buffalo	36	I-2	90	1.00	0.87	0.71	70	70	60
NY	New York	1	E-8	120	1.00	0.80	0.54	80	70	60
NY	Rochester	41	I-2	90	1.00	0.87	0.71	70	70	60
NY	Syracuse	59	I-2	90	1.00	0.87	0.71	70	70	60
OH	Cincinnati	23	I-4	90	1.00	0.87	0.71	80	70	60
OH	Cleveland	14	I-4	90	1.00	0.87	0.71	80	70	60
OH	Columbus	30	I-2	90	1.00	0.87	0.71	70	70	60
OH	Dayton	50	I-6	90	1.00	0.87	0.71	80	80	60
OH	Toledo	68	I-6	90	1.00	0.87	0.71	80	80	60
OH	Youngstown	69	I-2	90	1.00	0.87	0.71	70	70	60
OK	Oklahoma City	44	I-5	90	1.00	0.87	0.71	80	70	70
OK	Tulsa	58	I-2	90	1.00	0.87	0.71	70	70	60
OR	Burns		W-5	85	1.00	0.87	0.71	80	70	60
OR	Pendleton		W-5	85	1.00	0.87	0.71	80	70	60
OR	Portland	22	W-8	SWR	N/A	N/A	N/A	90	80	70
OR	Roseburg		W-3	85	1.00	0.87	0.71	70	60	60
PA	Allentown	67	E-1	100	1.00	0.87	0.71	70	70	60
PA	Harrisburg	66	I-2	90	1.00	0.87	0.71	70	70	60
PA	Philadelphia	6	E-2	100	1.00	0.87	0.71	80	70	60
PA	Pittsburgh	19	I-2	90	1.00	0.87	0.71	70	70	60
PA	Scranton	64	I-2	90	1.00	0.87	0.71	70	70	60
RI	Providence	39	E-9	120	1.00	0.80	0.54	80	70	70
SC	Charleston		E-10	120	1.00	0.80	0.54	90	90	80
SC	Columbia		I-7	90	1.00	0.87	0.71	80	80	70
SC	Greenville	52	I-7	90	1.00	0.87	0.71	80	80	70
SD	Huron		I-5	90	1.00	0.87	0.71	80	70	70
SD	Rapid City		I-7	90	1.00	0.87	0.71	80	80	70
TN	Knoxville	63	I-4	90	1.00	0.87	0.71	80	70	60
TN	Memphis	42	I-2	90	1.00	0.87	0.71	70	70	60
TN	Nashville	40	I-2	90	1.00	0.87	0.71	70	70	60
TX	Abilene		I-4	90	1.00	0.87	0.71	80	70	60

Table A—1. List of Cities, Sorted by State. (Continued)

				Proposed AASHTO Specifications (1999)				Current AASHTO Specifications (1994)		
State	City	Pop. Ranking	Site	Wind Speed (mph)	Imp. Factor (50-yr)	Imp. Factor (25-yr)	Imp. Factor (10-yr)	Wind Speed, 50-year (mph)	Wind Speed, 25-year (mph)	Wind Speed, 10-year (mph)
TX	Amarillo		I-7	90	1.00	0.87	0.71	80	80	70
TX	Austin	43	I-2	90	1.00	0.87	0.71	70	70	60
TX	Brownsville		E-8	120	1.00	0.80	0.54	80	70	60
TX	Dallas	9	I-2	90	1.00	0.87	0.71	70	70	60
TX	DelRio		I-2	90	1.00	0.87	0.71	70	70	60
TX	El Paso	60	I-2	90	1.00	0.87	0.71	70	70	60
TX	Houston	10	E-5	110	1.00	0.80	0.58	80	70	60
TX	San Antonio	29	I-2	90	1.00	0.87	0.71	70	70	60
UT	Milford		I-4	90	1.00	0.87	0.71	80	70	60
UT	Salt Lake City	34	I-7	90	1.00	0.87	0.71	80	80	70
VA	Norfolk	27	E-7	110	1.00	0.80	0.58	90	80	70
VA	Richmond	51	I-4	90	1.00	0.87	0.71	80	70	60
VT	Burlington		I-2	90	1.00	0.87	0.71	70	70	60
WA	Seattle	13	W-6	85	1.00	0.87	0.71	80	80	70
WA	Spokane		W-4	85	1.00	0.87	0.71	70	70	60
WI	Green Bay		I-8	90	1.00	0.87	0.71	90	80	70
WI	Milwaukee	25	I-4	90	1.00	0.87	0.71	80	70	60
WV	Charleston		I-2	90	1.00	0.87	0.71	70	70	60
WY	Cheyenne		I-7	90	1.00	0.87	0.71	80	80	70
WY	Lander		I-8	90	1.00	0.87	0.71	90	80	70

Table A—1. List of Cities, Sorted by State. (Continued)

				Proposed AASHTO Specifications (1999)				Current AASHTO Specifications (1994)		
State	City	Pop. Ranking	Site	Wind Speed (mph)	Imp. Factor (50-yr)	Imp. Factor (25-yr)	Imp. Factor (10-yr)	Wind Speed, 50-year (mph)	Wind Speed, 25-year (mph)	Wind Speed, 10-year (mph)
Interior Wind Region										
AZ	Yuma		I-1	90	1.00	0.87	0.71	70	60	60
AL	Birmingham	53	I-2	90	1.00	0.87	0.71	70	70	60
AR	Little Rock	72	I-2	90	1.00	0.87	0.71	70	70	60
AZ	Phoenix	16	I-2	90	1.00	0.87	0.71	70	70	60
AZ	Tucson	57	I-2	90	1.00	0.87	0.71	70	70	60
DC	Washington	4	I-2	90	1.00	0.87	0.71	70	70	60
IL	Chicago	3	I-2	90	1.00	0.87	0.71	70	70	60
IL	Springfield		I-2	90	1.00	0.87	0.71	70	70	60
KY	Lexington		I-2	90	1.00	0.87	0.71	70	70	60
LA	Shreveport		I-2	90	1.00	0.87	0.71	70	70	60
ME	Caribou		I-2	90	1.00	0.87	0.71	70	70	60
MI	Sault Ste. Marie		I-2	90	1.00	0.87	0.71	70	70	60
MN	Duluth		I-2	90	1.00	0.87	0.71	70	70	60
MN	International Falls		I-2	90	1.00	0.87	0.71	70	70	60
MO	St. Louis	18	I-2	90	1.00	0.87	0.71	70	70	60
MS	Jackson		I-2	90	1.00	0.87	0.71	70	70	60
MT	Havre		I-2	90	1.00	0.87	0.71	70	70	60
NC	Charlotte	32	I-2	90	1.00	0.87	0.71	70	70	60
NC	Greensboro	38	I-2	90	1.00	0.87	0.71	70	70	60
ND	Williston		I-2	90	1.00	0.87	0.71	70	70	60
NV	Las Vegas	35	I-2	90	1.00	0.87	0.71	70	70	60
NV	Tonopah		I-2	90	1.00	0.87	0.71	70	70	60
NY	Albany	54	I-2	90	1.00	0.87	0.71	70	70	60
NY	Buffalo	36	I-2	90	1.00	0.87	0.71	70	70	60
NY	Rochester	41	I-2	90	1.00	0.87	0.71	70	70	60
NY	Syracuse	59	I-2	90	1.00	0.87	0.71	70	70	60
OH	Columbus	30	I-2	90	1.00	0.87	0.71	70	70	60
OH	Youngstown	69	I-2	90	1.00	0.87	0.71	70	70	60
OK	Tulsa	58	I-2	90	1.00	0.87	0.71	70	70	60
PA	Harrisburg	66	I-2	90	1.00	0.87	0.71	70	70	60
PA	Pittsburgh	19	I-2	90	1.00	0.87	0.71	70	70	60
PA	Scranton	64	I-2	90	1.00	0.87	0.71	70	70	60
TN	Memphis	42	I-2	90	1.00	0.87	0.71	70	70	60
TN	Nashville	40	I-2	90	1.00	0.87	0.71	70	70	60
TX	Austin	43	I-2	90	1.00	0.87	0.71	70	70	60
TX	Dallas	9	I-2	90	1.00	0.87	0.71	70	70	60
TX	DelRio		I-2	90	1.00	0.87	0.71	70	70	60
TX	El Paso	60	I-2	90	1.00	0.87	0.71	70	70	60
TX	San Antonio	29	I-2	90	1.00	0.87	0.71	70	70	60
VT	Burlington		I-2	90	1.00	0.87	0.71	70	70	60
WV	Charleston		I-2	90	1.00	0.87	0.71	70	70	60
MO	Kansas City	24	I-3	90	1.00	0.87	0.71	70	70	70

Table A—2. List of Cities, Sorted by Site.

				Proposed AASHTO Specifications (1999)				Current AASHTO Specifications (1994)		
State	City	Pop. Ranking	Site	Wind Speed (mph)	Imp. Factor (50-yr)	Imp. Factor (25-yr)	Imp. Factor (10-yr)	Wind Speed, 50-year (mph)	Wind Speed, 25-year (mph)	Wind Speed, 10-year (mph)
Interior Wind Region (Continued)										
ND	Bimarck		I-3	90	1.00	0.87	0.71	70	70	70
GA	Atlanta	11	I-4	90	1.00	0.87	0.71	80	70	60
ID	Boise		I-4	90	1.00	0.87	0.71	80	70	60
KY	Louisville	49	I-4	90	1.00	0.87	0.71	80	70	60
MI	Detroit	8	I-4	90	1.00	0.87	0.71	80	70	60
MI	Grand Rapids	46	I-4	90	1.00	0.87	0.71	80	70	60
MI	Lansing		I-4	90	1.00	0.87	0.71	80	70	60
MT	Missoula		I-4	90	1.00	0.87	0.71	80	70	60
NC	Raleigh	45	I-4	90	1.00	0.87	0.71	80	70	60
NV	Reno		I-4	90	1.00	0.87	0.71	80	70	60
NV	Winnemucca		I-4	90	1.00	0.87	0.71	80	70	60
OH	Cincinnati	23	I-4	90	1.00	0.87	0.71	80	70	60
OH	Cleveland	14	I-4	90	1.00	0.87	0.71	80	70	60
TN	Knoxville	63	I-4	90	1.00	0.87	0.71	80	70	60
TX	Abilene		I-4	90	1.00	0.87	0.71	80	70	60
UT	Milford		I-4	90	1.00	0.87	0.71	80	70	60
VA	Richmond	51	I-4	90	1.00	0.87	0.71	80	70	60
WI	Milwaukee	25	I-4	90	1.00	0.87	0.71	80	70	60
IO	Des Moines		I-5	90	1.00	0.87	0.71	80	70	70
MN	Minneapolis	15	I-5	90	1.00	0.87	0.71	80	70	70
ND	Fargo		I-5	90	1.00	0.87	0.71	80	70	70
NE	Lincoln		I-5	90	1.00	0.87	0.71	80	70	70
NE	Omaha	61	I-5	90	1.00	0.87	0.71	80	70	70
NM	Albuquerque	62	I-5	90	1.00	0.87	0.71	80	70	70
OK	Oklahoma City	44	I-5	90	1.00	0.87	0.71	80	70	70
SD	Huron		I-5	90	1.00	0.87	0.71	80	70	70
OH	Dayton	50	I-6	90	1.00	0.87	0.71	80	80	60
OH	Toledo	68	I-6	90	1.00	0.87	0.71	80	80	60
CO	Grand Junction		I-7	90	1.00	0.87	0.71	80	80	70
ID	Pocatello		I-7	90	1.00	0.87	0.71	80	80	70
IO	Dubuque		I-7	90	1.00	0.87	0.71	80	80	70
KS	Dodge City		I-7	90	1.00	0.87	0.71	80	80	70
MT	Billings		I-7	90	1.00	0.87	0.71	80	80	70
NE	North Platte		I-7	90	1.00	0.87	0.71	80	80	70
SC	Columbia		I-7	90	1.00	0.87	0.71	80	80	70
SC	Greenville	52	I-7	90	1.00	0.87	0.71	80	80	70
SD	Rapid City		I-7	90	1.00	0.87	0.71	80	80	70
TX	Amarillo		I-7	90	1.00	0.87	0.71	80	80	70
UT	Salt Lake City	34	I-7	90	1.00	0.87	0.71	80	80	70
WY	Cheyenne		I-7	90	1.00	0.87	0.71	80	80	70
IN	Indianapolis	28	I-8	90	1.00	0.87	0.71	90	80	70
WI	Green Bay		I-8	90	1.00	0.87	0.71	90	80	70
WY	Lander		I-8	90	1.00	0.87	0.71	90	80	70

Table A—2. List of Cities, Sorted by Site. (Continued)

				Proposed AASHTO Specifications (1999)				Current AASHTO Specifications (1994)		
State	City	Pop. Ranking	Site	Wind Speed (mph)	Imp. Factor (50-yr)	Imp. Factor (25-yr)	Imp. Factor (10-yr)	Wind Speed, 50-year (mph)	Wind Speed, 25-year (mph)	Wind Speed, 10-year (mph)
Interior Wind Region (Continued)										
CO	Denver	20	I-9	SWR	N/A	N/A	N/A	80	80	70
MT	Great Falls		I-10	SWR	N/A	N/A	N/A	80	70	70
West Coast Wind Region										
CA	Bakersfield	65	W-1	85	1.00	0.87	0.71	60	50	50
CA	Fresno	56	W-1	85	1.00	0.87	0.71	60	50	50
CA	San Diego	17	W-1	85	1.00	0.87	0.71	60	50	50
CA	Stockton	73	W-1	85	1.00	0.87	0.71	60	50	50
CA	Sacramento	26	W-2	85	1.00	0.87	0.71	70	60	50
CA	San Francisco	5	W-2	85	1.00	0.87	0.71	70	60	50
CA	Eureka		W-3	85	1.00	0.87	0.71	70	60	60
OR	Roseburg		W-3	85	1.00	0.87	0.71	70	60	60
WA	Spokane		W-4	85	1.00	0.87	0.71	70	70	60
OR	Burns		W-5	85	1.00	0.87	0.71	80	70	60
OR	Pendleton		W-5	85	1.00	0.87	0.71	80	70	60
WA	Seattle	13	W-6	85	1.00	0.87	0.71	80	80	70
CA	Los Angeles	2	W-7	SWR	N/A	N/A	N/A	60	50	50
OR	Portland	22	W-8	SWR	N/A	N/A	N/A	90	80	70
East Coast Wind Region										
MA	Springfield	70	E-1	100	1.00	0.87	0.71	70	70	60
NH	Concord		E-1	100	1.00	0.87	0.71	70	70	60
PA	Allentown	67	E-1	100	1.00	0.87	0.71	70	70	60
PA	Philadelphia	6	E-2	100	1.00	0.87	0.71	80	70	60
ME	Portland		E-3	100	1.00	0.87	0.71	80	80	70
CT	Hartford	37	E-4	110	1.00	0.80	0.58	70	70	60
TX	Houston	10	E-5	110	1.00	0.80	0.58	80	70	60
LA	Baton Rouge	71	E-6	110	1.00	0.80	0.58	90	70	70
MA	Boston	7	E-7	110	1.00	0.80	0.58	90	80	70
VA	Norfolk	27	E-7	110	1.00	0.80	0.58	90	80	70
FL	Jacksonville	47	E-8	120	1.00	0.80	0.54	80	70	60
NY	New York	1	E-8	120	1.00	0.80	0.54	80	70	60
TX	Brownsville		E-8	120	1.00	0.80	0.54	80	70	60
RI	Providence	39	E-9	120	1.00	0.80	0.54	80	70	70
SC	Charleston		E-10	120	1.00	0.80	0.54	90	90	80
AL	Mobile	75	E-11	130	1.00	0.80	0.54	90	70	60
FL	Orlando	31	E-11	130	1.00	0.80	0.54	90	70	60
FL	Pensacola		E-12	130	1.00	0.80	0.54	90	80	60
FL	Sarasota	74	E-13	130	1.00	0.80	0.54	90	80	70
FL	Tampa	21	E-13	130	1.00	0.80	0.54	90	80	70
LA	New Orleans	33	E-13	130	1.00	0.80	0.54	90	80	70
NC	Wilmington		E-14	130	1.00	0.80	0.54	100	100	80
FL	West Palm Beach	48	E-15	140	1.00	0.80	0.54	100	90	80
NC	Hatteras		E-16	140	1.00	0.80	0.54	110	100	80
FL	Miami	12	E-17	150	1.00	0.80	0.54	110	100	80

Table A—2. List of Cities, Sorted by Site. (Continued)

				Proposed AASHTO Specifications (1999)				Current AASHTO Specifications (1994)		
State	City	Pop. Ranking	Site	Wind Speed (mph)	Imp. Factor (50-yr)	Imp. Factor (25-yr)	Imp. Factor (10-yr)	Wind Speed, 50-year (mph)	Wind Speed, 25-year (mph)	Wind Speed, 10-year (mph)
Alaska										
AK	Fairbanks		A-1	90	1.00	0.89	0.76	70	70	60
AK	Ft. Yukon		A-1	90	1.00	0.89	0.76	70	70	60
AK	Northway		A-1	90	1.00	0.89	0.76	70	70	60
AK	Anchorage		A-2	100	1.00	0.89	0.76	90	80	70
AK	Juneau		A-2	100	1.00	0.89	0.76	90	80	70
AK	Annette		A-3	110	1.00	0.89	0.76	90	80	70
AK	Barter Is.		A-4	110	1.00	0.89	0.76	100	90	80
AK	Barrow		A-5	120	1.00	0.89	0.76	90	90	80
AK	Sitka		A-6	120	1.00	0.89	0.76	100	90	80
AK	Yakutat		A-6	120	1.00	0.89	0.76	100	90	80
AK	Bethel		A-7	130	1.00	0.89	0.76	100	90	80
AK	Cold Bay		A-7	130	1.00	0.89	0.76	100	90	80
AK	Kodiak		A-7	130	1.00	0.89	0.76	100	90	80
AK	Seward		A-7	130	1.00	0.89	0.76	100	90	80
AK	Nome		A-8	130	1.00	0.89	0.76	110	100	90
AK	St. Paul Is.		A-8	130	1.00	0.89	0.76	110	100	90
Hawaii										
HI	Adak		H-1	105	1.00	0.80	0.64	105	98	90
HI	Honolulu	55	H-1	105	1.00	0.80	0.64	105	98	90
HI	Shemya		H-1	105	1.00	0.80	0.64	105	98	90

Table A—2. List of Cities, Sorted by Site. (Continued)

Ratio of Wind Pressures (Proposed to Current Specification) for 50-year Mean Recurrence Interval				
Site / No. of Cities Represented	For z<15'	Average for z>15'	Maximum for z>15'	Minimum. for z>15'
Interior Wind Region				
Site I-1 (1)	1.18	1.05	1.12	0.95
Site I-2 (40)	1.18	1.05	1.12	0.95
Site I-3 (2)	1.18	1.05	1.12	0.95
Site I-4 (17)	0.91	0.80	0.86	0.72
Site I-5 (8)	0.91	0.80	0.86	0.72
Site I-6 (2)	0.91	0.80	0.86	0.72
Site I-7 (12)	0.91	0.80	0.86	0.72
Site I-8 (3)	0.72	0.63	0.68	0.57
Site I-9 (1)	N/A	N/A	N/A	N/A
Site I-10 (1)	N/A	N/A	N/A	N/A
West Coast Wind Region				
Site W-1 (4)	1.44	1.27	1.36	1.15
Site W-2 (2)	1.06	0.93	1.00	0.84
Site W-3 (2)	1.06	0.93	1.00	0.84
Site W-4 (1)	1.06	0.93	1.00	0.84
Site W-5 (2)	0.81	0.71	0.76	0.65
Site W-6 (1)	0.81	0.71	0.76	0.65
Site W-7 (1)	N/A	N/A	N/A	N/A
Site W-8 (1)	N/A	N/A	N/A	N/A
East Coast Wind Region				
Site E-1 (3)	1.46	1.29	1.38	1.17
Site E-2 (1)	1.12	0.99	1.06	0.89
Site E-3 (1)	1.12	0.99	1.06	0.89
Site E-4 (1)	1.77	1.56	1.67	1.41
Site E-5 (1)	1.35	1.20	1.28	1.08
Site E-6 (1)	1.07	0.95	1.01	0.86
Site E-7 (2)	1.07	0.95	1.01	0.86
Site E-8 (3)	1.61	1.42	1.52	1.29
Site E-9 (1)	1.61	1.42	1.52	1.29

Table A—3. Ratio of Wind Pressures (Proposed to Current Specification) for 50-year Mean Recurrence Interval

Ratio of Wind Pressures (Proposed to Current Specification) for 50-year Mean Recurrence Interval				
Site / No. of Cities Represented	For z<15'	Average for z>15'	Maximum for z>15'	Minimum. for z>15'
East Coast Wind Region (Continued)				
Site E-10 (1)	1.27	1.13	1.20	1.02
Site E-11 (2)	1.49	1.32	1.41	1.19
Site E-12 (1)	1.49	1.32	1.41	1.19
Site E-13 (3)	1.49	1.32	1.41	1.19
Site E-14 (1)	1.21	1.07	1.14	0.97
Site E-15 (1)	1.40	1.24	1.32	1.12
Site E-16 (1)	1.16	1.03	1.09	0.93
Site E-17 (1)	1.33	1.18	1.26	1.06
Alaska				
Site A-1 (3)	1.18	1.05	1.12	0.95
Site A-2 (2)	0.88	0.78	0.83	0.71
Site A-3 (1)	1.07	0.95	1.01	0.86
Site A-4 (1)	0.87	0.77	0.82	0.69
Site A-5 (1)	1.27	1.13	1.20	1.02
Site A-6 (2)	1.03	0.91	0.97	0.82
Site A-7 (4)	1.21	1.07	1.14	0.97
Site A-8 (2)	1.00	0.88	0.94	0.80
Hawaii				
Site H-1 (3)	0.72	0.63	0.68	0.57

Table A—3. Ratio of Wind Pressures (Proposed to Current Specification) for 50-year Mean Recurrence Interval (Continued)

Ratio of Wind Pressures (Proposed to Current Specification) for 25-year Mean Recurrence Interval				
Site / No. of Cities Represented	For z<15'	Average for z>15'	Maximum for z>15'	Minimum. for z>15'
Interior Wind Region				
Site I-1 (1)	1.40	1.24	1.32	1.12
Site I-2 (40)	1.03	0.91	0.97	0.82
Site I-3 (2)	1.03	0.91	0.97	0.82
Site I-4 (17)	1.03	0.91	0.97	0.82
Site I-5 (8)	1.03	0.91	0.97	0.82
Site I-6 (2)	0.79	0.70	0.74	0.63
Site I-7 (12)	0.79	0.70	0.74	0.63
Site I-8 (3)	0.79	0.70	0.74	0.63
Site I-9 (1)	N/A	N/A	N/A	N/A
Site I-10 (1)	N/A	N/A	N/A	N/A
West Coast Wind Region				
Site W-1 (4)	1.80	1.59	1.70	1.44
Site W-2 (2)	1.25	1.11	1.18	1.00
Site W-3 (2)	1.25	1.11	1.18	1.00
Site W-4 (1)	0.92	0.81	0.87	0.73
Site W-5 (2)	0.92	0.81	0.87	0.73
Site W-6 (1)	0.70	0.62	0.66	0.56
Site W-7 (1)	N/A	N/A	N/A	N/A
Site W-8 (1)	N/A	N/A	N/A	N/A
East Coast Wind Region				
Site E-1 (3)	1.27	1.12	1.20	1.02
Site E-2 (1)	1.27	1.12	1.20	1.02
Site E-3 (1)	0.97	0.86	0.92	0.78
Site E-4 (1)	1.41	1.25	1.33	1.13
Site E-5 (1)	1.41	1.25	1.33	1.13
Site E-6 (1)	1.41	1.25	1.33	1.13
Site E-7 (2)	1.08	0.96	1.02	0.87
Site E-8 (3)	1.68	1.49	1.59	1.35
Site E-9 (1)	1.68	1.49	1.59	1.35

Table A—4. Ratio of Wind Pressures (Proposed to Current Specification) for 25-year Mean Recurrence Interval

Ratio of Wind Pressures (Proposed to Current Specification) for 25-year Mean Recurrence Interval				
Site / No. of Cities Represented	For z<15'	Average for z>15'	Maximum for z>15'	Minimum. for z>15'
East Coast Wind Region (Continued)				
Site E-10 (1)	1.02	0.90	0.96	0.81
Site E-11 (2)	1.97	1.75	1.86	1.58
Site E-12 (1)	1.51	1.34	1.43	1.21
Site E-13 (3)	1.51	1.34	1.43	1.21
Site E-14 (1)	0.97	0.86	0.91	0.77
Site E-15 (1)	1.39	1.23	1.31	1.11
Site E-16 (1)	1.12	0.99	1.06	0.90
Site E-17 (1)	1.29	1.14	1.22	1.03
Alaska				
Site A-1 (3)	1.05	0.93	0.99	0.84
Site A-2 (2)	1.00	0.88	0.94	0.80
Site A-3 (1)	1.20	1.07	1.14	0.96
Site A-4 (1)	0.95	0.84	0.90	0.76
Site A-5 (1)	1.13	1.00	1.07	0.91
Site A-6 (2)	1.13	1.00	1.07	0.91
Site A-7 (4)	1.33	1.18	1.25	1.06
Site A-8 (2)	1.08	0.95	1.02	0.86
Hawaii				
Site H-1 (3)	0.66	0.58	0.62	0.53

Table A—4. Ratio of Wind Pressures (Proposed to Current Specification) for 25-year Mean Recurrence Interval (Continued)

Ratio of Wind Pressures (Proposed to Current Specification) for 10-year Mean Recurrence Interval				
Site / No. of Cities Represented	For z<15'	Average for z>15'	Maximum for z>15'	Minimum. for z>15'
Interior Wind Region				
Site I-1 (1)	1.14	1.01	1.08	0.91
Site I-2 (40)	1.14	1.01	1.08	0.91
Site I-3 (2)	0.84	0.74	0.79	0.67
Site I-4 (17)	1.14	1.01	1.08	0.91
Site I-5 (8)	0.84	0.74	0.79	0.67
Site I-6 (2)	1.14	1.01	1.08	0.91
Site I-7 (12)	0.84	0.74	0.79	0.67
Site I-8 (3)	0.84	0.74	0.79	0.67
Site I-9 (1)	N/A	N/A	N/A	N/A
Site I-10 (1)	N/A	N/A	N/A	N/A
West Coast Wind Region				
Site W-1 (4)	1.47	1.30	1.39	1.17
Site W-2 (2)	1.47	1.30	1.39	1.17
Site W-3 (2)	1.02	0.90	0.96	0.82
Site W-4 (1)	1.02	0.90	0.96	0.82
Site W-5 (2)	1.02	0.90	0.96	0.82
Site W-6 (1)	0.75	0.66	0.71	0.60
Site W-7 (1)	N/A	N/A	N/A	N/A
Site W-8 (1)	N/A	N/A	N/A	N/A
East Coast Wind Region				
Site E-1 (3)	1.41	1.25	1.33	1.13
Site E-2 (1)	1.41	1.25	1.33	1.13
Site E-3 (1)	1.04	0.92	0.98	0.83
Site E-4 (1)	1.40	1.23	1.32	1.12
Site E-5 (1)	1.40	1.23	1.32	1.12
Site E-6 (1)	1.03	0.91	0.97	0.82
Site E-7 (2)	1.03	0.91	0.97	0.82
Site E-8 (3)	1.55	1.37	1.46	1.24
Site E-9 (1)	1.14	1.00	1.07	0.91

Table A—5. Ratio of Wind Pressures (Proposed to Current Specification) for 10-year Mean Recurrence Interval

Ratio of Wind Pressures (Proposed to Current Specification) for 10-year Mean Recurrence Interval				
Site / No. of Cities Represented	For z<15'	Average for z>15'	Maximum for z>15'	Minimum. for z>15'
East Coast Wind Region (Continued)				
Site E-10 (1)	0.87	0.77	0.82	0.70
Site E-11 (2)	1.81	1.60	1.71	1.45
Site E-12 (1)	1.81	1.60	1.71	1.45
Site E-13 (3)	1.33	1.18	1.26	1.07
Site E-14 (1)	1.02	0.90	0.96	0.82
Site E-15 (1)	1.18	1.05	1.12	0.95
Site E-16 (1)	1.18	1.05	1.12	0.95
Site E-17 (1)	1.36	1.20	1.28	1.09
Alaska				
Site A-1 (3)	1.22	1.08	1.16	0.98
Site A-2 (2)	1.11	0.98	1.05	0.89
Site A-3 (1)	1.34	1.19	1.27	1.07
Site A-4 (1)	1.03	0.91	0.97	0.82
Site A-5 (1)	1.22	1.08	1.16	0.98
Site A-6 (2)	1.22	1.08	1.16	0.98
Site A-7 (4)	1.44	1.27	1.36	1.15
Site A-8 (2)	1.13	1.00	1.07	0.91
Hawaii				
Site H-1 (3)	0.62	0.55	0.59	0.50

Table A—5. Ratio of Wind Pressures (Proposed to Current Specification) for 10-year Mean Recurrence Interval (Continued)

Base Shears for Proposed and Current Specification for Non-Cantilevered Overhead Sign (50-year M.R.I.)			
Site / No. of Cities Represented	Base Shear for Proposed Specification (lb)	Base Shear for Current Specification (lb)	Ratio of Base Shears (Proposed to Current Spec.)
Interior Wind Region			
Site I-1 (1)	30,944	29,461	1.05
Site I-2 (40)	30,944	29,461	1.05
Site I-3 (2)	30,944	29,461	1.05
Site I-4 (17)	30,944	38,479	0.80
Site I-5 (8)	30,944	38,479	0.80
Site I-6 (2)	30,944	38,479	0.80
Site I-7 (12)	30,944	38,479	0.80
Site I-8 (3)	30,944	48,700	0.64
Site I-9 (1)	N/A	N/A	N/A
Site I-10 (1)	N/A	N/A	N/A
West Coast Wind Region			
Site W-1 (4)	27,602	21,645	1.28
Site W-2 (2)	27,602	29,461	0.94
Site W-3 (2)	27,602	29,461	0.94
Site W-4 (1)	27,602	29,461	0.94
Site W-5 (2)	27,602	38,479	0.72
Site W-6 (1)	27,602	38,479	0.72
Site W-7 (1)	N/A	N/A	N/A
Site W-8 (1)	N/A	N/A	N/A
East Coast Wind Region			
Site E-1 (3)	38,203	29,461	1.30
Site E-2 (1)	38,203	38,479	0.99
Site E-3 (1)	38,203	38,479	0.99
Site E-4 (1)	46,225	29,461	1.57
Site E-5 (1)	46,225	38,479	1.20
Site E-6 (1)	46,225	48,700	0.95
Site E-7 (2)	46,225	48,700	0.95
Site E-8 (3)	55,012	38,479	1.43
Site E-9 (1)	55,012	38,479	1.43

Table A—6. Base Shears for Proposed and Current Specification for Non-Cantilevered Overhead Sign (50-year M.R.I.)

Base Shears for Proposed and Current Specification for Non-Cantilevered Overhead Sign (50-year M.R.I.)			
Site / No. of Cities Represented	Base Shear for Proposed Specification (lb)	Base Shear for Current Specification (lb)	Ratio of Base Shears (Proposed to Current Spec.)
East Coast Wind Region (Continued)			
Site E-10 (1)	55,012	48,700	1.13
Site E-11 (2)	64,563	48,700	1.33
Site E-12 (1)	64,563	48,700	1.33
Site E-13 (3)	64,563	48,700	1.33
Site E-14 (1)	64,563	60,124	1.07
Site E-15 (1)	74,878	60,124	1.25
Site E-16 (1)	74,878	72,750	1.03
Site E-17 (1)	85,956	72,750	1.18
Alaska			
Site A-1 (3)	30,944	29,461	1.05
Site A-2 (2)	38,203	48,700	0.78
Site A-3 (1)	46,225	48,700	0.95
Site A-4 (1)	46,225	60,124	0.77
Site A-5 (1)	55,012	48,700	1.13
Site A-6 (2)	55,012	60,124	0.91
Site A-7 (4)	64,563	60,124	1.07
Site A-8 (2)	64,563	72,750	0.89
Hawaii			
Site H-1 (3)	42,119	66,287	0.64

Table A—6. Base Shears for Proposed and Current Specification for Non-Cantilevered Overhead Sign (50-year M.R.I.) (Continued)

Base Shears for Proposed and Current Specification for Cantilevered Overhead Sign (50-year M.R.I.)			
Site / No. of Cities Represented	Base Shear for Proposed Specification (lb)	Base Shear for Current Specification (lb)	Ratio of Base Shears (Proposed to Current Spec.)
Interior Wind Region			
Site I-1 (1)	6,811	6,495	1.05
Site I-2 (40)	6,811	6,495	1.05
Site I-3 (2)	6,811	6,495	1.05
Site I-4 (17)	6,811	8,483	0.80
Site I-5 (8)	6,811	8,483	0.80
Site I-6 (2)	6,811	8,483	0.80
Site I-7 (12)	6,811	8,483	0.80
Site I-8 (3)	6,811	10,736	0.63
Site I-9 (1)	N/A	N/A	N/A
Site I-10 (1)	N/A	N/A	N/A
West Coast Wind Region			
Site W-1 (4)	6,075	4,772	1.27
Site W-2 (2)	6,075	6,495	0.94
Site W-3 (2)	6,075	6,495	0.94
Site W-4 (1)	6,075	6,495	0.94
Site W-5 (2)	6,075	8,483	0.72
Site W-6 (1)	6,075	8,483	0.72
Site W-7 (1)	N/A	N/A	N/A
Site W-8 (1)	N/A	N/A	N/A
East Coast Wind Region			
Site E-1 (3)	8,409	6,495	1.29
Site E-2 (1)	8,409	8,483	0.99
Site E-3 (1)	8,409	8,483	0.99
Site E-4 (1)	10,174	6,495	1.57
Site E-5 (1)	10,174	8,483	1.20
Site E-6 (1)	10,174	10,736	0.95
Site E-7 (2)	10,174	10,736	0.95
Site E-8 (3)	12,108	8,483	1.43
Site E-9 (1)	12,108	8,483	1.43

Table A—7. Base Shears for Proposed and Current Specification for Cantilevered Overhead Sign (50-year M.R.I.)

Base Shears for Proposed and Current Specification for Cantilevered Overhead Sign (50-year M.R.I.)			
Site / No. of Cities Represented	Base Shear for Proposed Specification (lb)	Base Shear for Current Specification (lb)	Ratio of Base Shears (Proposed to Current Spec.)
East Coast Wind Region (Continued)			
Site E-10 (1)	12,108	10,736	1.13
Site E-11 (2)	14,211	10,736	1.32
Site E-12 (1)	14,211	10,736	1.32
Site E-13 (3)	14,211	10,736	1.32
Site E-14 (1)	14,211	13,254	1.07
Site E-15 (1)	16,481	13,254	1.24
Site E-16 (1)	16,481	16,038	1.03
Site E-17 (1)	18,919	16,038	1.18
Alaska			
Site A-1 (3)	6,811	6,495	1.05
Site A-2 (2)	8,409	10,736	0.78
Site A-3 (1)	10,174	10,736	0.95
Site A-4 (1)	10,174	13,254	0.77
Site A-5 (1)	12,108	10,736	1.13
Site A-6 (2)	12,108	13,254	0.91
Site A-7 (4)	14,211	13,254	1.07
Site A-8 (2)	14,211	16,038	0.89
Hawaii			
Site H-1 (3)	9,270	14,613	0.63

Table A—7. Base Shears for Proposed and Current Specification for Cantilevered Overhead Sign (50-year M.R.I.) (Continued)

Base Shears for Proposed and Current Specification for High Mast Lighting Pole (50-year M.R.I.)			
Site / No. of Cities Represented	Base Shear for Proposed Specification (lb)	Base Shear for Current Specification (lb)	Ratio of Base Shears (Proposed to Current Spec.)
Interior Wind Region			
Site I-1 (1)	4,862	4,665	1.04
Site I-2 (40)	4,862	4,665	1.04
Site I-3 (2)	4,862	4,665	1.04
Site I-4 (17)	4,862	6,053	0.80
Site I-5 (8)	4,862	6,053	0.80
Site I-6 (2)	4,862	6,053	0.80
Site I-7 (12)	4,862	6,053	0.80
Site I-8 (3)	4,862	7,637	0.64
Site I-9 (1)	N/A	N/A	N/A
Site I-10 (1)	N/A	N/A	N/A
West Coast Wind Region			
Site W-1 (4)	4,354	3,479	1.25
Site W-2 (2)	4,354	4,665	0.93
Site W-3 (2)	4,354	4,665	0.93
Site W-4 (1)	4,354	4,665	0.93
Site W-5 (2)	4,354	6,053	0.72
Site W-6 (1)	4,354	6,053	0.72
Site W-7 (1)	N/A	N/A	N/A
Site W-8 (1)	N/A	N/A	N/A
East Coast Wind Region			
Site E-1 (3)	5,965	4,665	1.28
Site E-2 (1)	5,965	6,053	0.99
Site E-3 (1)	5,965	6,053	0.99
Site E-4 (1)	7,218	4,665	1.55
Site E-5 (1)	7,218	6,053	1.19
Site E-6 (1)	7,218	7,637	0.95
Site E-7 (2)	7,218	7,637	0.95
Site E-8 (3)	8,589	6,053	1.42
Site E-9 (1)	8,589	6,053	1.42

Table A—8. Base Shears for Proposed and Current Specification for High Mast Lighting Pole (50-year M.R.I.)

Base Shears for Proposed and Current Specification for High Mast Lighting Pole (50-year M.R.I.)			
Site / No. of Cities Represented	Base Shear for Proposed Specification (lb)	Base Shear for Current Specification (lb)	Ratio of Base Shears (Proposed to Current Spec.)
East Coast Wind Region (Continued)			
Site E-10 (1)	8,589	7,637	1.12
Site E-11 (2)	10,081	7,637	1.32
Site E-12 (1)	10,081	7,637	1.32
Site E-13 (3)	10,081	7,637	1.32
Site E-14 (1)	10,081	9,427	1.07
Site E-15 (1)	11,691	9,427	1.24
Site E-16 (1)	11,691	11,406	1.02
Site E-17 (1)	13,421	11,406	1.18
Alaska			
Site A-1 (3)	4,862	4,665	1.04
Site A-2 (2)	5,965	7,637	0.78
Site A-3 (1)	7,218	7,637	0.95
Site A-4 (1)	7,218	9,427	0.77
Site A-5 (1)	8,589	7,637	1.12
Site A-6 (2)	8,589	9,427	0.91
Site A-7 (4)	10,081	9,427	1.07
Site A-8 (2)	10,081	11,406	0.88
Hawaii			
Site H-1 (3)	6,576	10,393	0.63

Table A—8. Base Shears for Proposed and Current Specification for High Mast Lighting Pole (50-year M.R.I.) (Continued)

Base Shears for Proposed and Current Specification for Cantilevered Traffic Signal Structure (25-year M.R.I.)			
Site / No. of Cities Represented	Base Shear for Proposed Specification (lb)	Base Shear for Current Specification (lb)	Ratio of Base Shears (Proposed to Current Spec.)
Interior Wind Region			
Site I-1 (1)	972	809	1.20
Site I-2 (40)	972	1,051	0.92
Site I-3 (2)	972	1,051	0.92
Site I-4 (17)	972	1,051	0.92
Site I-5 (8)	972	1,051	0.92
Site I-6 (2)	972	1,328	0.73
Site I-7 (12)	972	1,328	0.73
Site I-8 (3)	972	1,328	0.73
Site I-9 (1)	N/A	N/A	N/A
Site I-10 (1)	N/A	N/A	N/A
West Coast Wind Region			
Site W-1 (4)	881	612	1.44
Site W-2 (2)	881	809	1.09
Site W-3 (2)	881	809	1.09
Site W-4 (1)	881	1,051	0.84
Site W-5 (2)	881	1,051	0.84
Site W-6 (1)	881	1,328	0.66
Site W-7 (1)	N/A	N/A	N/A
Site W-8 (1)	N/A	N/A	N/A
East Coast Wind Region			
Site E-1 (3)	1,169	1,051	1.11
Site E-2 (1)	1,169	1,051	1.11
Site E-3 (1)	1,169	1,328	0.88
Site E-4 (1)	1,086	1,051	1.03
Site E-5 (1)	1,086	1,051	1.03
Site E-6 (1)	1,086	1,051	1.03
Site E-7 (2)	1,086	1,328	0.82
Site E-8 (3)	1,510	1,051	1.44
Site E-9 (1)	1,510	1,051	1.44

Table A—9. Base Shears for Proposed and Current Specification for Cantilevered Traffic Signal Structure (25-year M.R.I.)

Base Shears for Proposed and Current Specification for Cantilevered Traffic Signal Structure (25-year M.R.I.)			
Site / No. of Cities Represented	Base Shear for Proposed Specification (lb)	Base Shear for Current Specification (lb)	Ratio of Base Shears (Proposed to Current Spec.)
East Coast Wind Region (Continued)			
Site E-10 (1)	1,510	1,651	0.91
Site E-11 (2)	1,759	1,051	1.67
Site E-12 (1)	1,759	1,328	1.32
Site E-13 (3)	1,759	1,328	1.32
Site E-14 (1)	1,759	2,023	0.87
Site E-15 (1)	2,034	1,651	1.23
Site E-16 (1)	2,034	2,023	1.01
Site E-17 (1)	2,333	2,023	1.15
Alaska			
Site A-1 (3)	992	1,051	0.94
Site A-2 (2)	1,192	1,328	0.90
Site A-3 (1)	1,417	1,328	1.07
Site A-4 (1)	1,417	1,651	0.86
Site A-5 (1)	1,671	1,651	1.01
Site A-6 (2)	1,671	1,651	1.01
Site A-7 (4)	1,952	1,651	1.18
Site A-8 (2)	1,952	2,023	0.96
Hawaii			
Site H-1 (3)	1,183	1,945	0.61

Table A—9. Base Shears for Proposed and Current Specification for Cantilevered Traffic Signal Structure (25-year M.R.I.) (Continued)

Base Shears for Proposed and Current Specification for Streetlighting Pole (25-year M.R.I.)			
Site / No. of Cities Represented	Base Shear for Proposed Specification (lb)	Base Shear for Current Specification (lb)	Ratio of Base Shears (Proposed to Current Spec.)
Interior Wind Region			
Site I-1 (1)	470	417	1.13
Site I-2 (40)	470	510	0.92
Site I-3 (2)	470	510	0.92
Site I-4 (17)	470	510	0.92
Site I-5 (8)	470	510	0.92
Site I-6 (2)	470	607	0.77
Site I-7 (12)	470	607	0.77
Site I-8 (3)	470	607	0.77
Site I-9 (1)	N/A	N/A	N/A
Site I-10 (1)	N/A	N/A	N/A
West Coast Wind Region			
Site W-1 (4)	437	309	1.41
Site W-2 (2)	437	417	1.05
Site W-3 (2)	437	417	1.05
Site W-4 (1)	437	510	0.86
Site W-5 (2)	437	510	0.86
Site W-6 (1)	437	607	0.72
Site W-7 (1)	N/A	N/A	N/A
Site W-8 (1)	N/A	N/A	N/A
East Coast Wind Region			
Site E-1 (3)	537	510	1.05
Site E-2 (1)	537	510	1.05
Site E-3 (1)	537	607	0.88
Site E-4 (1)	576	510	1.13
Site E-5 (1)	576	510	1.13
Site E-6 (1)	576	510	1.13
Site E-7 (2)	576	607	0.95
Site E-8 (3)	647	510	1.27
Site E-9 (1)	647	510	1.27

Table A—10. Base Shears for Proposed and Current Specification for Streetlighting Pole (25-year M.R.I.)

Base Shears for Proposed and Current Specification for Streetlighting Pole (25-year M.R.I.)			
Site / No. of Cities Represented	Base Shear for Proposed Specification (lb)	Base Shear for Current Specification (lb)	Ratio of Base Shears (Proposed to Current Spec.)
East Coast Wind Region (Continued)			
Site E-10 (1)	647	713	0.91
Site E-11 (2)	723	510	1.42
Site E-12 (1)	723	607	1.19
Site E-13 (3)	723	607	1.19
Site E-14 (1)	723	828	0.87
Site E-15 (1)	807	713	1.13
Site E-16 (1)	807	828	0.97
Site E-17 (1)	904	828	1.09
Alaska			
Site A-1 (3)	476	510	0.93
Site A-2 (2)	545	607	0.90
Site A-3 (1)	619	607	1.02
Site A-4 (1)	619	713	0.87
Site A-5 (1)	697	713	0.98
Site A-6 (2)	697	713	0.98
Site A-7 (4)	781	713	1.10
Site A-8 (2)	781	828	0.94
Hawaii			
Site H-1 (3)	542	804	0.67

Table A—10. Base Shears for Proposed and Current Specification for Streetlighting Pole (25-year M.R.I.) (Continued)

Base Shears for Proposed and Current Specification for Roadside Sign (10-year M.R.I.)			
Site / No. of Cities Represented	Base Shear for Proposed Specification (lb)	Base Shear for Current Specification (lb)	Ratio of Base Shears (Proposed to Current Spec.)
Interior Wind Region			
Site I-1 (1)	736	644	1.14
Site I-2 (40)	736	644	1.14
Site I-3 (2)	736	876	0.84
Site I-4 (17)	736	644	1.14
Site I-5 (8)	736	876	0.84
Site I-6 (2)	736	644	1.14
Site I-7 (12)	736	876	0.84
Site I-8 (3)	736	876	0.84
Site I-9 (1)	N/A	N/A	N/A
Site I-10 (1)	N/A	N/A	N/A
West Coast Wind Region			
Site W-1 (4)	657	447	1.47
Site W-2 (2)	657	447	1.47
Site W-3 (2)	657	644	1.02
Site W-4 (1)	657	644	1.02
Site W-5 (2)	657	644	1.02
Site W-6 (1)	657	876	0.75
Site W-7 (1)	N/A	N/A	N/A
Site W-8 (1)	N/A	N/A	N/A
East Coast Wind Region			
Site E-1 (3)	909	644	1.41
Site E-2 (1)	909	644	1.41
Site E-3 (1)	909	876	1.04
Site E-4 (1)	899	644	1.40
Site E-5 (1)	899	644	1.40
Site E-6 (1)	899	876	1.03
Site E-7 (2)	899	876	1.03
Site E-8 (3)	996	644	1.55
Site E-9 (1)	996	876	1.14

Table A—11. Base Shears for Proposed and Current Specification for Roadside Sign (10-year M.R.I.)

Base Shears for Proposed and Current Specification for Roadside Sign (10-year M.R.I.)			
Site / No. of Cities Represented	Base Shear for Proposed Specification (lb)	Base Shear for Current Specification (lb)	Ratio of Base Shears (Proposed to Current Spec.)
East Coast Wind Region (Continued)			
Site E-10 (1)	996	1,145	0.87
Site E-11 (2)	1,168	644	1.81
Site E-12 (1)	1,168	644	1.81
Site E-13 (3)	1,168	876	1.33
Site E-14 (1)	1,168	1,145	1.02
Site E-15 (1)	1,355	1,145	1.18
Site E-16 (1)	1,355	1,145	1.18
Site E-17 (1)	1,556	1,145	1.36
Alaska			
Site A-1 (3)	788	644	1.22
Site A-2 (2)	973	876	1.11
Site A-3 (1)	1,177	876	1.34
Site A-4 (1)	1,177	1,145	1.03
Site A-5 (1)	1,401	1,145	1.22
Site A-6 (2)	1,401	1,145	1.22
Site A-7 (4)	1,644	1,145	1.44
Site A-8 (2)	1,644	1,449	1.13
Hawaii			
Site H-1 (3)	903	1,449	0.62

Table A—11. Base Shears for Proposed and Current Specification for Roadside Sign (10-year M.R.I.) (Continued)

Appendix B

Figures for Wind Load Comparison

List of Figures

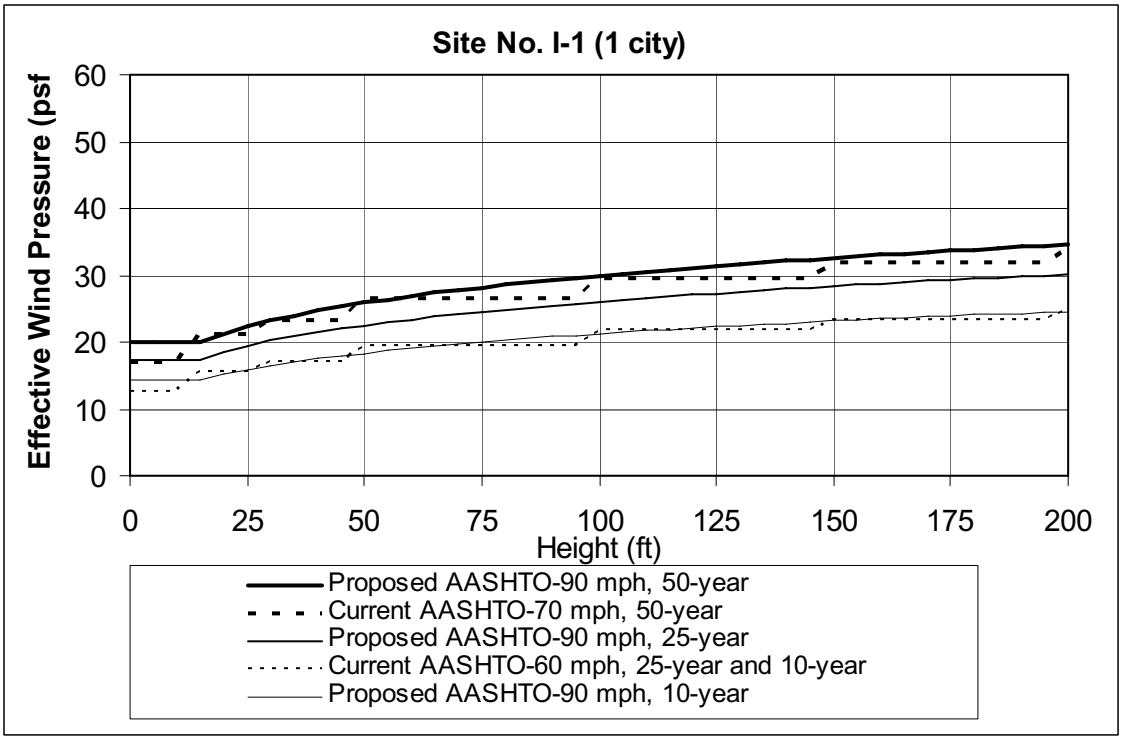

Figure B—1. Site No. I-1: Effective Wind Pressure

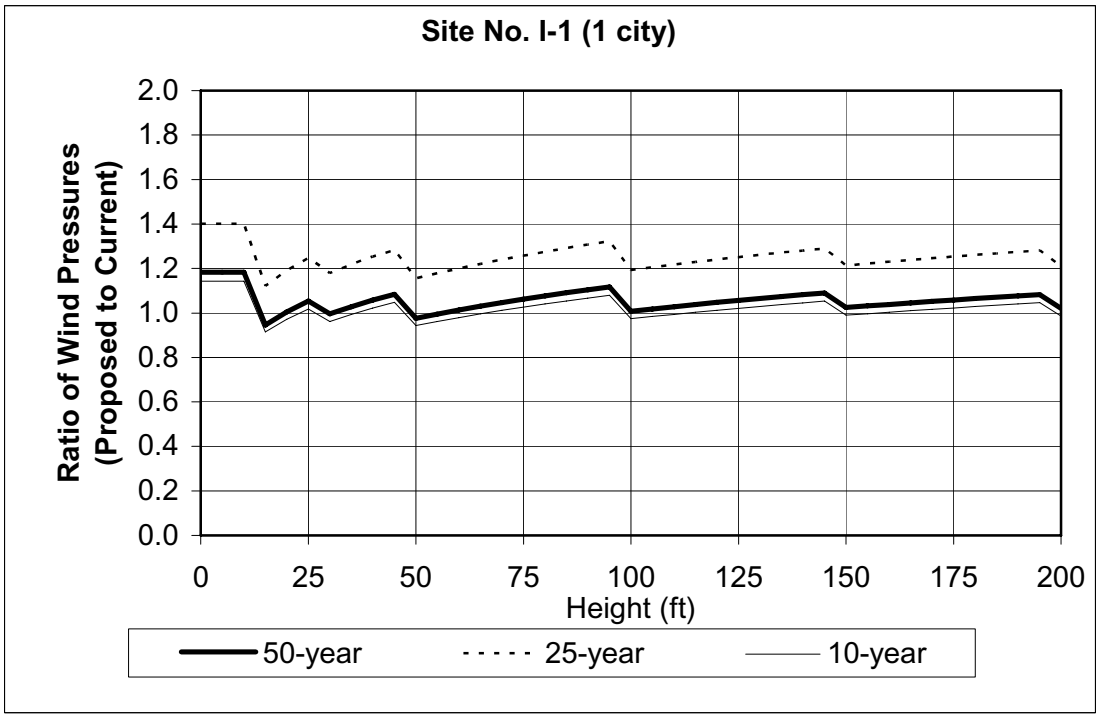

Figure B—2. Site No. I-1: Ratio of Wind Pressures (Proposed to Current Specification)

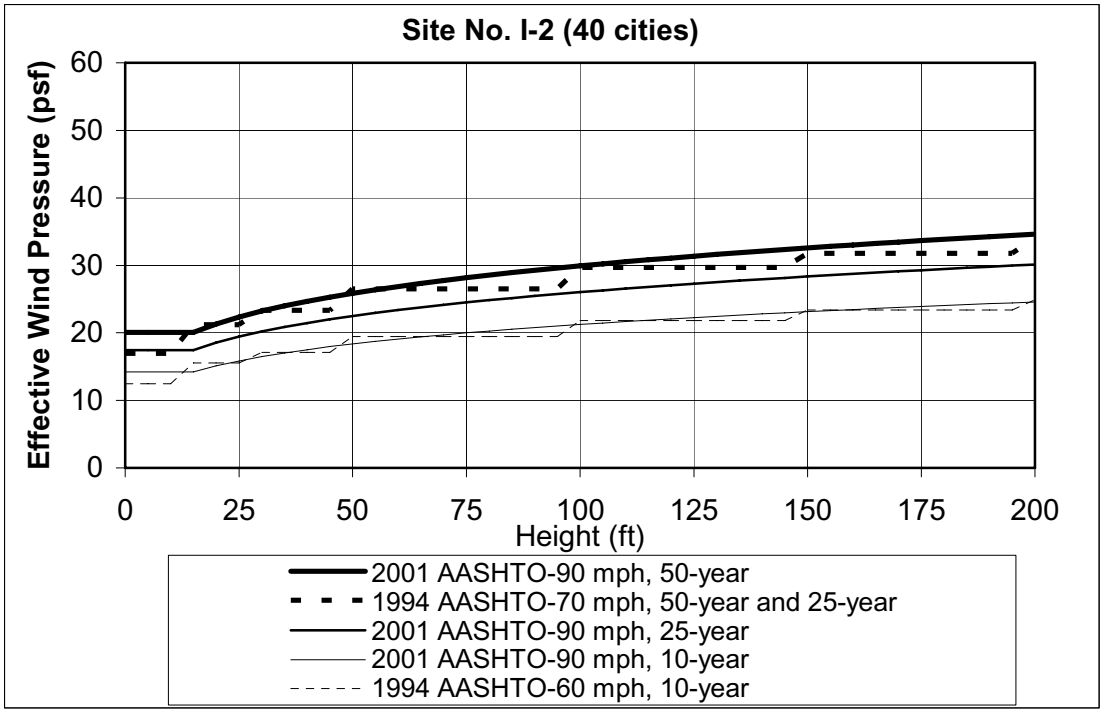

Figure B—3. Site No. I-2: Effective Wind Pressure

Figure B—4. Site No. I-2: Ratio of Wind Pressures (Proposed to Current Specification)

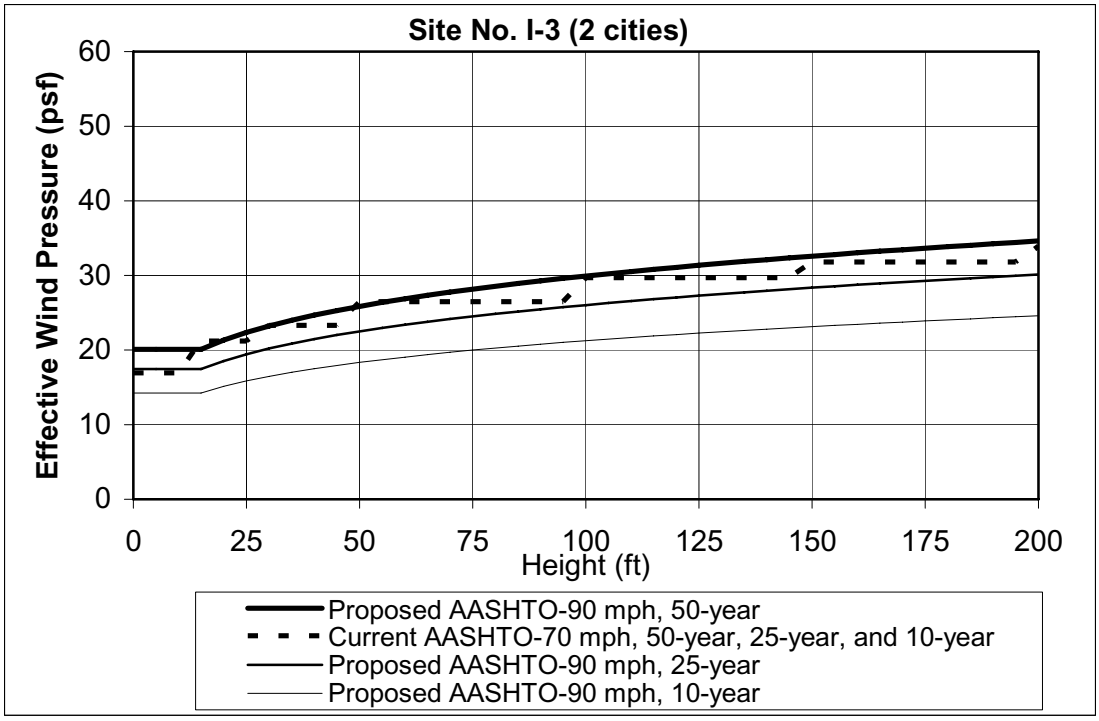

Figure B—5. Site No. I-3: Effective Wind Pressure

Figure B—6. Site No. I-3: Ratio of Wind Pressures (Proposed to Current Specification)

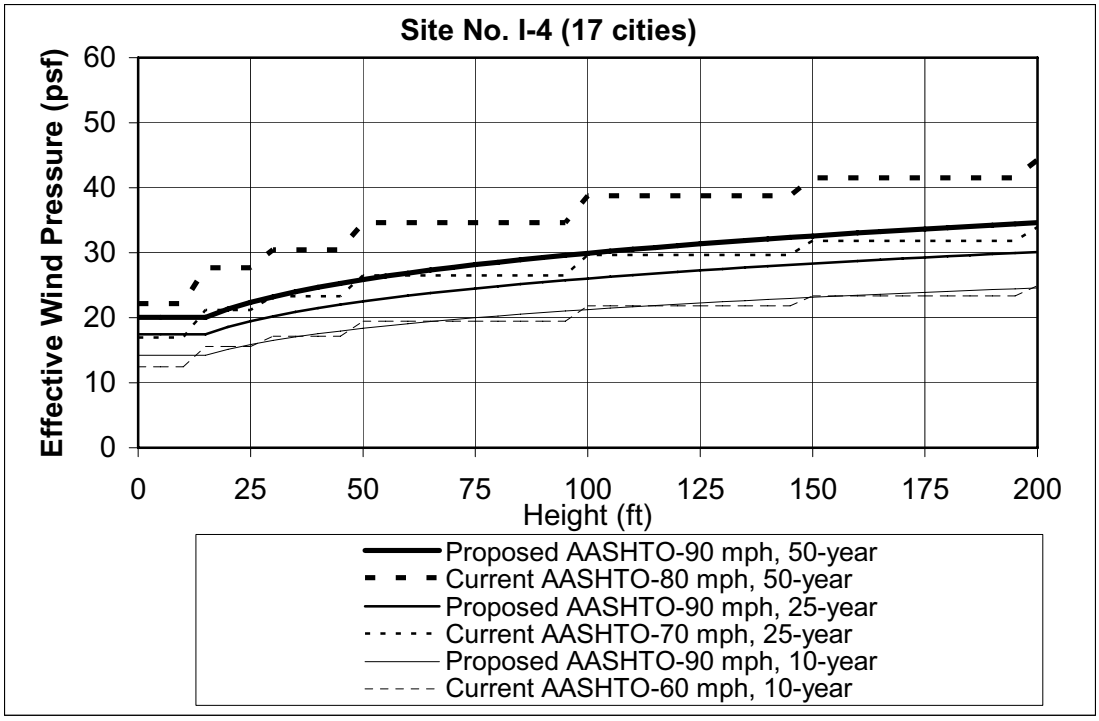

Figure B—7. Site No. I-4: Effective Wind Pressure

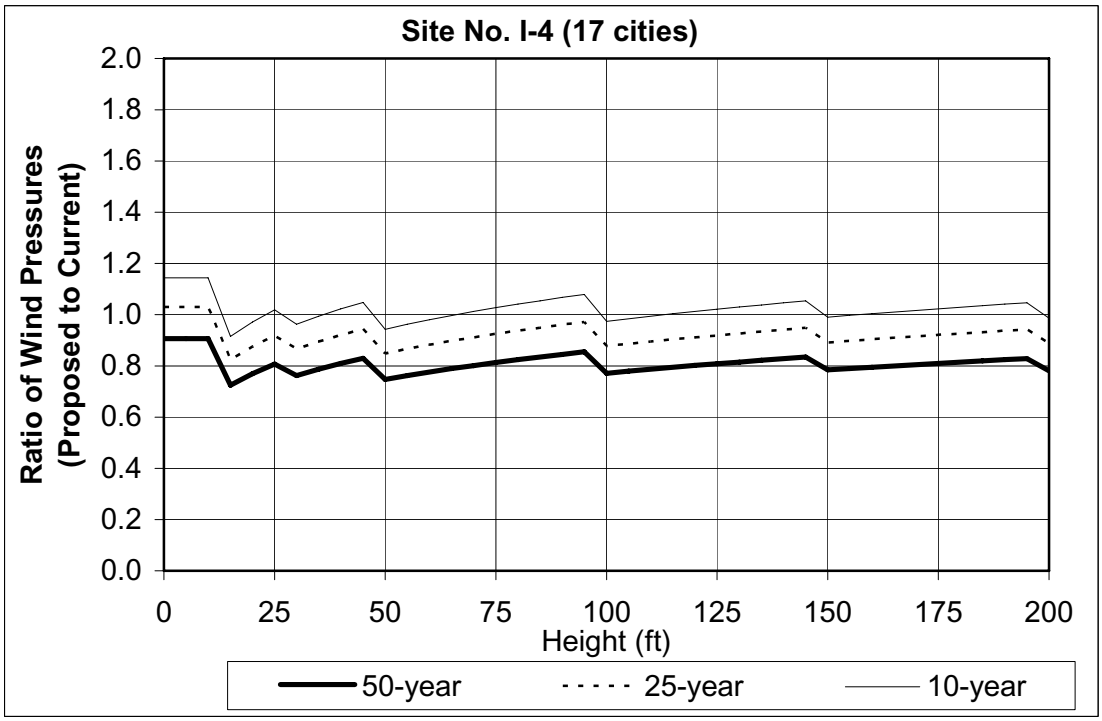

Figure B—8. Site No. I-4: Ratio of Wind Pressures (Proposed to Current Specification)

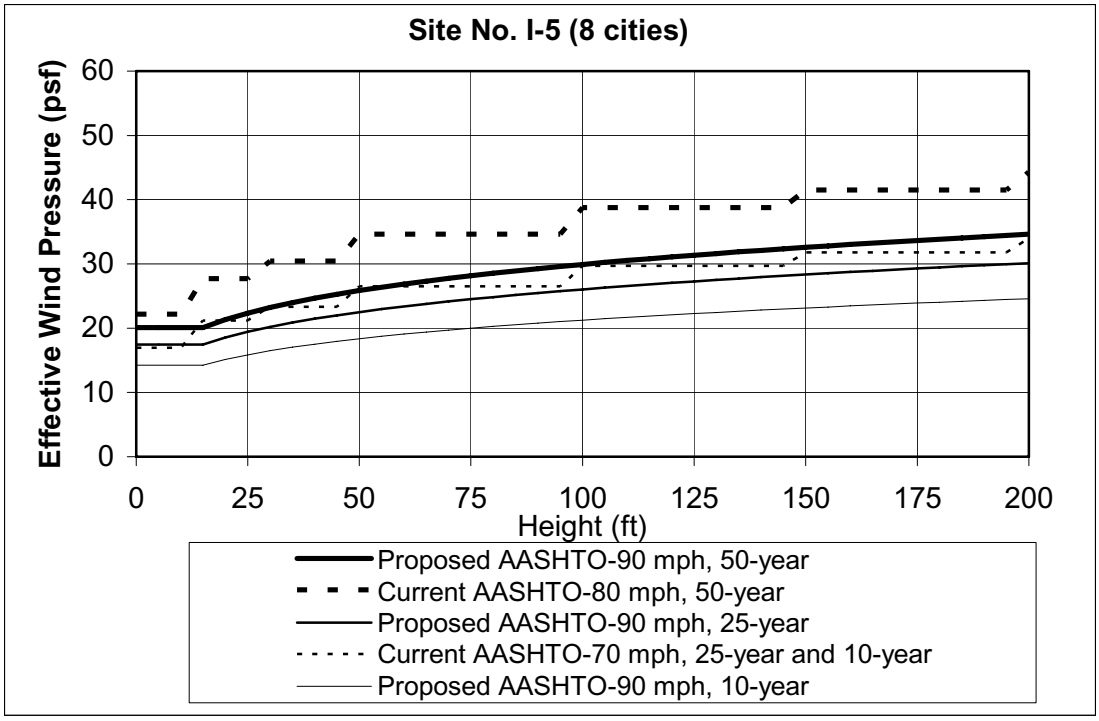

Figure B—9. Site No. I-5: Effective Wind Pressure

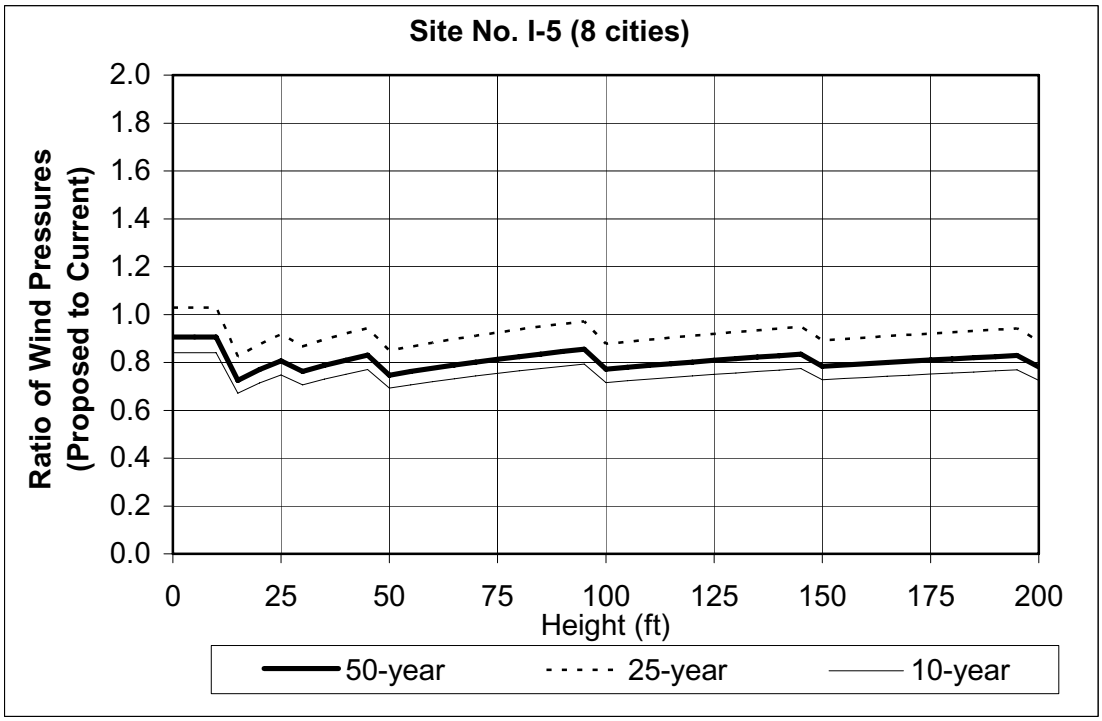

Figure B—10. Site No. I-5: Ratio of Wind Pressures (Proposed to Current Specification)

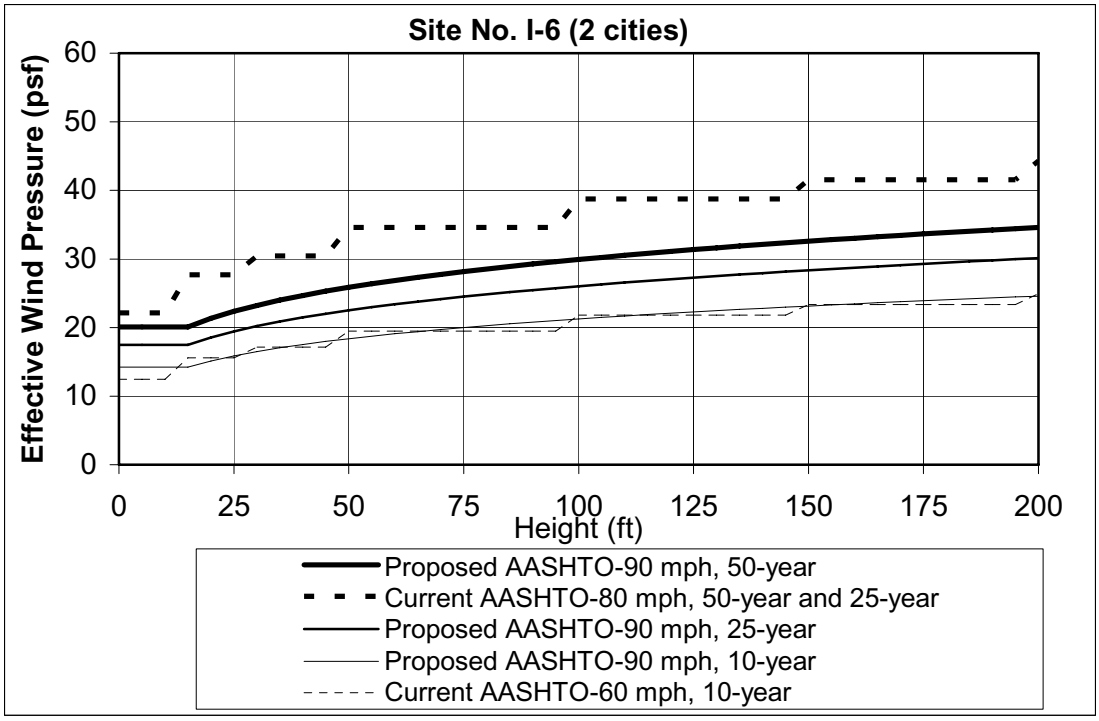

Figure B—11. Site No. I-6: Effective Wind Pressure

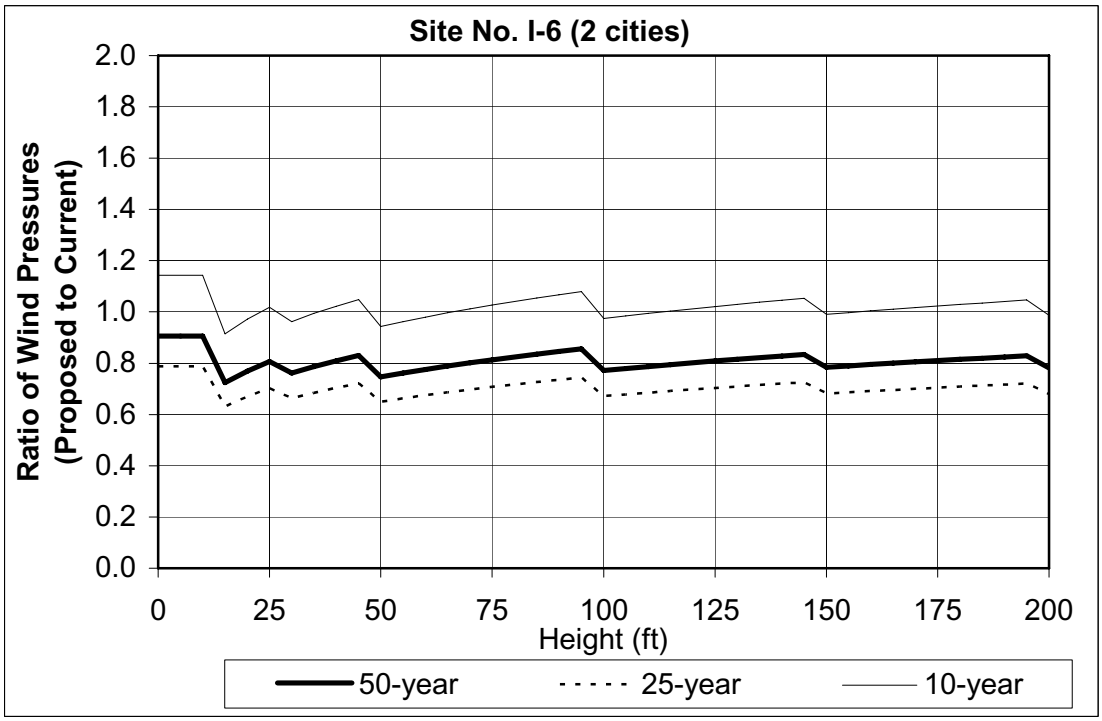

Figure B—12. Site No. I-6: Ratio of Wind Pressures (Proposed to Current Specification)

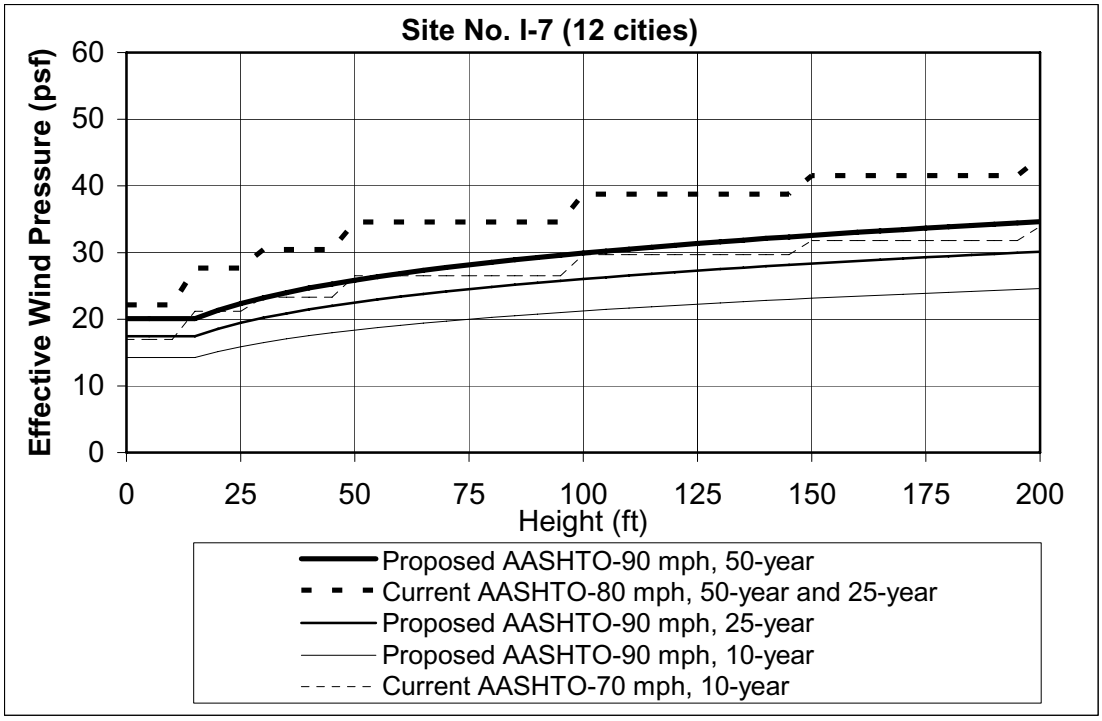

Figure B—13. Site No. I-7: Effective Wind Pressure

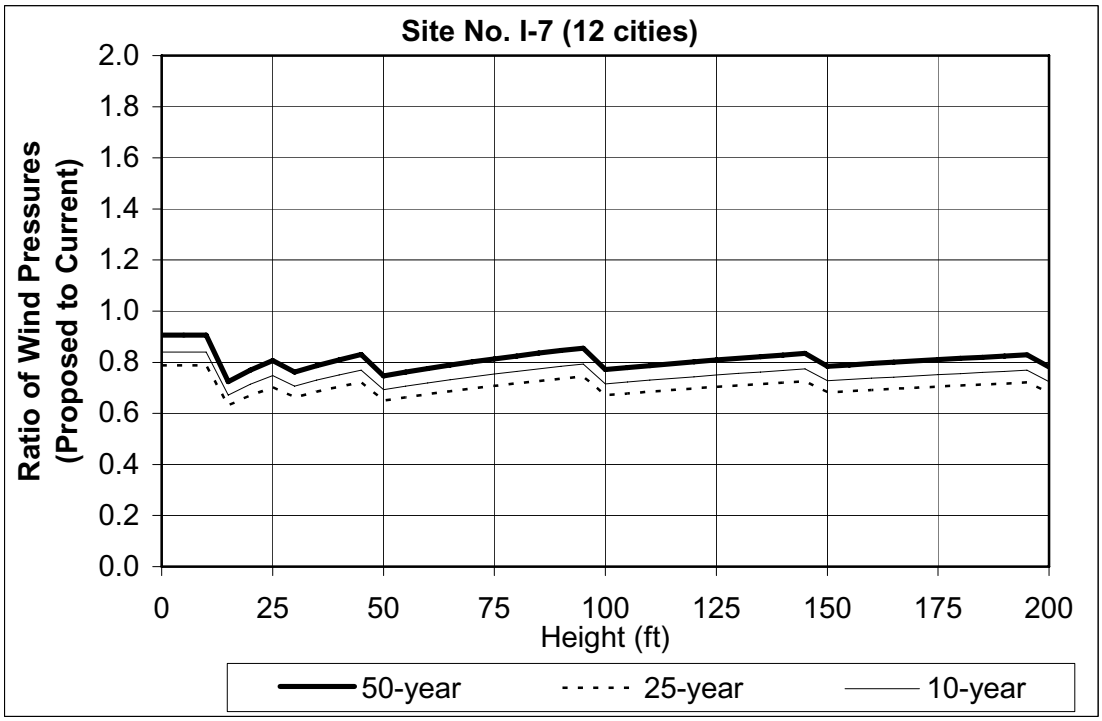

Figure B—14. Site No. I-7: Ratio of Wind Pressures (Proposed to Current Specification)

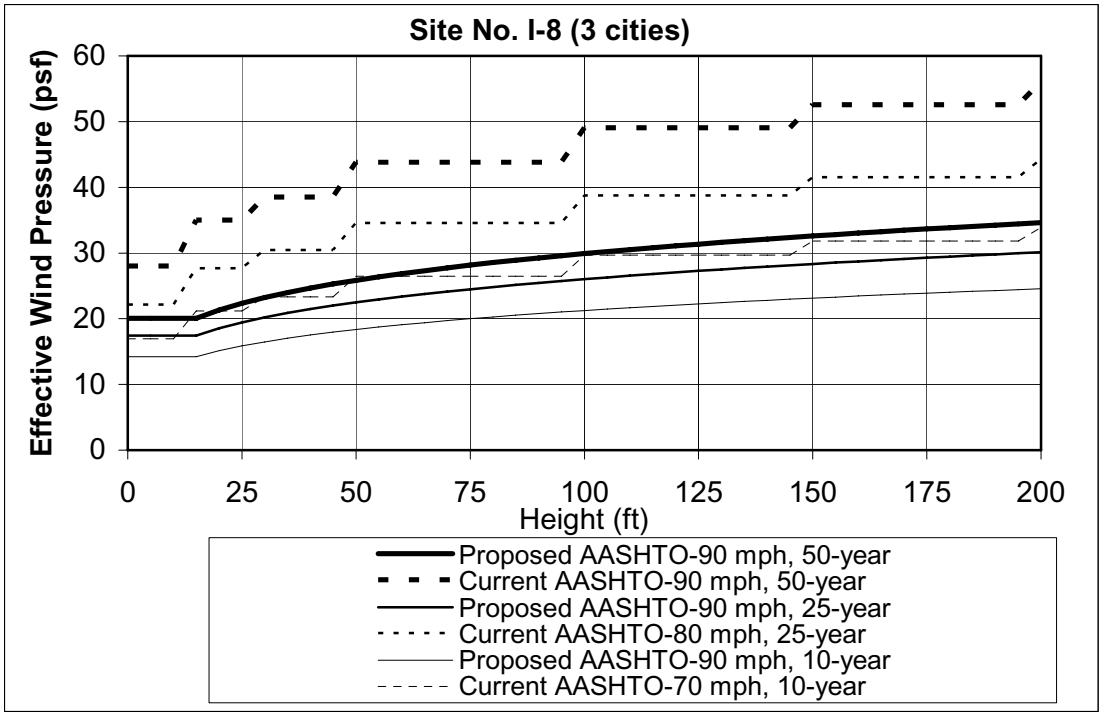

Figure B—15. Site No. I-8: Effective Wind Pressure

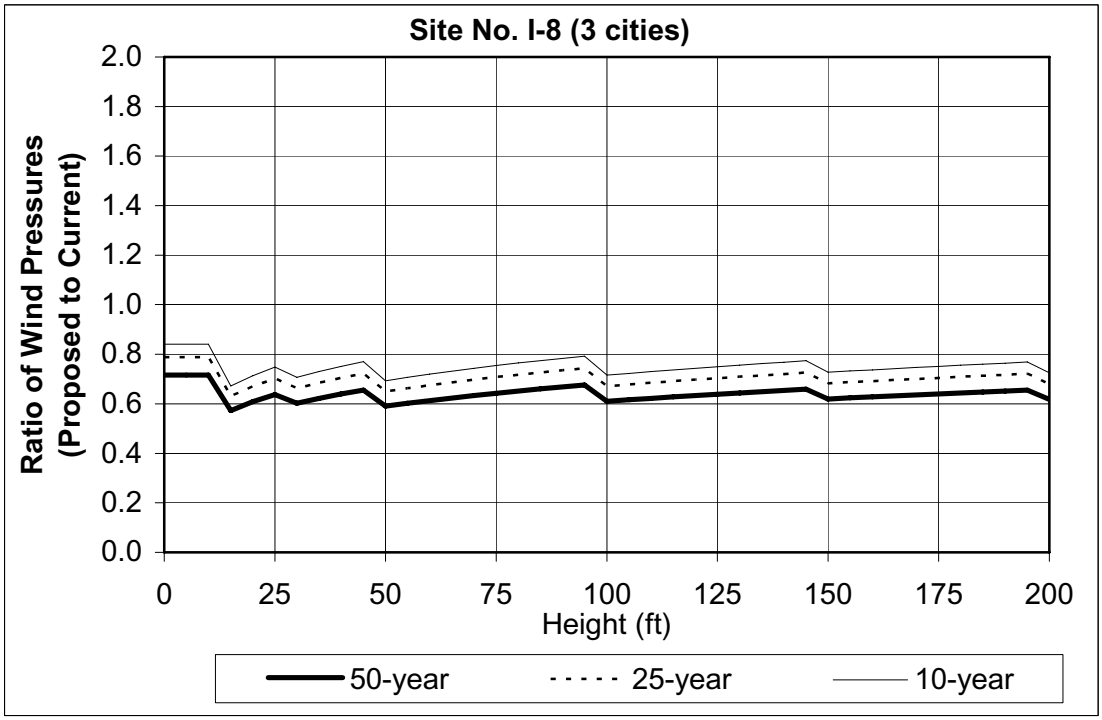

Figure B—16. Site No. I-8: Ratio of Wind Pressures (Proposed to Current Specification)

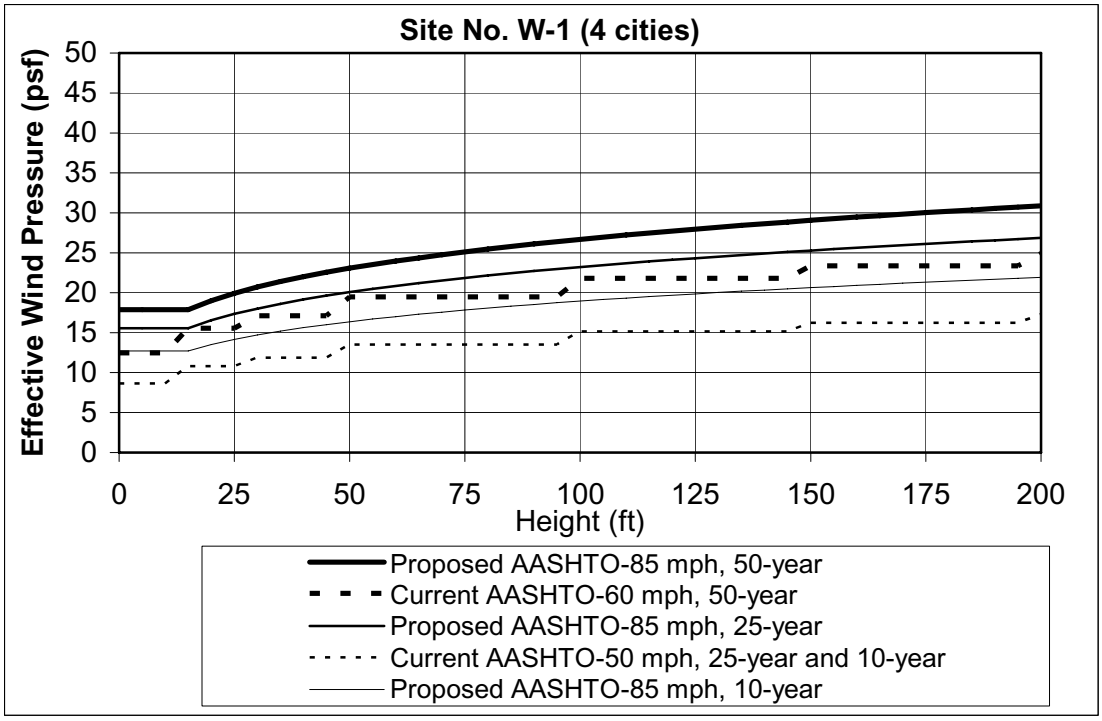

Figure B—17. Site No. W-1: Effective Wind Pressure

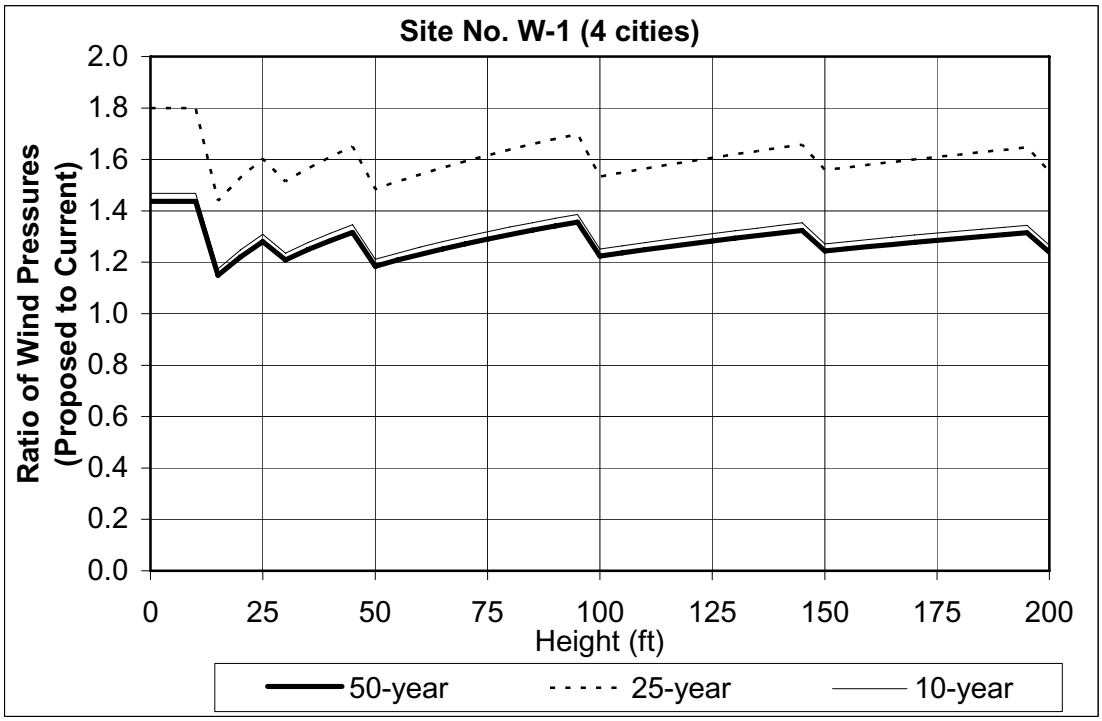

Figure B—18. Site No. W-1: Ratio of Wind Pressures (Proposed to Current Specification)

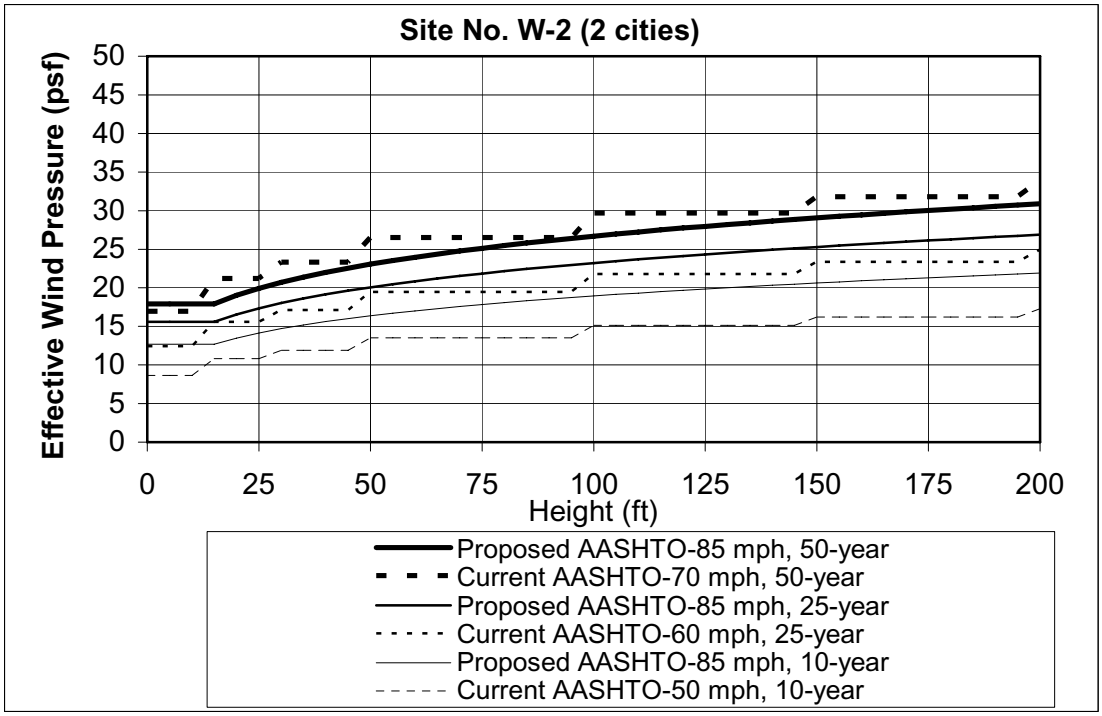

Figure B—19. Site No. W-2: Effective Wind Pressure

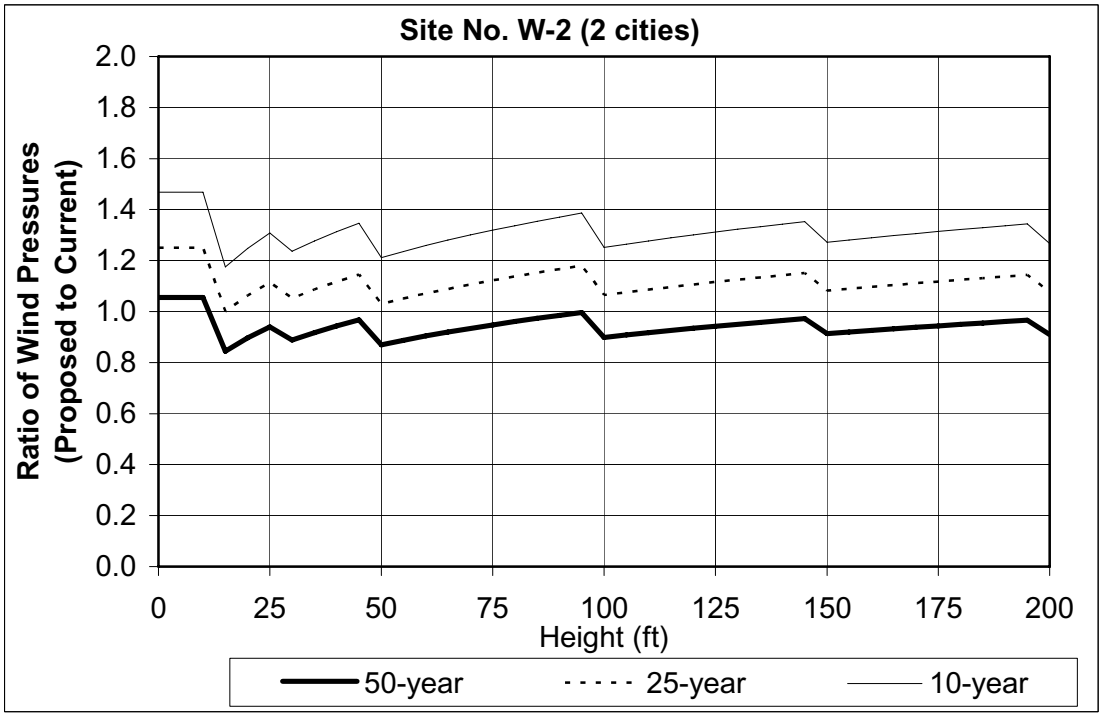

Figure B—20. Site No. W-2: Ratio of Wind Pressures (Proposed to Current Specification)

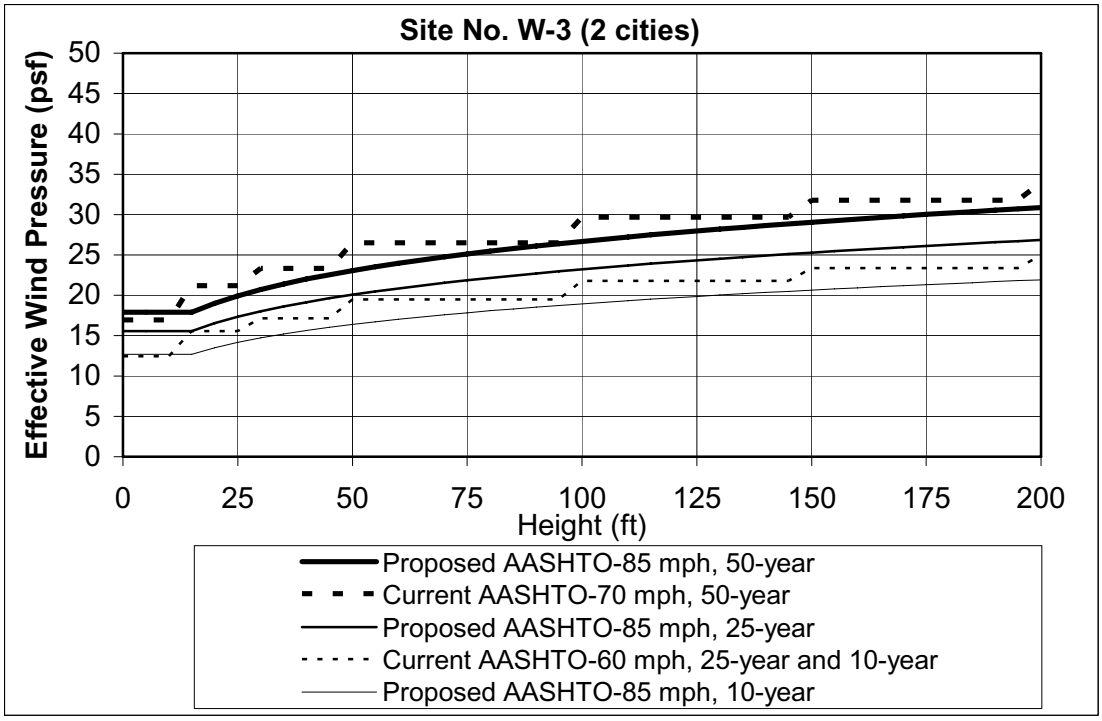

Figure B—21. Site No. W-3: Effective Wind Pressure

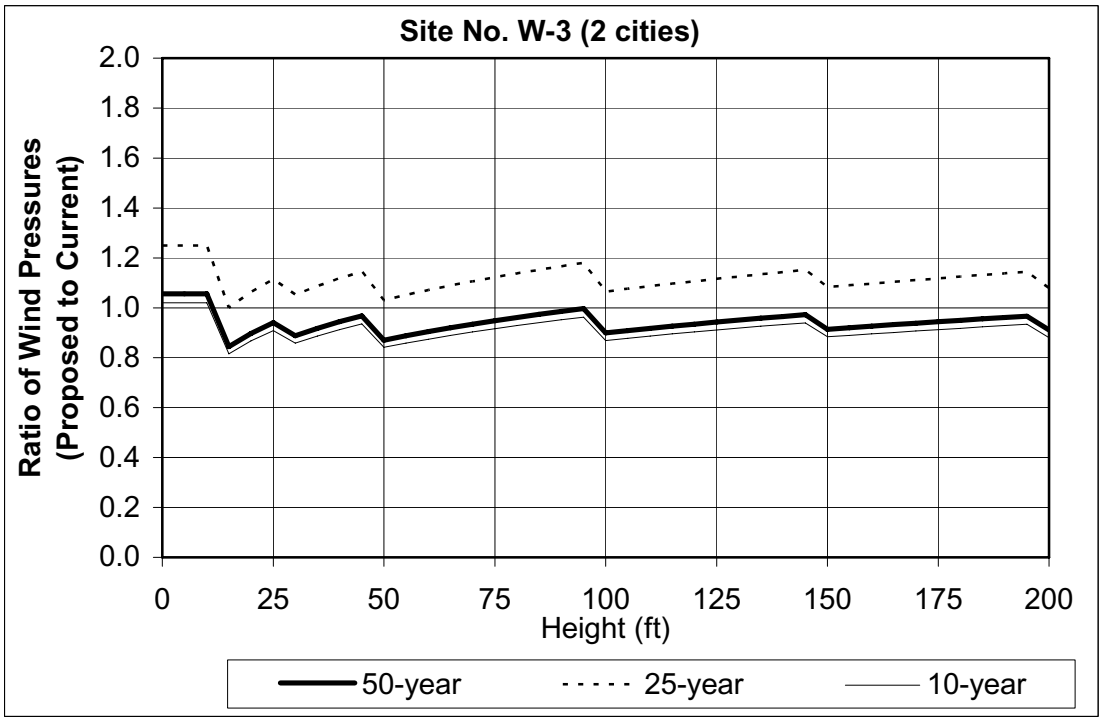

Figure B—22. Site No. W-3: Ratio of Wind Pressures (Proposed to Current Specification)

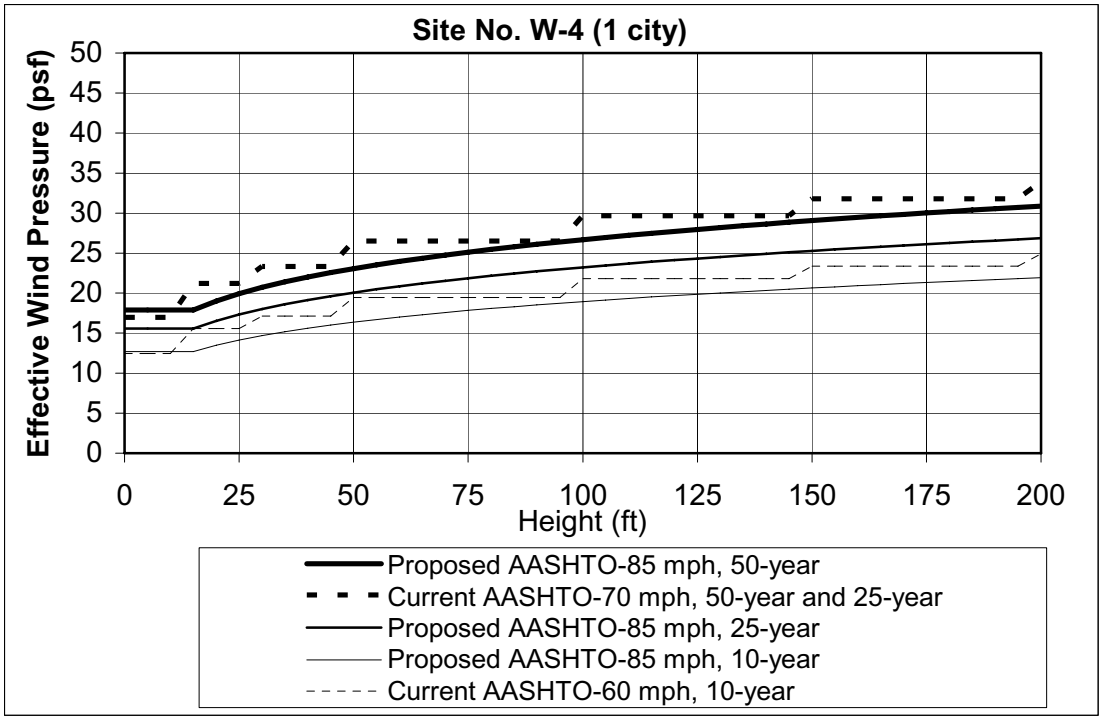

Figure B—23. Site No. W-4: Effective Wind Pressure

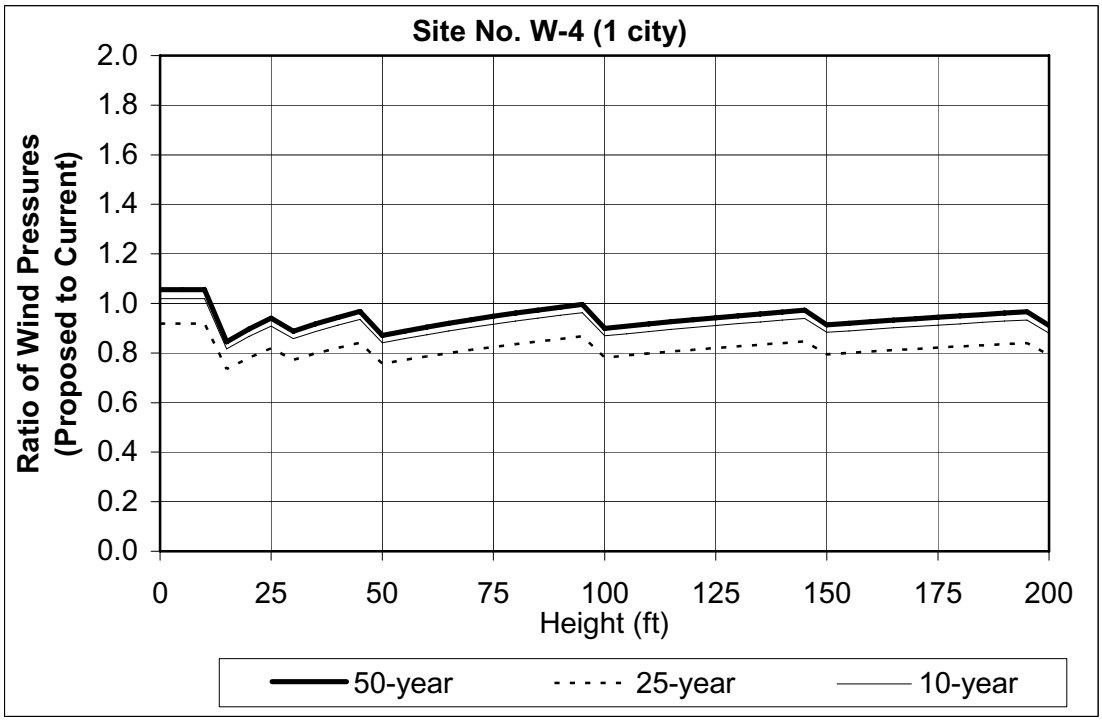

Figure B—24. Site No. W-4: Ratio of Wind Pressures (Proposed to Current Specification)

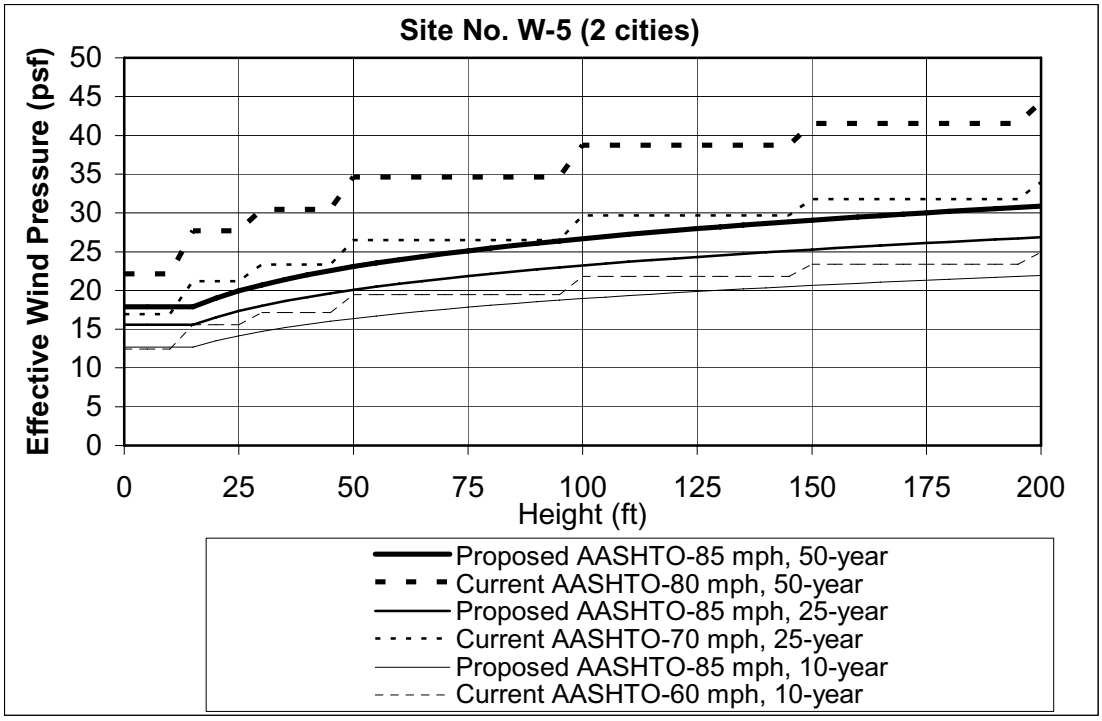

Figure B—25. Site No. W-5: Effective Wind Pressure

Figure B—26. Site No. W-5: Ratio of Wind Pressures (Proposed to Current Specification)

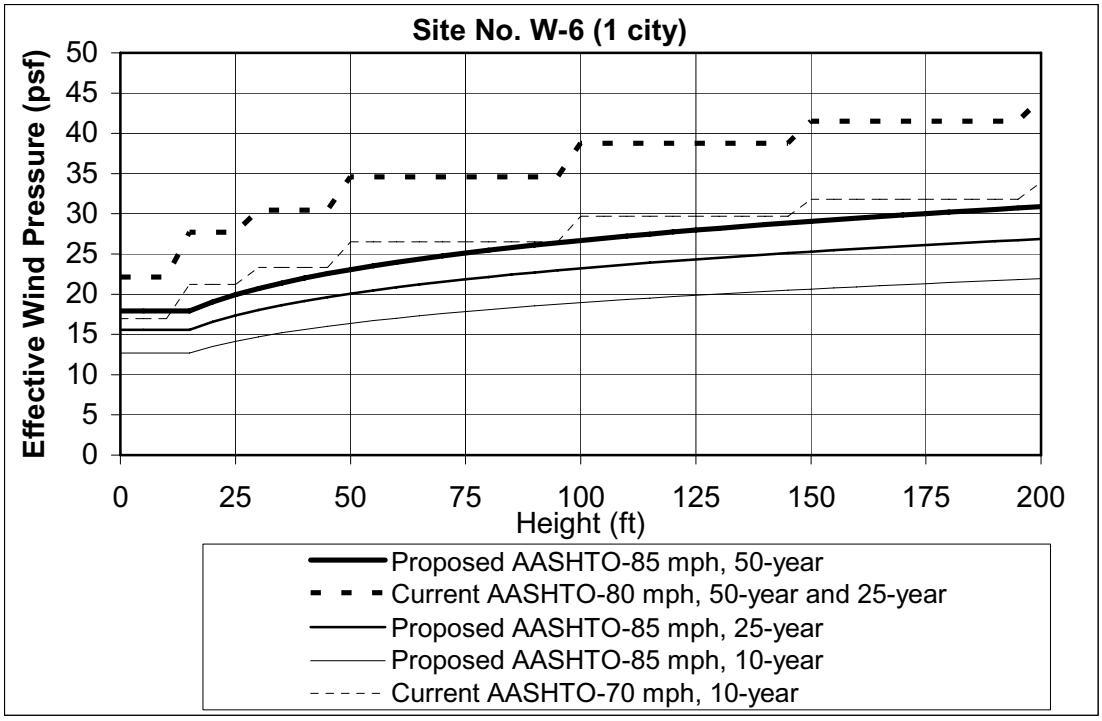

Figure B—27. Site No. W-6: Effective Wind Pressure

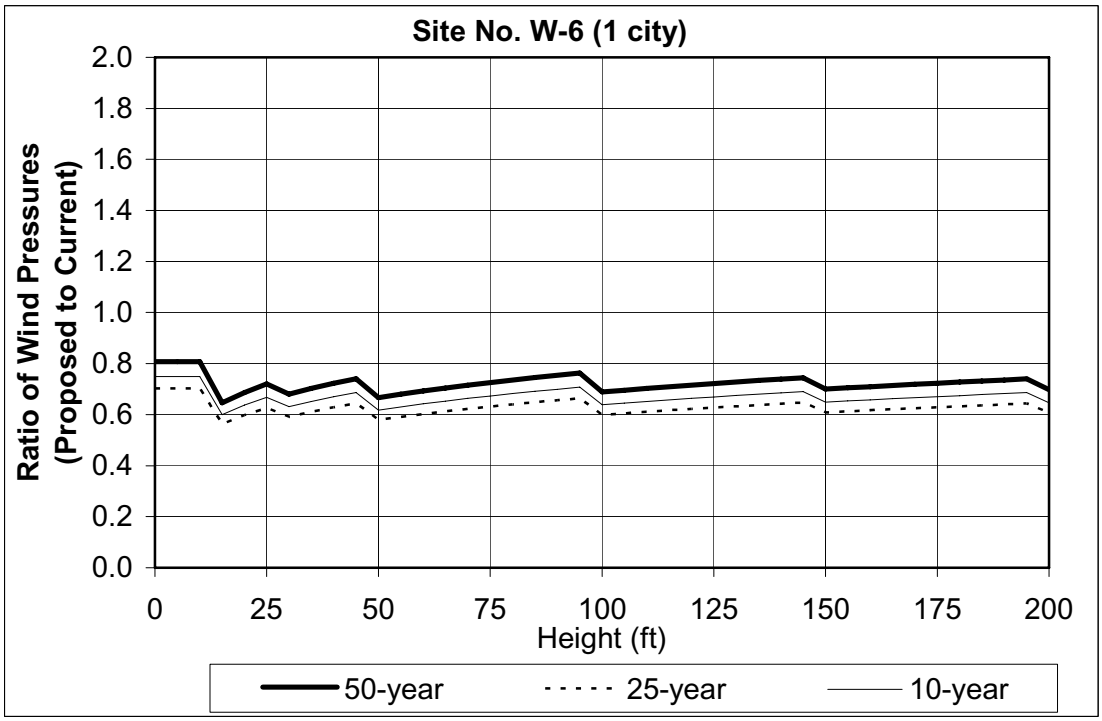

Figure B—28. Site No. W-6: Ratio of Wind Pressures (Proposed to Current Specification)

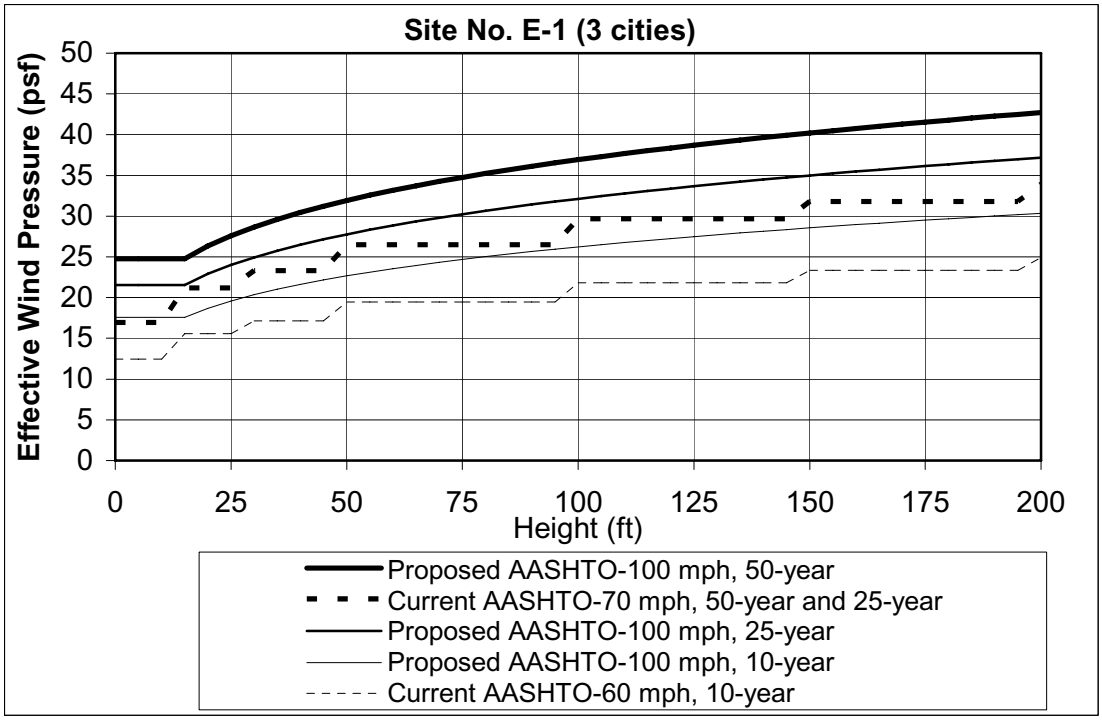

Figure B—29. Site No. E-1: Effective Wind Pressure

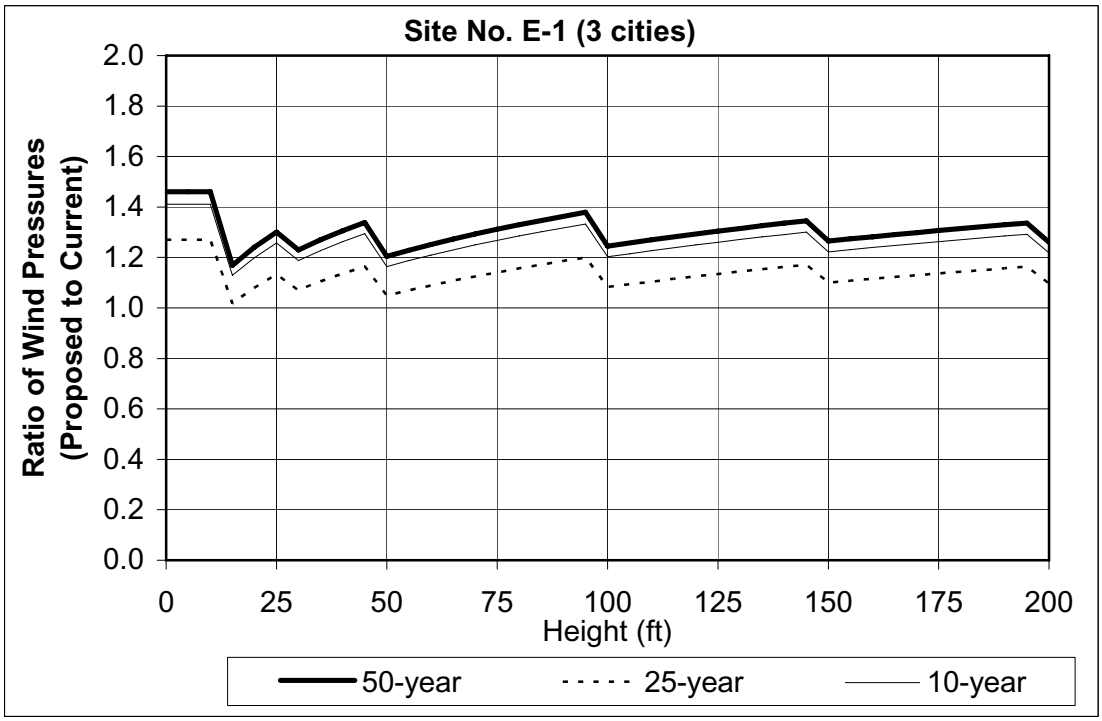

Figure B—30. Site No. E-1: Ratio of Wind Pressures (Proposed to Current Specification)

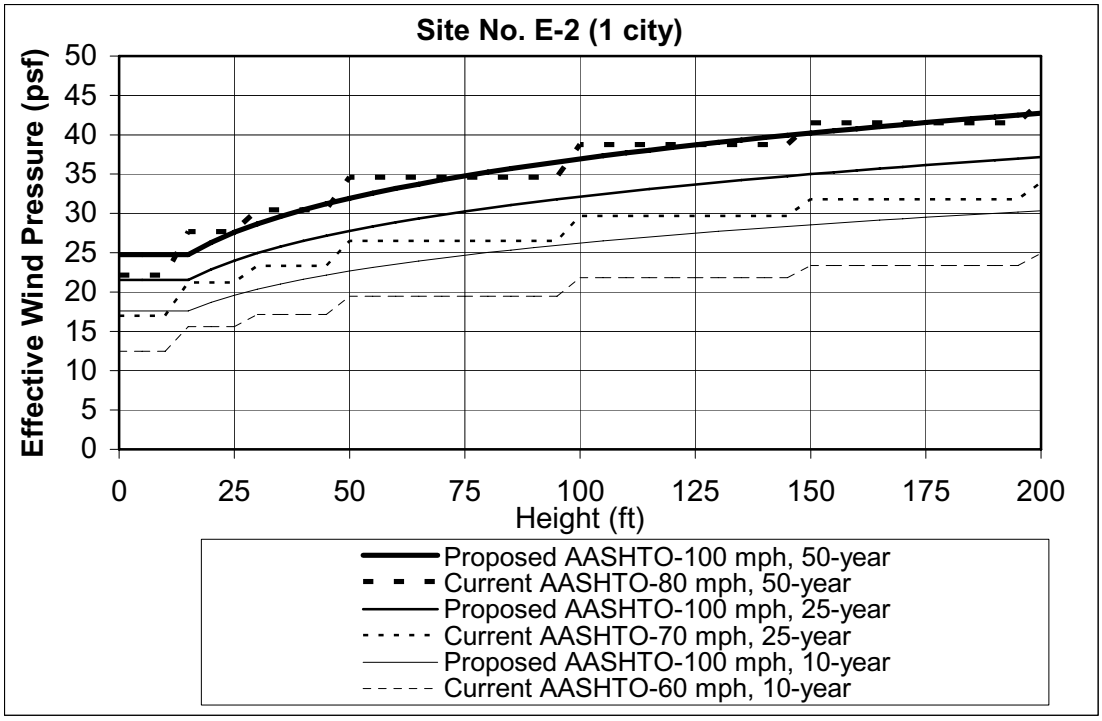

Figure B—31. Site No. E-2: Effective Wind Pressure

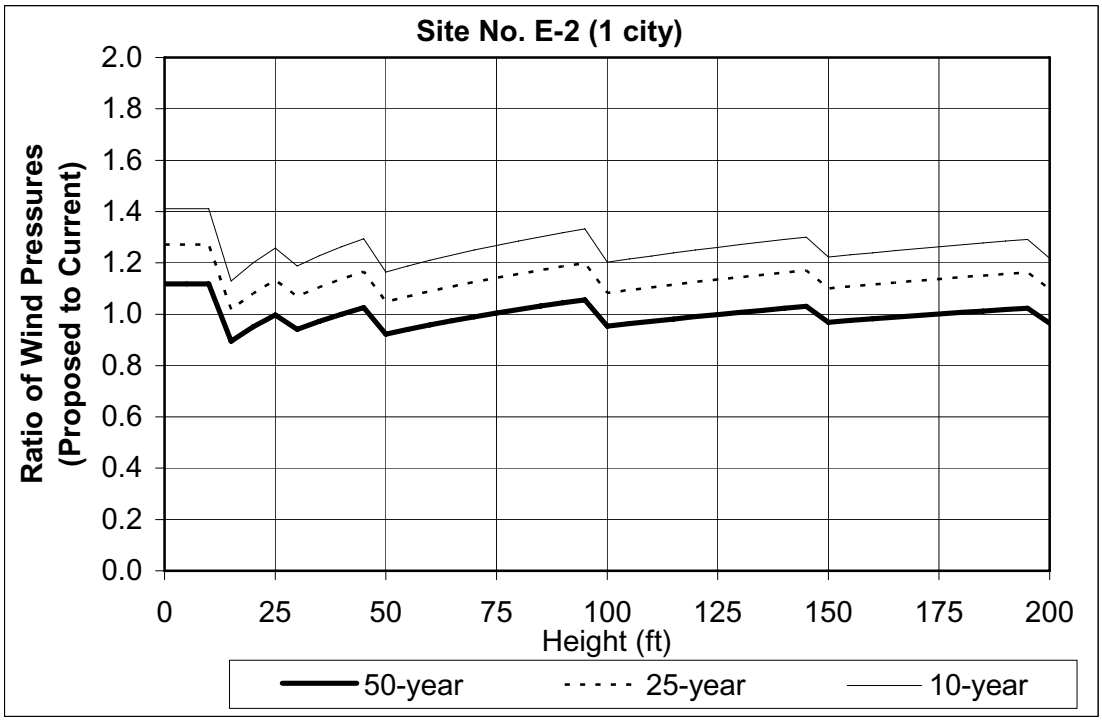

Figure B—32. Site No. E-2: Ratio of Wind Pressures (Proposed to Current Specification)

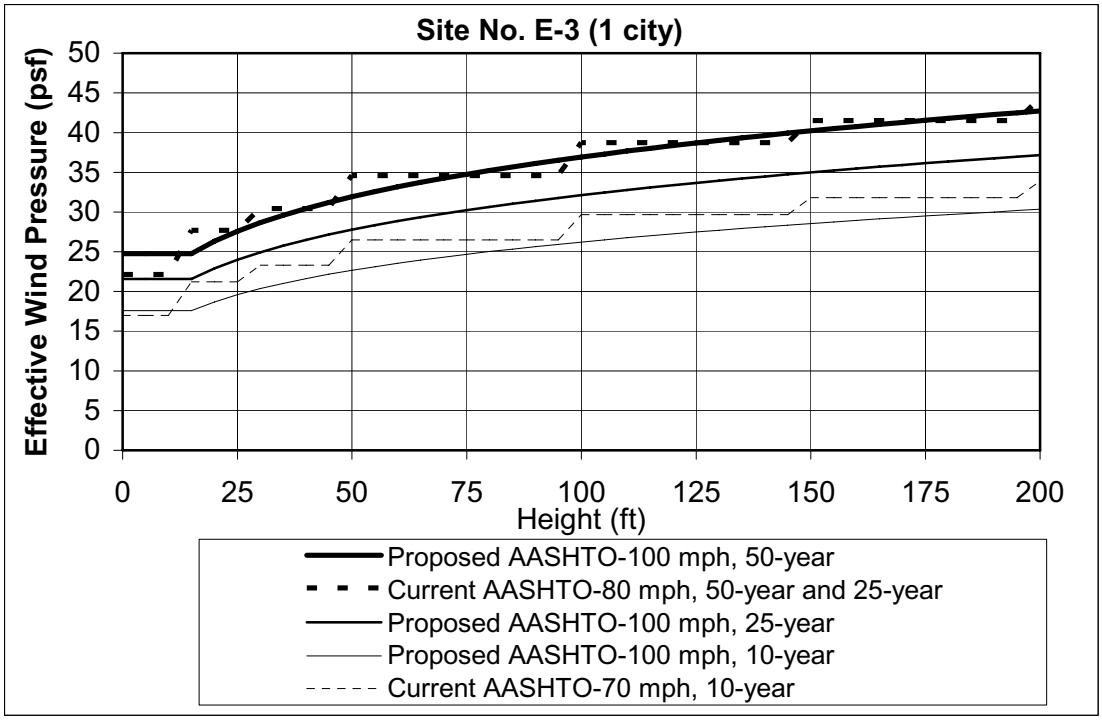

Figure B—33. Site No. E-3: Effective Wind Pressure

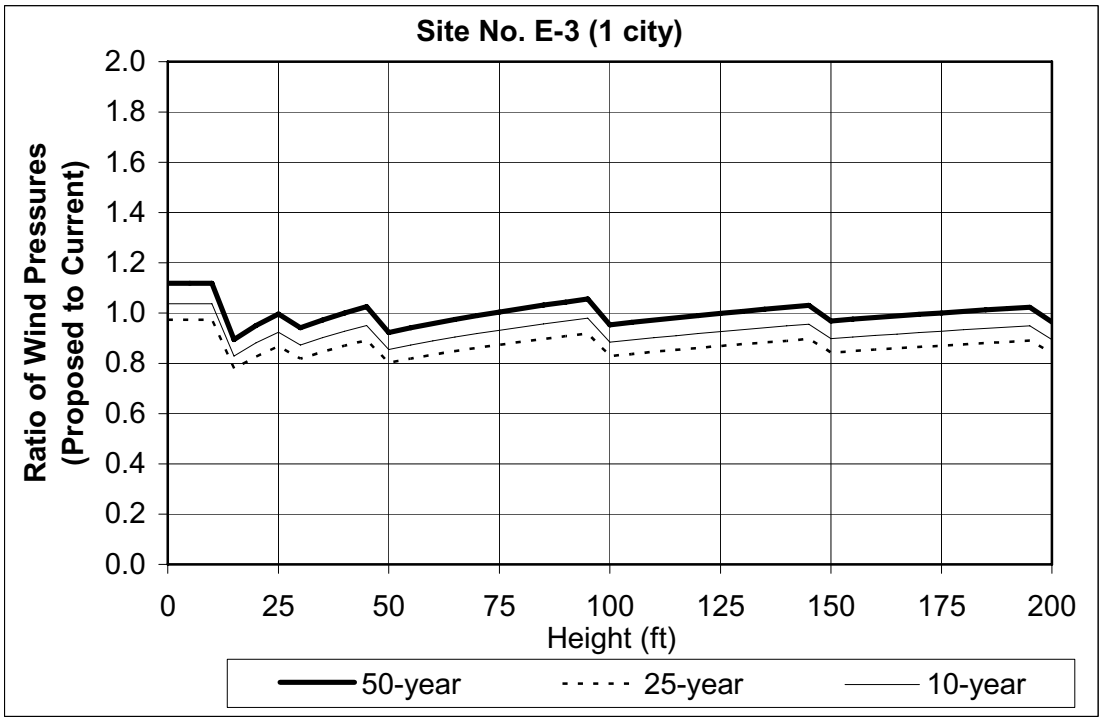

Figure B—34. Site No. E-3: Ratio of Wind Pressures (Proposed to Current Specification)

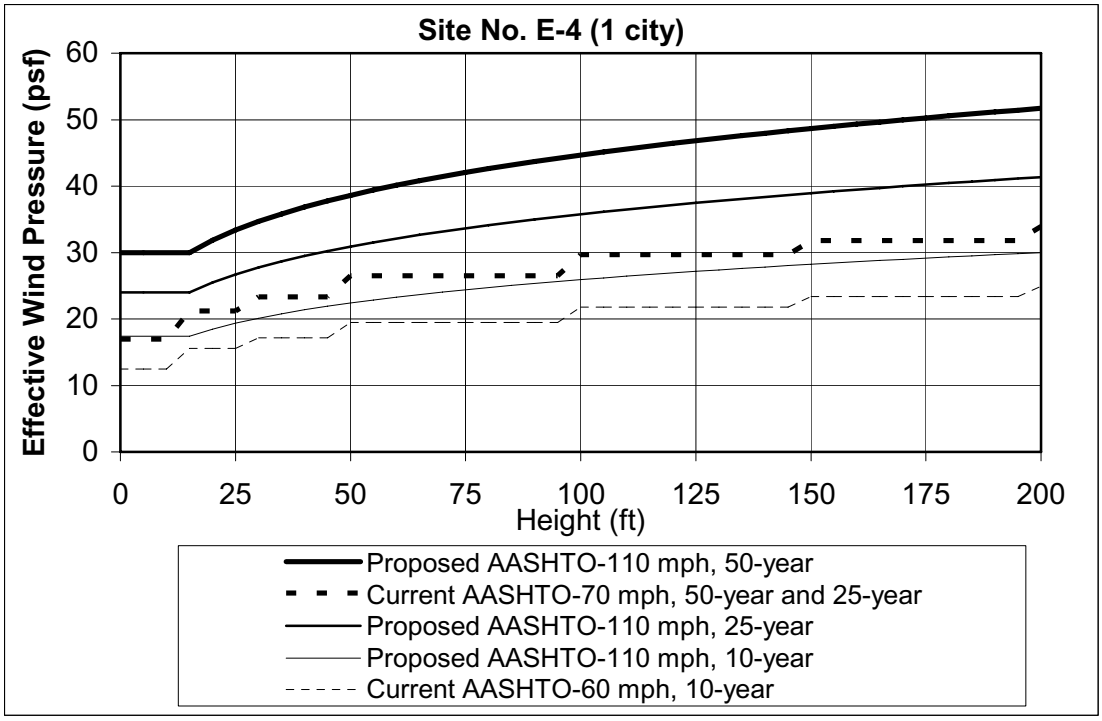

Figure B—35. Site No. E-4: Effective Wind Pressure

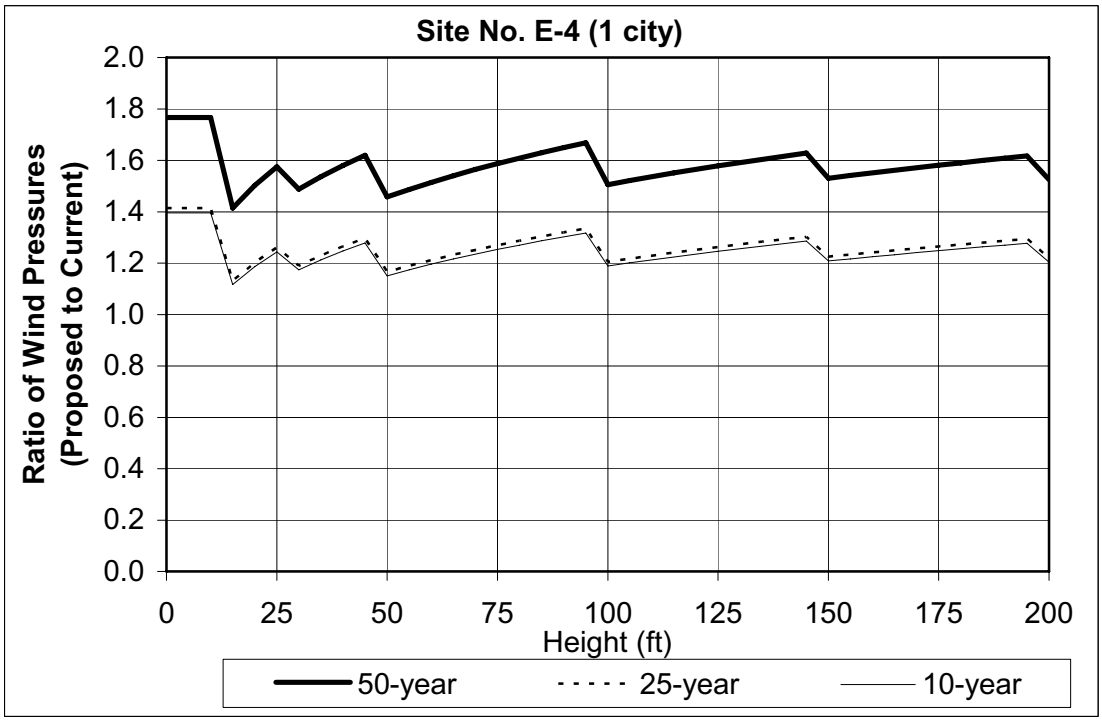

Figure B—36. Site No. E-4: Ratio of Wind Pressures (Proposed to Current Specification)

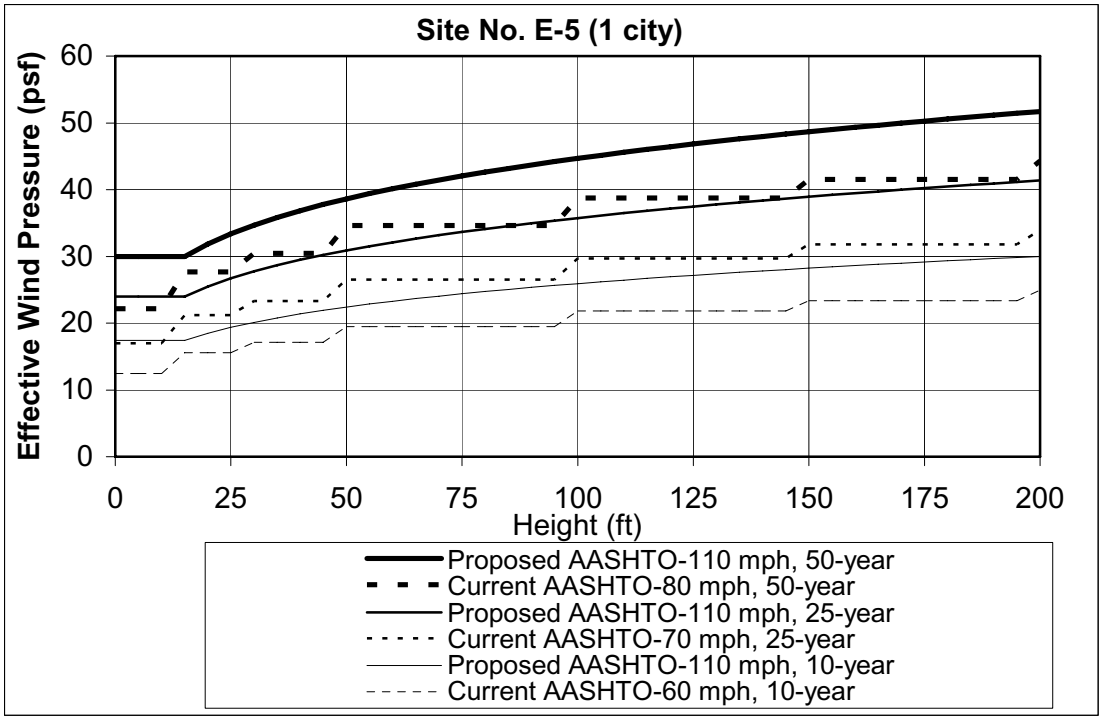

Figure B—37. Site No. E-5: Effective Wind Pressure

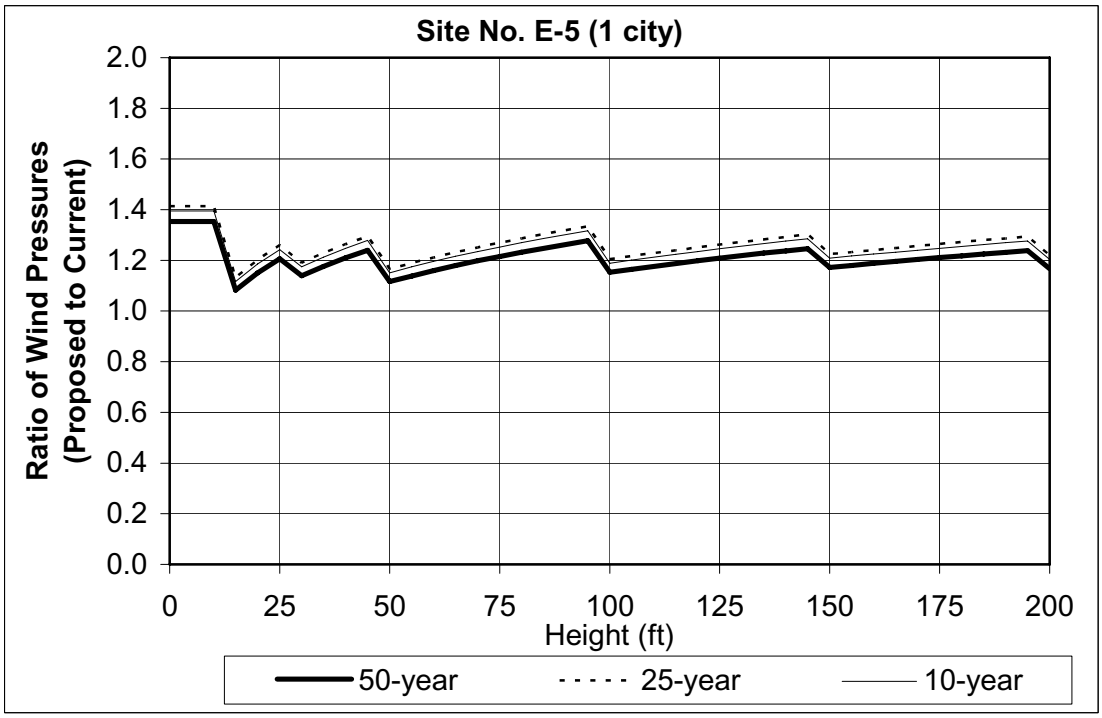

Figure B—38. Site No. E-5: Ratio of Wind Pressures (Proposed to Current Specification)

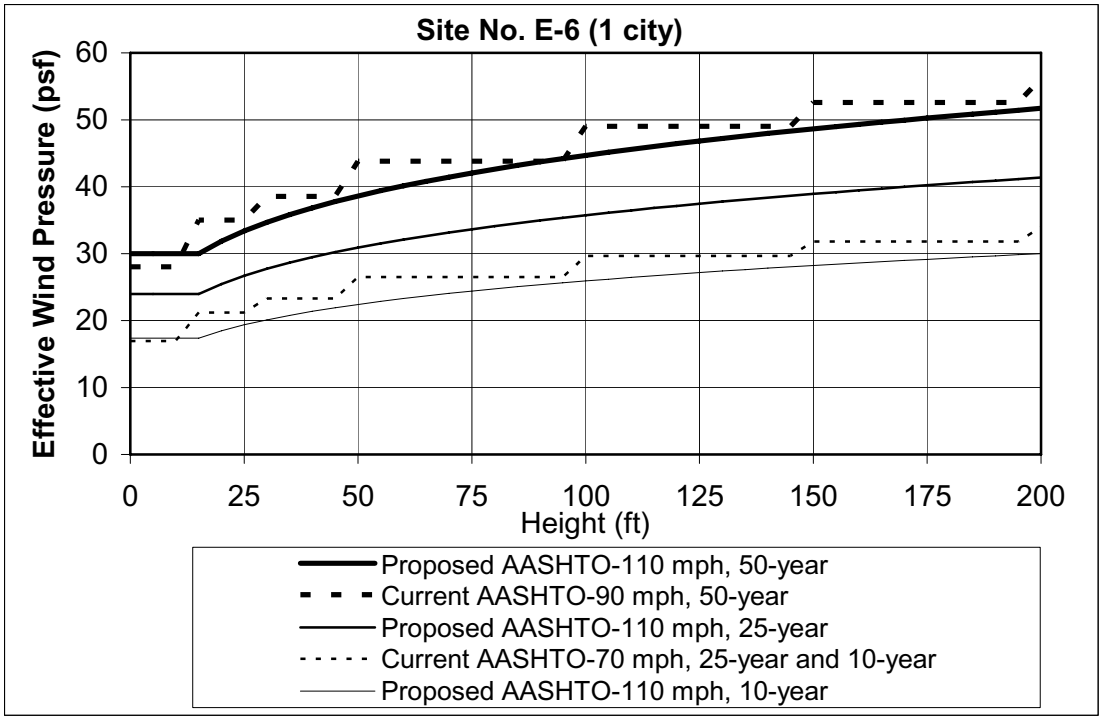

Figure B—39. Site No. E-6: Effective Wind Pressure

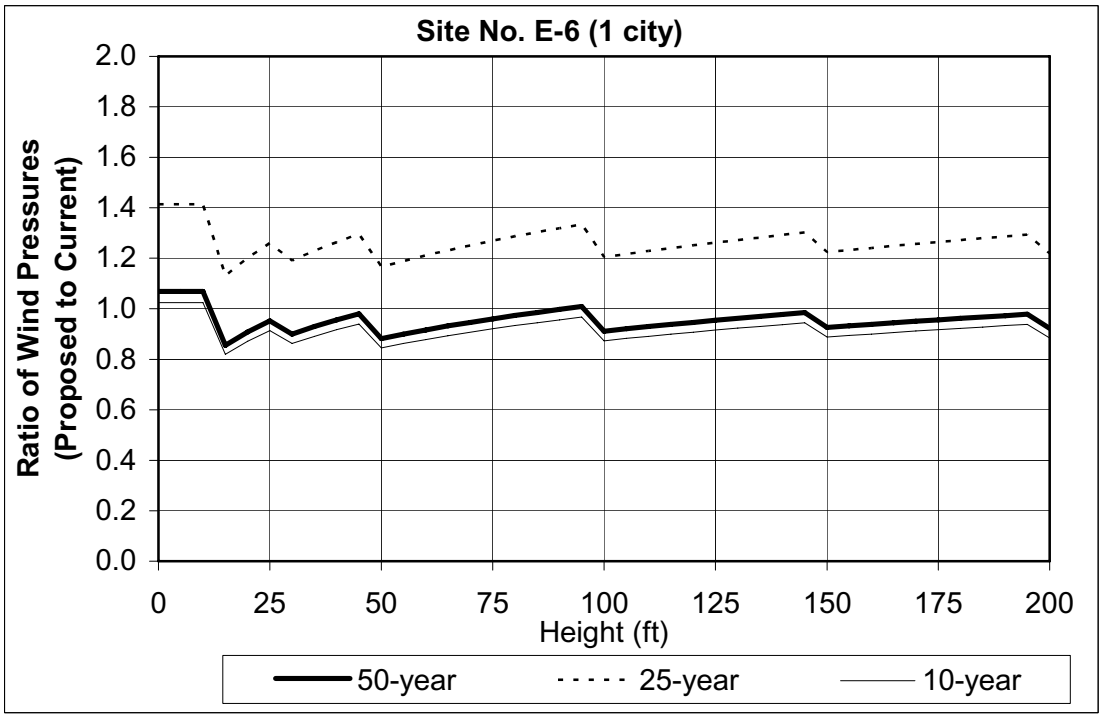

Figure B—40. Site No. E-6: Ratio of Wind Pressures (Proposed to Current Specification)

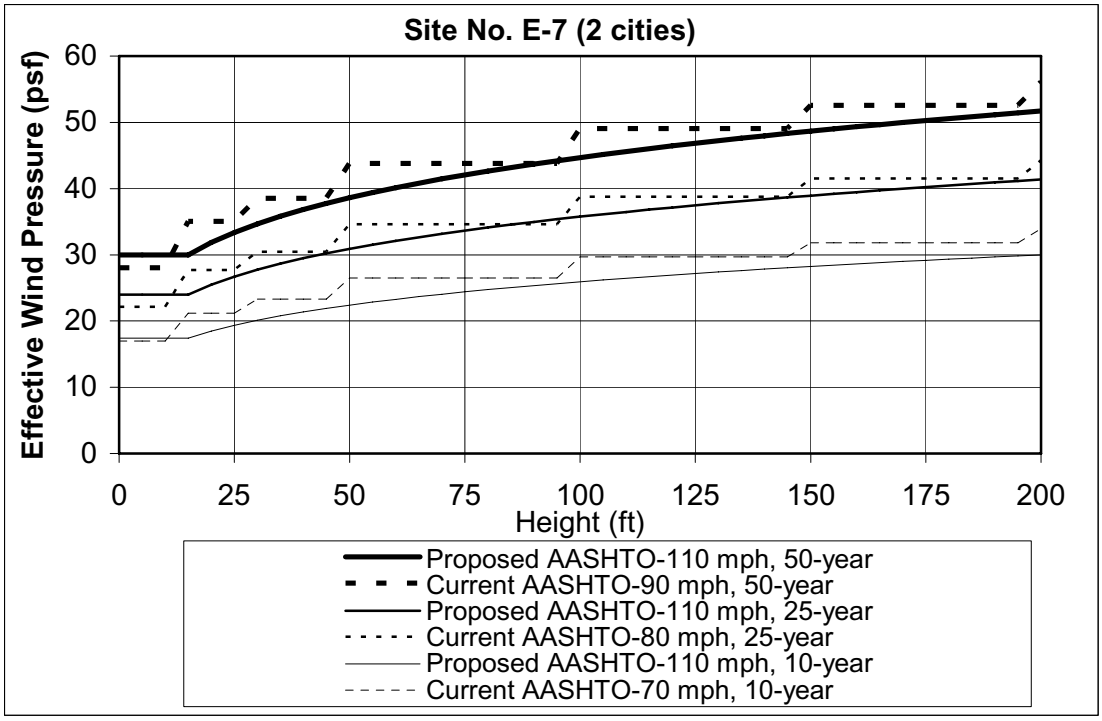

Figure B—41. Site No. E-7: Effective Wind Pressure

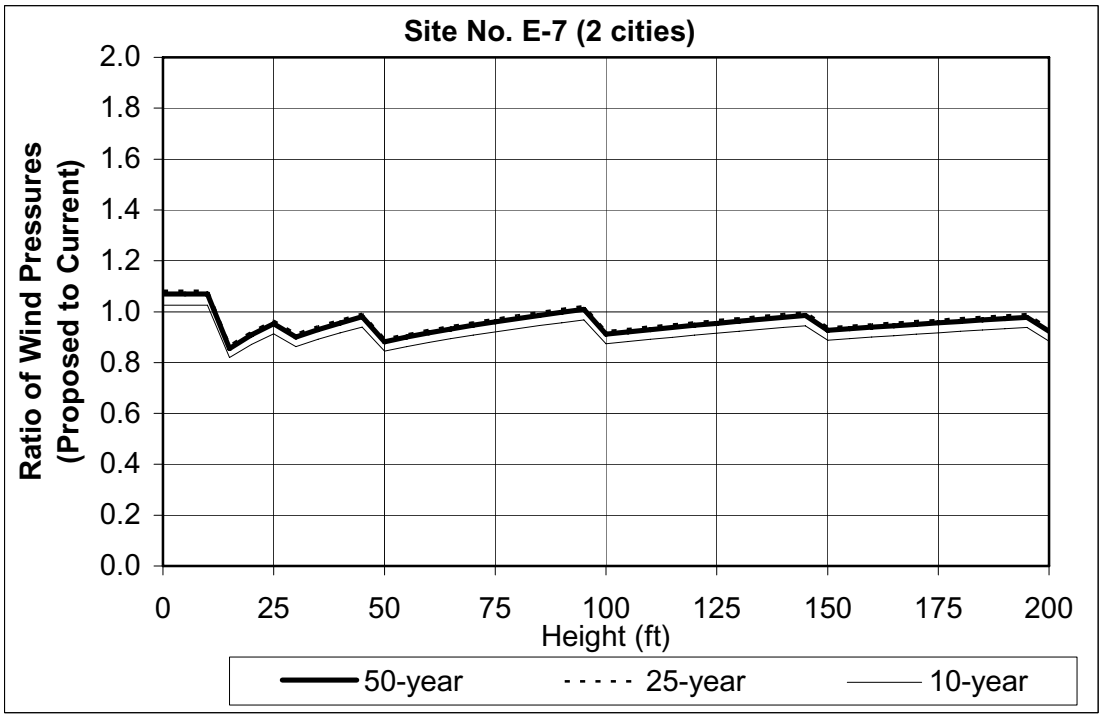

Figure B—42. Site No. E-7: Ratio of Wind Pressures (Proposed to Current Specification)

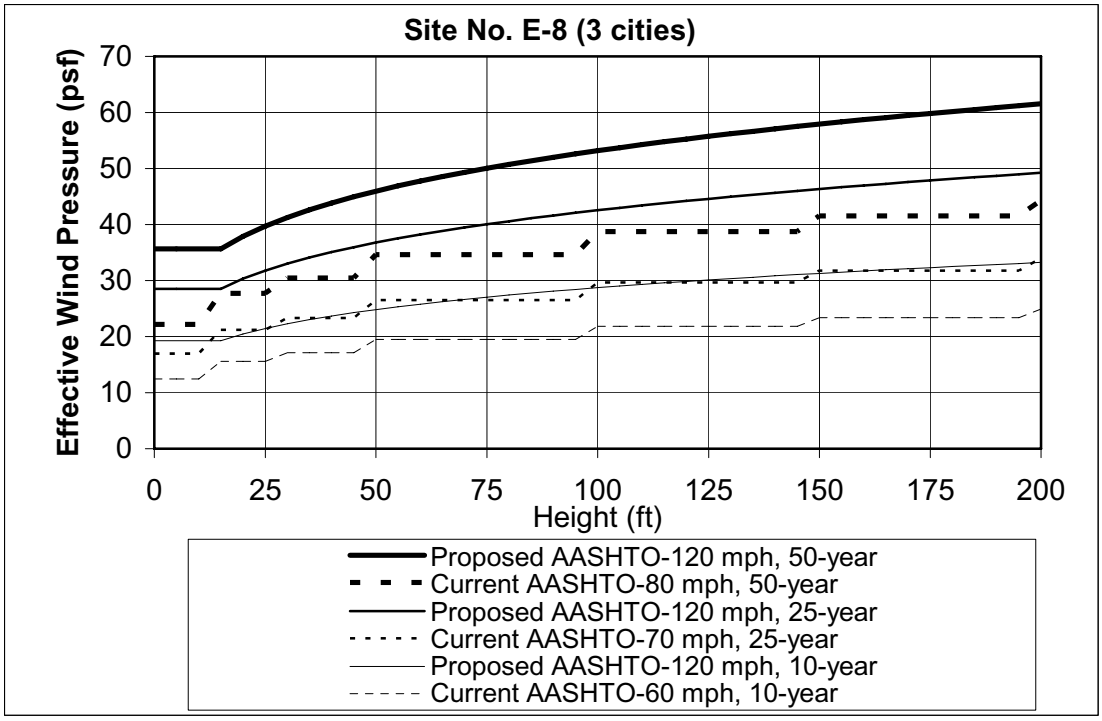

Figure B—43. Site No. E-8: Effective Wind Pressure

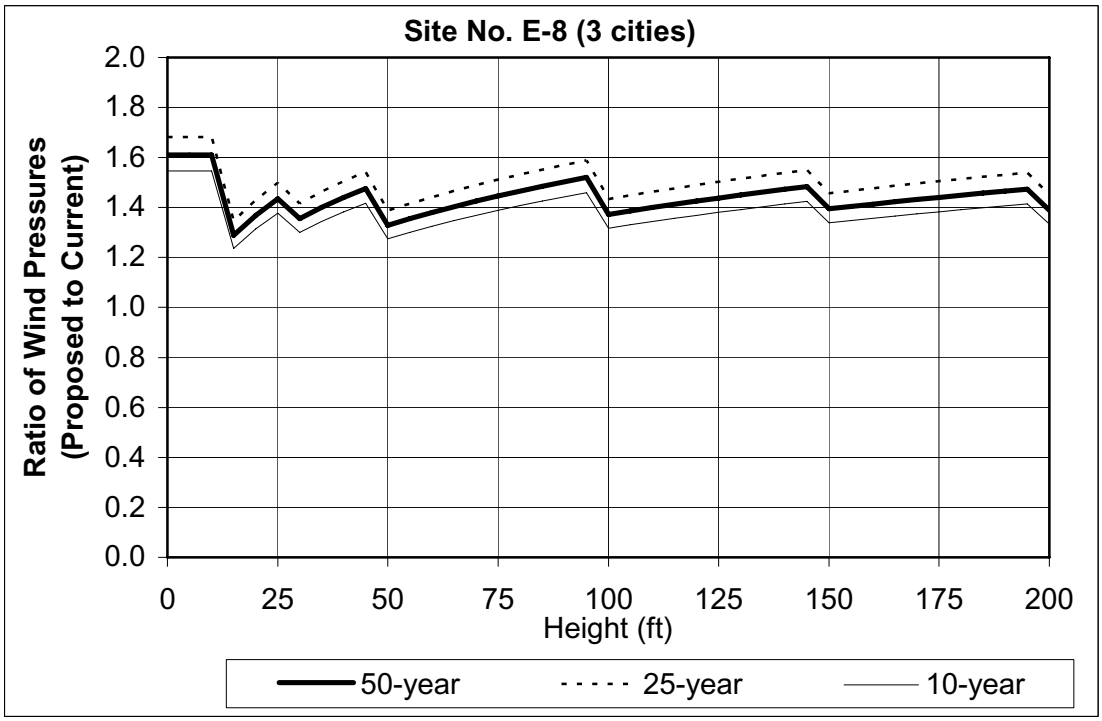

Figure B—44. Site No. E-8: Ratio of Wind Pressures (Proposed to Current Specification)

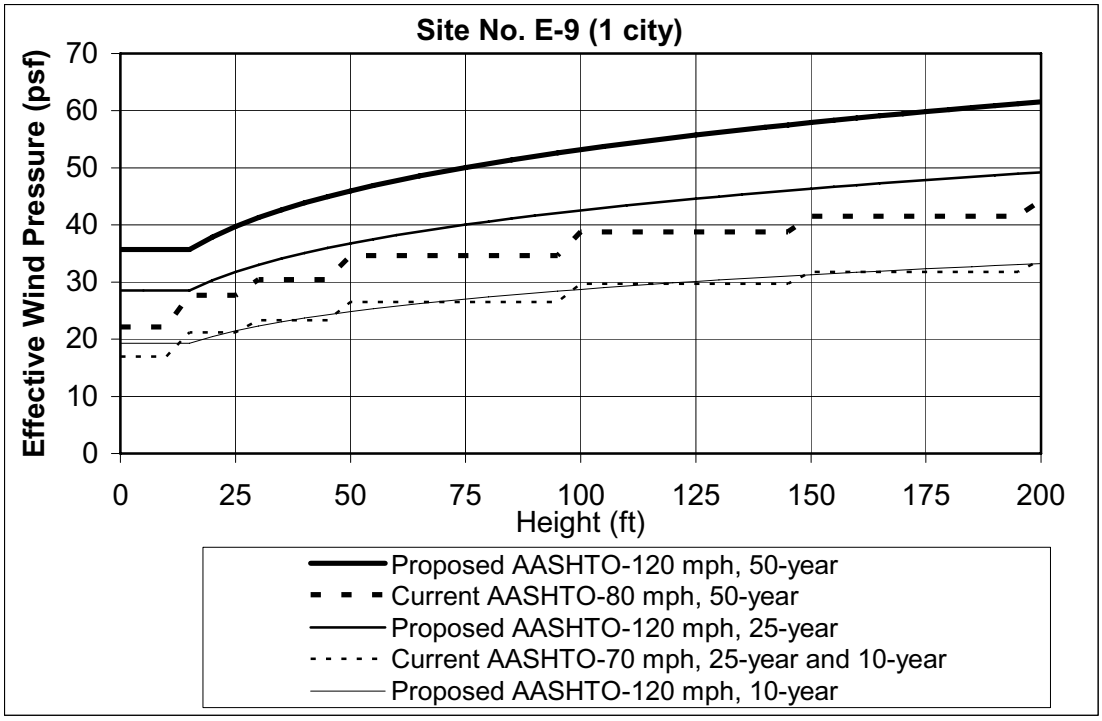

Figure B—45. Site No. E-9: Effective Wind Pressure

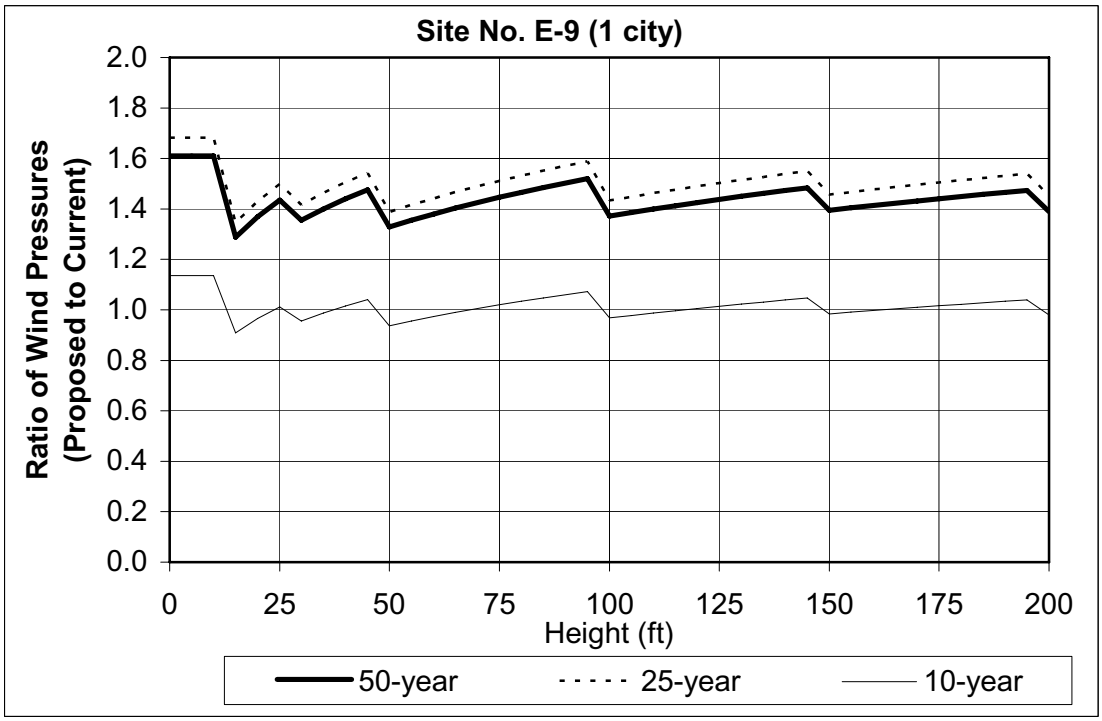

Figure B—46. Site No. E-9: Ratio of Wind Pressures (Proposed to Current Specification)

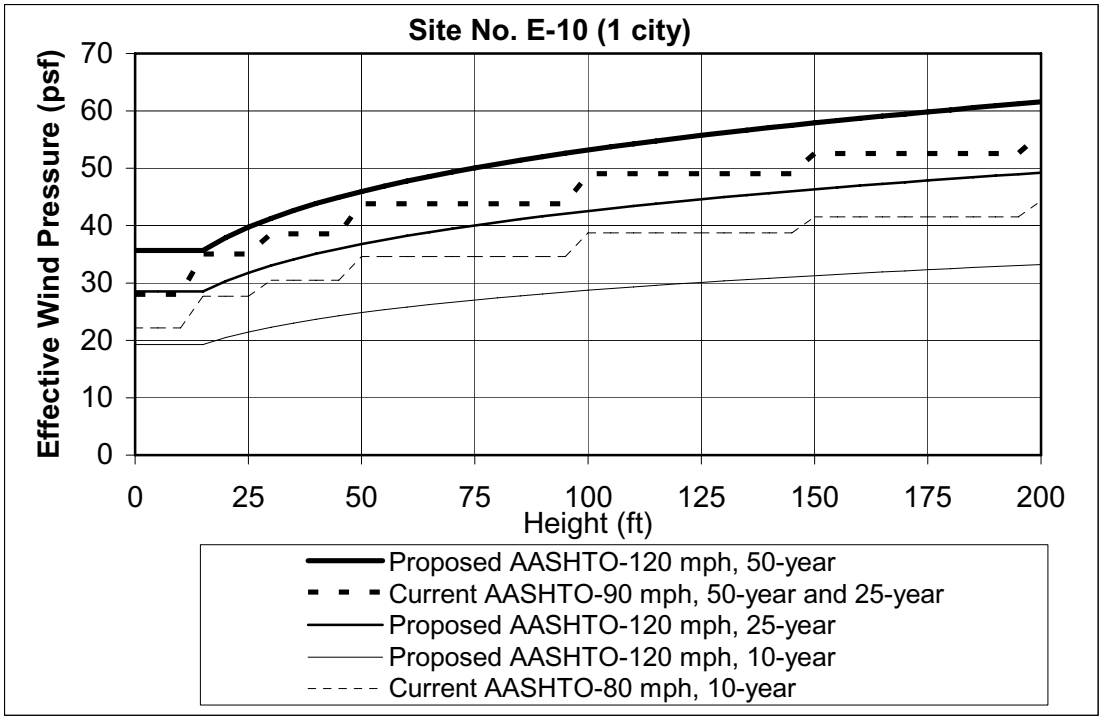

Figure B—47. Site No. E-10: Effective Wind Pressure

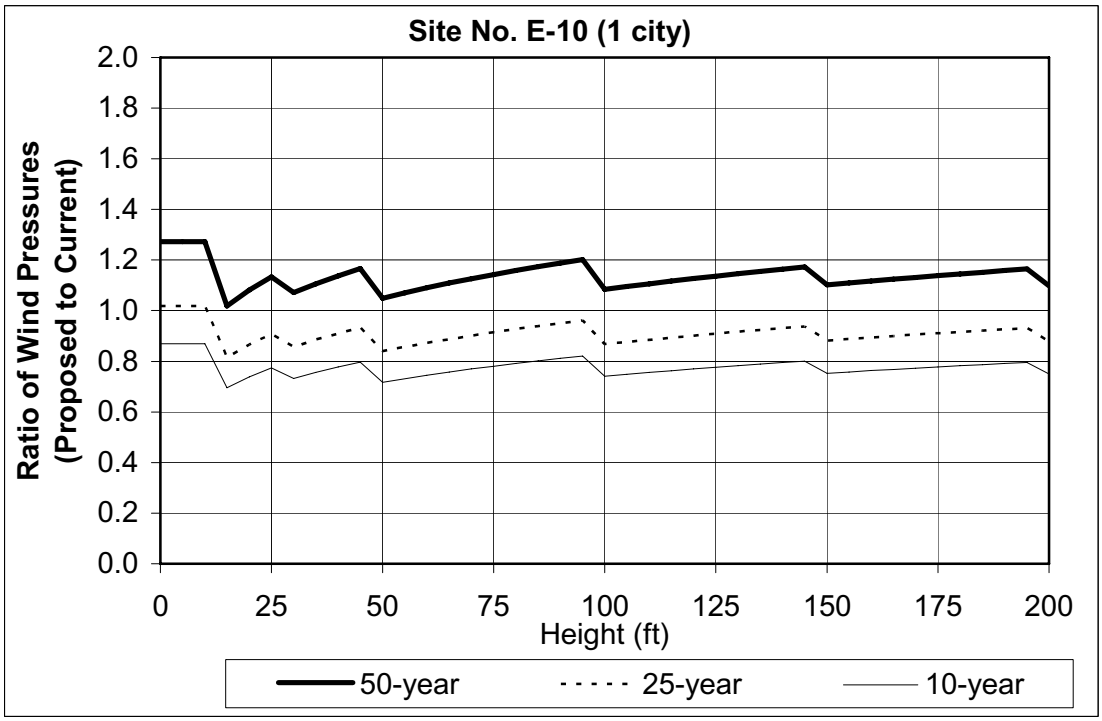

Figure B—48. Site No. E-10: Ratio of Wind Pressures (Proposed to Current Specification)

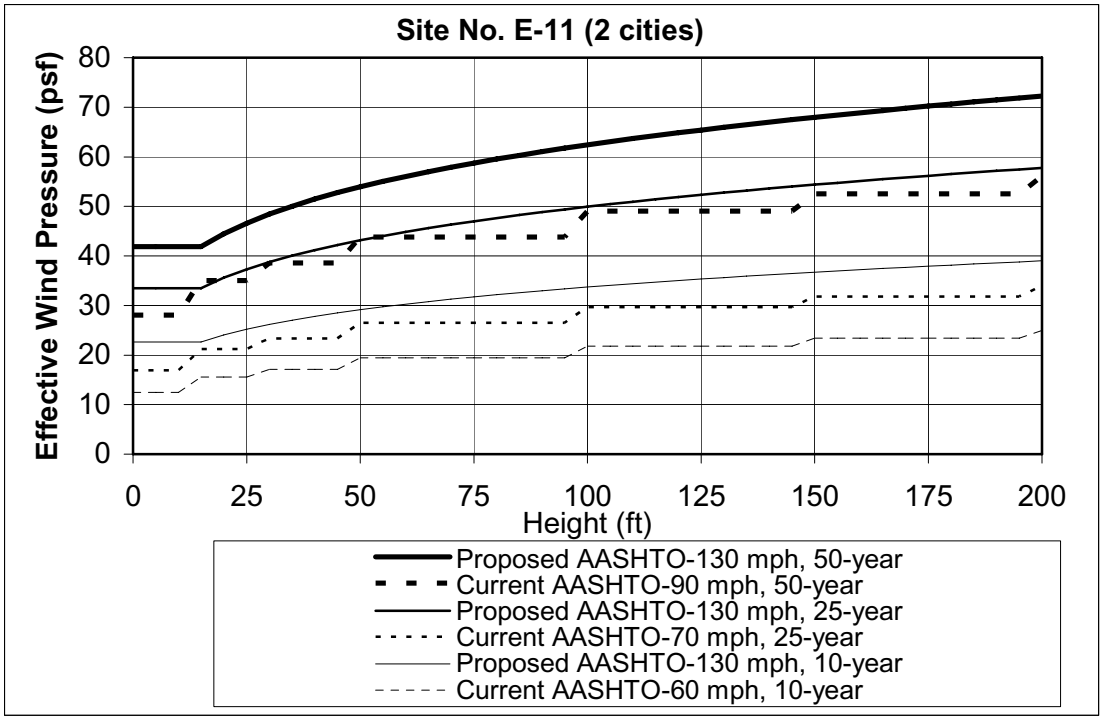

Figure B—49. Site No. E-11: Effective Wind Pressure

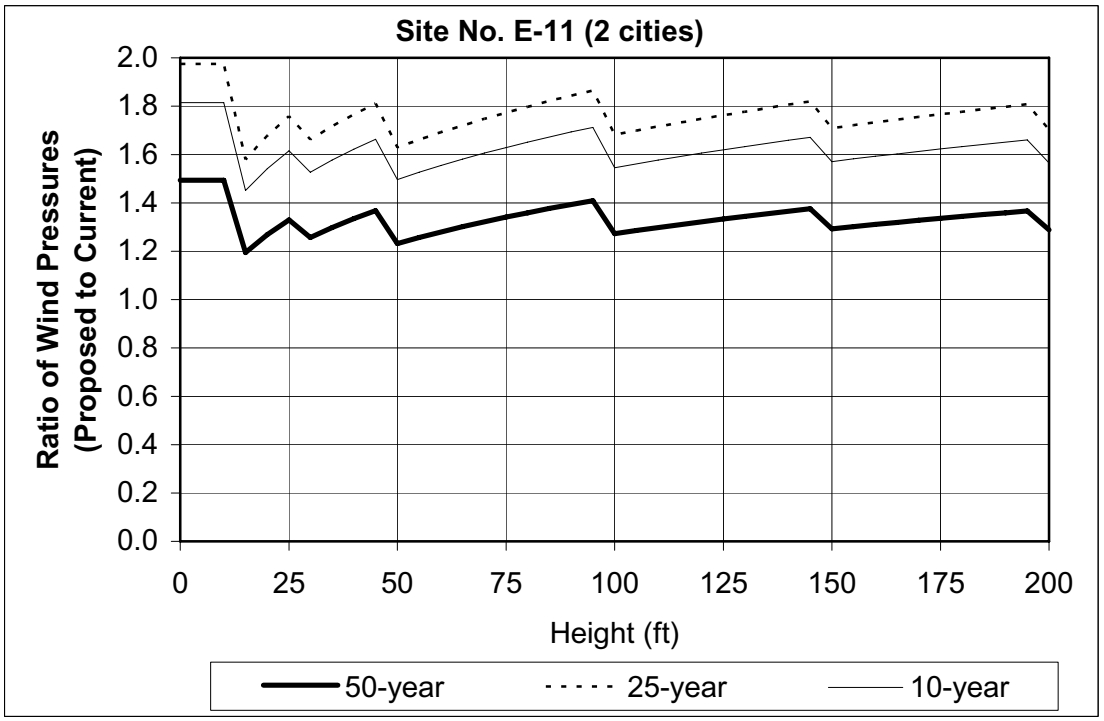

Figure B—50. Site No. E-11: Ratio of Wind Pressures (Proposed to Current Specification)

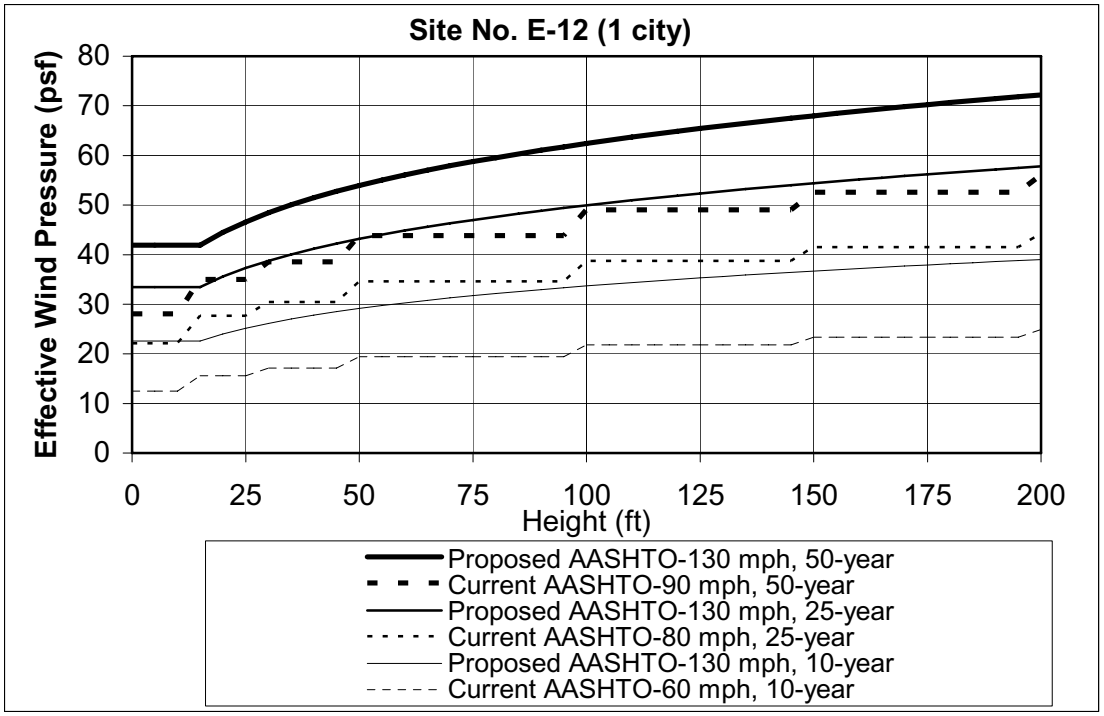

Figure B—51. Site No. E-12: Effective Wind Pressure

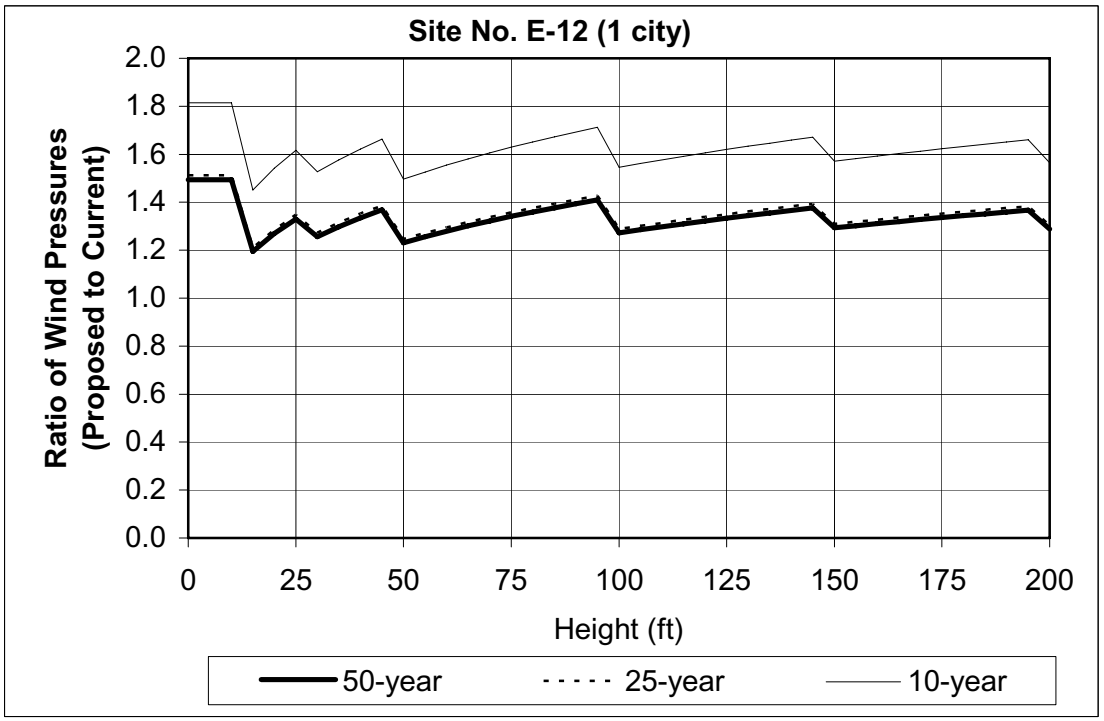

Figure B—52. Site No. E-12: Ratio of Wind Pressures (Proposed to Current Specification)

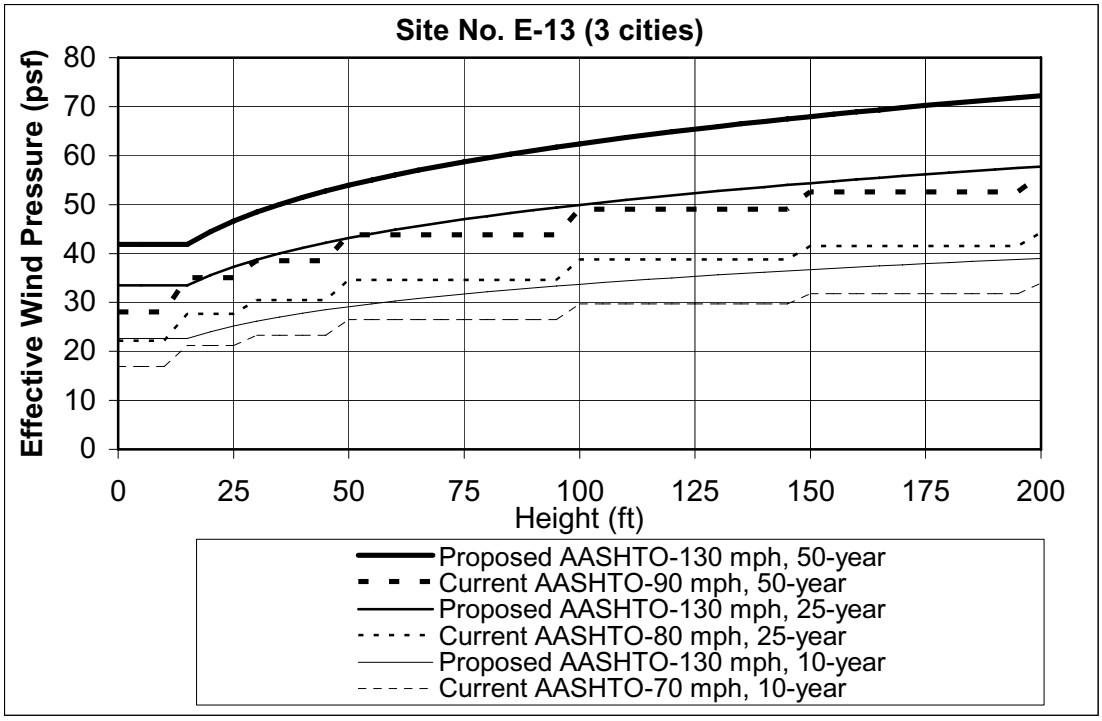

Figure B—53. Site No. E-13: Effective Wind Pressure

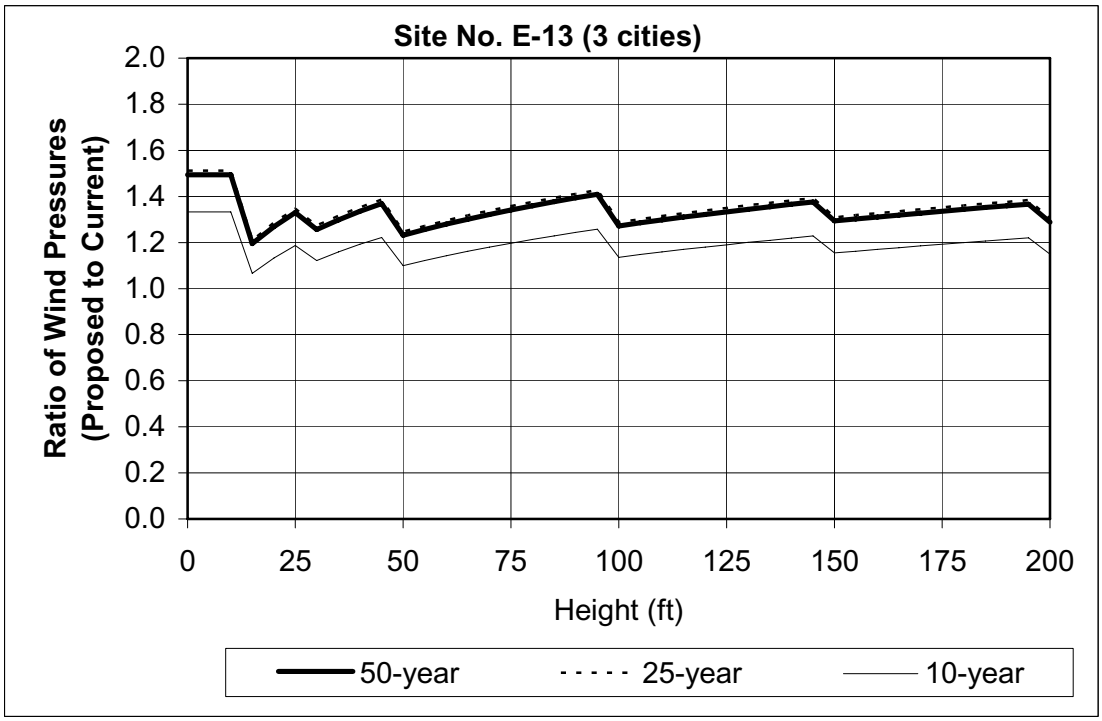

Figure B—54. Site No. E-13: Ratio of Wind Pressures (Proposed to Current Specification)

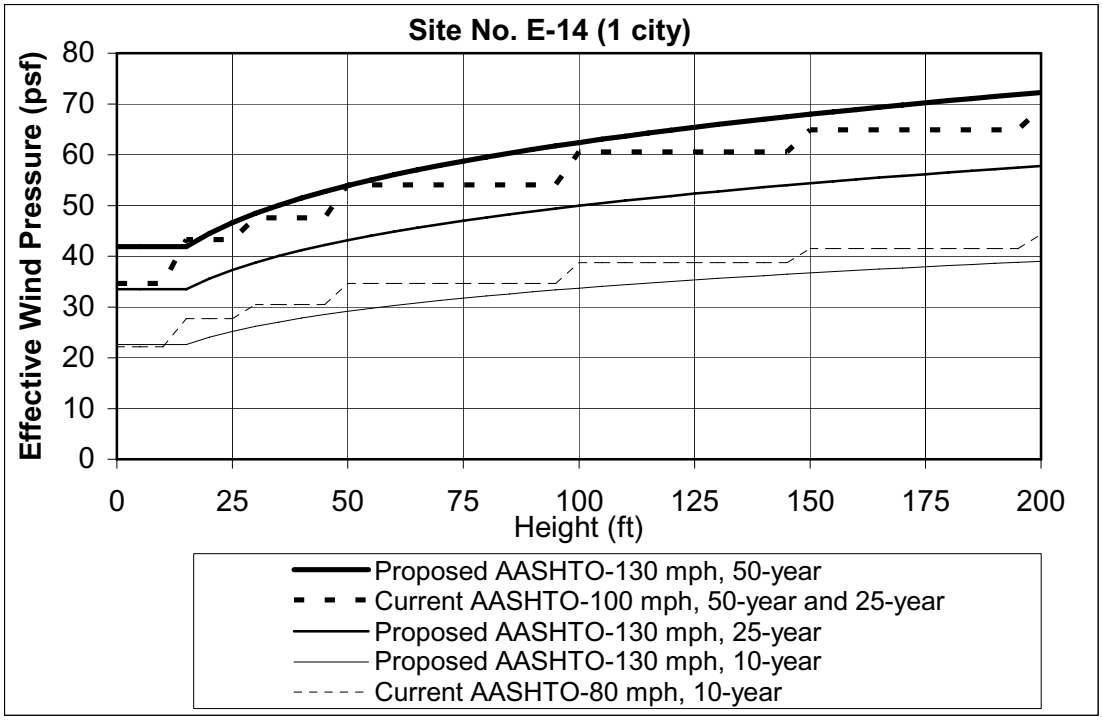

Figure B—55. Site No. E-14: Effective Wind Pressure

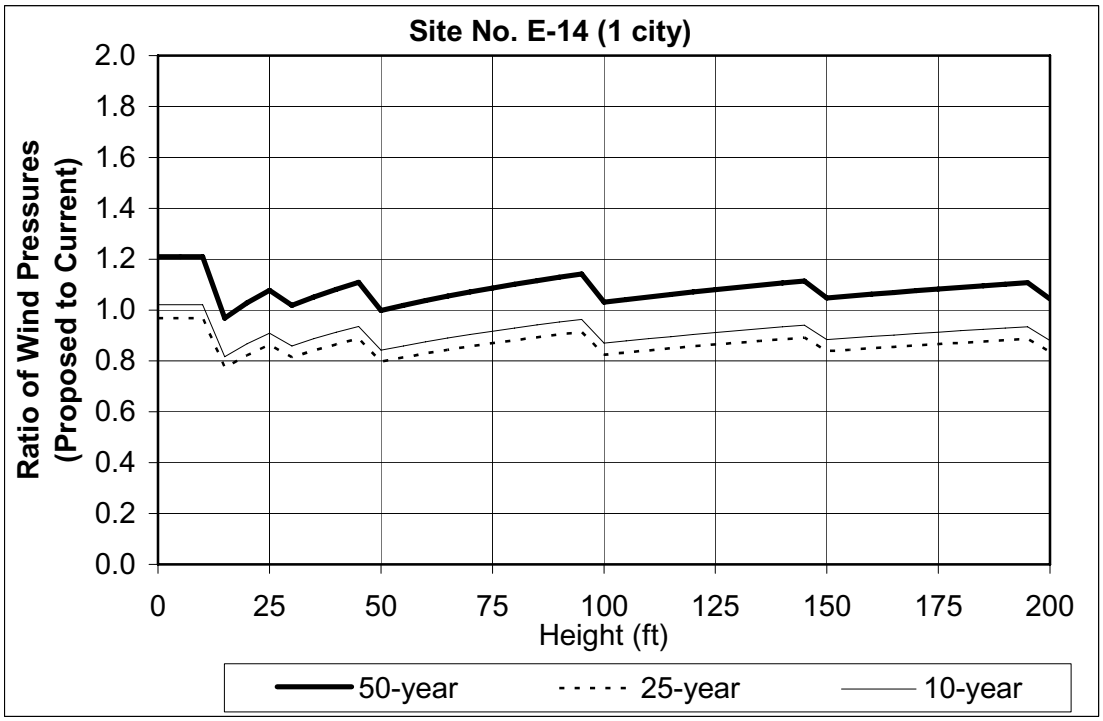

Figure B—56. Site No. E-14: Ratio of Wind Pressures (Proposed to Current Specification)

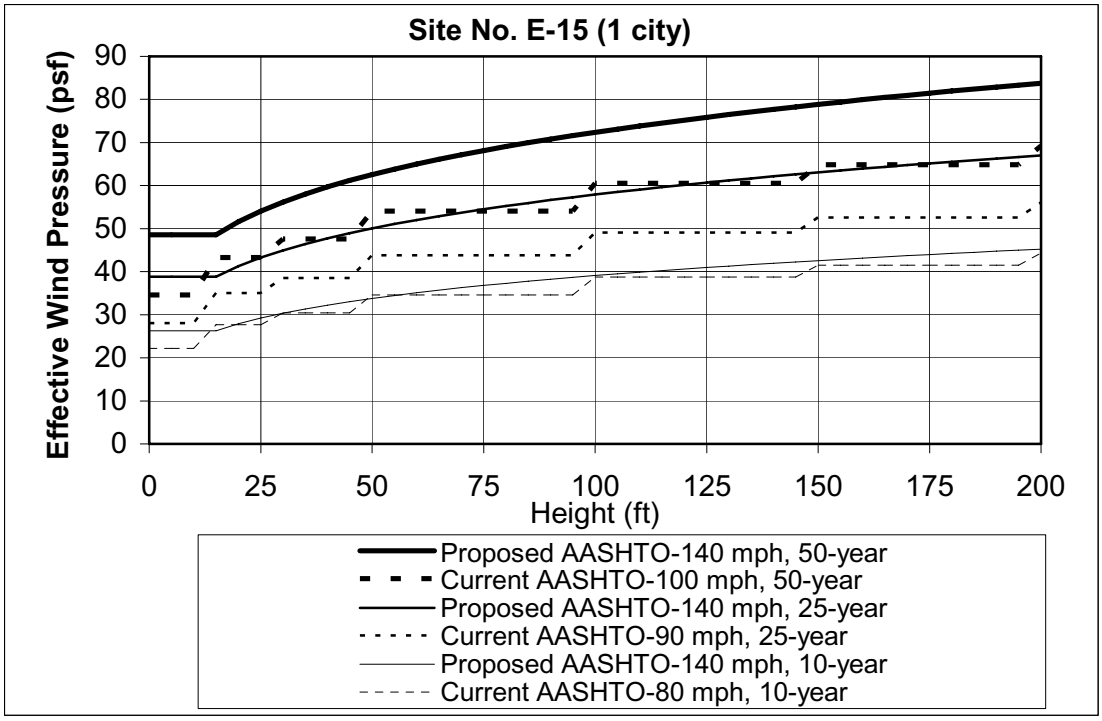

Figure B—57. Site No. E-15: Effective Wind Pressure

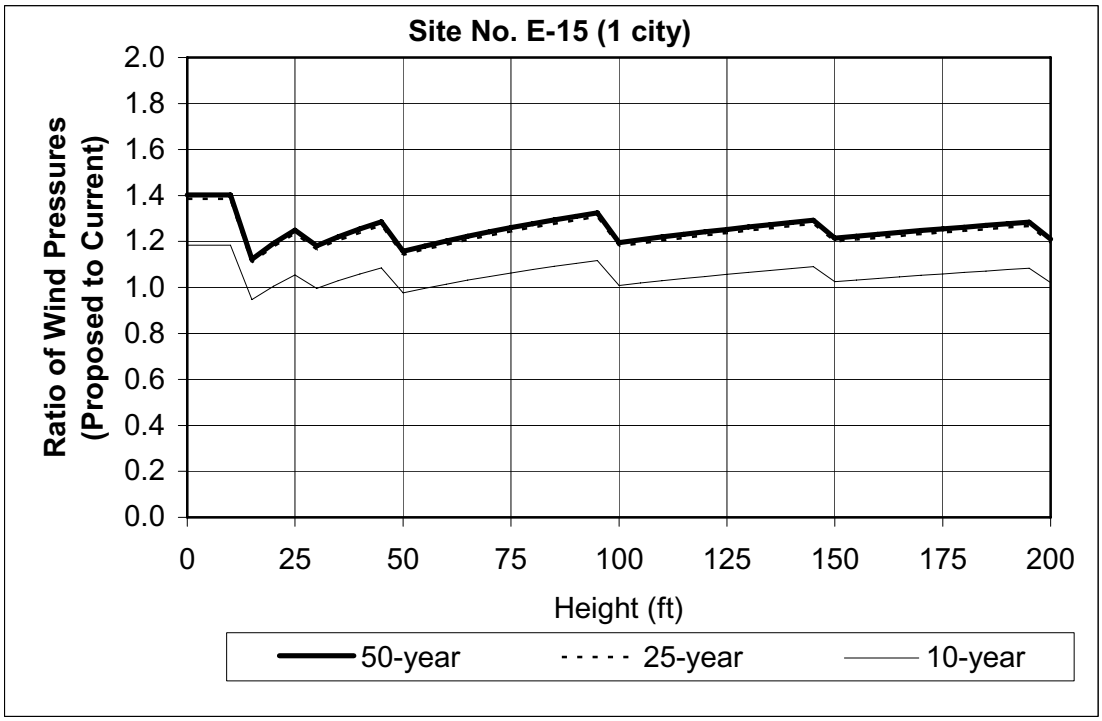

Figure B—58. Site No. E-15: Ratio of Wind Pressures (Proposed to Current Specification)

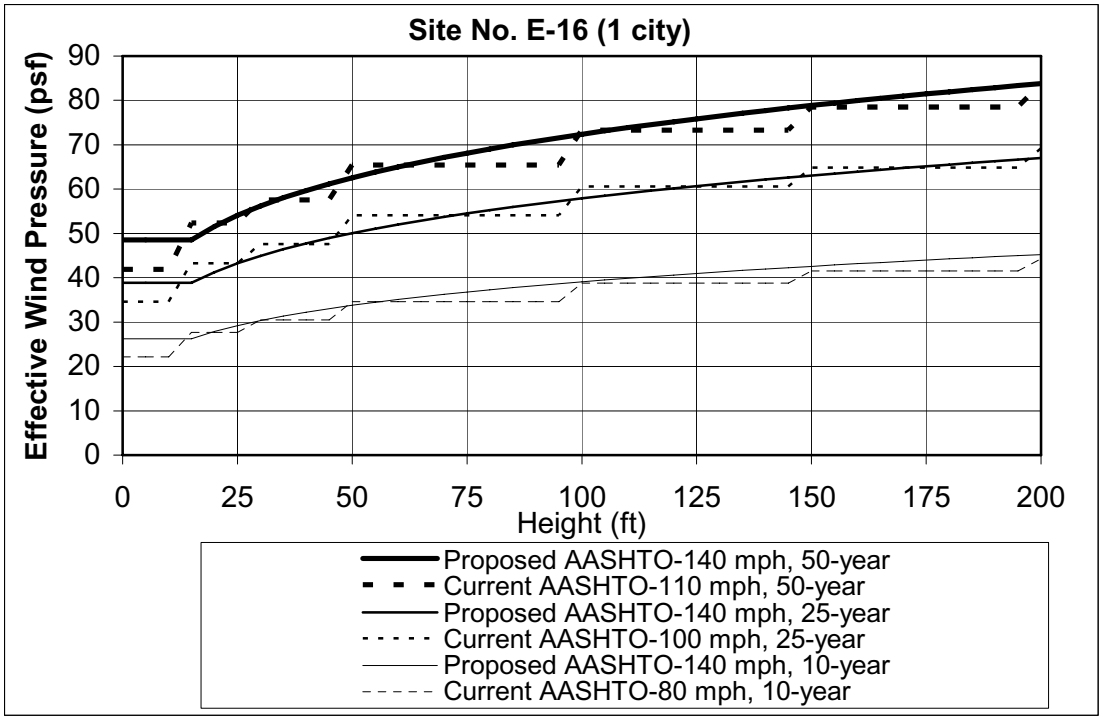

Figure B—59. Site No. E-16: Effective Wind Pressure

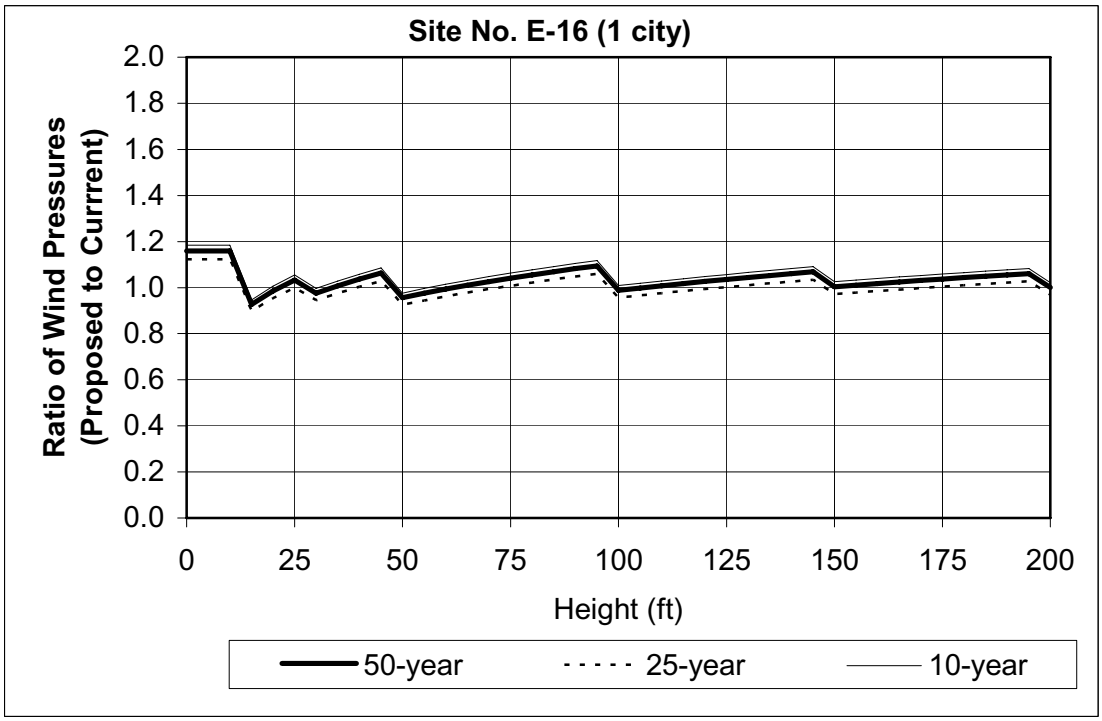

Figure B—60. Site No. E-16: Ratio of Wind Pressures (Proposed to Current Specification)

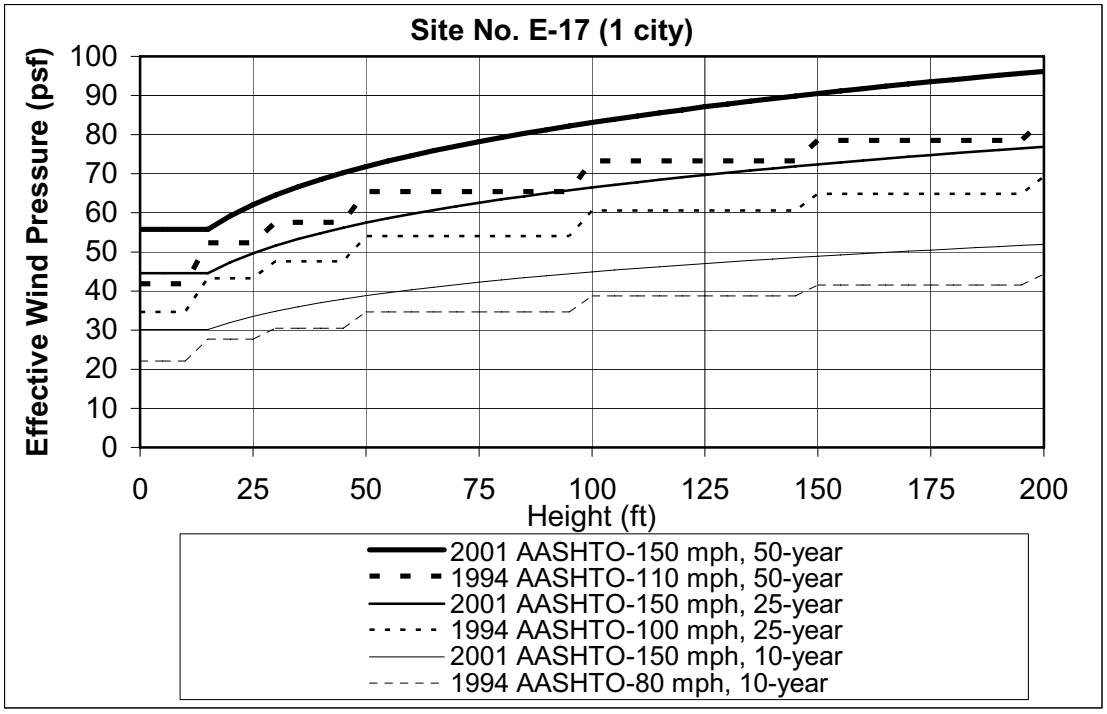

Figure B—61. Site No. E-17: Effective Wind Pressure

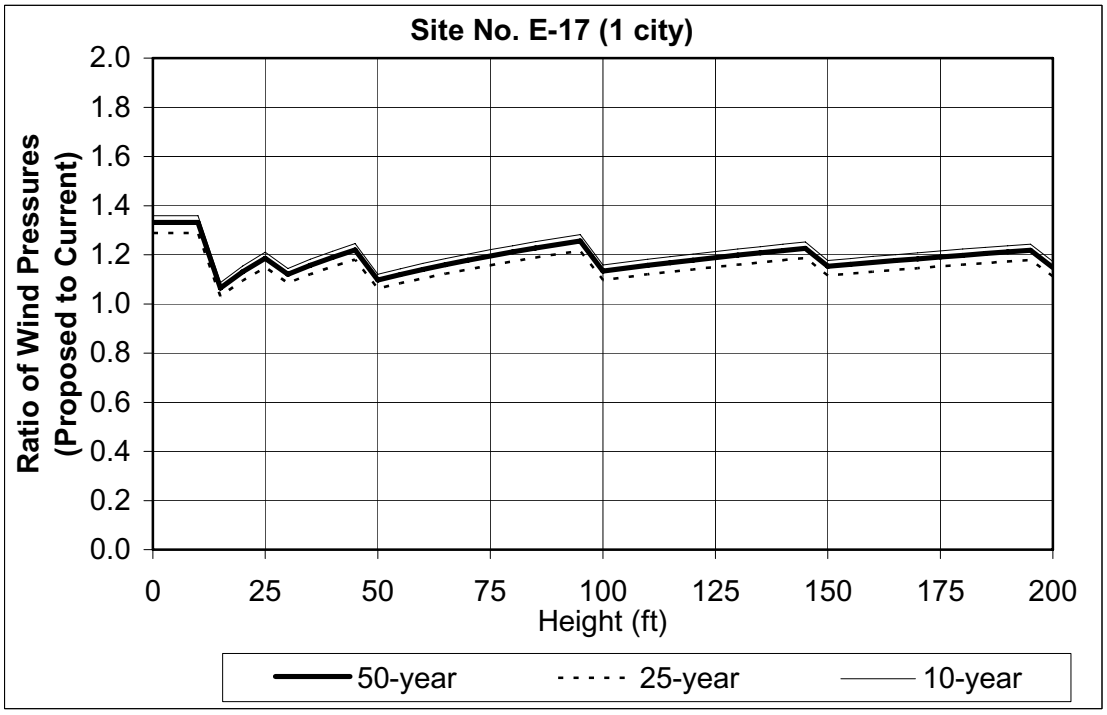

Figure B—62. Site No. E-17: Ratio of Wind Pressures (Proposed to Current Specification)

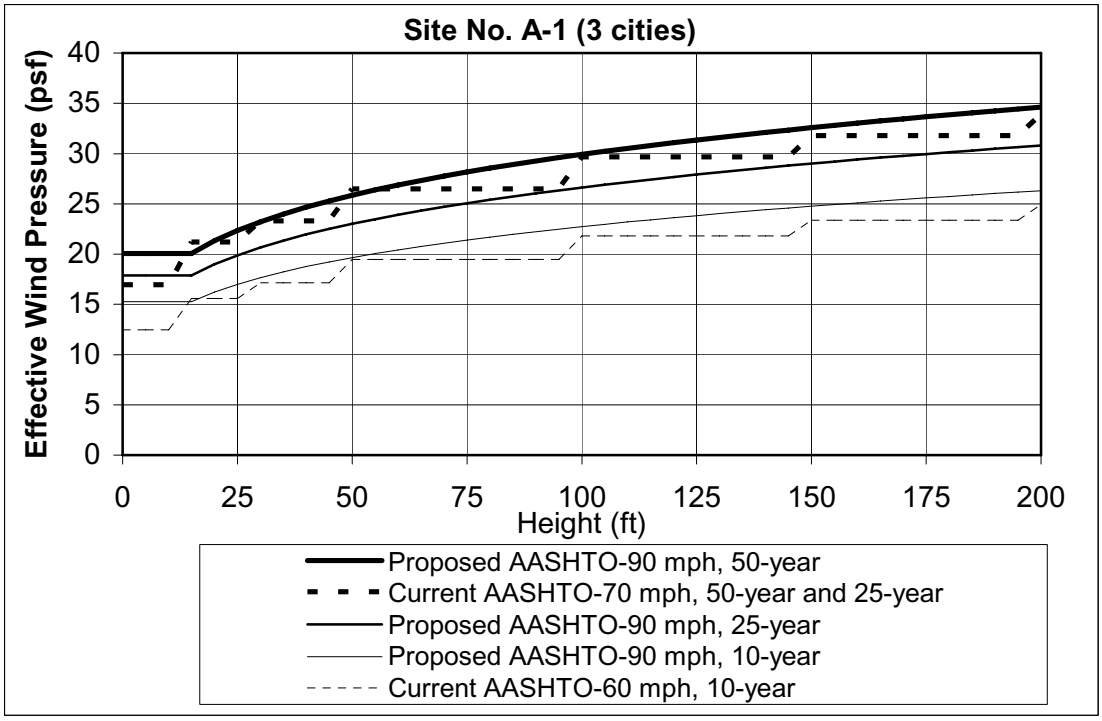

Figure B—63. Site No. A-1: Effective Wind Pressure

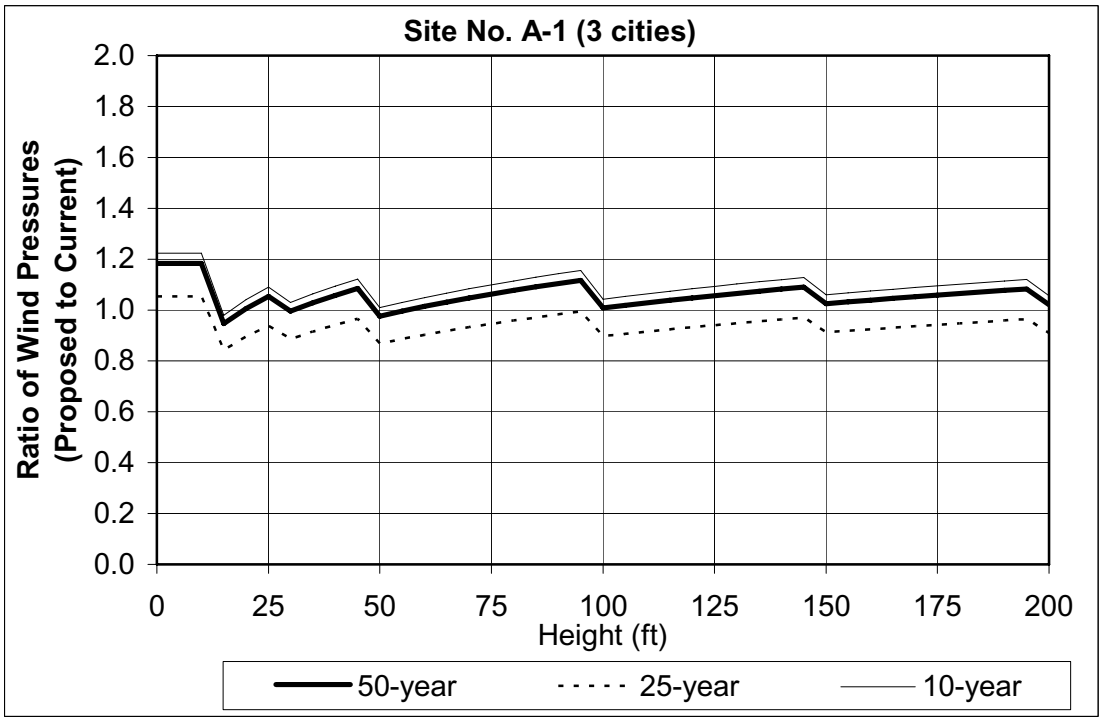

Figure B—64. Site No. A-1: Ratio of Wind Pressures (Proposed to Current Specification)

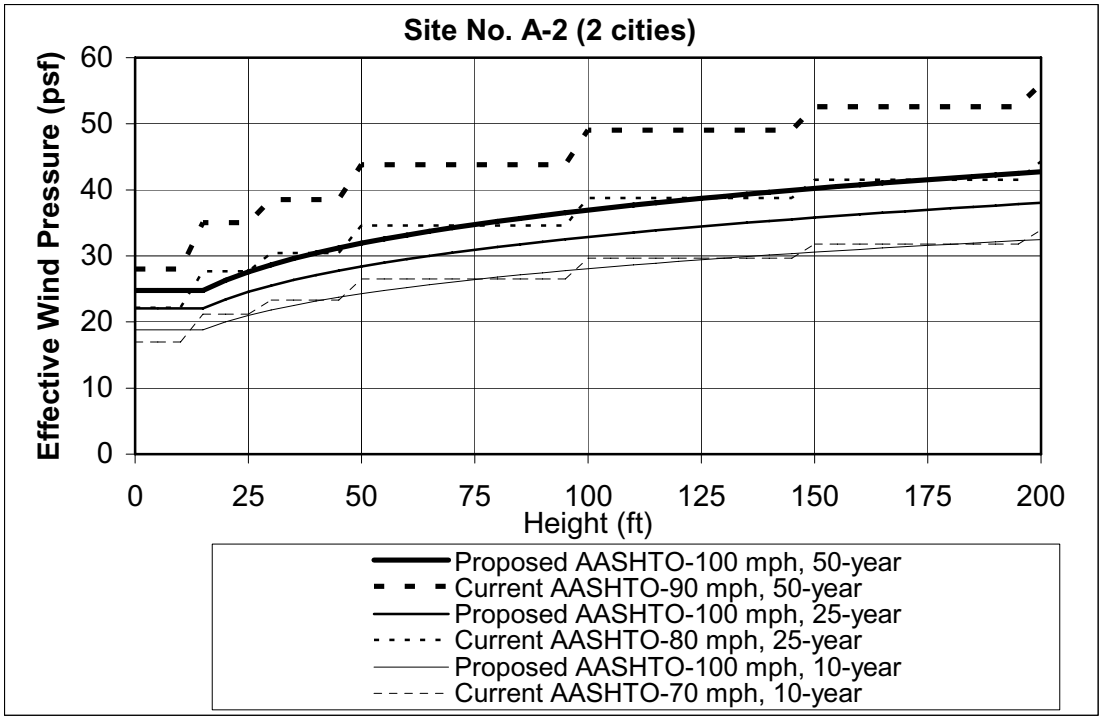

Figure B—65. Site No. A-2: Effective Wind Pressure

Figure B—66. Site No. A-2: Ratio of Wind Pressures (Proposed to Current Specification)

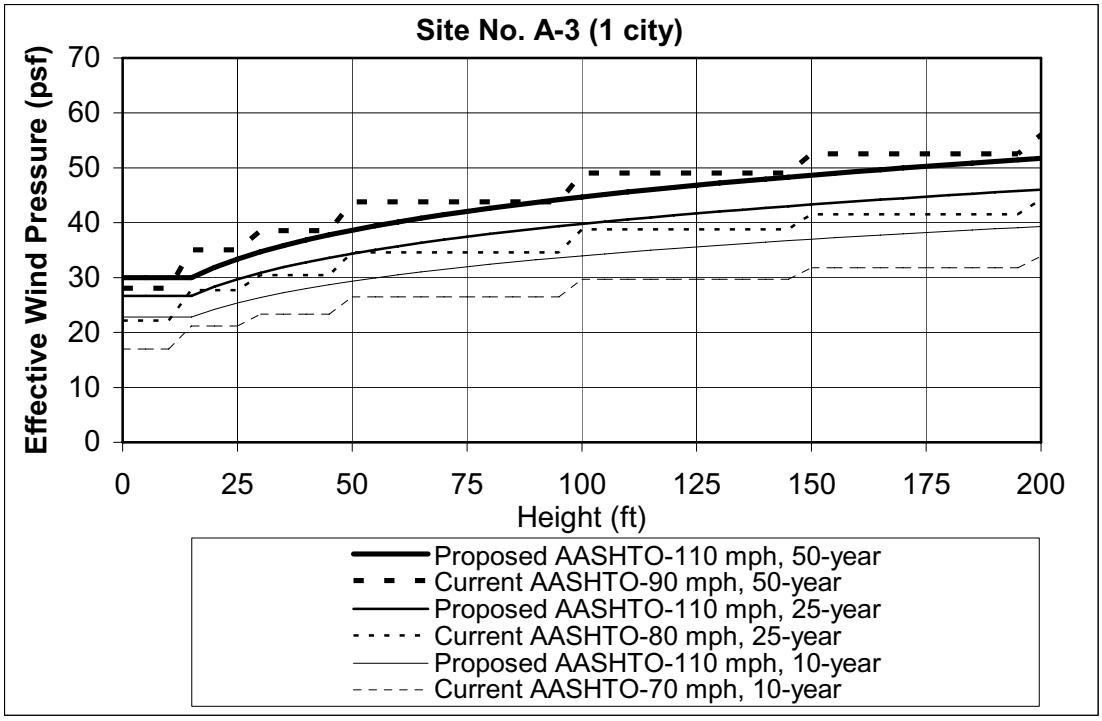

Figure B—67. Site No. A-3: Effective Wind Pressure

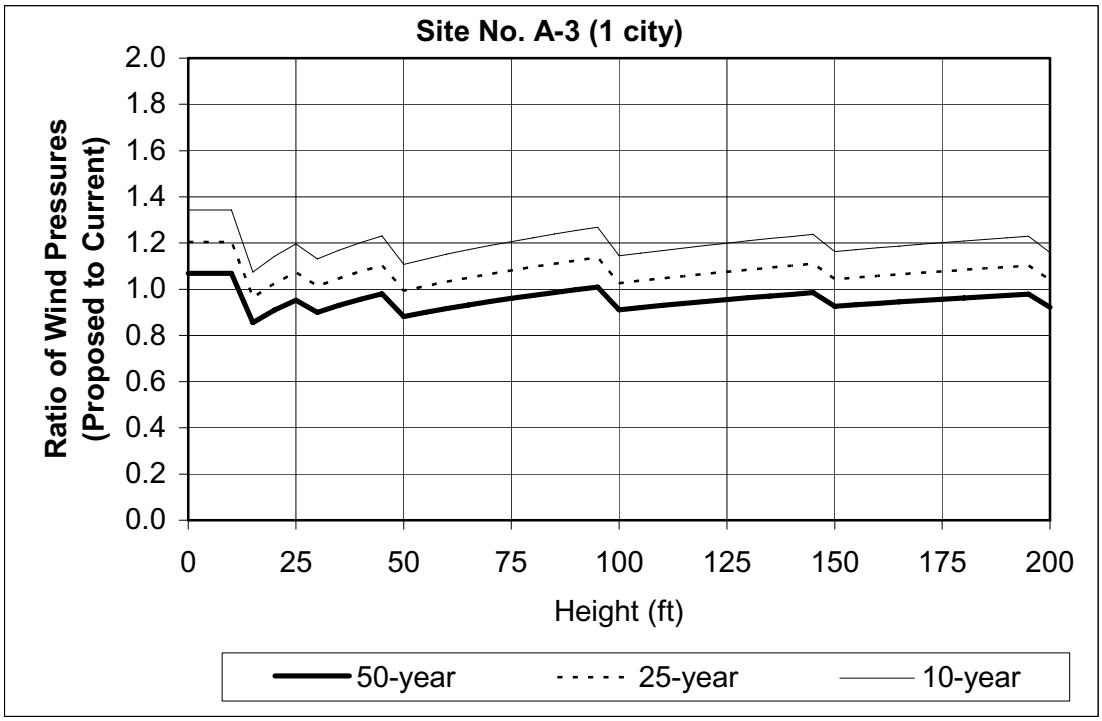

Figure B—68. Site No. A-3: Ratio of Wind Pressures (Proposed to Current Specification)

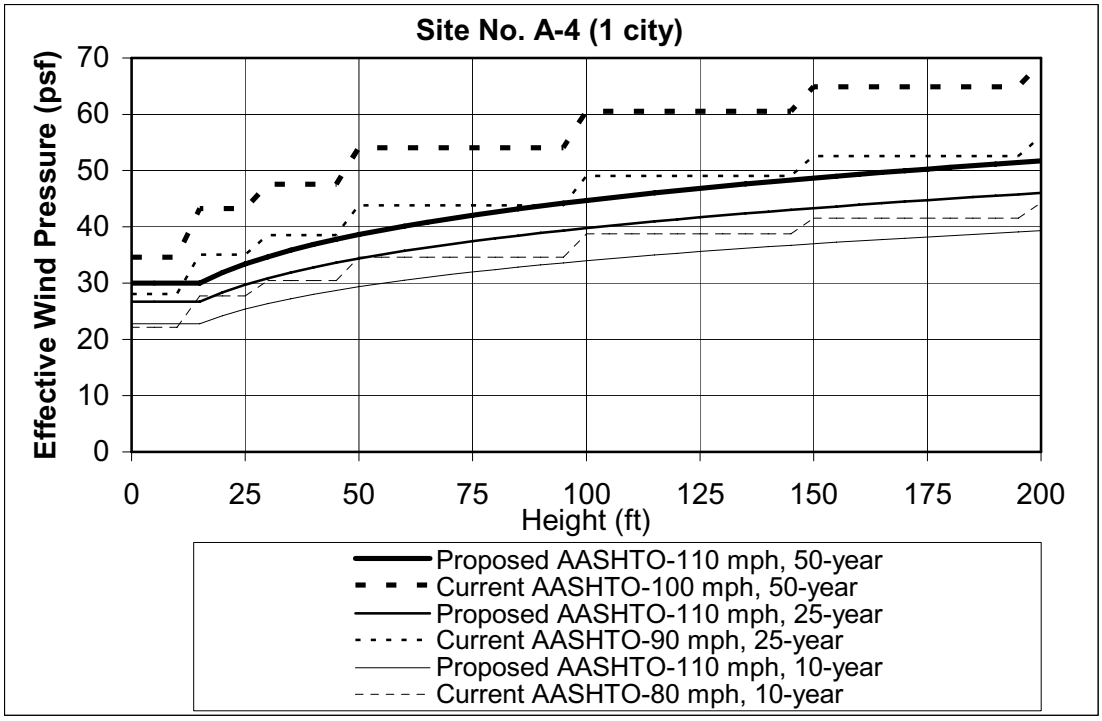

Figure B—69. Site No. A-4: Effective Wind Pressure

Figure B—70. Site No. A-4: Ratio of Wind Pressures (Proposed to Current Specification)

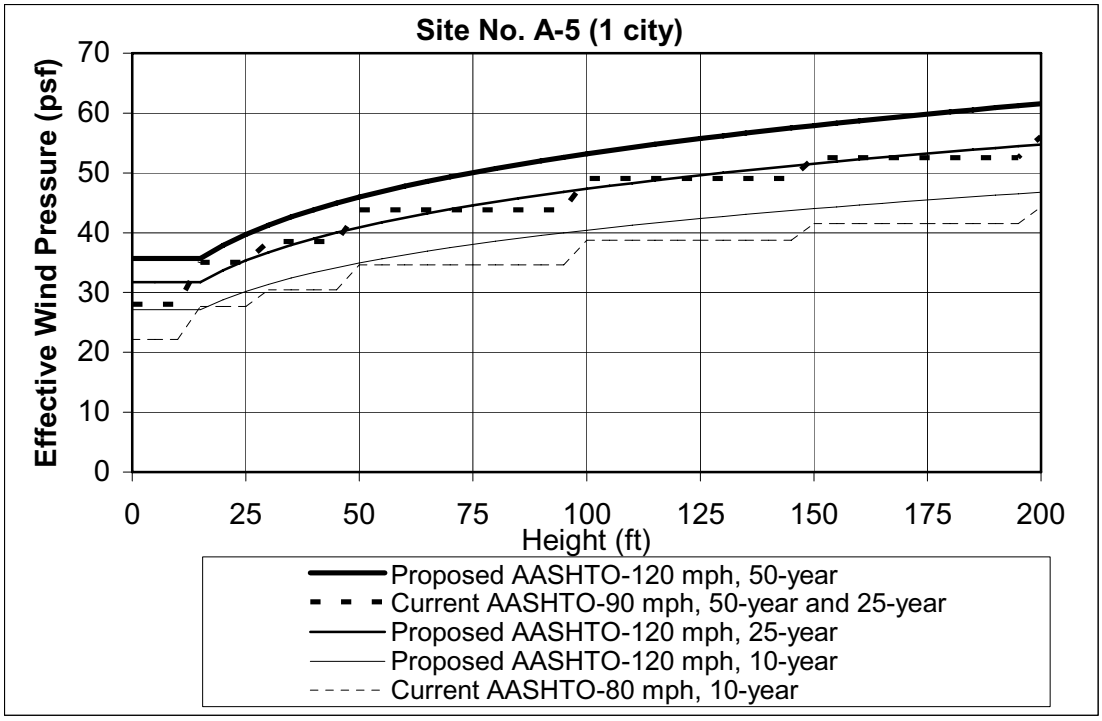

Figure B—71. Site No. A-5: Effective Wind Pressure

Figure B—72. Site No. A-5: Ratio of Wind Pressures (Proposed to Current Specification)

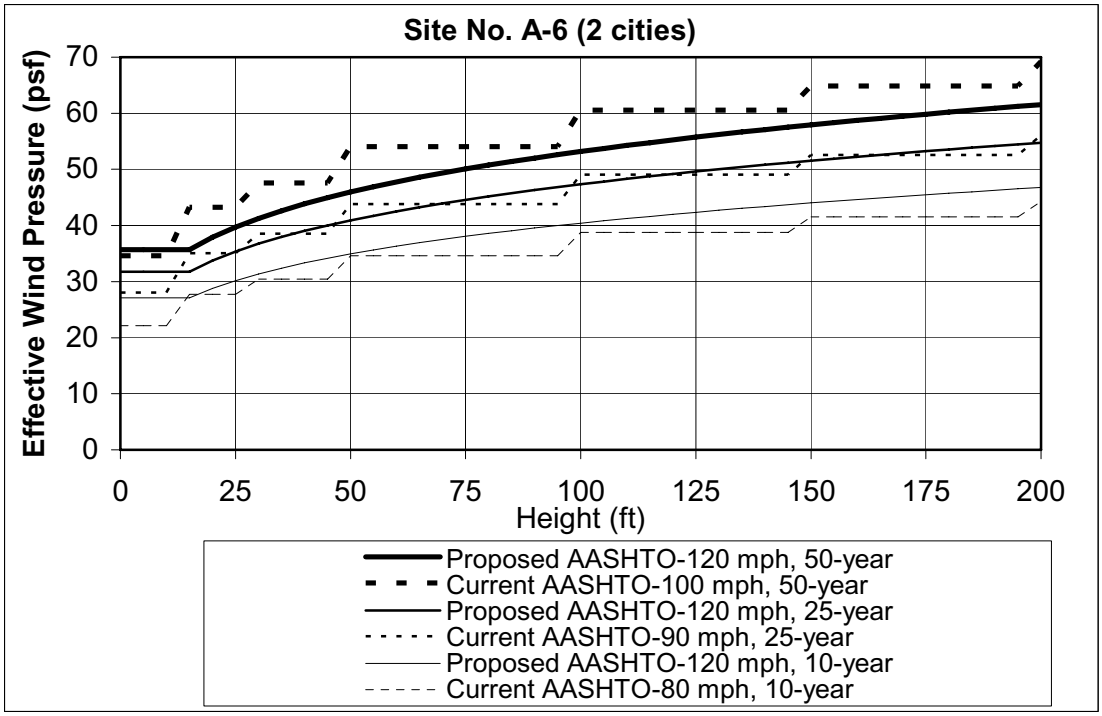

Figure B—73. Site No. A-6: Effective Wind Pressure

Figure B—74. Site No. A-6: Ratio of Wind Pressures (Proposed to Current Specification)

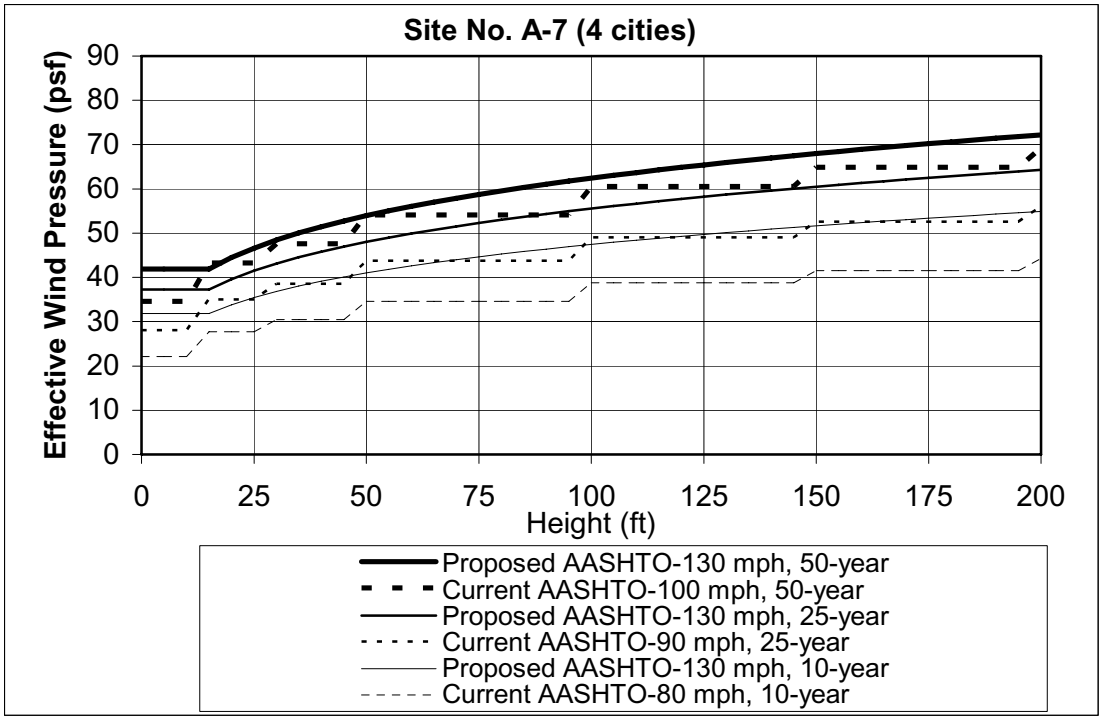

Figure B—75. Site No. A-7: Effective Wind Pressure

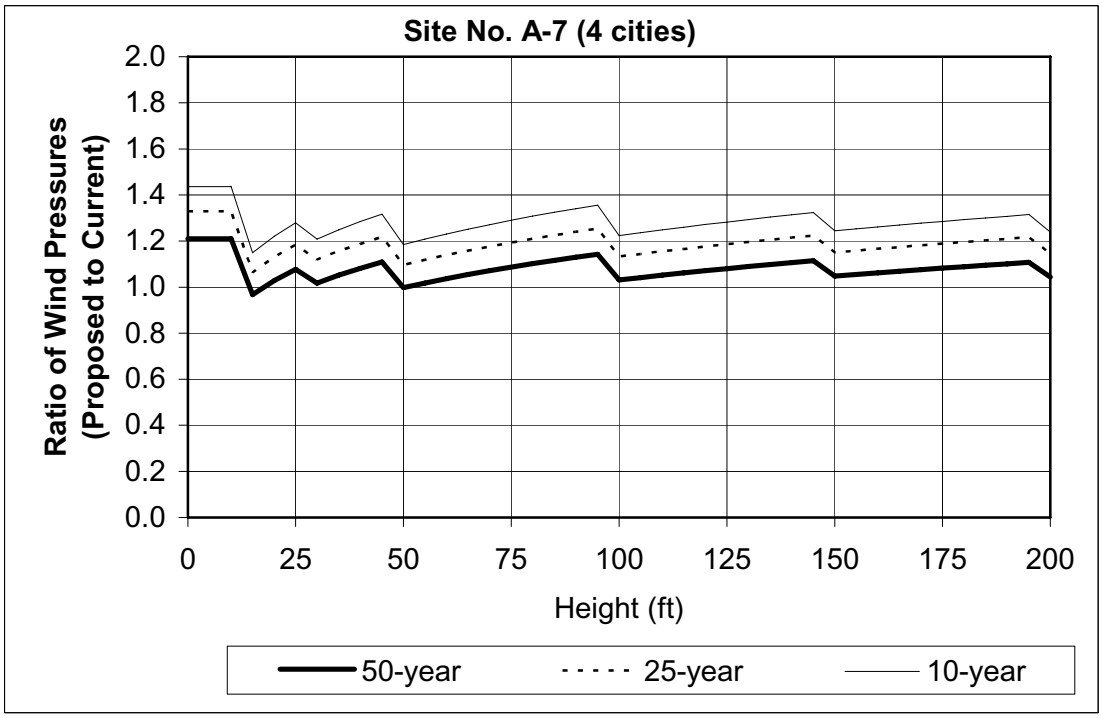

Figure B—76. Site No. A-7: Ratio of Wind Pressures (Proposed to Current Specification)

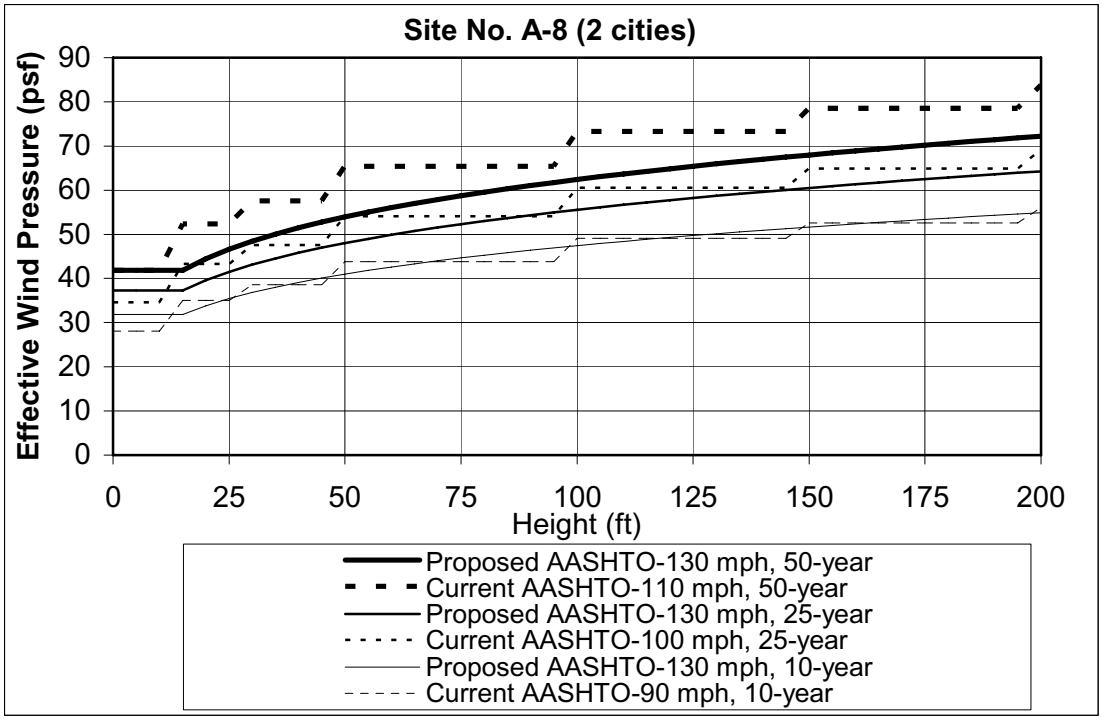

Figure B—77. Site No. A-8: Effective Wind Pressure

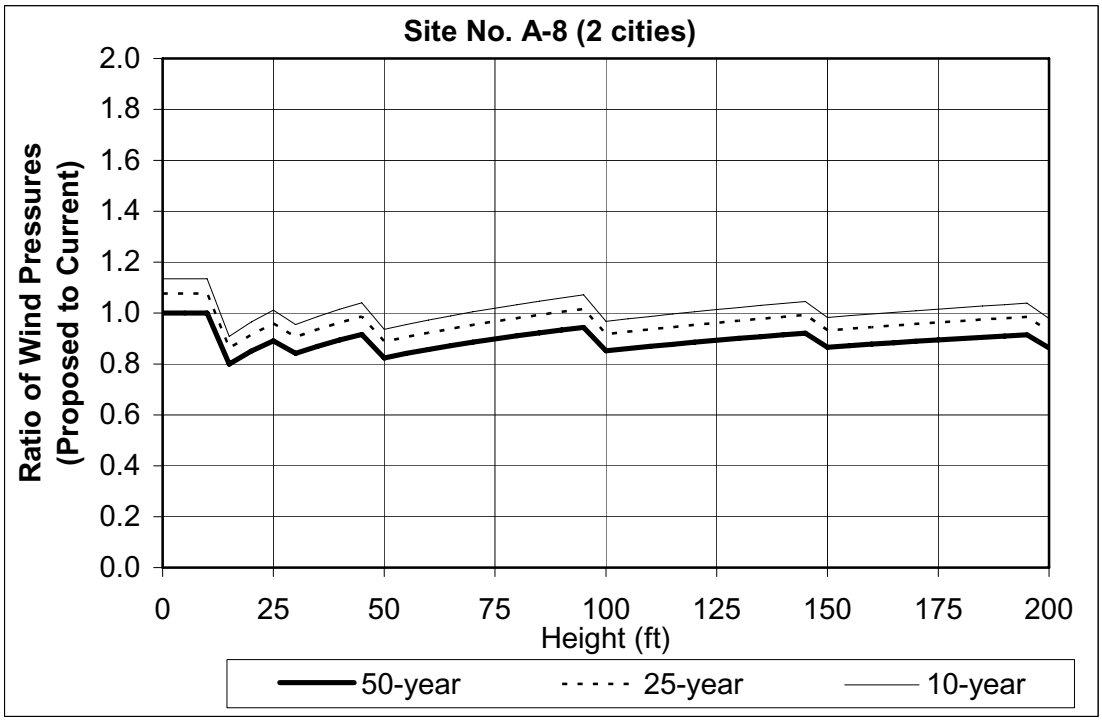

Figure B—78. Site No. A-8: Ratio of Wind Pressures (Proposed to Current Specification)

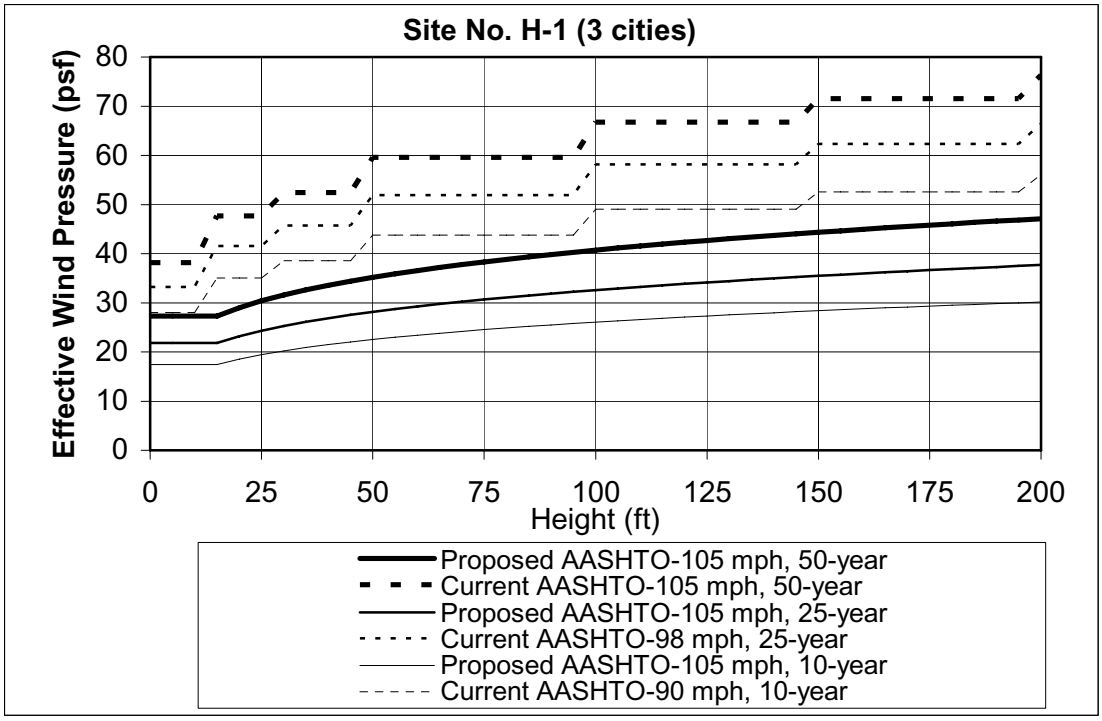

Figure B—79. Site No. H-1: Effective Wind Pressure

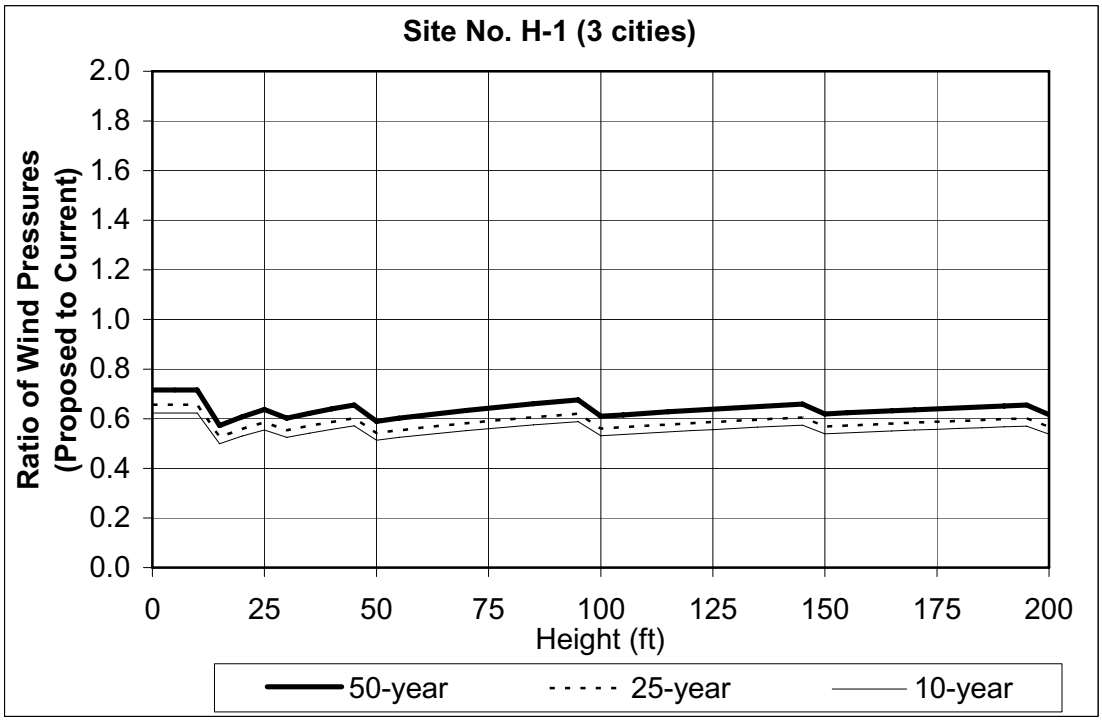

Figure B—80. Site No. H-1: Ratio of Wind Pressures (Proposed to Current Specification)

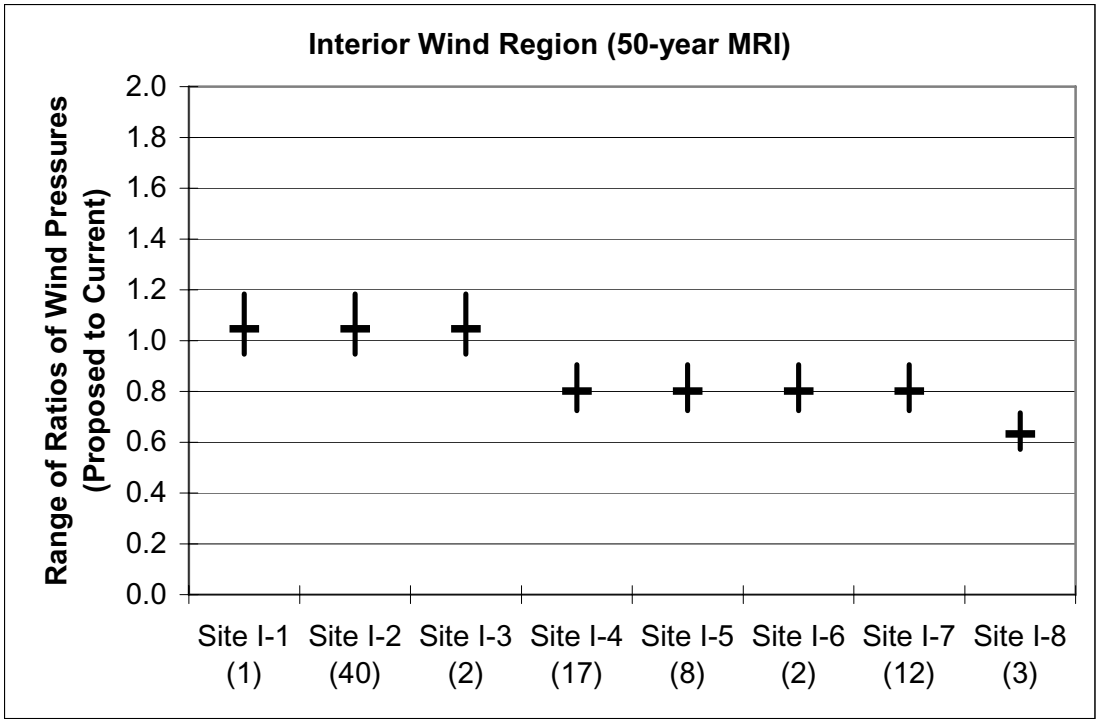

Figure B—81. Interior Wind Region (50-year MRI): Range of Ratios of Wind Pressures (Proposed to Current Specification)

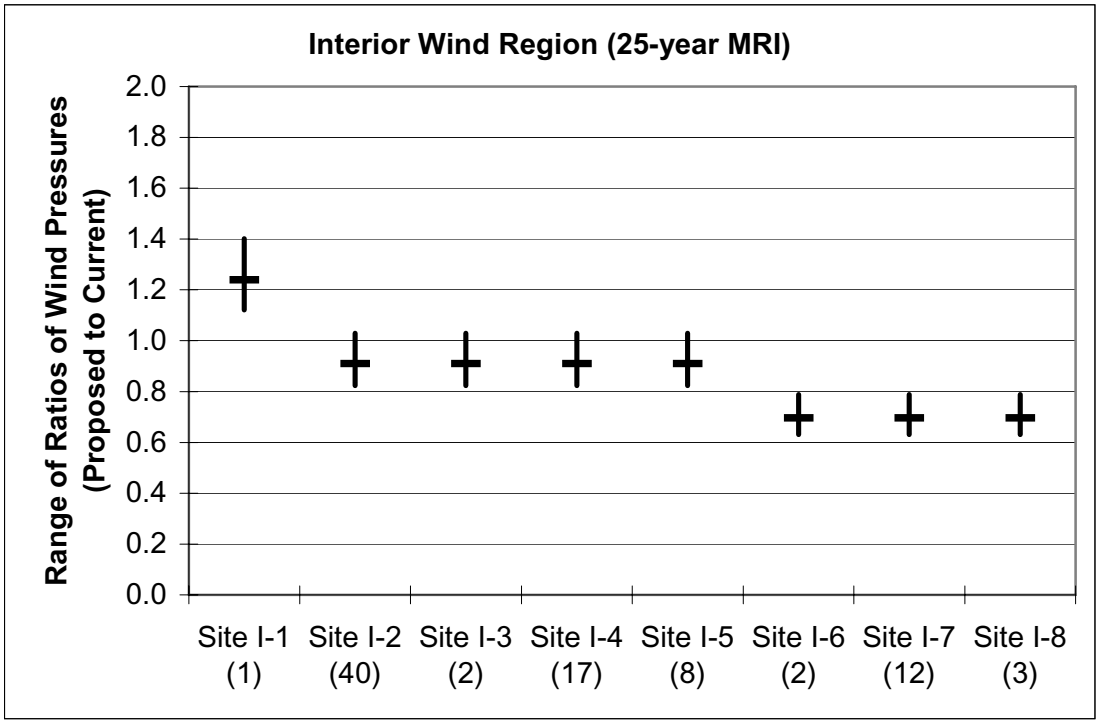

Figure B—82. Interior Wind Region (25-year MRI): Range of Ratios of Wind Pressures (Proposed to Current Specification)

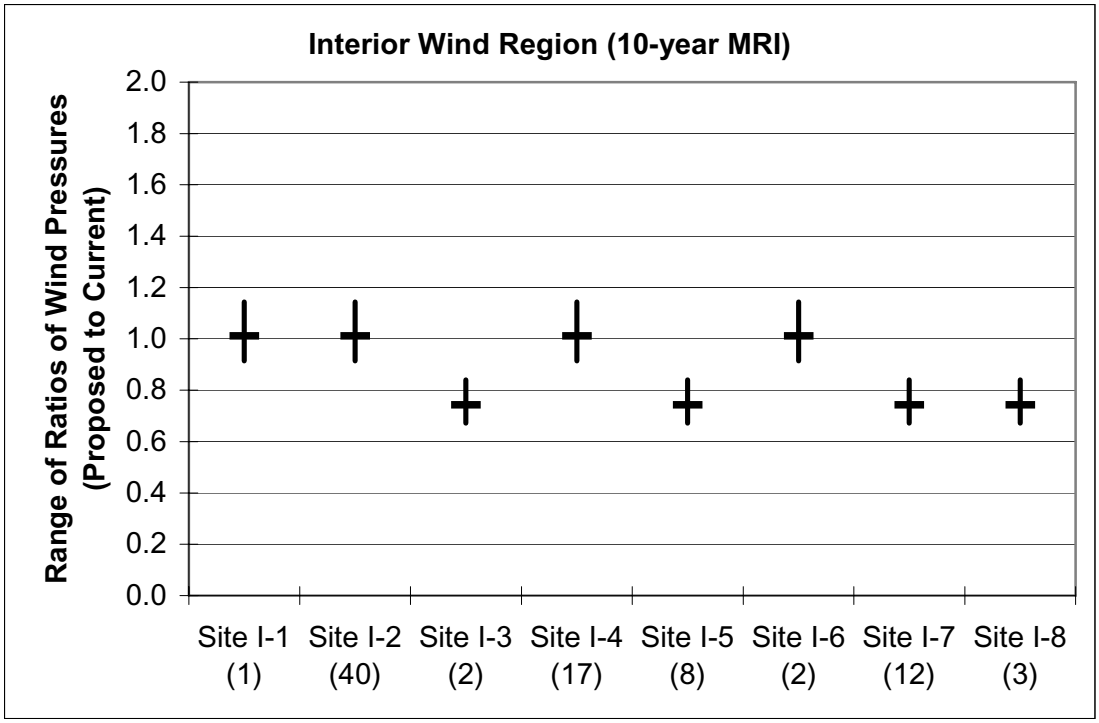

Figure B—83. Interior Wind Region (10-year MRI): Range of Ratios of Wind Pressures (Proposed to Current Specification)

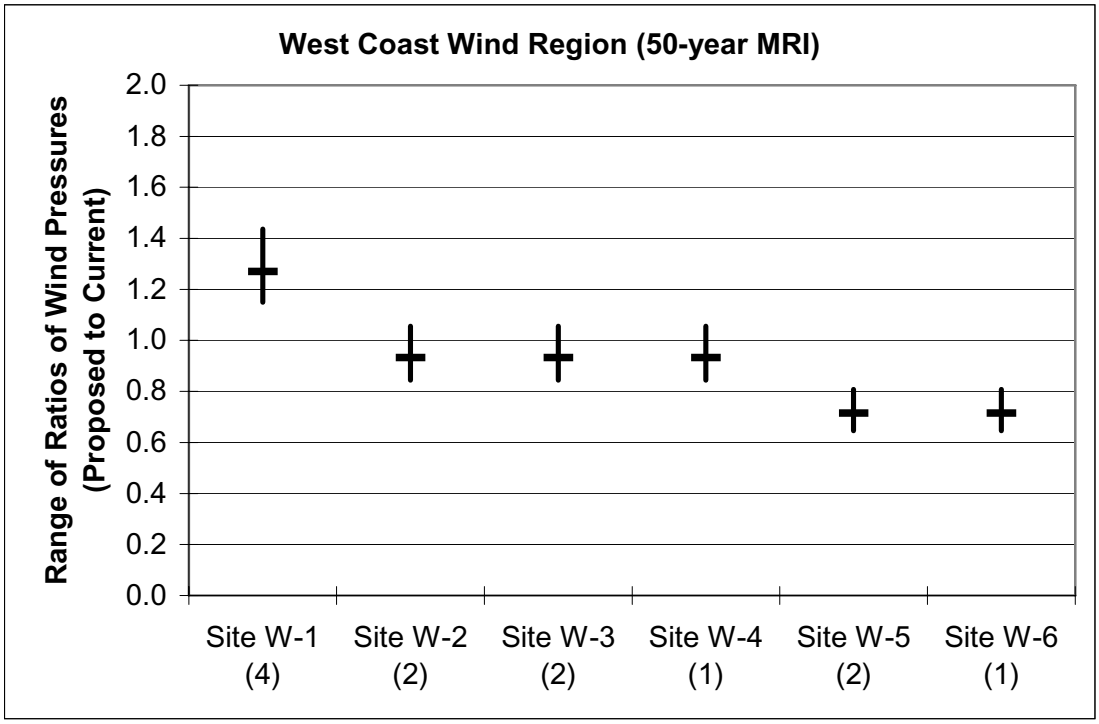

Figure B—84. West Coast Wind Region (50-year MRI): Range of Ratios of Wind Pressures (Proposed to Current Specification)

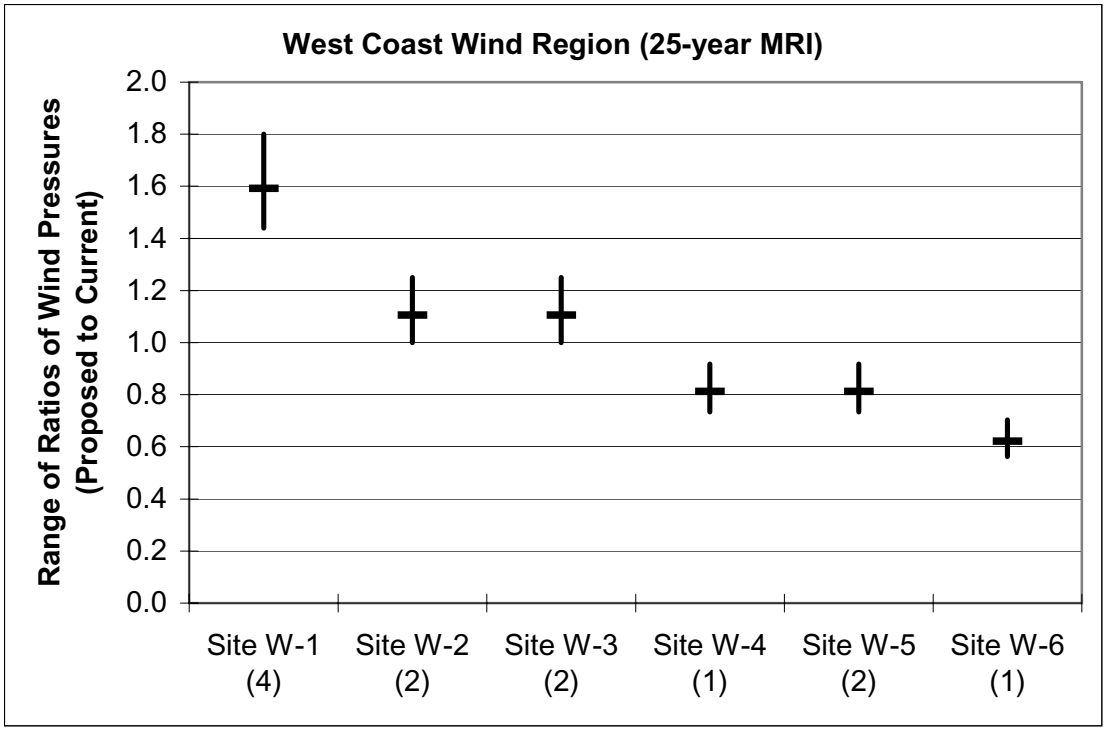

Figure B—85. West Coast Wind Region (25-year MRI): Range of Ratios of Wind Pressures (Proposed to Current Specification)

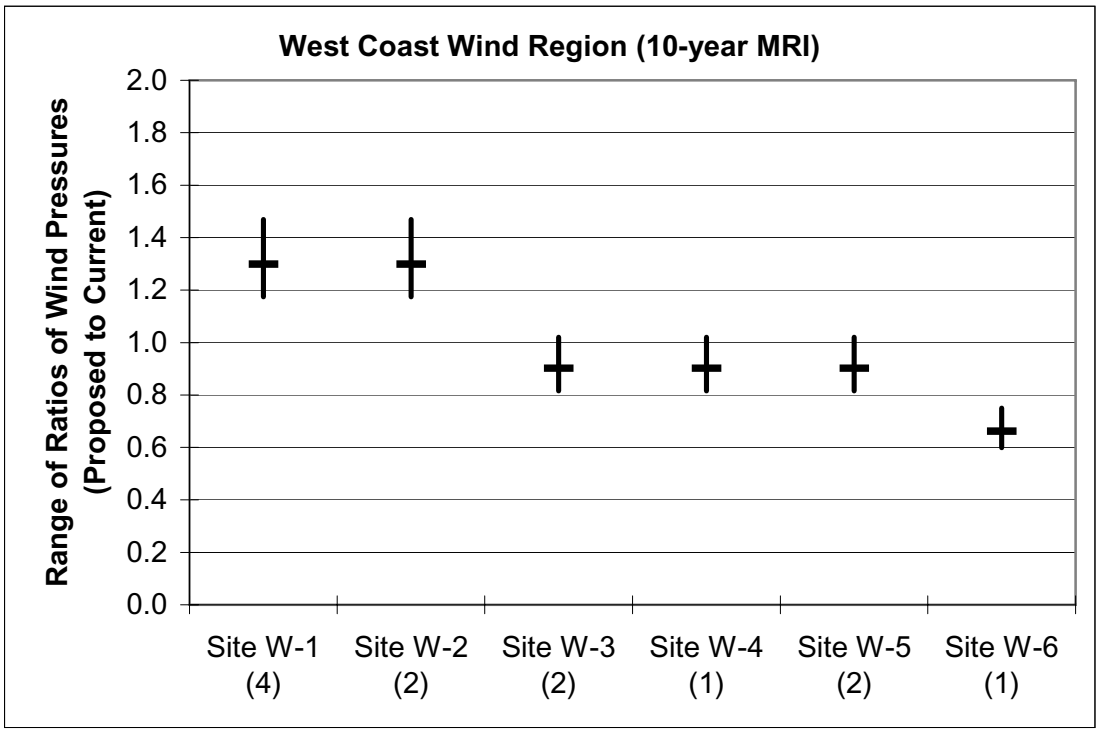

Figure B—86. West Coast Wind Region (10-year MRI): Range of Ratios of Wind Pressures (Proposed to Current Specification)

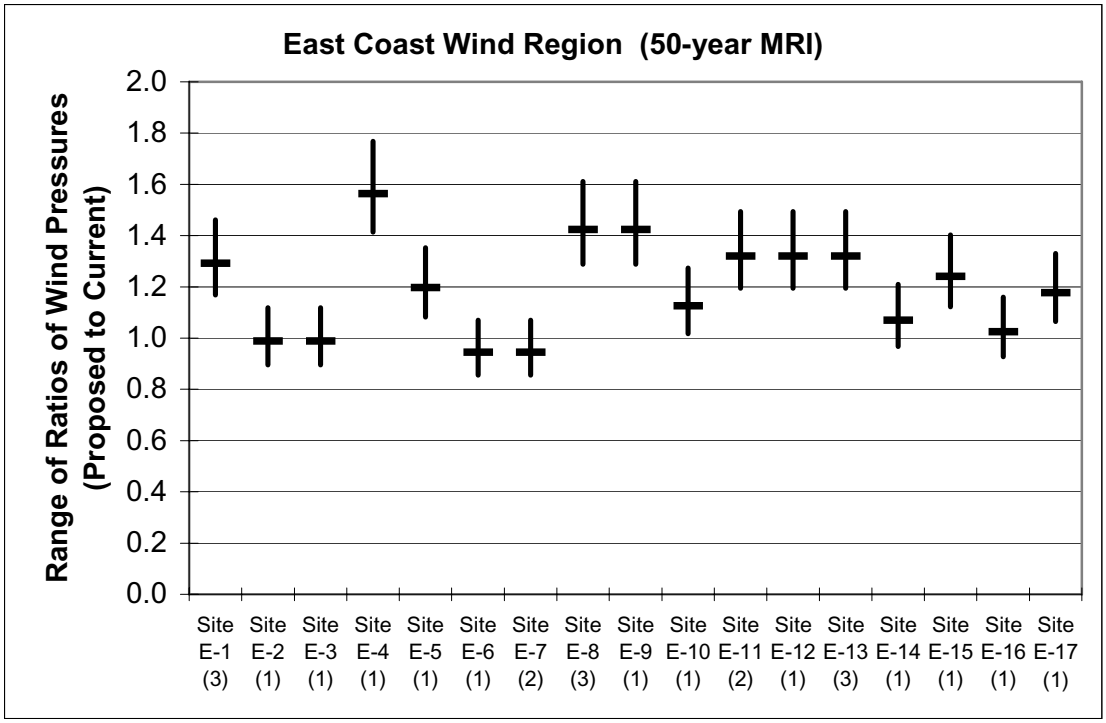

Figure B—87. East Coast Wind Region (50-year MRI): Range of Ratios of Wind Pressures (Proposed to Current Specification)

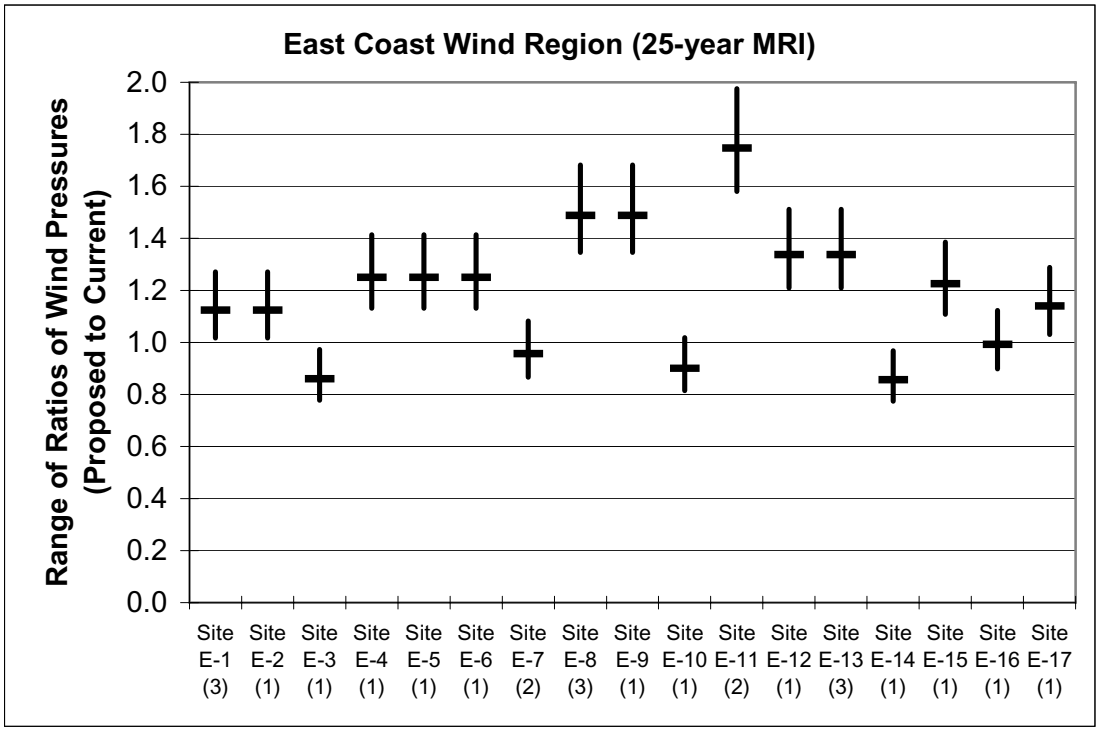

Figure B—88. East Coast Wind Region (25-year MRI): Range of Ratios of Wind Pressures (Proposed to Current Specification)

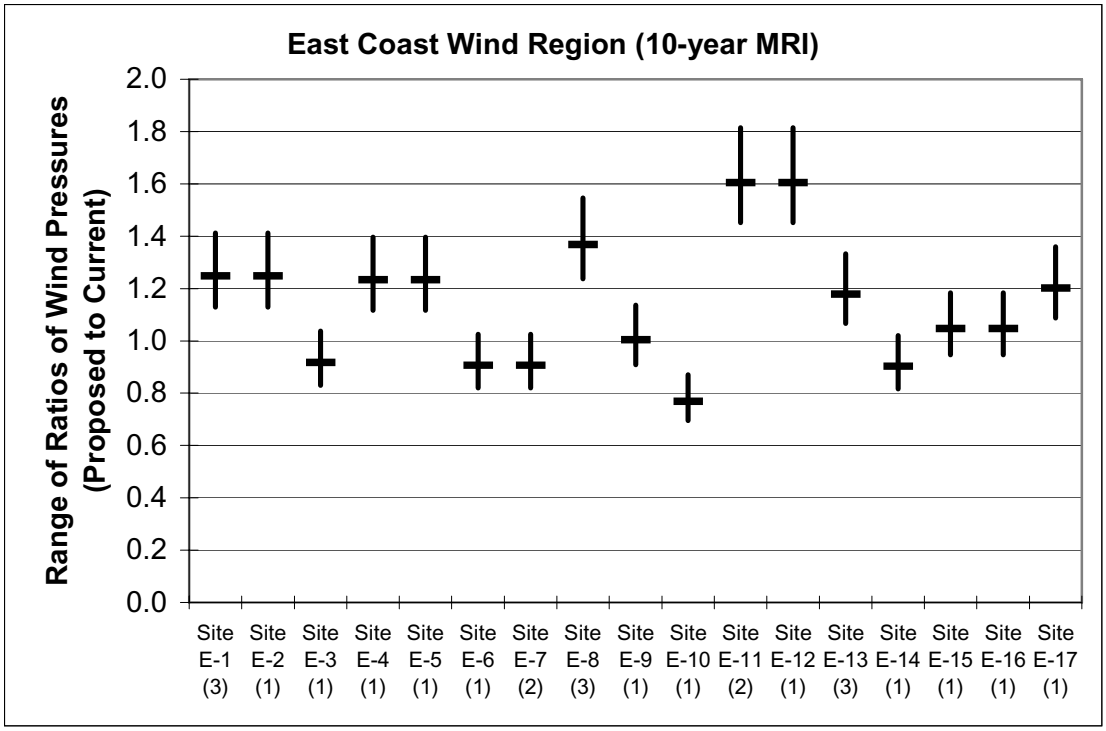

Figure B—89. East Coast Wind Region (10-year MRI): Range of Ratios of Wind Pressures (Proposed to Current Specification)

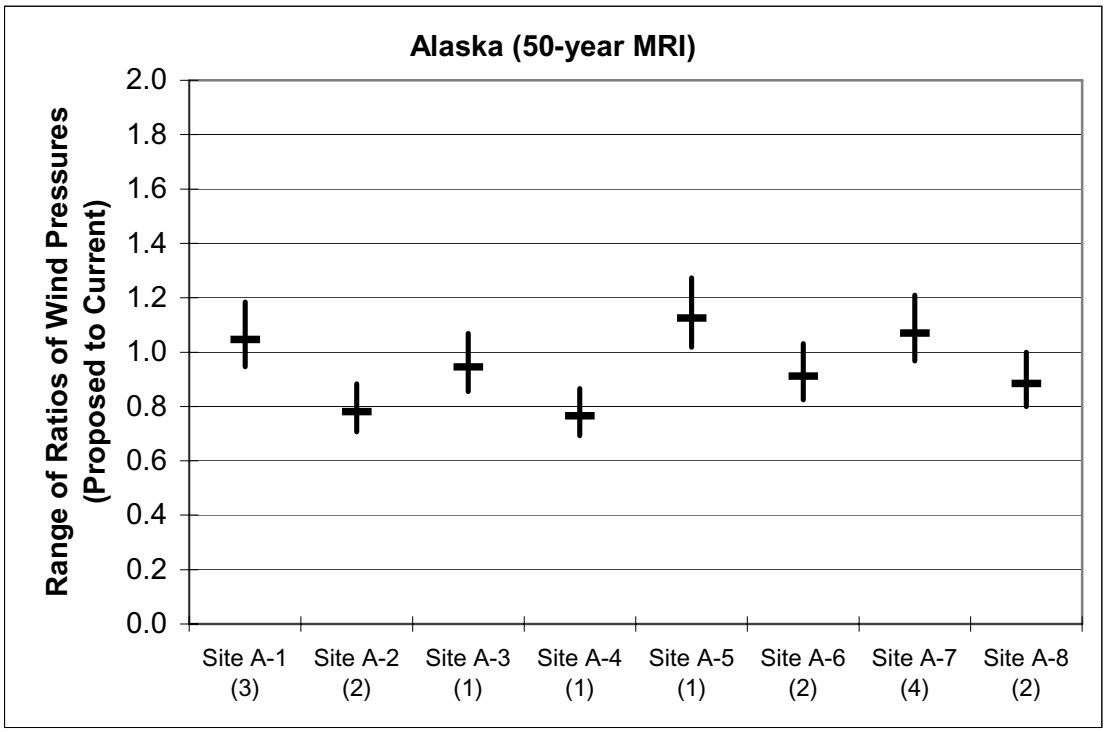

Figure B—90. Alaska (50-year MRI): Range of Ratios of Wind Pressures (Proposed to Current Specification)

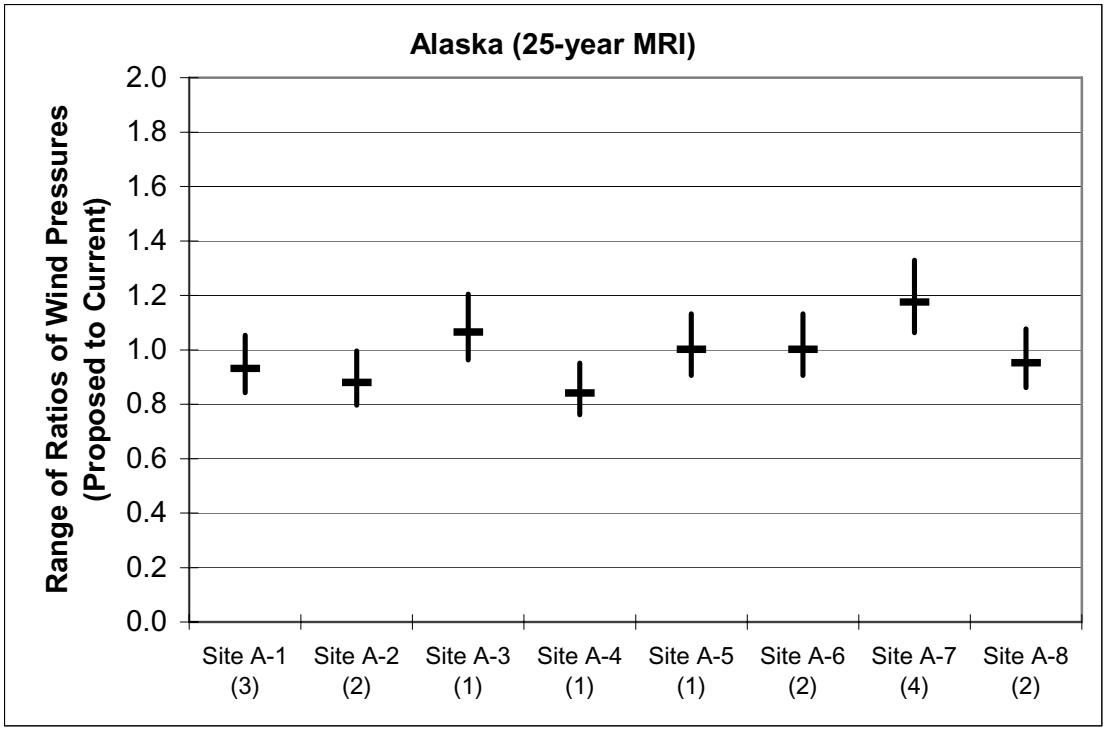

Figure B—91. Alaska (25-year MRI): Range of Ratios of Wind Pressures (Proposed to Current Specification)

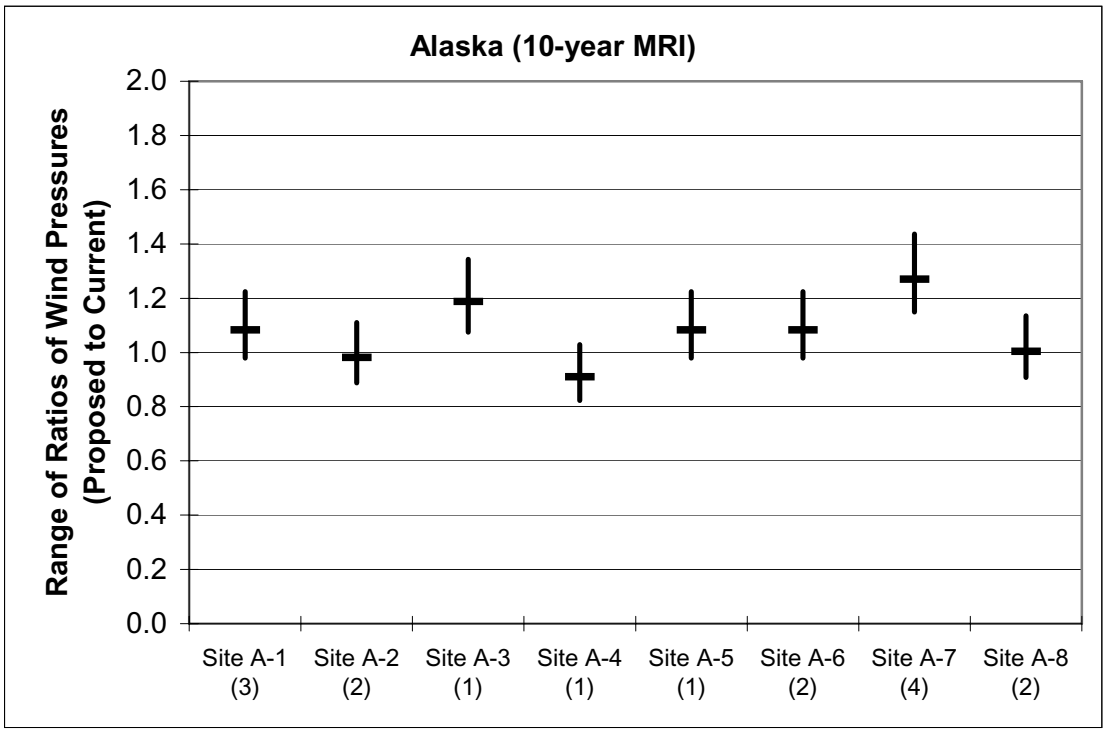

Figure B—92. Alaska (10-year MRI): Range of Ratios of Wind Pressures (Proposed to Current Specification)

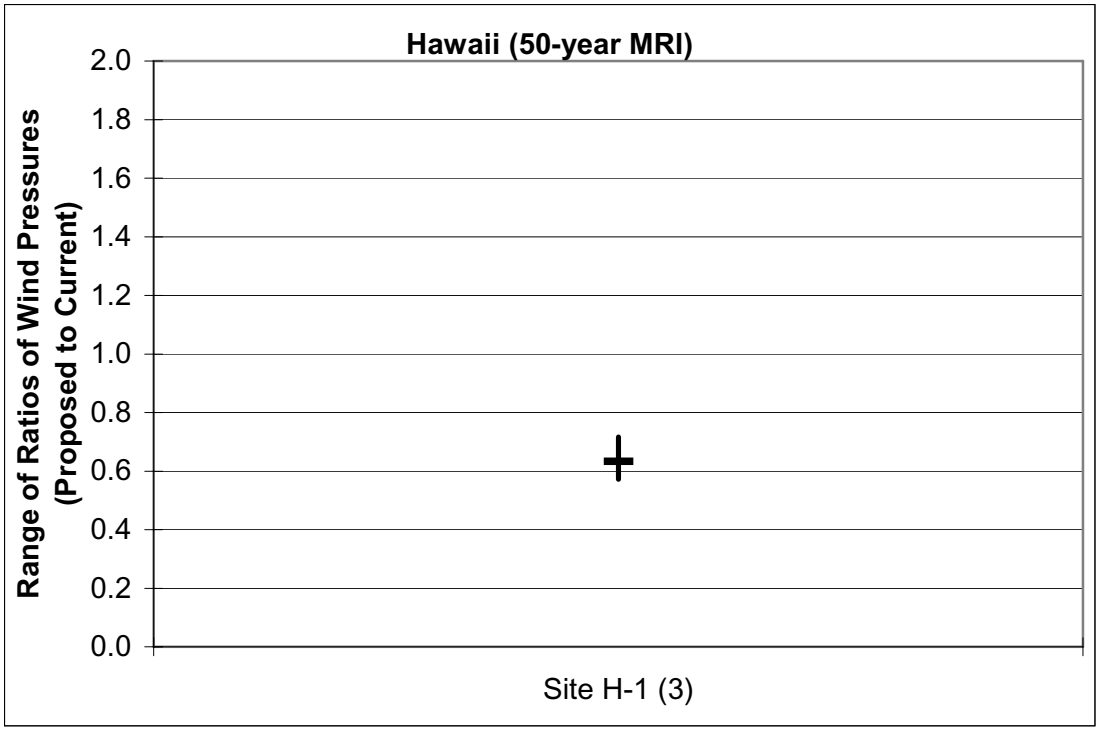

Figure B—93. Hawaii (50-year MRI): Range of Ratios of Wind Pressures (Proposed to Current Specification)

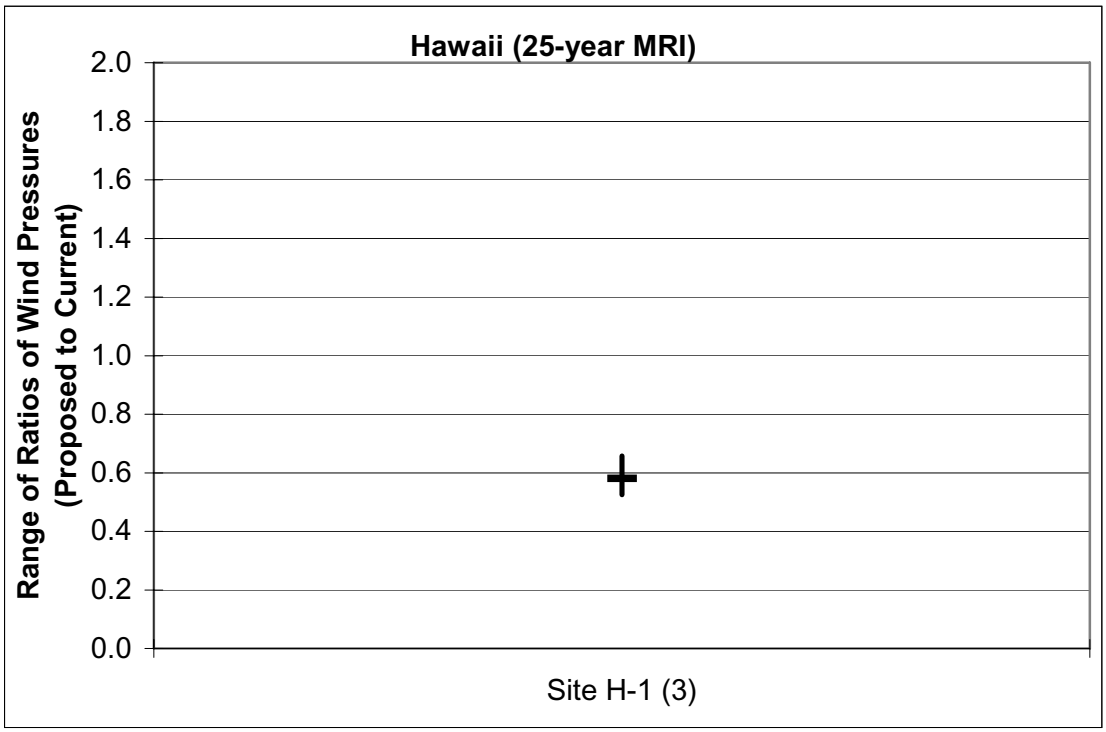

Figure B—94. Hawaii (25-year MRI): Range of Ratios of Wind Pressures (Proposed to Current Specification)

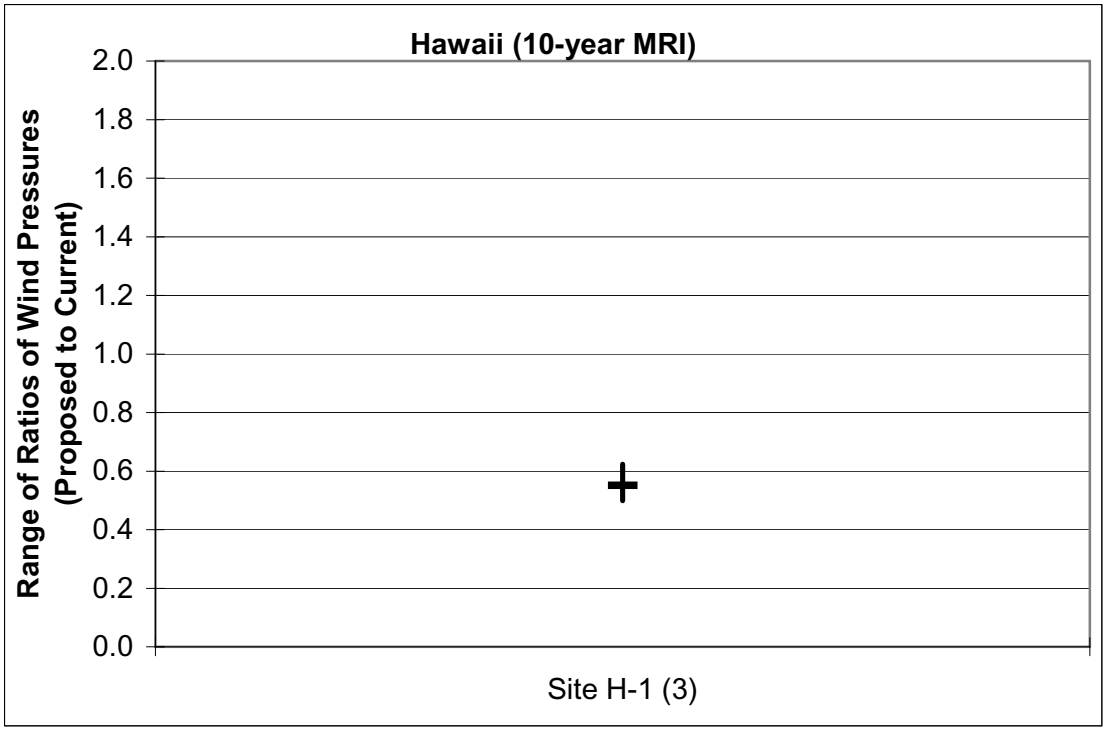

Figure B—95. Hawaii (10-year MRI): Range of Ratios of Wind Pressures (Proposed to Current Specification)

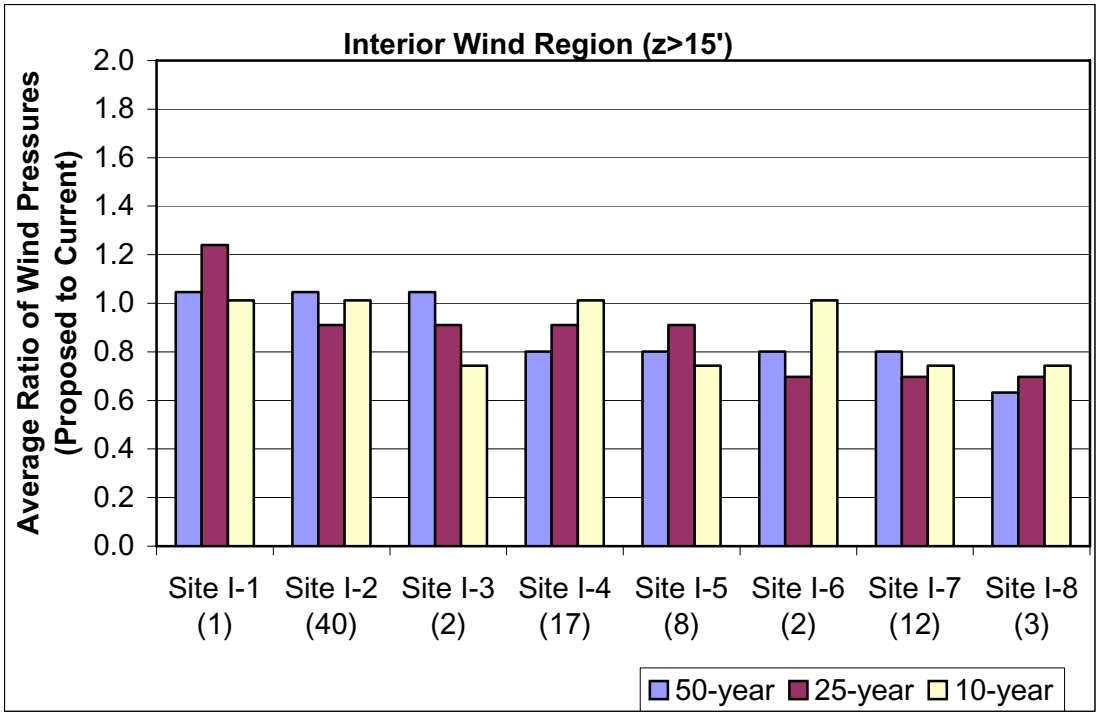

Figure B—96. Interior Wind Region: Average Ratio of Wind Pressures (Proposed to Current Specification) For Heights Greater Than 15 Feet

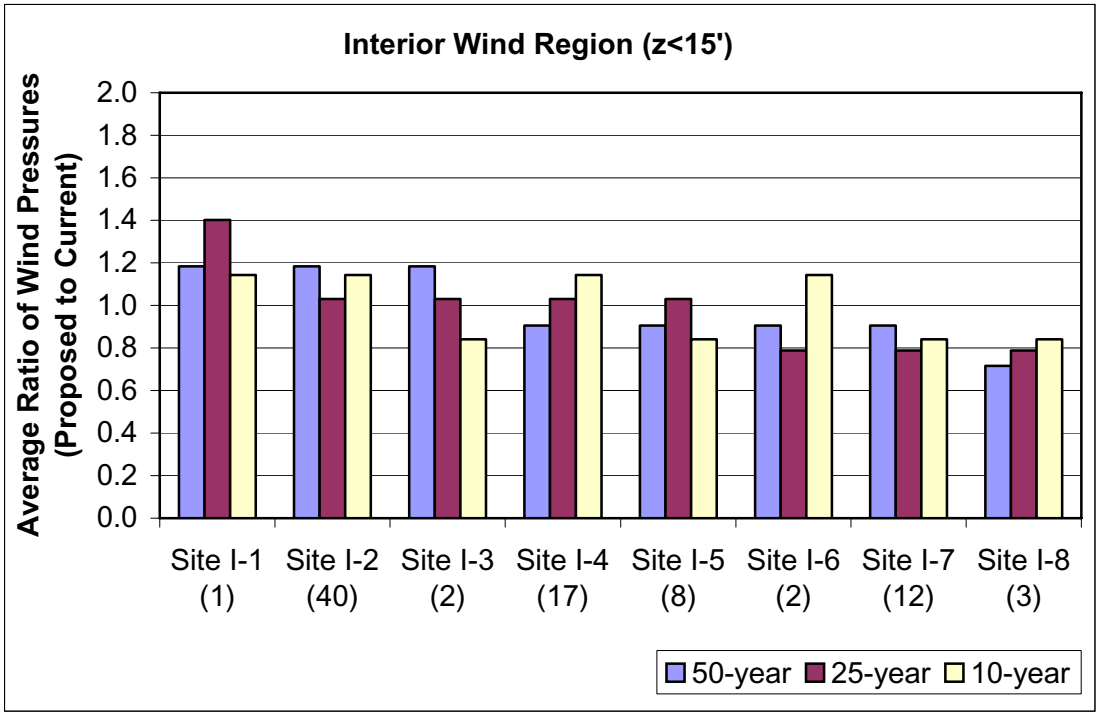

Figure B—97. Interior Wind Region: Average Ratio of Wind Pressures (Proposed to Current Specification) For Heights Less Than 15 Feet

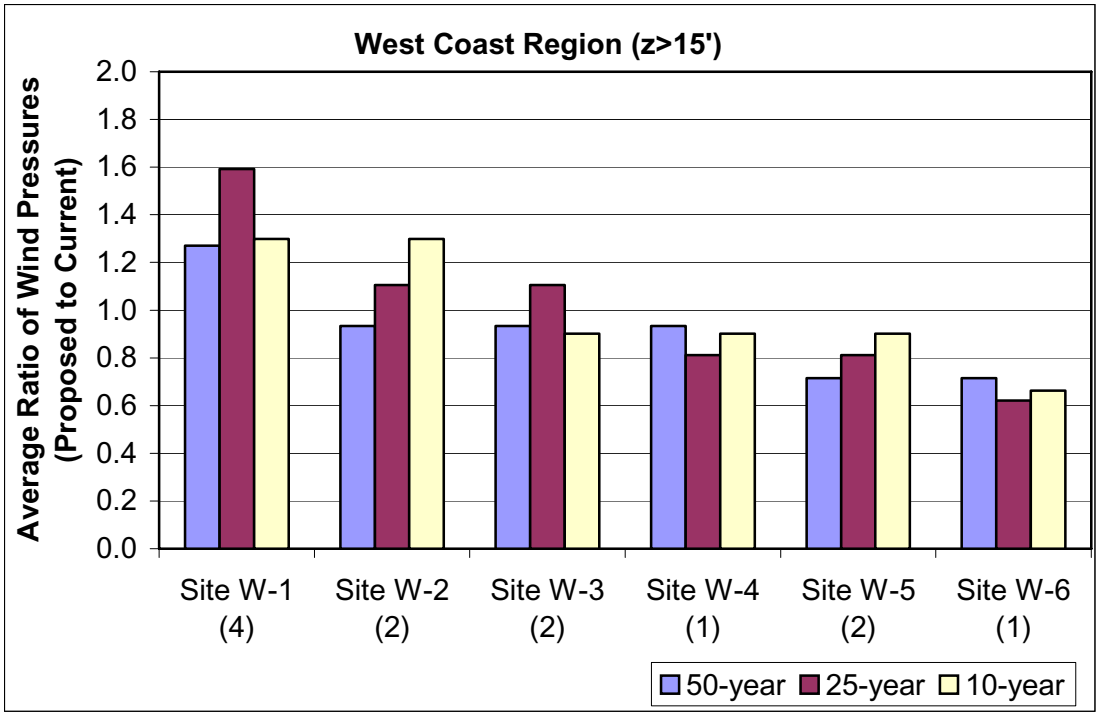

Figure B—98. West Coast Wind Region: Average Ratio of Wind Pressures (Proposed to Current Specification) For Heights Greater Than 15 Feet

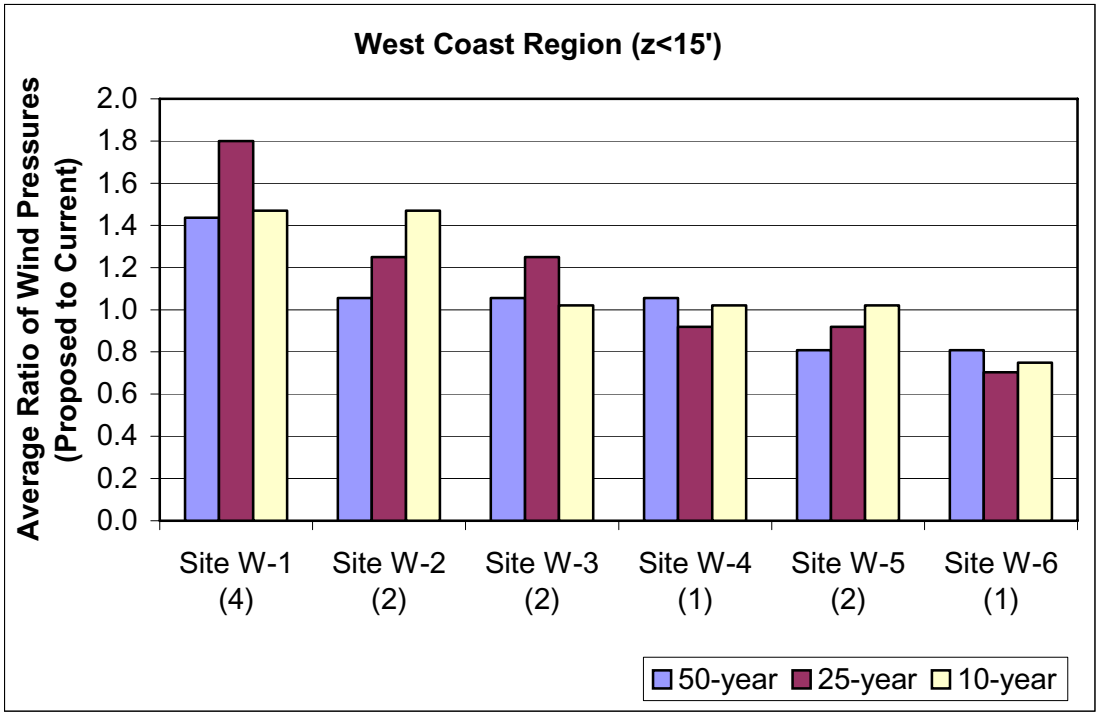

Figure B—99. West Coast Wind Region: Average Ratio of Wind Pressures (Proposed to Current Specification) For Heights Less Than 15 Feet

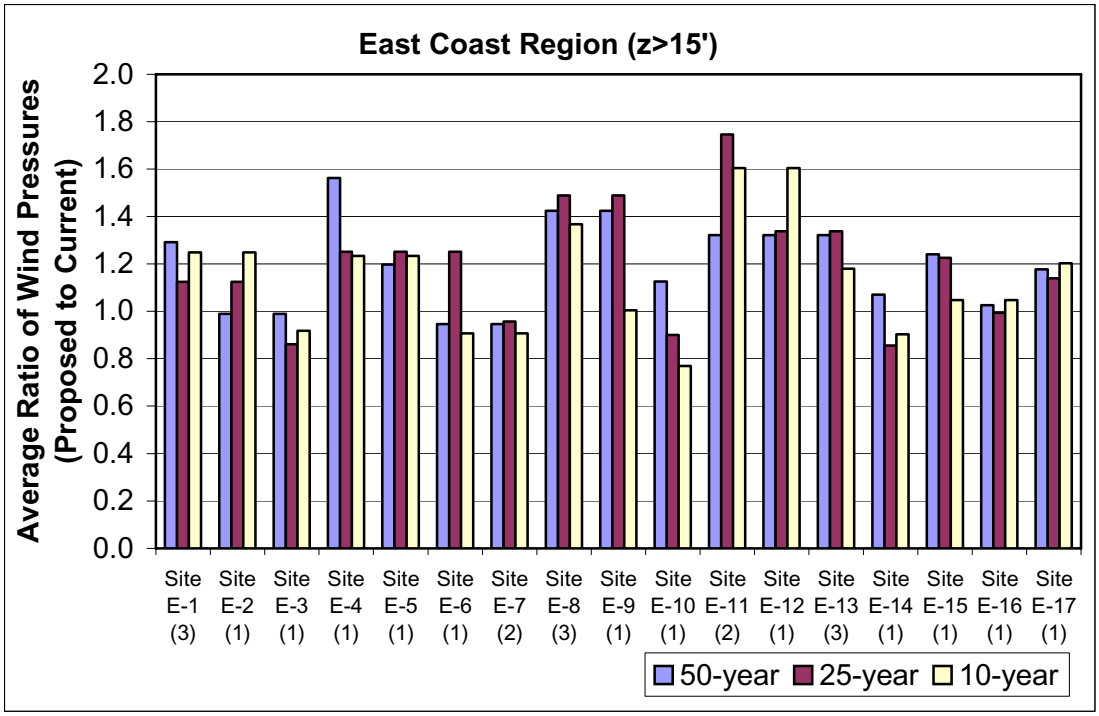

Figure B—100. East Coast Wind Region: Average Ratio of Wind Pressures (Proposed to Current Specification) For Heights Greater Than 15 Feet

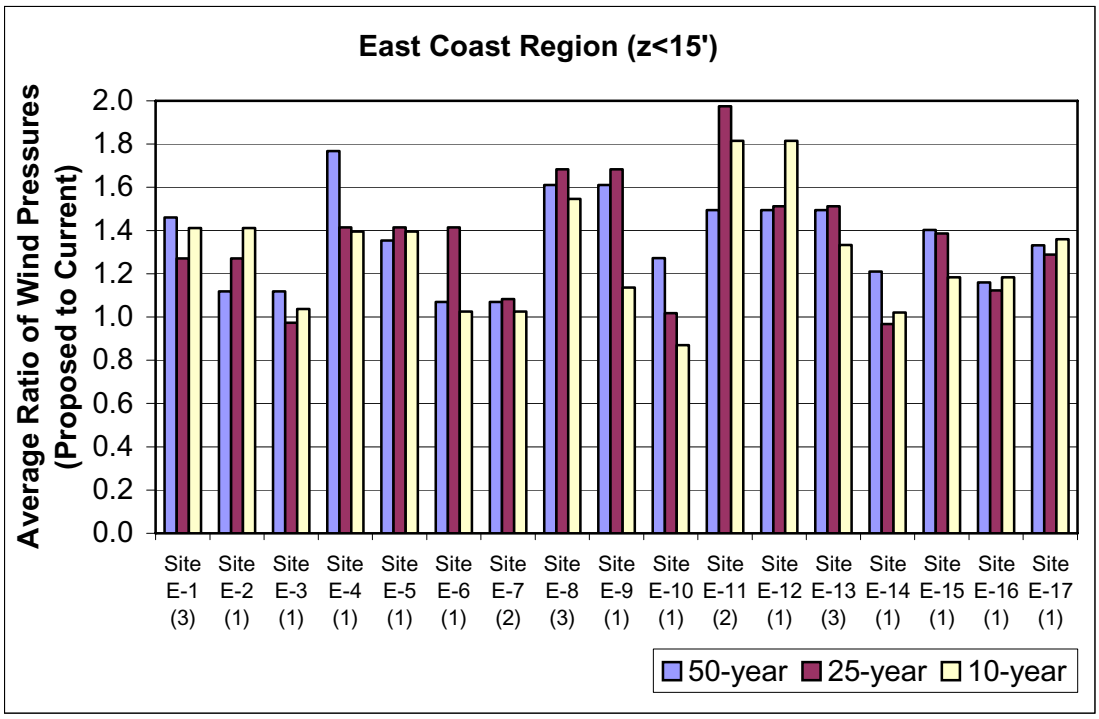

Figure B—101. East Coast Wind Region: Average Ratio of Wind Pressures (Proposed to Current Specification) For Heights Less Than 15 Feet

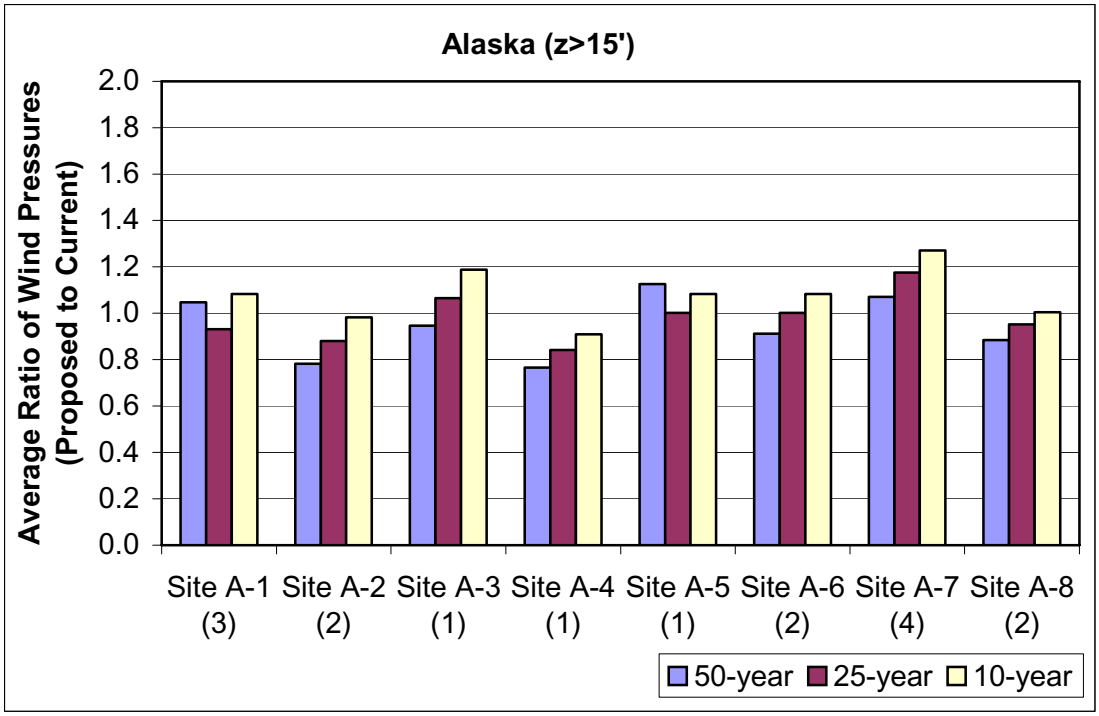

Figure B—102. Alaska: Average Ratio of Wind Pressures (Proposed to Current Specification) For Heights Greater Than 15 Feet

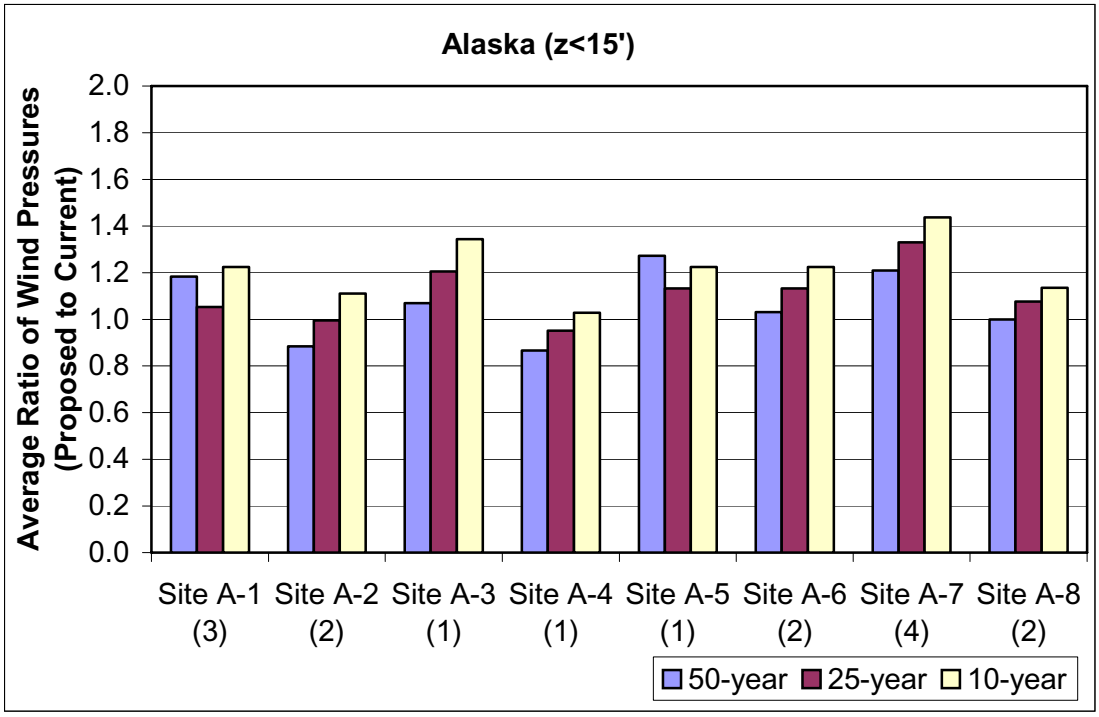

Figure B—103. Alaska: Average Ratio of Wind Pressures (Proposed to Current Specification) For Heights Less Than 15 Feet

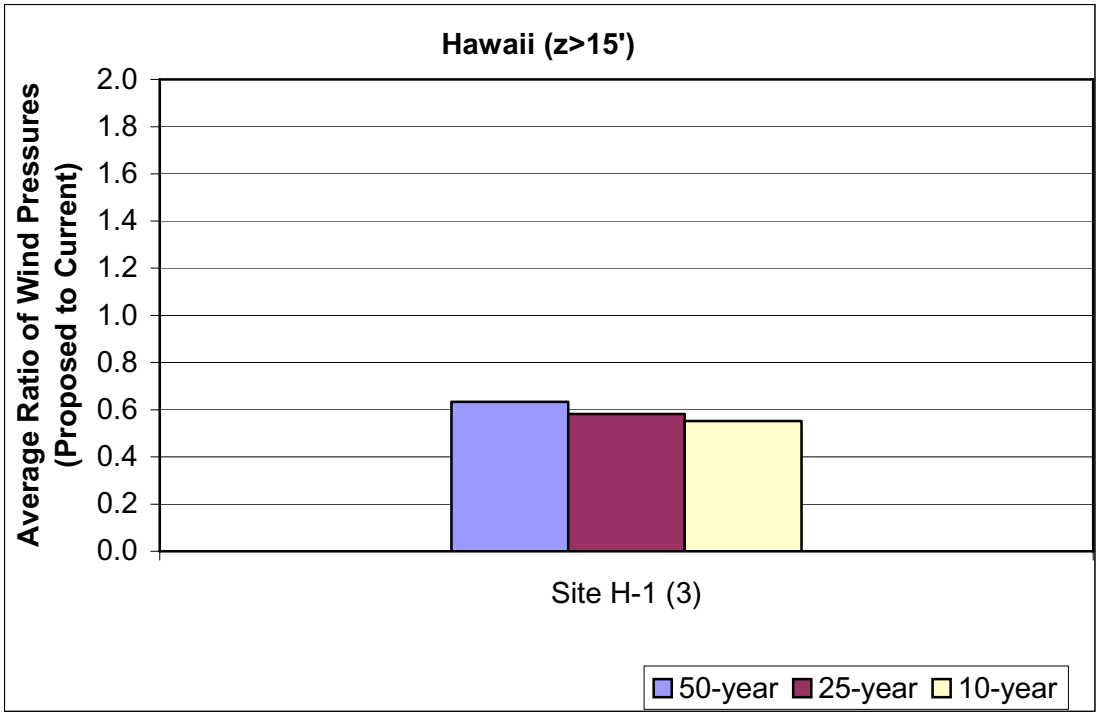

Figure B—104. Hawaii: Average Ratio of Wind Pressures (Proposed to Current Specification) For Heights Greater Than 15 Feet

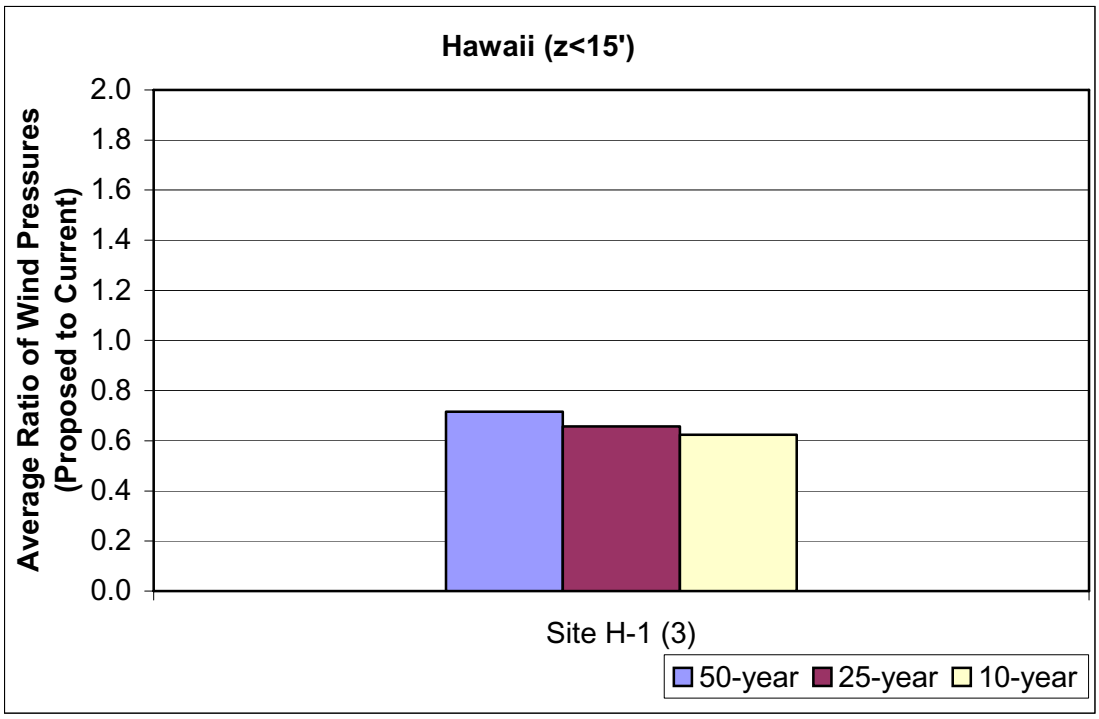

Figure B—105. Hawaii: Average Ratio of Wind Pressures (Proposed to Current Specification) For Heights Less Than 15 Feet

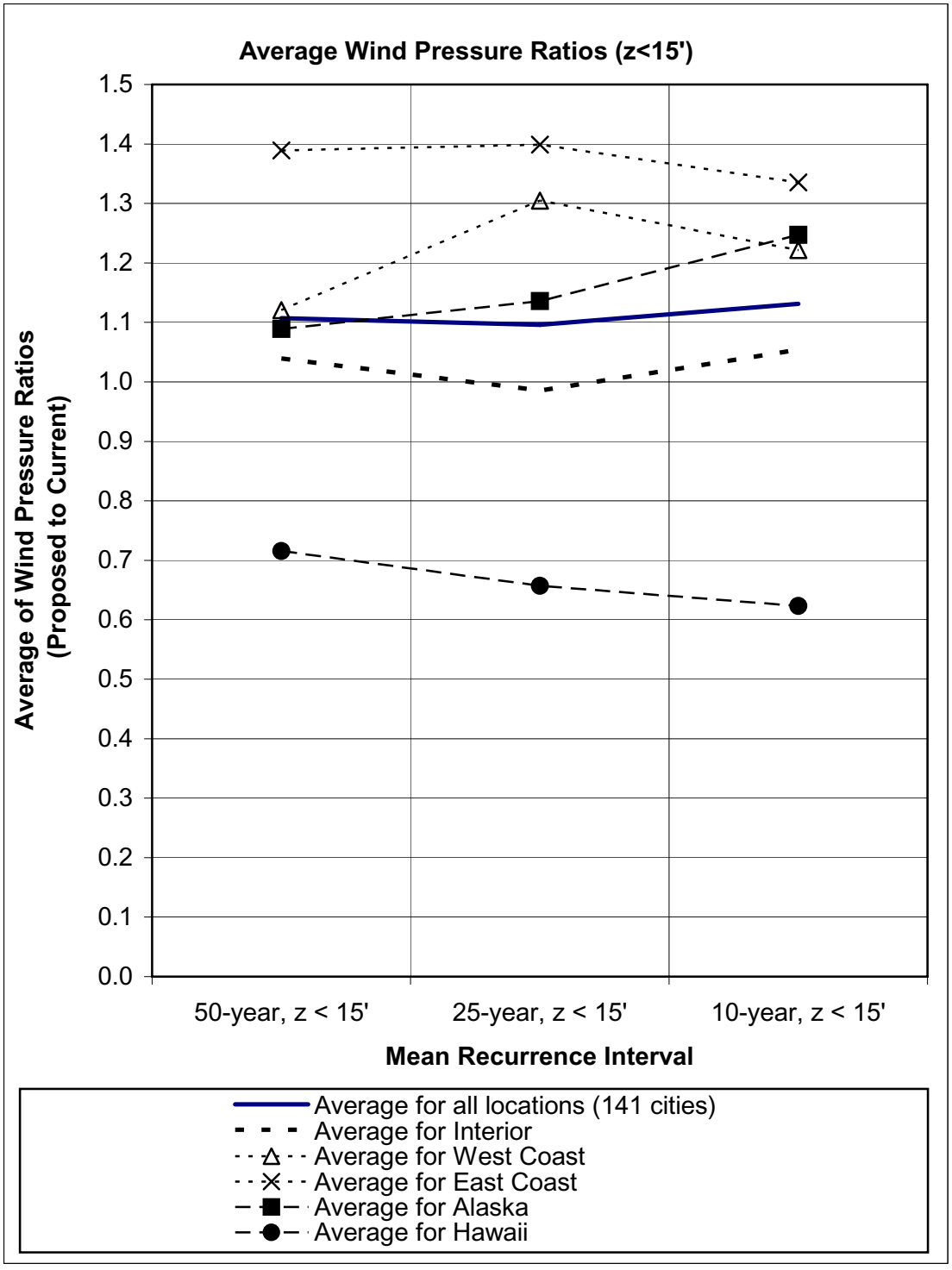

Figure B—106. All Regions (141 cities): Average Ratio of Wind Pressures (Proposed to Current Specification) For Heights Less Than 15 Feet

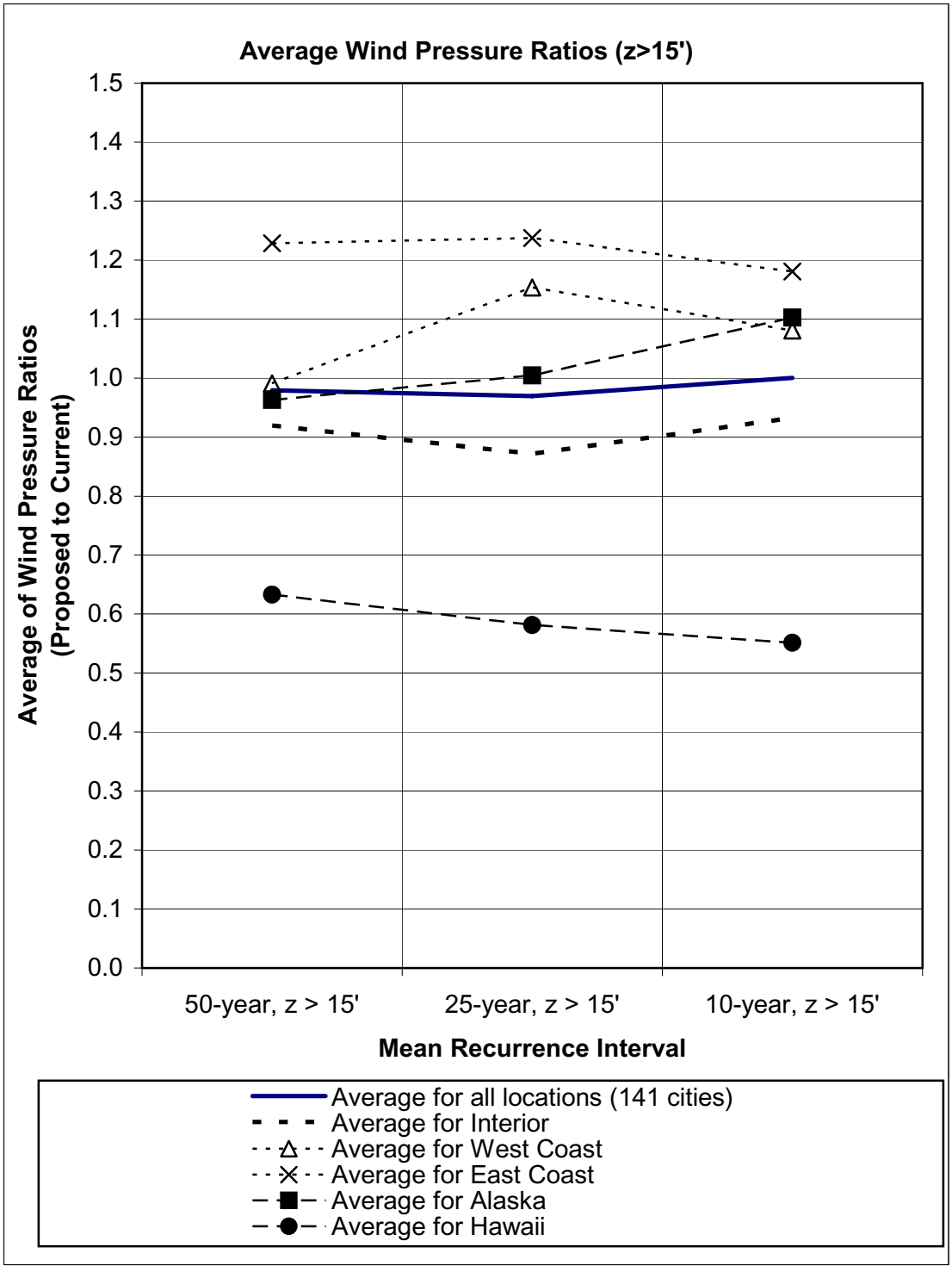

Figure B—107. All Regions (141 cities): Average Ratio of Wind Pressures (Proposed to Current Specification) For Heights Greater Than 15 Feet

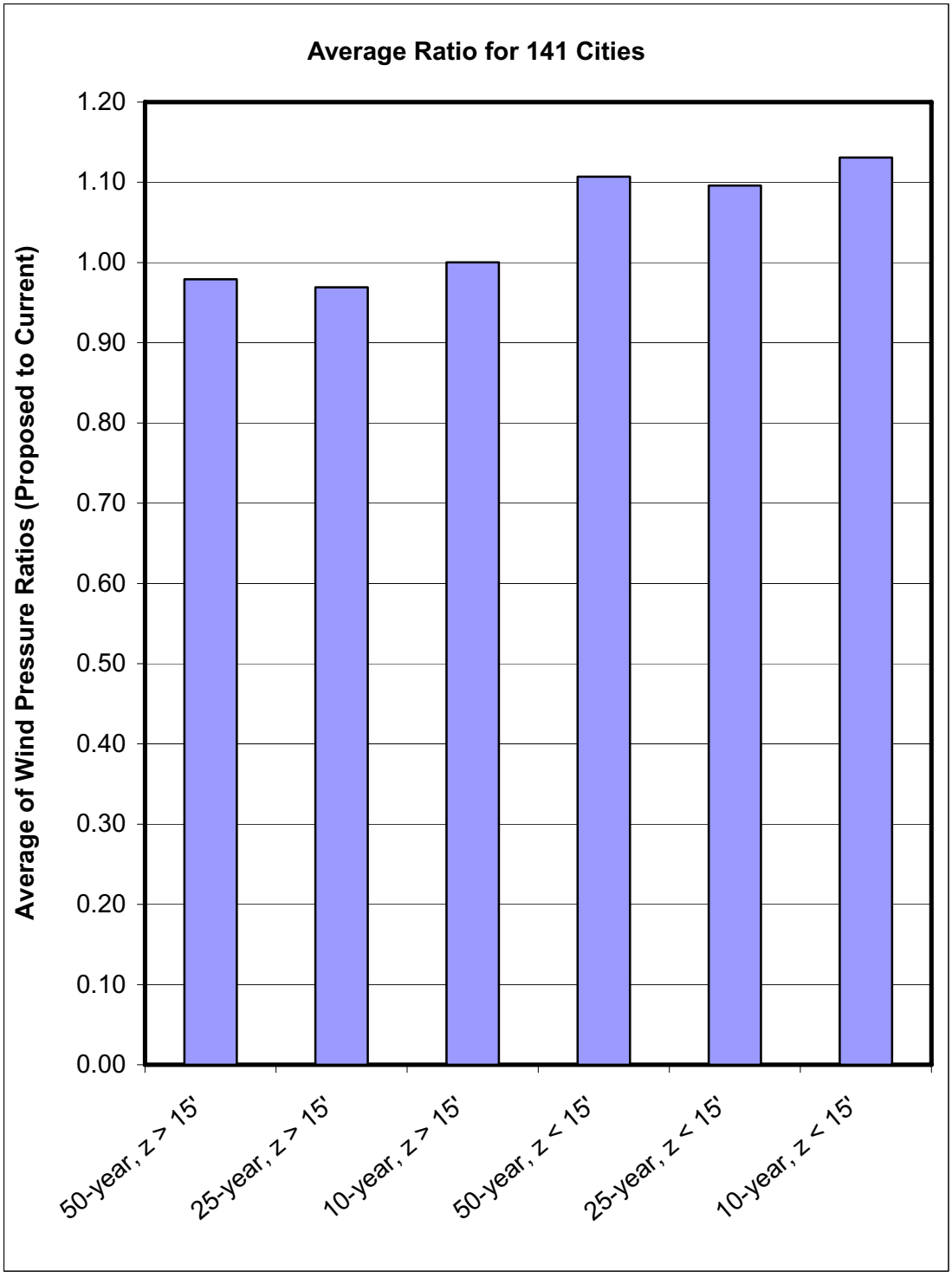

Figure B—108. All Regions (141 Cities): Average Ratio of Wind Pressures (Proposed to Current Specification)

Structure dimensions:

- Vertical support:
  - Columns: TS 12 x 12 x ½
  - Diagonals: TS 4 x 4 x 1/4
- Horizontal truss:
  - Chords: TS 8 x 8 x ½
  - Diagonals and struts: TS 3.5 x 3.5 x 3/16
- Other:
  - Sign area: 1000 $feet^2$
  - EPA of truss: 2.45 $feet^2$ per foot
- Notation:
  - A: 125 feet
  - B: 15 feet
  - C: 8 feet
  - D: 9 feet
  - H: 21 feet
  - L: 155 feet
  - M: 7 feet

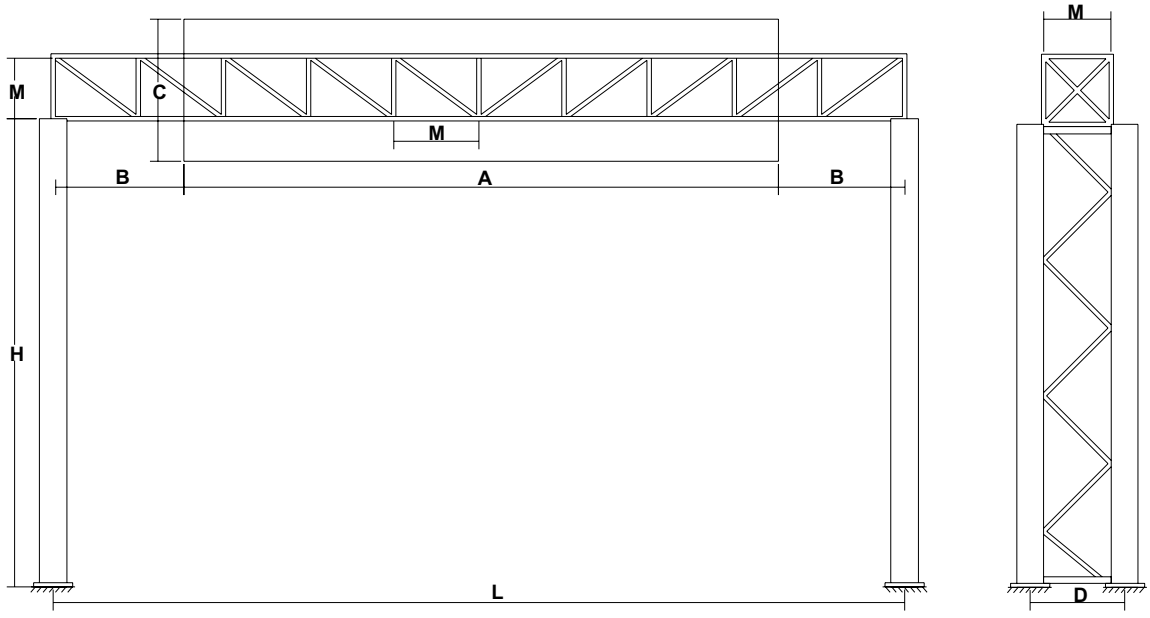

Figure B—109. Non-Cantilevered Overhead Sign Structure

Structure dimensions:

Vertical post: 24-inch diameter

Cantilevered truss:

Top and bottom chords: 2.5 inch standard pipe

Diagonal and strut: 1 inch standard pipe

Other:

Sign area: 220 $feet^2$

EPA of truss: 1.88 $feet^2$ per foot

Notation:

A: 11 feet

B: 10 feet

C: 22 feet

D: 4 feet

D1: 2 feet

H: 25 feet

L: 24 feet

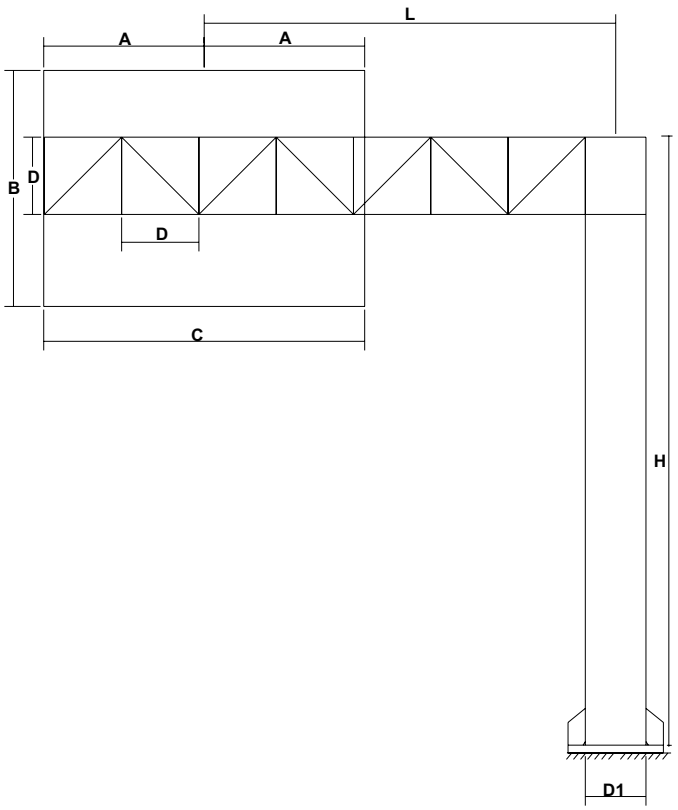

Figure B—110. Cantilevered Overhead Sign Structure

Structure dimensions:

Pole dimensions:

Round tubular tapered pole:

Tip diameter D_t: 7.75 inch

Base diameter D_b: 32.6 inch

Other:

EPA of luminaires + mounting device: 58 $feet^2$

Notation:

H: 150 feet

H1: 151 feet

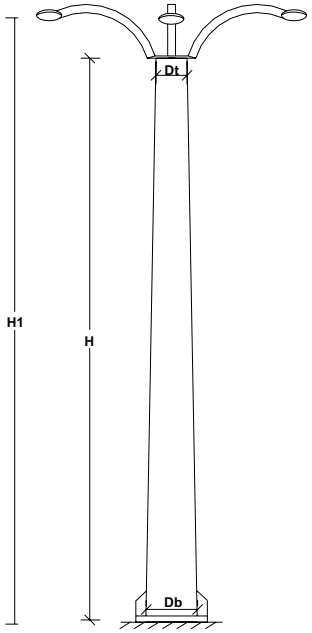

Figure B—111. High Mast Lighting Pole

Structure dimensions:

- Pole dimensions:
  - Top diameter: 12 inch
  - Bottom diameter: 16 inch
- Mast arm dimensions:
  - Diameter at connection: 10 inch
  - Diameter at tip: 7 inch
- Other:
  - EPA of signal: 8.7 feet^2
- Notation:
  - A: 10 feet
  - B: 8 feet
  - C: 5 feet
  - D: 2 feet
  - H: 25 feet

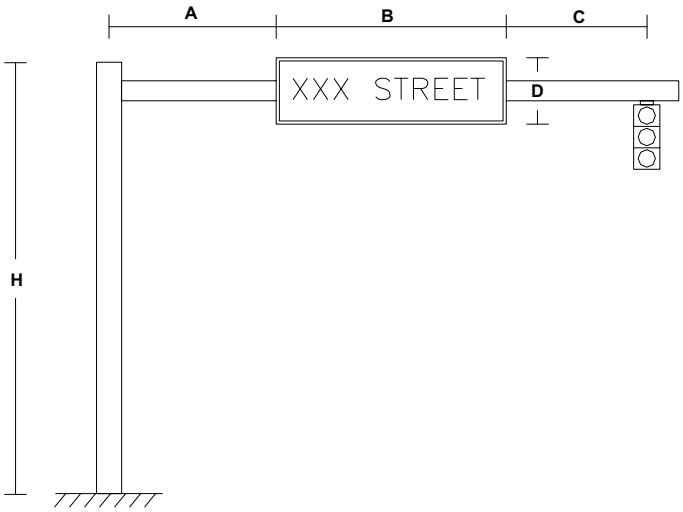

Figure B—112. Cantilevered Traffic Signal Structure

Structure dimensions:

Pole:

Top diameter: 6.0 inch
Bottom diameter: 8.0 inch

Arm:

Tip diameter: 3.5 inch
Connection diameter: 3.5 inch

Other:

EPA of luminaire: 3.3 $feet^2$
EPA of arm: 6.5 $feet^2$

Notation:

A: 0.5 feet
B: 1.5 feet
H: 30.75 feet
H1: 33.5 feet
H2: 32.07 feet
L: 12 feet
L1: 4.8 feet.

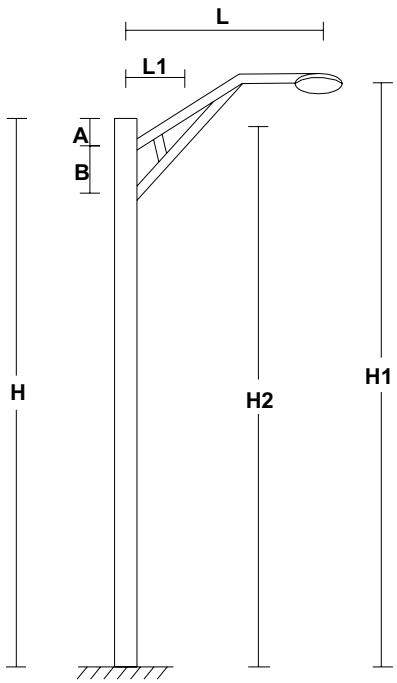

Figure B—113. Streetlighting Pole

Structure dimensions:

Post dimensions: 8 x 8 inch square post

Notation:

A: 4 feet
B: 8 feet
C: 1 feet
D: 6 feet
H: 6 feet.

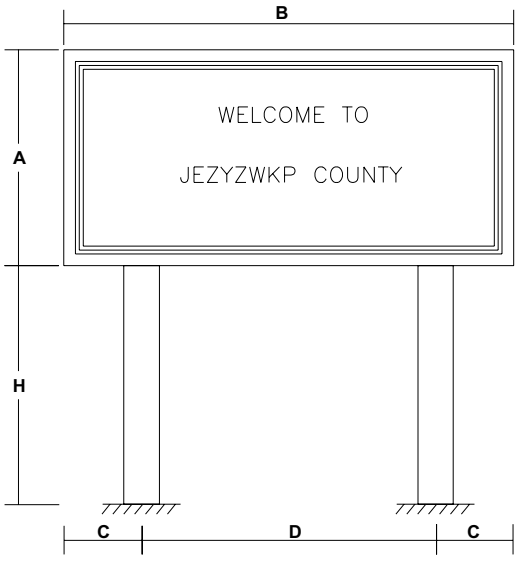

Figure B—114. Roadside Sign

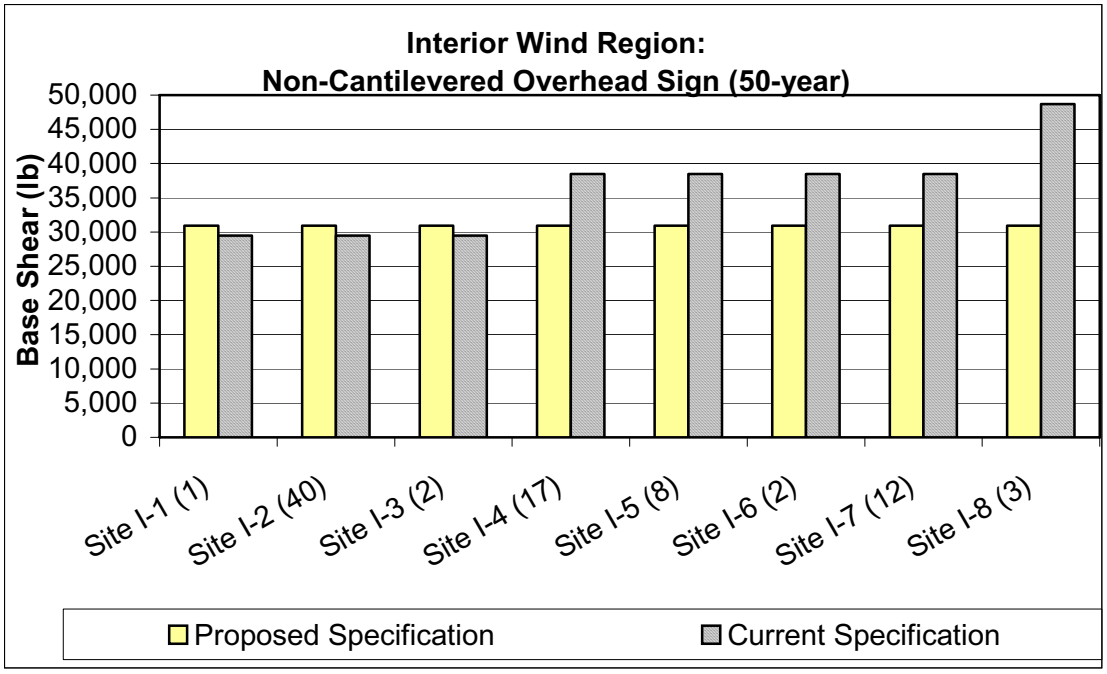

Figure B—115. Interior Wind Region: Base Shear Comparison for Non-Cantilevered Overhead Sign (50-year)

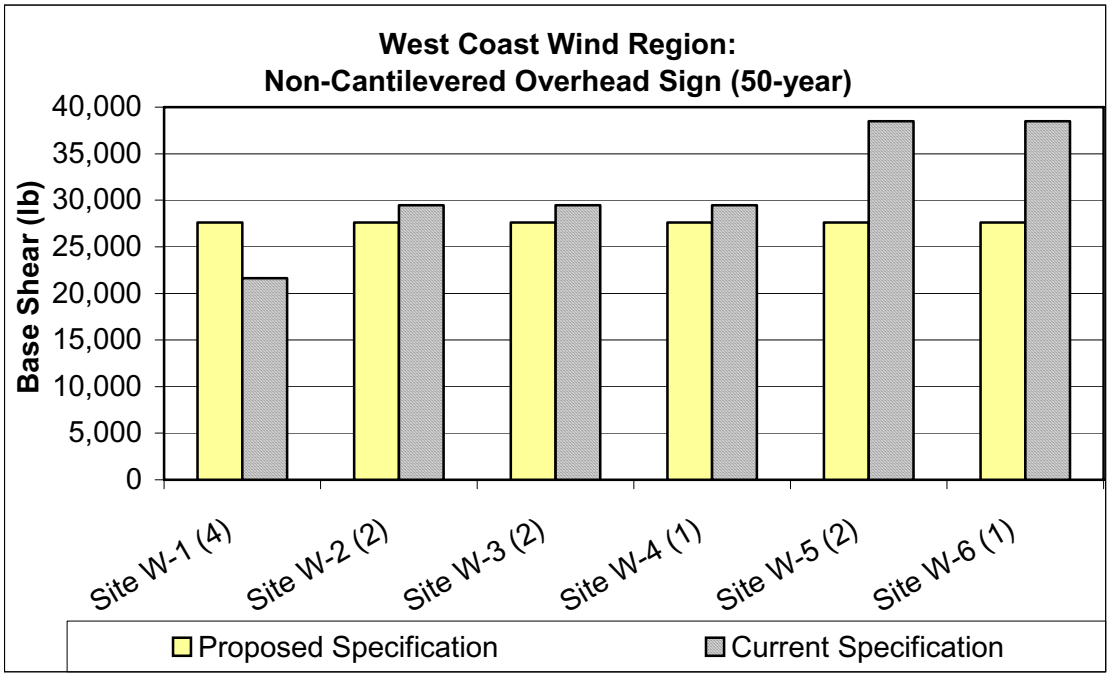

Figure B—116. West Coast Wind Region: Base Shear Comparison for Non-Cantilevered Overhead Sign (50-year)

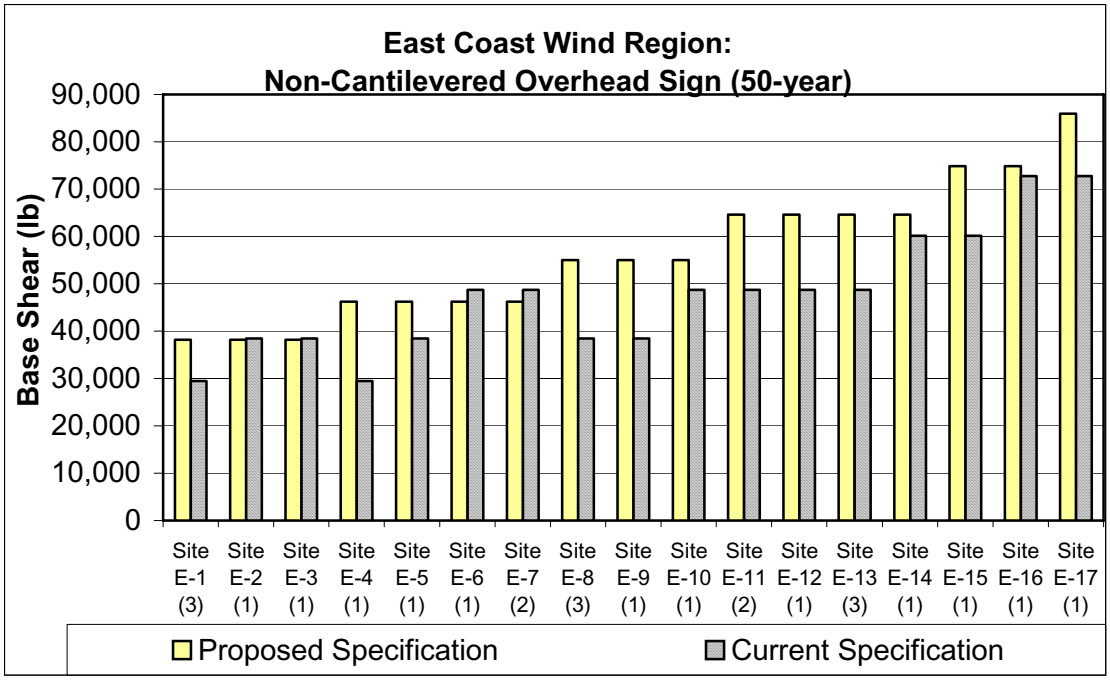

Figure B—117. East Coast Wind: Base Shear Comparison for Non-Cantilevered Overhead Sign (50-year)

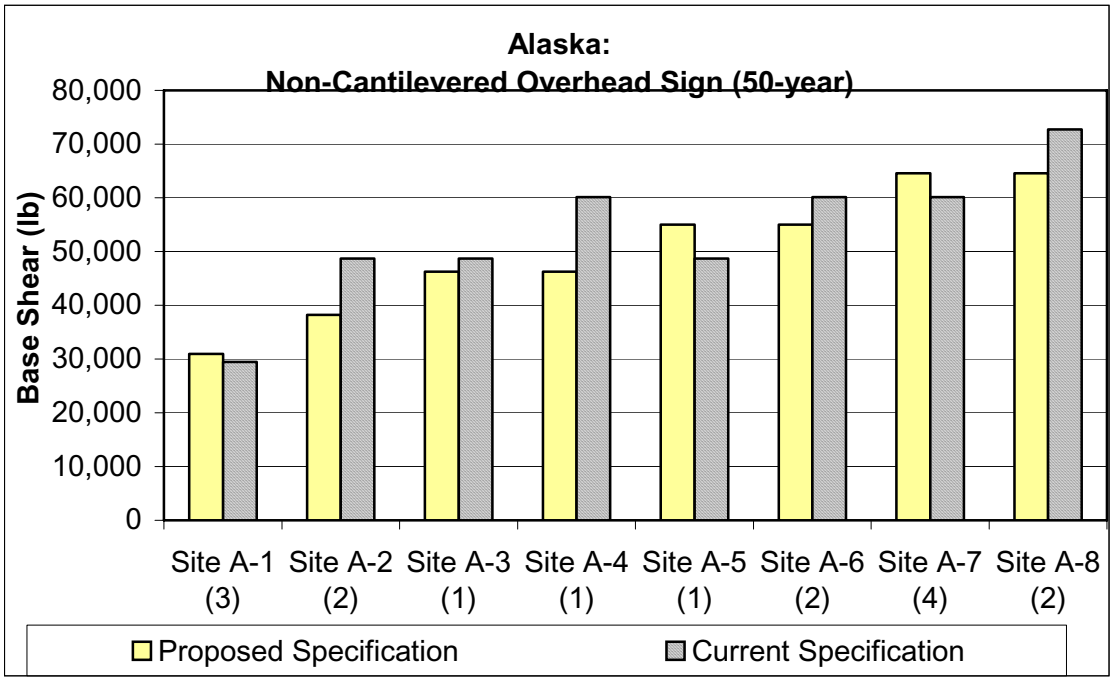

Figure B—118. Alaska: Base Shear Comparison for Non-Cantilevered Overhead Sign (50-year)

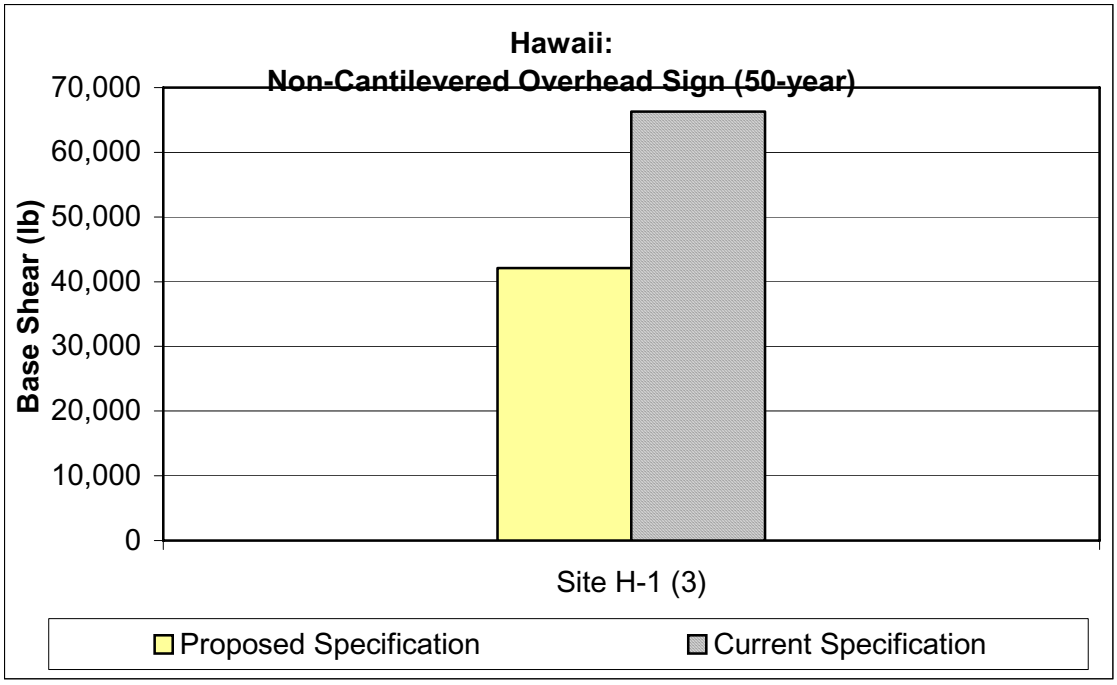

Figure B—119. Hawaii: Base Shear Comparison for Non-Cantilevered Overhead Sign (50-year)

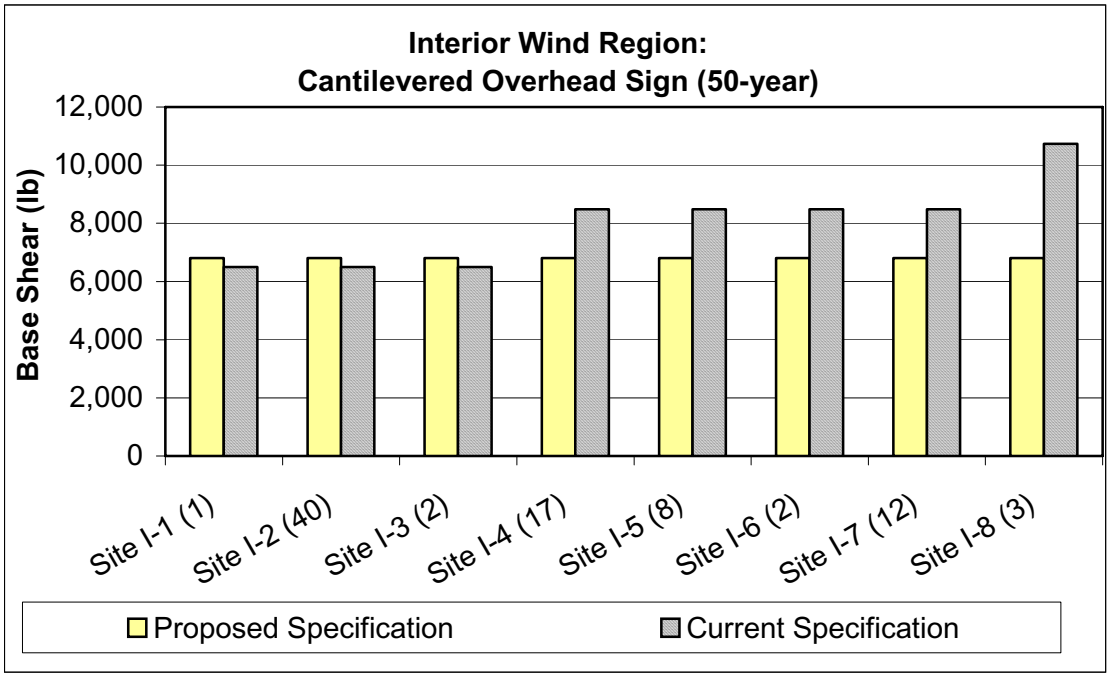

Figure B—120. Interior Wind Region: Base Shear Comparison for Cantilevered Overhead Sign (50-year)

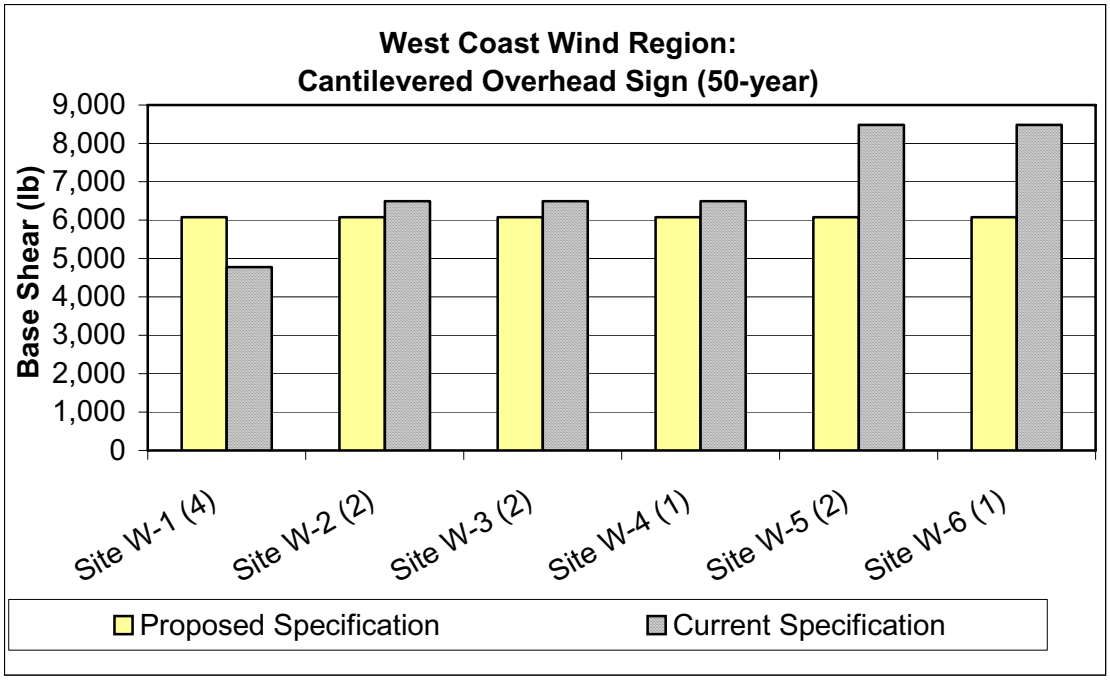

Figure B—121. West Coast Wind Region: Base Shear Comparison for Cantilevered Overhead Sign (50-year)

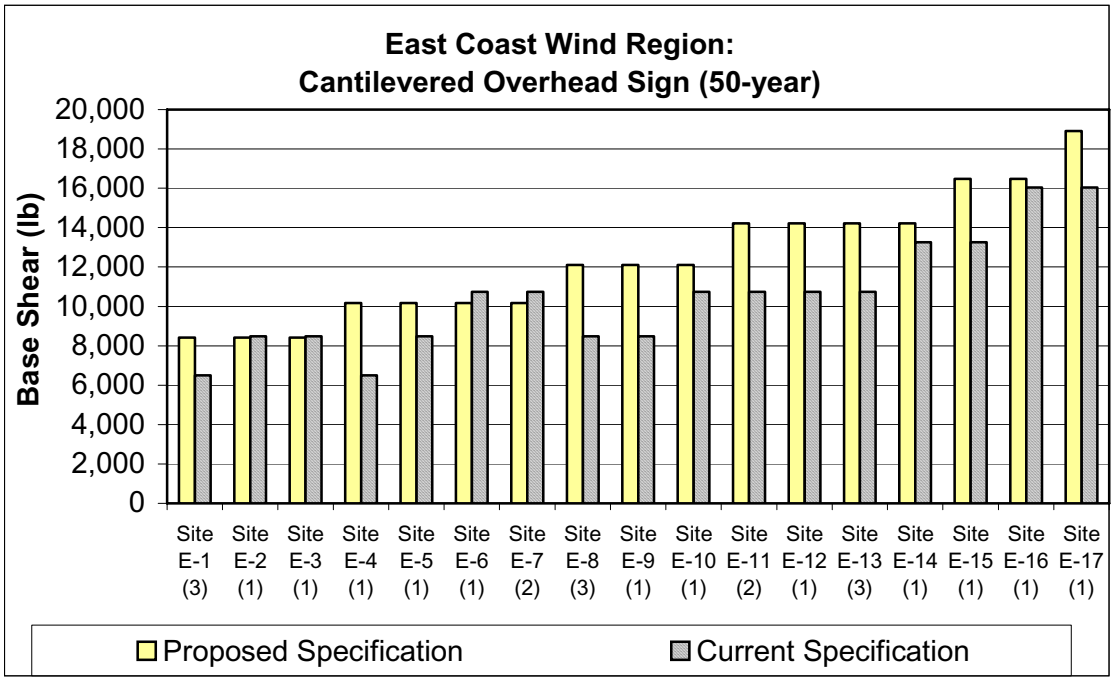

Figure B—122. East Coast Wind Region: Base Shear Comparison for Cantilevered Overhead Sign (50-year)

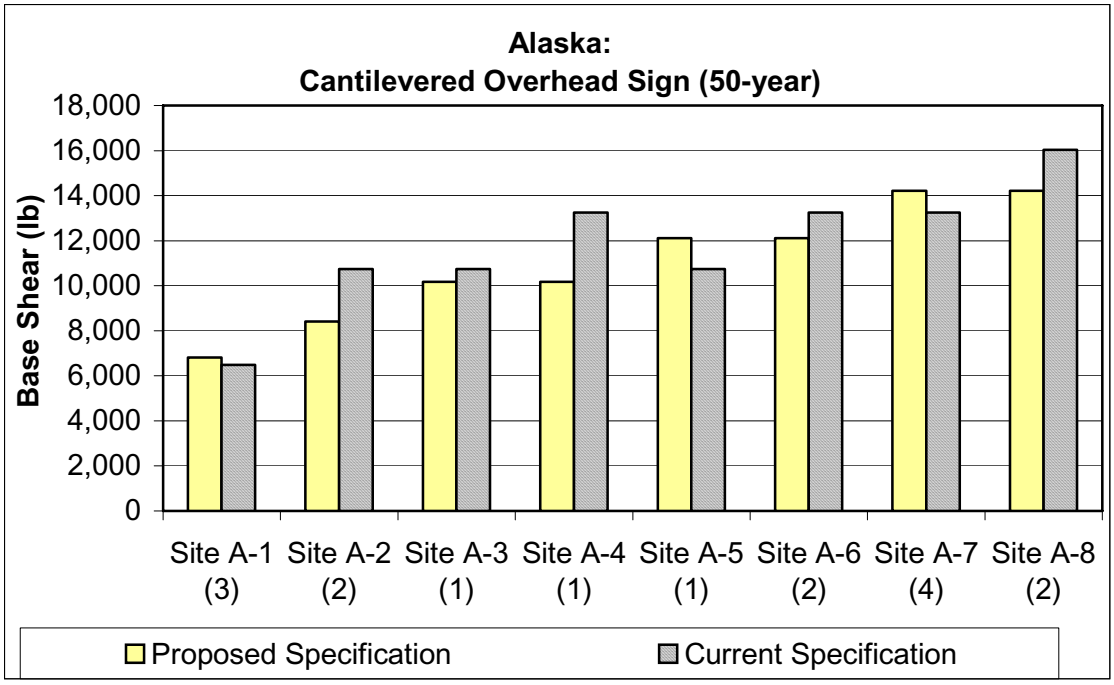

Figure B—123. Alaska: Base Shear Comparison for Cantilevered Overhead Sign (50-year)

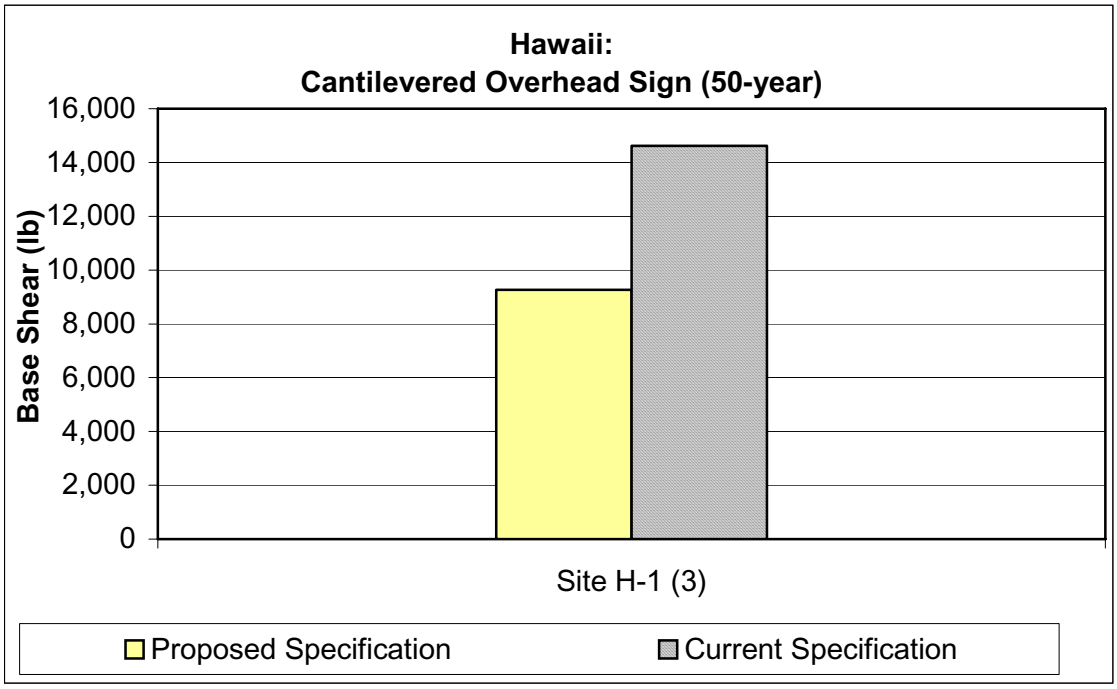

Figure B—124. Hawaii: Base Shear Comparison for Cantilevered Overhead Sign (50-year)

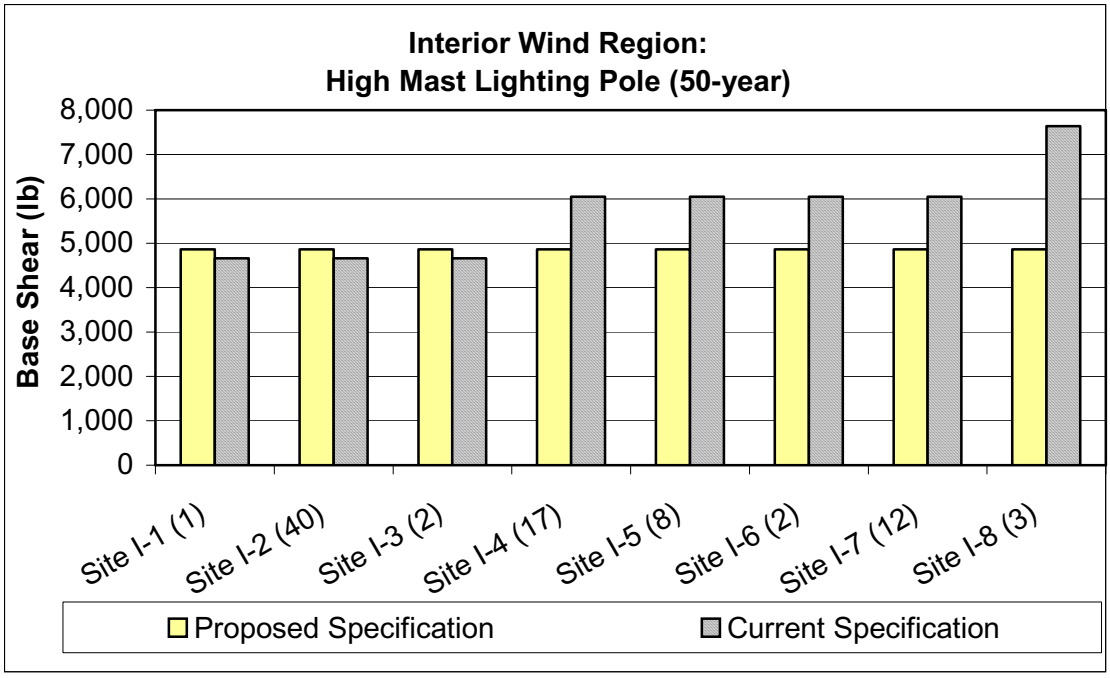

Figure B—125. Interior Wind Region: Base Shear Comparison for High Mast Lighting Pole (50-year)

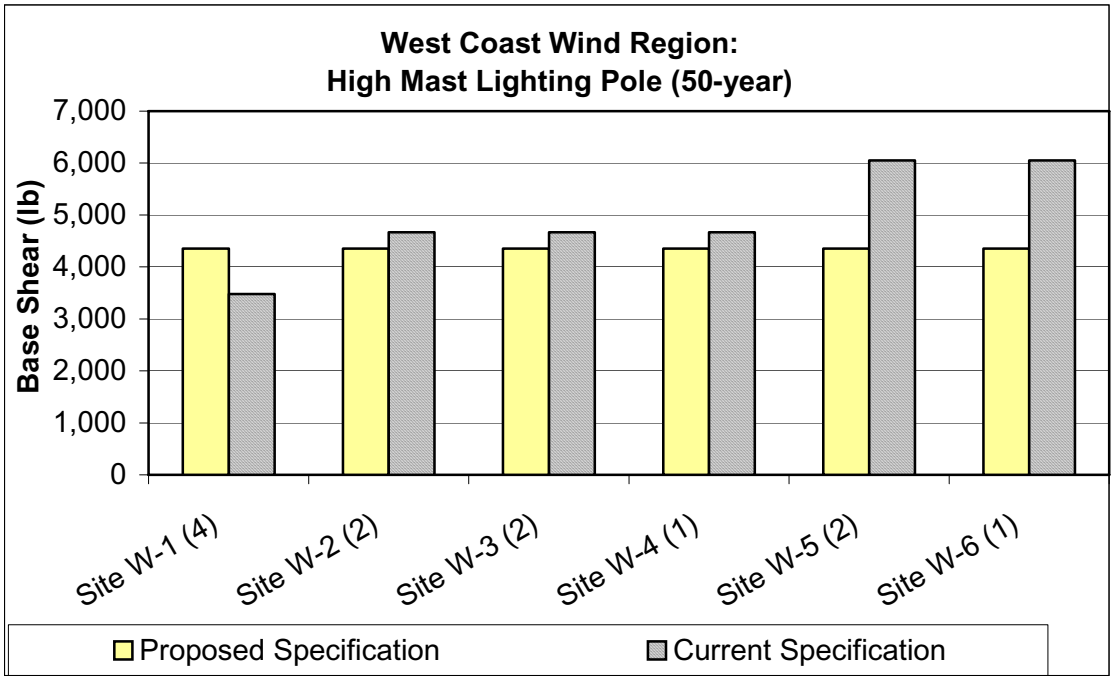

Figure B—126. West Coast Wind Region: Base Shear Comparison for High Mast Lighting Pole (50-year)

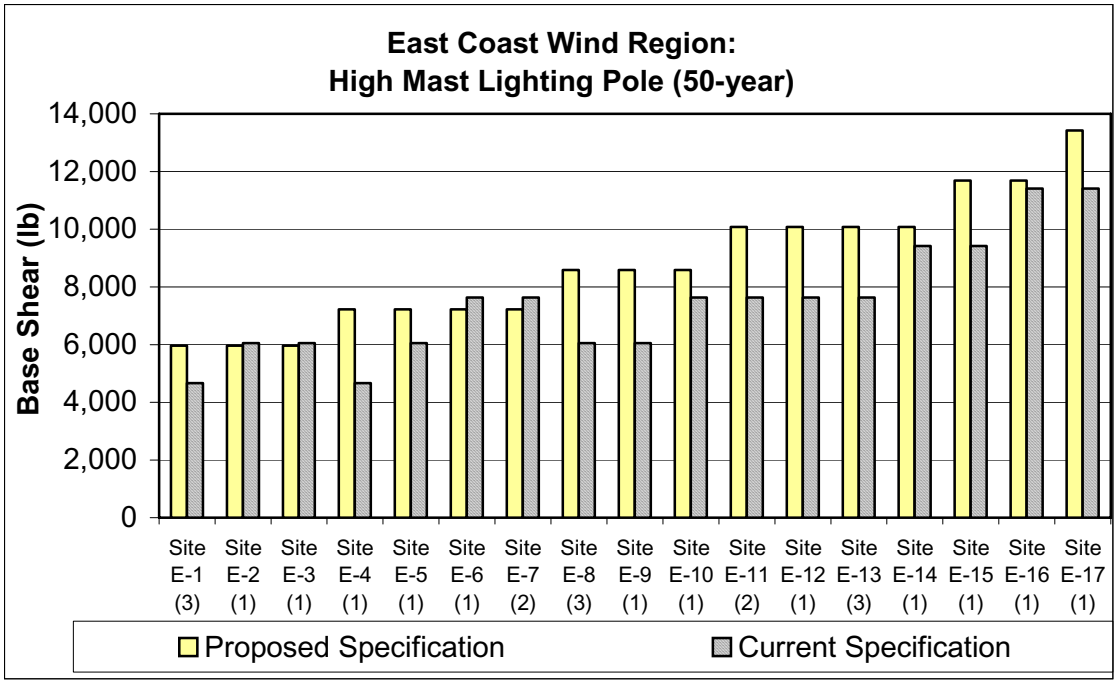

Figure B—127. East Coast Wind Region: Base Shear Comparison for High Mast Lighting Pole (50-year)

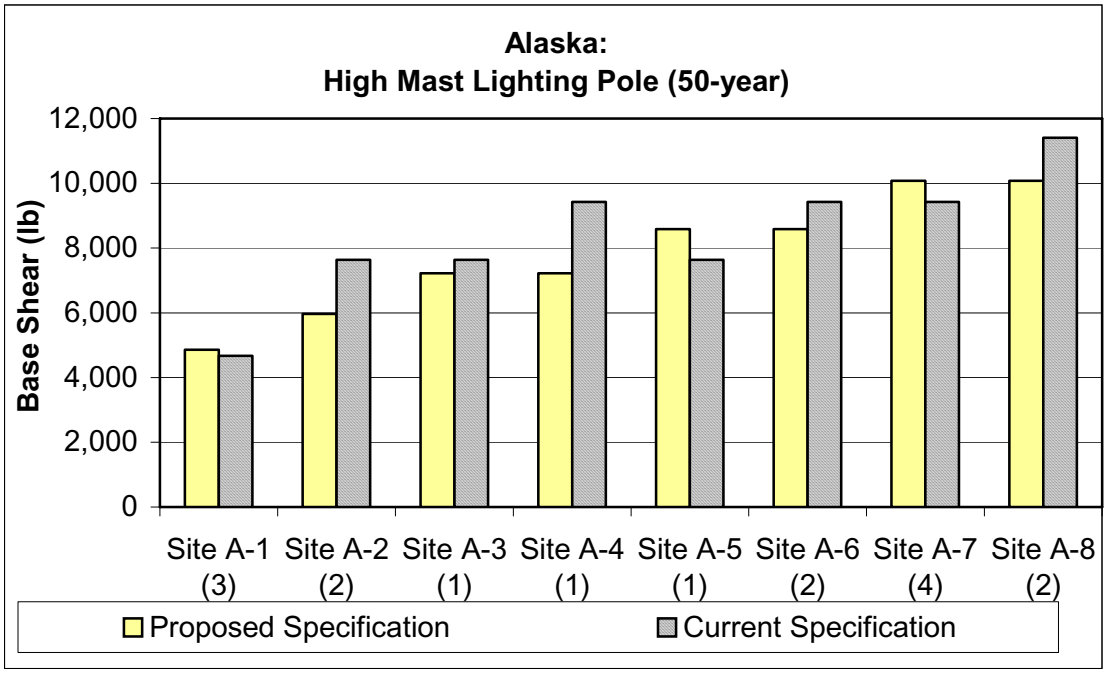

Figure B—128. Alaska: Base Shear Comparison for High Mast Lighting Pole (50-year)

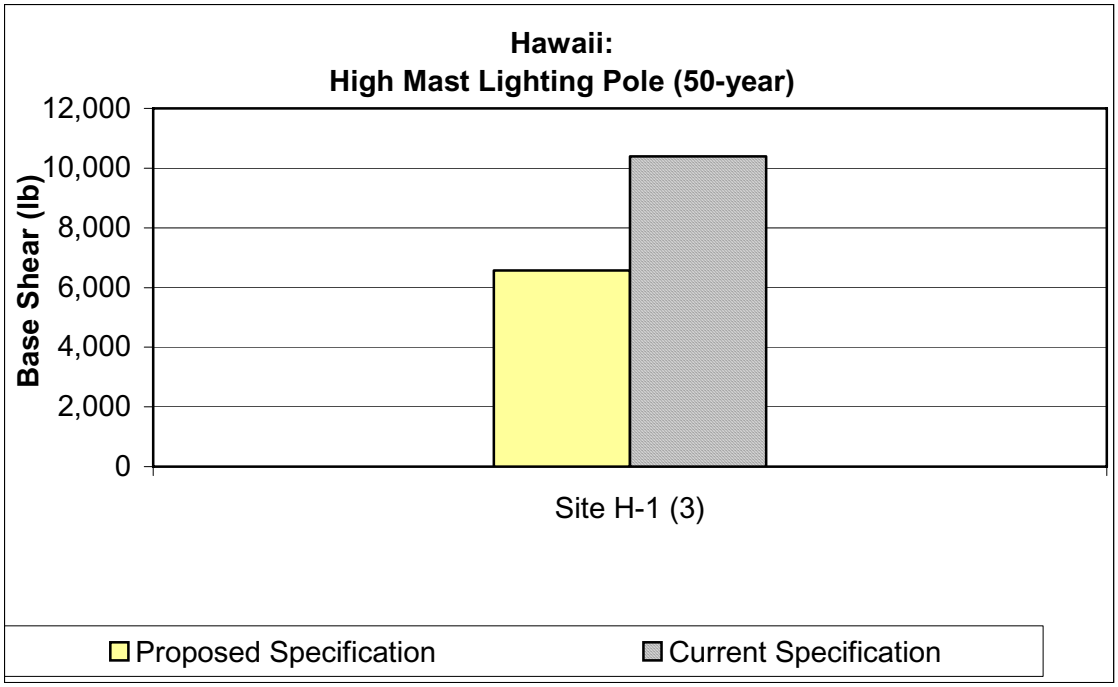

Figure B—129. Hawaii: Base Shear Comparison for High Mast Lighting Pole (50-year)

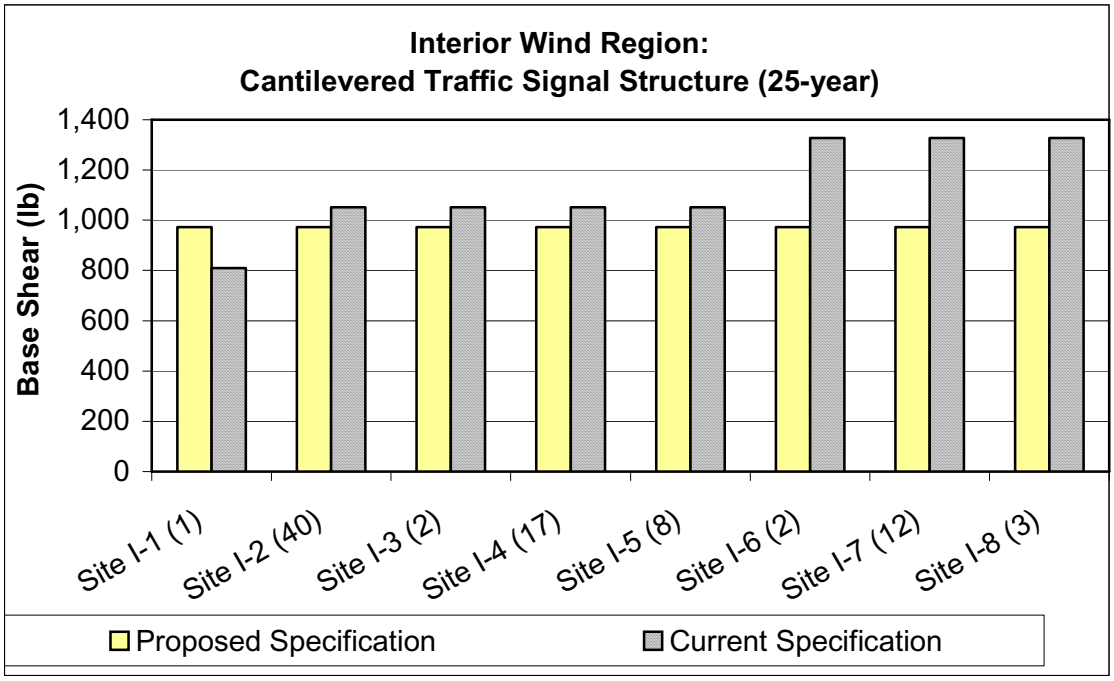

Figure B—130. Interior Wind Region: Base Shear Comparison for Cantilevered Traffic Signal Structure (25-year)

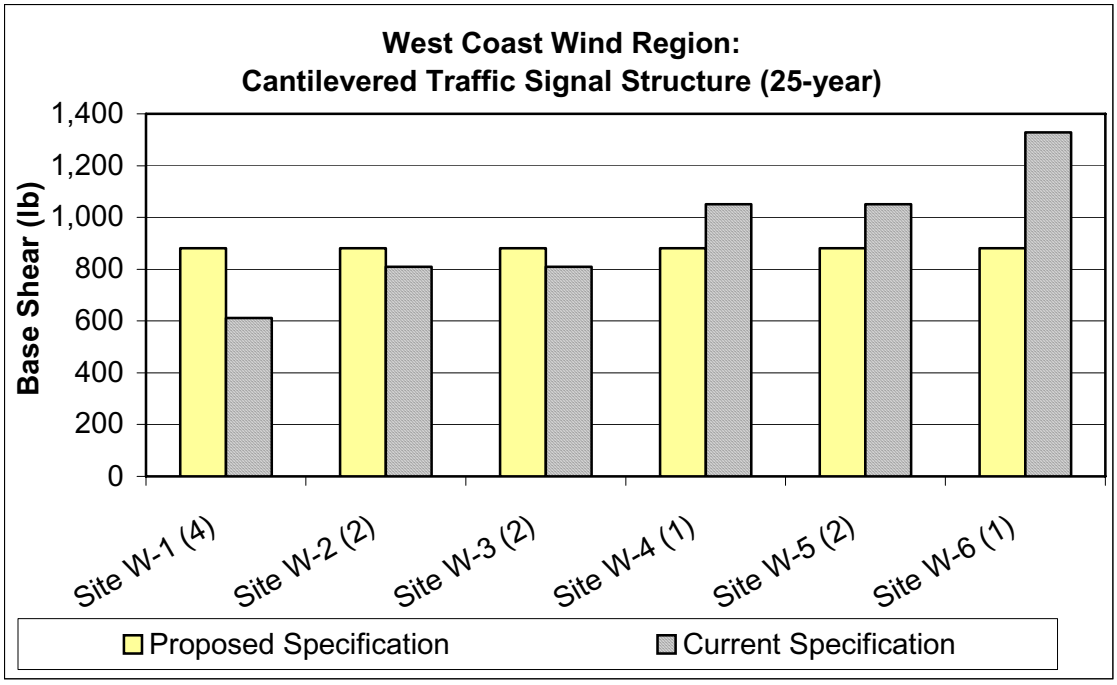

Figure B—131. West Coast Wind Region: Base Shear Comparison for Cantilevered Traffic Signal Structure (25-year)

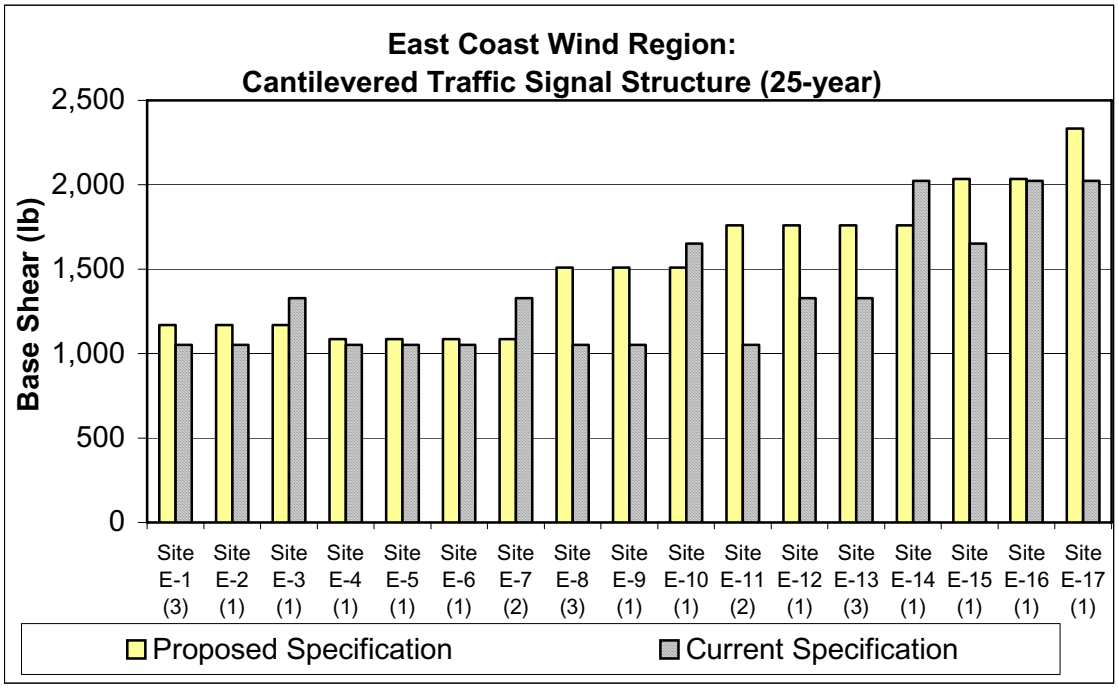

Figure B—132. East Coast Wind Region: Base Shear Comparison for Cantilevered Traffic Signal Structure (25-year)

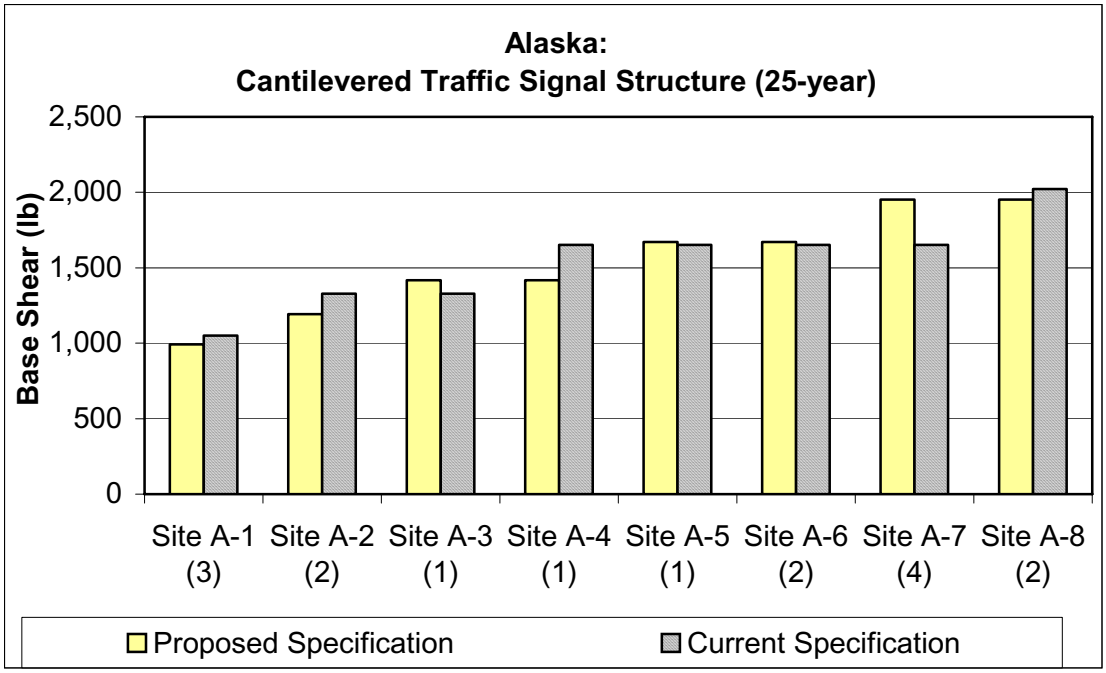

Figure B—133. Alaska: Base Shear Comparison for Cantilevered Traffic Signal Structure (25-year)

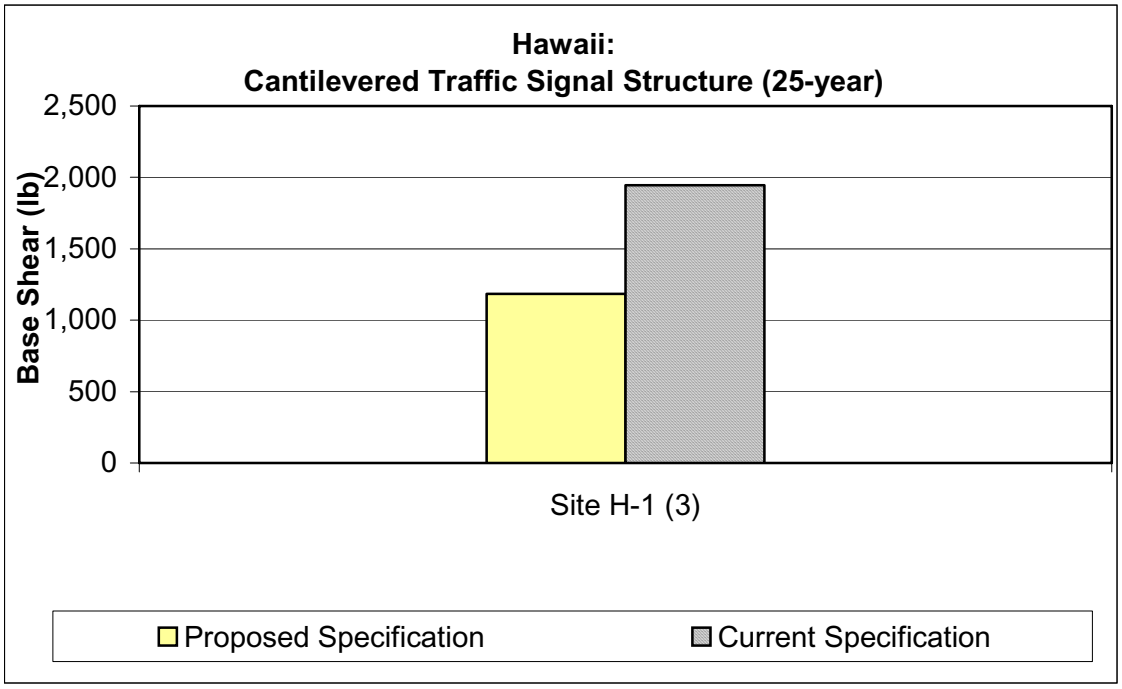

Figure B—134. Hawaii: Base Shear Comparison for Cantilevered Traffic Signal Structure (25-year)

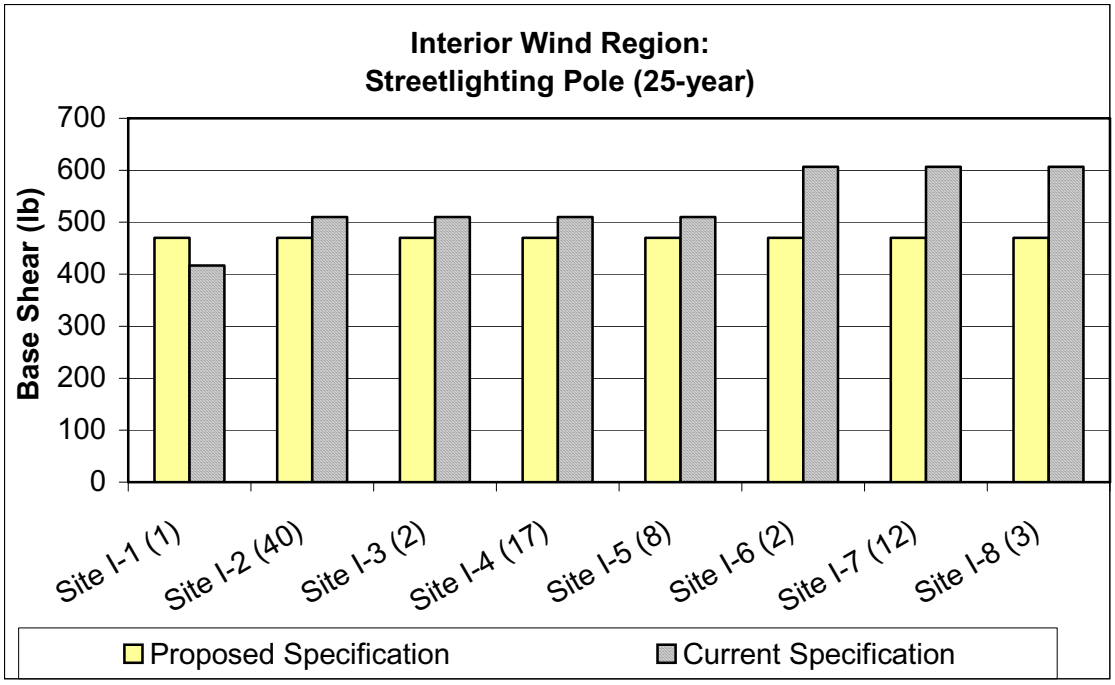

Figure B—135. Interior Wind Region: Base Shear Comparison for Streetlighting Pole (25-year)

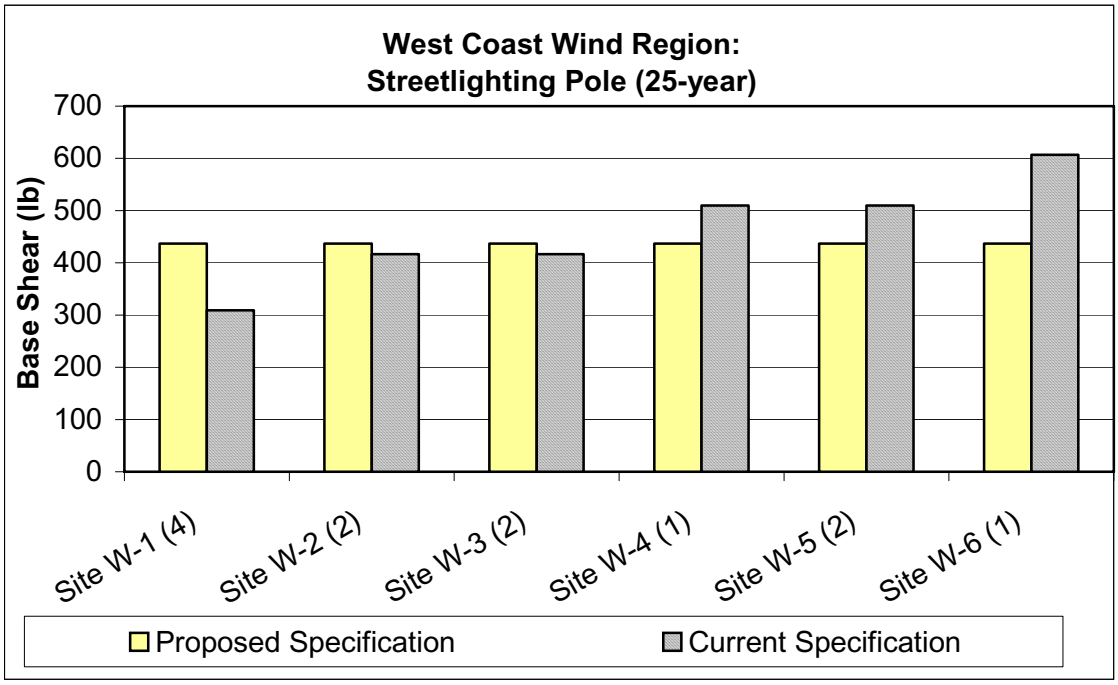

Figure B—136. West Coast Wind Region: Base Shear Comparison for Streetlighting Pole (25-year)

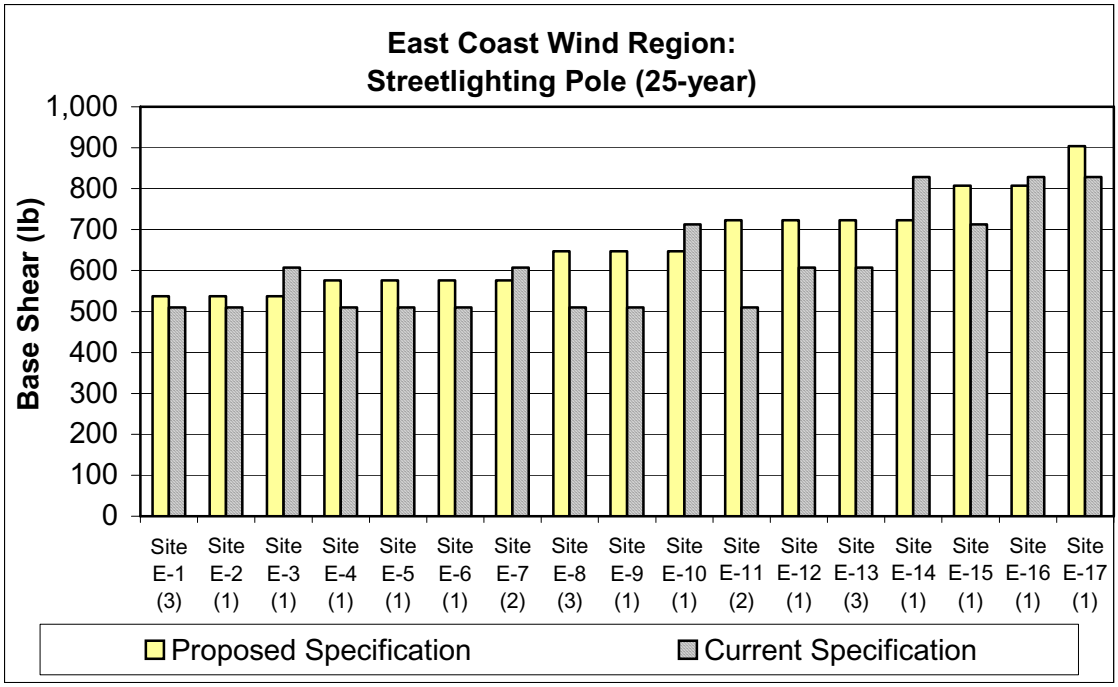

Figure B—137. East Coast Wind Region: Base Shear Comparison for Streetlighting Pole (25-year)

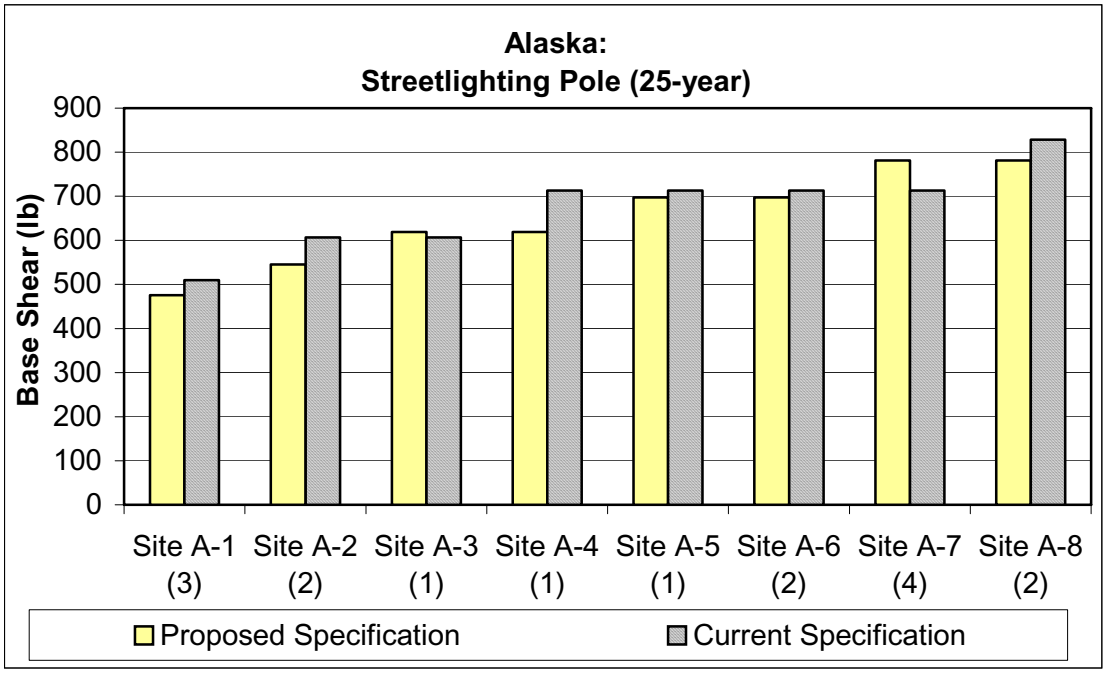

Figure B—138. Alaska: Base Shear Comparison for Streetlighting Pole (25-year)

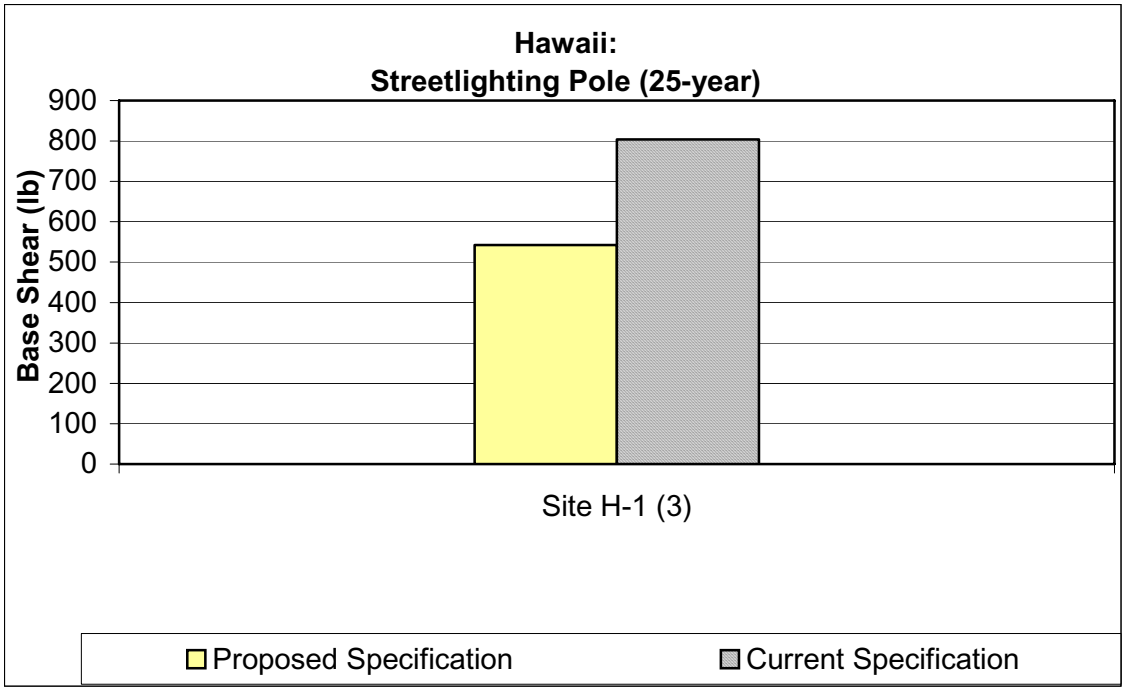

Figure B—139. Hawaii: Base Shear Comparison for Streetlighting Pole (25-year)

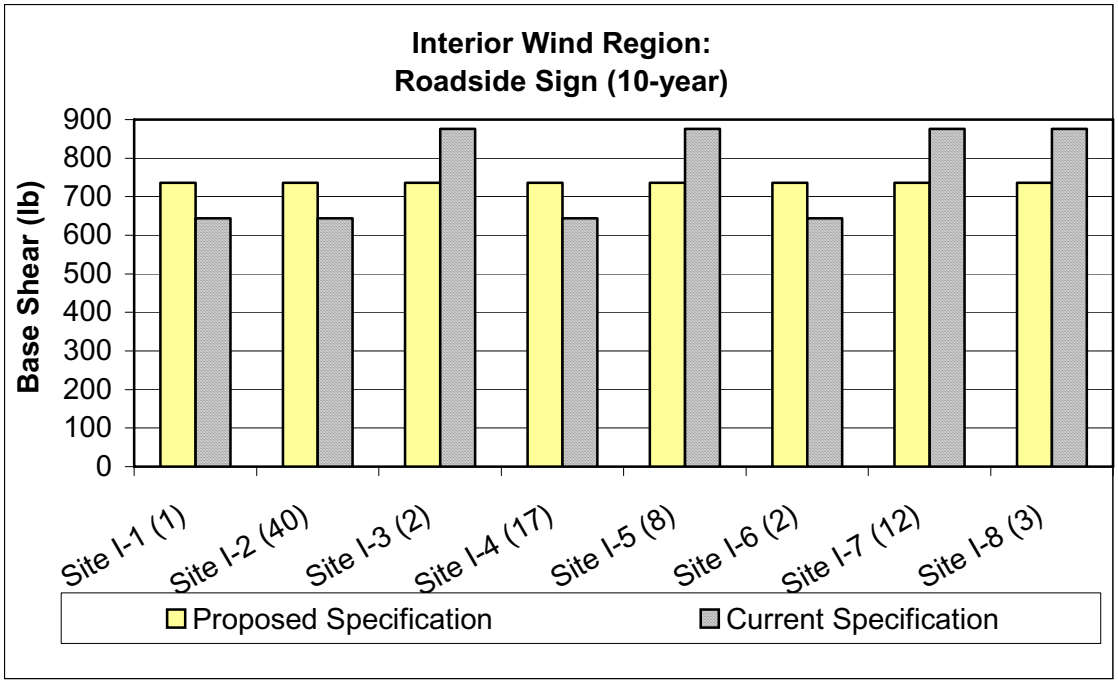

Figure B—140. Interior Wind Region: Base Shear Comparison for Roadside Sign (10-year)

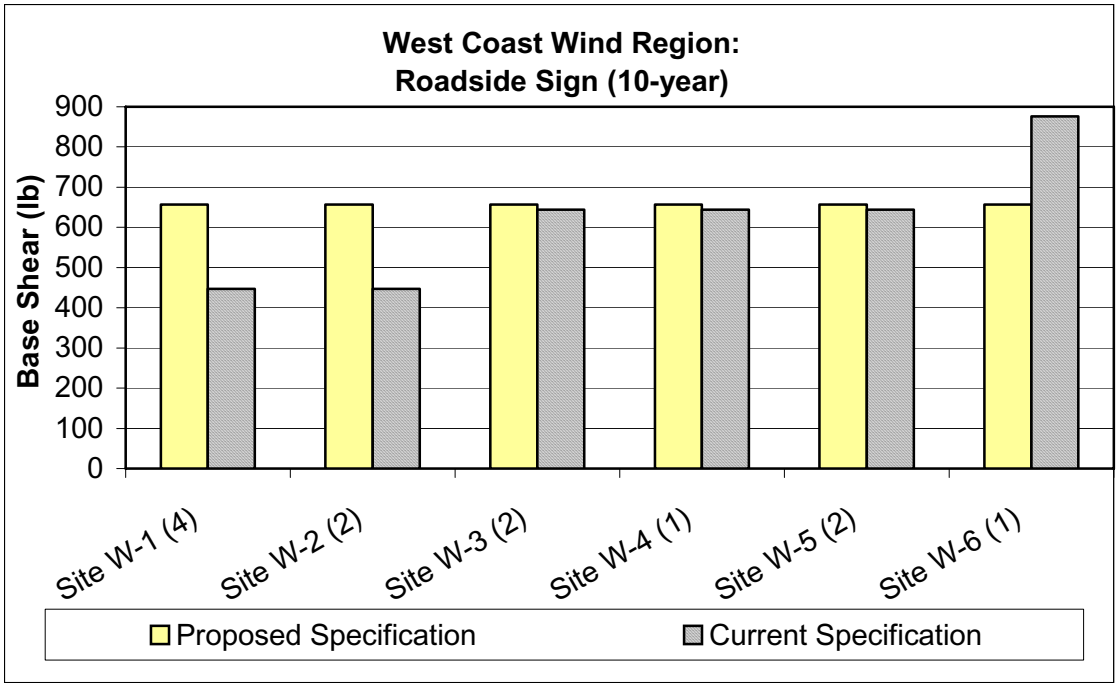

Figure B—141. West Coast Wind Region: Base Shear Comparison for Roadside Sign (10-year)

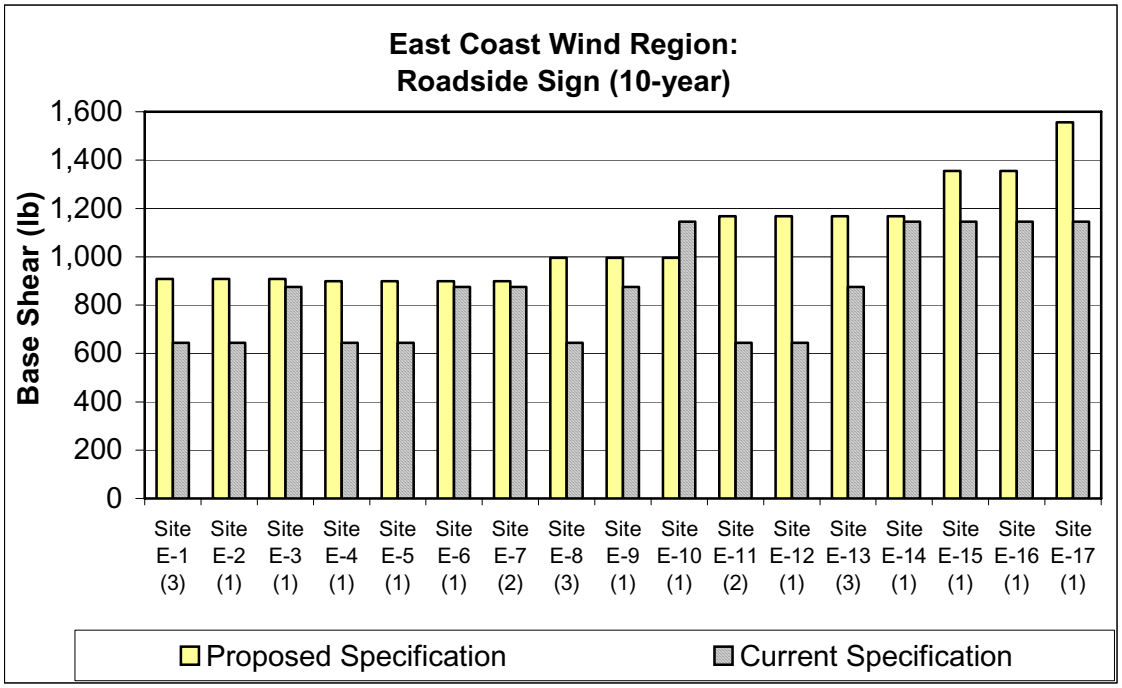

Figure B—142. East Coast Wind Region: Base Shear Comparison for Roadside Sign (10-year)

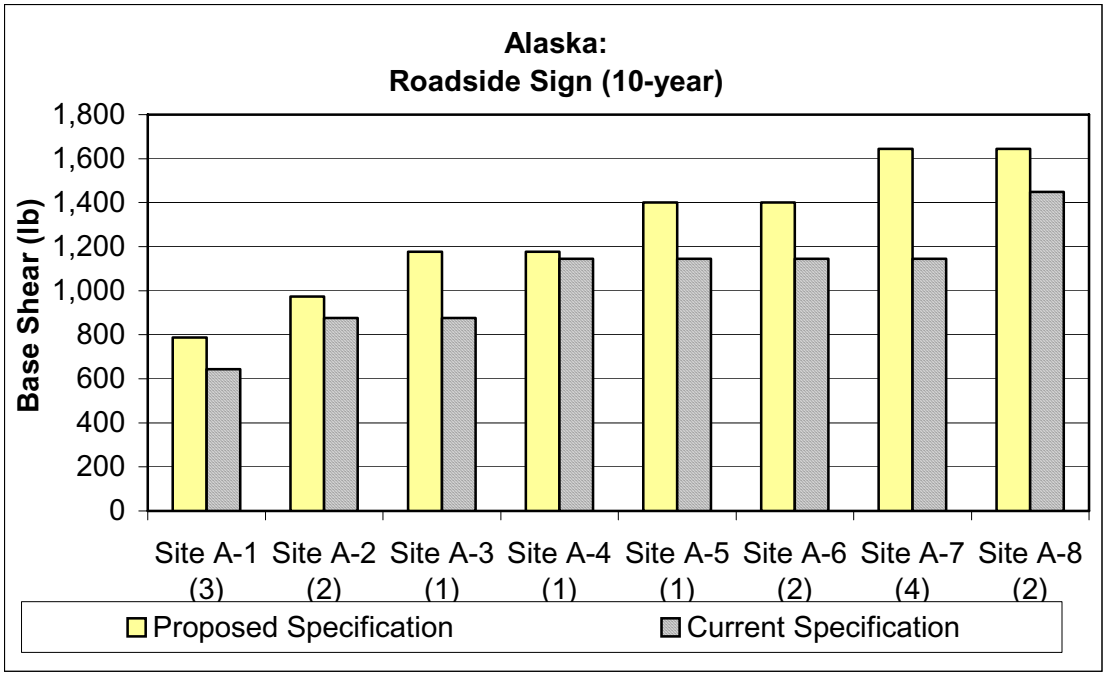

Figure B—143. Alaska: Base Shear Comparison for Roadside Sign (10-year)

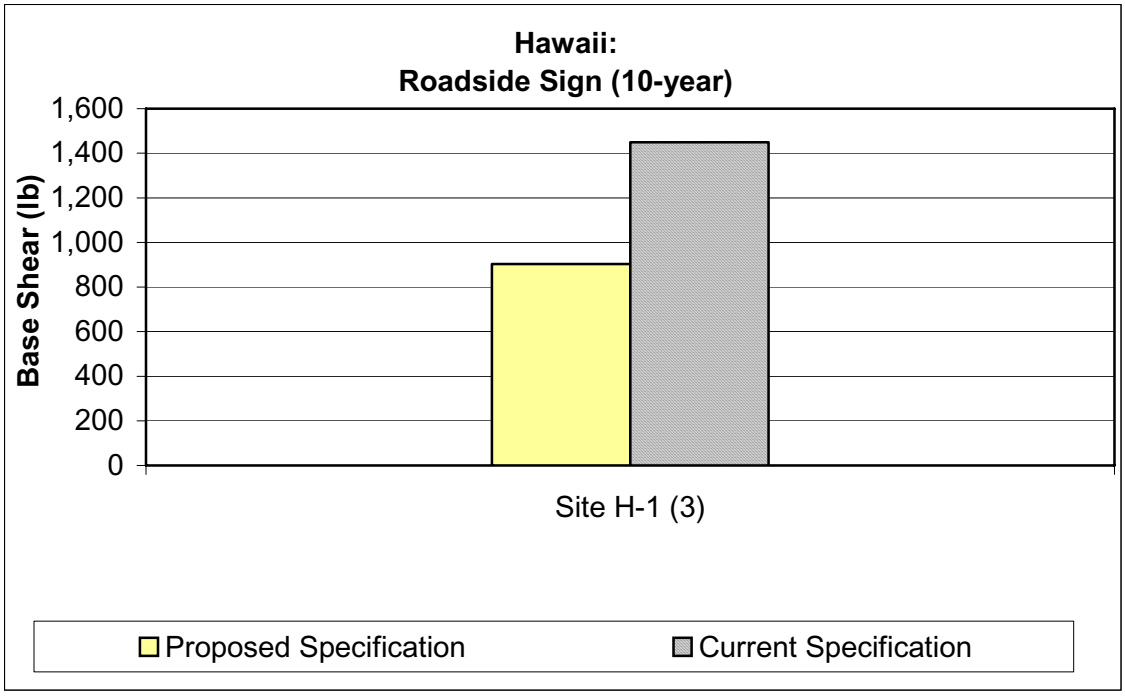

Figure B—144. Hawaii: Base Shear Comparison for Roadside Sign (10-year)

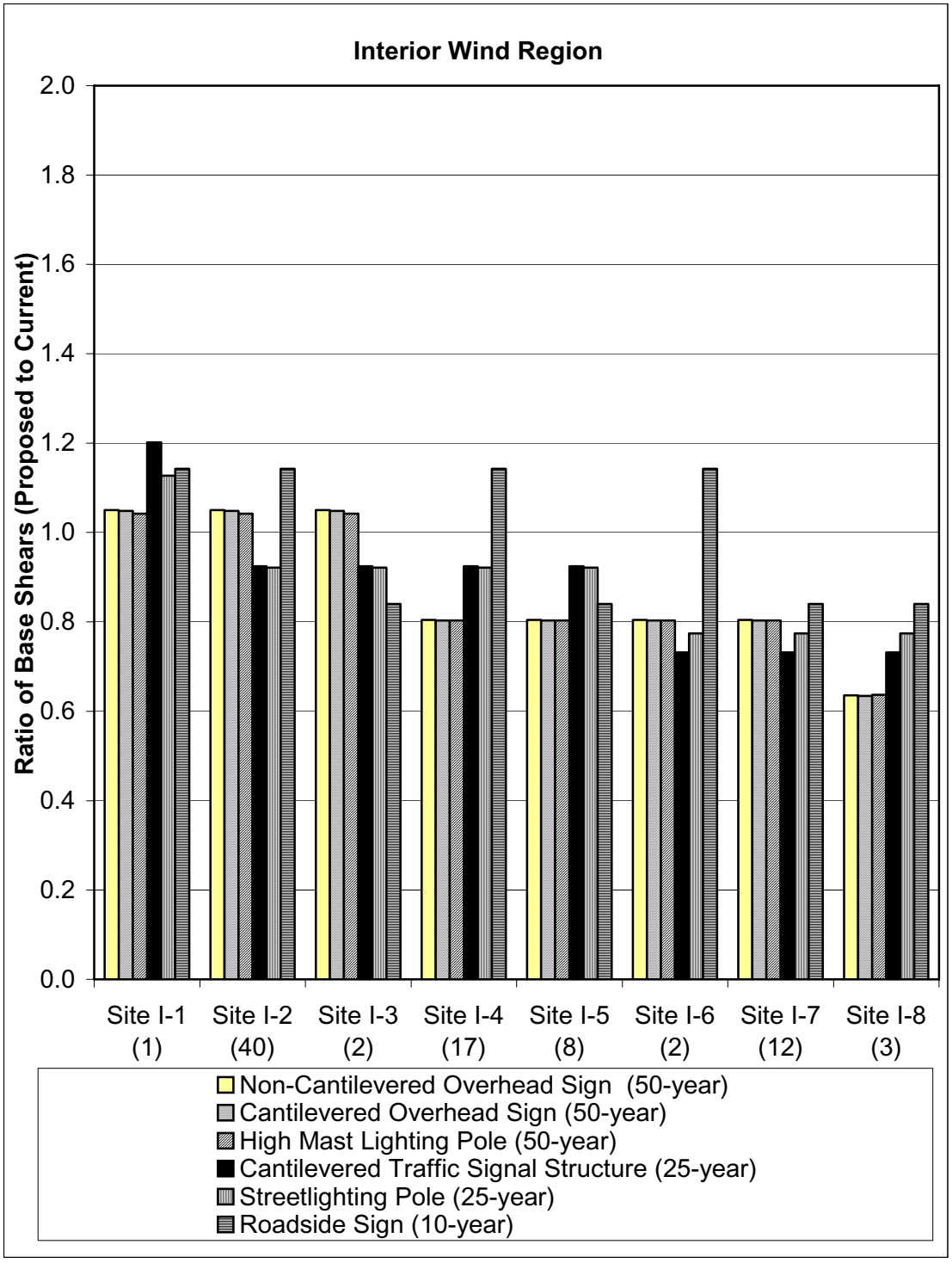

Figure B—145. Interior Wind Region: Ratio of Base Shears (Proposed to Current Specification)

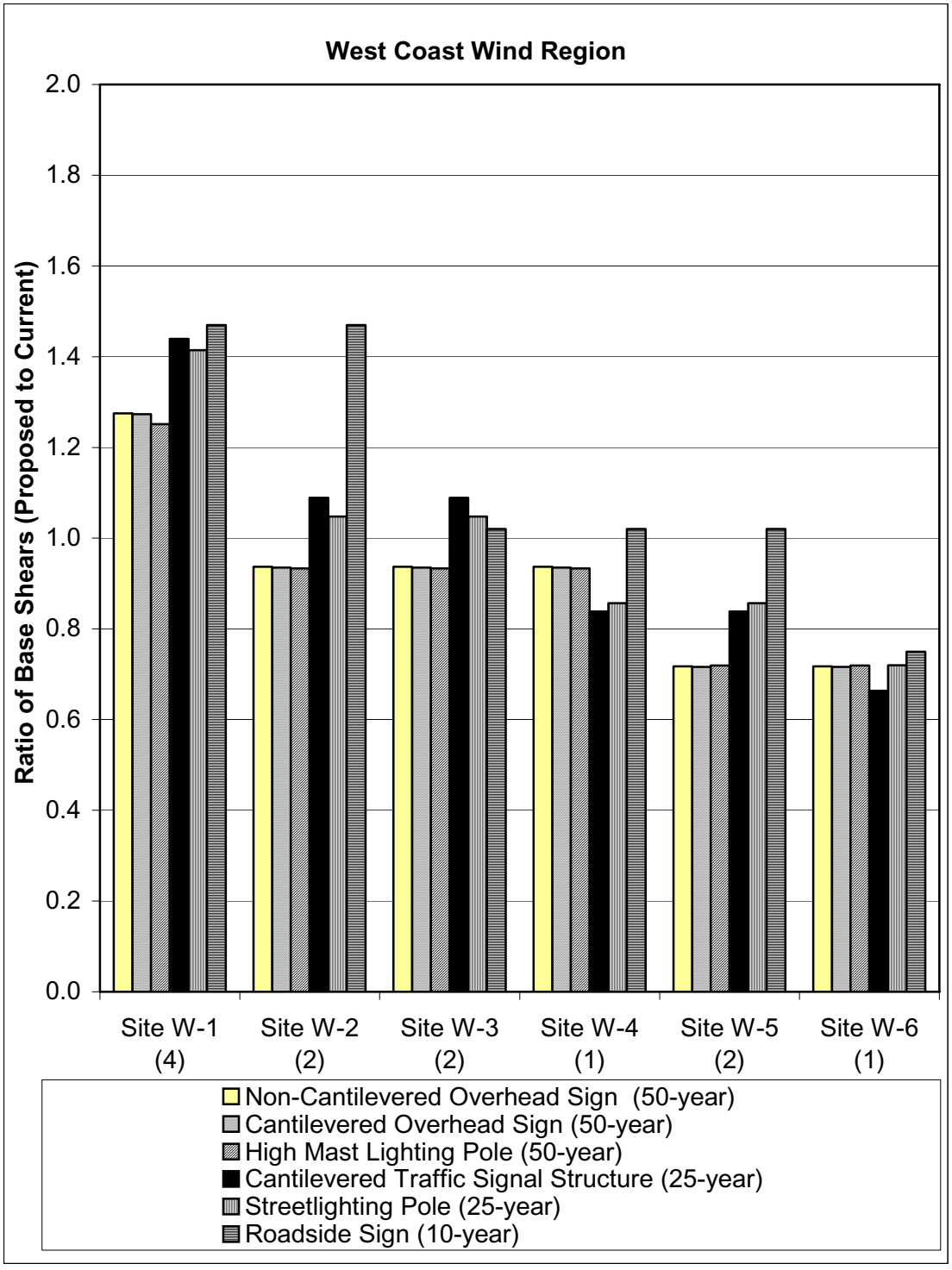

Figure B—146. West Coast Wind Region: Ratio of Base Shears (Proposed to Current Specification)

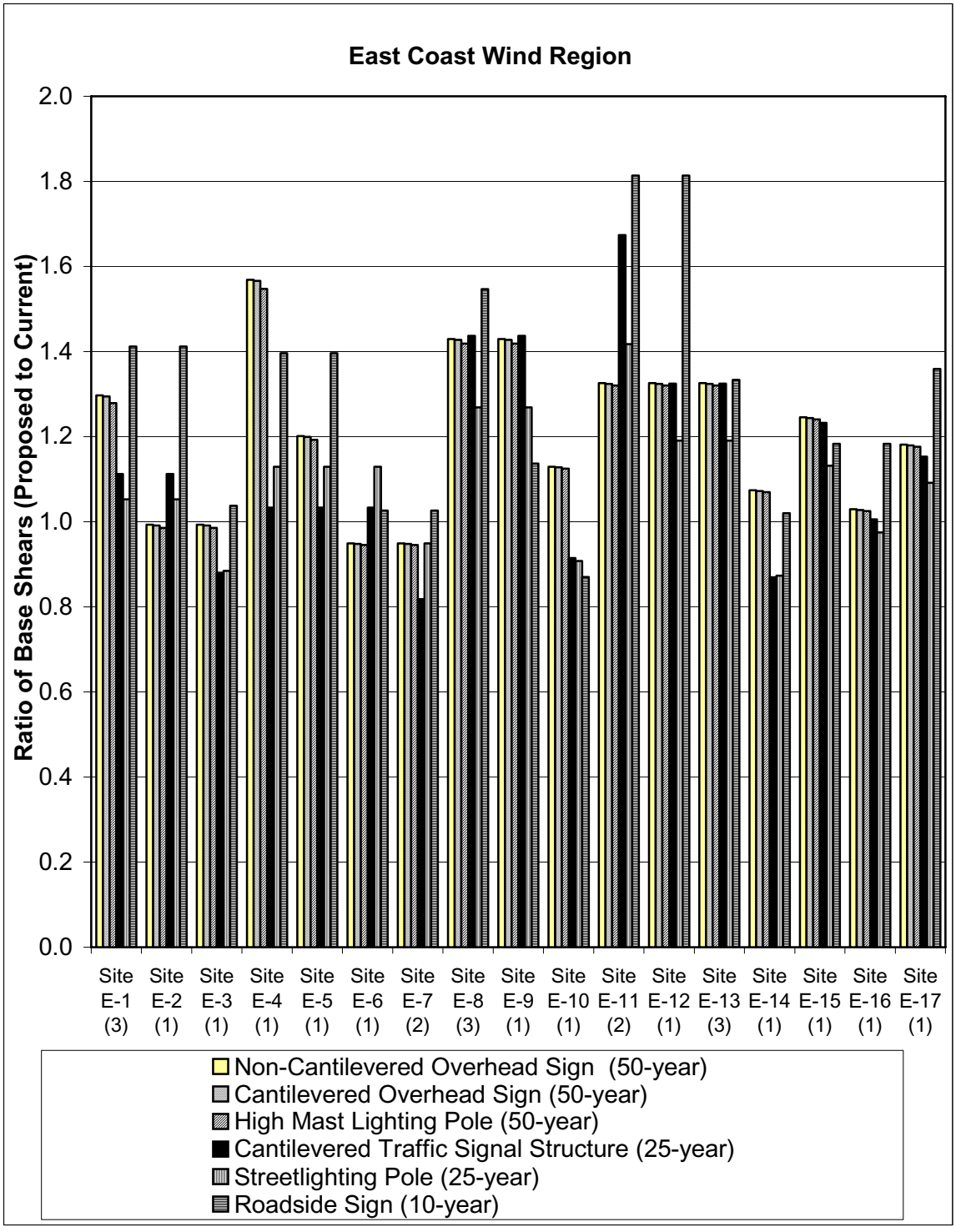

Figure B—147. East Coast Wind Region: Ratio of Base Shears (Proposed to Current Specification)

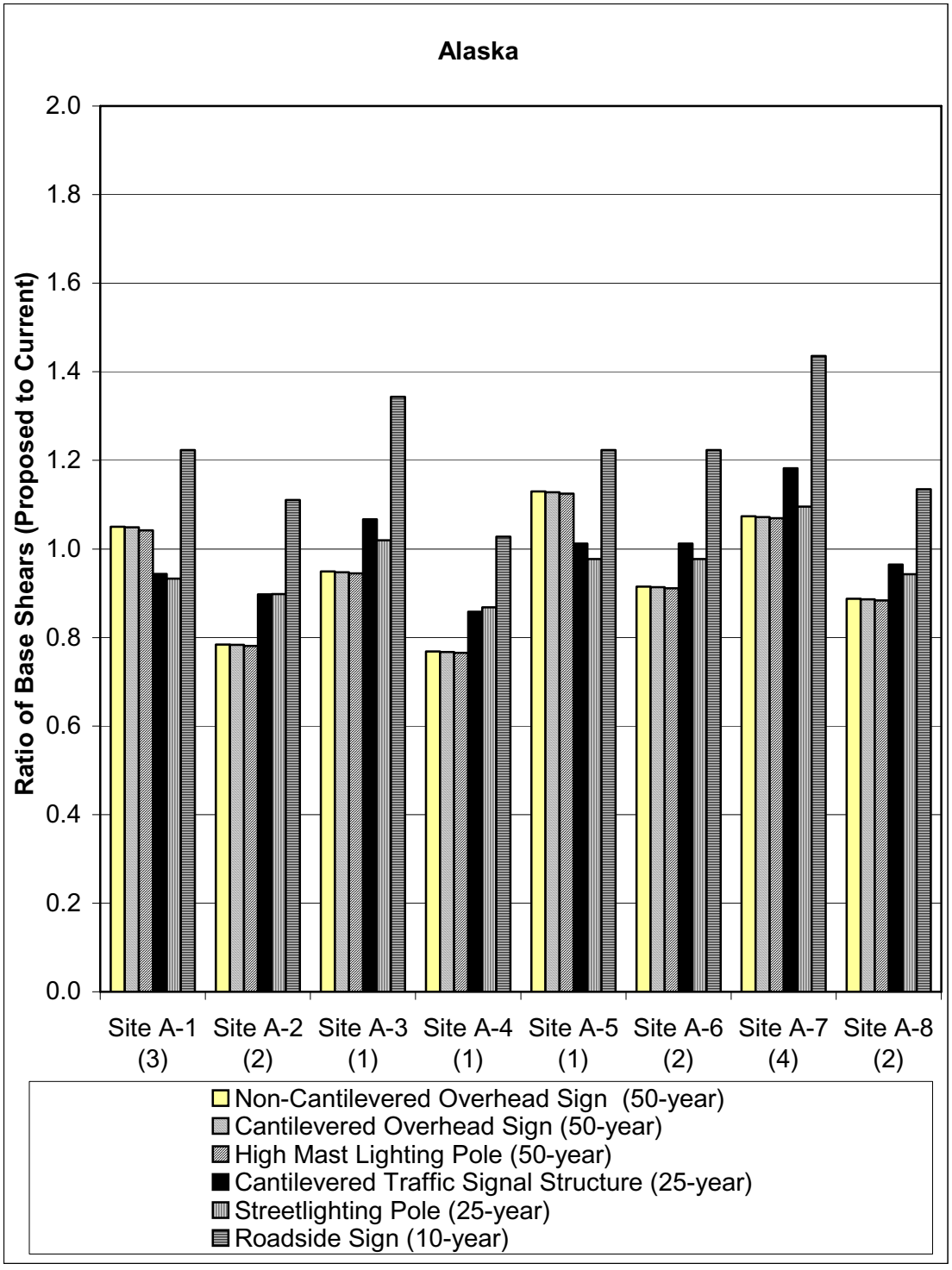

Figure B—148. Alaska: Ratio of Base Shears (Proposed to Current Specification)

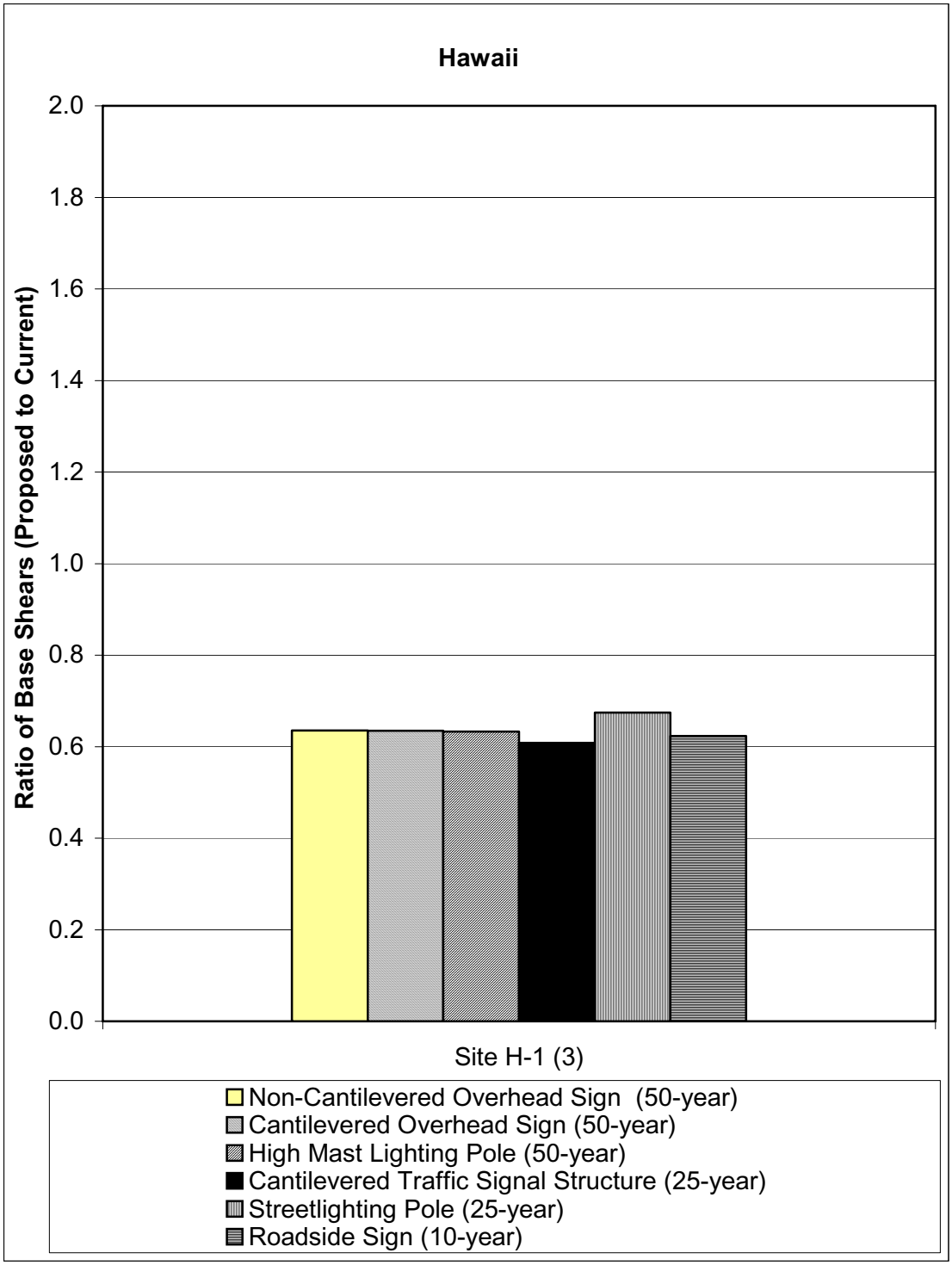

Figure B—149. Hawaii: Ratio of Base Shears (Proposed to Current Specification)

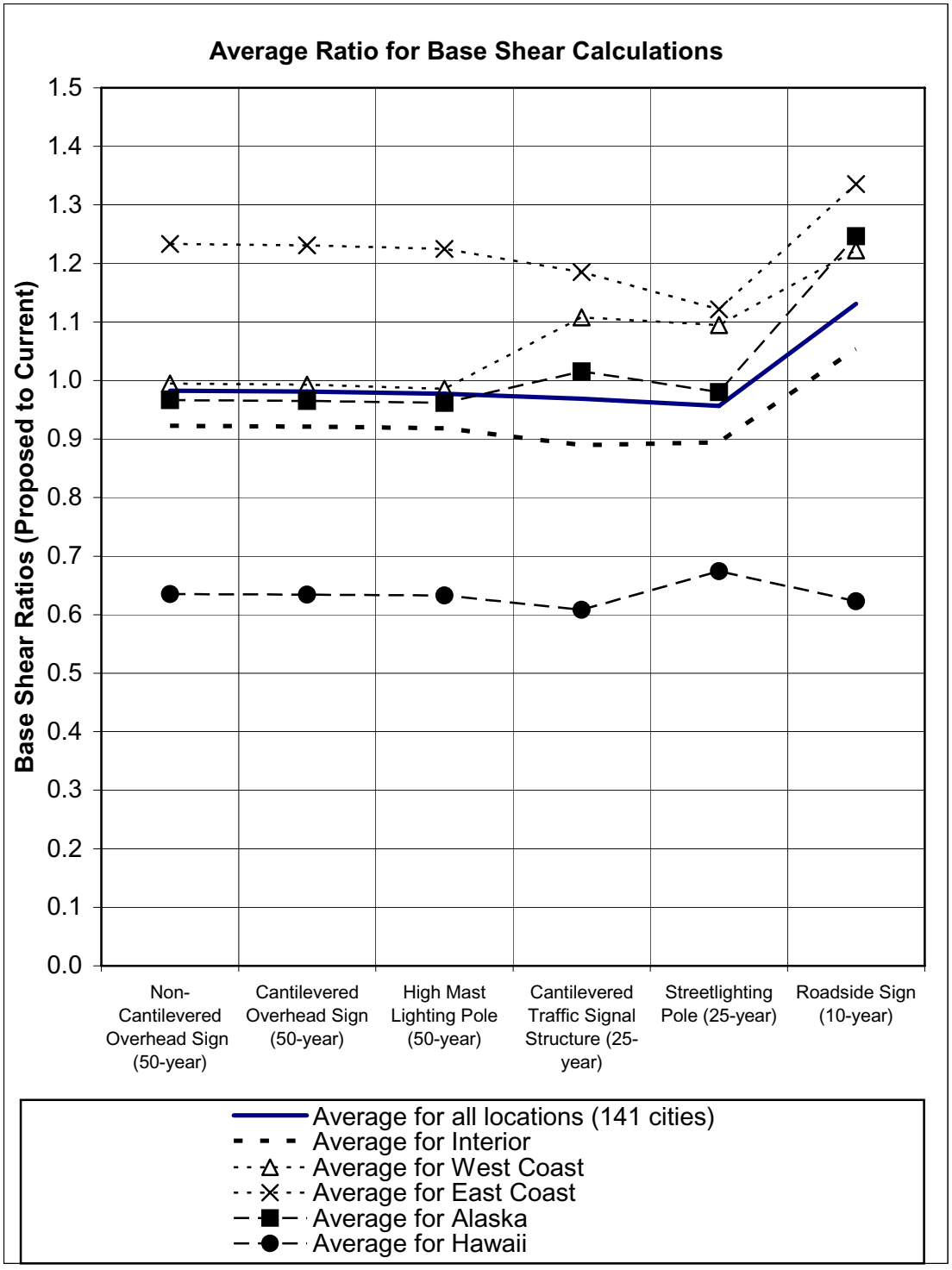

Figure B—150. All Regions (141 Cities): Average Ratio of Base Shears (Proposed to Current Specification)

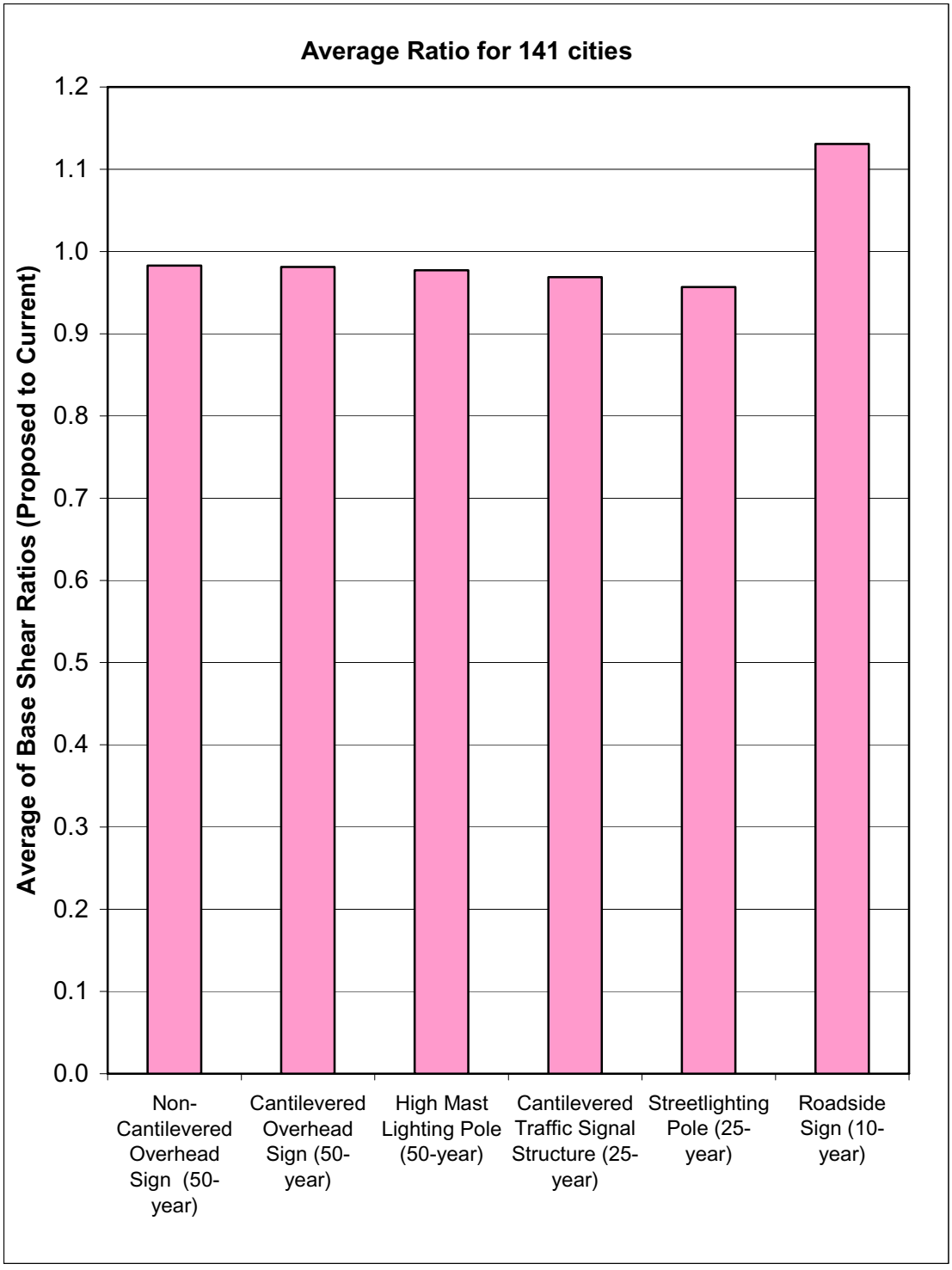

Figure B—151. All Regions (141 Cities): Average Ratio of Base Shears (Proposed to Current Specification)

Appendix C

Proposed Specification and Commentary for the Gust Effect Factor for Wind Sensitive Structural Supports

SPECIFICATION COMMENTARY

Suggested Revisions to (1999) *Supports Specifications*
March, 2000

3.8.5 Gust Effect Factor *G*

The gust effect factor ***G*** shall be taken as a minimum of 1.14.

G is the gust effect factor and it corrects the effective velocity pressure for the dynamic interaction of the structure with the gustiness of the wind. The gust effect factor, ***G***, should not be confused with the gust coefficient that was incorporated in earlier versions of these Specifications. While the two factors accomplish essentially the same purpose, the gust effect factor, ***G***, is multiplied by the pressure, while the gust coefficient is multiplied by the wind speed. Hence, the gust effect factor, ***G***, is the square of the gust coefficient. The proper procedure to calculate either the gust effect factor, ***G***, or the gust coefficient depends upon whether a structure is classified as wind sensitive or not.

Information presented in ANSI/ASCE 7-98 states that if the fundamental frequency of a structure is less than 1 Hz or if the ratio of the height to least horizontal dimension is greater than 4, the structure should be designed as a wind sensitive structure. Thus, it is clear that virtually all structures covered by these Specifications should be classified as wind sensitive structures based on the height to least horizontal dimension ratio. Therefore, it is not appropriate to use a non-wind sensitive gust effect factor, ***G***, for the design of sign, luminaire, and traffic signal structures. Special procedures are presented in the commentary of ANSI/ASCE 7-98 for the calculation of the gust effect factor for wind sensitive structures. The problem is that the use of the gust effect calculation procedure presented in ANSI/ASCE 7-98 for wind sensitive structures would significantly complicate these Specifications. The ANSI/ASCE 7-98 calculation procedure requires reasonable estimates of critical factors such as the damping ratio and fundamental frequency of the structure. These factors are site and structure dependent. Relatively small errors in the estimation of these factors result in significant variations in the calculated gust effect factor. Therefore, even though signs, luminaires, and traffic signal support structures are wind sensitive, the benefits of using the ANSI/ASCE 7-98 gust effect factor calculation do not outweigh the complexities and confusion introduced by its use.

Previous versions of these AASHTO Specifications dealt with the wind sensitivity question by incorporating an increased gust coefficient of 1.3. This gust coefficient corresponds to a gust effect factor of 1.69 = (1.3) (1.3) for use with fastest-mile design

wind speeds. The 1.3 gust coefficient has been with these Specifications since around 1961. It was intended to reflect the wind sensitivity of the types of structures addressed by these Specifications. Its origin can be traced back to a paper by Sherlock (1947) and subsequent wind engineering literature through the 1950's and 1960's. Use of this factor results in higher wind loads than would be expected for structures that are not wind sensitive. As discussed above, it is clear that structures supporting signs, signals, and luminaires are wind sensitive. Thus, the types of structures addressed by these Specifications should be designed for wind loads that are higher than those used to design typical buildings per ANSI/ASCE 7-98. Finally, use of the traditional gust coefficient of 1.3 has resulted in successful designs. Therefore, it was decided to use a three-second gust effect factor, ***G***, that is derived from the traditional fastest mile gust coefficient of 1.3.

First, the fastest-mile gust coefficient of 1.3 must be converted to a three-second gust coefficient. This is accomplished by multiplying the gust coefficient of 1.3 by the ratio of the fastest-mile wind speed to the three-second gust wind speed. This ratio is approximately equal to 0.82 based on information presented in ANSI/ASCE 7-98. The equivalent three-second gust coefficient is thus found to be equal to 1.07 =(1.3)(0.82). The corresponding gust effect factor, ***G***, is then found to be approximately equal to 1.14 by squaring the three-second gust coefficient. It is thus recommended that a gust effect factor, ***G***, of 1.14 be used for the design of structural supports for signs, signals, and luminaires. Structural supports for signs, luminaires, and traffic signals that have been designed with this past philosophy have performed well. Therefore, use of this philosophy is continued.

The following illustrates the relationship between the gust effect factor, ***G***, and the fastest-mile gust coefficient. Neglecting the effects from height above ground, exposure and drag, the use of the gust effect factor of 1.14 with an assumed three-second gust speed will result in essentially the same wind pressure as was determined by the 1994 edition of these Specifications using the 1.3 gust coefficient and the equivalent fastest-mile wind speed. The equivalent fastest-mile wind speed is 82 percent of the three-second gust wind speed.

If the designer wishes to perform a more rigorous analysis than the use of the 1.14 gust effect factor, it is suggested that the gust effect calculation procedure for flexible or dynamically sensitive structures presented in ANSI/ASCE 7-98 be used. The use of the ANSI/ASCE 7-98 gust effect calculation procedure for flexible or dynamically sensitive structures can result in a reduction or increase in the

wind loads depending on the dynamic characteristics of the structure.

Use of Gust Effect Factor of ASCE 7-98 Commentary for Wind-Sensitive Structures

The (1999) *Supports Specifications* has incorporated a single value for the gust effect factor of 1.14. It is recommended that this value be used for wind sensitive as well as non-wind sensitive structures. This value will produce about the same wind pressure on the average as that computed using the current (1994) *Supports Specifications*. Structures with a natural frequency in the along wind direction less than 1 Hertz are considered wind-sensitive; GEF equations for such structures are available in the literature and usually have values exceeding 1.0.

These gust effect factors for wind sensitive structures, however, should be verified by physical wind tunnel testing on typical support structures. Insufficient research is available on gust effect factors for flexible support structures, and the only published information was developed primarily for buildings.

Flexible structures with fundamental frequency less than 1 Hz (period of vibration greater than 1 second) are considered wind-sensitive structures because they can have resonance response in addition to response due to turbulence in wind. The procedure to determine GEF (also called gust response factor) has evolved from the work by Davenport in 1961 (Davenport, 1961). Graphical and analytical procedures are included in the national standards ANSI A58.1-1982, ASCE 7-88, ASCE 7-95 and the latest ASCE 7-98.

GEF Procedure from ASCE 7-98 Commentary

For wind-sensitive structures, GEF in ASCE 7-98 is calculated using the following equation:

$$G = 0.925\left[\frac{1+1.7 I_Z \sqrt{g_Q^2 Q^2 + g_R^2 R^2}}{1+1.7 g_v I_Z}\right] \quad \text{Eq. C 3-1}$$

Parameters in the above equation are determined using a series of equations. Peak factors g_V and g_Q are given as a constant value of ***3.4***. Peak factor g_R is determined as:

$$g_R = \sqrt{2\ ln\ (3600\ n)} + \frac{0.577}{\sqrt{2\ ln\ (3600\ n)}} \quad \text{Eq. C 3-2}$$

where n is the natural frequency of structure in the

SPECIFICATION

COMMENTARY

along wind direction, Hz
ln is the natural logarithm.

Turbulence intensity I_z is determined as:

$$I_z = c\left(\frac{33}{z}\right)^{1/6} \qquad \text{Eq. C 3-3}$$

where ***z*** is the height at which turbulence intensity is assessed; in ASCE 7-98, it is taken as 0.6 times the height of the structure with minimum value shown in Table C3-1
c is a constant (values shown in Table C3-1).

Background response factor ***Q*** is determined using the following equation:

$$Q^2 = \frac{1}{1 + 0.63\left(\frac{B+h}{L_z}\right)^{0.63}} \qquad \text{Eq. C 3-4}$$

where ***B*** is the width of the structure
h is the height of the structure.

Integral length scale L_z is determined as:

$$L_z = \ell\left(\frac{z}{33}\right)^{\epsilon} \qquad \text{Eq. C 3-5}$$

where ℓ and ϵ are constants given in Table C3-1
z is the height above ground used in Eq. C 3-3.

Resonance response factor ***R*** is determined using the following equation:

$$R^2 = \frac{1}{\beta} R_n R_h R_B \left(0.53 + 0.47 R_L\right) \qquad \text{Eq. C 3-6}$$

where β is the critical damping ratio.

Other parameters are determined using the following series of equations:

$$R_n = \frac{7.47N}{\left(1 + 10.3N\right)^{5/3}} \qquad \text{Eq. C 3-7}$$

$$N = \frac{nL_z}{\overline{V}} \qquad \text{Eq. C 3-8}$$

$$\overline{V} = b\left(\frac{z}{33}\right)^{\overline{\alpha}} V\sqrt{I}\left(\frac{88}{60}\right) \qquad \text{Eq. C 3-9}$$

SPECIFICATION

COMMENTARY

where V is the basic design wind speed, mph
I is the importance factor
z is the height above ground used in Eq. C 3-3
$\bar{\alpha}$ and b are constants given in Table C3-1
n is the natural frequency of structure in the along wind direction, Hz, and
L_z is from Eq. C 3-5.

$$R_h = \frac{1}{\eta} - \frac{1}{2\eta^2}\left(1 - e^{-2\eta}\right) \geq 1.0 \qquad \text{Eq. C 3-10}$$

using $\eta = 4.6\frac{nh}{\bar{V}}$

where **n** is the natural frequency of structure in the along wind direction, Hz
$\bar{V}$ is from Eq. C 3-9
h is the height of the structure.

$$R_B = \frac{1}{\eta} - \frac{1}{2\eta^2}\left(1 - e^{-2\eta}\right) \geq 1.0 \qquad \text{Eq. C 3-11}$$

using $\eta = 4.6\frac{nB}{\bar{V}}$

where n is the natural frequency of structure in the along wind direction, Hz
$\bar{V}$ is from Eq. C 3-9
B is the width of the structure across wind.

$$R_L = \frac{1}{\eta} - \frac{1}{2\eta^2}\left(1 - e^{-2\eta}\right) \geq 1.0 \qquad \text{Eq. C 3-12}$$

using $\eta = 15.4\frac{nL}{\bar{V}}$

where n is the natural frequency of structure in the along wind direction, Hz
$\bar{V}$ is from Eq. C 3-9
L is the length of the structure in the direction of wind.

Simplified GEF Equation

Highway structures have limited dimensions. For example, length in the direction of wind is generally small compared to other dimensions. Also, for high-level lighting poles, the dimensions across and along wind are small compared to the height. These specific geometrical characteristics permit simplification of the calculations for GEF. Parametric studies and simplified equations are presented in the subsequent sections.

To assess what are the most critical parameters for GEF, a parametric study is conducted

for the ASCE 7-98 equations. According to the detailed procedure of the ASCE, the variables involved in the equations could be divided into three groups:

Geometric Variables: These variables include the height and width of the structure. It should be noted that for the high-level lighting posts the width is quite small compared to the height.

Wind Characteristics Variables: These variables include turbulence intensity I_z, design wind speed V, longitudinal integral scale L_z, and correlation of gusts.

*Structure Related Variable*s: These variables are structure's natural frequency of vibration n, and critical damping ratio β. There is no analytical procedure to determine critical damping ratio β; it can only be determined from full-scale testing.

For high-level lighting poles, the three parameters that have a significant effect on GEF are found to be wind speed V, structure's frequency of vibration n, and critical damping ratio β. Other parameters such as width and space correlation are taken into account for rigid structures (non-wind sensitive), but are not significant for wind sensitive structures.

Damping is made up of two components, 1) structural (mechanical) damping and 2) aerodynamic damping. The structural damping depends on the material, type of connection, flexibility of structure and rigidity of foundation. Structural damping is not a constant number since it depends on the amplitude of vibration and the participation of different modes of vibration. As a rule, higher modes of vibration will have higher damping. Consequently, the more there is participation of the higher modes, the more the structural damping. For welded steel structures, structural (mechanical) damping may be as low as 0.5% or as high as 2.0% depending on the amplitude of vibration, higher modes of vibration and flexibility of foundation. The aerodynamic damping depends on the amplitude of vibration, the shape of the structure and the wind speed. Therefore, aerodynamic damping can be significant in the case of tall flexible structure with large deflection. There is no theoretical procedure for obtaining damping ratios. Precise damping values could only be determined through full-scale experiments. More information on damping can be obtained from Kareem (1996) and Watanabe (1995). Figure 4.3 shows GEFs calculated using damping range of 0.5% to 3.5%. GEF values vary significantly with the value of the damping ratio. When the damping ratio decreases from 0.02 to 0.01 the GEF increases by about 20%.

SPECIFICATION

COMMENTARY

Simplified Equation for High-Level Lighting Poles

The rational procedure for obtaining GEF for flexible structures given in ASCE 7-98 has been studied thoroughly for the following characteristics of high-level lighting poles:

1. Poles are located in exposure "C".
2. Pole height range from 70 to 200 feet with a practical average of 125 feet.
3. Natural frequency of structures range from 0.2 Hz to 1.0 Hz.
4. Design wind speed range from 90 mph to 150 mph.

The rational procedure of the ASCE 7-98 is modified with series expansion, assumptions, and simplification to yield the following simplified equation:

$$G = \left[0.8 + C\left(\frac{V\sqrt{I}}{n}\right)^{0.64}\left(\frac{1}{\beta}\right)\right] \times \left[0.68 + 16\,\beta\right] \quad \text{Eq. C 3-13}$$

where V is design wind speed, mph
I is the importance factor
n is the natural frequency of structure in along wind direction, Hz
β is the damping ratio
C is a constant = 2.75×10^{-4} (C = 4.6×10^{-4} SI)

Assumptions:

1. Pole width is negligible compared to pole height.
2. Turbulence intensity I_z is taken as 0.20.
3. Since the pole has very small width and depth (in direction of wind), it is assumed that gust space components are perfectly correlated.

In Eq. C 3-13, the second bracketed term becomes 1.0 for damping ratio of $\beta = 0.02$. The correlation of the proposed equation with the ASCE 7-98 rational procedure is studied. It is found that the proposed equation is well correlated for $\frac{V\sqrt{I}}{n}$ in the range of 200 up to 700 where V is expressed in mph. In case $\frac{V\sqrt{I}}{n}$ exceeds the limiting value, it is recommended to use the ASCE 7-98 rational procedure.

In Eq. C 3-13, as well as in the ASCE 7-98

rational procedure, all the terms are well established except for the damping ratio β. As mentioned previously, there is no theoretical or analytical procedure to determine a specific value of damping ratio. However, based on engineering judgment, a damping ratio of 0.02 is quite acceptable for welded steel high-level lighting poles. It is felt that this value is reasonable, and perhaps conservative, because high mast poles are likely to have some aerodynamic damping value in addition to mechanical damping.

Simplified Equation for Signal and Sign Structures

Traffic signal and sign structures are different from high-level lighting poles in two aspects: 1) they are shorter in height and 2) the width of the fixtures is significant compared to the height. This makes the background response component larger than that of the high-level lighting post. Additionally, the resonant response component in the GEF becomes less significant compared to the background one.

In signal light structures, the structures might have cantilever arms with fixtures of significant width, i.e., the ***B*** dimension is significant. To perform calculations using the rational procedure of the ASCE 7-98, some assumptions are made, these are:

1. ***B*** dimension (width of signal fixtures) is 8 feet, equivalent to two signal fixtures.
2. For short lighting poles (h = 25 feet), the ***B*** dimension is 7 feet for the arm length.
3. For structures supporting signs, the width of the sign ***B*** can be 20 feet.
4. The damping ratio is taken as 0.01 and 0.02; results for both values are reported.
5. Wind speeds are considered to be 90 and 150 mph to establish upper and lower bound values of wind speeds.

It is expected that the highest wind speed (150-mph) together with the lowest damping ratio (0.01) will yield the highest GEF. Conversely, the lowest wind speed (90-mph) together with the highest damping expected will yield the lowest GEF. Both combinations of values are used within the ASCE 7-98 procedure to demonstrate the complete range of GEF.

A simplified equation for GEF for such structures is developed. It is similar to that of the high-level lighting posts. The equation is in the following form:

SPECIFICATION

COMMENTARY

$$G = \left[0.95 + C\left(\frac{V\sqrt{I}}{n}\right)^{0.64}\left(\frac{1}{\beta}\right)\right] \quad \text{Eq. C 3-14}$$

where V is design wind speed, mph
I is the importance factor
n is the natural frequency of structure in the along wind direction, Hz
β is the damping ratio
$C = 2.75 \times 10^{-4}$ ($C = 4.6 \times 10^{-4}$ SI)

Assumptions:

1. Turbulence intensity I_z is taken as 0.20.
2. Since the dimensions are relatively small, gust space components are correlated.

It should be noted that the constant term in the equation is larger in value compared to that of the high-level lighting posts. This is due to the fact that the height is not large (i.e., the wind forces are well-correlated over the structure). Moreover, the equation does not need the correction factor $[0.68 + 16\,\beta]$ that appeared in Eq. C 3-13 since resonance response is not dominating.

Attention should be given to the variable n since it is not the across (perpendicular to) wind natural frequency of vibration, but it is the along (in the direction of) wind one.

The damping ratio for such structures is recommended to be taken as 0.015 as they are not supposed to have as large amplitudes as the high mast poles; therefore, the aerodynamic damping will be low.

Eq. C 3-14 gives well-correlated results for $\frac{V\sqrt{I}}{n}$ values up to 400 where V is expressed in mph.

Summary

Gust effect factor for non-wind sensitive highway structures, which have an along-wind natural frequency greater than 1 Hertz, will usually be in the range of 0.8 to 1.0. However, for simplicity, and in order to account for the flexibility of support structures in general, a unified gust effect factor (GEF) of 1.14 could be used, as provided by the proposed AASHTO (1999) specification.

In general, for wind sensitive highway support structures, which have an along-wind natural frequency less than 1 Hertz, the GEF that is provided by ASCE 7-98 (Eq. C 3-1) may be used.

SPECIFICATION

COMMENTARY

The GEF for wind sensitive structures has been simplified for certain support structures. For tubular steel high mast lighting structures with heights greater than 70 feet, Eq. C 3-13 may be used, where $\frac{V\sqrt{I}}{n}$ is in the range of 200 up to 700.

For traffic signal structures, overhead sign structures, and streetlighting poles, Eq. C 3-14 may be used and is valid for $\frac{V\sqrt{I}}{n}$ values up to 400.

Roadside signs are not anticipated to be wind-sensitive. Since most of these structures will have an along wind natural frequency greater than 1 Hertz, the gust factor of 1.14 can be applied to these structure types.

Until further research is performed to verify the GEF for wind sensitive and non-wind sensitive structural supports, it is recommended to use the GEF of 1.14 for all structure types as provided in the proposed *Supports Specifications*. While this factor is greater than the GEF for non-wind sensitive structures, it is smaller than the GEF for wind sensitive structures. Additionally, the use of the GEF of 1.14 will result in wind pressures that are on the average comparable to the wind pressures computed using the current (1994) *Supports Specifications*, for which satisfactory structural performance has been demonstrated.

Table C3-1. Constants for GEF (ASCE 7-98)

Exposure	b	c	ℓ (ft)	$\in$	$\bar{\alpha}$	z_{min} (ft)
Suburban B	0.45	0.30	320	1/3	1/4.0	30
Open C	0.65	0.20	500	1/5	1/6.5	15
Water D	0.80	0.15	650	1/8	1/9.0	7

REFERENCES

Davenport, A.G., “The Application of Statistical Concepts to the Wind Loading of Structures,” *Proceedings*, Institution of Civil Engineers, Vol. 19, Paper 6480, 1961.

Minimum Design Loads for Buildings and Other Structures, ANSI A58.1-1982, American National Standards Institute, New York, NY, 1982.

Standard Minimum Design Loads for Buildings and Other Structures, ANSI/ASCE 7-88, American Society of Civil Engineers, New York, NY, 1990.

Standard Minimum Design Loads for Buildings and Other Structures, ANSI/ASCE 7-93, American Society of Civil Engineers, New York, NY, 1994.

Standard Minimum Design Loads for Buildings and Other Structures, ANSI/ASCE 7-95, American Society of Civil Engineers, New York, NY, 1996.

Minimum Design Loads for Buildings and Other Structures, ASCE 7-98, American Society of Civil Engineers, New York, NY, 1999.

Appendix C

Fatigue Resistant Design of Noncantilevered Sign Support Structures

TABLE OF CONTENTS

LIST OF FIGURES

LIST OF TABLES

CHAPTER 1. INTRODUCTION AND RESEARCH APPROACH

1.1 Background

Highway sign support structures are designed in accordance with the American Association of State Highway and Transportation Officials (AASHTO) "Standard Specifications for Structural Supports for Highway Signs, Luminaires and Traffic Signals", (adopted in 1994). These specifications contain provisions that specify that support structures should be designed for infinite fatigue life in accordance with the procedure outlined in the AASHTO "Standard Specification for Highway Bridges"(1994). As a result, designers are faced with significant uncertainty when applying the provisions of the AASHTO bridge specifications to the design of sign support structures for fatigue.

In 1993, the National Cooperative Highway Research Program (NCHRP) initiated Project 10-38, "Fatigue-Resistant Design of Cantilevered Signal, Sign, and Light Supports," to develop guidelines for the fatigue resistant design of cantilevered sign, signal, and luminaire support structures. At approximately the same time (1994), NCHRP initiated Project 17-10, "Structural Supports for Highway Signs, Luminaires, and Traffic Signals," to update the 1994 edition of the "Standard Specifications for Structural Supports for Highway Signs." Neither of these projects addressed the design of noncantilevered sign support structures. In January 1998, NCHRP Project 17-10(2) was initiated to address sign support issues that were not adequately addressed under Project 17-10, including the fatigue-resistant design of noncantilevered support structures.

The report presented herein addresses issues related to fatigue and vibration in noncantilevered sign support structures. It begins by investigating the applicability of some aspects of the results of Project 10-38 and 10-38(2) to noncantilevered structures. This includes static fatigue limit load ranges, maximum dynamic deflection limits, connection details to minimize fatigue effects, and other related aspects.

1.2 Research Objectives

The primary objective of this research was to develop guidelines for fatigue resistant design for noncantilevered sign support structures. In order to achieve this goal, a comprehensive research program, including a review of the related literature and analytical study, has been performed. The following specific points were investigated:

1. Current vibration and fatigue concerns for noncantilevered support structures.
2. Equivalent static load ranges.
3. Allowable deflection limits.

4. Evaluating and categorizing connection details according to fatigue resistance.
5. Effectiveness of gussets.
6. Vibration mitigation measures.

1.3 Scope

NCHRP Project 10-38 dealt with fatigue resistant design of cantilever sign support structure. This study considers the noncantilevered overhead bridge structures (supported at both ends), including monotube and truss structures. The structures selected for analytical studies were chosen to encompass spans and materials that are typically used for noncantilevered sign support structures.

1.4 Research Approach

The first task of the research was to identify the present vibration and fatigue concerns for noncantilevered sign support structures. As part of NCHRP Project 17-10(2), surveys were sent to state DOTs and manufacturers to determine fatigue concerns for noncantilevered support structures.

A major part of this research was to establish equivalent static load ranges that represent the fatigue loads for noncantilevered structures. This was done through static and dynamic finite element analysis on selected structures. First, selected cantilevered structures were analyzed to obtain the dynamic load configuration that represents the various wind load phenomena, and then this dynamic load was applied to cantilevered support structures. Finally, a static analysis was done for the noncantilevered support structure to determine the applicability of the equivalent static load used for cantilevered to noncantilevered support structures.

Typical connection details used for noncantilevered structures were categorized following the same approach used by NCHRP Project 10-38. The drawings and standards obtained from state department of transportation (DOT) offices were reviewed, and factors that affect the fatigue resistance were studied.

1.5 Organization

CHAPTER 1 - INTRODUCTION AND RESEARCH APPROACH, begins with a general introduction. Then, the main objectives of this research are summarized. Finally, the scope and the research approach are discussed before introducing the organization of the report.

CHAPTER 2 - LITERATURE REVIEW, provides a review of related research. First, the different wind phenomena associated with support structures are introduced. Then, the susceptibility of the noncantilevered support structures for these loading phenomena is assessed, followed by an explanation of the variable amplitude fatigue. The next section

describes previous research that deals with static and dynamic behavior of noncantilevered sign support structures. The last section reviews recent research on fatigue resistant design of cantilevered structures.

CHAPTER 3 - EQUIVALENT STATIC FATIGUE LOADS FOR NONCANTILEVERED SUPPORT STRUCTURES presents the findings of this research by first specifying the vibrations and fatigue concerns for noncantilevered structures and then moving to a step-by-step illustration for the work done to develop the equivalent static ranges.

CHAPTER 4 - FATIGUE CATEGORIZATION OF CONNECTION DETAILS FOR NONCANTILEVERED SUPPORT STRUCTURES presents proposed categorization of connection details and the bases for this categorization.

CHAPTER 5 - EFFECTIVENESS OF GUSSETS IN SIGN SUPPORT STRUCTURES introduces the findings of the latest literature available and provides an example to demonstrate the effect of gussets.

CHAPTER 6 - VIBRATION MITIGATION MEASURES IN SIGN SUPPORT STRUCTURES shows vibration mitigation measures for each wind phenomena and then introduces the findings of the research done in Florida and Wyoming. Finally the effect of increasing the damping on the response of support structures to dynamic loads is illustrated.

CHAPTER 7 - INTERPRETATION AND APPLICATION, provides a review of specific areas of the current specifications. These areas include the static loads that represent fatigue for support structures, allowable deflection limits, and fatigue resistance of connection details. Chapter 4 also introduces proposed modifications to Chapter 11 of the support specifications.

CHAPTER 8 - SUMMARY, CONCLUSION, AND SUGGESTED RESEARCH, summarizes the main conclusions of this study and provides recommendations for future research.

CHAPTER 2. LITERATURE REVIEW

2.1 Wind Loads on Support Structures

Wind loads are the primary dynamic loads to which sign support structures are exposed. Wind loads develop variable amplitude stresses. Support structures are subjected to several types of wind loading phenomena. Four types of the most common wind loading cases are galloping, vortex shedding, natural wind gust, and truck-induced wind gust.

2.1.1 Galloping

Galloping is a phenomenon where large amplitude oscillations occur in a direction normal to the wind flow at frequencies lower than those of vortex shedding. It is an aeroelastic phenomenon caused by coupling between the aerodynamic forces and the structural vibrations. It can be explained by considering the "D"-shaped cross-section shown in Figure 2.1 that is exposed to a flow velocity normal to face *AB* at rest. When this body moves with a velocity $Y^{\cdot}$, the relative velocity of the flow will be *V'*. This will make the flow asymmetric, causing a difference in pressure between points and *B* and, hence, generating a lift force in the *y* direction. The resulting force will accelerate the motion of the body. This force will change periodically as the structural element is subjected to a periodic change in the angle of attack of the wind flow.

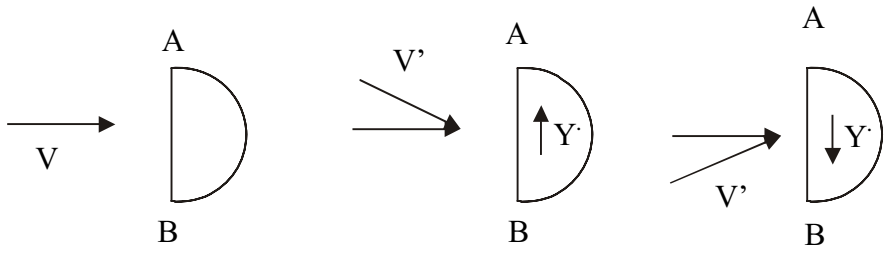

Figure 2.1. Galloping of D-Shape (Asymmetric Cross Section)

Hartog defined the condition necessary for galloping instability as

$$\left(\frac{\partial C_L}{\partial \alpha} + C_D\right)\Big|_{(\alpha=0)} < 0 \tag{2.1}$$

where C_L is the lift force coefficient, C_D is the drag coefficient, and α is the angle of attack is given by

$$\alpha = \tan^{-1}(\frac{\dot{Y}}{V}) \tag{2.2}$$

Circular cylinders, which are used in many support structures, will not gallop because of symmetry. However, rectangular sections representing the attachments to these structures are susceptible to galloping. Novak (1972) and Parkinson *et al*. (1961) proposed analytical models based on experimental information and nonlinear analytical models to describe galloping of prismatic structures. These models cannot be used for complicated cases such as sign support structures.

2.1.2 Vortex Shedding

When a uniform steady flow is obstructed by a structural element, vortices are shed in the wake of the structural element. If the frequency of the developed vortices approaches one of the natural frequencies of the structure, significant displacement would take place in a plane normal to the direction of flow. Von Karman studied this phenomenon for perfect fluid. He found that the double row vortices would be stable if the vortices of one row are halfway between the vortices of the other rows and the two rows are spaced at 0.281 times the distance between two vortices. This configuration is shown in Figure 2.2.

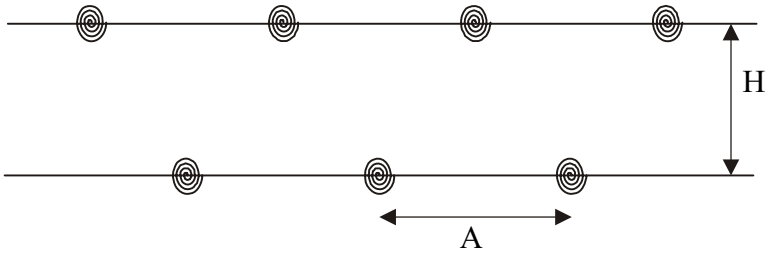

H/A = 0.281

Figure 2.2. Von Karman Vortex Sheet

For a wind flow over cylindrical structural members with small Reynolds number (*R*), the flow is smooth and unsupported. As *R* increases, two vortices are developed in the wake of the element, as shown in Figure 2.2. Vortices start to shed when *R* approaches 40 as the two vortices move downstream. The vortices are stable and can be modeled using the Karman sheet up to *R*=300. Above *R*=300, vortices still have deterministic frequency but variable amplitude. For *R* greater than $3x10^5$, the flow becomes turbulent. Previous research (Kaczinski *et al*. 1996) found that the three dimensional characteristics of the attachment (signs and signals) interfere with the formation of a stable set of vortices at a specified frequency. The frequency for vortex shedding is given by the Strouhal relation:

$$f_s = \frac{S \cdot V}{D} \tag{2.3}$$

S is the Strouhal number, D is the across wind dimension of the element, and V is the wind flow velocity. For monotube structures, the Reynolds number R is given by Equation 2.4.

$$R = (780.5)(V)(D) \tag{2.4}$$

where V is the wind speed in miles per hour and D is the cylinder diameter in inches. For the diameters typical of sign support structures (10-15 inch), the maximum value of $3x10^5$ for R after which the vortices do not shed is reached at 25-40 mph. Also, the magnitude of the vortex shedding force developed by winds below 10 mph will not develop significant displacement in sign support structures. However, the support structure can exhibit vortex shedding vibration for wind velocities between 10 and 25 mph.

2.1.3 Natural Wind Gusts

Both velocity and direction of wind are random. This tends to develop vibration in light structures at different frequencies. At frequencies near the natural frequencies of the structure, the structure will vibrate in the corresponding mode shape, causing large displacement and forces. The static component of the drag is given by Equation 2.5.

$$D = (1/2)\, \rho\, C_D\, A\, V'^2 \tag{2.5}$$

Where ρ = the air density (0.0024 slugs/ft^3), C_D = drag coefficient, A = the exposed area of structure to wind, and V' = mean wind velocity. This value of drag is magnified by a gust factor to account for turbulence. AASHTO uses a value of 1.3 for C_D . The resulting value of maximum expected wind pressure is used in ultimate strength design but cannot be used in fatigue design since the design for fatigue is based on service load.

2.1.4 Truck-induced Wind Gusts

When a truck passes under overhead sign support structures, two types of pressure are developed. The first type is horizontal in the direction of traffic, and is a function of the frontal area of the sign and the structure elements. The second type acts vertically normal to the direction of traffic and is a function of the projected area of the sign, attachment, and structure elements. Several research efforts have been conducted to estimate the loads due to truck passage. Creamer, *et al*. (1979) represented these two loads by a horizontal triangular pressure distribution with a peak of 60 Pa (1.25 psf) at the center of the sign and a uniform vertical pressure distribution of 60 Pa (1.25 psf). Based on experimental results, they concluded that forces due to truck passage are not critical for fatigue. However, Kaczinski *et al*. (1996) used the values Desantis and Haig (1996)

proposed for the vertical pressure anticipated for truck passage since these values agreed with the analysis of some variable message sign (VMS) support structures that failed due to fatigue. This is presented in more detail in the following chapters.

2.2. Susceptibility of Noncantilevered Support Structures to Wind Induced Vibration

The survey that was conducted as part of NCHRP Project 17-10(2) revealed that eight states out of the 48 replies received identified problems with overhead bridge structures. Unfortunately, little documentation of such vibration problems is available and therefore it is difficult to analyze the susceptibility of these structures to various wind phenomena. To help determine the susceptibility of noncantilevered support structures for different fatigue loading phenomena, the research team communicated directly with researchers, manufacturers, and state DOT engineers.

In a meeting with researchers of NCHRP Project 10-38, it was explained that it is difficult to get galloping to occur in lab conditions, except when wind is applied at 45 degrees, where some galloping has been observed in two-chord cantilevered trusses. NCHRP Project 10-38 researchers indicated that it is not likely that noncantilevered truss support structures are susceptible to galloping. However, no experimental work has been done to support whether galloping can occur. In meeting with engineers at a local sign support manufacturer with many years of experience in sign support design and manufacturing, it was described that steel noncantilevered very rarely have vibration problems. More problems have been noted in aluminum structures. Furthermore, it was noted that, when vibration problems have occurred, there was usually substantially less mass attached to the structure than called for in the design.

Several studies investigated the dynamic behavior of noncantilevered support structures (Mirza *et al*. (trichord), Ehsani *et al*. (monotube), Lundgren (monotube)). In these studies, vibration in the vertical direction was assumed to be due to loads that represent vortex shedding. The conditions necessary for galloping to occur can be summarized as a periodic change in angle of wind attack and the asymmetry due to the sign panel attached to support structures. Galloping forces will change periodically as the structural element is subjected to a periodic change in the angle of attack of the wind flow. The conditions necessary for vortex shedding to occur can be summarized as vortices that develop in the wake of the structural element under steady wind flow at specific range of frequency. The conditions necessary for natural wind to occur can be summarized as exposure to natural wind gusts. The conditions necessary for truck-induced gust to occur can be summarized as having the structure height less than 33.67 ft and exposed to the pressures due to the passage of trucks.

Since the conditions needed for each wind load case do exist and vibration attributed to these phenomena has been observed, it was conservatively assumed in this study that the support structures are susceptible to all four vibration inducing wind load phenomenon identified for cantilevered support structures. The finite element method can be used to determine the natural frequency of the structures and therefore help to

understand some susceptibility issues. However, the answer to the question of whether noncantilevered structures are susceptible to galloping is not totally resolved due to a lack of data. Additional research using other methods such as wind tunnel tests and field observations is needed and is beyond the scope of this research.

2.3 Variable Amplitude Fatigue

The AASHTO (1994) bridge specifications define the nominal fatigue resistance as a function of the number of stress cycles, which can be estimated in terms of average daily traffic (ADT). Also, the maximum load can be predicted using the heaviest truck load. For these reasons, S-N curves based on constant amplitude loading are used. In addition, several studies have been conducted to evaluate the effect of variable amplitude loading and infrequent exceeding of the load above the constant amplitude fatigue limit. Fisher *et al*. (1993) concluded that the existence of a fatigue limit below which fatigue cracks propagate is assured only if none of the stress range cycles exceeds this constant amplitude fatigue limit. If any of the stress range cycles (as few as 1 per 1000 cycles) exceed the limit, fatigue crack propagation will likely occur.

For structural sign supports, the main fatigue loading is wind. Unlike bridge fatigue loads, the wind loading varies widely and rapidly, which causes many more loading cycles. Kaczinski *et al*. (1996) used the infinite life approach for cantilevered sign support structures. They developed equivalent static ranges for "fatigue limit-state" that will produce a static response similar to the dynamic response. Stress ranges at critical details calculated using the fatigue limit-state load ranges should not exceed the constant amplitude fatigue limit (CAFL) of these details. This approach is also used in the present research.

2.4. Static and Dynamic Behavior of Noncantilevered Sign Support Structures

Evaluation of noncantilevered sign support structures has been investigated by many researchers. An early study on static and dynamic behavior of two tri-chord truss overhead sign support structures was performed by Mirza, *et al*. (1975). The chord column connection was examined experimentally by applying static loads to get a relationship among moment, load, and angle change. Repeated load tests were conducted on the flange connection of the chord splice, which revealed a high endurance limit. There were no signs of fatigue for a specimen with 6-inch (150-mm) diameter and 3/16-inch (4.7-mm) thickness after 1 million cycles of load varying from 10 to 42 kips (69 to 290 MPa) at 2 cycles per second.

Mirza *et al*. (1975) also performed dynamic and static analyses for two structures by considering two types of wind loads: random drag force in the direction of wind flow and vortex shedding transverse to wind flow. The largest response was found to be at a wind velocity of 5 to 11 mph near the center of the span with no signs attached. The study concluded that the Stockbridge damper, which is commonly used with electrical

wires near the center of the span, can reduce the vibration amplitude and that the AASHTO gust factor of 1.3 was sufficient. Finally, an approximate method was developed for predicting behavioral information needed for final design checks.

Ehsani, *et al*. (1985), studied another type of noncantilevered sign support structure. Using the finite element method, eight models of monotube span structures were analyzed to examine the effect of beam stiffness, column stiffness, span length, and sign location along the beam. Based on these analyses a value of 1/100 of the span for deflection was suggested instead of $d^2/400$ used by the specification and concluded that the in-plane and out-of-plane static responses of the structure can be determined separately. They also concluded that the dynamic deflection due to vortex shedding for wind speeds up to 29 mph was small compared to the static deflection due to gravity and ice.

Ehsani *et al*. (1986), later extended research work on monotube structures. They monitored two structures using strain gauges placed at critical points to test these two structures under service loads and analyzed the structures for static and dynamic loads. The field measurements agreed with finite element analyses. A value of 1/150 of the span for the deflection was proposed for the allowable limits for monotube structures.

Lundgren (1989) conducted another study on monotube support structures. He reviewed the existing specifications and Ehsani's (1985) reports. Lundgren concluded that the work of Ehsani *et al*. was limited by their assumptions for wind velocity of 29 mph or less. He also claimed that the reports of Ehsani *et al*. have an apparent unit error that causes the natural frequency calculations to be in error by as much as a factor of 2. His major finding was to develop a procedure that can be used to determine the deflection that occurs during crosswind oscillation. Hence, the maximum stresses can be estimated and compared to the fatigue reduced allowable stresses. This procedure was similar to the approach used in the Ontario Highway Bridge Design Code (Ontario Ministry of Transportation, 1992) and assumes lock-in resonance. Large amplitude vibration is developed when the vortices frequency matches one of the natural frequencies of the structure. This approach eliminates the need to know either the wind velocity or the natural frequencies of the structures.

2.5 Fatigue Resistant Design of Cantilevered Signal, Sign, and Light Supports

Kaczinski *et al*. (1996) investigated the susceptibility of cantilevered support structures to dynamic wind loads. Galloping and vortex shedding were investigated through wind tunnel tests, and load models for natural wind gusts and truck-induced gusts were gathered from the literature. The researchers conducted both dynamic and static finite element analyses for a range of cantilevered support structures to determine the equivalent static load range that could be used in fatigue design. Static tests were conducted on anchor bolts to evaluate the effect of factors such as misalignment, exposed length, and looseness. Full-scale fatigue tests were also performed to estimate the finite and infinite life fatigue strength of axially loaded anchor bolts. Finally, connection details were categorized by the existing AASHTO fatigue design curves based on their

knowledge of previous research work that had led to the existing fatigue design curves, on their experience with fatigue problems, and on limited fatigue tests. The natural wind force spectrum used was derived from a standard velocity spectrum presented by Davenport (1961). The truck-induced wind loads were obtained by using the static wind pressure formula in the specification, considering V = 65 mph, C_h = 1, and a gust factor of C_d = 1.3. The value was then doubled to account for the vertical lifting of the mast arm. This approach was proposed by Desantis and Haig (1996) in research that analyzed fatigue-damaged VMSs. It was preferred over the pressure distribution proposed by Creamer *et al*. (1979) and described in Chapter 1.

In recent research by Johns and Dexter (1999), truck-induced wind loads on highway sign support structures were studied by monitoring a cantilevered VMS structure while trucks were driven at varying speeds beneath the support structure. A modification for the truck-induced wind load was proposed that correlates the value of the pressure with the elevation above the road surface.

CHAPTER 3. RESEARCH FINDINGS

3.1 Current Vibration and Fatigue Concerns for Noncantilevered Support Structures

A survey was conducted as a part of NCHRP Project 17-10(2). Forty-eight state DOTs replied to this survey. Twenty-five states reported fatigue-related failure of different types of support structures, which slightly exceeds half of the states that responded. Out of these 25, 8 identified problems associated with overhead bridge structures. That ranks this type of sign support structure second, after the cantilevered supports, in fatigue concerns. The survey also revealed that 20 DOTs investigated or used some kind of vibration mitigation devices or practices. However, only 8 DOTs stated that they have special details for fatigue-resistant design. The DOTs that reported fatigue problems associated with bridge type sign support structures were contacted for further detailed information. From the previous summary of survey results, it can be concluded that noncantilevered structures also have fatigue-related problems. Furthermore, the survey results revealed the lack of use of special connection details to resist fatigue and, hence, confirmed the need to develop fatigue-resistant design checks for noncantilevered sign support structures.

3.2 Establishing loads for overhead bridge structures

To establish equivalent static fatigue loads, finite-element analyses were needed. The analyses were accomplished using MSC/NASTRAN running on the CRAY supercomputer of the Alabama Supercomputer Network. The results were then processed and visualized using MSC/PATRAN on the School of Engineering Unix workstations. These following analyses were needed:

1. Dynamic analysis to determine the natural modes and natural frequencies of the structures.
2. Static analysis to determine the response of the cantilevered signal and sign support structures due to fatigue loads.
3. Dynamic analysis to determine the dynamic loads configurations that result in the same response for cantilevered signal and sign support structures.
4. Dynamic analysis to determine the dynamic response for noncantilevered sign support structures due to dynamic loads estimated in the previous step.
5. Static analysis to determine the equivalent static load that will give the same response.

Presented in the next sections is a description of the selected structures followed by a presentation of the various analyses and their results. Later, a summary of the deflection values calculated is provided. Finally, the main conclusions are summarized.

3.2.1 Selected Structures and Finite-Element Models

Six structures were selected from literature for analysis. The main reason for choosing structures that were used by other researchers was to correlate the results of the present analyses with the available field and experimental test results that have been done in the past. The structures chosen were selected to reflect various aspects in these types of structures. For example, some structures were made of steel while other structures were made of aluminum, which are the two most commonly used materials in sign support structures. Another example was the use of tapered versus prismatic sections.

Two cantilevered sign supports were chosen from Kaczinski's report (1996) to develop the dynamic load configuration for galloping. The first structure is a steel cantilevered signal support that has two signals attached. Both the mast arm and the column are tapered. Figure 3.1 gives the dimension of *Structure 1*. The second structure is a steel cantilevered sign support structure with a prismatic column and a cantilevered two-chord truss made of prismatic tubular sections and is shown in Figure 3.2.

Two structures were chosen from Ehsani's research (1985) on monotube support structures. *Structure 3* is a 100-foot (30 m) span steel frame that has five signs attached to it. Both of its vertical members and the horizontal member are tapered. *Structure 4* is a 60 -foot (18 m) span steel frame that has four signs attached. The details of these structures are shown in Figure 3.3 and Figure 3.4, respectively.

The last two structures, *Structures 5* and *6*, were chosen from Mirza's report (1975). These structures are two tri-chord truss sign support structures. *Structure 5* is an 82-foot (24.6 m) span steel frame that has three signs attached. *Structure 6* is a 150-foot (45 m) span aluminum frame and has two signs attached. The details of the two structures are presented in Figures 3.5 and 3.7. The area and locations of the attached signs are shown in Figures 3.6 and 3.8.

To correlate the results from this effort with the results of the analyses by others, each structure was modeled in a manner as similar as possible to the model used in its original source. As an example, the same element properties used for the beam to column connection for the two-monotube structures by Ehsani *et al*. (1985) were used in the present study. However, the modeling approach used by Mirza *et al*. (1975) in the early 1970's was not followed in the present analyses. A higher fidelity model was used for the tri-chord truss structures (using bar elements to model each truss member), as opposed to using single beam elements that represent the stiffness of the truss used by Mirza *et al*. In all cases, the structures in this study were modeled with two-node bar elements, with each node having six degrees of freedom (three translations and three rotations). The signs were modeled as concentrated masses attached to locations along the span that correspond to the center of mass location of each sign. The foundation was considered fixed, therefore, the effect of soil/structure interaction was neglected. The values for overall damping of the structures used in the previous research studies were used in the analyses.

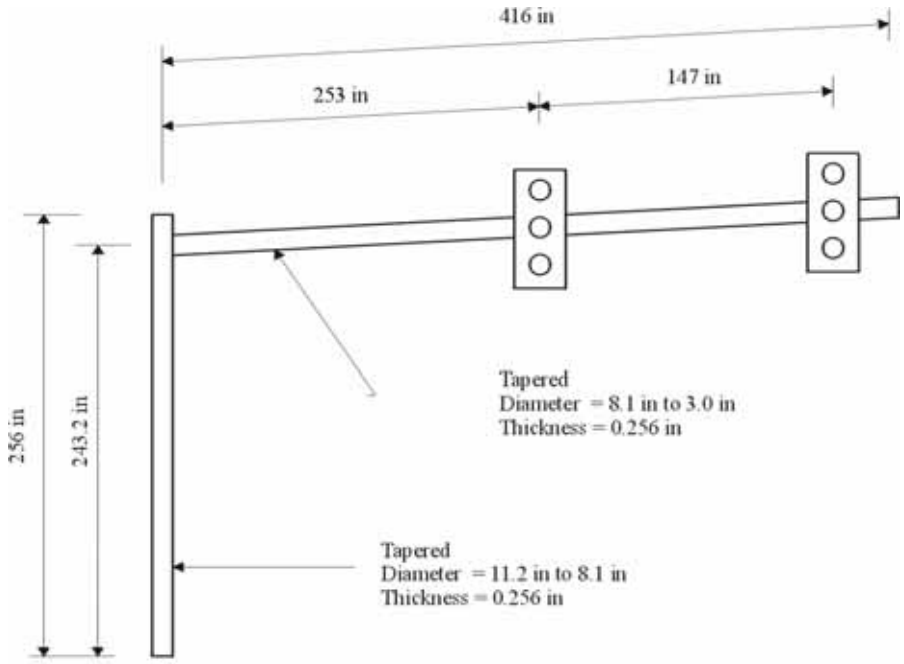

Figure 3.1. Dimensions of Support Structure 1

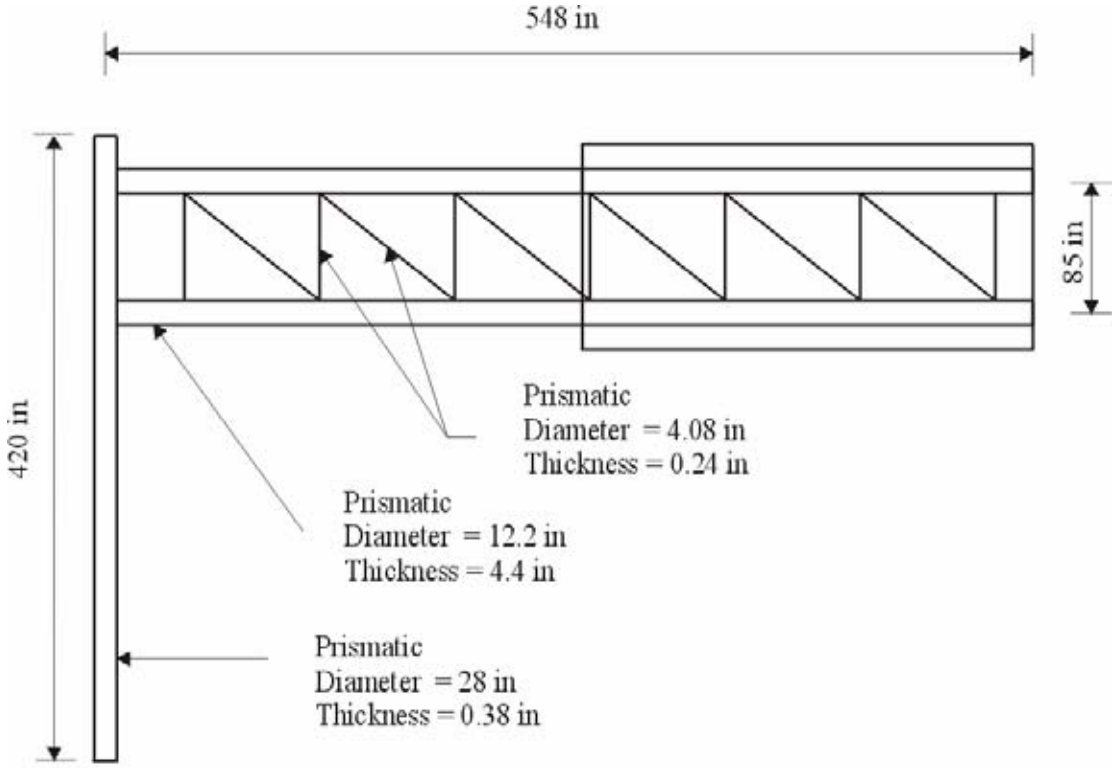

Figure 3.2. Dimensions of Support Structure 2

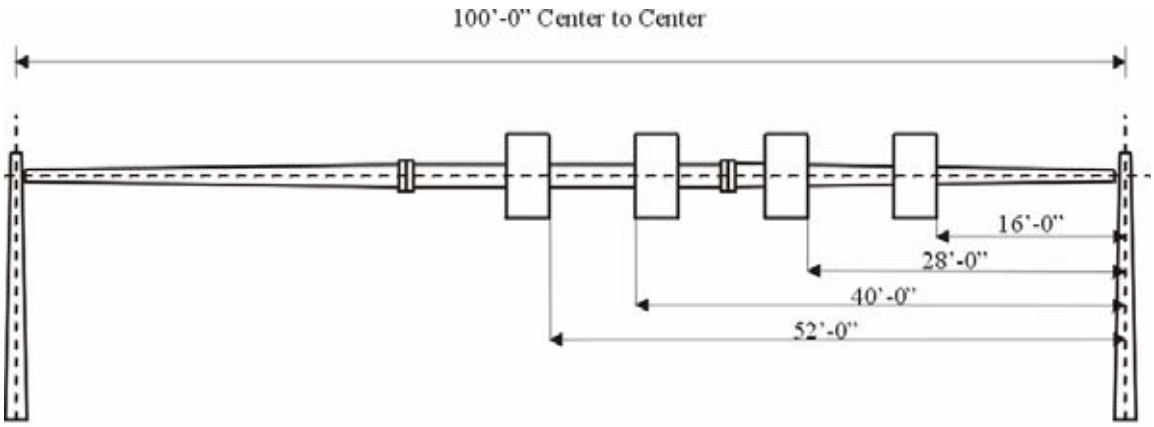

Figure 3.3. Dimensions of Support Structure 3

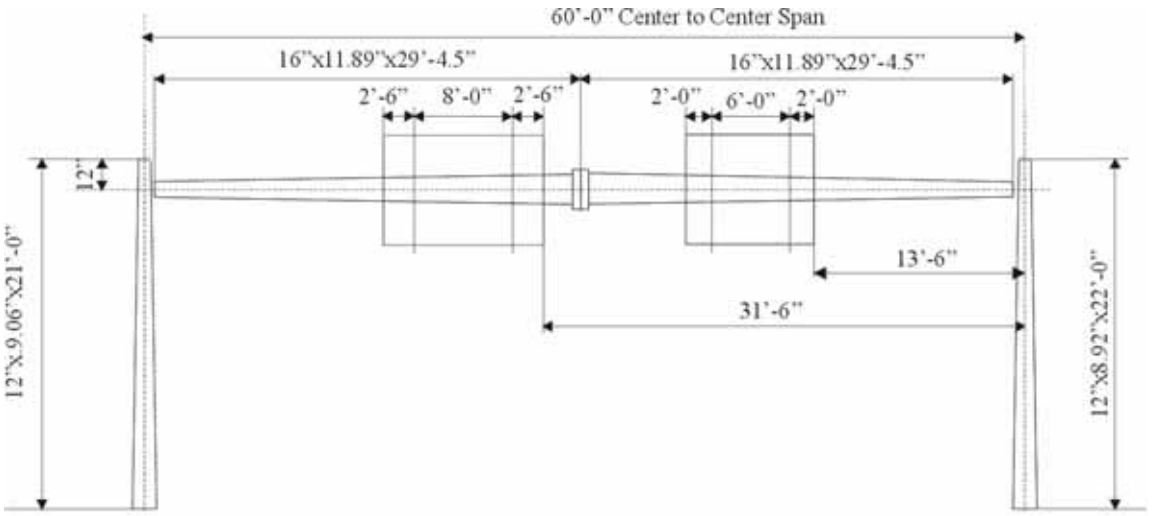

Figure 3.4. Dimensions of Support Structure 4

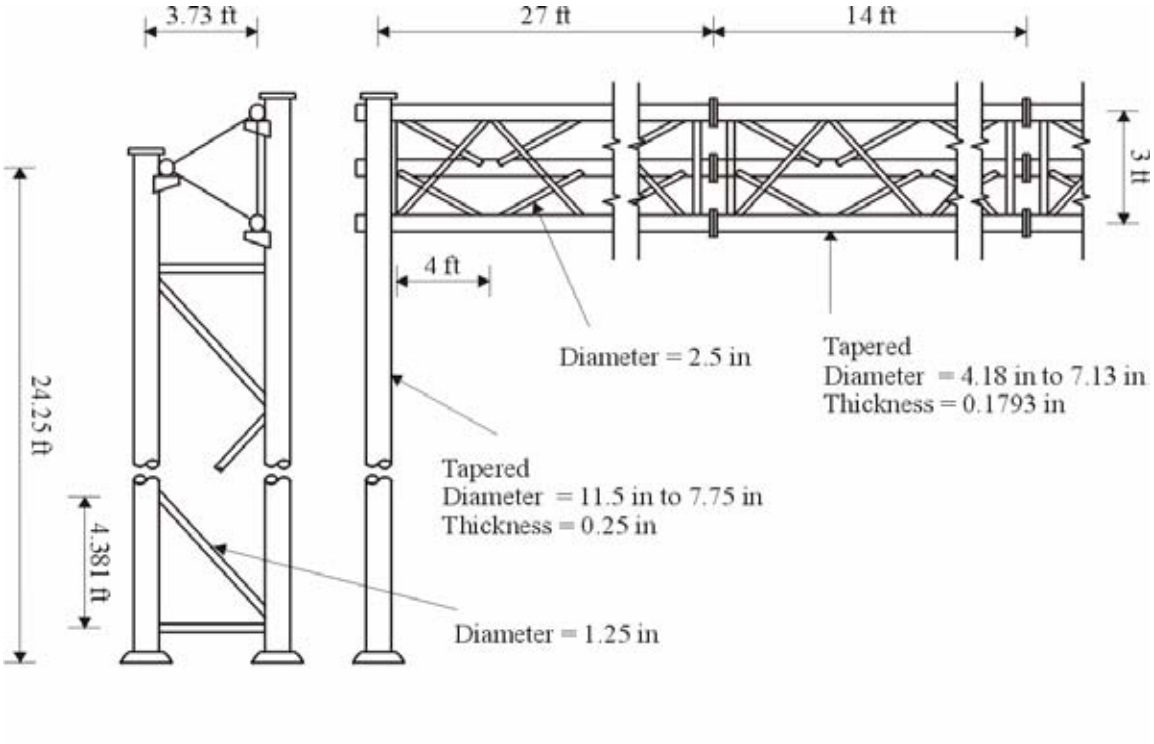

Figure 3.5. Dimensions of Support Structure 5 (Span = 82 ft)

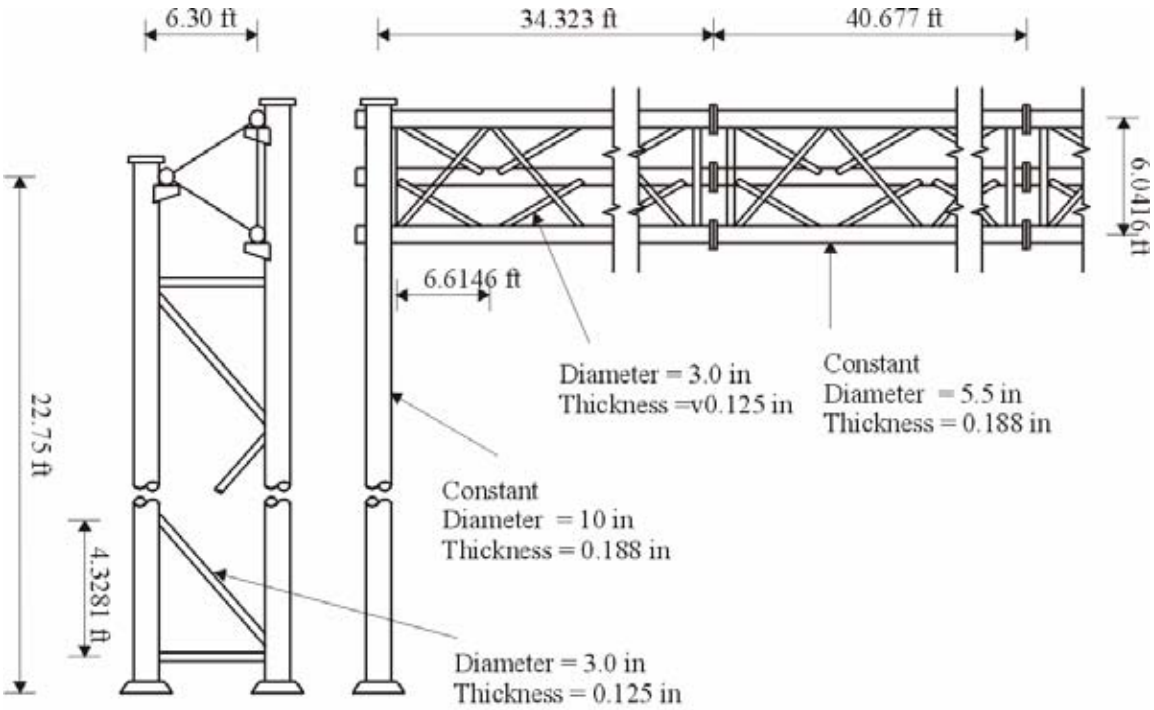

Figure 3.6. Dimensions of Support Structure 6 (Span = 150 ft)

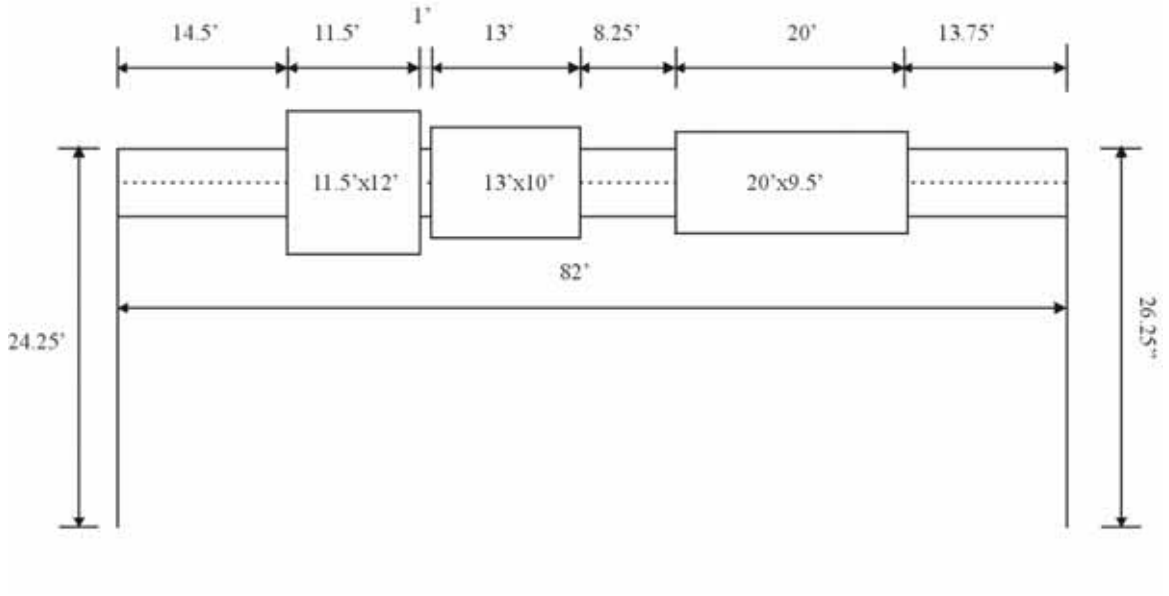

Figure 3.7. Sign Sizes and Locations of Support Structure 5

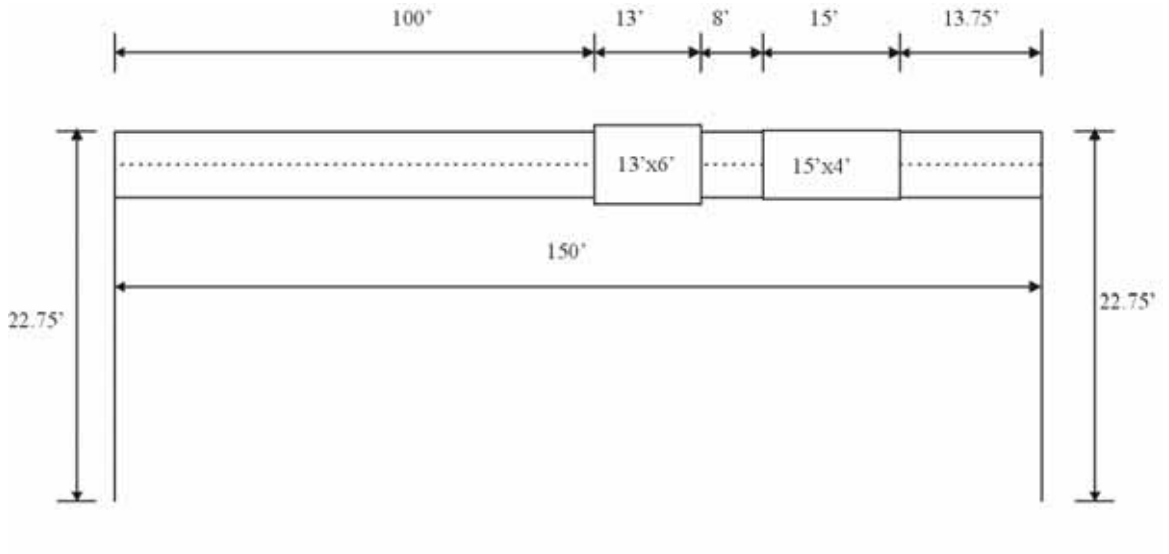

Figure 3.8. Sign Sizes and Locations of Support Structure 6

3.2.2 Natural Modes of Vibration

The natural modes of vibration of a structure represent the free vibration (no dynamic force applied) of the structure. These mode shapes and their frequencies are important structural characteristics of the structure, especially when dealing with dynamic loads. The natural frequencies were calculated using the same MSC/NASTRAN models.

The general equation of dynamic equilibrium used in MSC/NASTRAN is given by equation 3.1.

$$[M]\{u^{\bullet\bullet}\}+[B]\{u^{\bullet}\}+[K]\{u\}=\{P(t)\}+\{N\}+\{Q\} \tag{3.1}$$

where $\{u\}$ is the vector of grid point displacements, $\{u^{\bullet}\}$ is the vector of grid point velocities, $\{u^{\bullet\bullet}\}$ is the vector of grid point accelerations, [M] is the mass matrix, [B] is the damping matrix, [K] is the stiffness matrix, $\{P(t)\}$ is the time-dependent applied force vector, $\{N\}$ is a vector of forces which depends on $\{u\}$ and $\{u^{\bullet}\}$ in a nonlinear mode, and $\{Q\}$ is a vector of forces resulting from constraints.

Real eigenvalue analyses were used to compute the free vibration modes. With [B], $\{P(t)\}$, and $\{N\}$ zero (null), and assuming that all parts of the structure are vibrating sinusoidally with frequency:

$$f=\frac{\omega}{2\cdot\pi} \tag{3.2}$$

and

$$\{u\}=\{\phi\}\cos(\omega\cdot t) \tag{3.3}$$

where $\{\phi\}$ is the vector of real numbers and $\cos(\omega\, t)$ is the scalar multiplier. Substituting in the equation of motion yields

$$[K-\omega^2 M]\{\phi\}\cos(\omega\cdot t)=0. \tag{3.4}$$

The inverse power method (INV) was used to extract the eigenvalues. This method is described in more details in MSC/NASTRAN *Handbook for Dynamic Analysis* (Gockel, 1983). The first five natural frequencies were determined for all structures to get the principal mode shape in each direction. The first natural frequency in the vertical

direction was then used to configure the dynamic galloping load while the first natural frequency in the horizontal direction was used for the dynamic natural wind load. This was accomplished by setting the dynamic load values to a sine wave forcing function at the natural frequency.

The mass effect on the natural mode shapes was studied. The mode shapes and natural frequencies were also compared to the results of other researchers. The values of the natural frequencies are presented in Table 3.1 through 3.4. Figures 3.9 through 3.11 provide samples of the mode shapes.

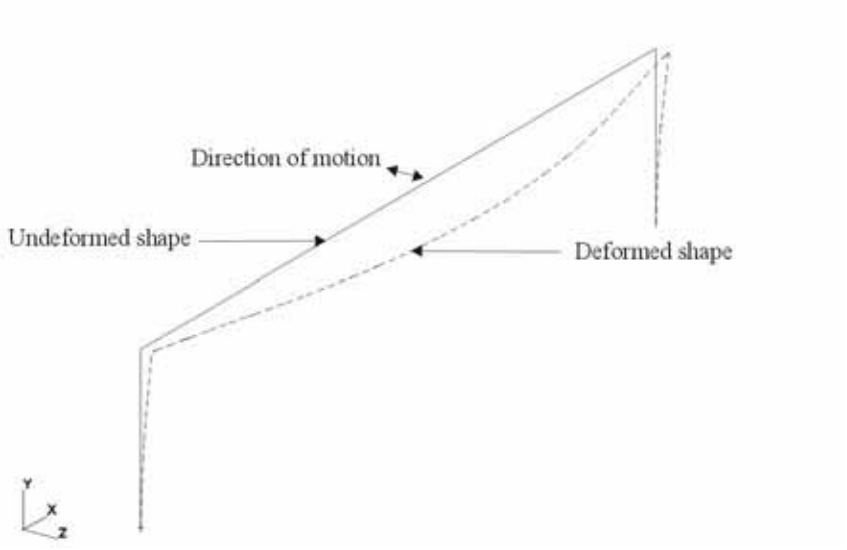

Figure 3.9. First Mode of Structure 3 (Natural Frequency = 0.89726 Hz)

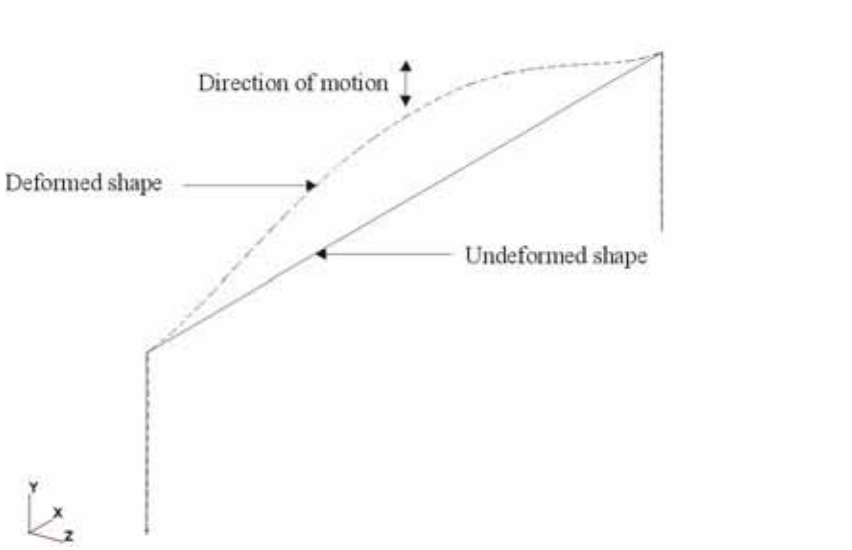

Figure 3.10. Second Mode of Structure 3 (Natural Frequency = 1.2003 Hz)

In most cases the first natural mode for each structure in each principal direction could be noticed, however for *Structures 5* and *6* the natural mode in the vertical and horizontal direction could not be identified. Instead the natural mode was found to be in a direction inclined to the horizontal and vertical direction. This was considered as a first mode in each direction.

Table 3.1. Natural Frequencies for Structures Without Attachments Mass

Support structure Mode Shape	1	2	3	4	5	6
(1)	(2)	(3)	(4)	(5)	(6)	(7)
1	1.2996	1.0633	1.0624	1.5902	2.0270	1.5608
2	1.4010	1.6484	1.4312	2.8394	4.0517	2.1899
3	3.8740	3.7787	2.4003	3.3196	5.2616	2.3524
4	4.2701	6.2166	2.7728	3.5591	8.4125	4.1762
5	8.1543	6.6485	4.3218	5.3727	12.4670	5.8228

Table 3.2. Natural Frequencies for Structures With Attachments Mass

Support structure Mode Shape	1	2	3	4	5	6
(1)	(2)	(3)	(4)	(5)	(6)	(7)
1	1.2257	1.0633	0.8973	1.0765	1.6708	1.4047
2	1.3211	1.6241	1.2003	2.0743	3.1421	1.9887
3	3.7559	3.7586	2.1190	2.1396	4.0958	2.0931
4	4.1674	6.1107	2.5050	3.0227	7.0858	3.7127
5	7.6650	6.5764	3.9197	4.9902	9.7508	5.2384

Table 3.3. Natural Frequencies for Structures Without Mass from Previous Literature

Support structure Mode Shape	1	2	3	4	5	6
(1)	(2)	(3)	(4)	(5)	(6)	(7)
1	1.130	1.270	1.467	2.295	2.254	2.638
2			1.479	2.834	3.479	3.229
3			3.055	3.265	3.833	3.432
4			3.868	4.293	7.749	9.787
5			5.001	7.925	11.857	10.501

Table 3.4. Natural Frequencies for Structures With Mass from Previous Literature

Support structure Mode Shape	1	2	3	4	5	6
(1)	(2)	(3)	(4)	(5)	(6)	(7)
1	-	-	1.467	2.295	1.913	2.094
2	-	-	1.479	2.834	2.909	2.496
3	-	-	3.055	3.265	3.072	2.574
4	-	-	3.868	4.293	5.681	5.966
5	-	-	5.001	7.925	7.806	7.837

3.2.3 Dynamic and Static Analysis to Simulate Galloping

Kaczinski *et al*. (1996), used wind tunnel tests to determine the dynamic response of cantilevered sign support structures to galloping and vortex shedding. They also conducted static and dynamic finite element analyses on these models and other prototype structures that have experienced vibration to quantify the equivalent static load that results in the same response. The finite element results revealed that an equivalent static load between 1150 and 1770 Pa (24 and 37 psf, respectively) gave the same response as the wind tunnel tests while, equivalent static pressures of 775 to 1290 Pa (16.2 to 27.0 psf) were calculated for actual structures that experience vibrations. A median value of 1000 Pa (21 psf) for equivalent static load was recommended by Kaczinski for the actual structural loads of cantilevered structures.

In this research, a static pressure of 1000 Pa (21 psf) was applied to two cantilevered structures (*Structures 1* and *2*). This pressure was represented by a series of concentrated loads applied at the nodes corresponding to where signals or signs are attached. A maximum vertical displacement of 12.1 inches at the free end of the cantilever resulted for *Structure 1*. This displacement is associated with a normal force of 376 lb, a moment of 1.23×10^5 lb-in at the column base, and a maximum shear force and moment on the cantilever of 375 lb and 1.05×10^5 lb-in, respectively. A transient analysis was conducted for the same structure using varying dynamic load configurations to get maximum displacement that resulted from the previous static analysis. The load was assumed to be sinusoidal with a frequency that matches the first natural frequency of vibration of the structure in the vertical direction. Matching the load with the natural frequency results in maximum response, and thus is conservative. This applied load can be written as:

$$P(t) = P_o \cdot \sin(\omega \cdot t) \tag{3.5}$$

Where :

$P(t)$ = the load value at any time (t);
Po = the load amplitude; and
ω = the first natural frequency in the vertical direction.

To represent accurately the dynamic load, the time interval was set to 1/8 of the periodical time to the appropriate number of significant digits. This causes the load to be calculated nine times for each cycle, in which two correspond to the peak values of the load during the cycle.

The vertical displacement of the cantilevered tip was used to match the displacement response between the response from the static and dynamic analyses. The displacement of 12.1 inch was reached at a value of 19.75 lb at the two nodes where the signals were attached. The maximum normal force at the column base was 439 lb and

the maximum moment was 1.80 $x10^5$ lb-in. For the cantilever arm, the maximum shear was 440 lb and the maximum moment was 1.05 $x10^5$ lb-in. The dynamic pressure was calculated to be 2.2 lb/ft^2 of the signal.

The same procedure was followed with *Structure 2*. Applying the static load of 21 lb/ft^2 yields a vertical deflection of 3.84 inch at the free end of the cantilever with a maximum moment at the column base of $1.91x10^6$ lb-in and maximum normal force in the chords of $1.42x10^4$ lb and $7.23x10^3$ lb. The dynamic analysis revealed that a value of 61.75 lb at each node at the sign would result in a maximum displacement in the vertical direction of the same value. The maximum base moment was 2.53 $x10^5$ lb-in, and the maximum normal force in the two chords was 8.67 $x10^5$ lb. The dynamic pressure was calculated as 2.27 lb/ft^2 of the sign.

Based on the analysis described above, a value of 2.25 lb/ft^2 was assumed for the dynamic pressure to simulate galloping effects on structures. Thus, a dynamic load with this value was applied to the other four structures.

For *Structure 3*, a vertical deflection of 5.64 inch at the center of the beam resulted from the dynamic analysis. This vertical deflection was accompanied by 0.174 inch of horizontal deflection at the column end, a maximum moment value at the column base of $2.41*10^5$ lb-in, and a maximum moment in the beam elements of $1.10*10^5$ lb-in. The static pressure value that was found to give the same deflection of 5.64 was 23.7 psf. This static load results in a horizontal deflection at the column of 0.286 inch, a moment at the column base of $2.50*10^5$ lb-in, and a maximum moment value in the beam element of $1.49x10^5$ lb-in.

Similarly, for *Structure 4*, the maximum vertical deflection at the beam center due to the dynamic load was 3.16 inch with a horizontal deflection at the column end of 0.518 inch. The maximum moment at the column base was $2.53*10^5$ lb-in, and $1.71x10^5$ lb-in resulted in the horizontal part of the structure. The static pressure required to match dynamic analysis was 21.2 psf; the accompanied values were 0.315 inches for horizontal deflection at the column end, $2.55*10^5$ lb-in for the column base moment, and $1.49*10^5$ lb-in for the maximum moment in the beam elements.

For *Structure 5*, the maximum dynamic vertical deflection at the beam center was 2.19 inches, 0.261 inches horizontal deflection at the column end, $6.07*10^4$ lb-in moment at the column base, and $6.04*10^4$ lb-in moment at the beam column connection. The static pressure was calculated to be 22.3 psf. That results in a 0.255-inch horizontal deflection at the column end, $5.64*10^4$ lb-in moment at the column base, and $6.46*10^4$ lb-in moment at the beam column connection.

Finally, for *Structure 6*, the maximum vertical deflection from the dynamic analysis at the beam center was 2.3 inches, 0.209 inches for horizontal deflection, $1.34*10^4$ lb-in moment at the column base, and $1.12*10^4$ lb-in moment at the beam column connection. To get an equivalent vertical deflection, 17.9-psf static pressure was required. That static load results in a 0.256-inch horizontal displacement at the column

end, $1.36*10^4$ lb-in column base moment, and $1.30*10^4$ lb-in beam column connection moment.

A summary of these results is presented in Tables 3.5 through 3.8. Table 3.5 shows the results of the static analysis performed on *Structures 1* and *2*, while Table 3.6 shows the dynamic analysis results for these structures. Table 3.7 shows the results of the dynamic analysis for *Structures 3*, *4*, *5*, and *6*; and Table 3.8 shows the static analysis results.

Figure 3.11 shows a sample of the time history dynamic response (in this case, the displacement at the tip of the cantilevered part in *Structure 1*). The average of the static pressure calculated for *Structures 3* through *6* was 21.3 psf. It was noticed that, although the maximum vertical deflection of the structure was chosen to compare the static and dynamic behavior of the support structures, the other values such as the moments and the normal force correlate well.

Table 3.5. Static Analysis Results of Cantilevered Signal and Sign Support to Simulate Galloping

Support structure	Equivalent static pressure range	Amplitude Cant. Tip Displacement	Amplitude column end Displacement	Amplitude Column base moment	Amplitude Column Beam moment
	(psf)	(in)	(in)	(lb-in)	(lb-in)
(1)	(2)	(3)	(4)	(5)	(6)
1	21.00	12.10	1.35	1.23E+05	1.04E+05
2	21.00	3.84	1.17	1.91E+06	1.05E+05

Table 3.6. Dynamic Analysis Results of Cantilevered Signal and Sign Support to Simulate Galloping

Support structure	Natural Frequency	Assumed damping	Dynamic Pressure	Amplitude Cant. tip Displace-ment	Amplitude column end Displace-ment	Amplitude Column base moment	Amplitude Column Beam moment
	Hz	%	(lb/ft^2)	(in)	(in)	(lb-in)	(lb-in)
(1)	(2)	(3)	(4)	(5)	(6)	(7)	(8)
1	1.3211	0.75	2.2	12.1		1.80E+05	9.92E+04
2	1.6241	1.00	2.268	3.84	1.85	2.53E+06	7.81E+04

Table 3.7. Dynamic Analysis Results of Noncantilevered Sign Support to Simulate Galloping

Support structure	Natural Frequency	Assumed damping	Dynamic Pressure	Amplitude Beam center Displace-ment	Amplitude column end Displace-ment	Amplitude Column base moment	Amplitude Column Beam moment
	Hz	%	(psf)	(in)	(in)	(lb-in)	(lb-in)
(1)	(2)	(3)	(4)	(5)	(6)	(7)	(8)
3	1.2003	0.5	2.25	5.64	0.174	2.41E+05	1.10E+05
4	2.1396	0.5	2.25	3.16	0.518	2.53E+05	1.71E+05
5	3.1421	0.5	2.25	2.19	0.261	6.07E+04	6.04E+04
6	2.0931	0.5	2.25	2.3	0.209	1.34E+04	1.12E+04

Table 3.8. Static Analysis Results of Noncantilevered Sign Support to Simulate Galloping

Support Structure	Equivalent static pressure range	Amplitude Beam center Displacement	Amplitude column end displacement	Amplitude Column base moment	Amplitude column beam moment
	(psf)	(in)	(in)	(lb-in)	(lb-in)
(1)	(2)	(3)	(4)	(5)	(6)
3	23.69	5.64	0.286	2.50E+05	1.49E+05
4	21.20	3.16	0.315	2.55E+05	1.49E+05
5	22.33	2.19	0.255	5.64E+04	6.46E+04
6	17.95	2.30	0.256	1.36E+04	1.30E+04

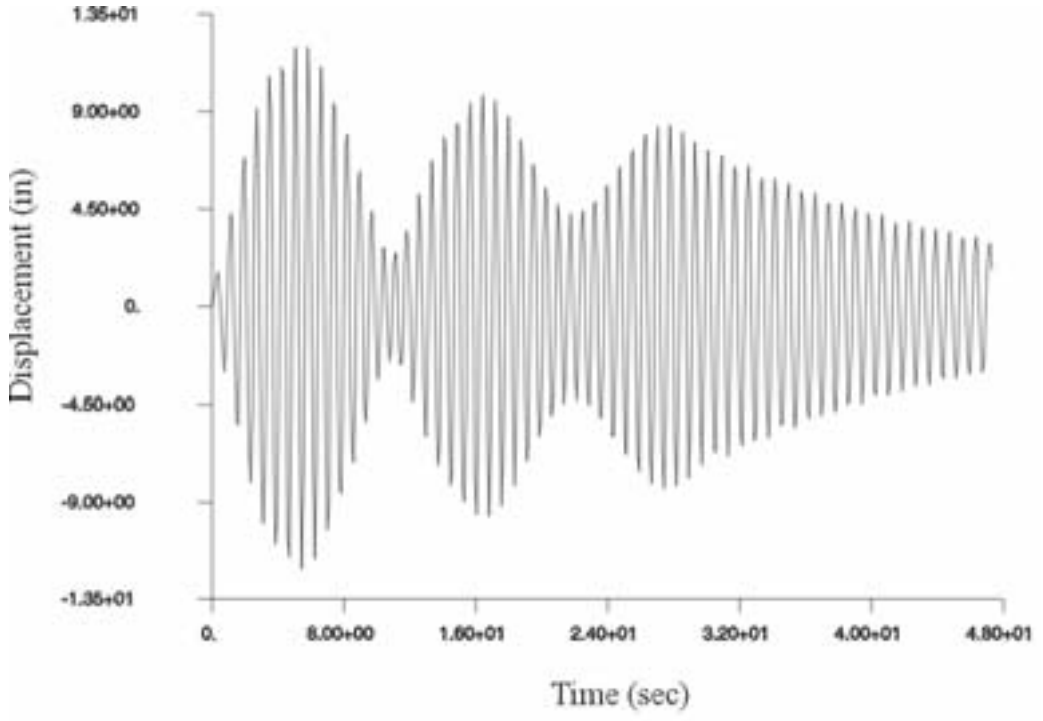

Figure 3.11. Sample Time History of the Dynamic Response Due to Galloping (Displacement at the Tip of Cantilever of Structure 1)

3.2.4 Dynamic and Static Analysis to Simulate Natural Wind Gusts

Kaczinski *et al*. (1996) selected a standard wind velocity spectrum from the literature and modeled the response of cantilevered structures to natural wind gust using spectral finite element analyses. They performed spectral analysis over a range of mean hourly wind velocities. Finally, they conducted static analyses to calculate the static pressure range that results in the same response. The static pressure range was determined to be from 170 Pa to 300 Pa (3.6 to 6.3 psf).

The same approach used in the last section to get the galloping load for noncantilevered structures was used for natural wind gusts. This approach concluded that applying the static pressure range recommended by Kaczinski *et al*. (1996) on the two cantilevered structures and calculating the response (along wind displacement of the tip of the cantilevered part in this case). A dynamic load was then applied to the nodes with the same distribution of the static load and with a maximum load value of unity. From these two analyses the dynamic pressure range that simulates the natural wind load was calculated. The calculated value of the dynamic pressure was then applied to the four noncantilevered structures. Finally, a static analysis was conducted to calculate the value of the equivalent static pressure. All of the dynamic loads were applied to the nodes in the form of a sine wave. The load function can be written as

$$P(t) = P_o \cdot \sin(\omega \cdot t) \tag{3.6}$$

where

$P(t)$ = the load value at any time (t),
P_o = the load amplitude, and
ω = the natural frequency of the structure in the (along-wind) direction.

The same values for the damping that were used in the last section were used in these calculations. Also, the time interval was set to 1/8 of the natural period. Applying the static loads calculated by Kaczinski *et al*. (1996) to *Structure 1* yielded a displacement of 5.6 inches at the tip of the cantilever, while applying a dynamic load with the same distribution with the maximum load value equal to unity yields a maximum displacement of 0.93 inches in the same location. A maximizing ratio of 6.02 was needed to give an equivalent response to the static response. A value of 0.571 psf results when dividing this load by the projected area of the structure plus the area of the sign attached to the node that has the largest load value.

Following the same steps with *Structure 2*, the maximum displacement from static loads was 4.22 inches, and the maximum displacement from the dynamic load with a maximum load value set equal to unity was 0.26 inches. The required dynamic scale ratio was 16.2 and the dynamic pressure was found to be 0.596 psf. Based on these results, a value of 0.6 lb/ft^2 was assumed as a dynamic pressure that represents the natural wind service load. This value was used with the other four structures.

For *Structure 3*, a horizontal deflection of 4.33 inches at the center of the beam resulted from the dynamic analysis. This deflection was accompanied by a small deflection of 0.577 inches at the column end, a maximum moment value at the column base of $1.36*10^5$ lb-in, and a maximum moment in the beam elements of $6.48*10^4$ lb-in. The static pressure value found to give an equivalent deflection was 4.5 psf. This static load gives deflection at the column of 0.578 inches, a moment at the column base of $1.67*10^5$ lb-in, and a maximum moment value in the beam element of $6.56*10^4$ lb-in.

Similarly, for *Structure 4*, the maximum horizontal deflection at the beam center due to the dynamic load was 4.24 inches with a deflection at the column end of 1.7 inches. The maximum moment at the column base was $1.87*10^5$ lb-in and at the beam elements was $1.23*10^4$ lb-in. The static pressure required was 4.24 psf; the accompanying values were 1.98 inches for horizontal deflection at the column end, $1.88*10^5$ lb-in for the column base moment, and $1.22*10^4$ lb-in for the maximum moment in the beam elements.

For *Structure 5*, the maximum dynamic horizontal deflection at the beam center was 0.424 inches with 0.11 inches horizontal deflection at the column end, $1.52*10^4$ lb-in moment at the column base, and $6.99*10^3$ lb-in moment at the beam column connection. The static pressure was calculated to be 2.98 psf, which results in 0.0878 inches

deflection at the column end, $1.71*10^4$ lb-in moment at the column base, and $7.55*10^3$ lb-in moment at the beam column connection.

Finally, for *Structure 6*, the maximum horizontal deflection from the dynamic analysis at the beam center was 1.46, 0.195 inches for horizontal deflection, $4.29*10^3$ lb-in moment at the column base, and $1.52*10^4$ lb-in moment at the beam column connection. To get the same horizontal deflection, a 3.95-psf static pressure was applied. That static load results in 0.097 inches horizontal displacement at the column end, a $4.57*10^3$ lb-in column base moment, and $2.01*10^4$ lb-in beam column connection moment.

A summary of these results is presented in Tables 3.9 through 3.12. Table 3.9 shows the results of the static analysis performed on *Structures 1* and *2*, while Table 3.10 shows the dynamic analysis results for these structures. Table 3.11 shows the results of the dynamic analysis for *Structures 3* through *6*. Table 3.12 shows the static analysis results. Figure 3.12 shows a sample of the time history dynamic response (in this case, the displacement at the tip of the cantilevered part in *Structure 1*).

It can be noticed from the previous results that static loads required to achieve the same dynamic pressure for truss structures (average of 3.47 psf) are smaller than those of monotube structures (average of 4.89 psf). This is because the truss structures are stiffer than the monotube structures, which corresponds to greater resistance to dynamic load. The overall average for the static pressure was 4.17 psf. The values of the moments and axial force from static analysis were found to agree well with the corresponding values from dynamic analysis.

Table 3.9. Static Analysis Results of Cantilevered Signal and Sign Support to Simulate Natural Wind

Support Structure	Equivalent static pressure range	Amplitude Cant. Tip displacement	Amplitude column end displacement	Amplitude column base moment	Amplitude Column Beam moment
	(psf)	(in)	(in)	(lb-in)	(lb-in)
(1)	(2)	(3)	(4)	(5)	(6)
1	5.2	5.6	0.388	4.94E+04	4.01E+04
2	5.2	4.22	0.35	5.47E+05	1.78E+05

Table 3.10. Dynamic Analysis Results of Cantilevered Signal and Sign Support to Simulate Natural Wind

Support structure	Natural frequency	Assumed damping	Dynamic pressure	Amplitude Cant. Tip displace-ment	Amplitude column end displace-ment	Amplitude column base moment	Amplitude column beam moment
	Hz	%	(lb/ft2)	(in)	(in)	(lb-in)	(lb-in)
(1)	(2)	(3)	(4)	(5)	(6)	(7)	(8)
1	1.2257	0.75	0.571	5.60	0.373	5.08E+04	4.12E+04
2	1.0463	1.00	0.596	4.22	0.560	5.54E+05	1.80E+05

Table 3.11. Dynamic Analysis Results of Noncantilevered Sign Support to Simulate Natural Wind

Support structure	Natural Frequency	Assumed damping	Dynamic pressure	Amplitude Beam center displacement	Amplitude column end displacement	Amplitude column base moment	Amplitude Column beam moment
	Hz	%	(psf)	(in)	(in)	(lb-in)	(lb-in)
(1)	(2)	(3)	(4)	(5)	(6)	(7)	(8)
3	0.897	0.5	0.6	4.33	0.577	1.36E+05	6.48E+04
4	1.0765	0.5	0.6	4.24	1.7	1.87E+05	1.23E+04
5	4.0958	0.5	0.6	0.424	0.11	1.52E+04	6.99E+03
6	2.0931	0.5	0.6	1.46	0.195	4.29E+03	1.52E+04

Table 3.12. Static Analysis Results of Noncantilevered Sign Support to Simulate Natural Wind

Support Structure	Equivalent static pressure range	Amplitude Beam center Displacement	Amplitude column Displacement	Amplitude Column base moment	Amplitude Column Beam moment
	(psf)	(in)	(in)	(lb-in)	(lb-in)
(1)	(2)	(3)	(4)	(5)	(6)
3	4.5	4.33	0.578	1.67E+05	6.56E+04
4	5.275	4.24	1.98	1.88E+05	1.22E+04
5	2.98	0.424	0.0848	1.71E+04	7.55E+03
6	3.952	1.46	0.097	4.57E+03	2.01E+04

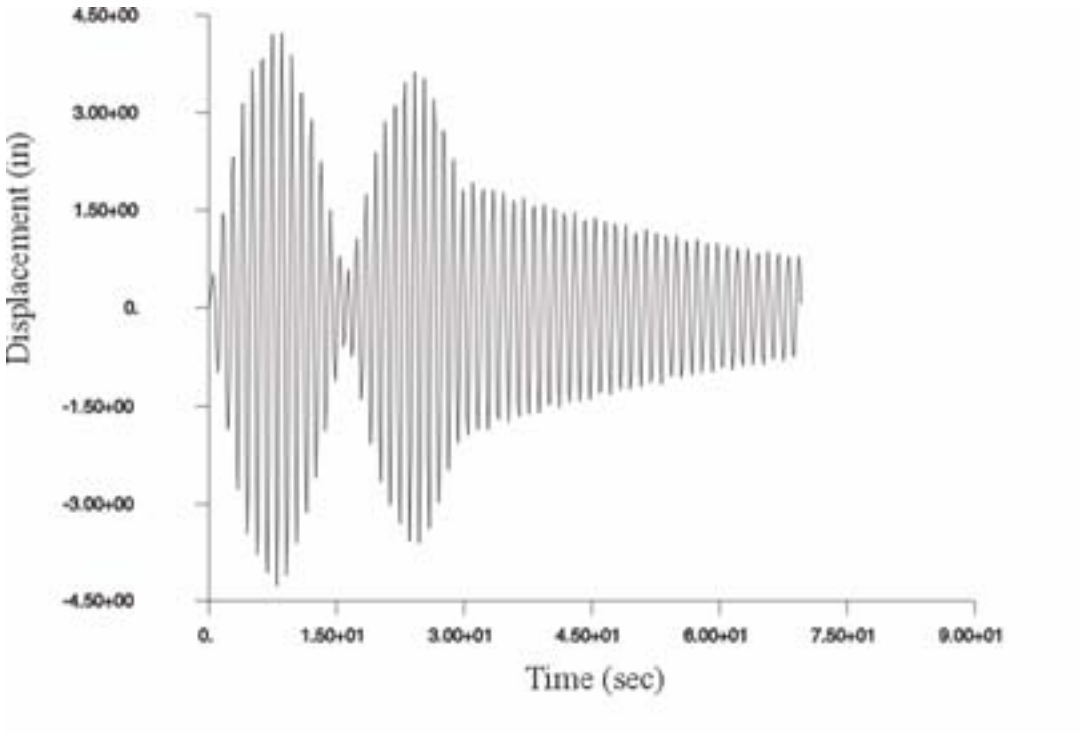

Figure 3.12. Sample Time History of the Dynamic Response Due to Natural Wind (Displacement at the Tip of Cantilever of Structure 1)

3.2.5 Dynamic and Static Analysis to Simulate Truck-induced Gusts

Creamer *et al*. (1979) conducted dynamic analyses for three structures that were previously instrumented with strain gauges to measure the stresses during the passage of trucks. The dynamic load used was in the form of a pressure triangle distribution, applied to the face of the sign, with a maximum value of 1.25 psf at the bottom of the sign and vanishes towards the top. That load was linear, starting at 0 time, reaching the peak after 0.125 sec, and vanishing at 0.375 sec. This load corresponds to the estimated time for passage of a 30-foot long truck at 55 mph. It results in a uniform pressure of 1.25 psf in the vertical direction. Creamer *et al*. also conducted static analyses to estimate the dynamic load factor. The dynamic load factors they calculated gave a maximum value of 2.1.

These load configurations were checked by Kaczinski *et al*. (1996) in their study of fatigue loads for cantilevered structures. However, in applying these load values on fatigue-damaged VMSs, they concluded that the loads proposed by Creamer *et al*. (1979) were not enough to represent loads from truck gusts, especially in the vertical direction. Therefore, they considered the load model proposed by Desantis and Haig (1996), in which the wind speed in the upward direction due to the passage of the truck is assumed to be the truck speed with a gust factor of 1.3. This increased the equivalent static load to 36.6 psf (1760 Pa), applied to the horizontally projected area along the greater length of the sign panel or to 12 ft (3.7 m).

This value was later modified by Johns and Dexter (1999) to account for the height of the structure above the truck. This modification was presented as a table and is reproduced here in Table 3.13. The value of the pressure is assumed to vanish at a height of 10.1 m above the road surface.

In a study by Cook *et al*. (1999), the pressure produced by 23 random trucks was measured with instrumentation on a bridge overpass. The height effect was also investigated by measuring the pressure at varying heights for the same truck speed. The maximum positive horizontal pressure was found to be 0.92 psf, the maximum negative pressure was -1.5 psf, and the maximum vertical pressures were 1.43 psf and the -2.1 psf. The time for these loads is approximately 0.5 sec for positive pressure and 1.0 sec for negative pressure. Cook *et al*. suggested 10% reduction in pressure for each foot and also recommended a value of 5 psf for all pressures to accommodate for the dynamic effects.

Table 3.13. Truck-induced Gust Values (After Johns and Dexter 1999)

Elevation Above Road Surface		Value of "TG"	
(m)	(ft)	(Pa)	(psf)
(1)	(2)	(3)	(4)
6 or less	0 or less	1760	36.6
6.1 to 7	20.1 to 23.33	1530	31.8
7.1 to 8	23.66 to 26.67	1150	23.9
8.1 to 9	27 to 30	690	14.3
9.1 to 10	30.33 to 33.33	380	7.9
10.1 and above	33.67 and above	0	0

In the present research, the pressures measured by Cook *et al*. (1999) were used as a dynamic load applied along the span of four noncantilevered structures (*Structures 3* though *6*) and the dynamic response was calculated. Then, a static pressure that would result in the same response was calculated. These static pressures were compared to the pressures recommended by Kaczinski *et al*. (1996). Finally, a value was recommended for the static pressure to represent truck loads.

Applying the dynamic pressure in the horizontal direction to *Structure 3* yields a maximum negative displacement value of 3.55 inches and positive value of 2.35 inches. These values were added together to get the total amplitude of the displacement, which is 5.9 inches. A unit static pressure in the same direction yields a displacement of 0.851 inches. The value of the pressure needed for 5.9 inches displacement was calculated to be 6.93 psf. On the other hand, the maximum values obtained from dynamic analysis for vertical displacement from applying loads in the vertical direction was -1.72 inches and 0.926 inches with total amplitude of 2.646 inches. The maximum value for vertical displacement obtained from applying a unit pressure in the vertical direction was 0.268 inches. This results in an equivalent static pressure of 9.87 psf to achieve the same maximum displacement.

Following the same approach with *Structure 4* yields a maximum negative displacement of 2.99 inches and positive displacement of 1.19 inches due to horizontal dynamic pressure. These values give a total displacement amplitude of 4.18 inches. The displacement caused by a unit static horizontal pressure was 0.681 inches. A value of 6.14 inches of static pressure is needed to get the same dynamic displacement. Regarding the vertical direction, the maximum positive displacement value was 0.12 inches and maximum negative value was -0.2 inches. The unit pressure load gives 0.0532 inches. The equivalent static pressure value was then calculated to be 6.02 psf.

Similarly, *Structure 5* displacements were positive 0.118 inches and negative 0.225 inches from the dynamic horizontal pressure and 0.0674 inches for the unit static horizontal pressure. This results in 5.09 psf for the horizontal pressure. Also, positive 0.0657 inches and negative 0.142 inches were obtained from vertical dynamic pressure; 0.024 inches were obtained for unit static pressure. The accompanied computed value for the equivalent static pressure was 8.65 psf.

Finally, *Structure 6* results were positive 0.574 inches and negative 0.985 inches for dynamic horizontal pressure and 0.32 inches for static horizontal pressure. The equivalent horizontal pressure value was 4.87 psf. Also, positive 0.559 inches and negative 1.44 inches for vertical dynamic pressure and 0.211 inches for static unit pressure. This gives a value of 6.83 psf for equivalent vertical static pressure.

A summary of the dynamic analysis results is presented in Table 3.14, and a summary of static results is presented in Table 3.15. Also, a sample of the displacement time history is shown in Figure 3.13. Figure 3.14 gives the displacement time history of Node 30 near the center of the span in *Structure 5* due to the horizontal dynamic load that represents the truck passage.

The typical noncantilevered, or bridge-type, sign support structures would have a greater span length than cantilevered structures, which have a two lane width requirement as the upper limit. The noncantilevered structures are frequently used over busy interstate roadways with at least three lanes. In a meeting with a local sign support manufacturer that designs and manufactures such structures for practically ever state in the country, they recommended to use a 2 lane width (24 ft).

It can be noticed from the summary of the results that the equivalent horizontal pressure value varies from 4.87 psf to 6.93 psf with an average of 5.76 psf and that the vertical equivalent static pressure is slightly higher, ranging from 6.02 psf to 9.87 psf and with an average of 7.84 psf. The average values were multiplied by a factor of 1.3 to account for increase in the relative truck speed due to head winds. It is recommended that the highest values of these pressures be used. Values of 7.5 psf and 10.2 psf are recommended for horizontal pressure and vertical pressure respectively. These pressures should be applied to a maximum of 24 ft.

Table 3.14. Dynamic Analysis Results of Noncantilevered Sign Supports to Simulate Truck Load

Support structure	Positive displacement due to horizontal pressure	Negative displacement due to horizontal pressure	Amplitude	Positive displacement due to vertical pressure	Negative displacement due to vertical pressure	Amplitude
	(in)	(in)	(in)	(in)	(in)	(in)
(1)	(2)	(3)	(4)	(5)	(6)	(7)
3	2.35	3.55	5.9	0.926	1.72	2.65
4	1.19	2.99	4.18	0.12	0.2	0.32
5	0.118	0.225	0.343	0.0657	0.142	0.21
6	0.574	0.985	1.559	0.559	0.882	1.44

Table 3.15. Static Analysis Results of Noncantilevered Sign Support to Simulate Truck Load

Support Structure	Displacement due to unit pressure	Equivalent static horizontal pressure	Displacement due to unit vertical pressure	Equivalent static vertical pressure
	(in)	(psf)	(in)	(Psf)
(1)	(2)	(3)	(4)	(5)
3	0.851	6.93	0.268	9.87
4	0.681	6.14	0.0532	6.02
5	0.0674	5.09	0.024	8.65
6	0.32	4.87	0.211	6.83

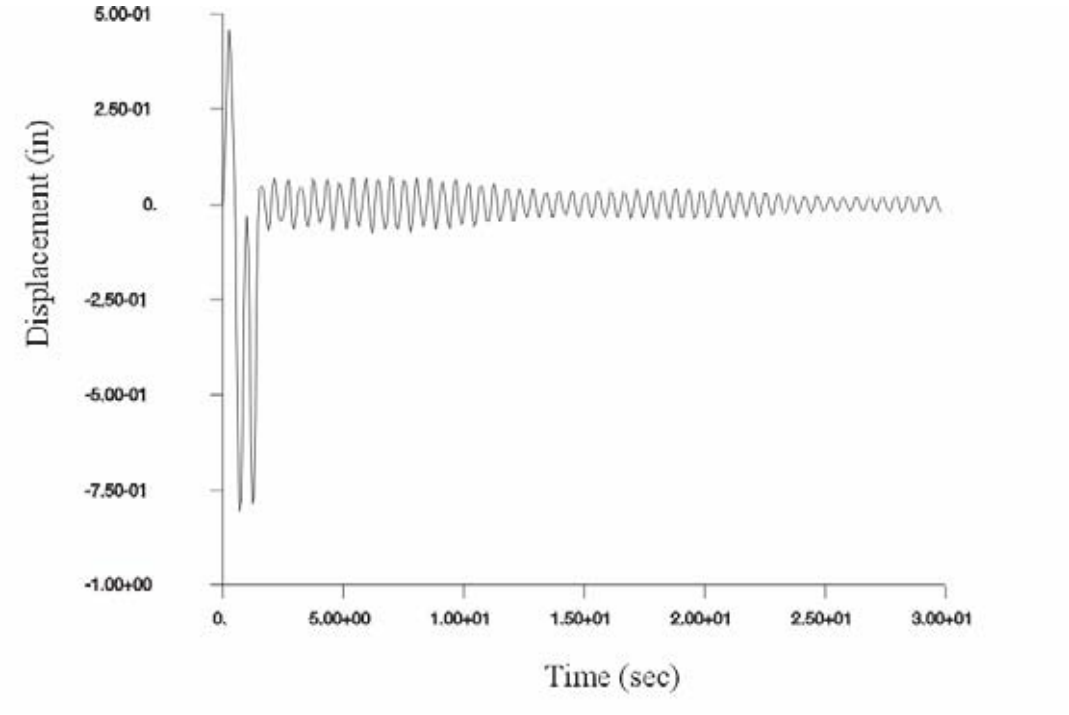

Figure 3.13. Sample Time History Response of the Dynamic Analysis to Simulate Truck Load (Horizontal Displacement of Mid-span joint in Structure 6)

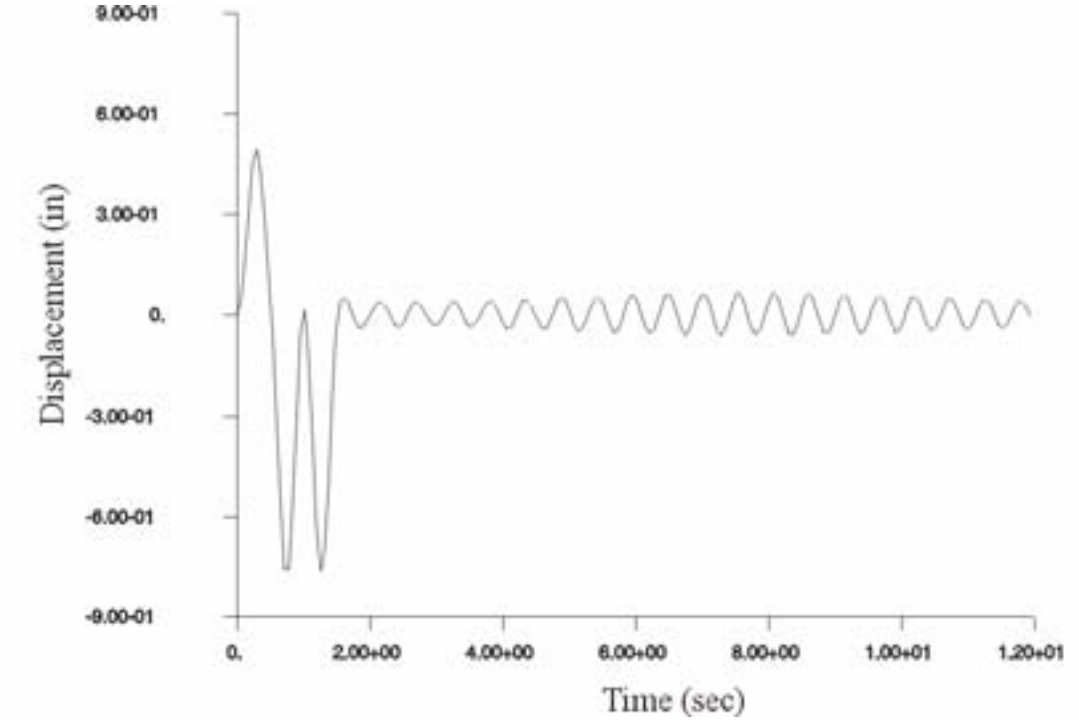

Figure 3.14. Sample Time History Response of the Dynamic Analysis to Simulate Truck Load (Vertical Displacement of Mid-span joint in Structure 6)

3.2.6 Deflection

The allowable deflection limits for in the 1994 standard AASHTO sign support specifications overhead bridge sign structures took the form of limiting the deflection from dead load and ice load. This analogy was used to ensure a minimum stiffness and to help reduce the vibration induced from wind phenomena that were not well identified. The approach suggested in the specification proposed by NCHRP 17-10 was to define the loads that cause different types of vibrations and to check the resulting stresses against the fatigue strength. This will help increase the allowable deflection limit from dead load. Applying appropriate camber can also reduce this deflection. In this research, the deflection values that result from applying the recommended equivalent static pressure loads were checked against the limits proposed by NCHRP Project 17-10. Table 3.15 gives a summary of these deflection values.

It can be seen that all of the deflection values due to fatigue loads are below the limit of 8 inches recommended by NCHRP Project 17-10 proposed specifications. Also, the deflection due to dead load and ice load calculated by others was checked. A value of 6.626 inches was obtained from Ehsani *et al*. (1985). It represents the maximum vertical deflection due to dead load and ice load. The deflection values for *Structures 5* and *6* were obtained from Mirza *et al*. (1975). These values represent the maximum vertical deflection from wind and self-weight. Table 3.16 provides a comparison of the available values calculated by other researchers and the allowable deflection limit for each structure.

Table 3.16 shows that the structures meet the deflection limit requirement of L/150. It can be noticed from both Tables 3.16 and 3.17 that the deflection for truss structures is small compared to monotube structures. It may be 50% less for the same span. The allowable deflections should vary for different types of structures.

Table 3.16. Deflection Values Due to Equivalent Static Loads

Structure	Galloping Deflection	Natural W. Deflection	Truck Gust Deflection	Deflection limit for fatigue loads
	(in)	(in)	(in)	(in)
(1)	(2)	(3)	(4)	(5)
3	5.64	4.33	5.9	8
4	3.16	4.24	4.18	8
5	2.19	0.424	0.343	8
6	2.3	1.46	1.559	8

Table 3.17. Deflection Values Obtained From the Literature

Structure (1)	D.L.+ICE Deflection (in) (2)	L/150 (in) (3)
3	6.626	8
4	NA	4.8
5	0.976	6.56
6	3.101	12

3.2.7 Conclusions Regarding Loads for Overhead bridge Structures

Based on the findings of the analytical research presented in the previous sections of this chapter, the following conclusions can be stated:

Galloping: The static pressure calculated for noncantilevered structures has an average of 21.291 psf, which is slightly higher than the value for cantilevered structures (21 psf). It is recommended to use the same value of 21 psf.

Vortex shedding: The static load model for vortex shedding of a simple pole in the support specifications suggested by NCHRP 17-10 can be applied to the nontapered element in the noncantilevered support structure.

Natural wind loads: The average static pressure calculated for noncantilevered structures is 4.17 psf, which is less than that applied to cantilevered structures. It is recommended to use the same value of 5.2 psf multiplied by the drag coefficient.

Truck-induced loads: It is recommended to use 7.5 psf for the horizontal pressure applied to the area of the sign and the area of the support structures and 10.2 psf for vertical pressure applied to the area of the support structure and the projected area of the sign. These pressures should be applied along at least two lanes (24 ft) of the span that gives the maximum effect. The state DOT may suggest more than two lanes for some highways based on the traffic spectrum.

Deflection: All deflection values were below the limits proposed by NCHRP Project 17-10. It is recommended to use these limits of L/150 for deflection due to dead load and ice load and 8 inches for deflection due to fatigue loads for noncantilevered overhead sign structures.

CHAPTER 4. FATIGUE CATEGORIZATION OF CONNECTION DETAILS FOR NONCANTILEVERED SUPPORT STRUCTURES

4.1 Fatigue Categorization of Connection Details

The 1994 standard sign support specifications require designing the support structures based on the infinite fatigue life (endurance limit) of the materials. The specifications also require that stress calculation for fatigue strength be as provided by the AASHTO bridge specification. The specifications proposed by NCHRP Project 17-10 (1996) (adopted 1999), in which the fatigue-related requirements are largely based on NCHRP Project 10-38, recognized the significant differences between support details and bridge details in terms of geometrical configuration and categorized connection details used for cantilevered support structures in compliance with the bridge specification. This categorization was made to be compliant with fatigue design curves in the AASHTO bridge specifications (1994) and its lower bound endurance limit. The fatigue categorization of details in the AASHTO Bridge Specifications (1994) was largely based on tests that were conducted on various types of details. NCHRP Project 10-38 categorized details based on review of previous research that led to the bridge details categorization, experience with fatigue structural failures and linkage between the cantilevered sign support structure details, and bridge details in terms of stress concentration and crack-formation locations. Test results from other researchers were also considered but were limited.

In research represented in this chapter, the noncantilevered sign support structures drawings and specifications provided by state DOTs were reviewed and various NCHRP reports dealing with fatigue in bridge connection, which provided the basis for bridge specification categorization were studied. Details of noncantilevered support structures were compared to the cantilevered structure details and were categorized as examples. The next few sections describe the findings. First, various types of connections are described in Section 4.2; then, in Section 4.3, factors that affect the fatigue resistance of welded connections are reviewed. The fatigue resistance of bolted connections is discussed in Section 4.4. Finally, the suggested categorization of details is provided in Section 4.5.

4.2 Types of Connections

Connection details used for noncantilevered structures vary widely across the country. Only a few examples are listed here as a guide. The AASHTO bridge specification (1994) classified the welded details into six categories based on their fatigue strength: *Category A* for rolled beams, *Category B* for longitudinal weld and flange splices, *Category C* for stiffeners and short 2-inches attachments, *Category D* for 4-inches attachments, *Category E* for cover-plated beams, and *Category E'* for thick cover-plates and long attachments. NCHRP Project 10-38 identified the following types of

cantilevered support structure details: plain members, mechanically fastened connections, groove welded connections, fillet welded connections, and attachments.

It should be noted here that two details belonging to two different categories might be the same type. The NCHRP Project 10-38 classification was used for noncantilevered support structures.

4.3 Fatigue of Welded Details

Several previous research projects studied issues related to fatigue of welded details for bridges (NCHRP Reports 102, 147, 188, 206, 286, 354). Factors that were thought to affect fatigue life were studied. These factors included stress variables, type of details, type of steel, and quality of fabrication. The stress range and detail type were found to affect the fatigue life significantly. Fisher *et al*. (1986) (NCHRP 286) stated that "all welding processes result in high residual stresses, which are at or near the yield point in the weldment and adjacent base metal." They also stated that "it is apparent that residual stresses play an important role in both the formation of cracks from discontinuities that reside in the tensile residual stress zone and the arrest of cracks as they grow into compression residual stress zone of a member subjected to compression alone." These two statements explain that the detail type should describe the effect of global stress concentration associated with the geometry of the detail, as well as the local stress concentration due to the geometry of the weld and the existence of any weld discontinuity.

4.4 Fatigue of Bolted Details

NCHRP Project 10-38 recommended *Category D* for most of the bolted connections, including U-bolts used to attach the signs and signals to the structures. It suggests that the stress be calculated in terms of net area of the section. NCHRP Project 10-38 also stated that the category could be improved to *Category B* for some details when a high strength bolted connection is fully tensioned. The basis for this categorization was extrapolation of fatigue strength of anchor bolts and other mechanically fastened steel connections, which all fall into *Category D*.

4.5 Categorization of Connection Details

The proposed specifications resulting from NCHRP Project 17-10 introduced the constant-amplitude fatigue thresholds for steel and aluminum for different categories in Table 11-5 of the proposed specifications. The same values for constant-amplitude fatigue threshold are applicable here. The proposed specifications also presented a summary of the typical fatigue-sensitive cantilevered support structures connection details. This summary includes 24 details explained in 13 example drawings. Provided later in this section is a description of the typical details for noncantilevered sign support

structures that were selected after reviewing the state DOTs' standard drawings and the their categories.

Table 4.1. Constant Amplitude Fatigue Threshold

Detail Category	Steel Threshold		Aluminum Threshold	
	(MPa)	(ksi)	(MPa)	(ksi)
(1)	(2)	(3)	(4)	(5)
A	165	24	70	10.2
B	110	16	41	6.0
B'	83	12	32	4.6
C	69	10	28	4.0
D	48	7	17	2.5
E	31	4.5	13	1.9
E'	18	2.6	7	1.0
ET	8	1.2	3	0.44

Presented in Figures 4.1 through 4.3 are 10 connection details that were selected to represent the typical details in noncantilevered support structures.

Example 1 shows a fillet welded tubular joint that is used in truss structures to connect the top or bottom chord to the diagonal and vertical members. This joint is the same as *Detail 19* in NCHRP Project 10-38 and falls into same category.

Example 2 shows another fillet welded tubular joint that connects the vertical and horizontal members and the diagonal in a four-chord truss. This joint also belongs to the same category (ET).

Example 3 shows typical beam column connections in monotube type structures. This connection contains two details. The first is the bolted connection and the recommended category is D, following the NCHRP Project 10-38 recommendation of *Category D* for axially, snug, and fully tightened anchor bolts. The second joint is the fillet welded socket connection. Comparing this detail to *Detail 16* in NCHRP Project 10-38 yields recommendation to use *Category E'*.

Example 4 shows the splice joint in monotube support structures. This connection also has two joints. The high tensioned bolts detail belongs to *Category D* and can be improved to *Category B* if the bolts are fully tensioned. The welded details similar to *Example 3* fall into *Category E'*.

Example 5 shows the column base connection for the monotube connection. For the two details included, one is bolted corresponding to *Category D* and the other welded detail is similar to *Detail 16* in NCHRP Project 10-38 and, hence, it can be categorized as *Category E'*.

Example 6 shows the bottom chord connection. U-bolts are used to keep the chord in place above the horizontal member of the side truss. The U-bolts as discussed above can be considered *Category D*.

Example 7 shows the double-angle truss gusset. This connection has some similarity to *Example 2* of NCHRP Project 10-38. *Category B* was recommended for the high tensioned bolts. The fillet weld detail can be classified as *Category E.*

Example 8 shows the splice connection used for the chord members. The high strength bolt connection can be considered *Category B* if fully tensioned; otherwise, it can be considered *Category D*.

Example 9 shows the column base connection using stiffeners. This connection was discussed in detail in NCHRP Project 10-38; and *Categories C, D*, and *E* were recommended based on the stiffener length. This is explained in NCHRP Project 10-38, *Example 14*.

Example 10 shows the detail of the upper clamp used in truss structures. The example demonstrates three details. The first detail is the U-bolt detail, which can be considered *Category D*. The fillet weld connection can be considered *Category E*, and the high strength tension bolts can be estimated to be *Category D* (improved to *Category B* if fully tensioned).

It should be noted that these recommendations for the categorization of the connection details are based on comparison of these details to similar details used for cantilevered sign support structures. Few details for cantilevered support structures have been tested. For the other details, fatigue resistance was assumed conservatively. Hence, the recommended category can be upgraded in the future if warranted by fatigue tests.

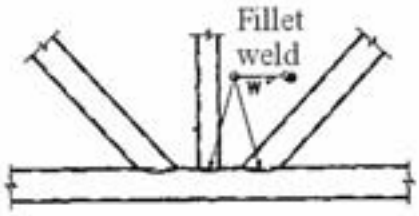

Example 1

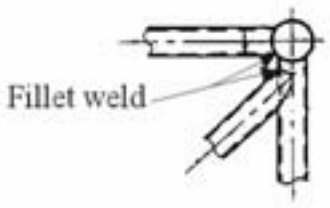

Example 2

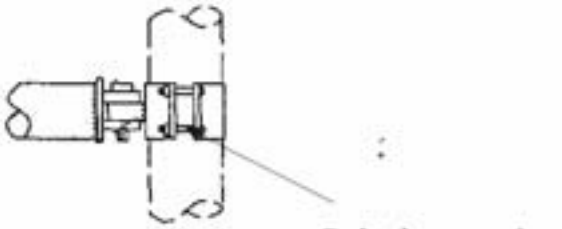

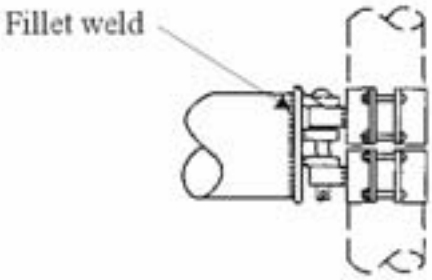

Example 3

Figure 4.1. Detail Examples 1 to 3

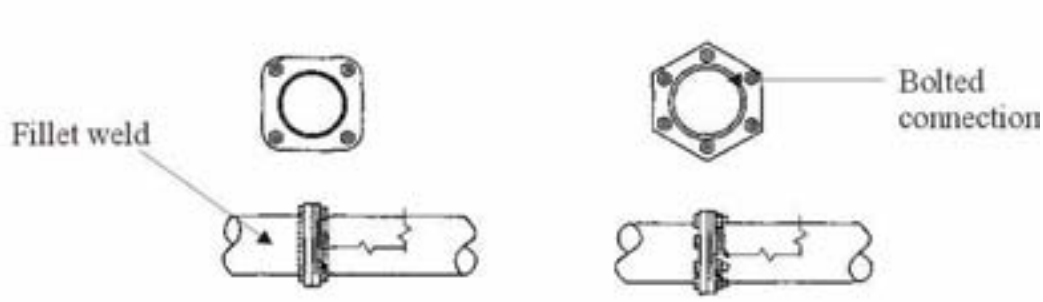

Example 4

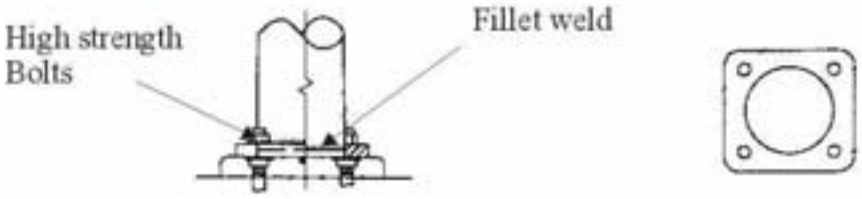

Example 5

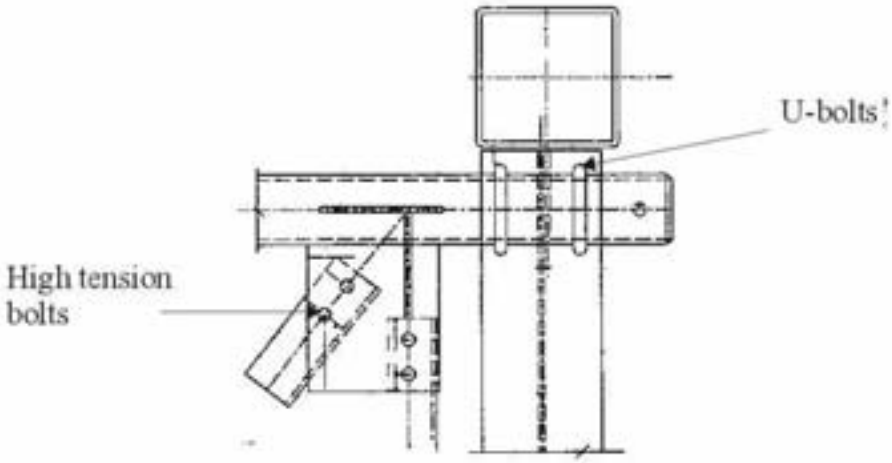

Example 6

Figure 4.2. Detail Examples 4 to 6

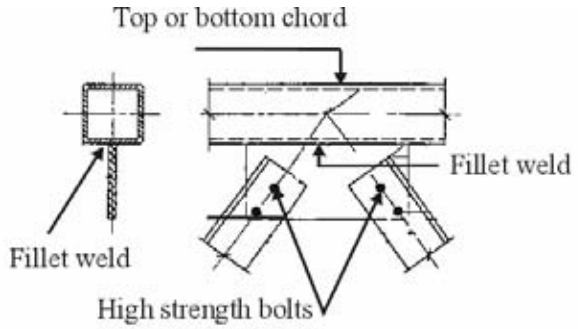

Example 7 Double Angle Truss Gusset

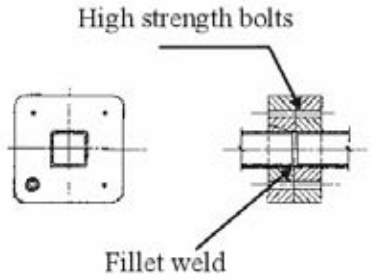

Example 8 Chord Connection Detail

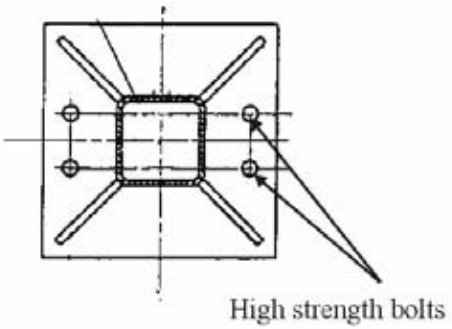

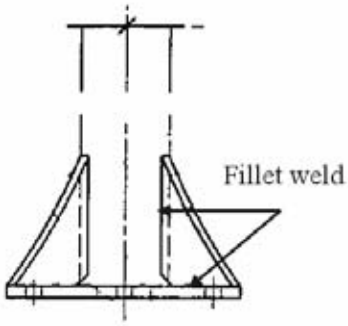

Example 9 Detail of Column-Base Connection

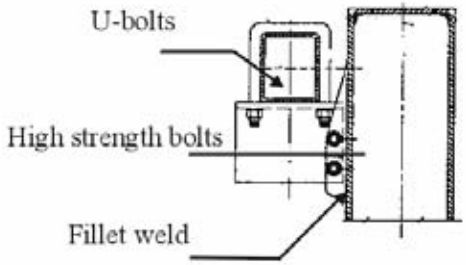

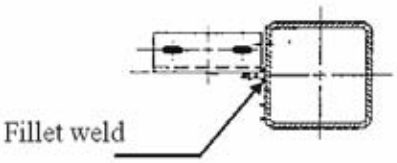

Example 10 Detail of Upper clamp

Figure 4.3. Detail Examples 7 to 10

CHAPTER 5. EFFECTIVENESS OF GUSSETS IN SIGN SUPPORT STRUCTURES

5.1 Effectiveness of Gussets

Gilani and Whittaker (2000) studied the fatigue-life evaluation of steel post structures and recommend revision of the values recommended for galloping loads based on field monitoring. They concluded that the gusset plates serve to substantially reduce the longitudinal and von Mises stresses in the post at locations remote from both the conduit hole and the upper tip of the gusset plates and will effectively protect the post baseplate weldment. However, the maximum stresses in the post (adjacent to the conduit hole) were not significantly affected by the addition of the gussets. Gilani and Whittaker proposed relocating the conduit hole up the post and away from the gusset as it was found that the stresses at the tip of the gussets were of the same order as the maximum stress around the conduit hole. Careful detailing and installation of the gusset plates was suggested. Several other factors, such as the size effect and the grinding of the weld tip, were not considered in their study.

5.2 Example to demonstrate the effect of gusset

Figure 5.1 shows an example of using the gusset at the post base as a stiffener. The drawings and dimensions were obtained from the survey reply of the Minnesota DOT. Using Post 2, 3, and 4, which has an outside diameter of 18 in (450 mm) and wall thickness of 0.375, .500, 0.562 in (9, 12 and 14 mm), respectively. Without using the gusset, the connection is classified as Detail 16 which falls into *Category E'*. The fatigue resistant stress for this category is 2.6 ksi (18 MPa) for steel. This will result in moment capacities of 233, 304, 338 kip-in (26, 34, 38 kN-m). With the gusset configuration provided, the gusset will upgrade this detail capacity. The critical stress range would be at the termination of the stiffener. This was verified by checking that the stress range at the groove-welded column to base plate connection was lower than the 2.6 ksi (18 MPa) limit of *Category E'*. Also, the stress range at the stiffener to base plate connection was checked for all cases to be lower than the 10 ksi (69 MPa) limit of *Category C* modified by the factor of 0.47 to account for the thickness calculated from the equation below

$$(\Delta F) = (\Delta F)_n^c \, x\left(\frac{0.094 + 1.23 * \frac{H}{t_p}}{t_p^{\frac{1}{6}}}\right) \qquad (5\text{-}1)$$

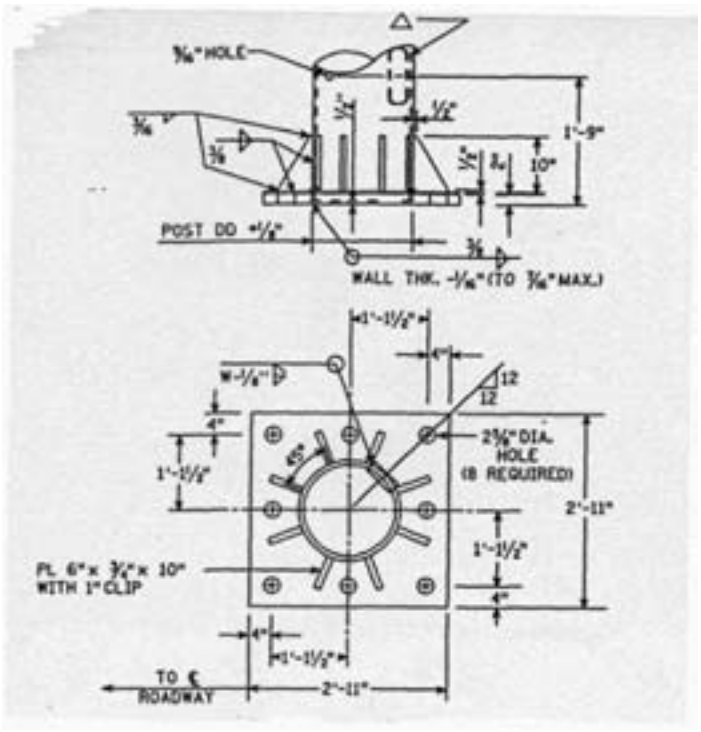

Figure 5.1. Gusset plate configuration

The stiffener length is 10 in., which is equal to 254 mm more than 102 mm. This will result in that detail to be *Detail 21*. The value of α was calculated to be approximately 31 degrees. Thus, the detail is *Category D,* which has a fatigue resistant stress of 7 ksi (48 MPa). The calculated moment capacity then becomes 627, 819, 911 kip-in (70, 91, 101 kN-m). Improving the gusset detail to satisfy the condition of α less than 15 degrees would upgrade the detail to *Category C,* which has a fatigue resistant stress of 10 ksi (69 MPa). The calculated moment capacity then become 896, 1170, 1302 kip-in. Table 5.1 summarizes this data, and Figure 5.2 presents the effect of gusset on the moment capacity of the connection.

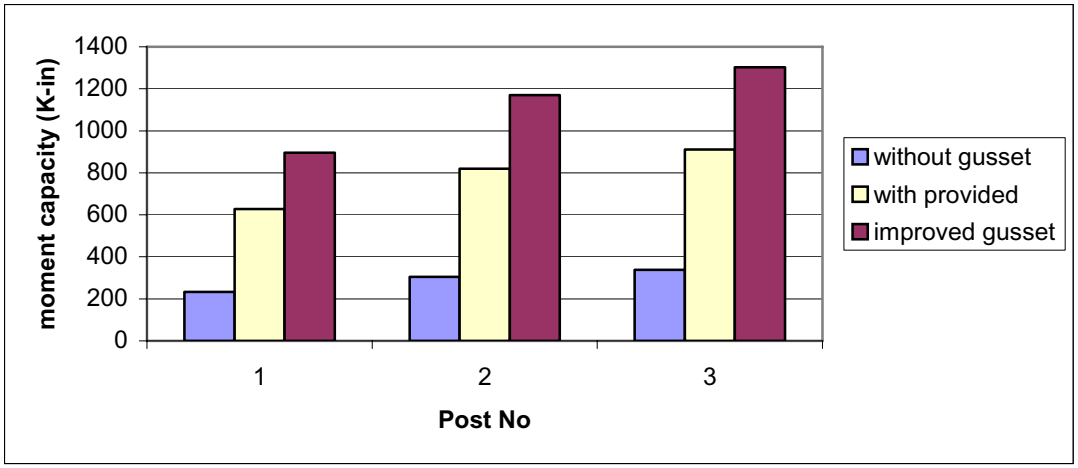

Figure 5.2. Effect of Gusset

Table 5.1. Moment capacity for connections with and without a gusset

Post No.	Post wall thickness	Moment Capacity		
		Without gusset	With provided gusset	Improved gusset
	(in)	(kip-in)	(kip-in)	(kip-in)
(1)	(2)	(3)	(4)	(5)
2	0.375	233	627	896
3	0.500	304	819	1170
4	0.562	338	911	1302

The results presented above shows that increasing the thickness of the post wall by 50 percent results in increasing the moment capacity by 45 percent while adding the gusset provided by the Minnesota standards will increase the moment capacity by approximately 170 percent. Adding another gusset that will meet the angle condition increase the moment capacity by approximately 285 percent.

From the previous calculations it can be concluded that updating the connection by providing a gusset plate will considerably increase the moment capacity of the connection. The moment capacity can even be increased more by appropriate design for the gusset.

5.3 Other Considerations

The material provided in Chapter 5 is based on existing literature. It may be noted that there is a lack of literature in terms of experimental work to verify the assumed fatigue categorization of different connections. The failure presented by Gilani and Whittaker (2000) happened near the conduit hole. Other factors like the size and weld tip treatment could not be demonstrated in the work by Gilani and Whittaker. These factors may govern the fatigue resistance due to the high stress concentration that may develop at the tips of the gusset. More fatigue test is needed to accurately calculate such effect.

CHAPTER 6. VIBRATION MITIGATION MEASURES FOR SIGN SUPPORT STRUCTURES

6.1 Vibration Mitigation Measures

Each of the main four wind loading cases has its own characteristics and hence requires a different type of mitigation measure. Kaczinski *et al*. (1996) suggested the following measures for cantilevered support structures.

A. Galloping

1. Change the dynamic characteristics of the structure such that the magnitude of the onset wind velocity is greater than the wind velocity for which steady-state flows are typically maintained.
2. Change the aerodynamic properties of the attachments such that the structure will experience positive aerodynamic damping when subjected to periodically varying angle of attack of the wind flow.

B. Vortex shedding

1. Alter the dynamic properties of structure.
2. Alter the aerodynamic characteristics of the structures. Altering the cross section of the element such that the formation of the a coherent pattern of vortices from members with circular cross section, helical strakes, shrouds, and the rectangular plate installed at intervals along the members have proven to be an effective method by which to mitigate vibrations in structures such as stacks and chimneys.

C. Natural wind

1. Alter the damping of the structure to lower dynamic amplification factor. Tune-mass and impact dampers have been proposed for galloping and vortex shedding, however, mixed results have been obtained.
2. Stiffening the structure will not mitigate it significantly since this type of loading is not aerodynamic.

D. Truck-Induced Gust vibration

1. Increase the vertical clearance of the sign panel above the tops of the trucks. The vertical clearance may be limited by roadway geometric constraints and sight distance. Recommended values are presented in Table 6.1 to reduce the equivalent static pressure. These values were obtained by rounding the values recommended by Dexter *et al.* (1999) presented in Table 3.13.
2. Use perforated panels and open grating to reduce the effective horizontal projected area.

Table 6.1. Recommended values to reduce truck-induced Gust

Elevation Above Road Surface		Percentage of the Pressure values
(m)	(ft)	%
(1)	(2)	(3)
6 or less	20 or less	100
6.1 to 7	20.1 to 23.33	85
7.1 to 8	23.66 to 26.67	65
8.1 to 9	27 to 30	40
9.1 to 10	30.33 to 33.33	20
10.1 and above	33.67 and above	0

NCHRP project 10-38(2) researchers were contacted to review their latest results regarding evaluating using different types of dampers. The damper devices developed or investigated by Florida DOT, Wyoming DOT, and Texas DOT, along with their effect in reducing the vibration for galloping and vortex shedding was discussed. The following sections describe dampers used and the types that were proven to be the most effective.

6.2 Work done by Cook *et al.* (Florida)

Cook *et al.* tested the following damping devices:

1. Dampers at arm-pole connection (disc springs and neoprene pads)
2. Stock bridge type dampers
3. Liquid tuned dampers
4. Tuned mass dampers
5. Spring/mass friction dampers
6. Spring/mass tapered friction dampers

The device that was chosen to be the most suitable in damping the vibrations of the arm was the tapered impact device shown in Figure 6.1. The device is composed of 102 mm (4 in) steel galvanized pipe, 686 mm (27.5 in) total length, a spring of 0.025 kg/mm (1.415 lb/in) and a mass of 6.8 kg (15 lb). This device was chosen because it provided a significant reduction in amplitude and number of cycles associated with the vibration of typical mast arm traffic signals. The device produced 3.6% critical damping on a 11.0 m

(36.7 ft) mast arm (0.7 Hz) and 2.8 critical damping on a 24.1 m (80.3 ft), mast arm (1.4 Hz) as compared to 0.2% and 0.6 % critical damping respectively without the devices.

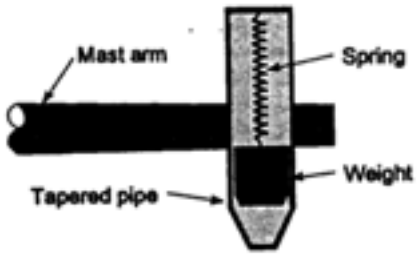

Figure 6.1. Tapered Impact Damping Device

6.3 Work done by Hamilton *et al.* (Wyoming)

Hamilton *et al.* reassembled cantilevered fatigue-damaged structure with a mast arm 50 ft (15.2 m) and tested the following types of damping devices:

1. Elastomeric pad
2. Strut
3. Hapco impact damper
4. Flat bar impact damper
5. Strand impact damper
6. Shot-put impact damper
7. Alcoa dumbbell damper

The configuration of some of these devices is shown in Figures 6.2 through 6.6.

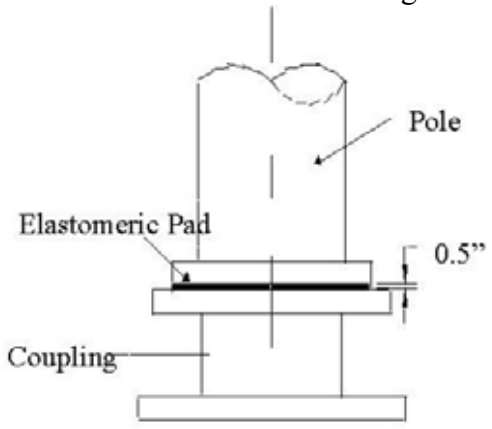

Figure 6.2. Pad at Base

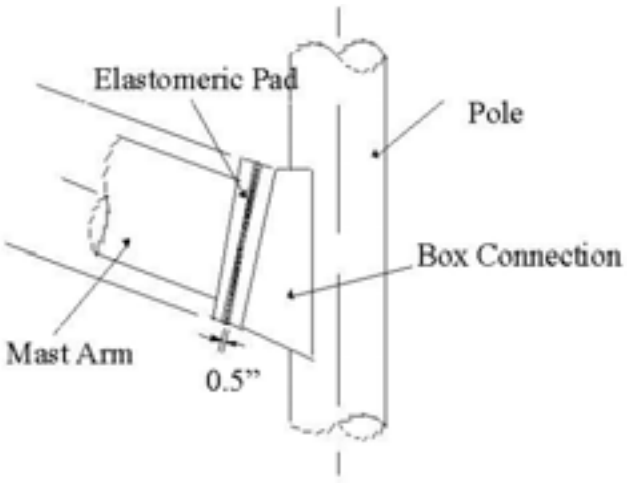

Figure 6.3. Pad at Mast Arm

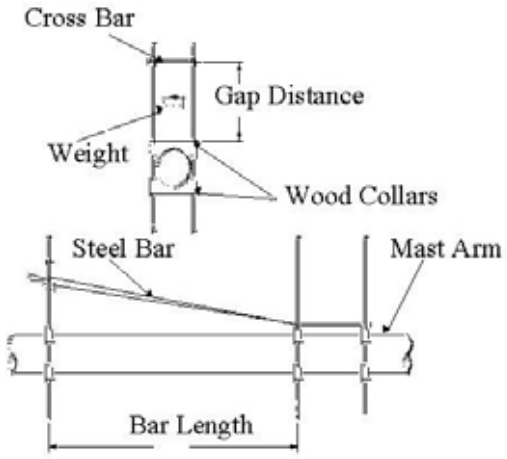

Figure 6.4. Flat Steel Bar

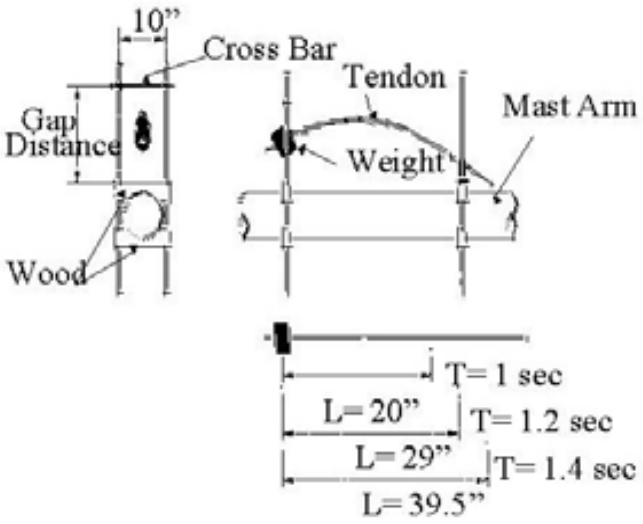

Figure 6.5. Strand Impact Damper

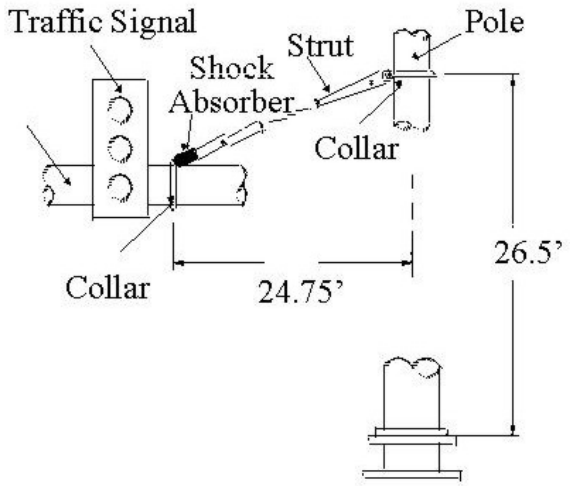

Figure 6.6. Strut and Shock Absorber Damper

The results can be summarized as the following:

In-plane:

- Structures with no damper exhibited a damping of 0.15%
- The most effective damping device was strut damper
- The order of effectiveness is strut, strand, Hapco impact, dumbbell, pads

Out of plane:

- Structures with no damper exhibited a damping of 0.47%
- The most effective damping device was the pad at base
- The order of effectiveness is pads, strand, shot put, Hapco impact, dumbbell, struts
- It was concluded that each retrofit increased damping, some significantly, but refinement and in service validation are necessary. It was also mentioned that to provide effective damping in both directions, a combination of two damping systems might be considered.

6.4 Vibration Mitigation Devices for Noncantilevered Support Structures

Varying values for damping ratio were applied to the galloping model of cantilever *Structure 1* to evaluate how increasing damping will affect the loads. The damping ratio values were selected within the range that was achieved in the previously described work. Figure 6.7 presents the results obtained. Close to 50 percent reduction in the displacement amplitude resulted. This will result in a 50 percent reduction in the equivalent static load.

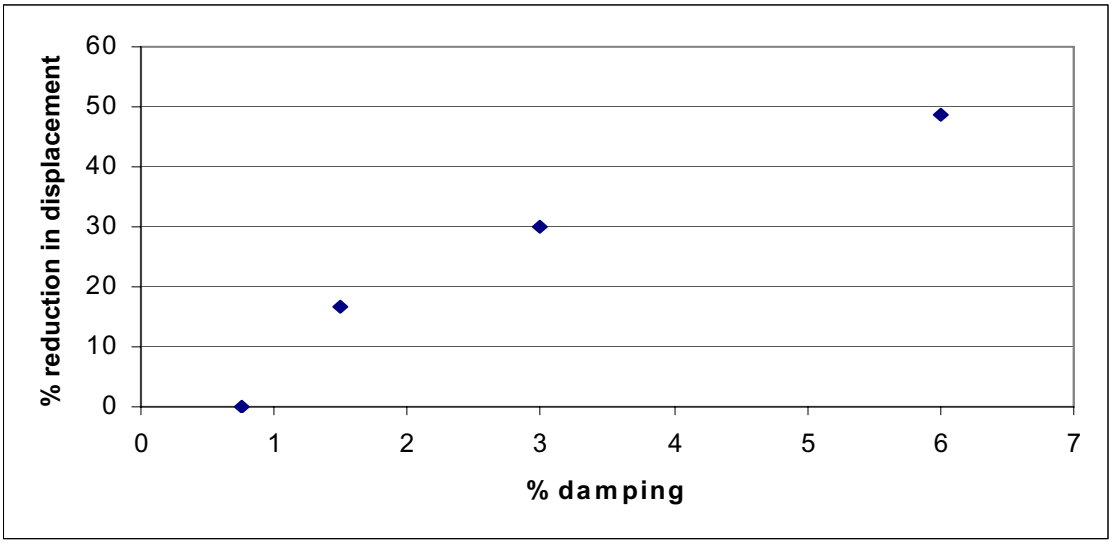

Figure 6.7. Percentage Reduction in Displacement due to Different Values of Damping Ratios.

The only way to verify the effectiveness of different vibration mitigation is through experimental and monitoring work for structures in service. Some devices can be ruled out for noncantilevered support structures. For example, while the strut and shock absorber seems to be the best device for cantilevered structures, it will not be practical for long span noncantilevered monotube structures. Also, the elastomeric pad at

the mast arm appears to not be applicable and the pad at the base appears to not be effective. Cook's damper and the strand impact damper, and flat steel bar damper might be a good choice for noncantilevered structures.

CHAPTER 7. INTERPRETATION AND APPLICATION

7.1 Review of the Existing Specifications

The 1994 "Standard Specifications for Structural Supports for Highway Signs, Luminaries and Traffic Signals", "Ontario Highway Bridge Design Code" (Ontario Ministry of Transportation 1992), NCHRP Project 17-10 proposed specifications (adopted in 1999), and the information provided by state DOTs were reviewed. The areas of wind induced vibration, allowable deflection limit, and fatigue resistance were of special interest. A summary of this review follows.

7.1.1 Wind Induced Limit State Fatigue Loads

The 1994 standard specifications limited the susceptibility of sign structures to vortex shedding vibration. The critical velocity that may cause lock-in phenomena is calculated using the equations 7.1 and 7.2.

$$V_c = \frac{f_n \cdot d}{S_n} \qquad \text{for circular sections} \qquad (7.1)$$

$$V_c = \frac{f_n \cdot b}{S_n} \qquad \text{for multisided sections} \qquad (7.2)$$

where V_c is the critical velocity, f_n is the first natural frequency, d is the diameter of the circular cross section, b is the width of the multisided section, and S_n is Strouhal number (0.15 -0.18).

F_n was estimated by the equation

$$f_n = \frac{1.75}{\pi \cdot (\frac{E \cdot I}{m \cdot l^4})} \qquad (7.3)$$

The equation was developed for cantilevered beams. The applicability of this equation for structures other than cantilevered beams, like cantilevered and noncantilevered sign support structures, was questioned by Kaczinski *et al.* (1996).

The specifications also state that the vibration in truss towers occurs primarily in individual members (locally), which limits the susceptibility to vibration for the slender tension members. This assumption neglects the possibility of vibration of the whole structure.

NCHRP Project 17-10 proposed a new section to address fatigue design based on the findings of NCHRP Project 10-38. The fatigue section is limited to steel and aluminum cantilevered support structures. It introduces four different mechanisms for vibration of such structures. These mechanisms were also quantified by applying equivalent static loads that represent the effect of each mechanism.

The first mechanism, galloping, was represented by an equivalent static pressure range equal to 1000 Pa (21 psf) applied vertically to the surface area of all signs and/or signals.

The second mechanism, vortex shedding, was expressed as transverse load applied along the length of the luminaries column and calculated as follows:

$$P_{vs} = \frac{0.613 \cdot V_{cr}^2 \cdot C_d}{2 \cdot B} \qquad \text{(Pa)} \qquad (7.4a)$$

$$P_{vs} = \frac{0.00118 \cdot V_{cr}^2 \cdot C_d}{2 \cdot B} \qquad \text{(psf)} \qquad (7.4b)$$

The proposed specifications exclude tapered elements from susceptibility to this mechanism if the element is uniformly tapered not less than 0.017 mm/mm (0.14 in/ft).

The third mechanism, natural wind gusts, was expressed as an equivalent pressure range applied horizontally (along wind direction) to the projected area of all exposed structure members and attachments. The value of this pressure range can be calculated from these formulas:

$$P_{NW} = 250 \cdot C_d \qquad \text{(Pa)} \qquad (7.5a)$$

$$P_{NW} = 5.2 \cdot C_d \qquad \text{(psf)} \qquad (7.5b)$$

The last mechanism, truck gusts, was represented by equivalent pressure applied in the vertical direction to the projected area on a horizontal plane of the structure members and attachments. The value of this pressure range can be calculated from

$$P_{TG} = 1760 \cdot C_d \qquad \text{(Pa)} \qquad (7.6a)$$

$$P_{TG} = 36.6 \cdot C_d \qquad \text{(psf)} \qquad (7.6b)$$

7.1.2 Allowable Deflection Limit

In dealing with deflection, the 1994 standard AASHTO specifications for structural supports for highway signs, luminaries, and traffic signals limit the ratio of the maximum deflection to the span length from dead loads plus ice for overhead steel monotube and steel truss structures to a maximum value of $L/150$. For aluminum structures, the specification requires the structures to be equipped with approved damping or energy absorbing devices both before and after installation of signs to prevent significant oscillations.

For cantilevered supports, luminaries, traffic signals, and signs, the deflection is controlled by limiting the angular rotation resulting from the effect of eccentric loads to an angle of 1^{o} 40' or a slope deviation of 0.35 inches (0.009 m) per 12 inches (0.305 m). The horizontal displacement of the top of the structure from the effects of overhead electric power cables or suspension cables is limited to 2.5 percent of the structure height. It also permits permanent camber of $L/100$, in addition to dead load camber for horizontal members of sign bridges, butterfly structures, and cantilevered structures.

The deflection limit for monotube and truss type structures under dead load plus ice load of $L/150$ was not changed in the NCHRP Project 17-10 proposed specifications. However, the deflection limit was reduced to 1.5 percent of height under loads from vertical supports. It also allowed the maximum deflection of the vertical support to reach 15 percent of the height for luminaire support structure under Group II (dead load plus wind load combination).

The NCHRP Project 17-10 proposed specifications introduced a new deflection limit of 8 inches under Group IV (for the range of galloping loads and truck-induced fatigue load combination).

7.1.3 Fatigue Resistance of Connection Details

As stated before, the 1994 AASHTO standard specification for structural supports for highway signs, and luminaries contains provisions that fatigue strength should be as specified by the AASHTO Standard Specifications for Highway Bridges (1994). The specifications consider the possibility of exceeding the number of cycles used in the bridge specifications due to the nature of wind loading by suggesting using infinite fatigue life (endurance limit) based design. The specification recognizes the importance of some connections (areas) by requiring exceeding care in fabrication and design. The areas mentioned are the junction of the base and shaft and the connection of the bracket arm and shaft.

The proposed specifications resulting from NCHRP Project 17-10 provided more guidance for fatigue resistance. It categorized the cantilevered support structure connection details using the same categories used by AASHTO Standard Specifications for Highway Bridges (1994) and by the American Welding Society (1992). NCHRP Project 10-38, which is the reference for such categorization, classified the connections

into four main groups: plain members, mechanically fastened connections, groove welded connections, and fillet weld connections. Each group has connections that may fall into different categories, depending on some other considerations. The details of each individual connection determine whether to improve or reduce the fatigue resistance. A complete listing of these connections can be found in Section 2.3 of the report and indicate changes to the specifications that deals with fatigue.

7.2 Proposed Modification

Based on the analytical study that was conducted as part of this research, the same values used for galloping, vortex shedding, and natural wind loads used for cantilevered support structures are recommended for noncantilevered support structures. Only truck-induced vibration load is recommended for modification. The deflection values that were recommended by Project 17-10 were found to be applicable. Few details were added to the detail categorization. Section 2.3 presents modifications to Chapter 11 of the specifications for support structures. This includes all the modifications described above.

Faced with the uncertainty associated with fatigue loads, the lack of fatigue case documentation regarding noncantilevered support structures, and the need to develop fatigue loads that address fatigue problems of such structures, the research team decided to use fatigue design loads established for cantilevered support structures as a basis and to correlate the loads for noncantilevered support structures with the loads used for cantilevered structures. Basing loads for noncantilevered support structures on those previously established for cantilevered structures will facilitate easy modifications to these loads in the future. Also, these loads may need to be adjusted through the use of importance factors. Importance factors for noncantilevered support structures are recommended below based on discussions with other researchers and NCHRP Project 17-10(2) panel comments. As a future enhancement, these importance factors should be evaluated based upon structures that exhibited fatigue problems. The following section provides a brief description of the importance factors, and introduces how these importance factors may be applied to the noncantilevered support structures.

7.3 Importance Factors

Importance factors account for the degree of hazard to traffic and damage to property. The importance factors for cantilevered support structures were introduced in the 2001 support structures specifications based on the findings of NCHRP Project 10-38. Support structures were classified according to their locations into the following three categories:

- Category I represents the essential facilities and it is applied to “critical support structures installed on major highways”

- Category II represents a substantial hazard to human life in the event of failure and it is applied to “other support structures installed on major highways and all support structures installed on secondary highways”

- Category III represents low-risk structures and it is applied to “support structures on all other locations”

Discussions with NCHRP Project 10-38(2) researchers, along with panel comments, were considered for developing importance factors for noncantilevered support structures. The importance factors presented in Table 7.1 are suggested and will be conservative. These factors are similar to the factors for cantilevered sign support structures. The factors for Category II are slightly higher than the factors in the 2001 specifications. These factors were obtained from the latest information from NCHRP Project 10-38(2). The "X" for galloping of truss support structures is based on experience of other researchers who have indicated that noncantilevered truss support structures are not susceptible to galloping. These factors were assumed conservatively and can be modified after developing a system to report the fatigue cases and gathering enough information to have accurate values.

Table 7.1. Importance Factors for Vibration and Fatigue Design for Noncantilevered Sign Support Structures

Category	Structure Type	Importance Factors			
		Galloping	Vortex shedding	Natural Wind	Truck Gust
I	Truss Monotube	X 1.0	X X	1.0 1.0	1.0 1.0
II	Truss Monotube	X 0.72	X X	0.85 0.85	0.9 0.9

CHAPTER 8. SUMMARY, CONCLUSIONS, AND SUGGESTED RESEARCH

8.1 Summary and Conclusions

The 1994 edition of the Support Specifications provided little guidance on fatigue-resistant design of sign support structures. NCHRP Project 17-10 introduced a new section on fatigue-resistant design, but it was limited to cantilevered structures. A major objective of this research was to establish fatigue resistant design guidelines for noncantilevered support structures.

In order to achieve this objective of this research the following steps were taken:

First, a survey was sent to state DOTs and sign support manufacturers to determine current vibration and fatigue concerns for noncantilevered support structures and research needs. Although most of the noncantilevered support structures indicate satisfactory performance in terms of fatigue, the survey response indicated that noncantilevered support structures have had problems attributed to fatigue. This indicates a need to develop fatigue loads for design. However, problems encountered were not accurately analyzed and documented, and therefore it is difficult to identify and quantify vibration phenomena that have caused fatigue problems.

A comprehensive literature review was then done to study the various phenomena associated with wind and the behavior of noncantilevered sign support structures and the conditions that lead to each phenomenon. The literature review also included a review of the existing specifications regarding the support structures and fatigue design. The survey and literature review led to an analytical investigation to calculate the fatigue loads that may be appropriate for noncantilevered support structures.

The analytical study developed static loads based on comparisons to cantilevered structures that represent each wind load phenomenon. This approach is conservative.

A summary of the general conclusions from this research is as follows:

1. Noncantilevered support structures have fatigue-related problems that rank second after cantilevered support structures among the seven types of sign support and luminaire structures in frequency of fatigue problems. Available data is too lacking to determine decisively which wind load phenomena are causing fatigue problems.
2. Equivalent static loads that represent various wind load phenomena were established. Loads for galloping, vortex shedding, and natural wind remained unchanged from cantilevered support structures. New values for truck-induced wind loads were recommended.
3. Deflection limits stated in Project 17-10 were found to be applicable.

4. Typical noncantilevered support structure connection details were categorized. Most of the details were found to be similar to those of cantilevered structures. Few other details were estimated in light of the previous literature and in agreement with Project 10-38 categorization.

8.2 Suggested Research

The following items are recommended for future research:

1. Fatigue test many typical details to categorize connection details accurately. As stated before, few tests have been performed and other details were categorized based on conservative assumptions that need to be verified with fatigue tests.
2. Develop a manual that recommends types of connections, welding methods that are more fatigue resistant, and methods of weld inspection. The fatigue-testing program mentioned above will help in developing this manual.
3. Develop mitigation measures. This will be studied as part of Task 11 of NCHRP Project 17-10(2) in light of the available literature. Limited information regarding this issue was found. Evaluation of different methods and devices used to mitigate vibrations in support structures is needed.
4. Evaluate the dynamic behavior of existing support structures. This can be done through monitoring programs that measure the displacement amplitude of some structures and comparing the response with the recommended equivalent static loads.
5. Collect data regarding fatigue and vibration from different inspection programs mentioned in the state-DOTs survey. This will help to build a database to improve fatigue-resistant design of support structures. The database should have information about the structure configuration, connection details, and structure location.
6. Conduct an analytical parametric study to get a structure-specific deflection limit. As mentioned before, the truss type structures have less deflection than mono-tube type structures. This study should consider the serviceability requirement.
7. Coordinate efforts with different DOT offices to identify vibration problems in the current noncantilevered structures that was designed based on the old specification. Analyze the data to gain more information regarding fatigue loads that cause such vibration. Improve loads and importance factors.
8. Conduct an analytical parametric study using the proposed fatigue loads in order to calibrate the loads for structure type, spans, material, and any other related parameter. The checked structures should include the structures that exhibit satisfactory performance in terms of fatigue and structures that have fatigue problems.

REFERENCES

American Association of State Highway and Transportation Officials. (1994), "AASHTO LFRD bridge design specifications," First Edition. Washington, D.C.

American Association of State Highway and Transportation Officials. (1994) "Standard Specifications for Structural Supports for Highway Signs, Luminaries and Traffic Signals," Washington, D.C.

American Welding Society. (1992). "Structural welding code." D1.1.

Cook R.A., Bloomquist, D., and Kalajian, M.A. (1999). "Mechanical damping system for mast arm traffic signal structures." *Proc. 1999 Structures Congress*, New Orleans, La.

Creamer, B.M., Frank, K.H., and Klingner, R.E. (1979). "Fatigue loading of cantilevered sign structures from truck-induced gusts," *Rep. No. FHWA/tx-79/10+209-1f,* Center for Highway Research, University of Texas, Austin, Tex.

Davenport, A.G., *et al.* (1976). "Vibration of structures induced by wind," *Shock and vibration handbook,* Second Edition. C.R. Harris, ed., McGraw-Hill, New York, N.Y.

Den Hartog, J.P. (1956) *Mechanical Vibrations*, Fourth Edition. McGraw-Hill, New York, N.Y.

Desantis, P.V., and Haig, P. (1996) "Unanticipated loading causes highway sign failure," Proc., of ANSYS Convention. Houston, PA.

Ehsani, M. R., Chakrabarti, S. K., and Bjorhovde, R. (1985) "Static and dynamic behavior of monotube span-type sign structures." *Report No. FHWA/AZ/194*, Vols. I & II, Arizona Department of Transportation, Phoenix.

Gilani, A. and Whittaker A. (2000) "Fatigue-life evaluation of steel post structures. I: Background and analysis." Journal of Structural Engineering, Vol. 126, ASCE.

Gilani, A. and Whittaker A. (2000) "Fatigue-life evaluation of steel post structures. II: Examination." Journal of Structural Engineering, Vol. 126, ASCE.

Fisher, J.W., *et al.* (1970). "Effect of weldments on the fatigue strength of steel beams." *National Cooperative Highway Research Program, Rep. No. 102*, Transportation Research Board, Washington, D.C.

Fisher, J.W., *et al.* (1986). "Fatigue strength of steel beams with welded stiffeners and attachments." *National Cooperative Highway Research Program, Rep. No. 286*, Transportation Research Board, Washington, D.C.

Fisher, J.W., *et al.* (1992). "Structural failure modes of advanced double-hull, fatigue and fracture failure modes." *TDL 91-01*, Vol. 3a, Lehigh University, Bethlehem, Pa.

Fisher, J.W., Nussbaumer, A., Keating, P.B., and Yen, B.T. (1993) "Resistance of welded details under variable amplitude loading.", *National Cooperative Highway Research Program Rep. No. 354*, Washington, D.C.

Fouad, F. H., Nunez, E, and Calvert, E. A., (1999). "Proposed revisions to AASHTO standard specifications for Highway Signs, Luminaires, and Traffic Signals." *Transportation Research Record, No. 1656*, 102-109. National Academy Press, Washington, D.C.

Fouad, F. H., Calvert, E., and Nunez, E. (1998). "Structural supports for highway signs, luminaires, and traffic signals," *National Cooperative Highway Research Program Rep. No. 411*, Transportation Research Board, National Research Council, Washington, D.C.

Gockel, M.A. (1983). *Handbook For dynamic analysis MSC/NASTRAN*. MacNeal-Schwendler Corp., Los Angeles.

Kaczinski, M.R., Dexter, R.J., and Van Dien, J.P. (1996). "Fatigue resistant design of cantilevered signal, sign and light supports." *National Cooperative Highway Research Program, Final report - NCHRP Project 10-38*, Transportation Research Board, Washington, D.C.

Keating, P.B., *et al.* (1986). "Evaluation of fatigue tests and design criteria on welded details," *National Cooperative Highway Research Program, Rep. No. 286*, Transportation Research Board, Washington D.C.

Johns, K.W., Dexter, R.J. (1999). "Truck-induced wind loads on highway sign support structures." *Proc., 1999 Structures Congress*, New Orleans, La.

Lundgren, H.R. (1989). "Evaluation of monotube sign support structures." Ariz. Dept. of Transp., *Rep. No. FHWA - AZ89 -829*,

Martin, K.A., Ehsani, M.R., and Bjorhoude, R. (1986). *Field testing of monotube span-type sign structures*. Ariz. Transp. and Traffic Institute, College of Engineering, Univ. of Arizona,

Mirza, J.F., Tung, C.C., and Smith, J.C. (1975). "Static and dynamic behavior of tri-chord truss' overhead sign support structures." North Carolina State University, NC.

Novak, M. (1972). "Galloping oscillations of prismatic structures." *J. Engrg. Mechanics Division*, ASCE, 98, (EM1).

Ontario Ministry of Transportation. (1992). *Ontario highway bridge design code*, Third Edition. Ontario, Canada.

Parkinson, G.V., *et al.* (1961). "On the aeroelastic instability of bluff cylinders." Transactions ASME, *J. App. Mechanics*, 83.

Appendix D

Drag Coefficient Transitions for Multi-Sided to Round Cross-Sections

Table of Contents

Drag Coefficient Transitions for Multi-Sided to Round Cross-Sections

D.1 GENERAL

Table 3-6 of the 2001 specifications (1) provides drag coefficients for round and multi-sided shapes, which are consistent with the 1994 *Supports Specifications* (2), except for some minor changes related to the use of SI units and the 3-second gust wind velocity. The drag coefficients do not appropriately address the condition of a tapered pole with a multi-sided cross section that has large bend radii or is small in size such that the cross-section approaches a round section.

In general, multi-sided shapes have higher drag coefficients than round shapes. Figure D-1 provides a comparison of drag coefficient values for the various round and multi-sided shapes. For example, for $C_vVd>78$, the drag coefficient is 0.45 for a round shape and between 0.55 and 0.83 for a 16-sided shape, where C_v is the square root of the importance factor, V is the basic wind velocity, and d is the depth of the member. This represents an increase of about 22 to 84 percent in drag coefficient for the multi-sided shape over that of a round shape. Considering a tapered pole with a multi-sided cross section, a drag coefficient of 0.55 to 0.83 would normally be used according to the *Supports Specifications*. At higher elevations on the tapered pole, where the pole dimensions become smaller, the shape of the cross section could approach that of a round shape. It may be justifiable to use a lower drag coefficient at the higher elevations.

A procedure has been developed that will provide a drag coefficient for the transition from multi-sided to round shape.

D.2 THE RATIO *r*

In Figure D-1, drag coefficients (shape factors) for round and multi-sided shapes are compared. The drag coefficients are based on the equations in Table 3-6 of the *Supports Specifications*, which are reproduced in Table D-1.

For multi-sided sections, the ratio r is defined as the ratio of the outside corner radius to the radius of the inscribed circle. The value r represents the percentage of the circumference of a multi-sided shape that is curved, i.e. the ratio r may be used as a

measure of the degree of roundness of a cross section. For *r* values of 0, the cross-section a "pure" multi-sided section with sharp corners. For *r* values of 1, the cross section is round. The values of *r* will be between 0 and 1.

Another roundness ratio R_D, on the other hand, is defined as the ratio of the diameter across flats to the diameter across the rounded corner. For 16-sided shapes, R_D can vary from 0.9808 to 1 ("pure" multi-sided shape to round). For 12-sided shapes, R_D can vary from 0.9659 to 1. For 8-sided shapes, R_D can vary from 0.9239 to 1.

Table D-2 provides a comparison of the two parameters *r* and R_D for selected diameters for 16, 12, and 8-sided sections and an outside bend radius at the corners of 4 inches. For a given flat-to-flat width and bend radius, the ratio *r* is the same for 16, 12, and 8-sided cross sections. The roundness ratio R_D vary with number of sides, flat-to-flat width, and bend radius at the corners. The ratio *r* is more sensitive to the dimensions of the cross section and the bend radius, and hence it is a better indicator when comparing round and multi-sided shapes than the roundness ratio R_D.

D.3 PROPOSED EQUATIONS

A drag coefficient transition equation has been developed for multi-sided tapered poles with geometry approaching round sections. The proposed transition method for drag coefficients may be expressed as follows:

$$\text{If } r \le r_m \text{, then } C_d = C_{dm} \qquad \text{Eq. D-1}$$

$$\text{If } r_m < r < r_r \text{, then } C_d = C_{dr} + \left(C_{dm} - C_{dr}\right)\left(\frac{r - r_r}{r_m - r_r}\right) \qquad \text{Eq. D-2}$$

$$\text{If } r \ge r_r \text{, then } C_d = C_{dr} \qquad \text{Eq. D-3}$$

Where C_d is the drag coefficient to be used in the design

C_{dm} is the drag coefficient for the multi-sided section

C_{dr} is the drag coefficient for the round section

r is the ratio of the corner radius to radius of inscribed circle for the multi-sided cross section

r_m is the ratio of the corner radius to radius of inscribed circle where the multi-sided-cross section is considered multi-sided, as shown in Table D-3.

r_r is the ratio of the corner radius to radius of inscribed circle where the multi-sided-cross section is considered round, as shown in Table D-3.

Figure D-2 illustrates the proposed equations for the multi-sided shapes. It is a linear equation that transition between the multi-sided and round cross sections. Limiting constants representing the range of applicability of the equation are given. These constants define the transition points. They were arbitrarily selected based on analytical studies and observation. Table D-3 presents four methods (equations) that were considered in the analytical study. The difference in the methods vary where the transition for multi-sided and round sections begin. For a 16-sided shape in Method No. 4, the shape is considered multi-sided when $r<0.26$ and round when $r>0.625$. The transition equation is applied for $0.26<r<0.625$.

D.4 COMPARISON OF PROPOSED DESIGN METHOD TO THE EXISTING EQUATIONS

Figures D-3 through D-6 show the transitional limits provided in Table D-3 for the four different methods. Comparisons of the proposed transition equation for Method Nos. 1, 2, 3, and 4 were made for the 16-, 12-, 8-sided and round cross-sections. The proposed transition equations are plotted in Figures D-7 through D-102 with bend radii of 2 and 4 inches, mean recurrence intervals of 50 and 25 years, and wind speeds of 90 and 150 mph. Tables D-4 through D-11 provide drag coefficients for various diameters for the four methods. Percentage difference between the proposed method and the multi-sided shape is provided also. When comparing the 2- and 4-inch bend radii, the change in the drag coefficient is larger for the 4-inch bend radius, and also affects a large range of diameters.

D.5 SAMPLE CALCULATION

Calculate the drag coefficient using Method 4 for a 16-sided section with a diameter of 20 inches, wall thickness of 1/4 inch, and an inside bend radius of 4 inches. The drag coefficient is to be calculated for a 25-year MRI and a 90 mph wind speed.

1. Calculate the ratio *r,*

$$r = \frac{4in + 0.25in}{20in/2} = 0.425$$

2. Calculate C_vVd,

$$C_v = 0.93 \qquad \text{(Table 3-4, } \textit{Supports Specifications}\text{)}$$

$$V = 90mph$$

$$d = \frac{20in}{12in/ft} = 1.667\,ft$$

$$C_vVd = 0.93 * 90mph * 1.667\,ft = 139.5mph * ft$$

3. Calculate the drag coefficient for a round section C_{dr}. Since $C_vVd>78$,

$$C_{dr} = 0.45 \qquad \text{(Table 3-6, } \textit{Supports Specifications}\text{)}$$

4. Calculate the drag coefficient for a 16-sided section C_{dm}. Since $C_vVd>78$ and $r>0.26$,

$$C_{dm} = 0.55 \qquad \text{(Table 3-6, } \textit{Supports Specifications}\text{)}$$

5. Determine r_m and r_r from Table D-3 for Method No. 4 for a 16-sided shape,

$$r_m = 0.26$$

$$r_r = 0.625$$

6. Since $r_m \le r \le r_r$, then calculate the drag coefficient using the transition Eq. D-2,

$$\text{For } r_m < r < r_r, \text{ then } C_d = C_{dr} + \left(C_{dm} - C_{dr}\right)\left(\frac{r - r_r}{r_m - r_r}\right)$$

$$\text{For } 0.26 < r < 0.625, \text{ then } C_d = 0.45 + \left(0.55 - 0.45\right)\left(\frac{0.425 - 0.26}{0.625 - 0.26}\right)$$

$$C_d = 0.4952$$

D.6 SUMMARY

A method was developed to determine the drag coefficient for the transition from multi-sided to round shape. The proposed method uses a linear equation with respect to the variable r to interpolate between the drag coefficient for round poles, C_{dr}, and the drag coefficient for multi-sided poles, C_{dm}, with respect to the variable r. The accuracy of the proposed design method should be verified through experimental results. Wind tunnel tests using a wide range of multi-sided pole sections with different values for r would be needed.

REFERENCES

1. AASHTO, *Standard Specifications for Structural Supports for Highway Signs, Luminaires and Traffic Signals*. Fourth Edition, American Association of State Highway and Transportation Officials, Washington, D.C. (2001) 270 pp.

2. AASHTO, *Standard Specifications for Structural Supports for Highway Signs, Luminaires and Traffic Signals*. Third Edition, American Association of State Highway and Transportation Officials, Washington, D.C. (1994) 78 pp.

ANNEX A

LIST OF TABLES

Table D–1. From Table 3-6, Wind Drag Coefficients, C_d in the *Supports Specifications*

	$C_vVd \le 5.33$ (39)	5.33 (39) < C_vVd < 10.66 (78)	$C_vVd \ge 10.66$ (78)
Hexdecagonal: $0 \le r < 0.26$	1.10	$1.37 + 1.08r - \frac{C_vVd}{19.8} - \frac{C_vVdr}{4.94}$ (SI) $1.37 + 1.08r - \frac{C_vVd}{145} - \frac{C_vVdr}{36}$ (U.S. Cust.)	0.83 - 1.08r
Hexdecagonal: $r \ge 0.26$	1.10	$0.55 + \frac{(10.66 - C_vVd)}{9.67}$ (SI) $0.55 + \frac{(78.2 - C_vVd)}{71}$ (U.S. Cust.)	0.55
Dodecagonal (See Note 5)	1.20	$\frac{3.28}{(C_vVd)^{0.6}}$ (SI) $\frac{10.8}{(C_vVd)^{0.6}}$ (U.S. Cust.)	0.79
Octagonal	1.20	1.20	1.20
Cylindrical	1.10	$\frac{9.69}{(C_vVd)^{1.3}}$ (SI) $\frac{129}{(C_vVd)^{1.3}}$ (U.S. Customary)	0.45

Note 5. Valid for members having a ratio of corner radius to distance between parallel faces equal to or greater than 0.125.

Table D–2. Sample Dimensions for Multi-Sided Cross-Sections

Number of sides	16		12		8	
Flat-to-flat width (in)	30.77	10.67	30.77	10.67	30.77	10.67
Rounded corner-to-corner dia. (in)	31.22	10.72	31.57	10.76	32.65	10.89
Bend radius at corners (in)	4.0	4.0	4.0	4.0	4.0	4.0
Ratio for bend radius to flat width, r	0.26	0.75	0.26	0.75	0.26	0.75
Portion of circumference that is curved	26 %	75 %	26 %	75 %	26 %	75 %
Portion of circumference that is flat	74 %	25 %	74 %	25 %	74 %	25 %
Roundness ratio, R_D	0.985	0.995	0.974	0.991	0.942	0.979

Table D–3. The Ratio *r* for the Drag Coefficient Transition Equations

		r_m	r_r
Method No. 1	16-sided	0.2752	0.4844
	12-sided	0.5975	0.7136
	8-sided	0.8277	0.8774
Method No. 2	16-sided	0.26	0.75
	12-sided		
	8-sided		
Method No. 3	16-sided	0.50	1.00
	12-sided		
	8-sided		
Method No. 4	16-sided	0.26	0.625
	12-sided	0.50	0.75
	8-sided	0.75	1.00

Table D–4. Drag Coefficient: Method No. 1 (4” bend radius)

Wind Speed (mph)	Imp. Fact.	Bend Rad. (in)	16-sided r_m 0.2752 r_r 0.4844			12-sided r_m 0.5975 r_r 0.7136			8-sided r_m 0.8277 r_r 0.8774		
			Dia. (in)	C_d Cd-16-M1	C_{dm} % diff.	Dia. (in)	C_d Cd-12-M1	C_{dm} % diff.	Dia. (in)	C_d Cd-8-M1	C_{dm} % diff.
50-year MRI											
90	1.00	4	8.0	0.6295	-22%	8.0	0.6295	-32%	8.0	0.6295	-48%
90	1.00	4	8.8	0.5529	-23%	10.4	0.4487	-43%	9.1	0.5337	-56%
90	1.00	4	10.2	0.4567	-20%	11.8	0.5510	-30%	9.3	0.7046	-41%
90	1.00	4	17.8	0.4667	-15%	12.2	0.6195	-22%	9.4	0.8758	-27%
90	1.00	4	20.5	0.4946	-10%	12.8	0.7037	-11%	9.5	1.0470	-13%
90	1.00	4	24.0	0.5219	-5%	13.0	0.7432	-6%			
90	1.00	4	29.0	0.5497	0%	13.3	0.7809	-1%			
150	1.00	4	8.0	0.4500	-18%	8.0	0.4500	-43%	8.0	0.4500	-63%
150	1.00	4	17.8	0.4667	-15%	11.2	0.4517	-43%	9.1	0.4531	-62%
150	1.00	4	20.5	0.4946	-10%	11.8	0.5510	-30%	9.3	0.6533	-46%
150	1.00	4	24.0	0.5219	-5%	12.2	0.6195	-22%	9.4	0.8474	-29%
150	1.00	4	29.0	0.5497	0%	12.8	0.7037	-11%	9.5	1.0359	-14%
150	1.00	4				13.0	0.7432	-6%			
150	1.00	4				13.3	0.7809	-1%			
25-year MRI											
90	0.87	4	8.0	0.6891	-20%	8.0	0.6891	-29%	8.0	0.6891	-43%
90	0.87	4	9.5	0.5482	-23%	11.1	0.4513	-43%	9.1	0.5838	-51%
90	0.87	4	10.9	0.4588	-20%	11.8	0.5510	-30%	9.3	0.7406	-38%
90	0.87	4	20.5	0.4946	-10%	12.3	0.6412	-19%	9.4	0.8986	-25%
90	0.87	4	24.1	0.5229	-5%	12.8	0.7037	-11%	9.5	1.0574	-12%
90	0.87	4	29.0	0.5497	0%	13.0	0.7432	-6%			
90	0.87	4				13.3	0.7809	-1%			
150	0.80	4	8.0	0.4500	-18%	8.0	0.4500	-43%	8.0	0.4500	-63%
150	0.80	4	17.8	0.4667	-15%	11.4	0.4775	-40%	9.1	0.4531	-62%
150	0.80	4	20.5	0.4946	-10%	11.8	0.5510	-30%	9.3	0.6533	-46%
150	0.80	4	24.1	0.5229	-5%	12.8	0.7037	-11%	9.4	0.8474	-29%
150	0.80	4	29.0	0.5497	0%	13.0	0.7432	-6%	9.5	1.0359	-14%
150	0.80	4				13.3	0.7809	-1%			

Table D–5. Drag Coefficient: Method No. 2 (4" bend radius)

Wind Speed (mph)	Imp. Fact.	Bend Rad. (in)	16-sided r_m 0.2600 r_r 0.7500			12-sided r_m 0.2600 r_r 0.7500			8-sided r_m 0.2600 r_r 0.7500		
			Dia. (in)	C_d Cd-16-M2	C_{dm} % diff.	Dia. (in)	C_d Cd-12-M2	C_{dm} % diff.	Dia. (in)	C_d Cd-8-M2	C_{dm} % diff.
50-year MRI											
90	1.00	4	8.0	0.6295	-22%	8.0	0.6295	-32%	8.0	0.6295	-48%
90	1.00	4	8.8	0.5529	-23%	10.4	0.4487	-43%	10.4	0.4487	-63%
90	1.00	4	10.2	0.4567	-20%	13.0	0.5447	-31%	12.3	0.6057	-50%
90	1.00	4	15.1	0.4952	-10%	16.4	0.6319	-20%	16.1	0.8384	-30%
90	1.00	4	20.2	0.5222	-5%	21.4	0.7115	-10%	19.2	0.9602	-20%
90	1.00	4	30.7	0.5498	0%	25.2	0.7503	-5%	23.7	1.0809	-10%
90	1.00	4				30.7	0.7895	0%	26.8	1.1404	-5%
90	1.00	4							30.7	1.1988	0%
150	1.00	4	8.0	0.4500	-18%	8.0	0.4500	-43%	8.0	0.4500	-63%
150	1.00	4	12.1	0.4677	-15%	11.1	0.4694	-41%	13.9	0.7158	-40%
150	1.00	4	15.1	0.4952	-10%	13.3	0.5537	-30%	16.1	0.8384	-30%
150	1.00	4	20.3	0.5227	-5%	16.4	0.6319	-20%	19.2	0.9602	-20%
150	1.00	4	30.7	0.5498	0%	21.4	0.7115	-10%	23.7	1.0809	-10%
150	1.00	4				25.2	0.7503	-5%	26.8	1.1404	-5%
150	1.00	4				30.7	0.7895	0%	30.7	1.1988	0%
25-year MRI											
90	0.87	4	8.0	0.6891	-20%	8.0	0.6891	-29%	8.0	0.6891	-43%
90	0.87	4	9.5	0.5482	-23%	10.7	0.4745	-42%	10.7	0.4745	-60%
90	0.87	4	15.1	0.4952	-10%	13.3	0.5537	-30%	13.9	0.7158	-40%
90	0.87	4	20.3	0.5227	-5%	16.4	0.6319	-20%	19.2	0.9602	-20%
90	0.87	4	30.7	0.5498	0%	21.4	0.7115	-10%	23.7	1.0809	-10%
90	0.87	4				25.2	0.7503	-5%	26.8	1.1404	-5%
90	0.87	4				30.7	0.7895	0%	30.7	1.1988	0%
150	0.80	4	8.0	0.4500	-18%	8.0	0.4500	-43%	8.0	0.4500	-63%
150	0.80	4	15.1	0.4952	-10%	11.1	0.4694	-41%	13.9	0.7158	-40%
150	0.80	4	20.3	0.5227	-5%	16.4	0.6319	-20%	19.2	0.9602	-20%
150	0.80	4	30.7	0.5498	0%	21.4	0.7115	-10%	23.7	1.0809	-10%
150	0.80	4				25.2	0.7503	-5%	26.8	1.1404	-5%
150	0.80	4				30.7	0.7895	0%	30.7	1.1988	0%

Table D–6. Drag Coefficient: Method No. 3 (4" bend radius)

Wind Speed (mph)	Imp. Fact.	Bend Rad. (in)	16-sided r_m 0.5000 r_r 1.0000			12-sided r_m 0.5000 r_r 1.0000			8-sided r_m 0.5000 r_r 1.0000		
			Dia. (in)	C_d Cd-16-M3	C_{dm} % diff.	Dia. (in)	C_d Cd-12-M3	C_{dm} % diff.	Dia. (in)	C_d Cd-8-M3	C_{dm} % diff.
50-year MRI											
90	1.00	4	8.0	0.62950	-22%	8.0	0.62950	-32%	8.0	0.6295	-48%
90	1.00	4	10.4	0.49741	-10%	10.9	0.63274	-20%	9.5	0.7265	-39%
90	1.00	4	12.5	0.52179	-5%	13.0	0.71282	-10%	10.8	0.8389	-30%
90	1.00	4	16.0	0.54987	0%	14.3	0.74958	-5%	12.1	0.9550	-20%
90	1.00	4				16.0	0.78957	0%	13.7	1.0766	-10%
90	1.00	4							14.9	1.1425	-5%
90	1.00	4							16.0	1.1991	0%
150	1.00	4	8.0	0.45000	-18%	8.0	0.45000	-43%	8.0	0.4500	-63%
150	1.00	4	10.4	0.49586	-10%	9.4	0.55128	-30%	8.8	0.5925	-51%
150	1.00	4	12.5	0.52179	-5%	10.9	0.63274	-20%	9.8	0.7280	-39%
150	1.00	4	16.0	0.54987	0%	13.0	0.71282	-10%	10.8	0.8389	-30%
150	1.00	4				14.3	0.74958	-5%	12.1	0.9550	-20%
150	1.00	4				16.0	0.78957	0%	13.7	1.0766	-10%
150	1.00	4							14.9	1.1425	-5%
150	1.00	4							16.0	1.1991	0%
25-year MRI											
90	0.87	4	8.0	0.68914	-20%	8.0	0.68914	-29%	8.0	0.6891	-43%
90	0.87	4	10.8	0.52915	-10%	10.8	0.64268	-20%	10.7	0.8366	-30%
90	0.87	4	12.5	0.52179	-5%	13.0	0.71282	-10%	12.1	0.9550	-20%
90	0.87	4	16.0	0.54987	0%	14.3	0.74958	-5%	13.7	1.0766	-10%
90	0.87	4				16.0	0.78957	0%	14.9	1.1425	-5%
90	0.87	4							16.0	1.1991	0%
150	0.80	4	8.0	0.45000	-18%	8.0	0.45000	-43%	8.0	0.4500	-63%
150	0.80	4	10.2	0.49375	-10%	9.4	0.55128	-30%	8.8	0.5925	-51%
150	0.80	4	12.5	0.52179	-5%	10.9	0.63274	-20%	9.8	0.7280	-39%
150	0.80	4	16.0	0.54987	0%	13.0	0.71282	-10%	10.8	0.8389	-30%
150	0.80	4				14.3	0.74958	-5%	12.1	0.9550	-20%
150	0.80	4				16.0	0.78957	0%	13.7	1.0766	-10%
150	0.80	4							14.7	1.1348	-5%
150	0.80	4							16.0	1.1991	0%

Table D–7. Drag Coefficient: Method No. 4 (4" bend radius)

Wind Speed (mph)	Imp. Fact.	Bend Rad. (in)	16-sided r_m 0.2600 r_r 0.6250			12-sided r_m 0.5000 r_r 0.7500			8-sided r_m 0.7500 r_r 1.0000		
			Dia. (in)	C_d Cd-16-M4	C_{dm} % diff.	Dia. (in)	C_d Cd-12-M4	C_{dm} % diff.	Dia. (in)	C_d Cd-8-M4	C_{dm} % diff.
50-year MRI											
90	1.00	4	8.0	0.6295	-22%	8.0	0.6295	-32%	8.0	0.6295	-48%
90	1.00	4	8.8	0.5529	-23%	10.4	0.4487	-43%	9.0	0.8291	-31%
90	1.00	4	17.4	0.4951	-10%	13.0	0.6356	-20%	9.5	0.9522	-21%
90	1.00	4	22.1	0.5222	-5%	14.3	0.7092	-10%	10.1	1.0763	-10%
90	1.00	4	30.7	0.5498	0%	15.1	0.7514	-5%	10.4	1.1378	-5%
90	1.00	4				16.0	0.7891	0%	10.7	1.1986	0%
150	1.00	4	8.0	0.4500	-18%	8.0	0.4500	-43%	8.0	0.4500	-63%
150	1.00	4	14.3	0.4680	-15%	10.9	0.4755	-40%	8.4	0.5996	-50%
150	1.00	4	17.4	0.4951	-10%	11.9	0.5572	-29%	8.8	0.7351	-39%
150	1.00	4	22.1	0.5222	-5%	13.0	0.6356	-20%	9.3	0.8582	-28%
150	1.00	4	30.7	0.5498	0%	14.3	0.7092	-10%	9.7	0.9707	-19%
150	1.00	4				15.1	0.7514	-5%	10.1	1.0738	-11%
150	1.00	4				16.0	0.7891	0%	10.4	1.1379	-5%
150	1.00	4							10.7	1.1986	0%
25-year MRI											
90	0.87	4	8.0	0.6891	-20%	8.0	0.6891	-29%	8.0	0.6891	-43%
90	0.87	4	9.5	0.5482	-23%	10.7	0.4745	-42%	8.8	0.8313	-31%
90	0.87	4	17.4	0.4951	-10%	11.9	0.5572	-29%	9.5	0.9691	-19%
90	0.87	4	22.1	0.5222	-5%	13.0	0.6356	-20%	10.1	1.0837	-10%
90	0.87	4	30.7	0.5498	0%	14.3	0.7092	-10%	10.4	1.1413	-5%
90	0.87	4				15.1	0.7514	-5%	10.7	1.1986	0%
90	0.87	4				16.0	0.7891	0%			
150	0.80	4	8.0	0.4500	-18%	8.0	0.4500	-43%	8.0	0.4500	-63%
150	0.80	4	17.2	0.4941	-10%	10.9	0.4755	-40%	8.4	0.5996	-50%
150	0.80	4	22.1	0.5222	-5%	11.9	0.5572	-29%	8.8	0.7351	-39%
150	0.80	4	30.7	0.5498	0%	13.0	0.6356	-20%	9.3	0.8582	-28%
150	0.80	4				14.3	0.7092	-10%	9.7	0.9707	-19%
150	0.80	4				15.1	0.7514	-5%	10.1	1.0738	-11%
150	0.80	4				16.0	0.7891	0%	10.4	1.1379	-5%
150	0.80	4							10.7	1.1986	0%

Table D–8. Drag Coefficient: Method No. 1 (2” bend radius)

Wind Speed (mph)	Imp. Fact.	Bend Rad. (in)	16-sided r_m 0.2752 r_r 0.4844			12-sided r_m 0.5975 r_r 0.7136			8-sided r_m 0.8277 r_r 0.8774		
			Dia. (in)	C_d Cd-16-M1	C_{dm} % diff.	Dia. (in)	C_d Cd-12-M1	C_{dm} % diff.	Dia. (in)	C_d Cd-8-M1	C_{dm} % diff.
50-year MRI											
90	1.00	2	4.0	1.1000	0%	4.0	1.1000	-8%	4.0	1.1000	-8%
90	1.00	2	5.1	1.1000	0%	5.7	0.9950	-12%	4.6	1.1004	-8%
90	1.00	2	6.0	0.9230	-10%	6.4	1.0057	-5%	4.7	1.1530	-4%
90	1.00	2	8.2	0.6096	-22%	6.7	1.0272	-1%			
90	1.00	2	10.3	0.5038	-11%						
90	1.00	2	12.0	0.5219	-5%						
90	1.00	2	14.5	0.5497	0%						
150	1.00	2	4.0	0.7979	-16%	4.0	0.7979	-23%	4.0	0.7979	-34%
150	1.00	2	5.3	0.5589	-23%	5.5	0.5224	-39%	4.6	0.6751	-44%
150	1.00	2	10.3	0.4959	-10%	6.1	0.6308	-21%	4.7	0.9400	-22%
150	1.00	2	12.0	0.5219	-5%	6.4	0.7037	-11%			
150	1.00	2	14.5	0.5497	0%	6.5	0.7432	-6%			
150	1.00	2				6.7	0.7809	-1%			
25-year MRI											
90	0.87	2	4.0	1.1000	0%	4.0	1.1000	-8%	4.0	1.1000	-8%
90	0.87	2	5.5	1.1000	0%	6.2	1.0573	-6%	4.6	1.1004	-8%
90	0.87	2	6.0	1.0104	-5%	6.7	1.0722	-1%	4.7	1.1530	-4%
90	0.87	2	6.4	0.9248	-10%						
90	0.87	2	8.2	0.6674	-21%						
90	0.87	2	10.7	0.5371	-10%						
90	0.87	2	12.0	0.5219	-5%						
90	0.87	2	14.5	0.5497	0%						
150	0.80	2	4.0	0.9224	-10%	4.0	0.9224	-16%	4.0	0.9224	-23%
150	0.80	2	6.0	0.5493	-23%	5.1	0.6692	-30%	4.6	0.7797	-35%
150	0.80	2	10.3	0.4959	-10%	6.1	0.6946	-19%	4.7	0.9875	-18%
150	0.80	2	12.0	0.5219	-5%	6.4	0.7504	-10%			
150	0.80	2	14.5	0.5497	0%	6.7	0.8043	-1%			

Table D–9. Drag Coefficient: Method No. 2 (2” bend radius)

Wind Speed (mph)	Imp. Fact.	Bend Rad. (in)	16-sided r_m 0.2600 r_r 0.7500			12-sided r_m 0.2600 r_r 0.7500			8-sided r_m 0.2600 r_r 0.7500		
			Dia. (in)	C_d Cd-16-M2	C_{dm} % diff.	Dia. (in)	C_d Cd-12-M2	C_{dm} % diff.	Dia. (in)	C_d Cd-8-M2	C_{dm} % diff.
50-year MRI											
90	1.00	2	4.0	1.1000	0%	4.0	1.1000	-8%	4.0	1.1000	-8%
90	1.00	2	5.1	1.1000	0%	5.4	1.0516	-10%	5.3	1.0857	-10%
90	1.00	2	5.5	1.0179	-5%	7.2	0.8254	-16%	7.5	0.9125	-24%
90	1.00	2	7.2	0.7871	-11%	10.7	0.7115	-10%	11.8	1.0809	-10%
90	1.00	2	10.3	0.5345	-5%	12.5	0.7491	-5%	13.4	1.1404	-5%
90	1.00	2	15.3	0.5498	0%	15.3	0.7895	0%	15.3	1.1988	0%
150	1.00	2	4.0	0.7979	-16%	4.0	0.7979	-23%	4.0	0.7979	-34%
150	1.00	2	5.3	0.5589	-23%	5.4	0.5462	-37%	5.4	0.5526	-54%
150	1.00	2	7.5	0.4942	-10%	8.2	0.6319	-20%	6.9	0.7158	-40%
150	1.00	2	10.2	0.5227	-5%	10.7	0.7115	-10%	8.1	0.8384	-30%
150	1.00	2	15.3	0.5498	0%	12.5	0.7491	-5%	9.6	0.9602	-20%
150	1.00	2				15.3	0.7895	0%	11.8	1.0809	-10%
150	1.00	2							13.4	1.1404	-5%
150	1.00	2							15.3	1.1988	0%
25-year MRI											
90	0.87	2	4.0	1.1000	0%	4.0	1.1000	-8%	4.0	1.1000	-8%
90	0.87	2	5.5	1.1000	0%	6.0	1.0332	-10%	5.7	1.0873	-9%
90	0.87	2	6.1	0.9938	-5%	7.6	0.8521	-14%	7.6	0.9481	-21%
90	0.87	2	7.6	0.8088	-10%	10.6	0.7351	-10%	11.8	1.0809	-10%
90	0.87	2	10.6	0.5777	-5%	12.7	0.7515	-5%	13.4	1.1404	-5%
90	0.87	2	15.3	0.5498	0%	15.3	0.7895	0%	15.3	1.1988	0%
150	0.80	2	4.0	0.9224	-10%	4.0	0.9224	-16%	4.0	0.9224	-23%
150	0.80	2	5.4	0.6278	-22%	5.4	0.6301	-32%	5.4	0.6353	-47%
150	0.80	2	7.5	0.4942	-10%	8.2	0.6319	-20%	8.1	0.8384	-30%
150	0.80	2	10.2	0.5227	-5%	10.7	0.7115	-10%	9.6	0.9602	-20%
150	0.80	2	15.3	0.5498	0%	12.7	0.7515	-5%	11.8	1.0809	-10%
150	0.80	2				15.3	0.7895	0%	13.4	1.1404	-5%
150	0.80	2							15.3	1.1988	0%

Table D–10. Drag Coefficient: Method No. 3 (2" bend radius)

Wind Speed (mph)	Imp. Fact.	Bend Rad. (in)	16-sided r_m 0.5000 r_r 1.0000			12-sided r_m 0.5000 r_r 1.0000			8-sided r_m 0.5000 r_r 1.0000		
			Dia. (in)	C_d Cd-16-M3	C_{dm} % diff.	Dia. (in)	C_d Cd-12-M3	C_{dm} % diff.	Dia. (in)	C_d Cd-8-M3	C_{dm} % diff.
50-year MRI											
90	1.00	2	4.0	1.10000	0%	4.0	1.10000	-8%	4.0	1.1000	-8%
90	1.00	2	5.1	1.10000	0%	6.4	1.00570	-5%	5.1	1.1438	-5%
90	1.00	2	6.2	0.95763	-3%	7.9	0.92847	0%	6.1	1.1052	-8%
90	1.00	2	7.9	0.81300	0%				7.1	1.1399	-5%
90	1.00	2							7.9	1.1943	0%
150	1.00	2	4.0	0.79786	-16%	4.0	0.79786	-23%	4.0	0.7979	-34%
150	1.00	2	4.3	0.75256	-16%	6.5	0.71282	-10%	6.0	0.9519	-21%
150	1.00	2	5.5	0.60785	-10%	7.2	0.75327	-5%	6.9	1.0854	-10%
150	1.00	2	7.9	0.54899	0%	7.9	0.78657	0%	7.4	1.1348	-5%
150	1.00	2							7.9	1.1924	-1%
25-year MRI											
90	0.87	2	4.0	1.10000	0%	4.0	1.10000	-8%	4.0	1.1000	-8%
90	0.87	2	5.5	1.10000	0%	5.0	1.13936	-5%	6.2	1.1300	-6%
90	0.87	2	6.5	0.98405	-2%	7.9	0.96841	0%	7.9	1.1949	0%
90	0.87	2	7.9	0.86932	0%						
90	0.87	2									
150	0.80	2	4.0	0.92240	-10%	4.0	0.92240	-16%	4.0	0.9224	-23%
150	0.80	2	4.7	0.79661	-13%	4.6	0.83760	-18%	4.6	0.8816	-27%
150	0.80	2	5.5	0.70131	-10%	6.4	0.75030	-10%	6.9	1.0855	-10%
150	0.80	2	6.5	0.59384	-5%	7.2	0.75327	-5%	7.4	1.1348	-5%
150	0.80	2	7.9	0.54899	0%	7.9	0.78657	0%	7.9	1.1924	-1%

Table D–11. Drag Coefficient: Method No. 4 (2" bend radius)

Wind Speed (mph)	Imp. Fact.	Bend Rad. (in)	16-sided r_m 0.2600 r_r 0.6250			12-sided r_m 0.5000 r_r 0.7500			8-sided r_m 0.7500 r_r 1.0000		
			Dia. (in)	C_d Cd-16-M4	C_{dm} % diff.	Dia. (in)	C_d Cd-12-M4	C_{dm} % diff.	Dia. (in)	C_d Cd-8-M4	C_{dm} % diff.
50-year MRI											
90	1.00	2	4.0	1.1000	0%	4.0	1.1000	-8%	4.0	1.1000	-8%
90	1.00	2	5.1	1.1000	0%	5.8	0.9942	-11%	4.4	1.1380	-5%
90	1.00	2	5.5	1.0150	-5%	7.4	0.9261	-5%	5.3	1.1952	0%
90	1.00	2	6.0	0.9230	-10%	7.9	0.9255	-1%			
90	1.00	2	7.2	0.7523	-15%						
90	1.00	2	9.5	0.5870	-10%						
90	1.00	2	11.1	0.5229	-5%						
90	1.00	2	15.3	0.5498	0%						
150	1.00	2	4.0	0.7979	-16%	4.0	0.7979	-23%	4.0	0.7979	-34%
150	1.00	2	5.3	0.5589	-23%	5.3	0.5589	-36%	4.7	0.9764	-19%
150	1.00	2	8.6	0.4941	-10%	6.5	0.6356	-20%	5.0	1.0723	-11%
150	1.00	2	11.1	0.5229	-5%	7.2	0.7165	-9%	5.1	1.1224	-6%
150	1.00	2	15.3	0.5498	0%	7.5	0.7447	-6%	5.3	1.1732	-2%
150	1.00	2				7.9	0.7831	-1%			
25-year MRI											
90	0.87	2	4.0	1.1000	0%	4.0	1.1000	-8%	4.0	1.1000	-8%
90	0.87	2	5.5	1.1000	0%	6.1	1.0390	-9%	4.4	1.1380	-5%
90	0.87	2	6.0	1.0104	-5%	7.2	0.9749	-5%	5.3	1.1958	0%
90	0.87	2	6.5	0.9025	-11%	7.9	0.9657	-1%			
90	0.87	2	7.6	0.7781	-13%						
90	0.87	2	9.6	0.6361	-10%						
90	0.87	2	11.1	0.5251	-5%						
90	0.87	2	15.3	0.5498	0%						
150	0.80	2	4.0	0.9224	-10%	4.0	0.9224	-16%	4.0	0.9224	-23%
150	0.80	2	6.0	0.5493	-23%	5.4	0.6355	-31%	5.0	1.0922	-9%
150	0.80	2	8.6	0.4941	-10%	6.4	0.6660	-20%	5.1	1.1336	-6%
150	0.80	2	11.1	0.5229	-5%	7.2	0.7165	-9%	5.3	1.1768	-2%
150	0.80	2	15.3	0.5498	0%	7.5	0.7447	-6%			
150	0.80	2				7.9	0.7831	-1%			

ANNEX B

LIST OF FIGURES

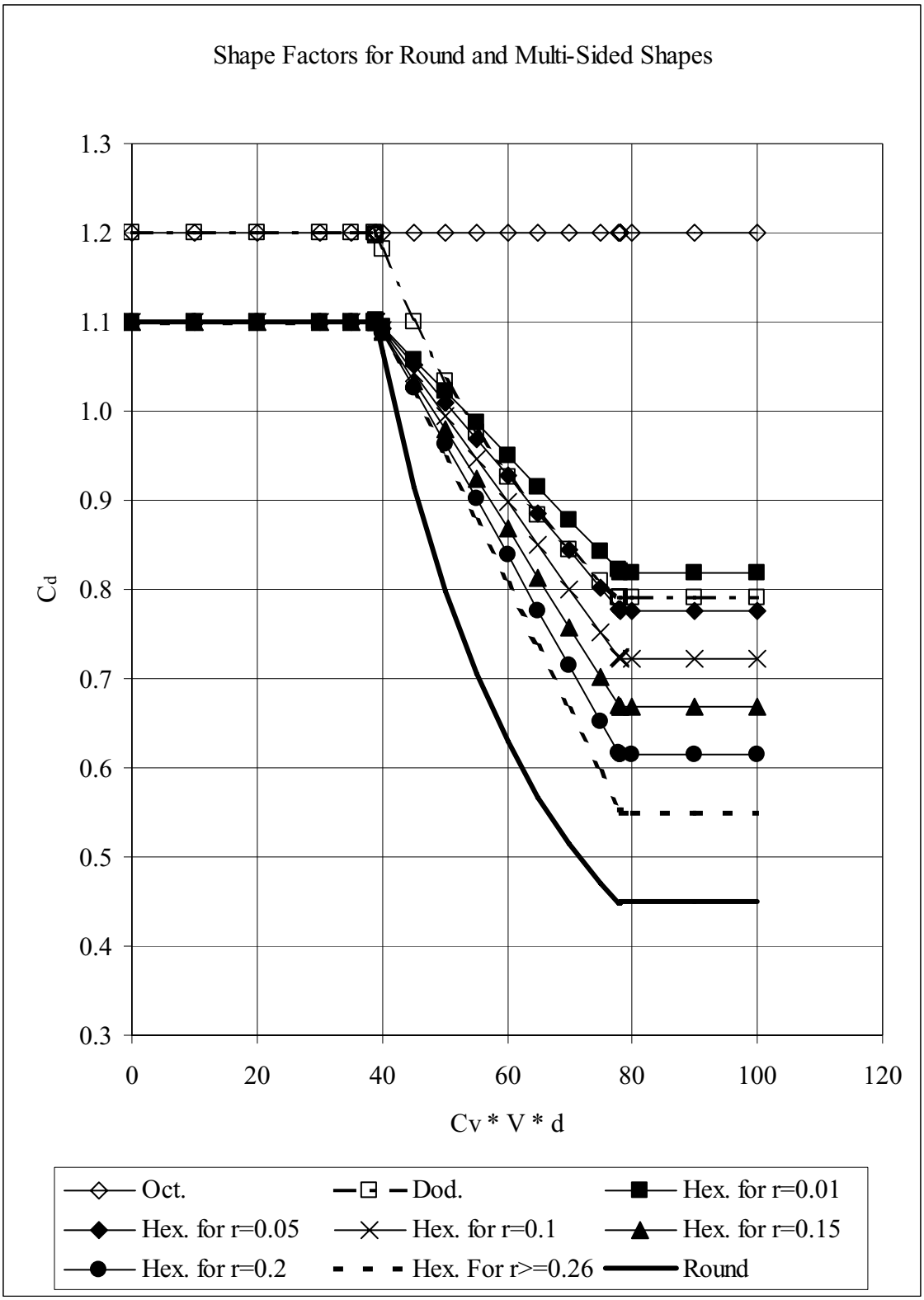

Figure D–1. Shape Factors for Round and Multi-Sided Sections

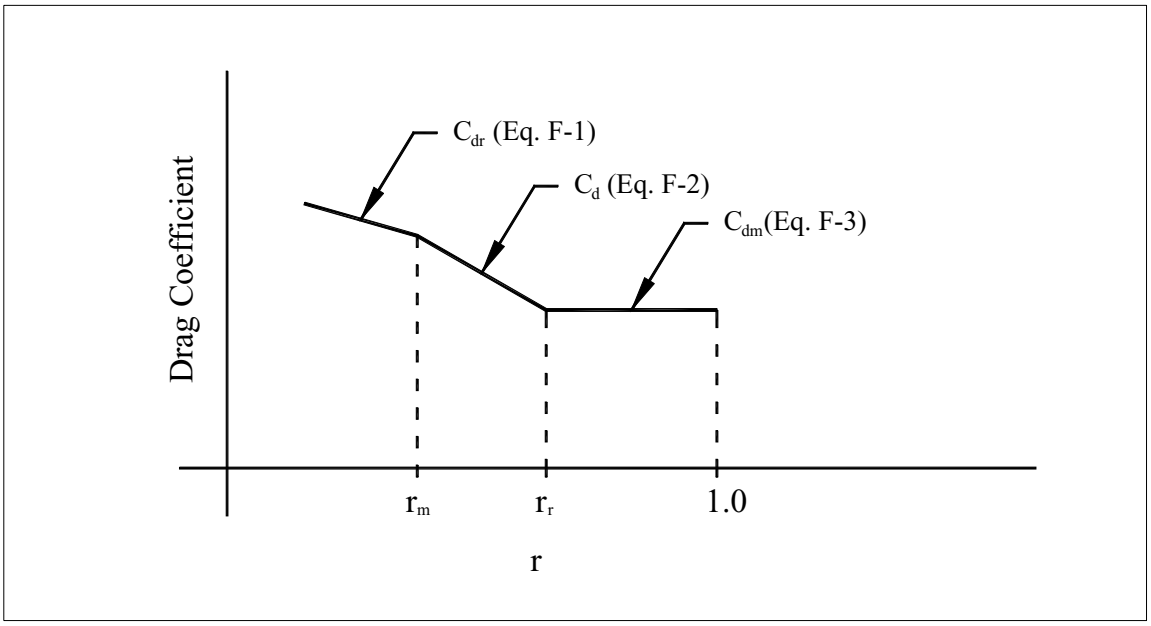

Figure D–2. Proposed Drag Coefficient for Multi-Sided Sections

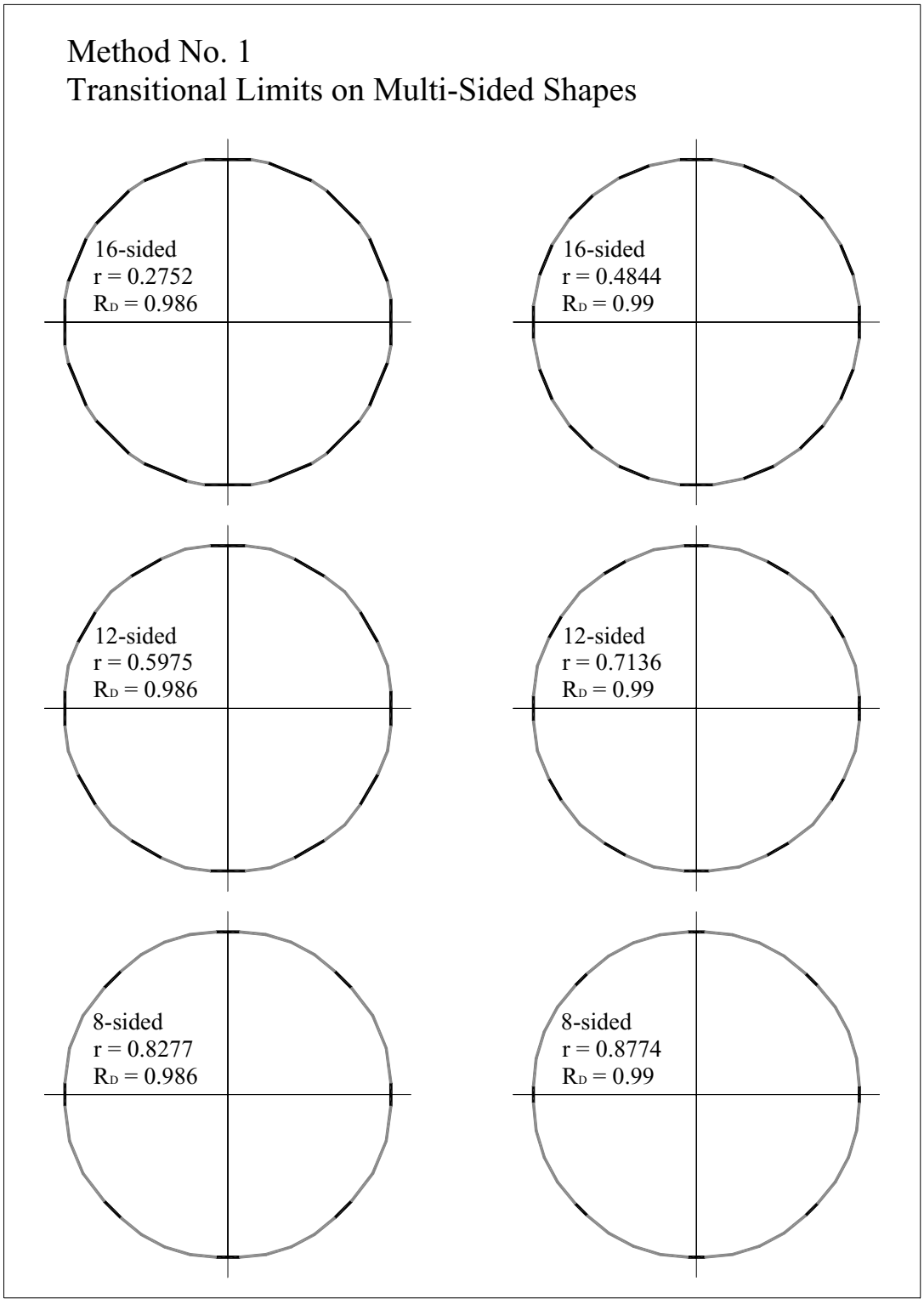

Figure D–3. Transitional Limits for Method No. 1

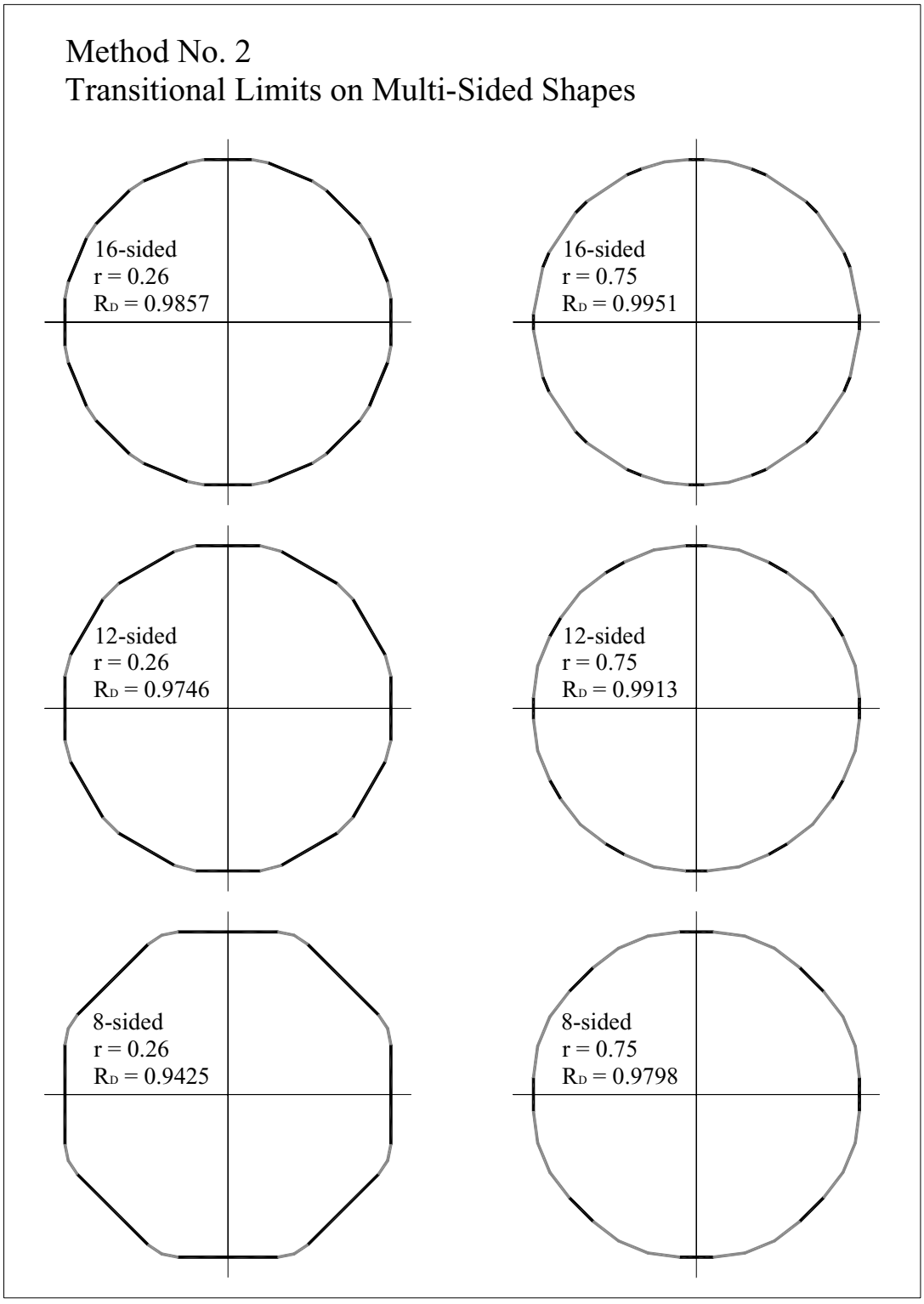

Figure D–4. Transitional Limits for Method No. 2

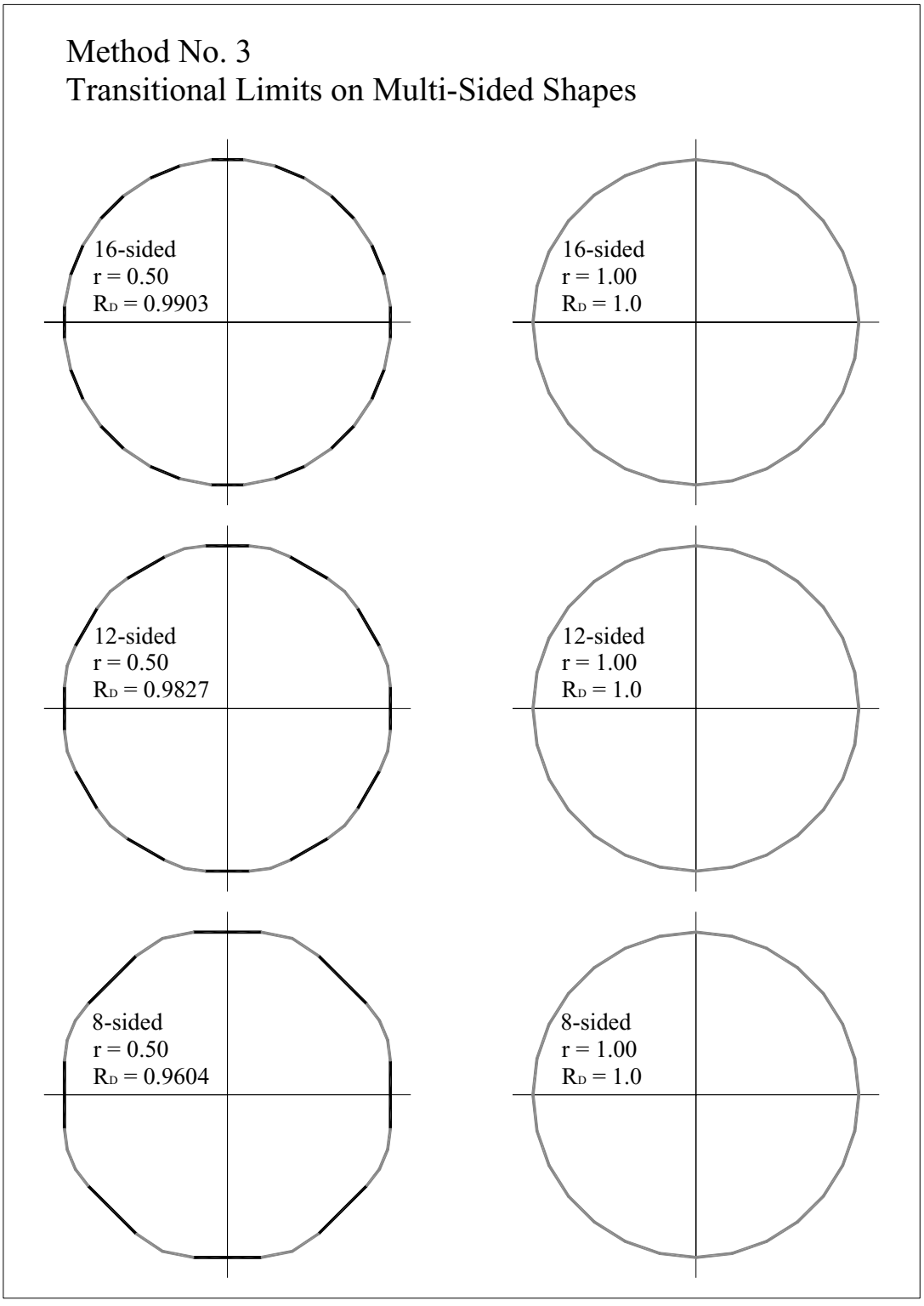

Figure D–5. Transitional Limits for Method No. 3

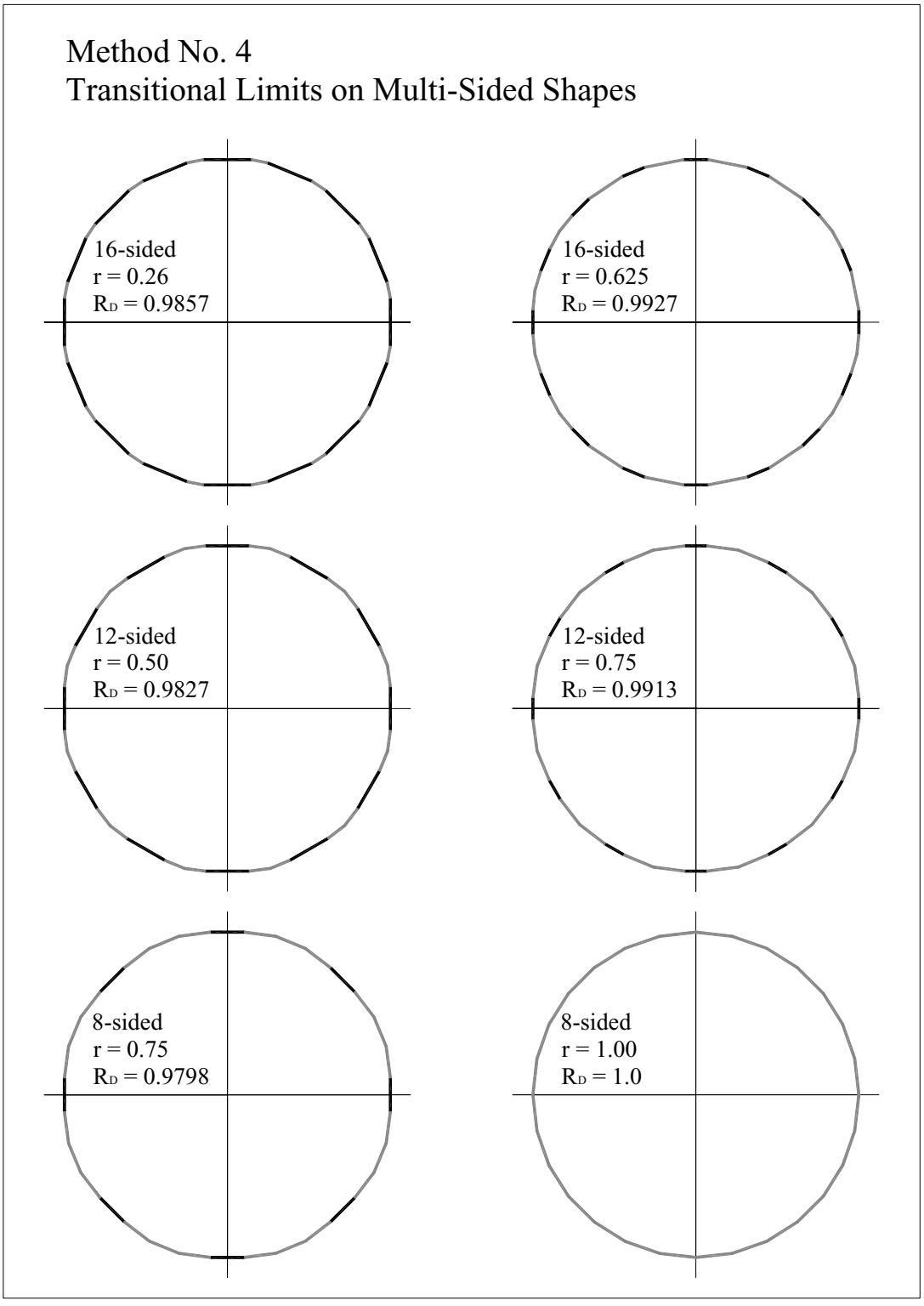

Figure D–6. Transitional Limits for Method No. 4

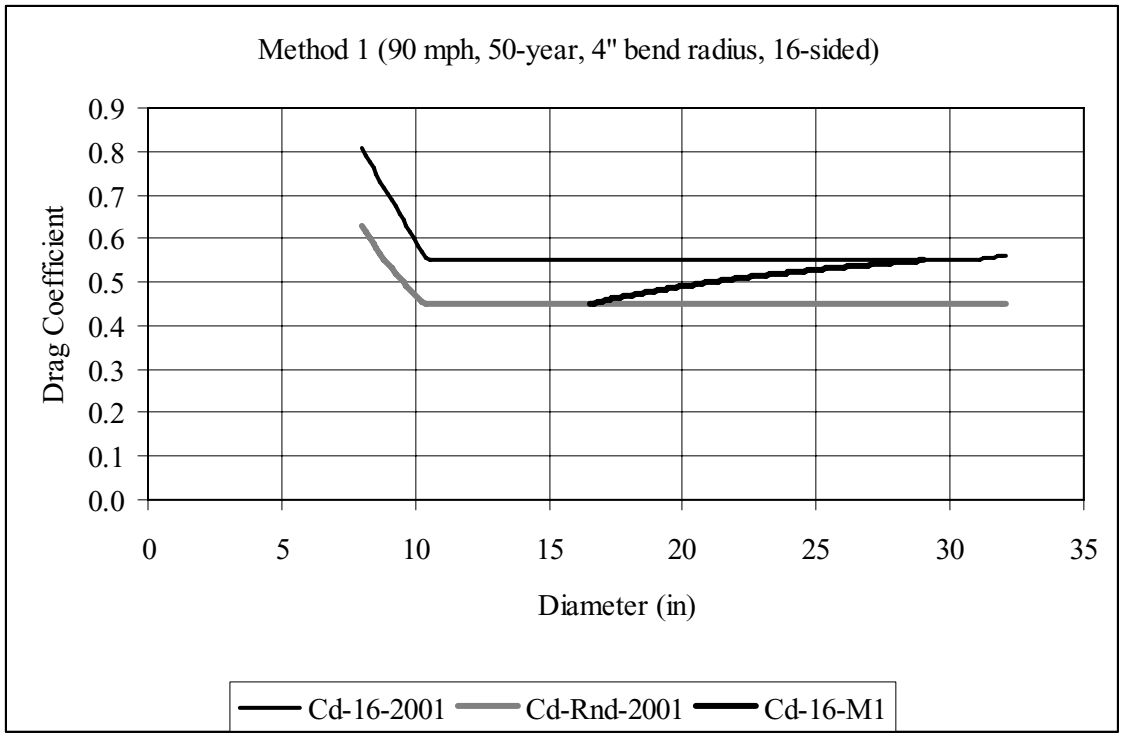

Figure D–7. Drag Coefficient Comparison: Method No. 1, 50-year MRI, 90 mph, 4" bend radius, 16-sided

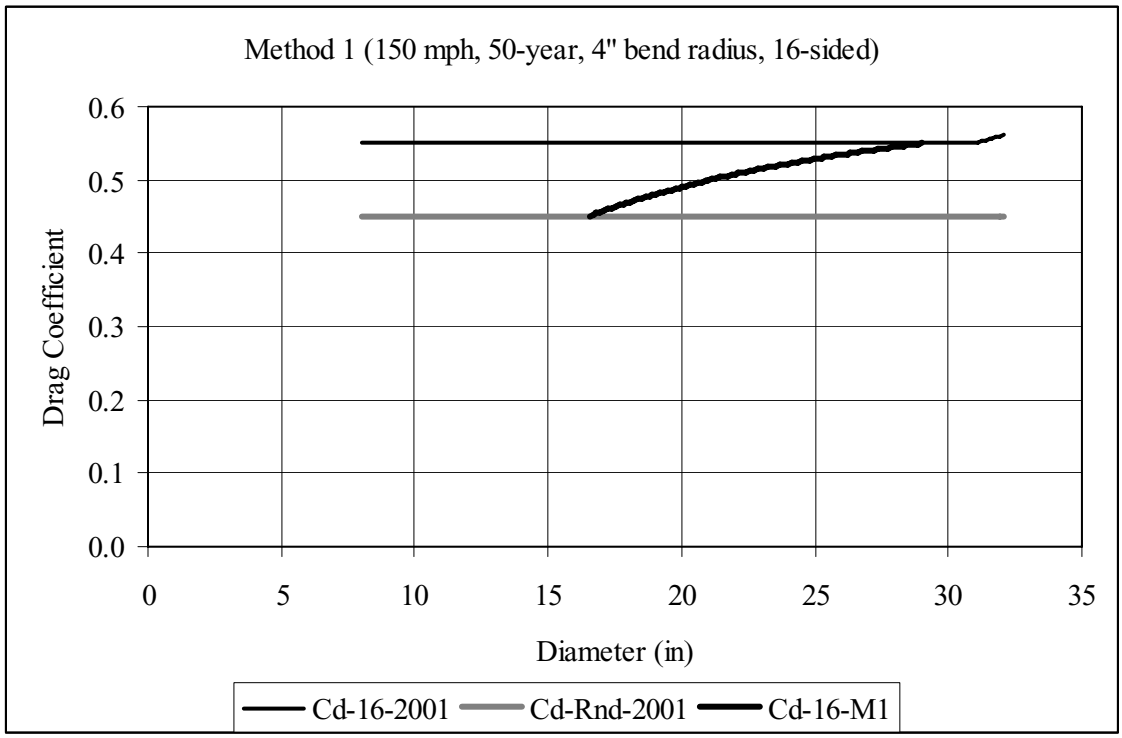

Figure D–8. Drag Coefficient Comparison: Method No. 1, 50-year MRI, 150 mph, 4" bend radius, 16-sided

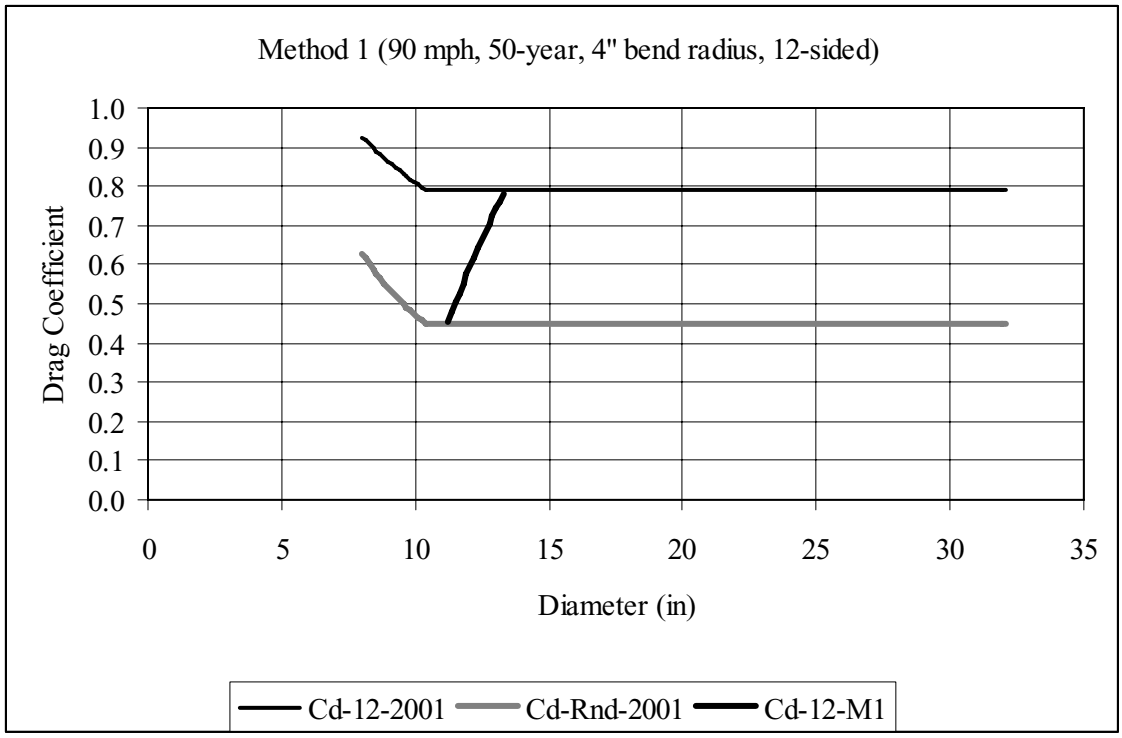

Figure D–9. Drag Coefficient Comparison: Method No. 1, 50-year MRI, 90 mph, 4" bend radius, 12-sided

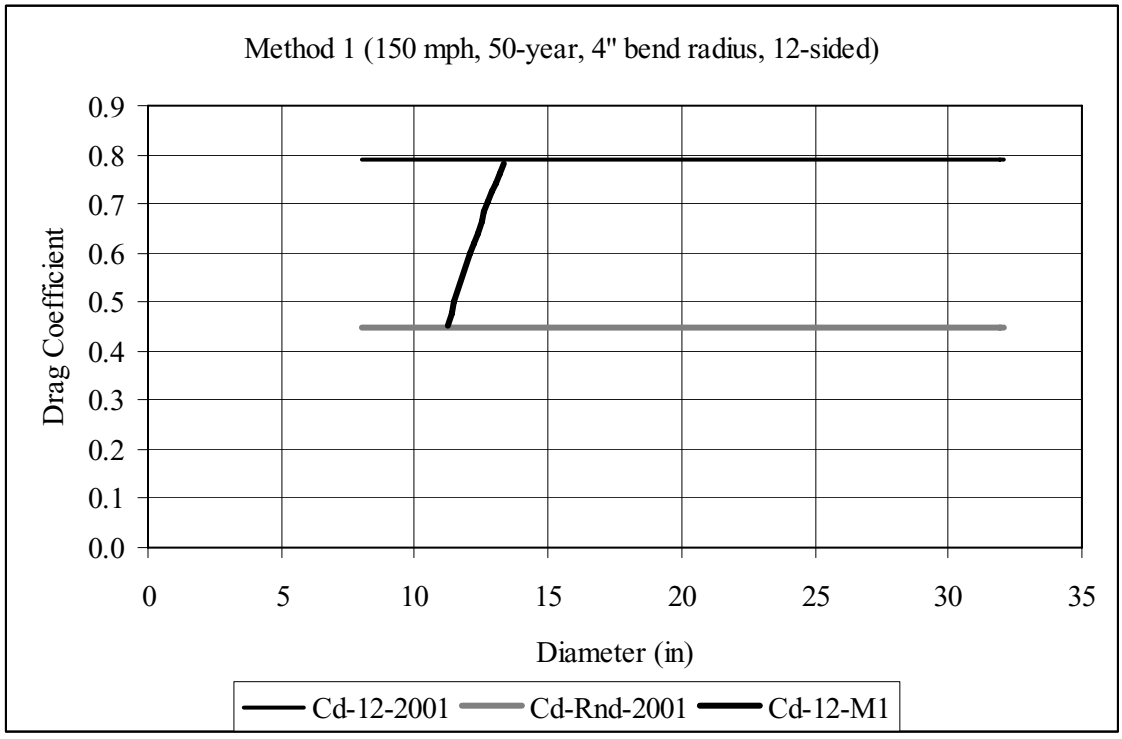

Figure D–10. Drag Coefficient Comparison: Method No. 1, 50-year MRI, 150 mph, 4" bend radius, 12-sided

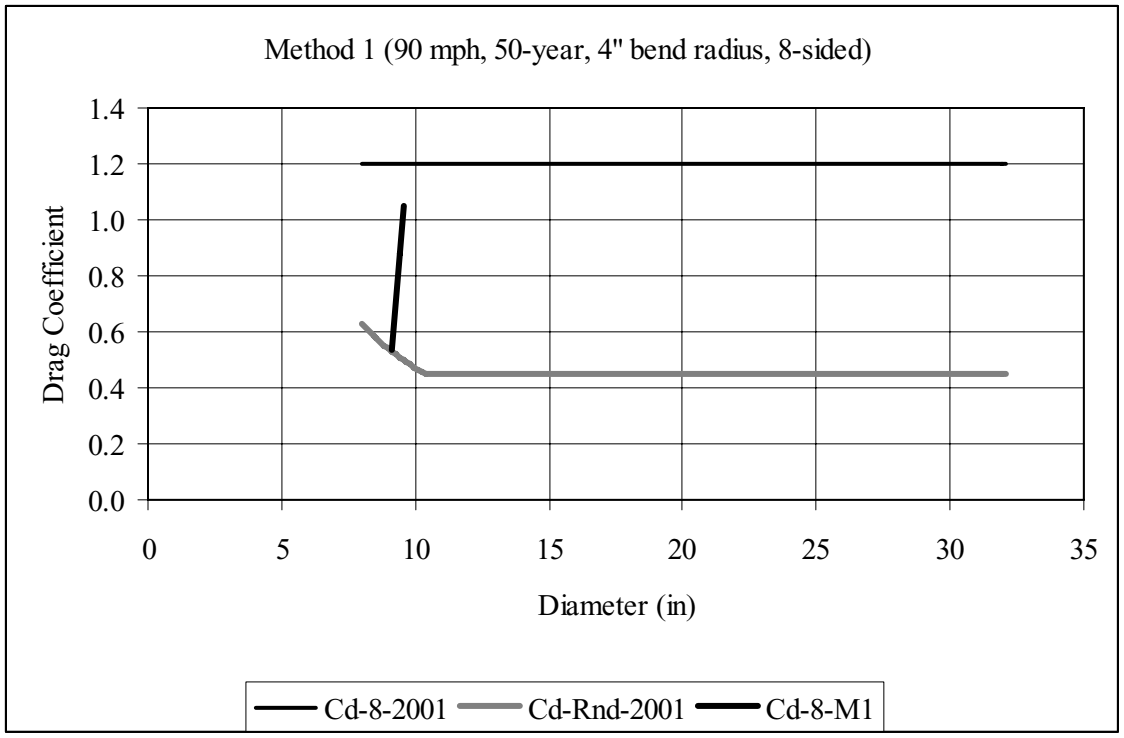

Figure D–11. Drag Coefficient Comparison: Method No. 1, 50-year MRI, 90 mph, 4” bend radius, 8-sided

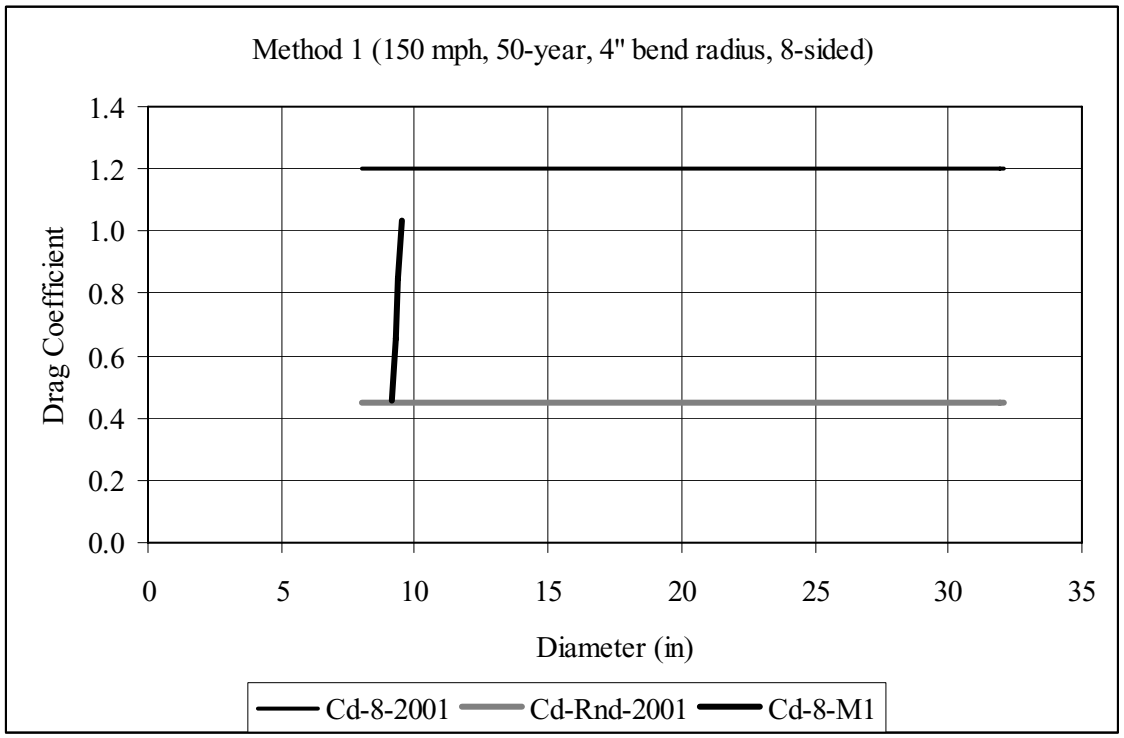

Figure D–12. Drag Coefficient Comparison: Method No. 1, 50-year MRI, 150 mph, 4” bend radius, 8-sided

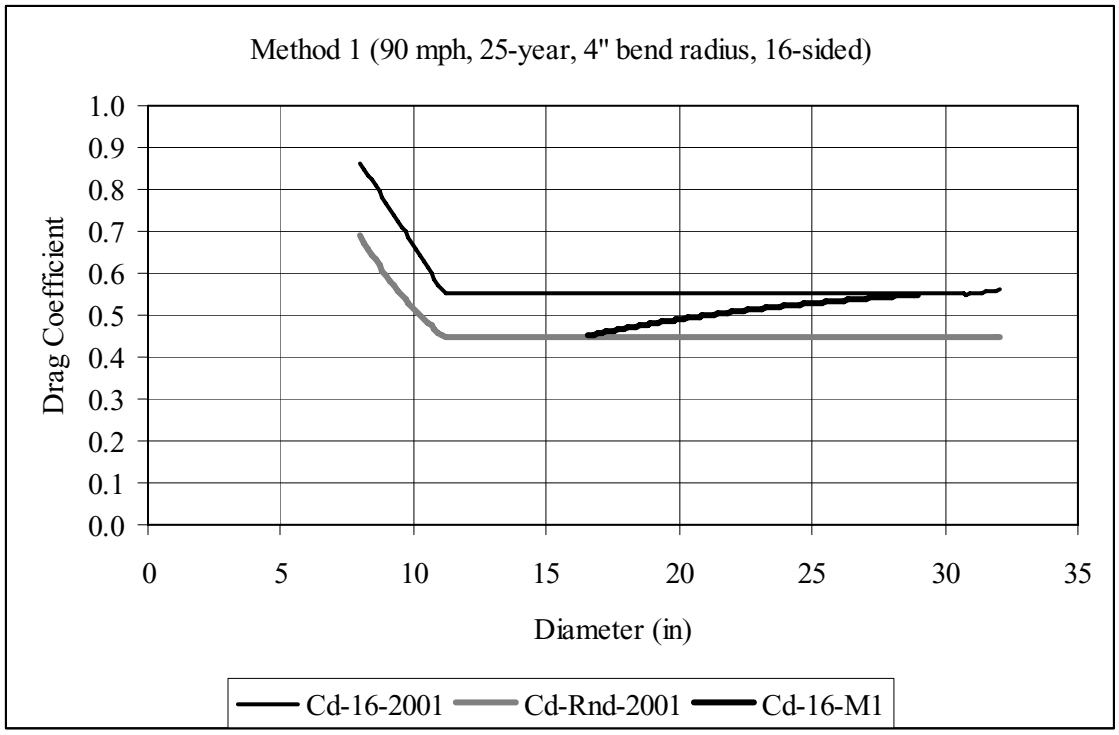

Figure D–13. Drag Coefficient Comparison: Method No. 1, 25-year MRI, 90 mph, 4” bend radius, 16-sided

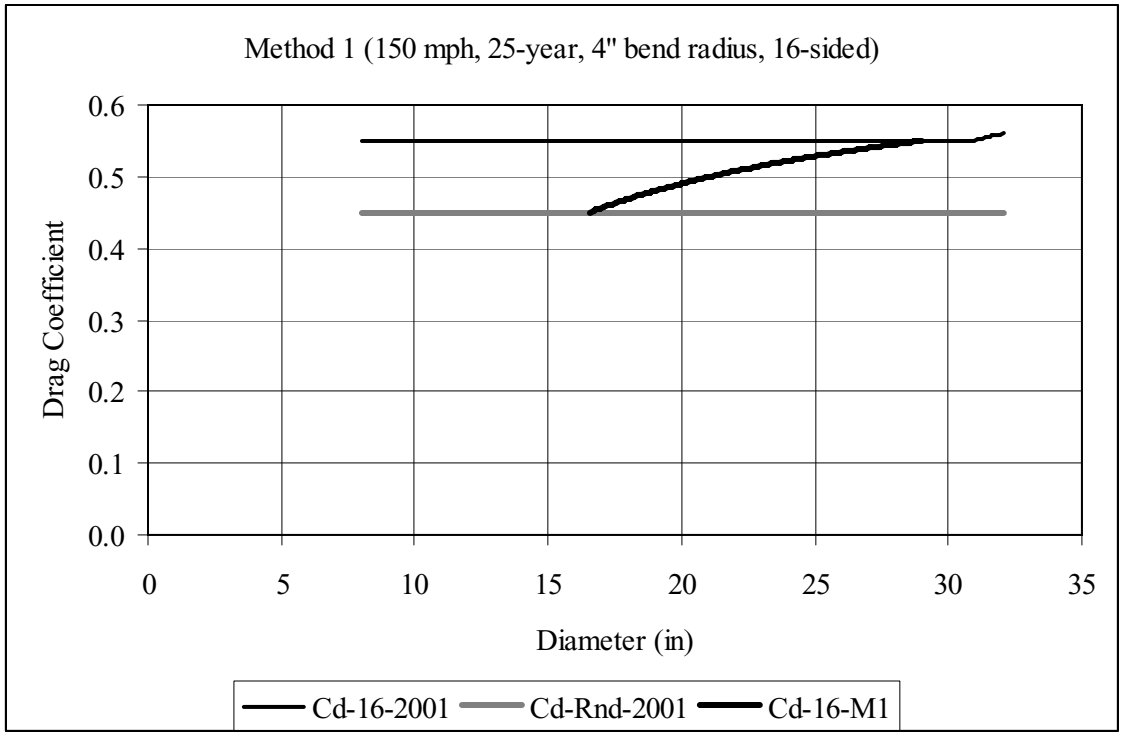

Figure D–14. Drag Coefficient Comparison: Method No. 1, 25-year MRI, 150 mph, 4” bend radius, 16-sided

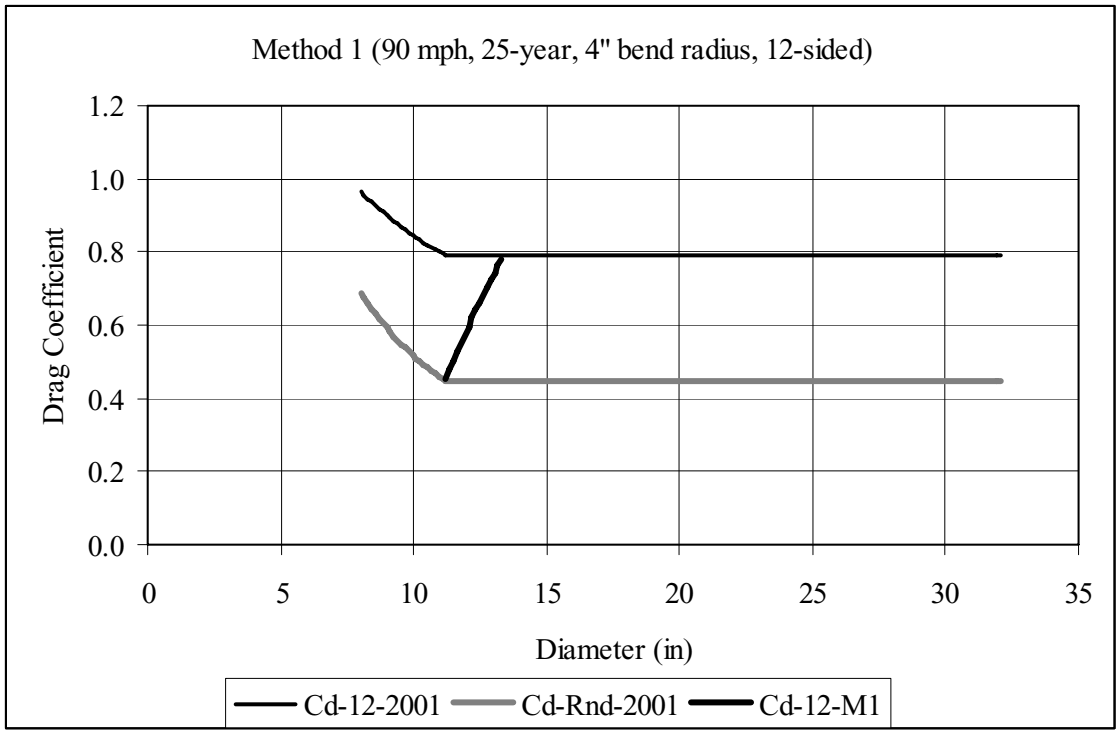

Figure D–15. Drag Coefficient Comparison: Method No. 1, 25-year MRI, 90 mph, 4" bend radius, 12-sided

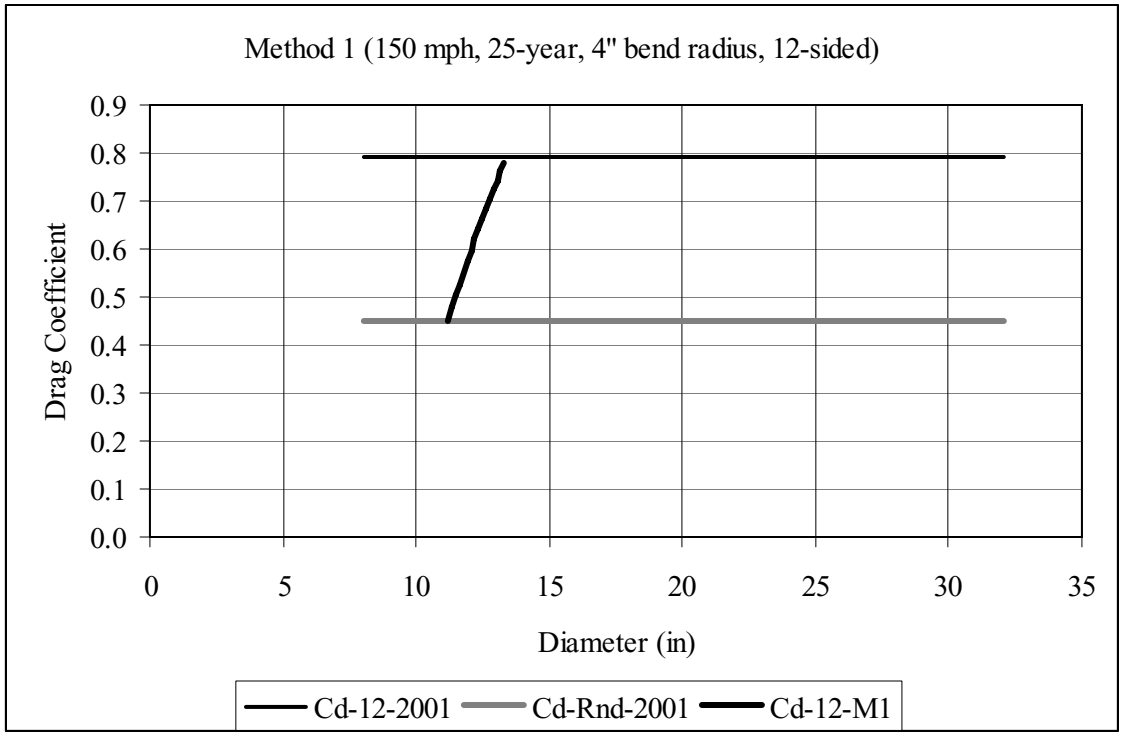

Figure D–16. Drag Coefficient Comparison: Method No. 1, 25-year MRI, 150 mph, 4" bend radius, 12-sided

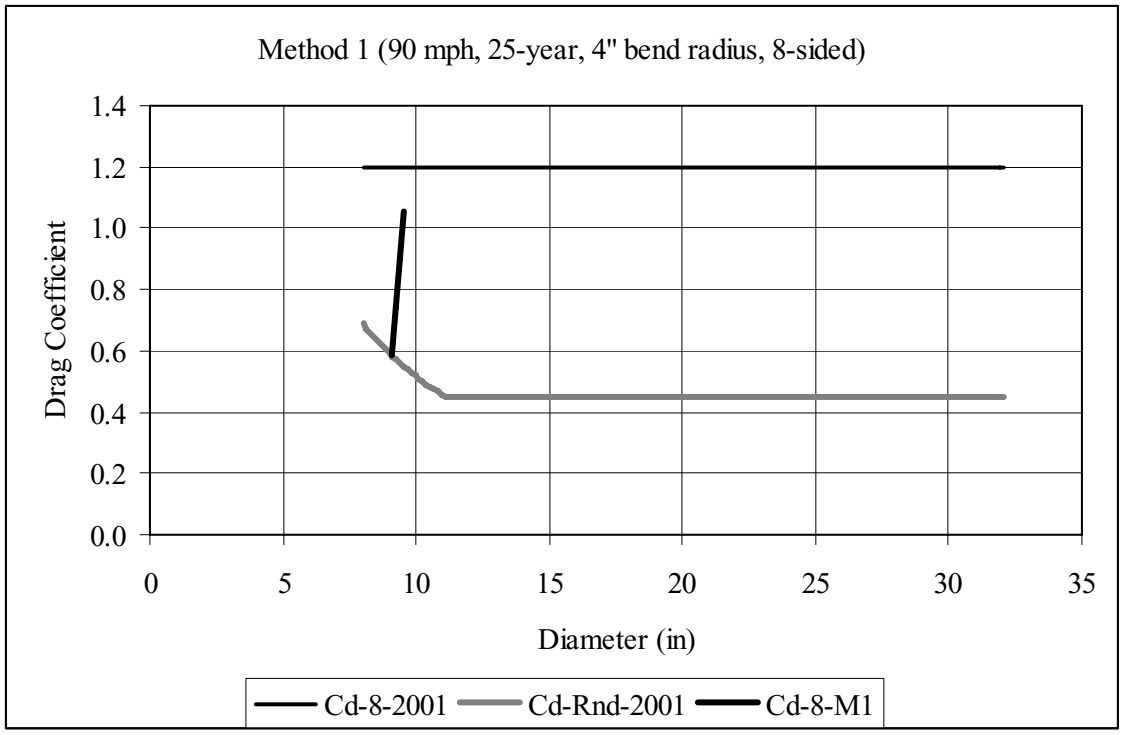

Figure D–17. Drag Coefficient Comparison: Method No. 1, 25-year MRI, 90 mph, 4” bend radius, 8-sided

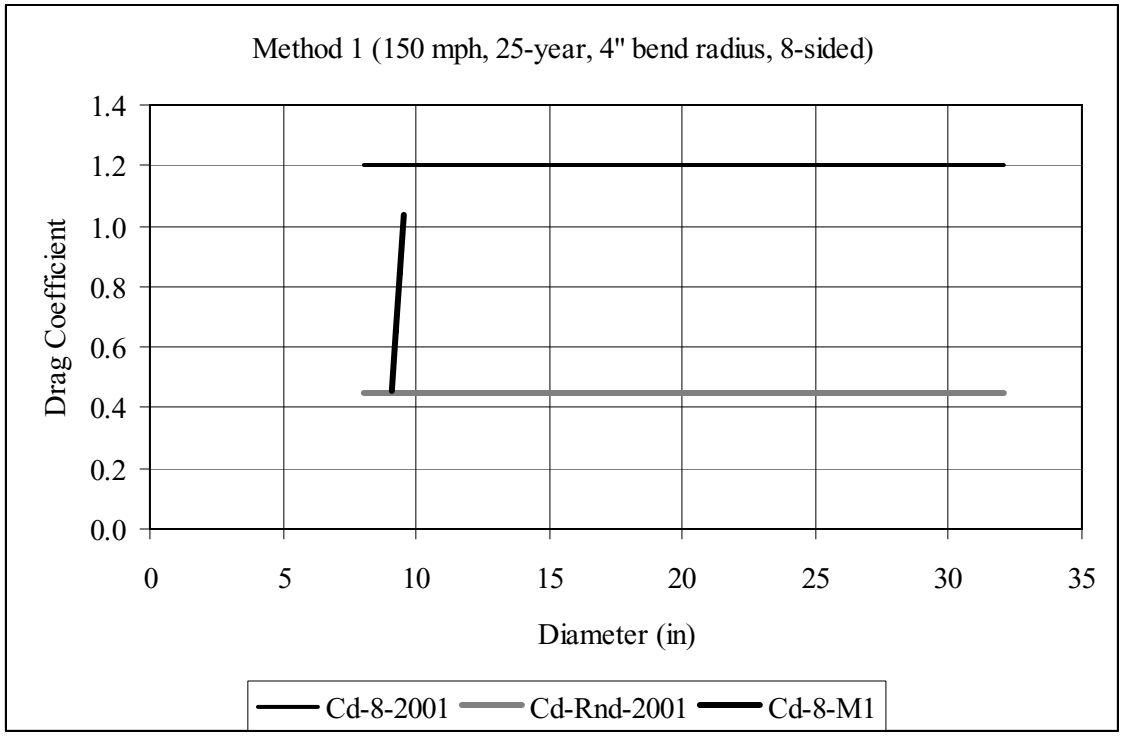

Figure D–18. Drag Coefficient Comparison: Method No. 1, 25-year MRI, 150 mph, 4” bend radius, 8-sided

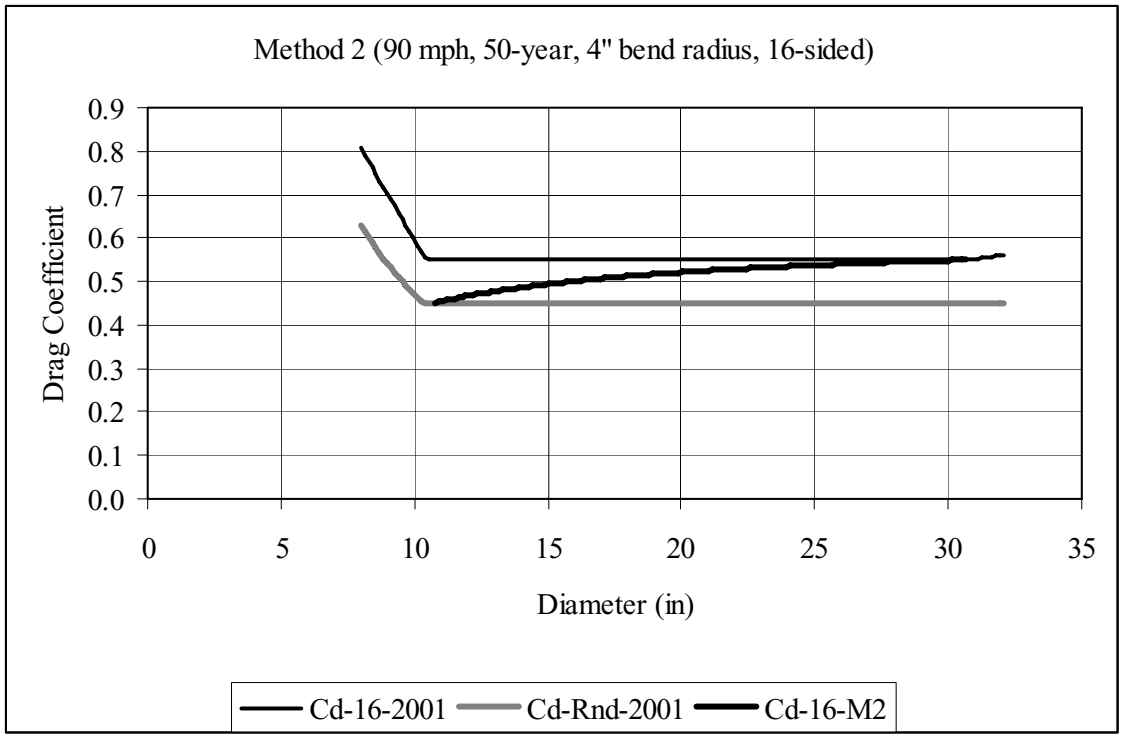

Figure D–19. Drag Coefficient Comparison: Method No. 2, 50-year MRI, 90 mph, 4” bend radius, 16-sided

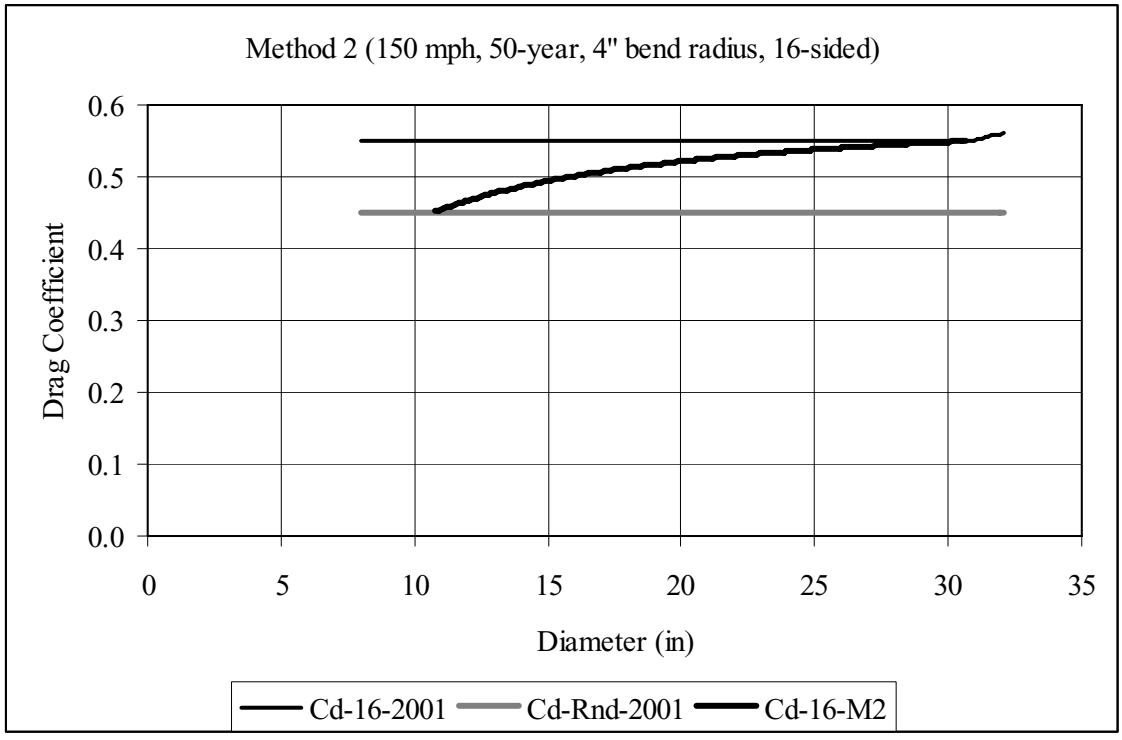

Figure D–20. Drag Coefficient Comparison: Method No. 2, 50-year MRI, 150 mph, 4” bend radius, 16-sided

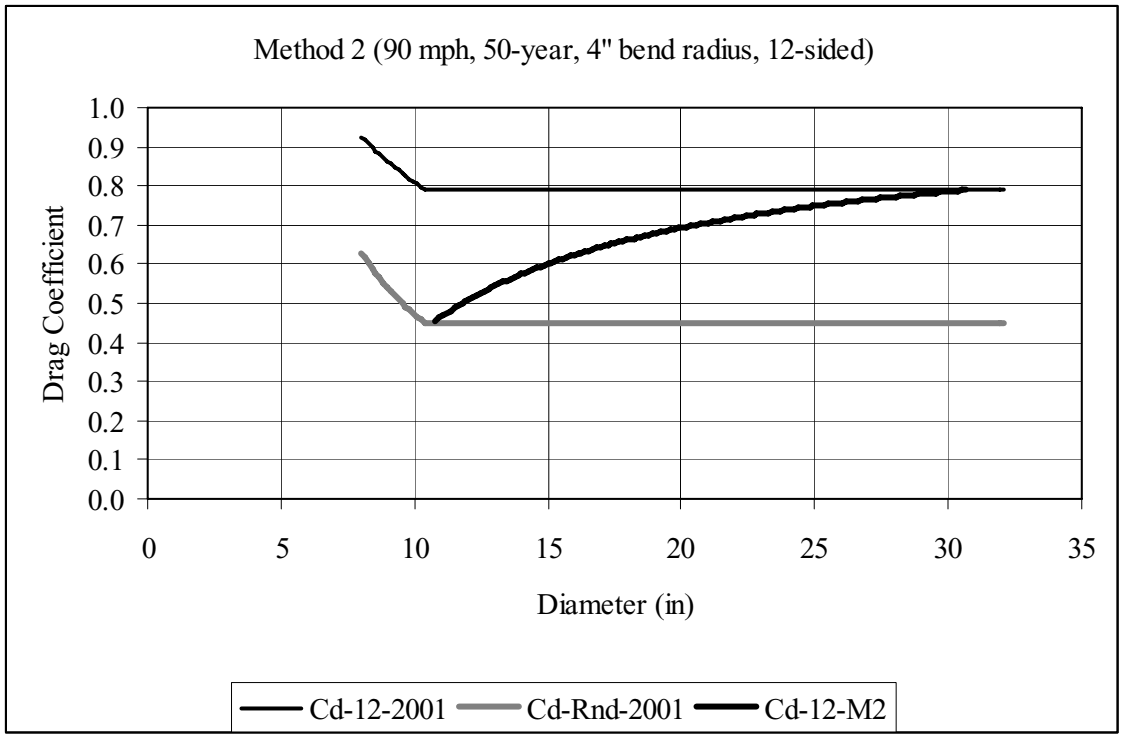

Figure D–21. Drag Coefficient Comparison: Method No. 2, 50-year MRI, 90 mph, 4” bend radius, 12-sided

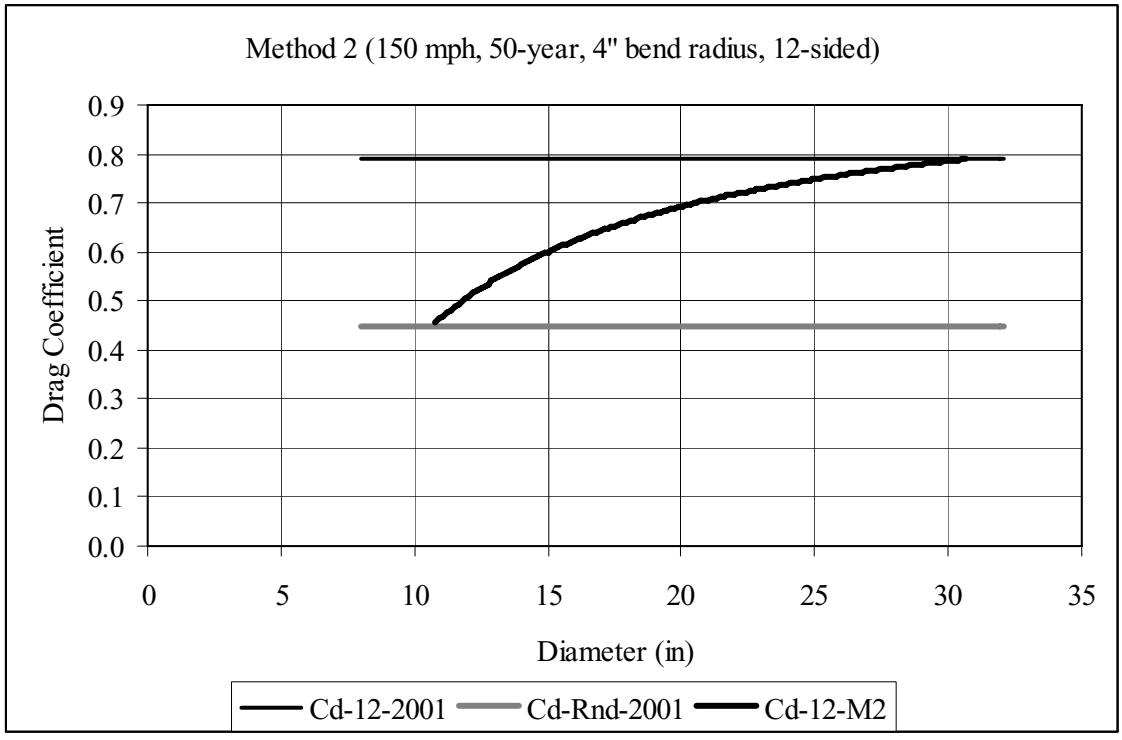

Figure D–22. Drag Coefficient Comparison: Method No. 2, 50-year MRI, 150 mph, 4” bend radius, 12-sided

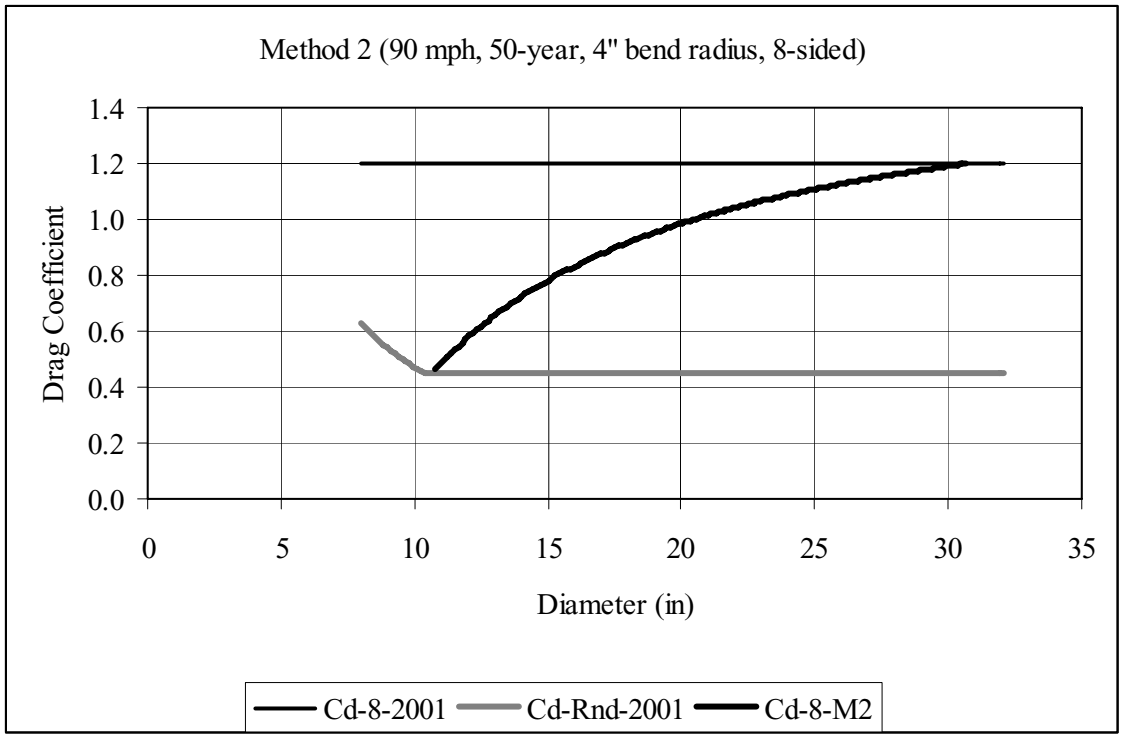

Figure D–23. Drag Coefficient Comparison: Method No. 2, 50-year MRI, 90 mph, 4” bend radius, 8-sided

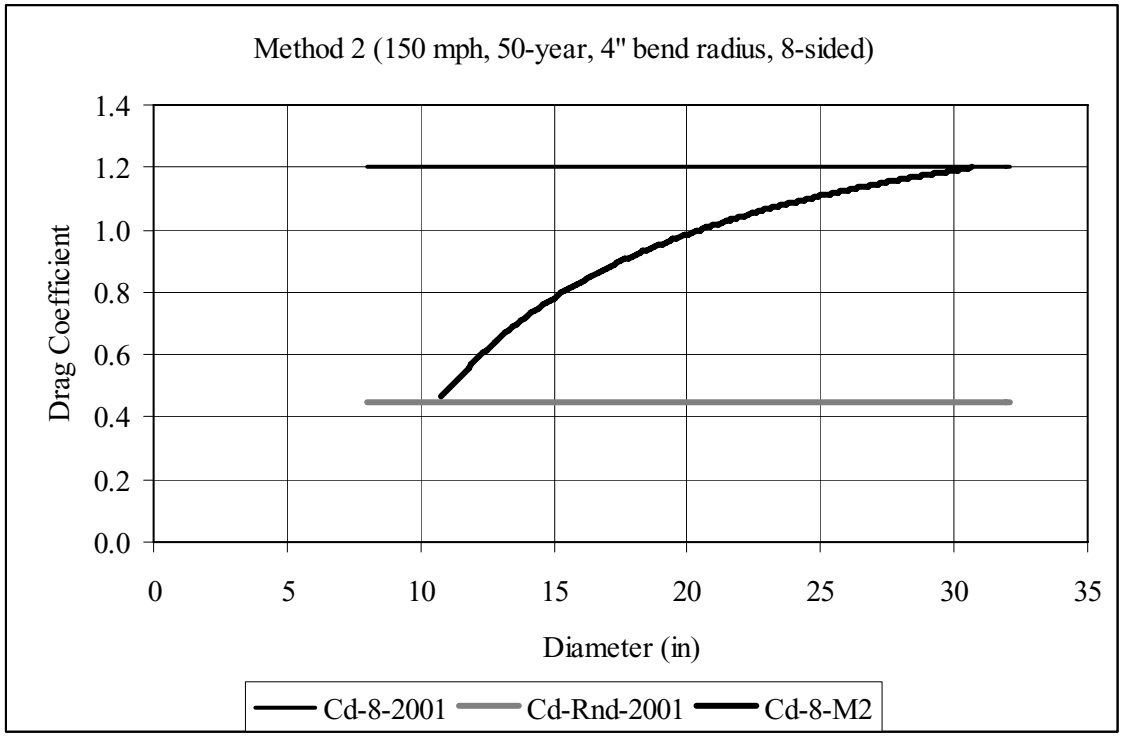

Figure D–24. Drag Coefficient Comparison: Method No. 2, 50-year MRI, 150 mph, 4” bend radius, 8-sided

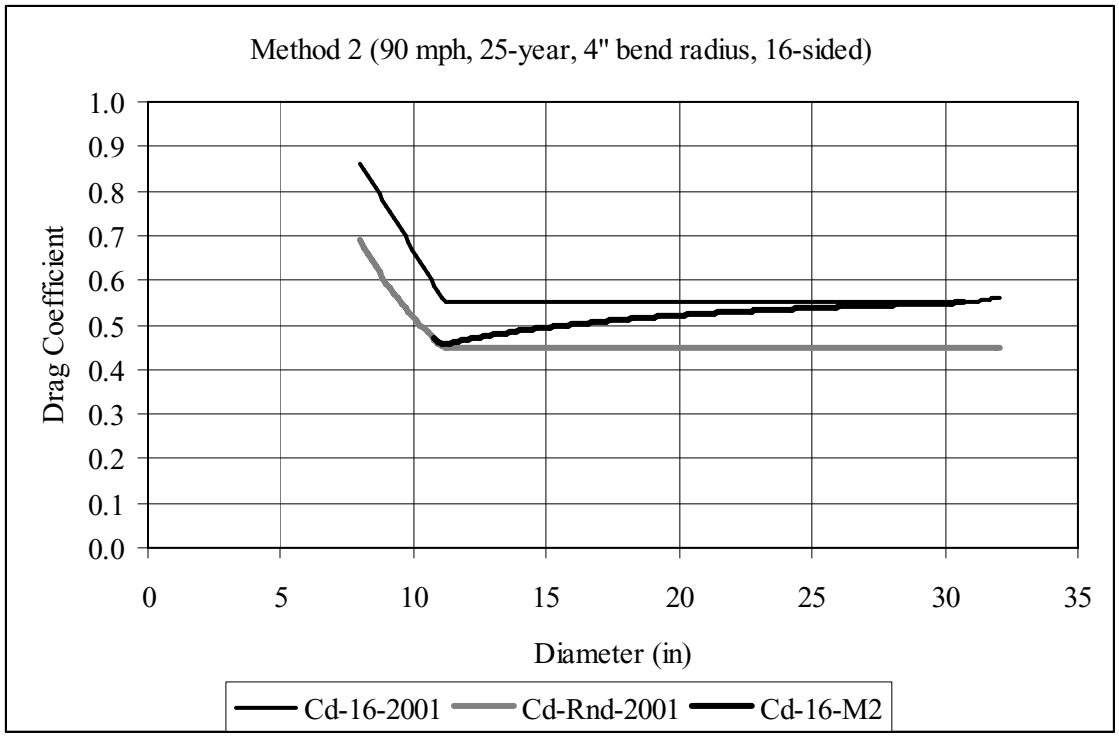

Figure D–25. Drag Coefficient Comparison: Method No. 2, 25-year MRI, 90 mph, 4” bend radius, 16-sided

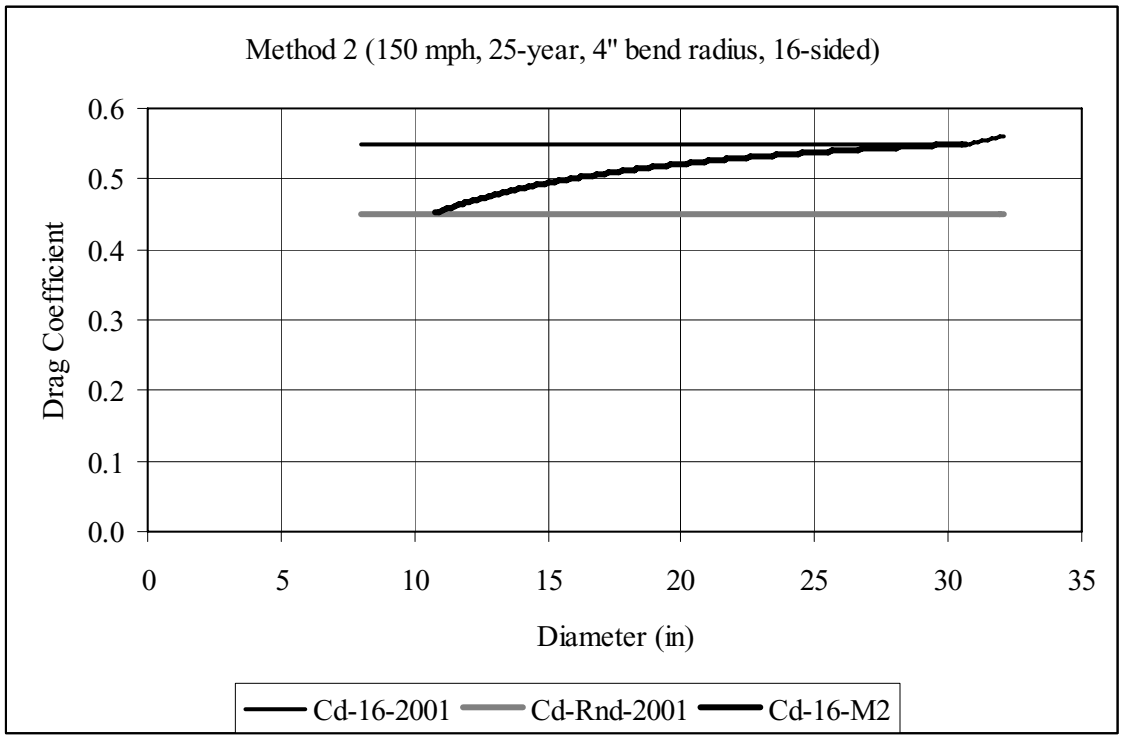

Figure D–26. Drag Coefficient Comparison: Method No. 2, 25-year MRI, 150 mph, 4” bend radius, 16-sided

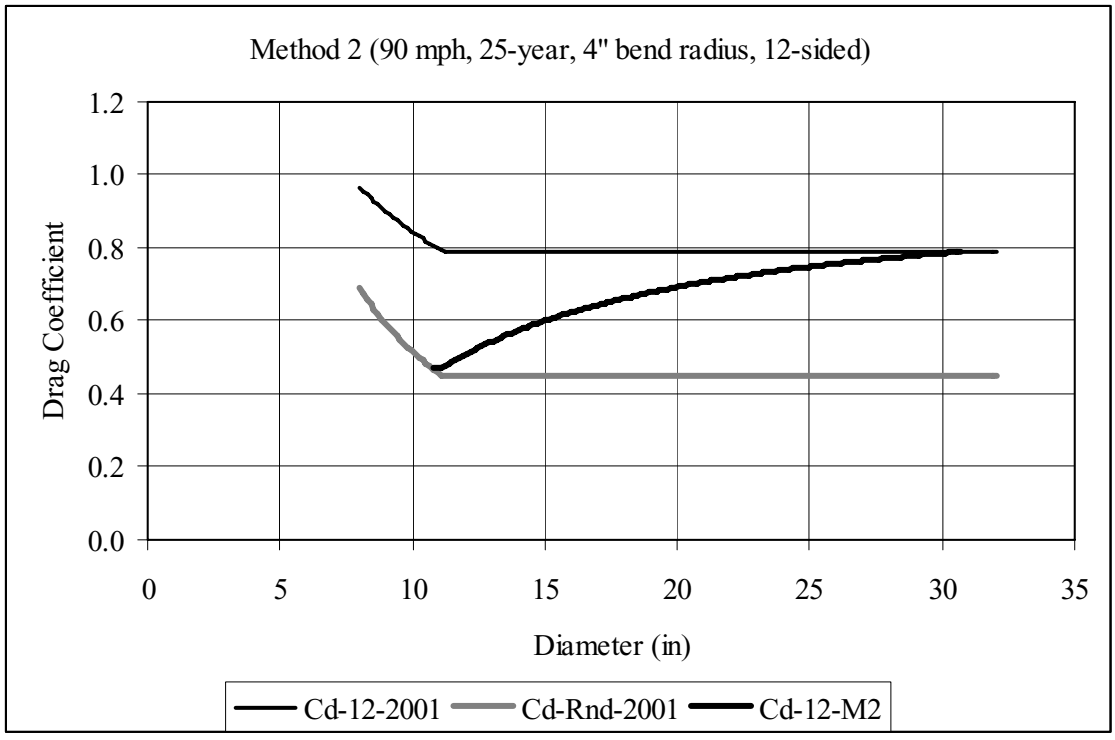

Figure D–27. Drag Coefficient Comparison: Method No. 2, 25-year MRI, 90 mph, 4” bend radius, 12-sided

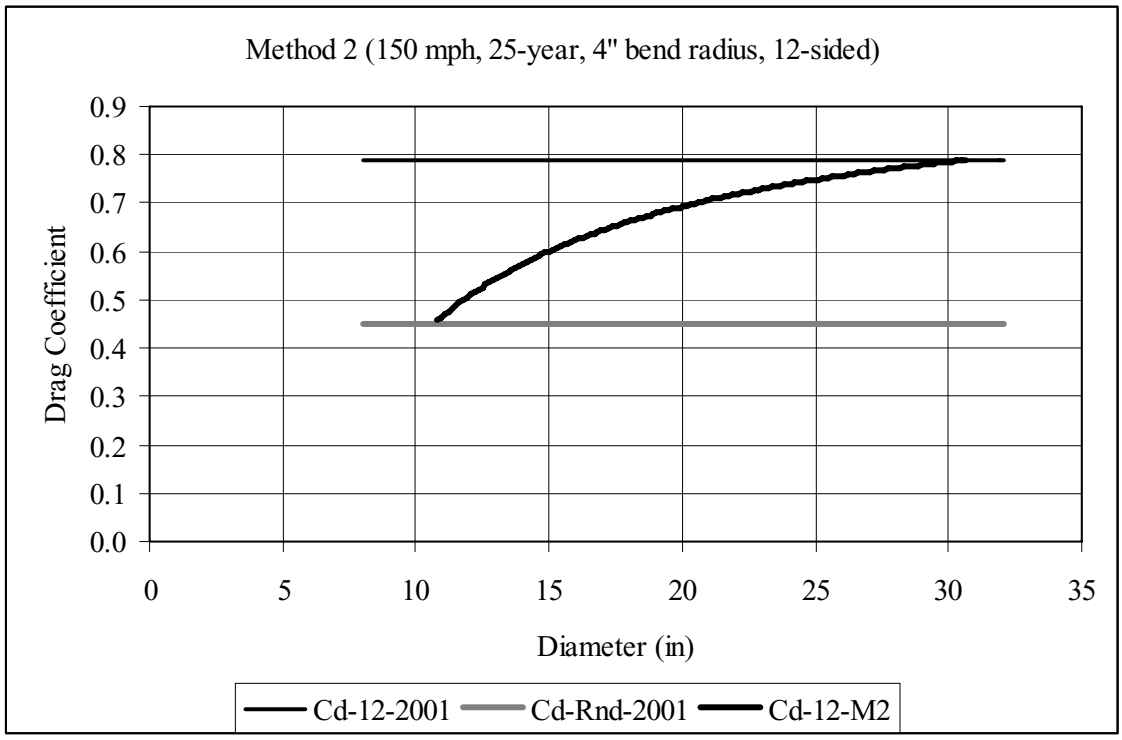

Figure D–28. Drag Coefficient Comparison: Method No. 2, 25-year MRI, 150 mph, 4” bend radius, 12-sided

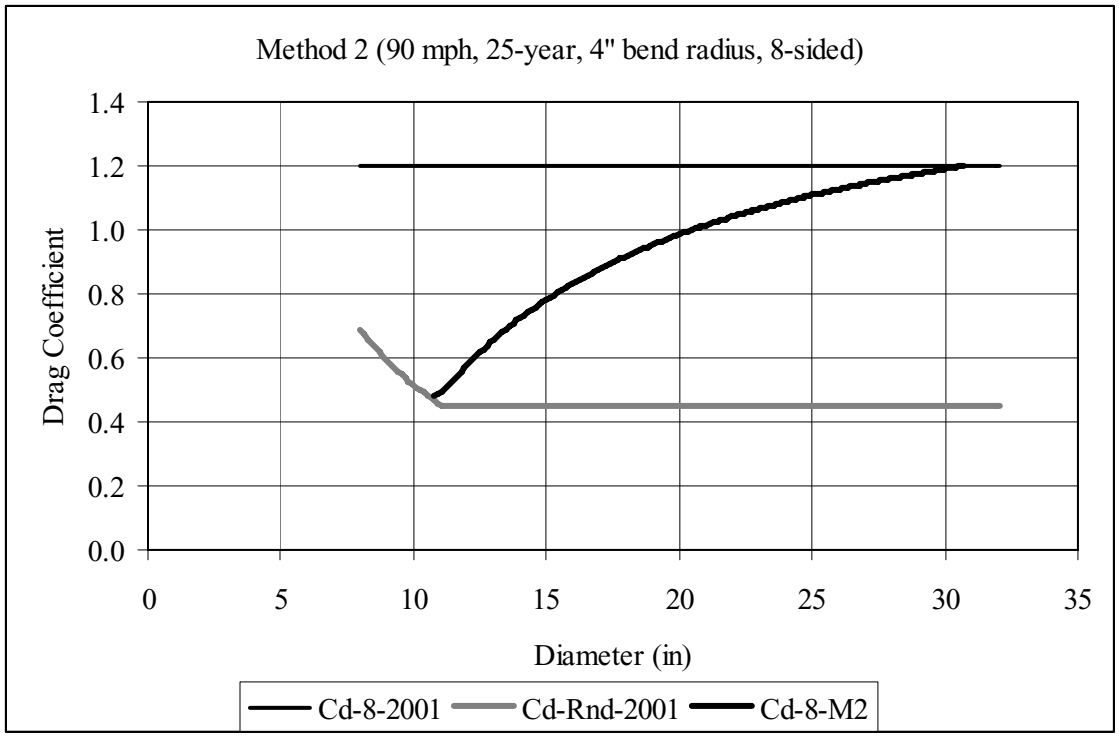

Figure D–29. Drag Coefficient Comparison: Method No. 2, 25-year MRI, 90 mph, 4” bend radius, 8-sided

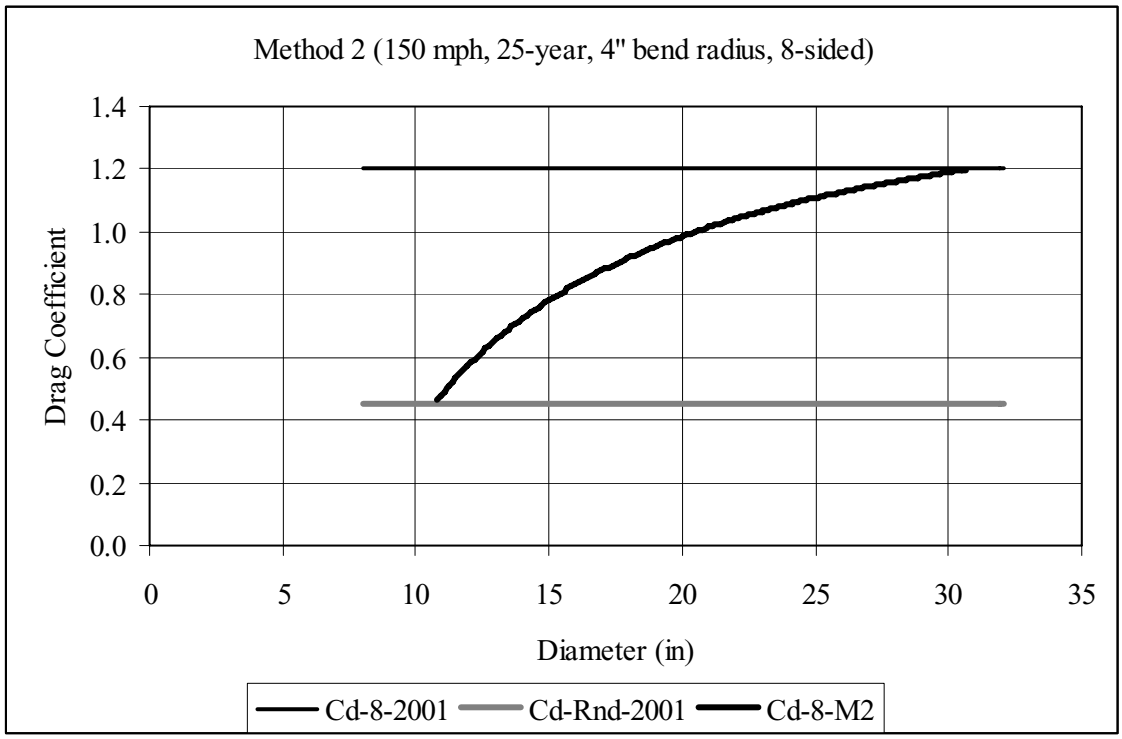

Figure D–30. Drag Coefficient Comparison: Method No. 2, 25-year MRI, 150 mph, 4” bend radius, 8-sided

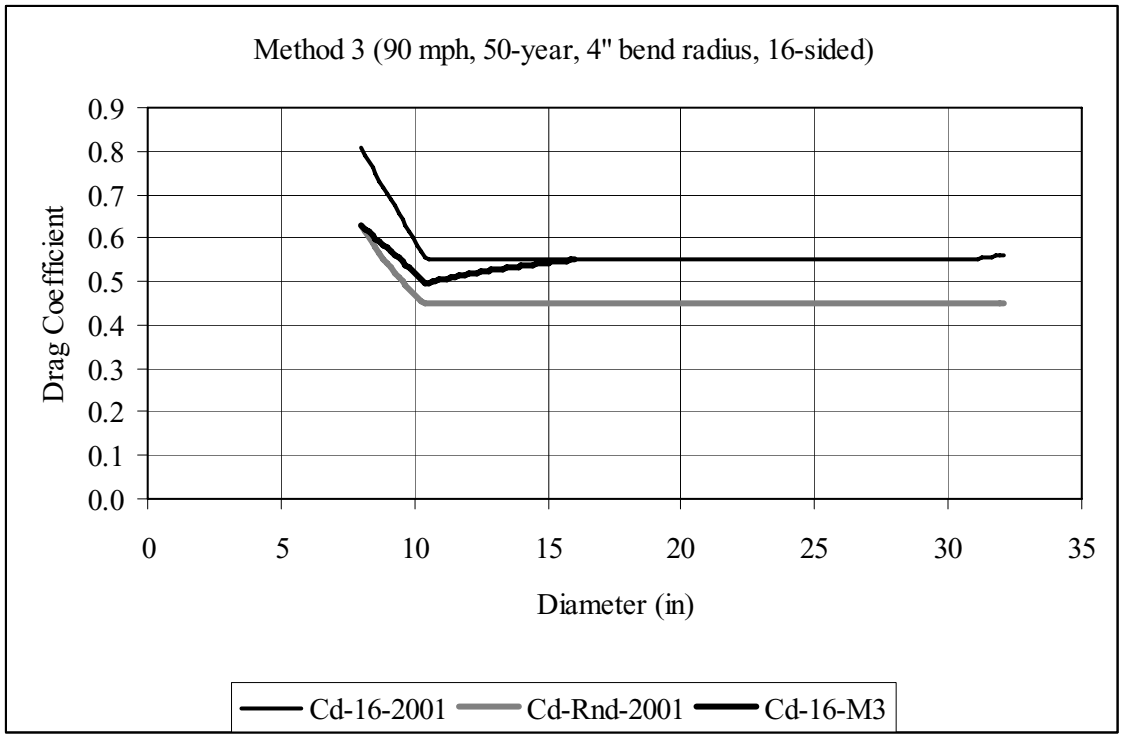

Figure D–31. Drag Coefficient Comparison: Method No. 3, 50-year MRI, 90 mph, 4” bend radius, 16-sided

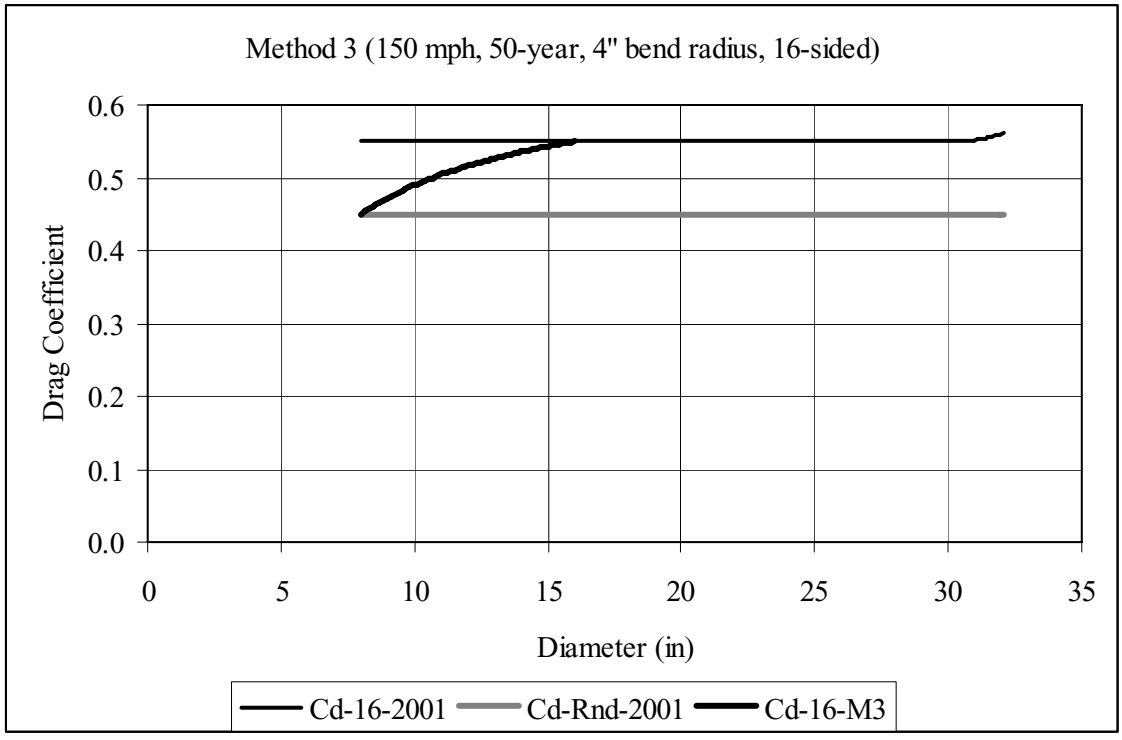

Figure D–32. Drag Coefficient Comparison: Method No. 3, 50-year MRI, 150 mph, 4” bend radius, 16-sided

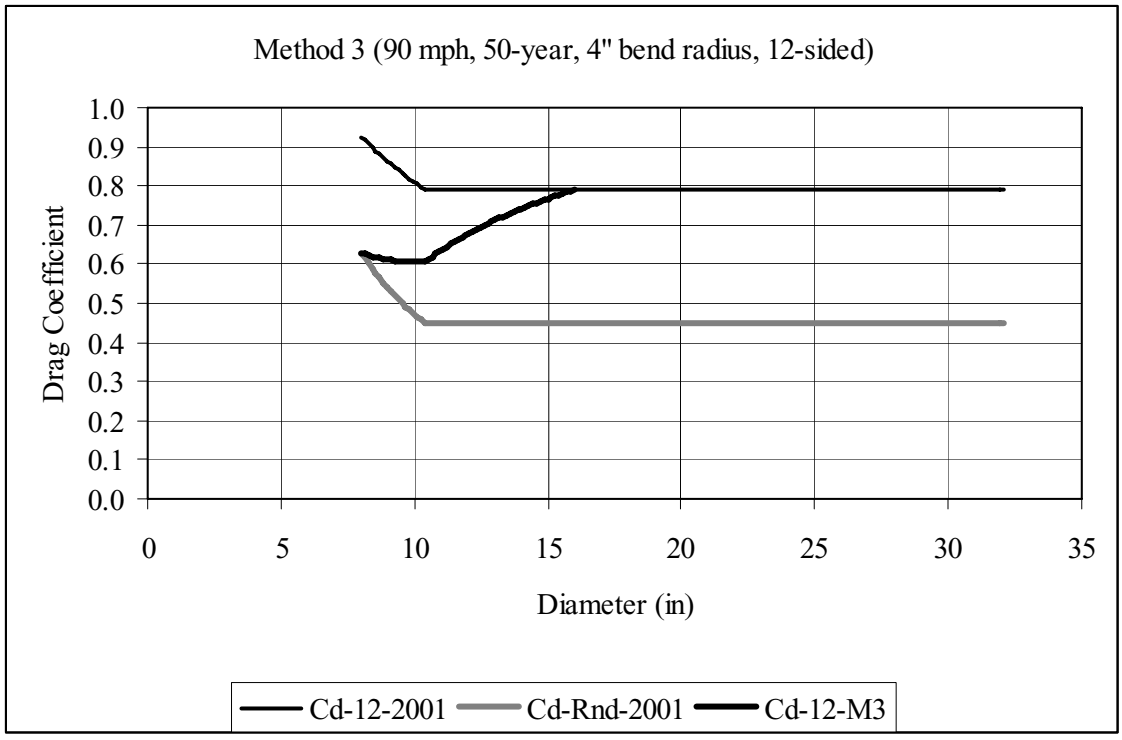

Figure D–33. Drag Coefficient Comparison: Method No. 3, 50-year MRI, 90 mph, 4” bend radius, 12-sided

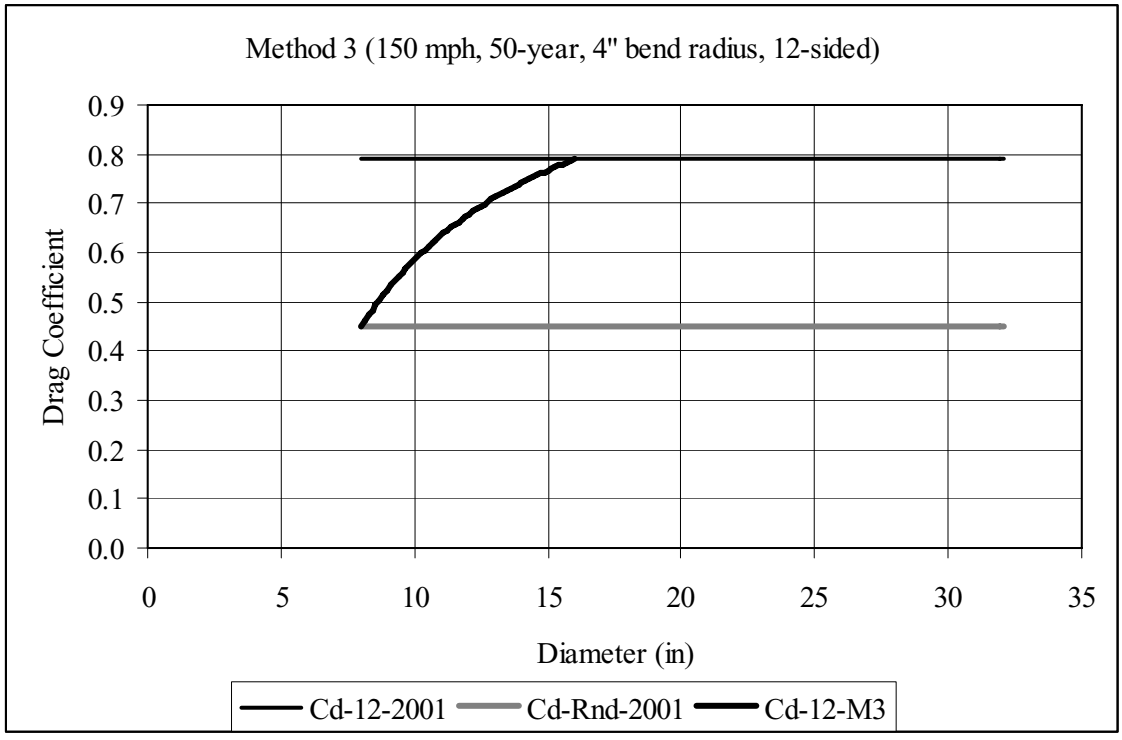

Figure D–34. Drag Coefficient Comparison: Method No. 3, 50-year MRI, 150 mph, 4” bend radius, 12-sided

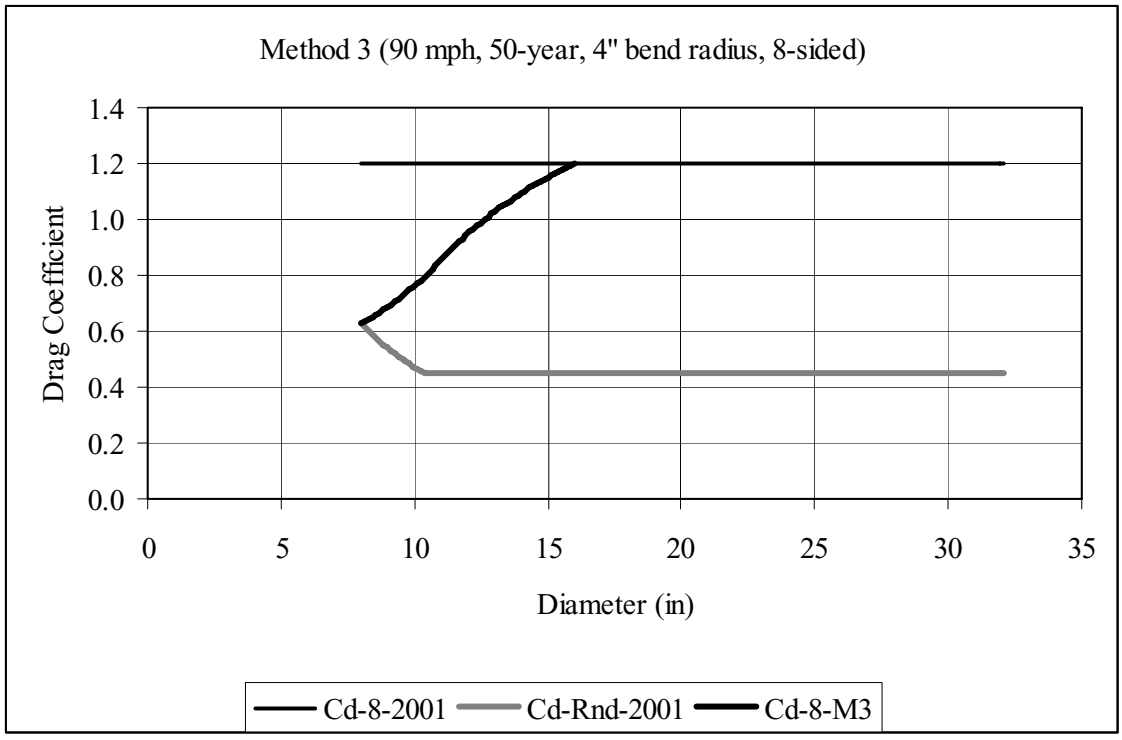

Figure D–35. Drag Coefficient Comparison: Method No. 3, 50-year MRI, 90 mph, 4” bend radius, 8-sided

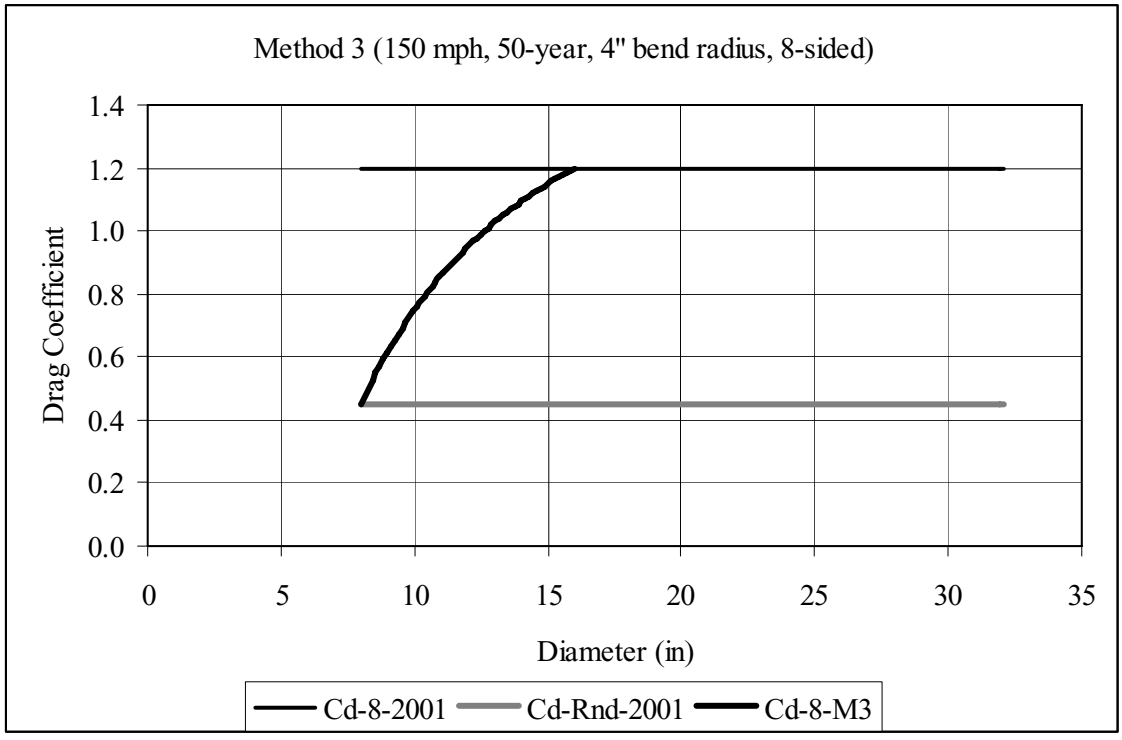

Figure D–36. Drag Coefficient Comparison: Method No. 3, 50-year MRI, 150 mph, 4” bend radius, 8-sided

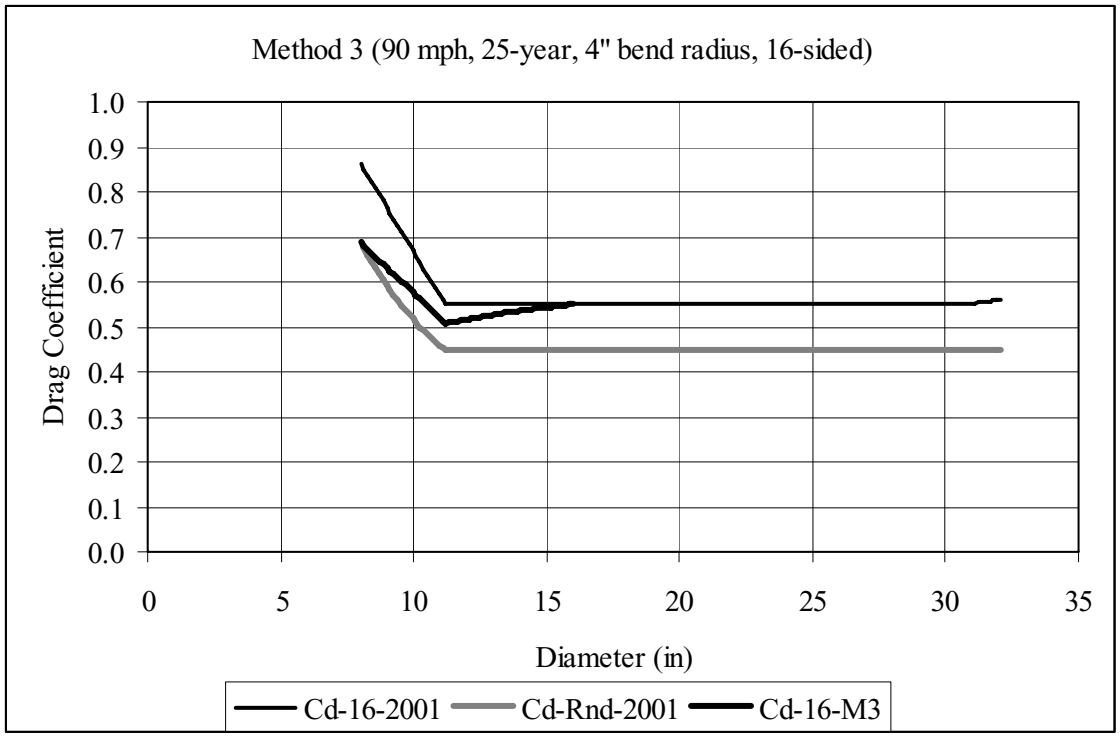

Figure D–37. Drag Coefficient Comparison: Method No. 3, 25-year MRI, 90 mph, 4” bend radius, 16-sided

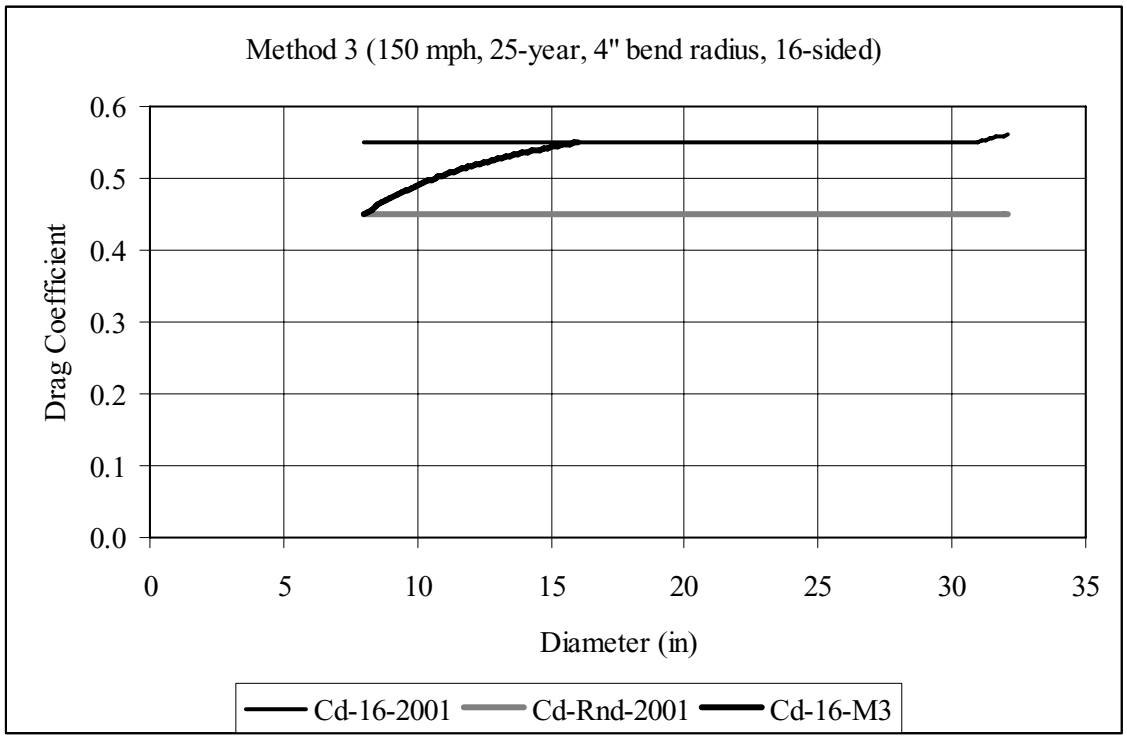

Figure D–38. Drag Coefficient Comparison: Method No. 3, 25-year MRI, 150 mph, 4” bend radius, 16-sided

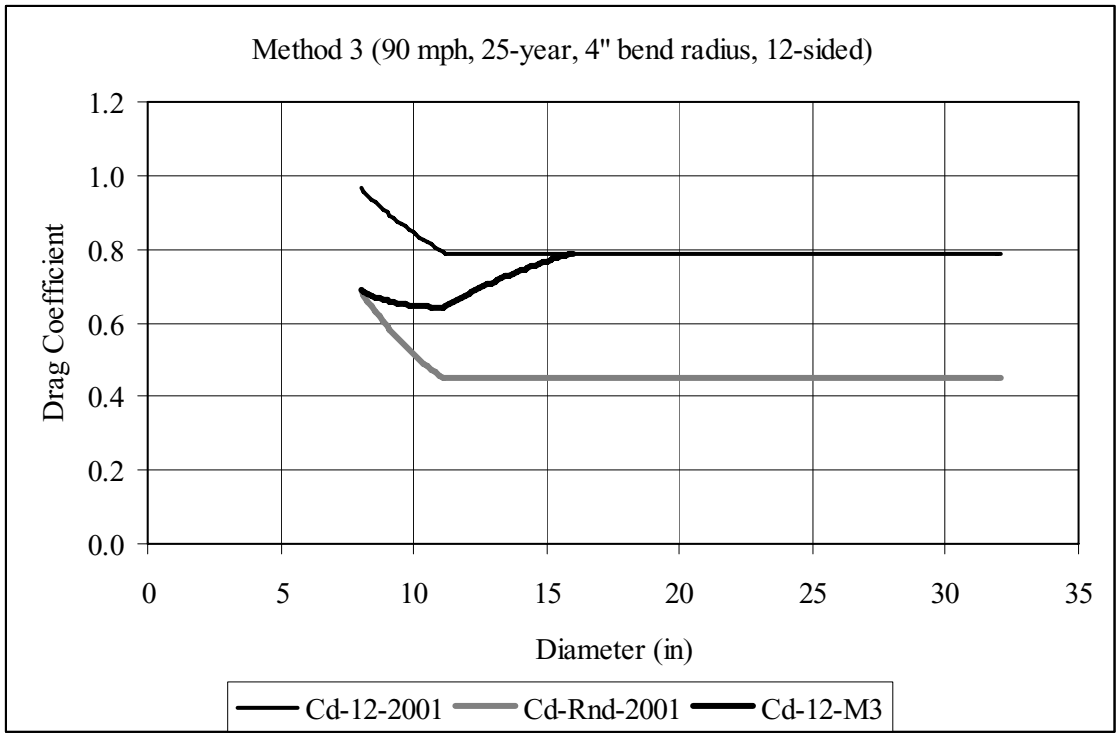

Figure D–39. Drag Coefficient Comparison: Method No. 3, 25-year MRI, 90 mph, 4” bend radius, 12-sided

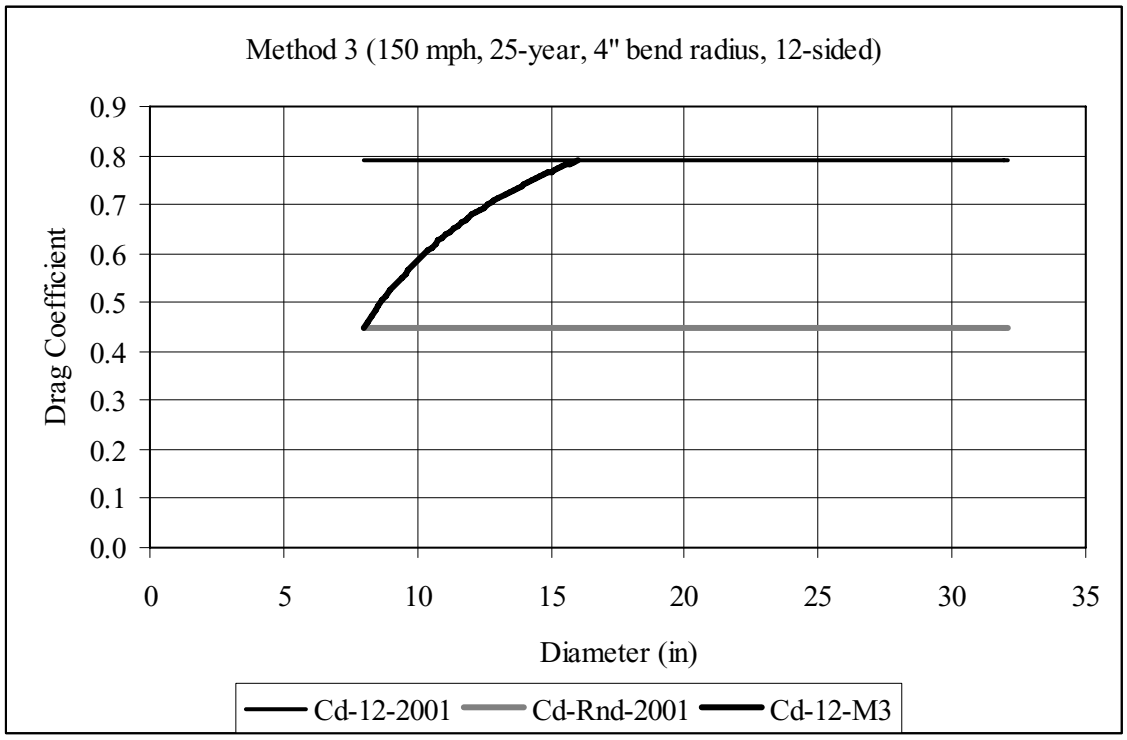

Figure D–40. Drag Coefficient Comparison: Method No. 3, 25-year MRI, 150 mph, 4” bend radius, 12-sided

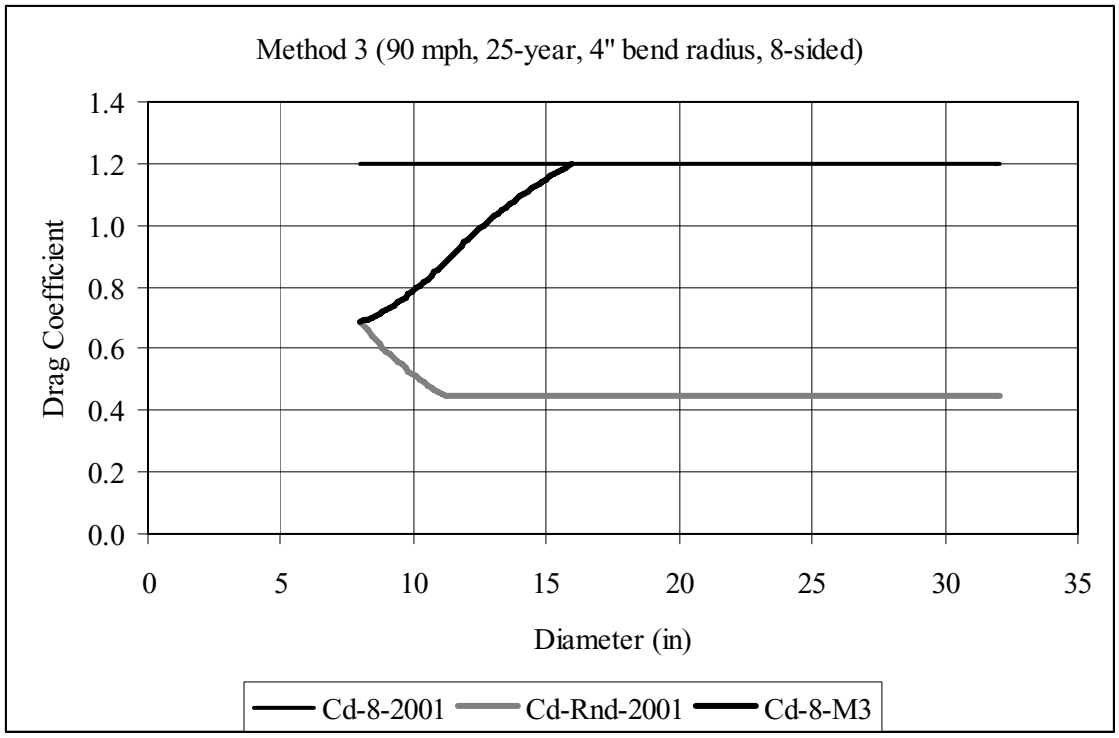

Figure D–41. Drag Coefficient Comparison: Method No. 3, 25-year MRI, 90 mph, 4” bend radius, 8-sided

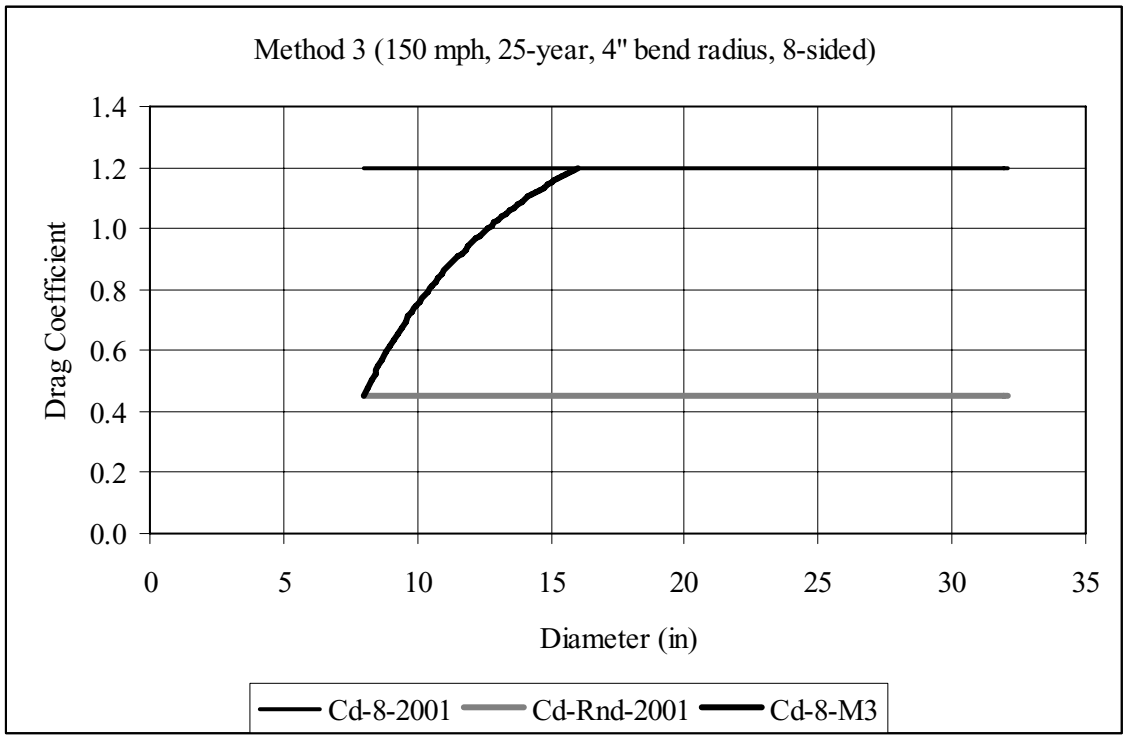

Figure D–42. Drag Coefficient Comparison: Method No. 3, 25-year MRI, 150 mph, 4” bend radius, 8-sided

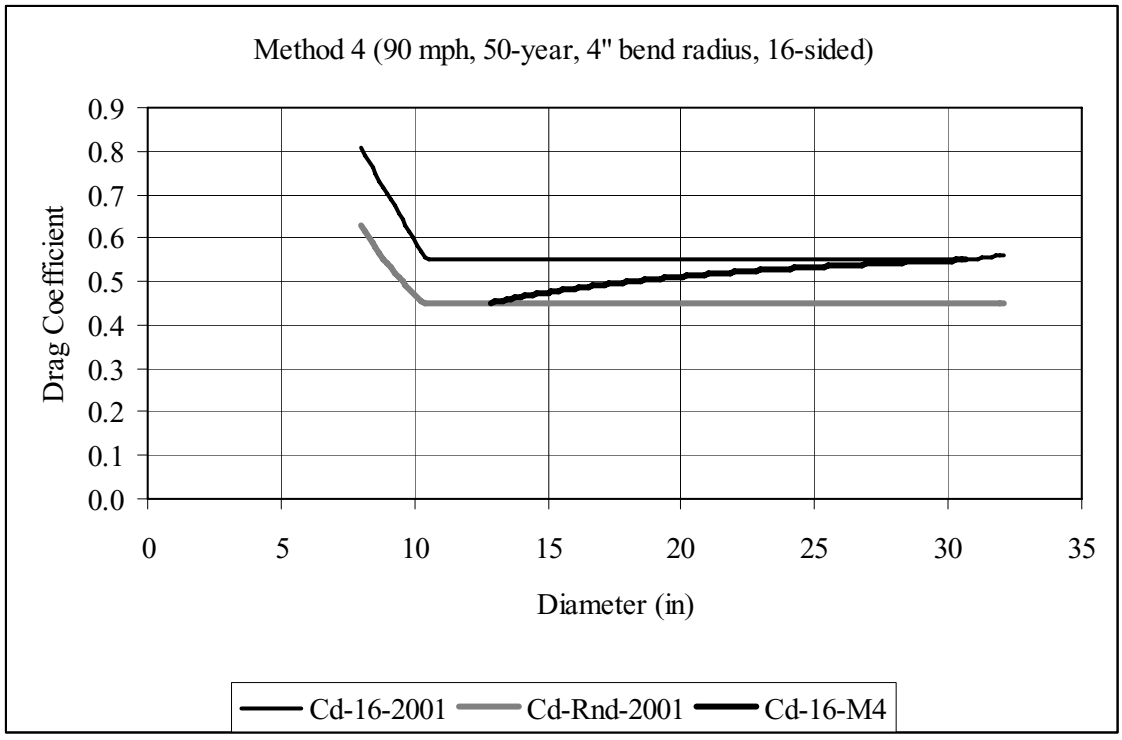

Figure D–43. Drag Coefficient Comparison: Method No. 4, 50-year MRI, 90 mph, 4” bend radius, 16-sided

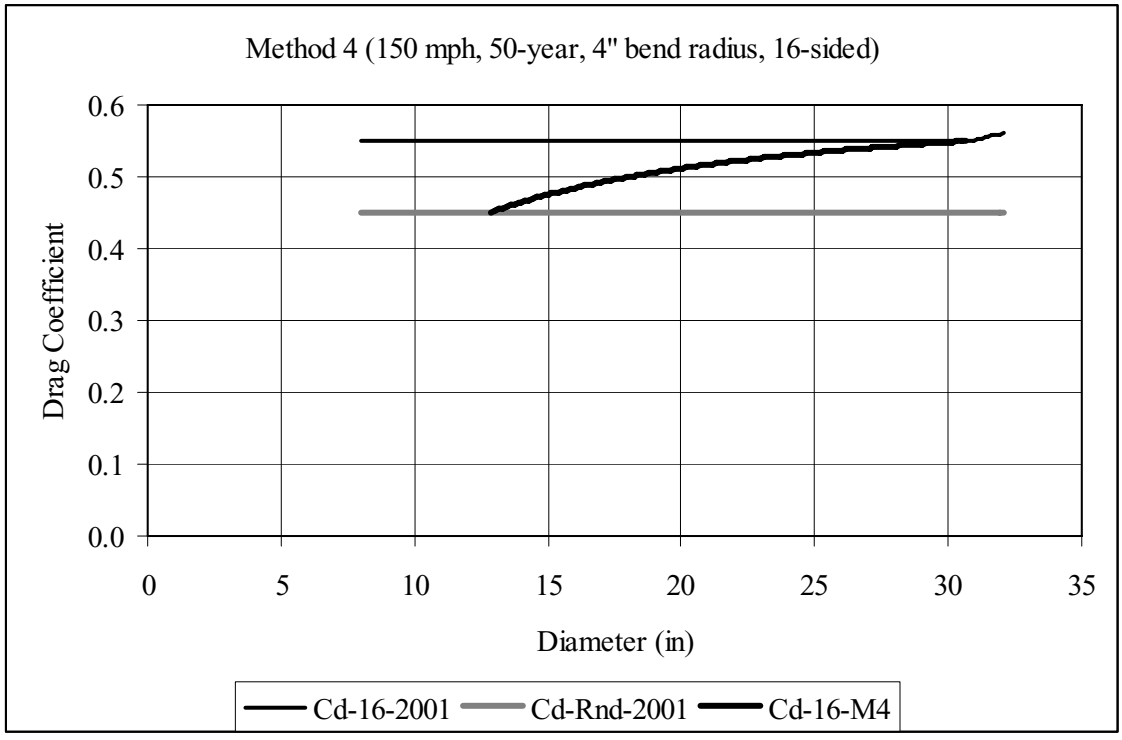

Figure D–44. Drag Coefficient Comparison: Method No. 4, 50-year MRI, 150 mph, 4” bend radius, 16-sided

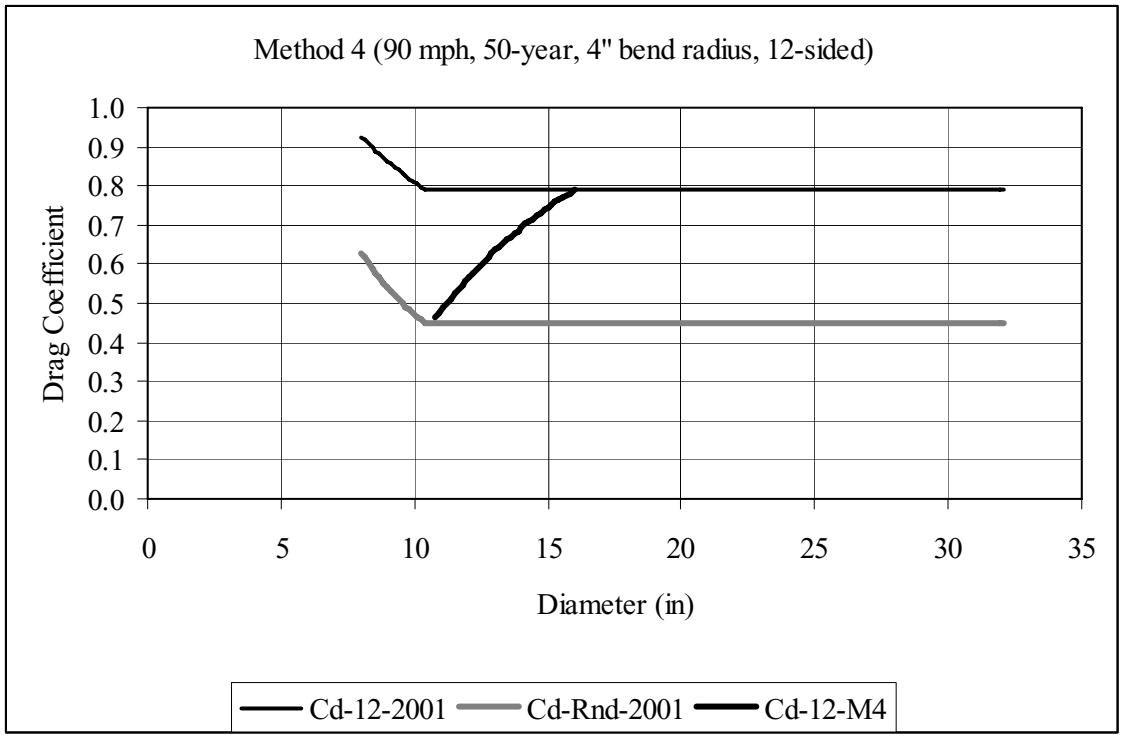

Figure D–45. Drag Coefficient Comparison: Method No. 4, 50-year MRI, 90 mph, 4” bend radius, 12-sided

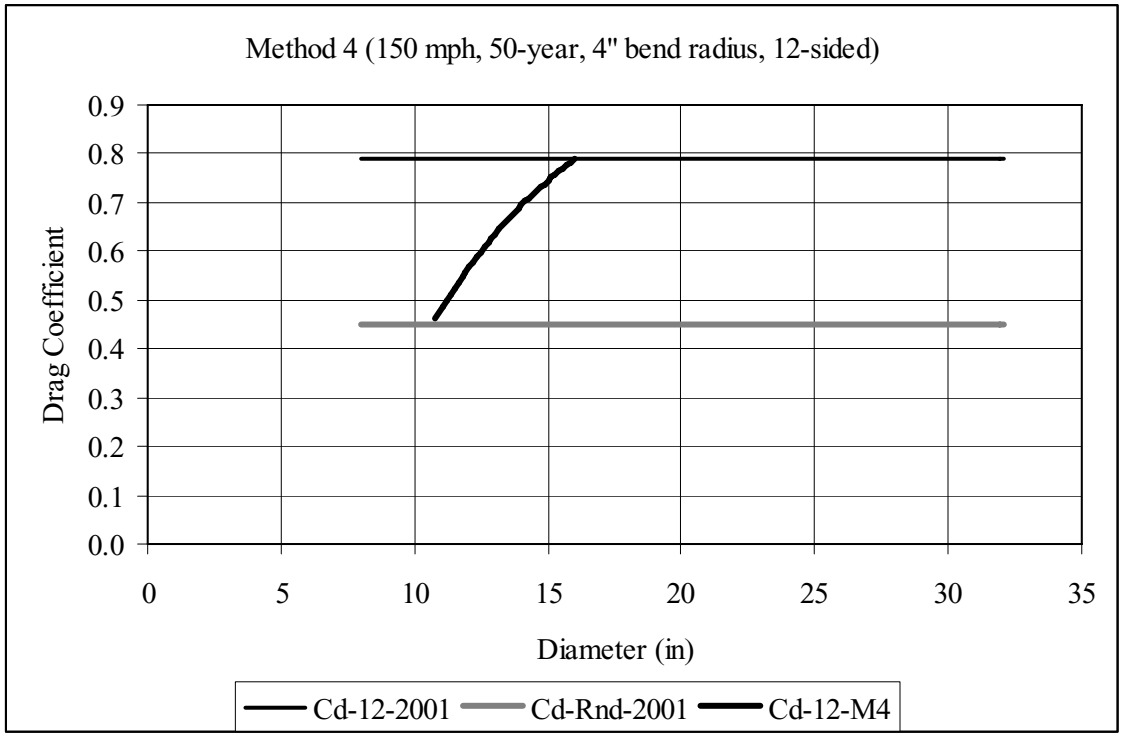

Figure D–46. Drag Coefficient Comparison: Method No. 4, 50-year MRI, 150 mph, 4” bend radius, 12-sided

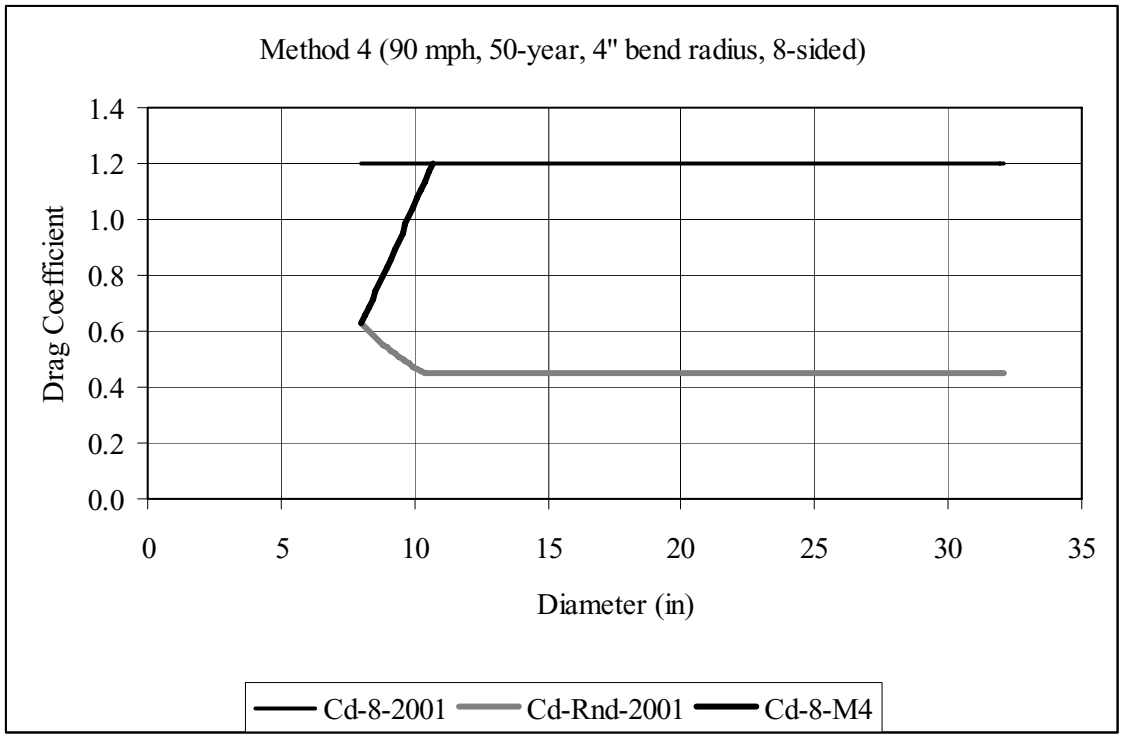

Figure D–47. Drag Coefficient Comparison: Method No. 4, 50-year MRI, 90 mph, 4” bend radius, 8-sided

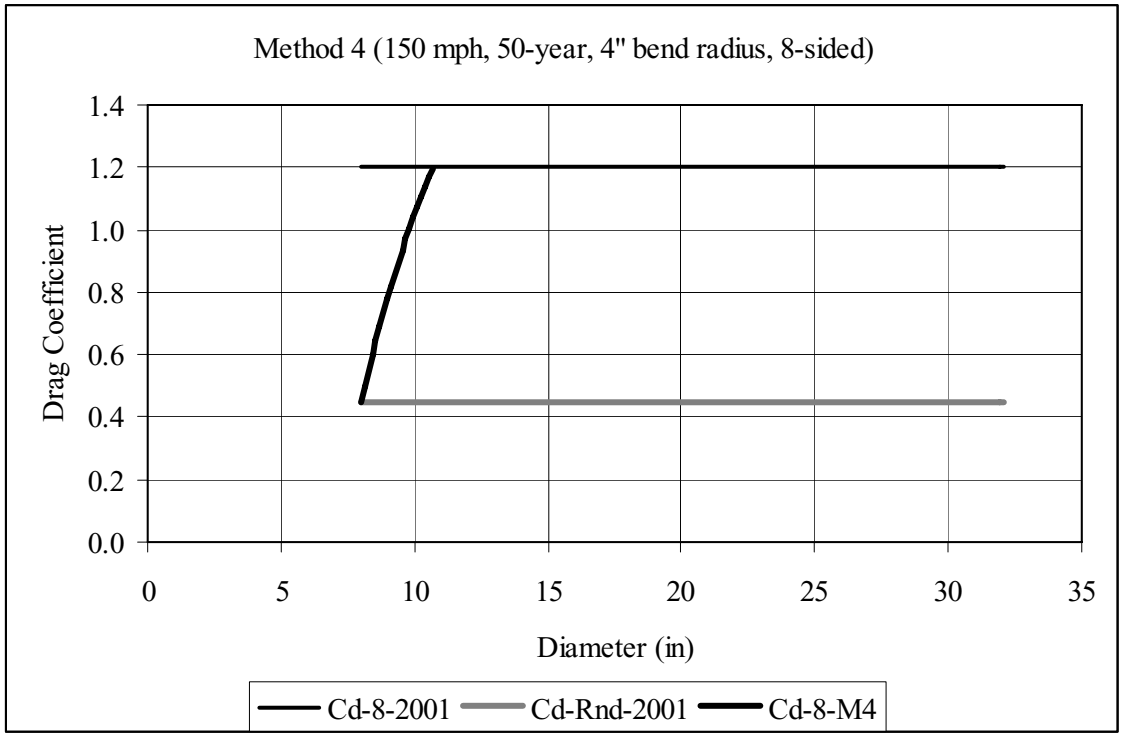

Figure D–48. Drag Coefficient Comparison: Method No. 4, 50-year MRI, 150 mph, 4” bend radius, 8-sided

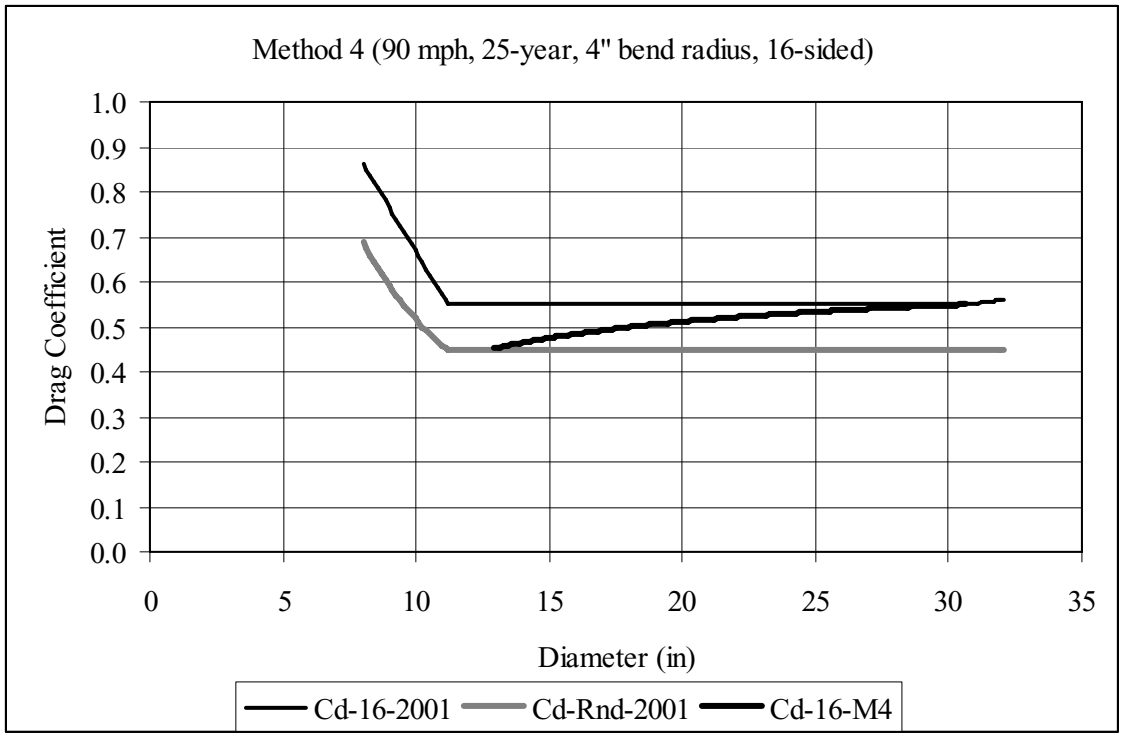

Figure D–49. Drag Coefficient Comparison: Method No. 4, 25-year MRI, 90 mph, 4” bend radius, 16-sided

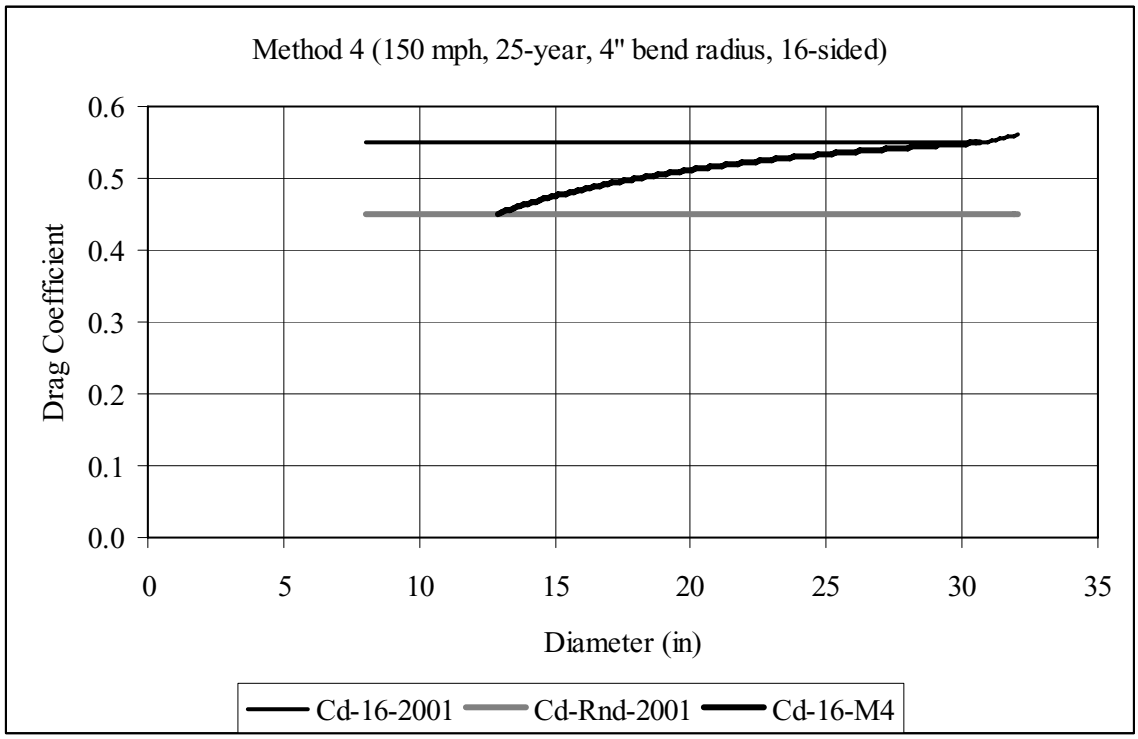

Figure D–50. Drag Coefficient Comparison: Method No. 4, 25-year MRI, 150 mph, 4” bend radius, 16-sided

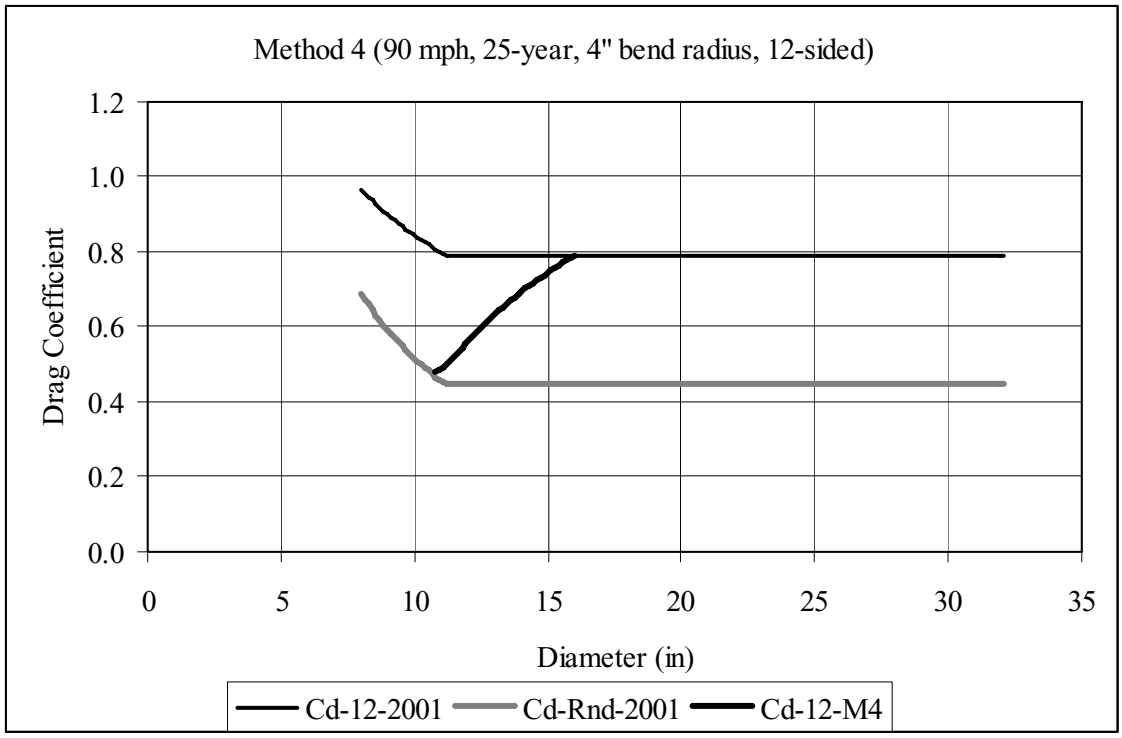

Figure D–51. Drag Coefficient Comparison: Method No. 4, 25-year MRI, 90 mph, 4" bend radius, 12-sided

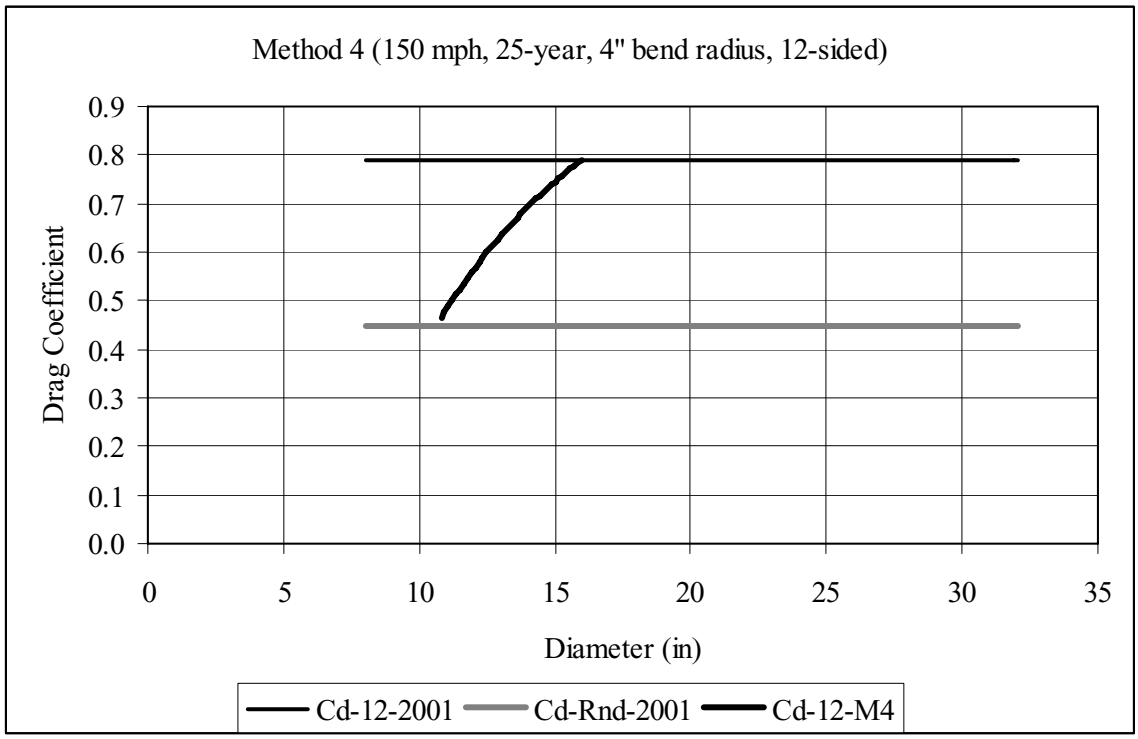

Figure D–52. Drag Coefficient Comparison: Method No. 4, 25-year MRI, 150 mph, 4" bend radius, 12-sided

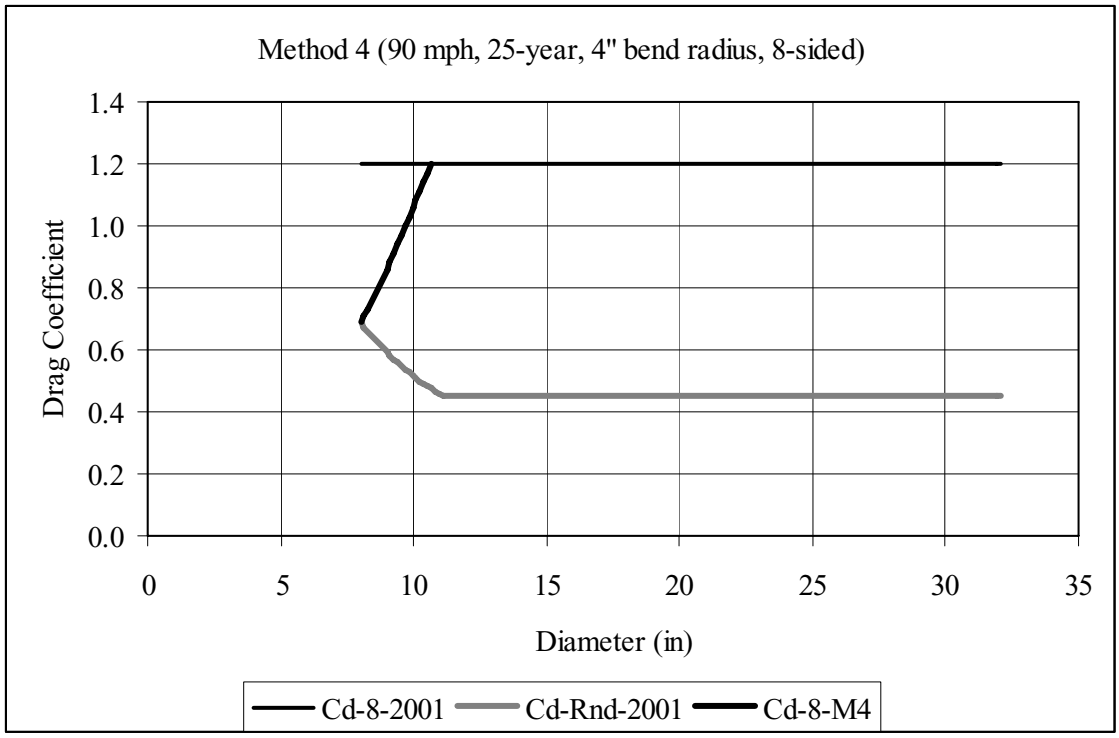

Figure D–53. Drag Coefficient Comparison: Method No. 4, 25-year MRI, 90 mph, 4” bend radius, 8-sided

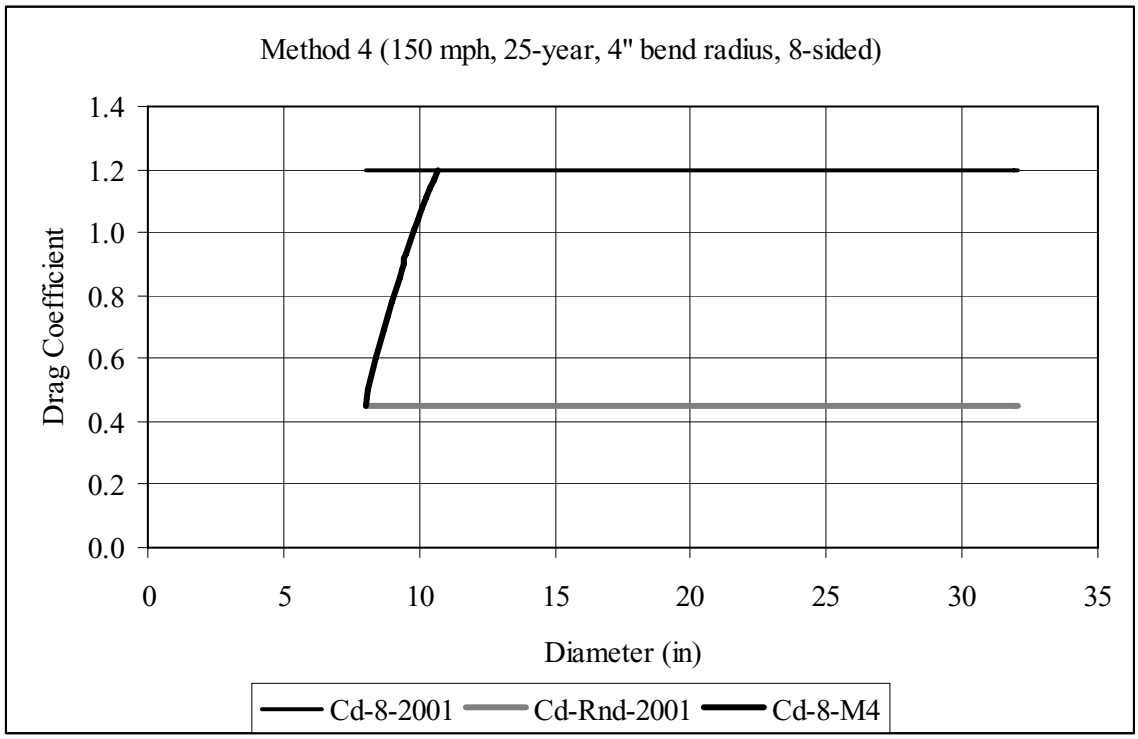

Figure D–54. Drag Coefficient Comparison: Method No. 4, 25-year MRI, 150 mph, 4” bend radius, 8-sided

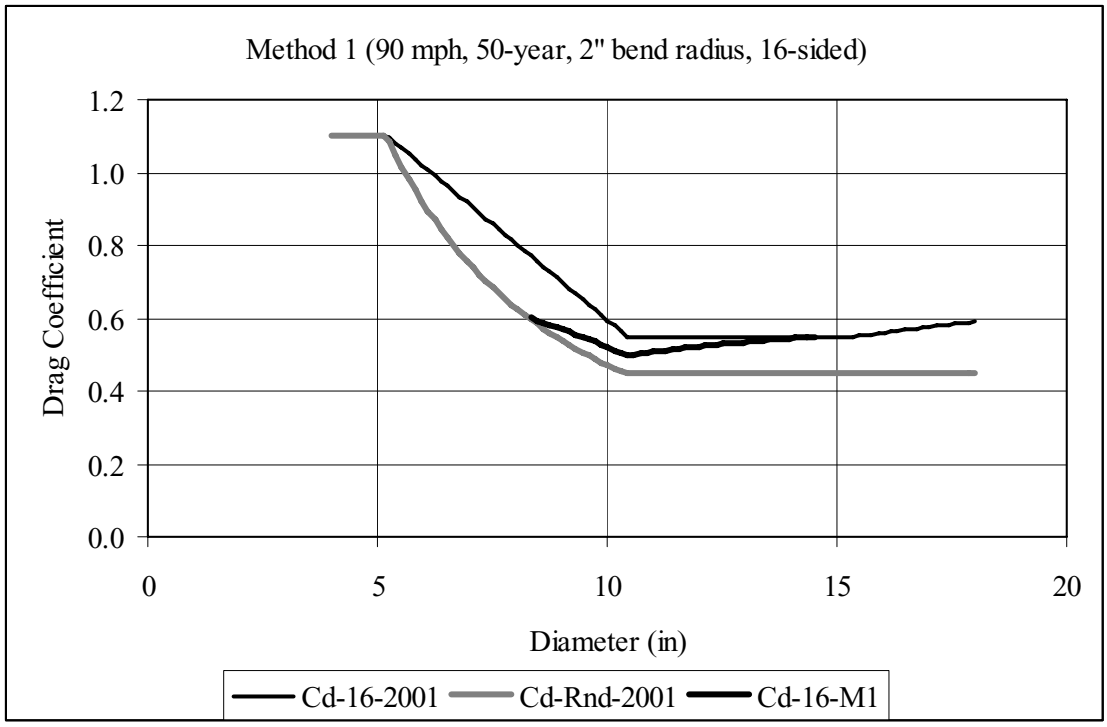

Figure D–55. Drag Coefficient Comparison: Method No. 1, 50-year MRI, 90 mph, 2" bend radius, 16-sided

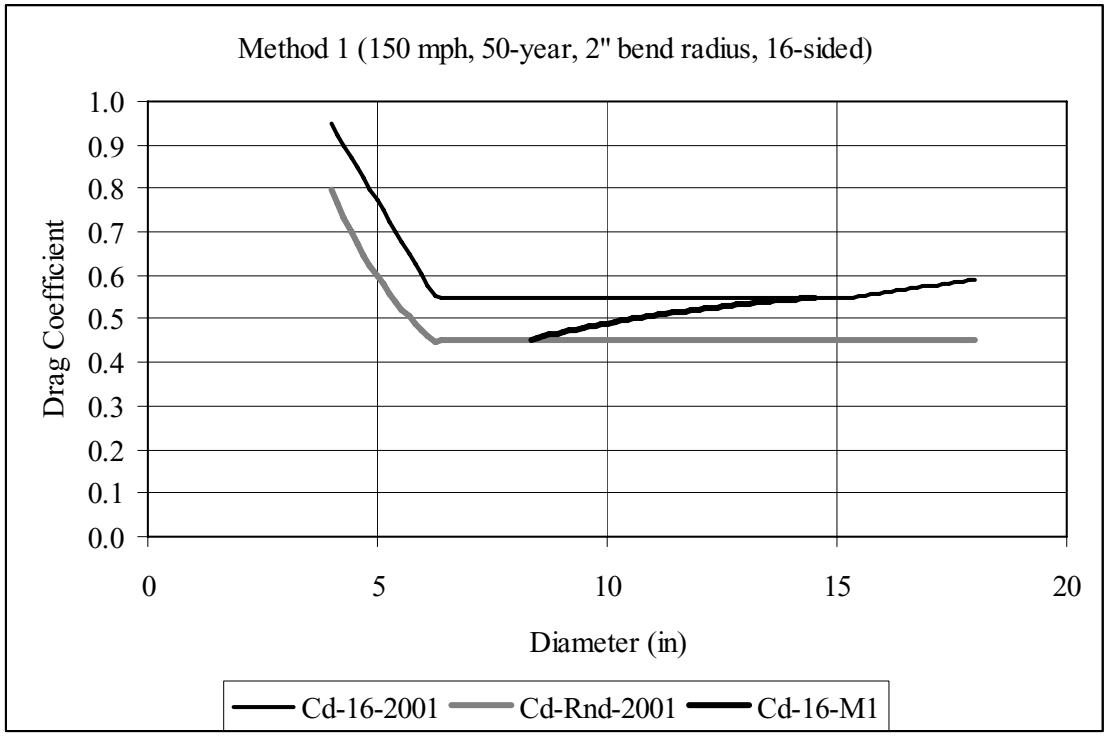

Figure D–56. Drag Coefficient Comparison: Method No. 1, 50-year MRI, 150 mph, 2" bend radius, 16-sided

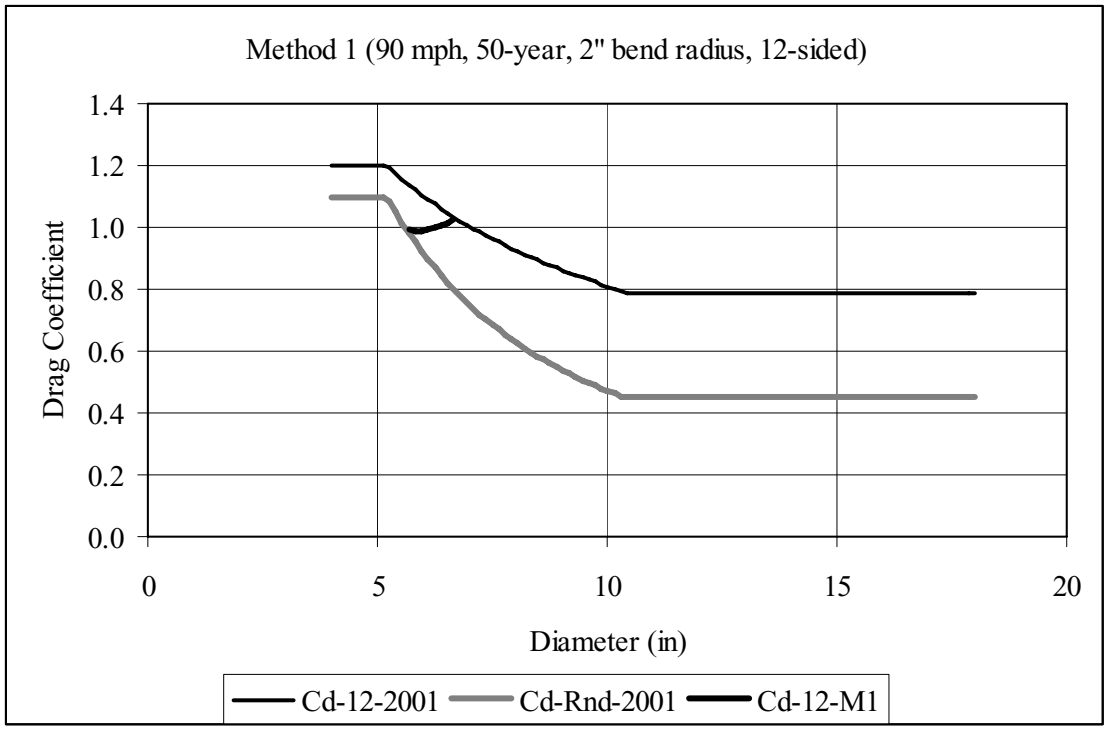

Figure D–57. Drag Coefficient Comparison: Method No. 1, 50-year MRI, 90 mph, 2” bend radius, 12-sided

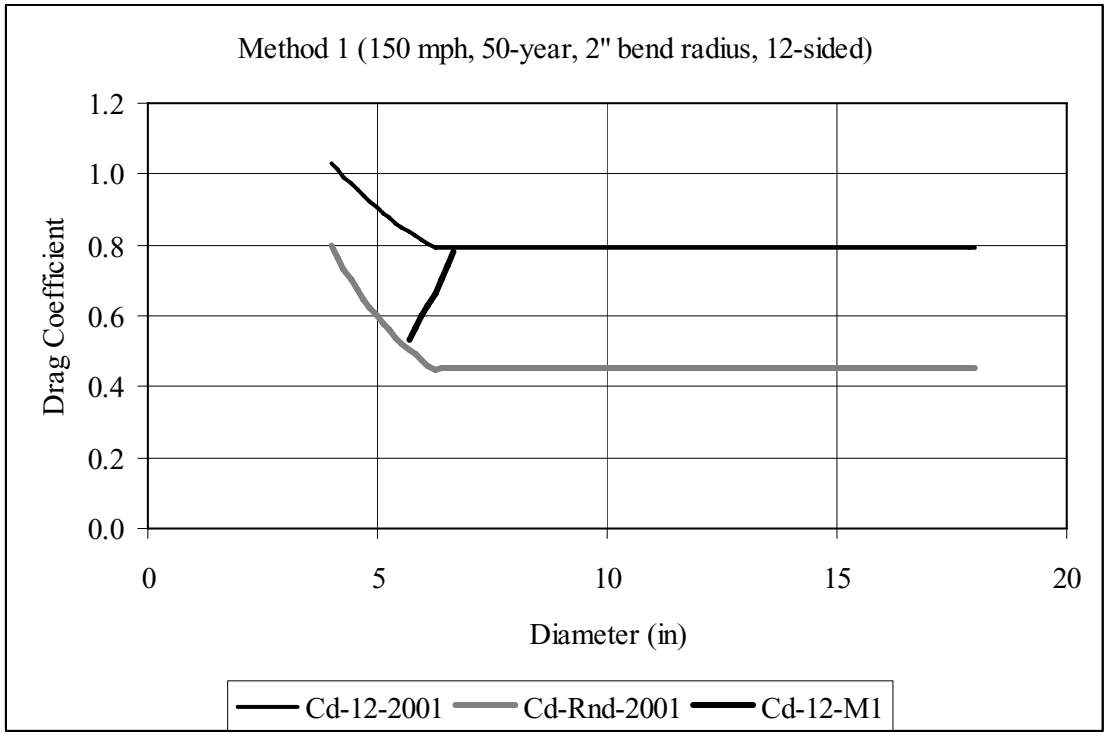

Figure D–58. Drag Coefficient Comparison: Method No. 1, 50-year MRI, 150 mph, 2” bend radius, 12-sided

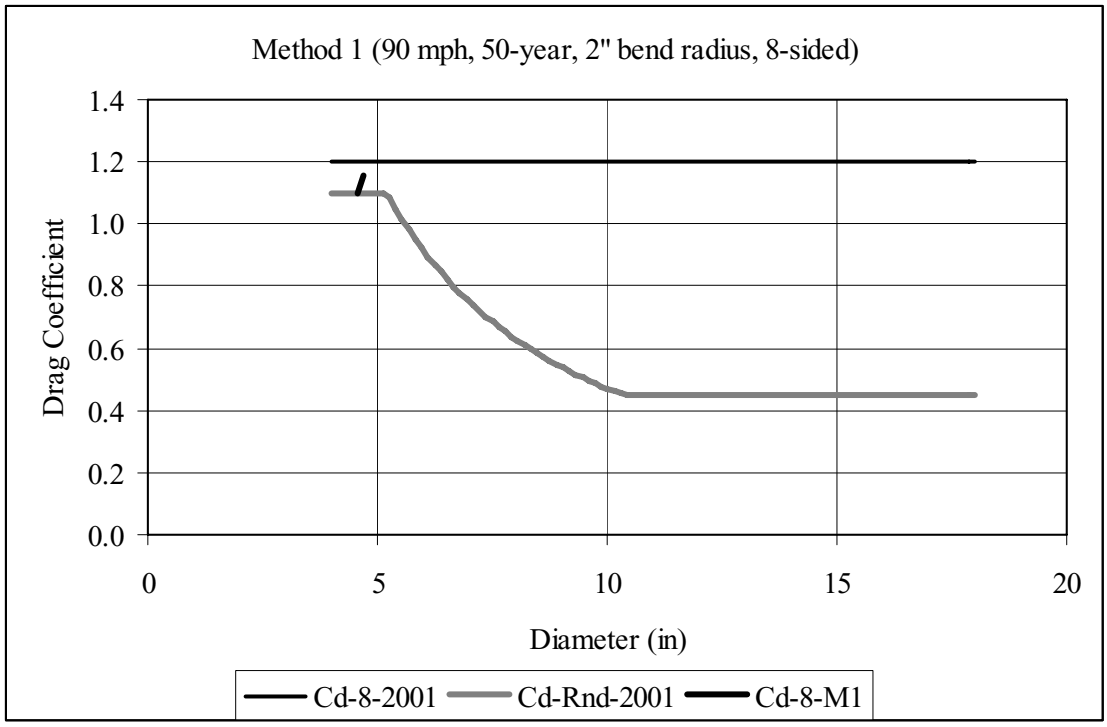

Figure D–59. Drag Coefficient Comparison: Method No. 1, 50-year MRI, 90 mph, 2" bend radius, 8-sided

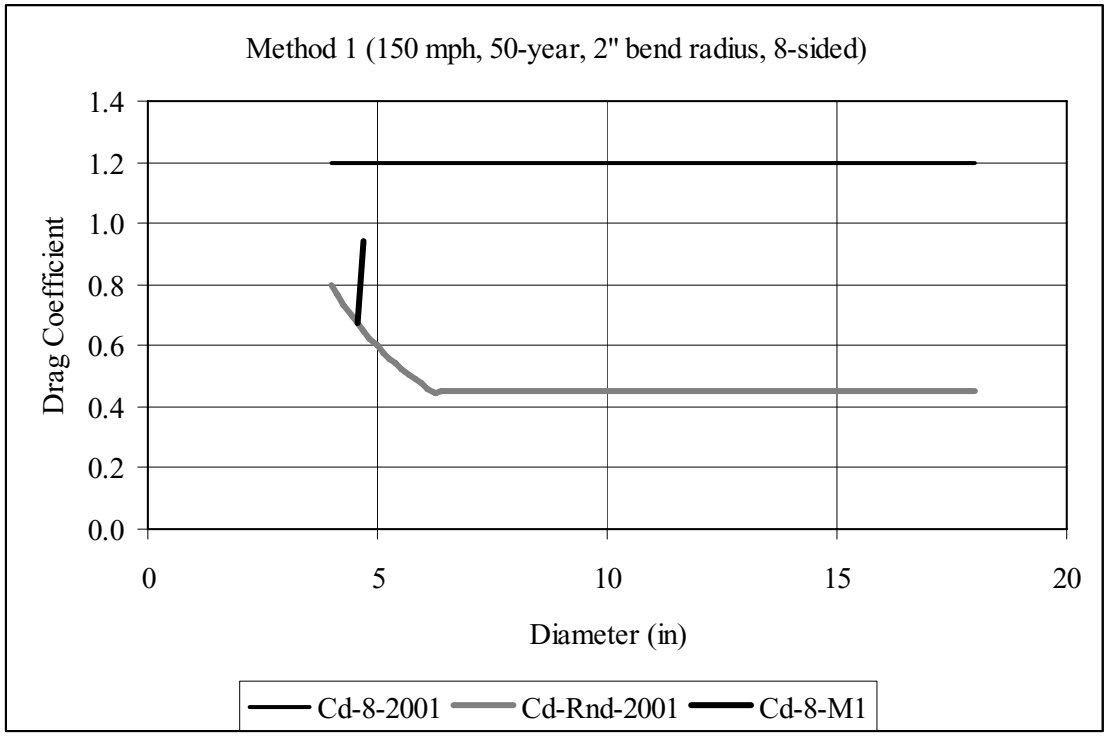

Figure D–60. Drag Coefficient Comparison: Method No. 1, 50-year MRI, 150 mph, 2" bend radius, 8-sided

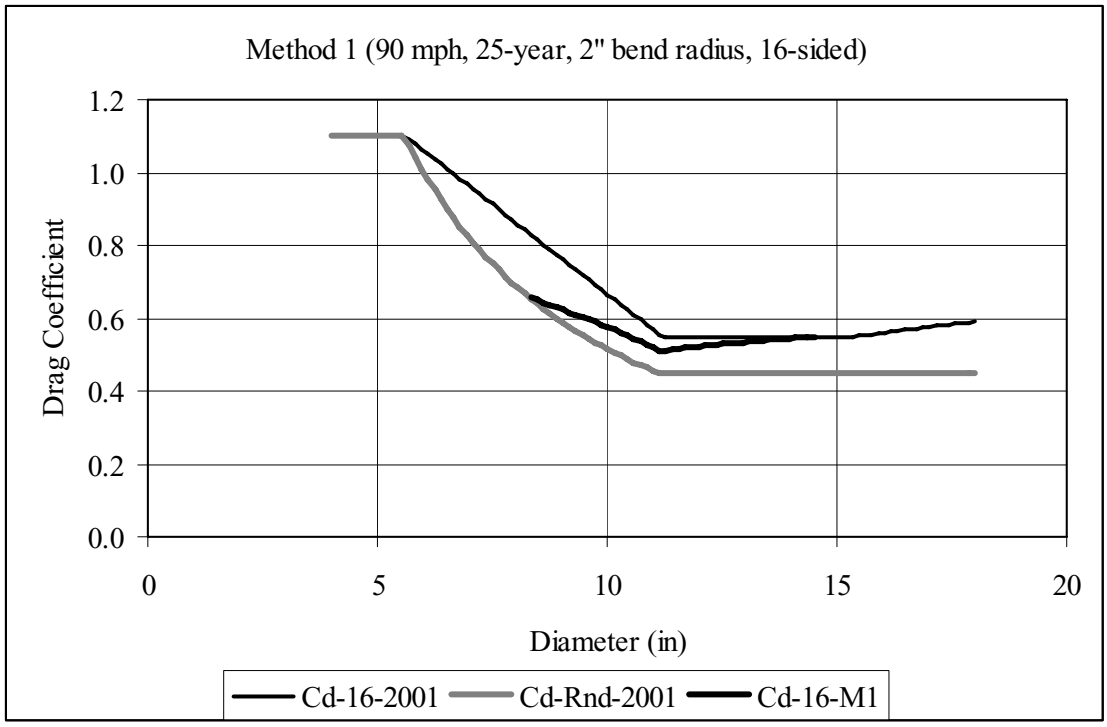

Figure D–61. Drag Coefficient Comparison: Method No. 1, 25-year MRI, 90 mph, 2" bend radius, 16-sided

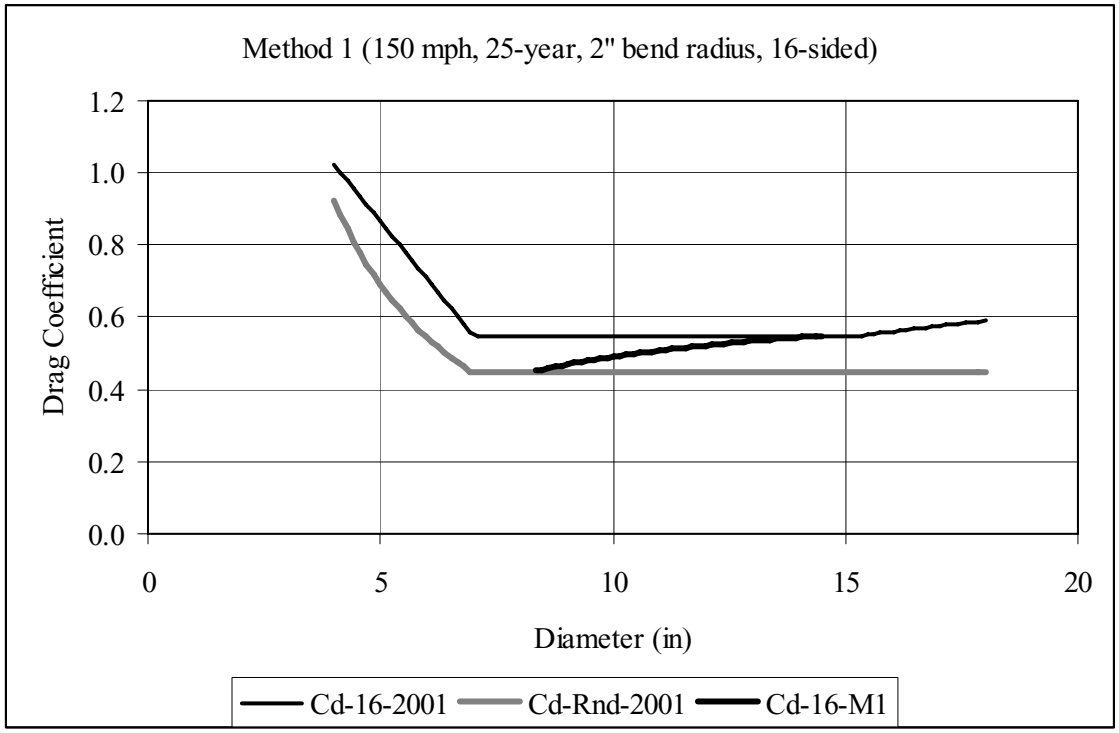

Figure D–62. Drag Coefficient Comparison: Method No. 1, 25-year MRI, 150 mph, 2" bend radius, 16-sided

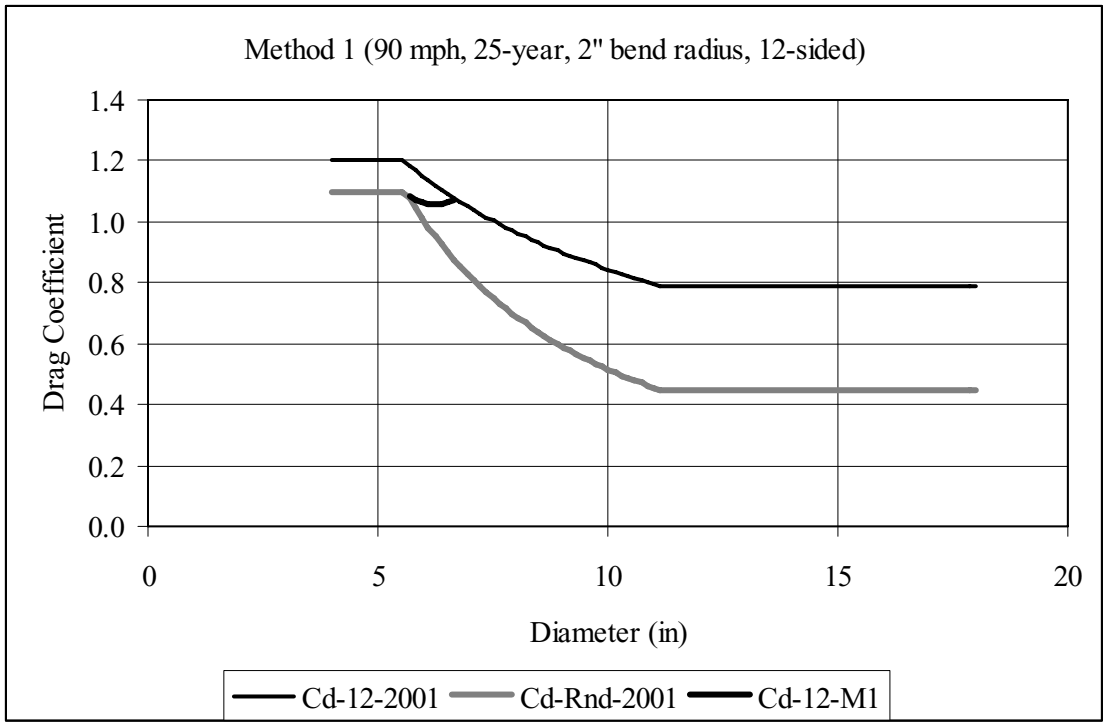

Figure D–63. Drag Coefficient Comparison: Method No. 1, 25-year MRI, 90 mph, 2” bend radius, 12-sided

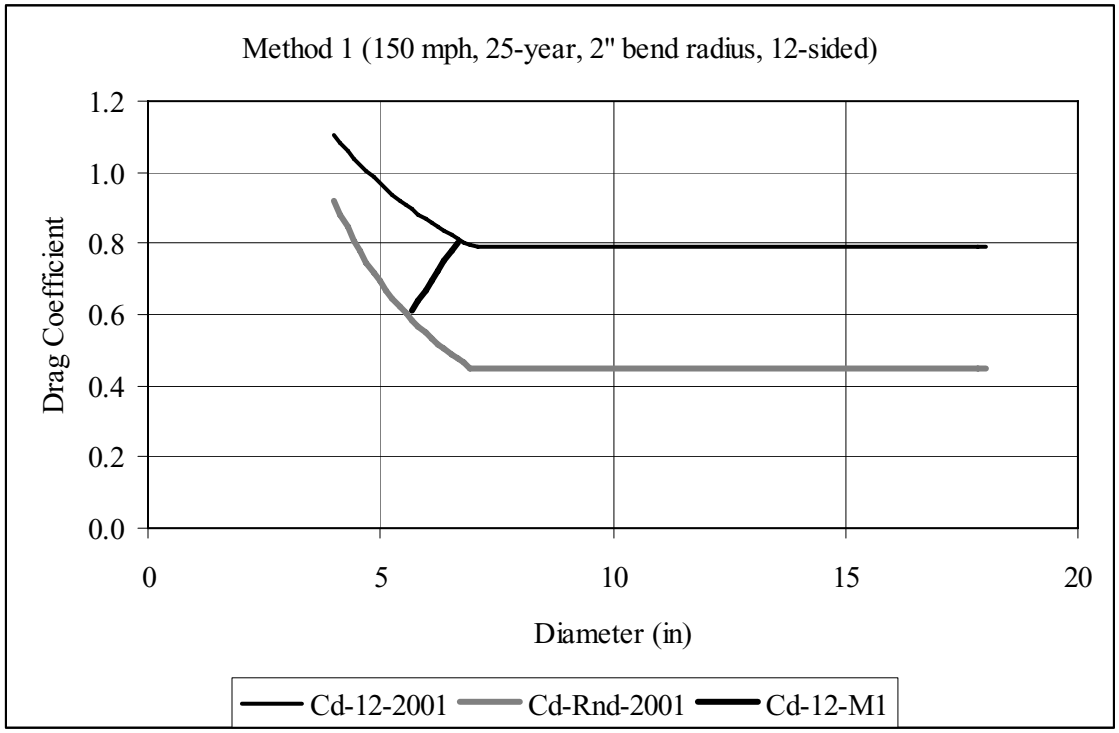

Figure D–64. Drag Coefficient Comparison: Method No. 1, 25-year MRI, 150 mph, 2” bend radius, 12-sided

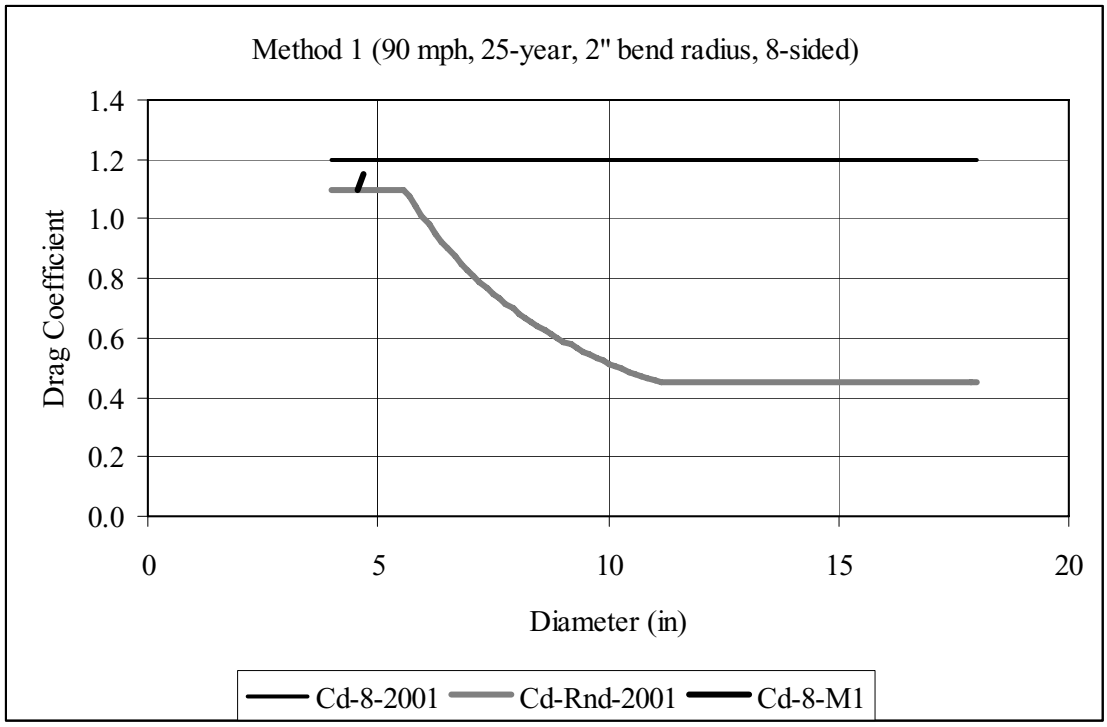

Figure D–65. Drag Coefficient Comparison: Method No. 1, 25-year MRI, 90 mph, 2” bend radius, 8-sided

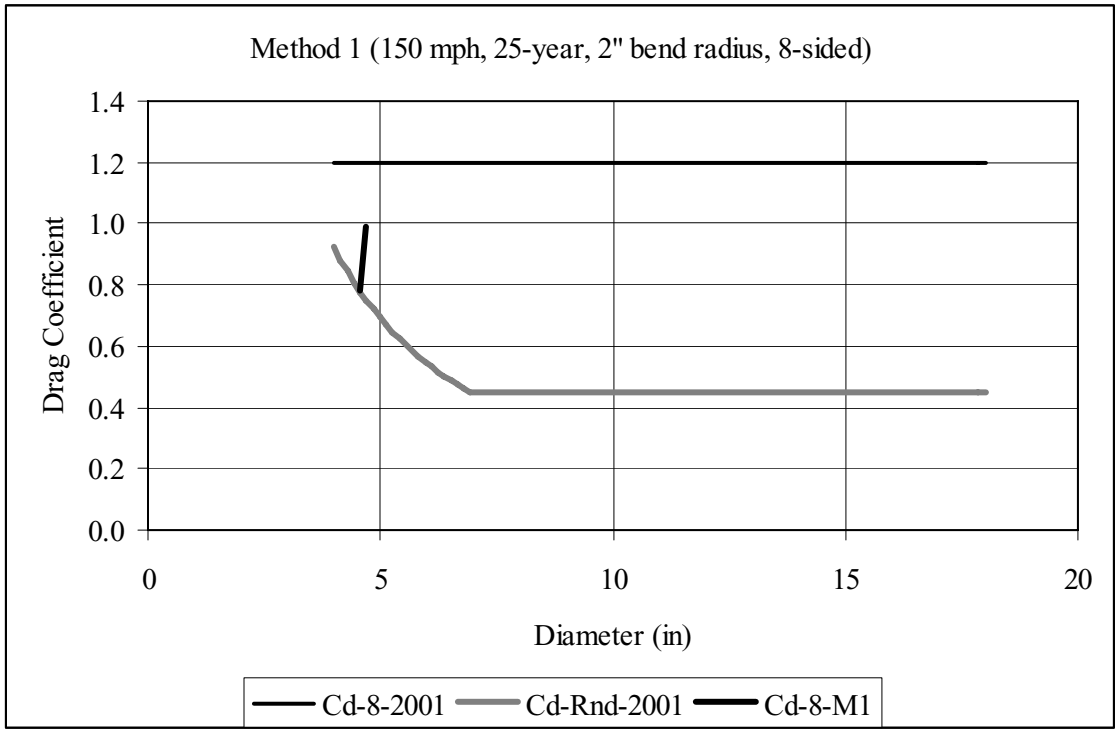

Figure D–66. Drag Coefficient Comparison: Method No. 1, 25-year MRI, 150 mph, 2” bend radius, 8-sided

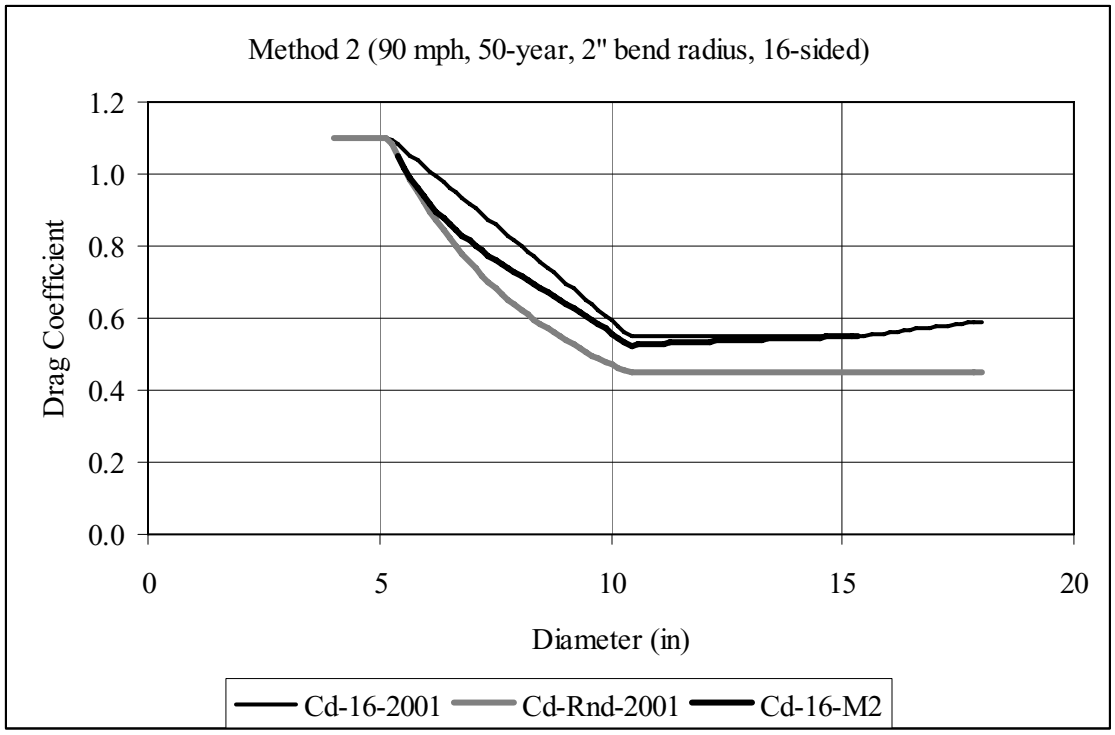

Figure D–67. Drag Coefficient Comparison: Method No. 2, 50-year MRI, 90 mph, 2” bend radius, 16-sided

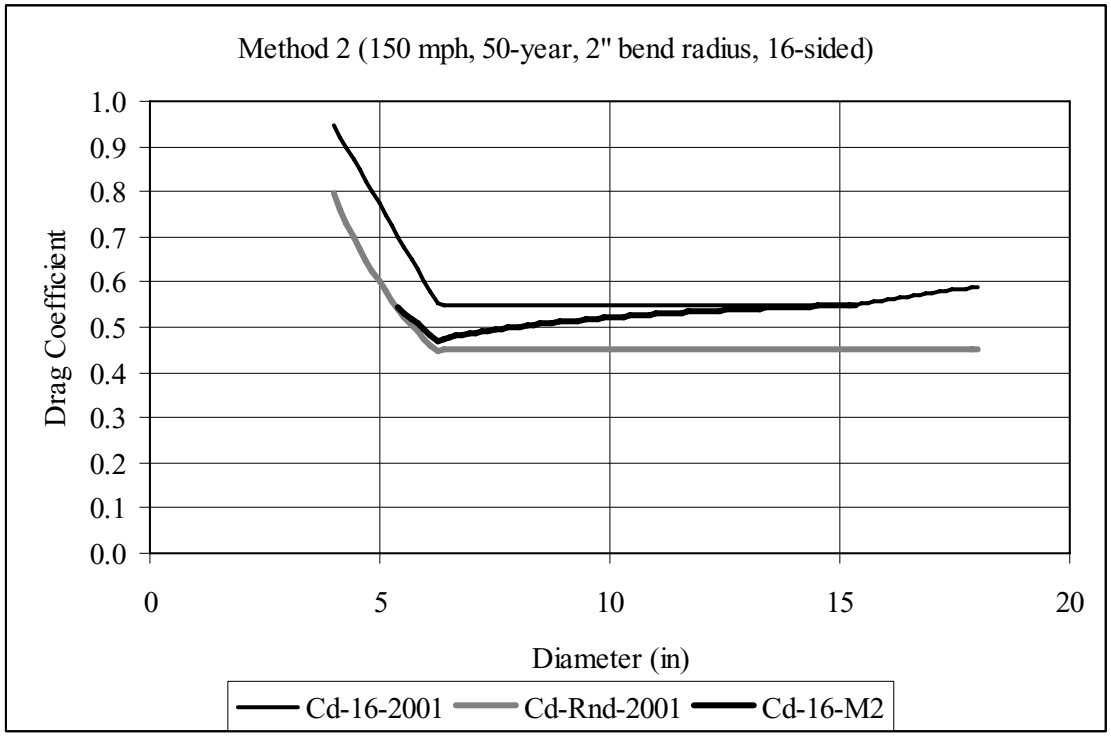

Figure D–68. Drag Coefficient Comparison: Method No. 2, 50-year MRI, 150 mph, 2” bend radius, 16-sided

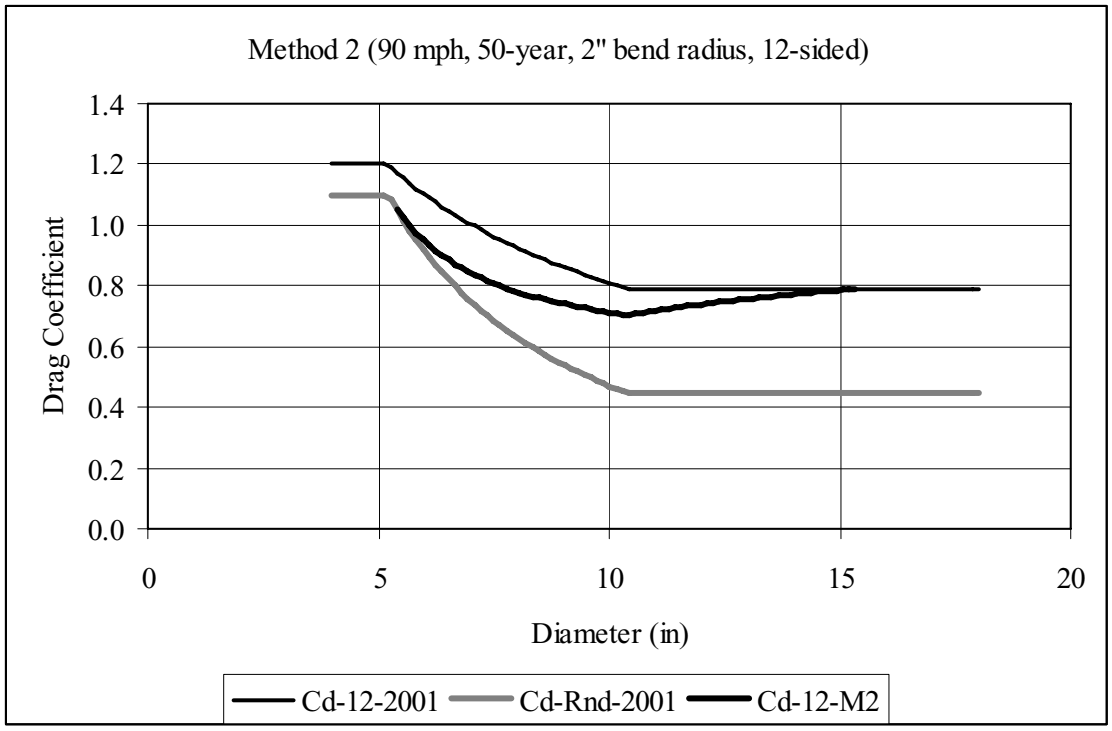

Figure D–69. Drag Coefficient Comparison: Method No. 2, 50-year MRI, 90 mph, 2” bend radius, 12-sided

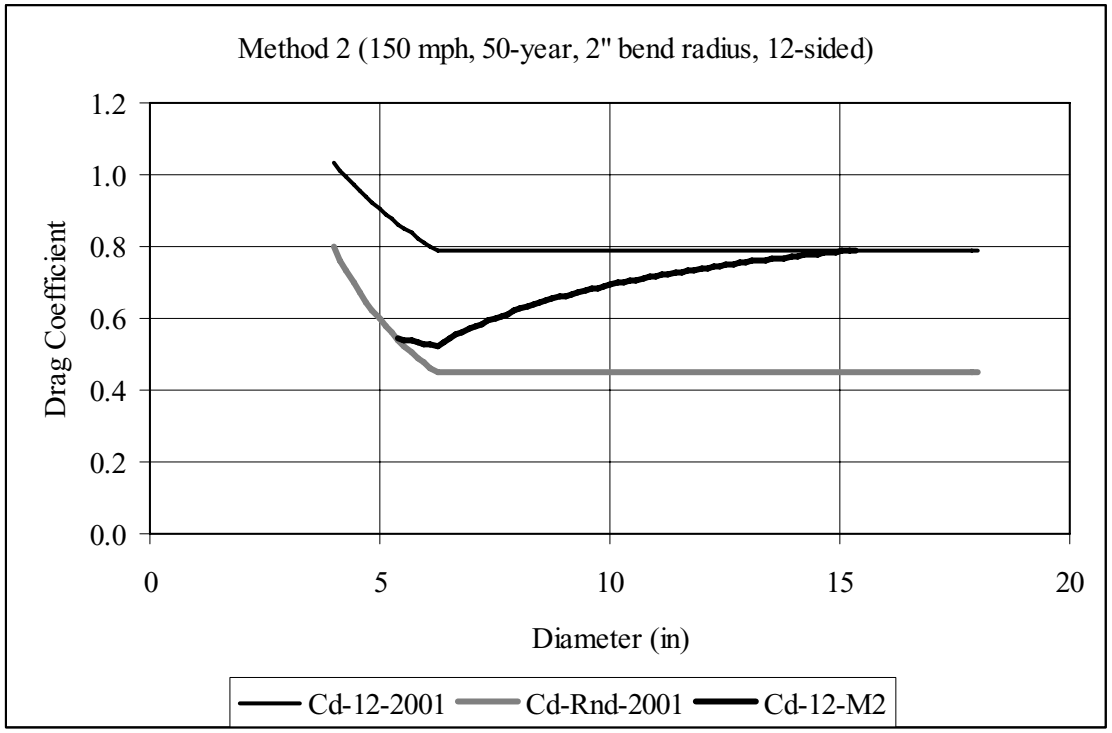

Figure D–70. Drag Coefficient Comparison: Method No. 2, 50-year MRI, 150 mph, 2” bend radius, 12-sided

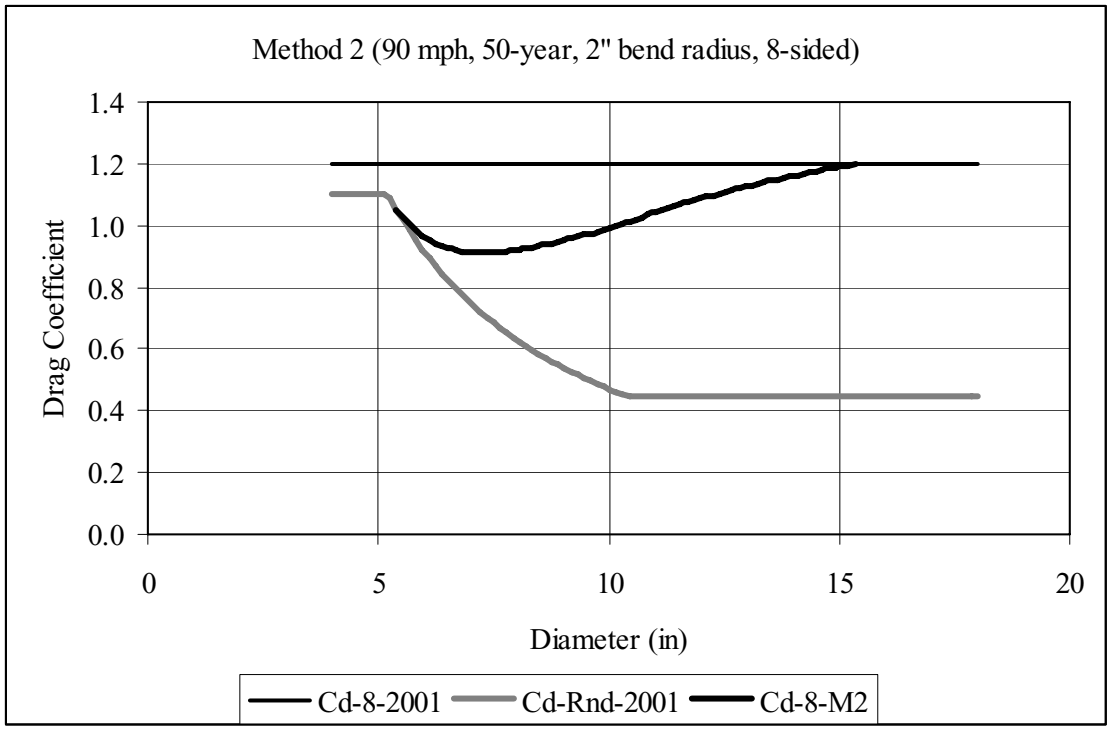

Figure D–71. Drag Coefficient Comparison: Method No. 2, 50-year MRI, 90 mph, 2” bend radius, 8-sided

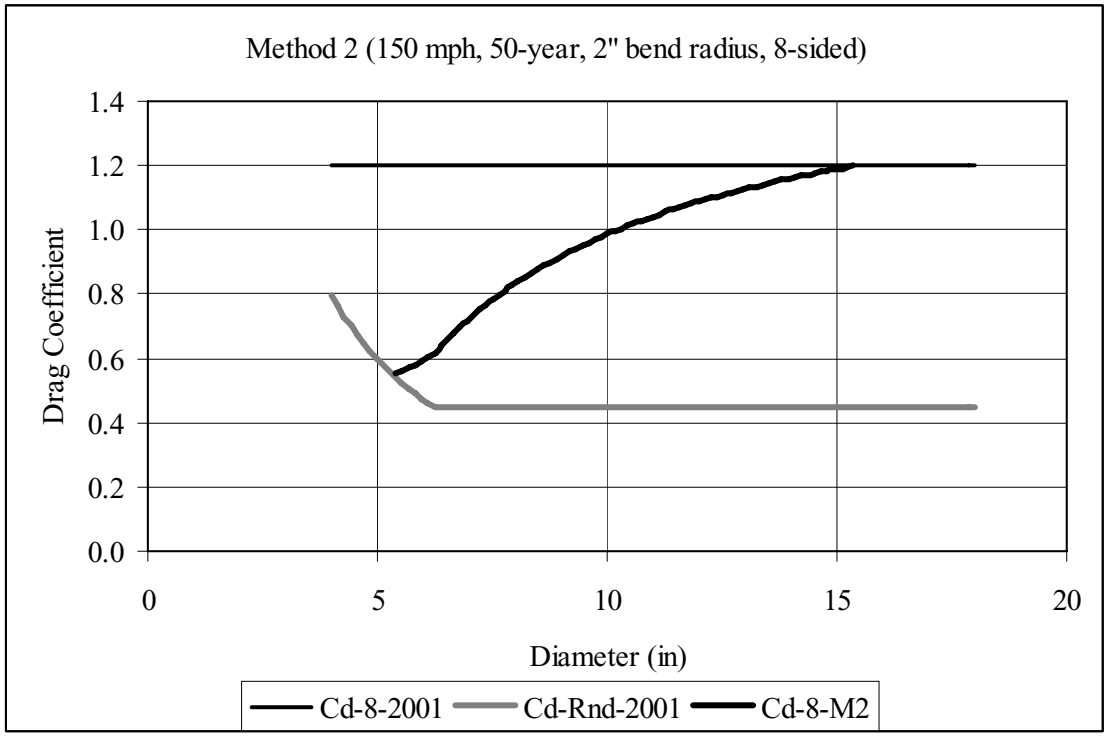

Figure D–72. Drag Coefficient Comparison: Method No. 2, 50-year MRI, 150 mph, 2” bend radius, 8-sided

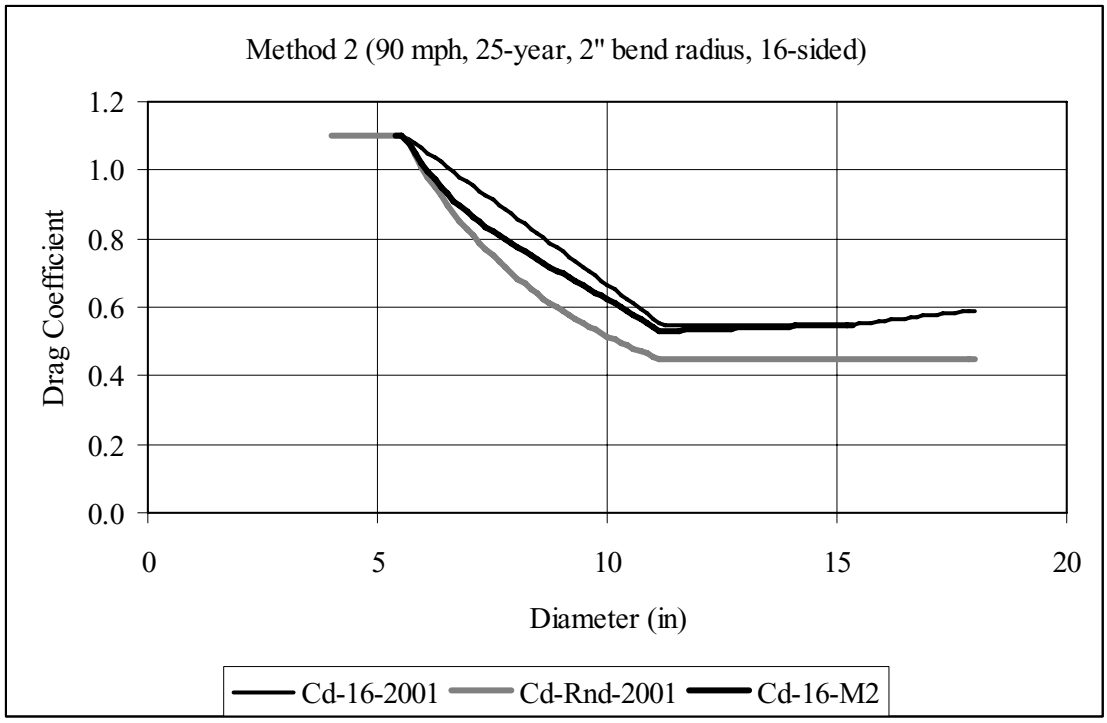

Figure D–73. Drag Coefficient Comparison: Method No. 2, 25-year MRI, 90 mph, 2” bend radius, 16-sided

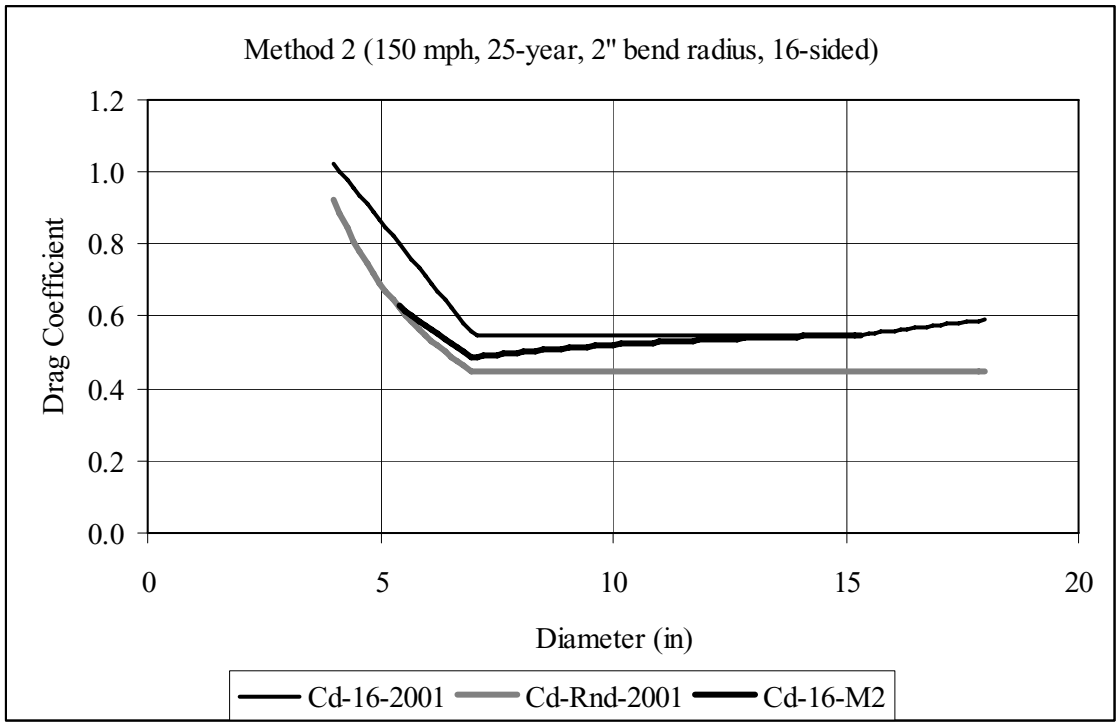

Figure D–74. Drag Coefficient Comparison: Method No. 2, 25-year MRI, 150 mph, 2” bend radius, 16-sided

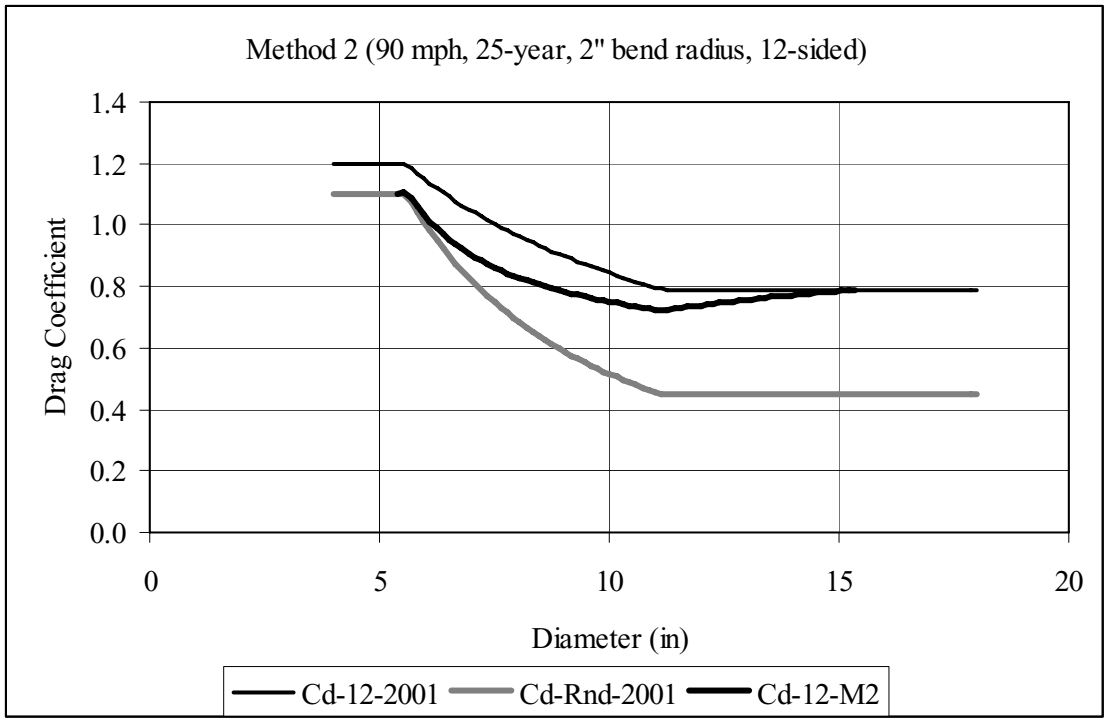

Figure D–75. Drag Coefficient Comparison: Method No. 2, 25-year MRI, 90 mph, 2” bend radius, 12-sided

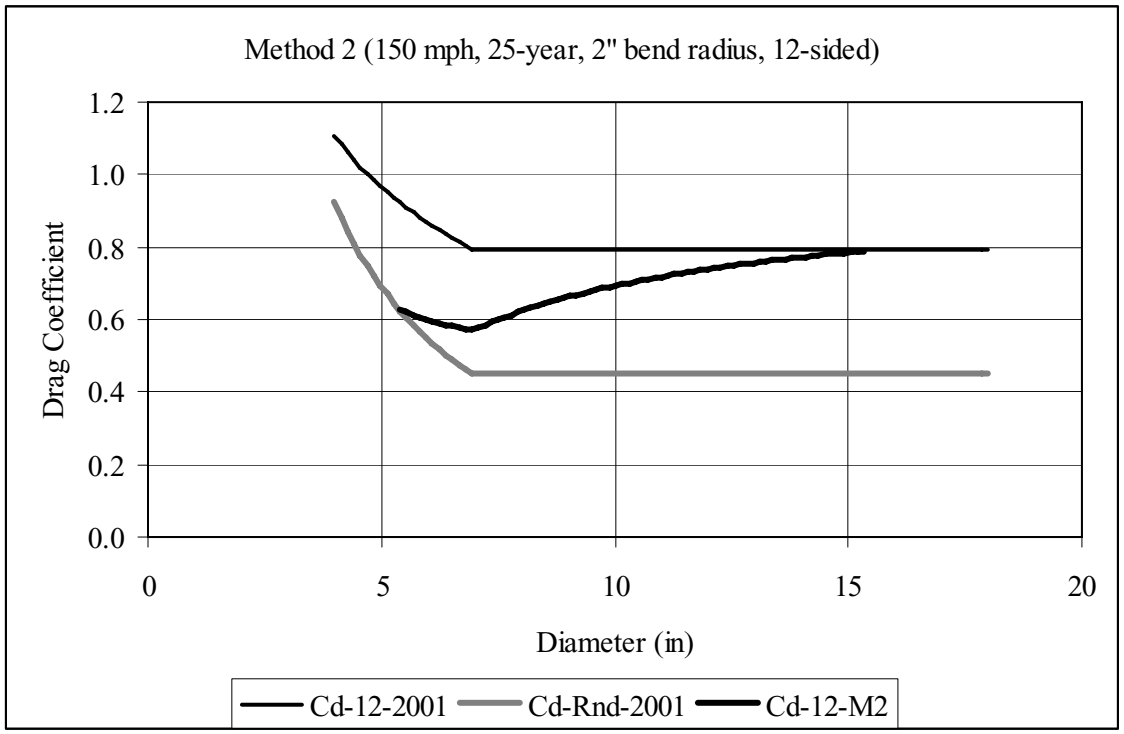

Figure D–76. Drag Coefficient Comparison: Method No. 2, 25-year MRI, 150 mph, 2” bend radius, 12-sided

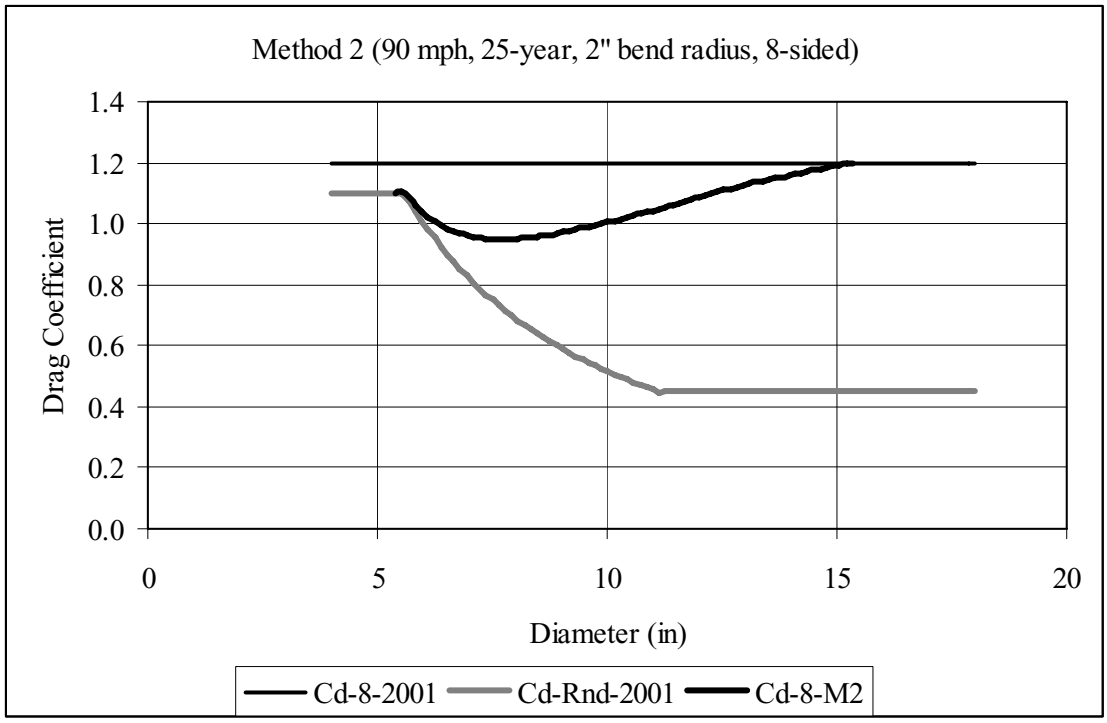

Figure D–77. Drag Coefficient Comparison: Method No. 2, 25-year MRI, 90 mph, 2” bend radius, 8-sided

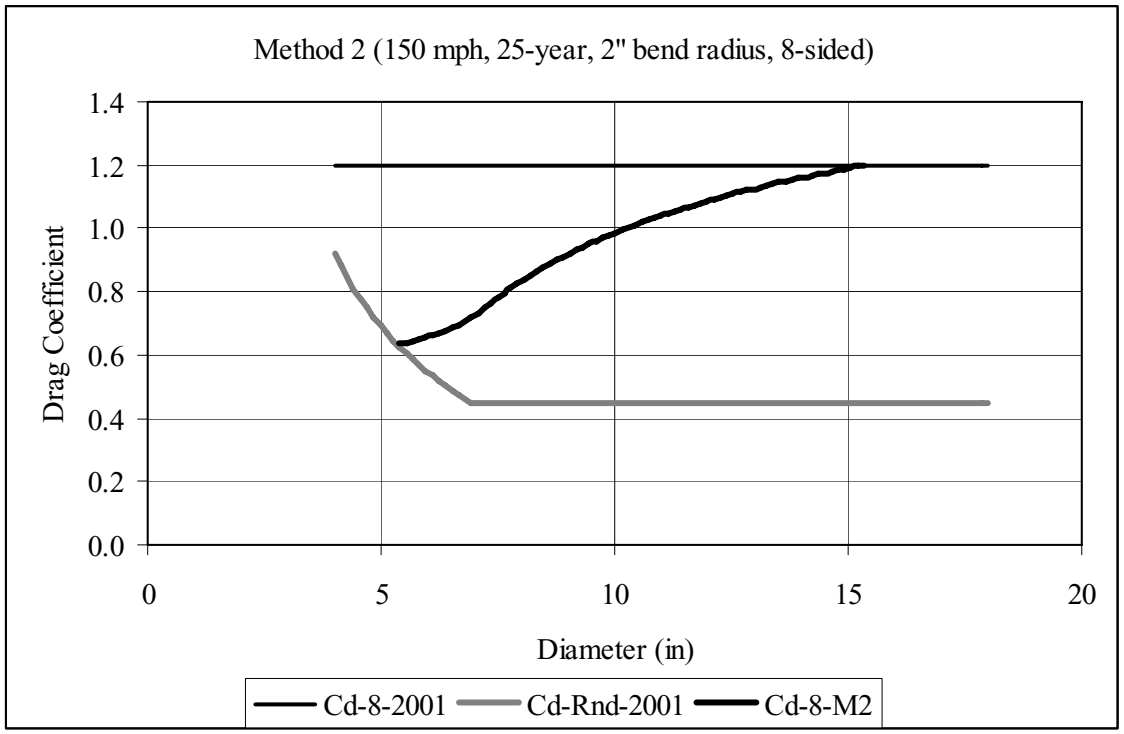

Figure D–78. Drag Coefficient Comparison: Method No. 2, 25-year MRI, 150 mph, 2” bend radius, 8-sided

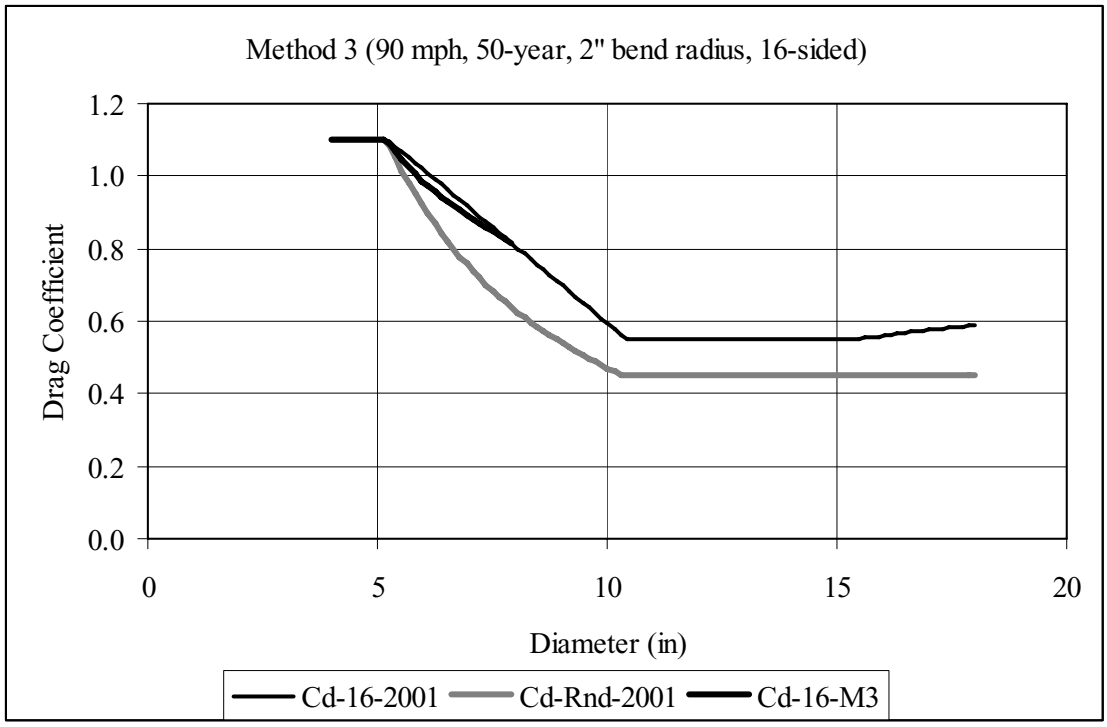

Figure D–79. Drag Coefficient Comparison: Method No. 3, 50-year MRI, 90 mph, 2" bend radius, 16-sided

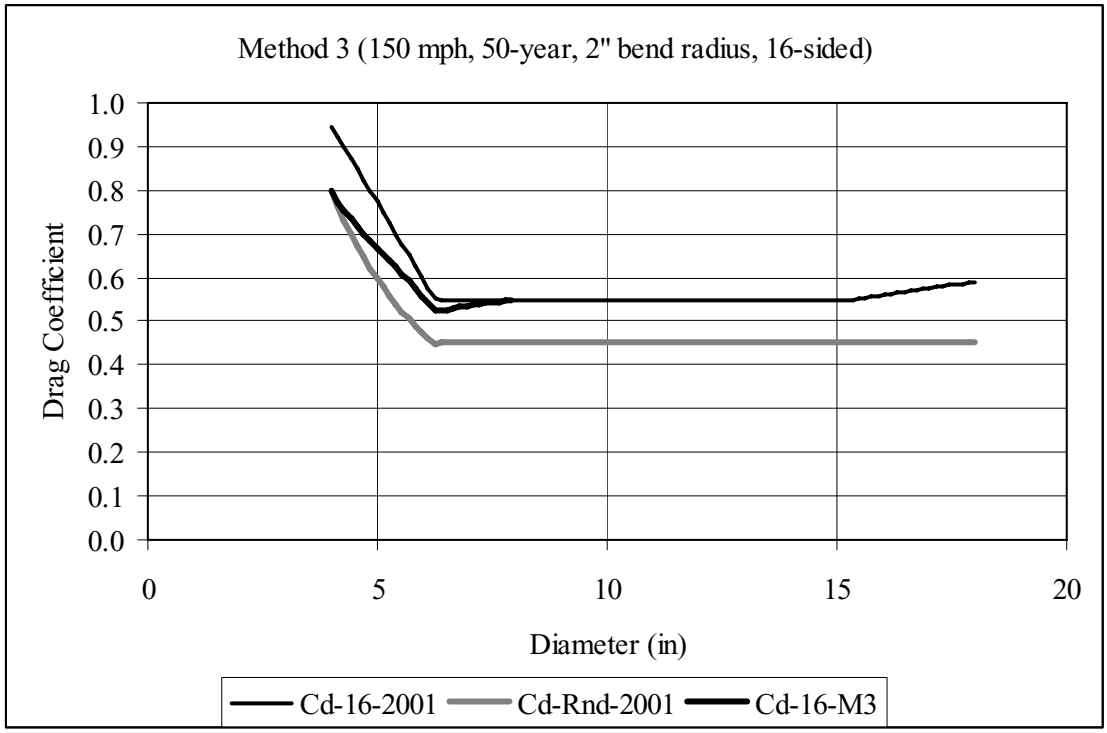

Figure D–80. Drag Coefficient Comparison: Method No. 3, 50-year MRI, 150 mph, 2" bend radius, 16-sided

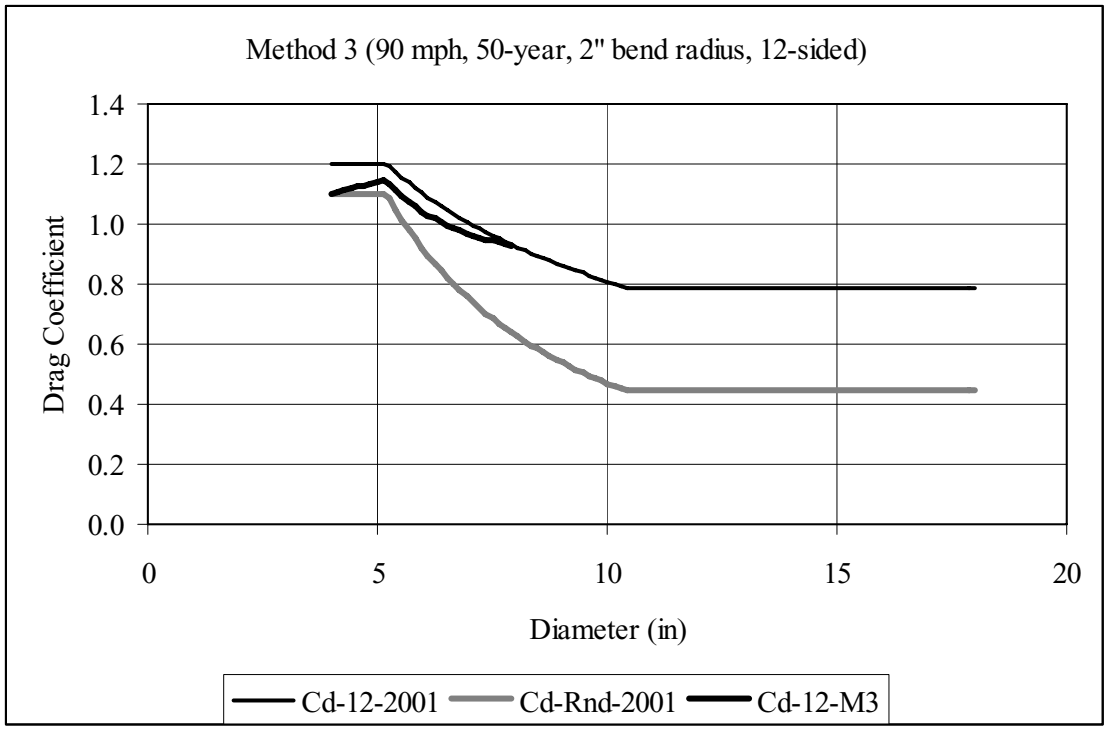

Figure D–81. Drag Coefficient Comparison: Method No. 3, 50-year MRI, 90 mph, 2” bend radius, 12-sided

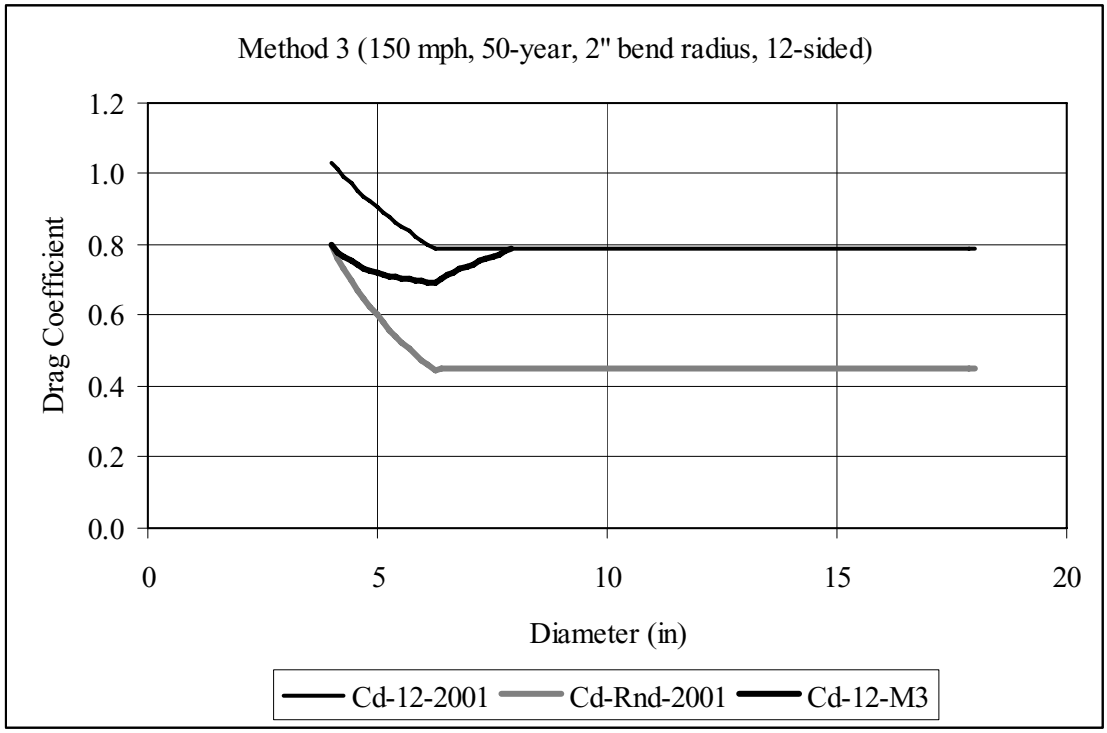

Figure D–82. Drag Coefficient Comparison: Method No. 3, 50-year MRI, 150 mph, 2” bend radius, 12-sided

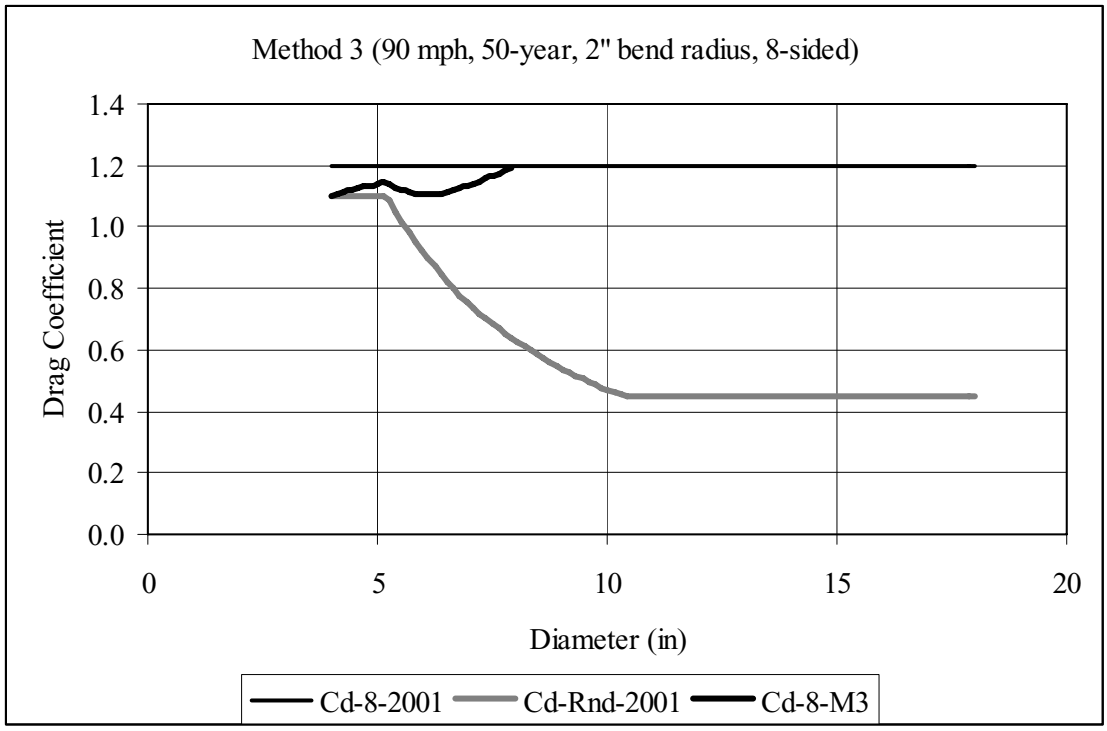

Figure D–83. Drag Coefficient Comparison: Method No. 3, 50-year MRI, 90 mph, 2” bend radius, 8-sided

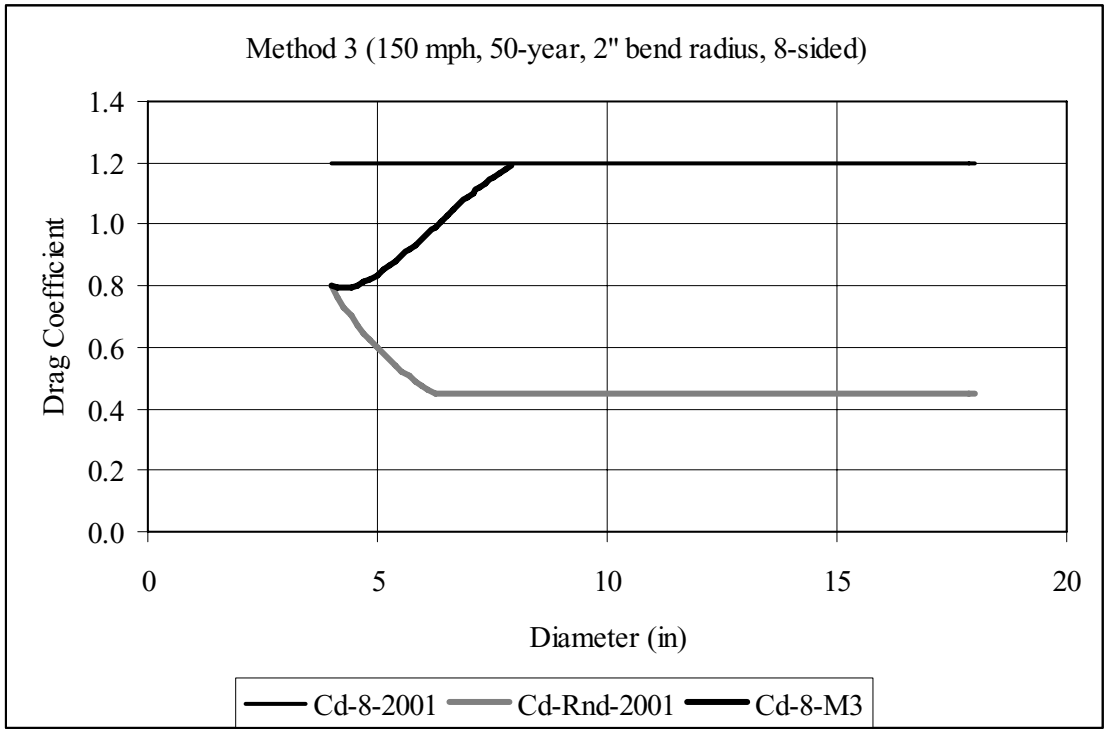

Figure D–84. Drag Coefficient Comparison: Method No. 3, 50-year MRI, 150 mph, 2” bend radius, 8-sided

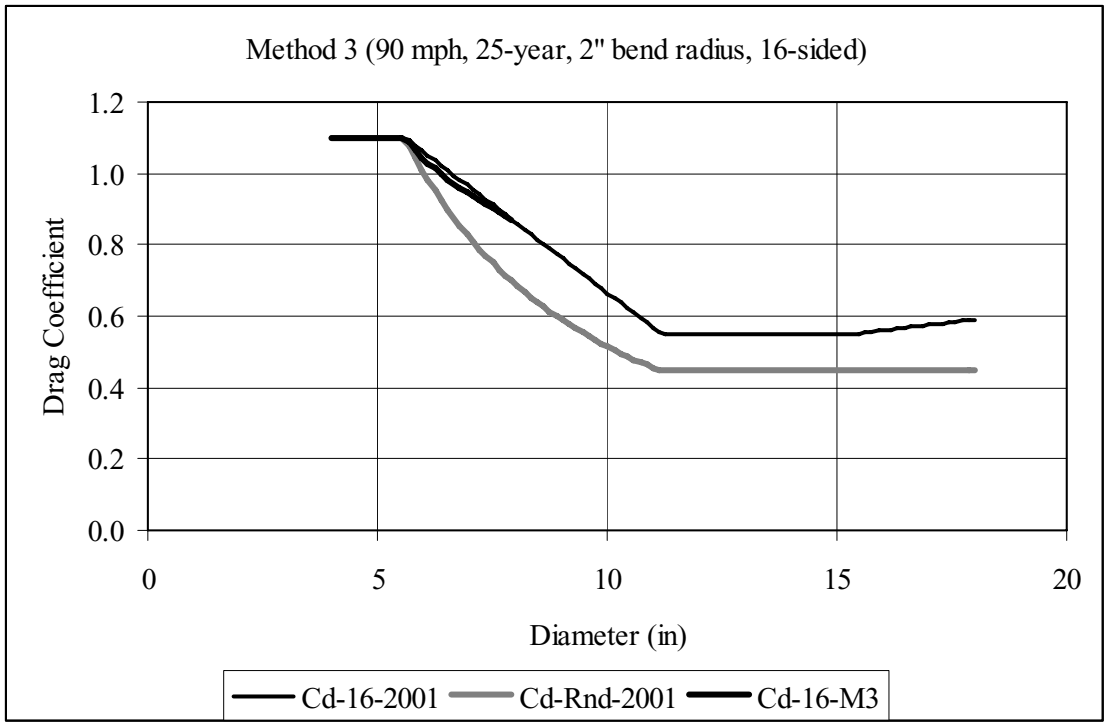

Figure D–85. Drag Coefficient Comparison: Method No. 3, 25-year MRI, 90 mph, 2" bend radius, 16-sided

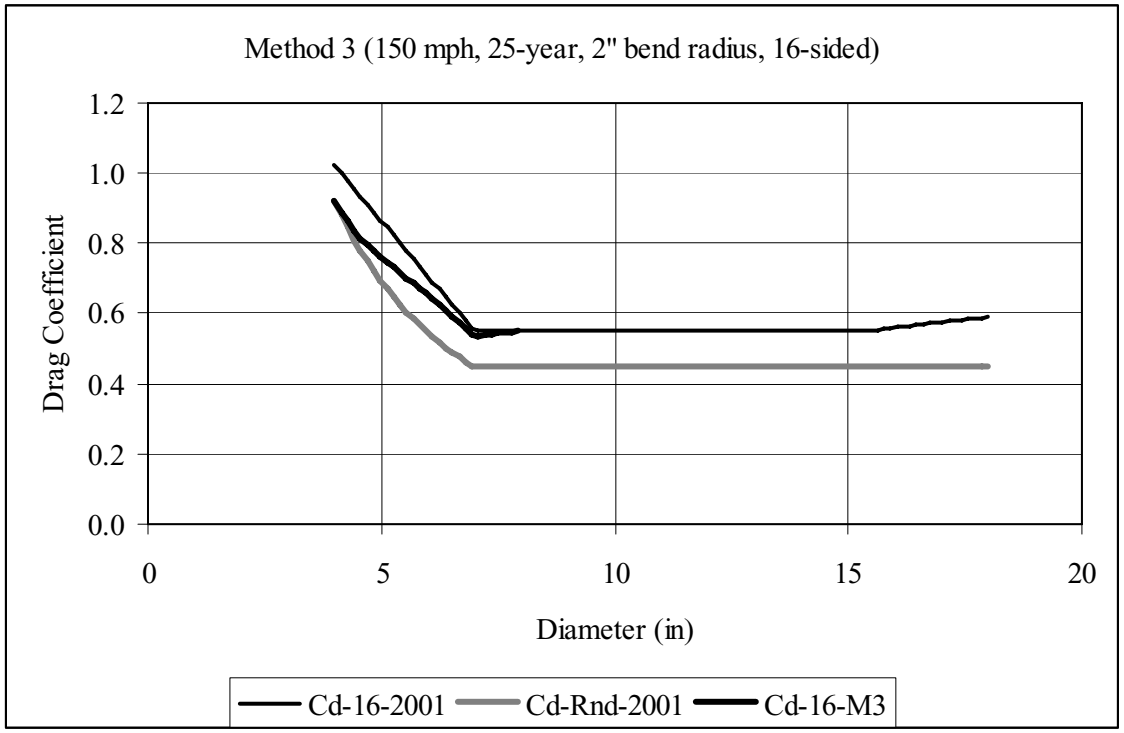

Figure D–86. Drag Coefficient Comparison: Method No. 3, 25-year MRI, 150 mph, 2" bend radius, 16-sided

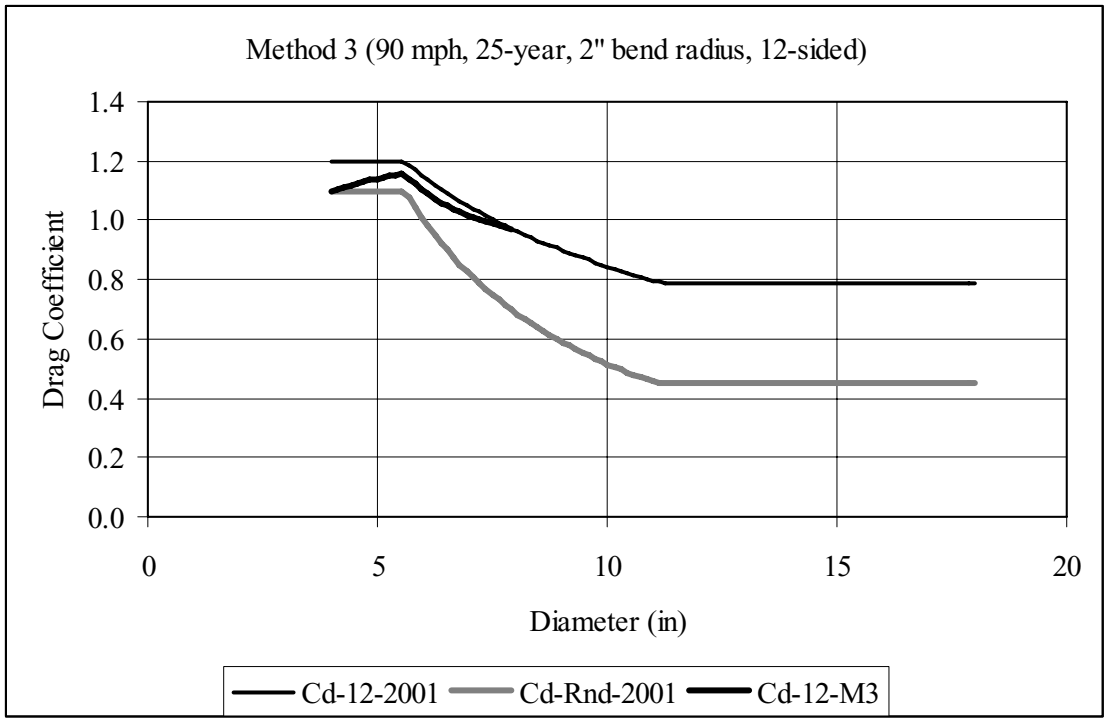

Figure D–87. Drag Coefficient Comparison: Method No. 3, 25-year MRI, 90 mph, 2" bend radius, 12-sided

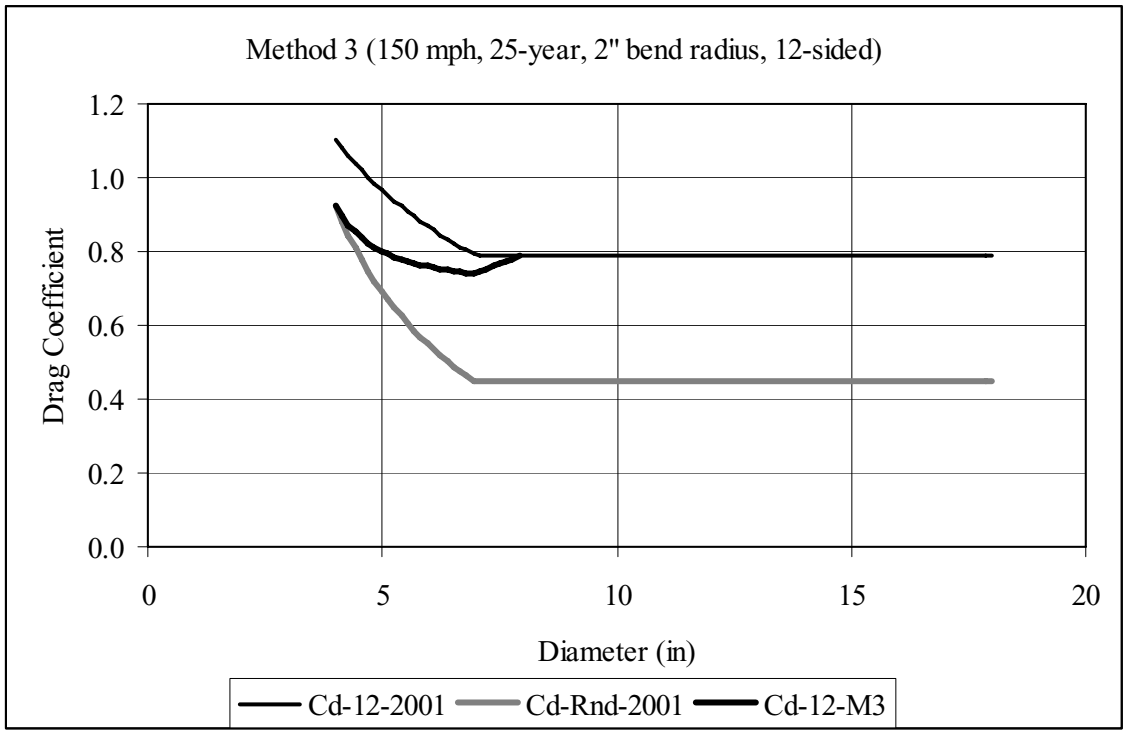

Figure D–88. Drag Coefficient Comparison: Method No. 3, 25-year MRI, 150 mph, 2" bend radius, 12-sided

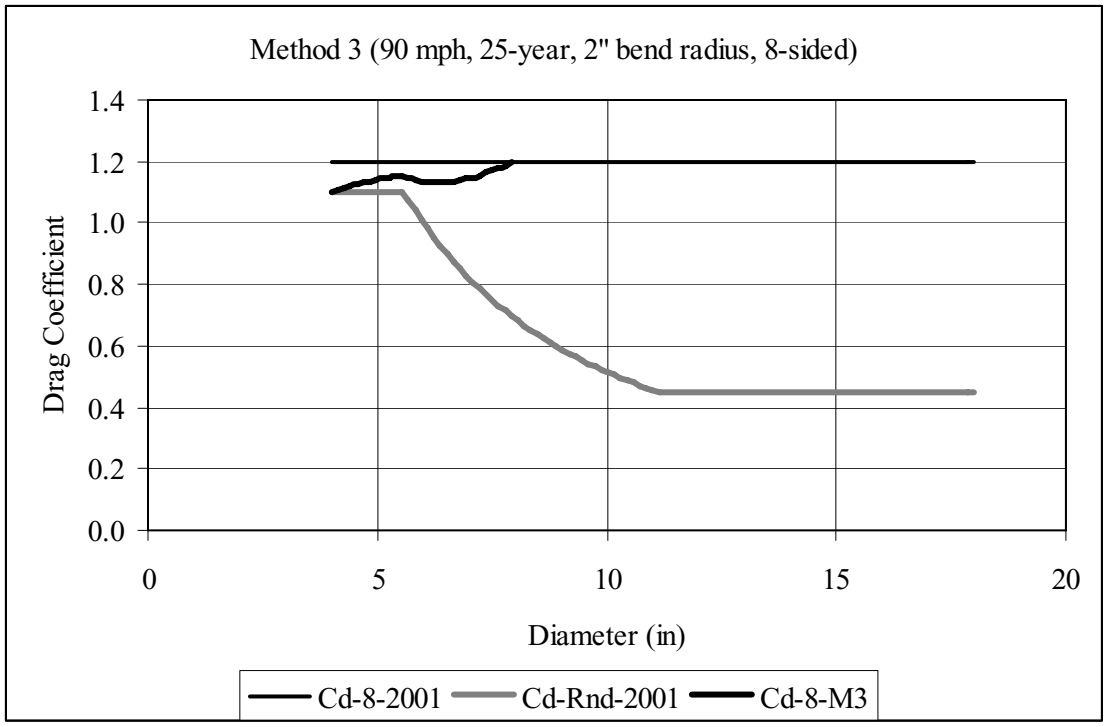

Figure D–89. Drag Coefficient Comparison: Method No. 3, 25-year MRI, 90 mph, 2” bend radius, 8-sided

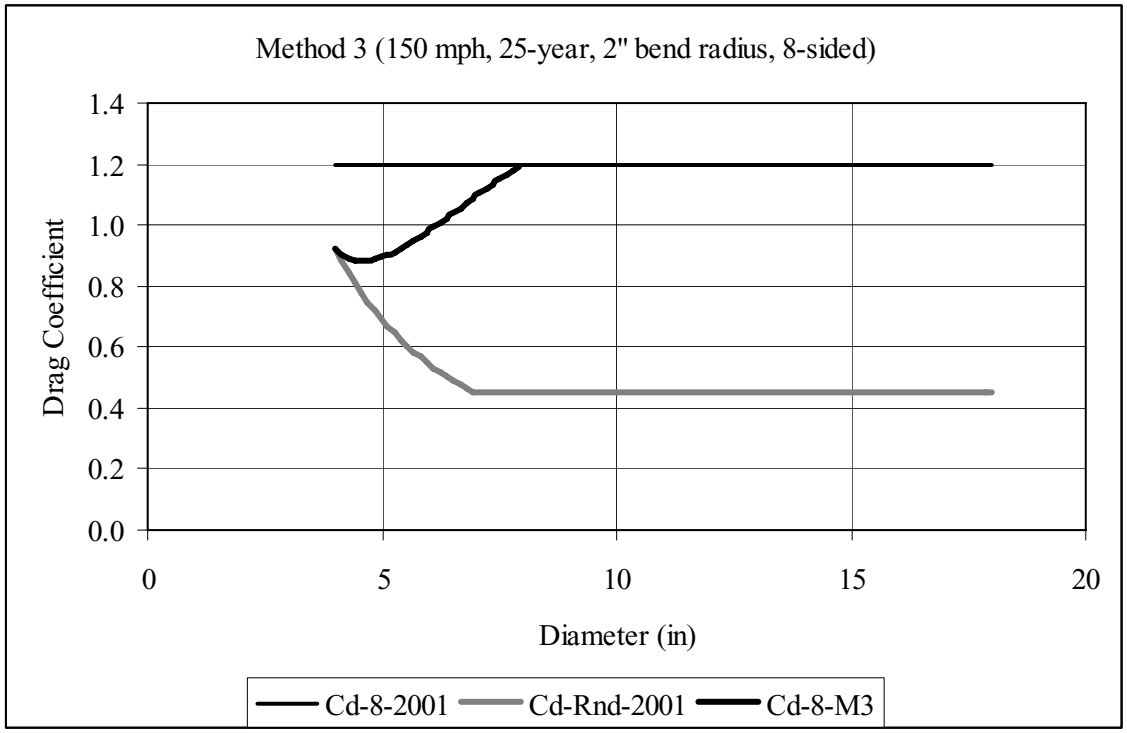

Figure D–90. Drag Coefficient Comparison: Method No. 3, 25-year MRI, 150 mph, 2” bend radius, 8-sided

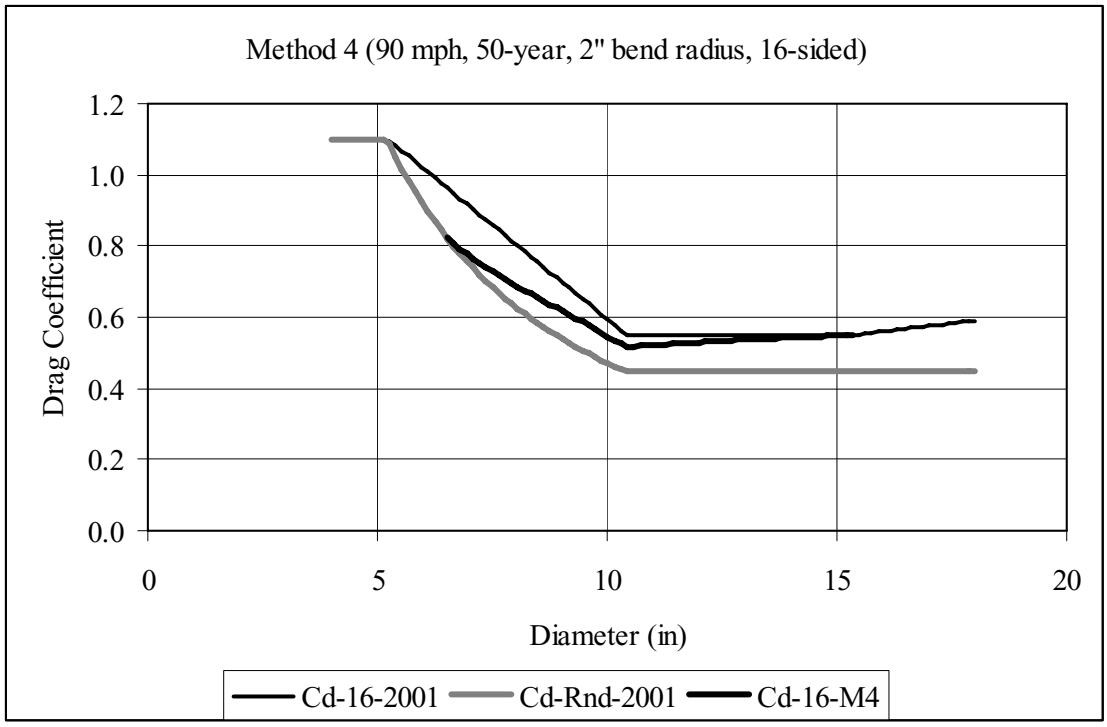

Figure D–91. Drag Coefficient Comparison: Method No. 4, 50-year MRI, 90 mph, 2" bend radius, 16-sided

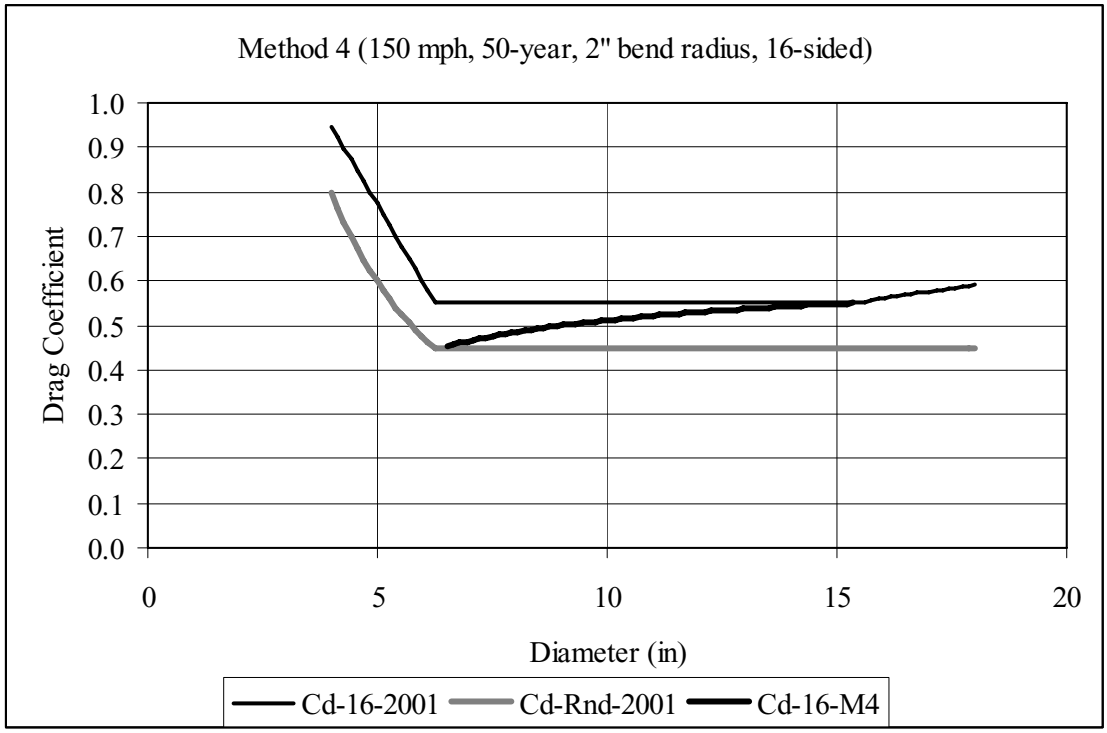

Figure D–92. Drag Coefficient Comparison: Method No. 4, 50-year MRI, 150 mph, 2" bend radius, 16-sided

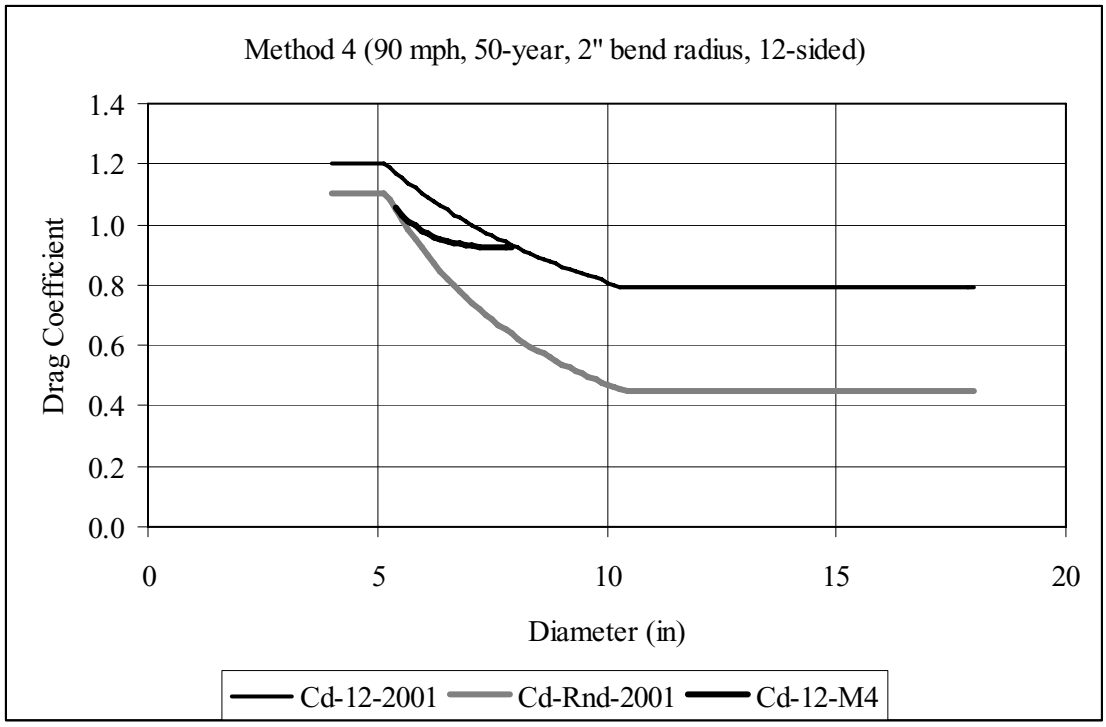

Figure D–93. Drag Coefficient Comparison: Method No. 4, 50-year MRI, 90 mph, 2” bend radius, 12-sided

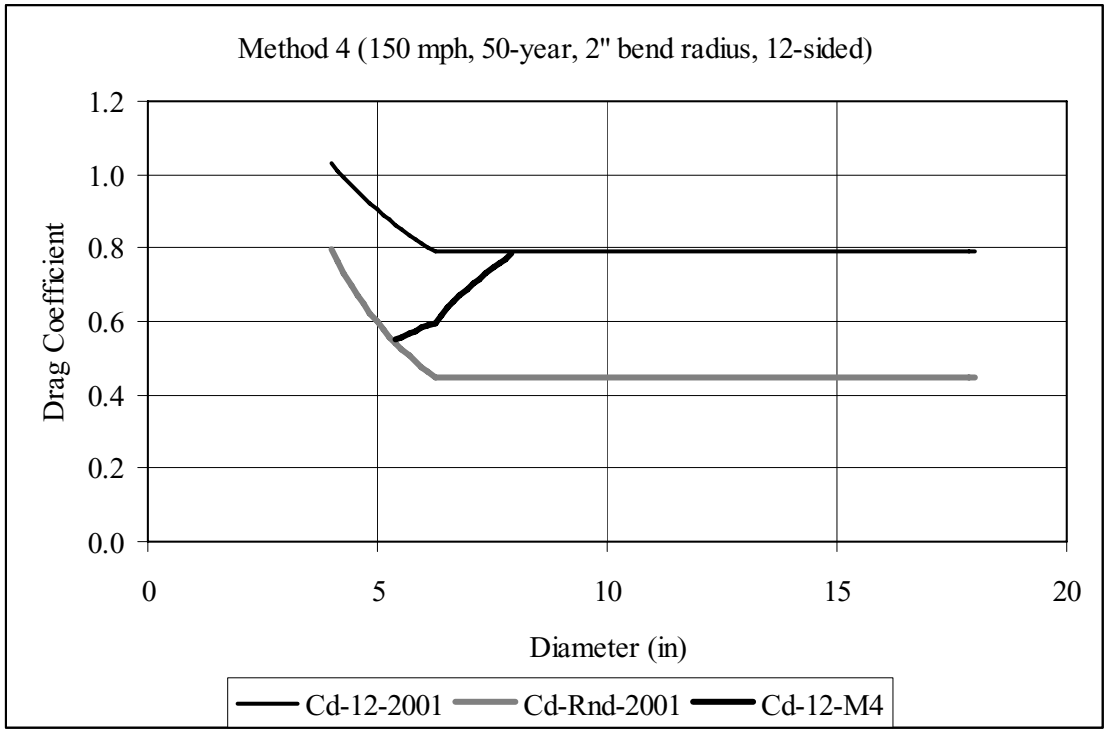

Figure D–94. Drag Coefficient Comparison: Method No. 4, 50-year MRI, 150 mph, 2” bend radius, 12-sided

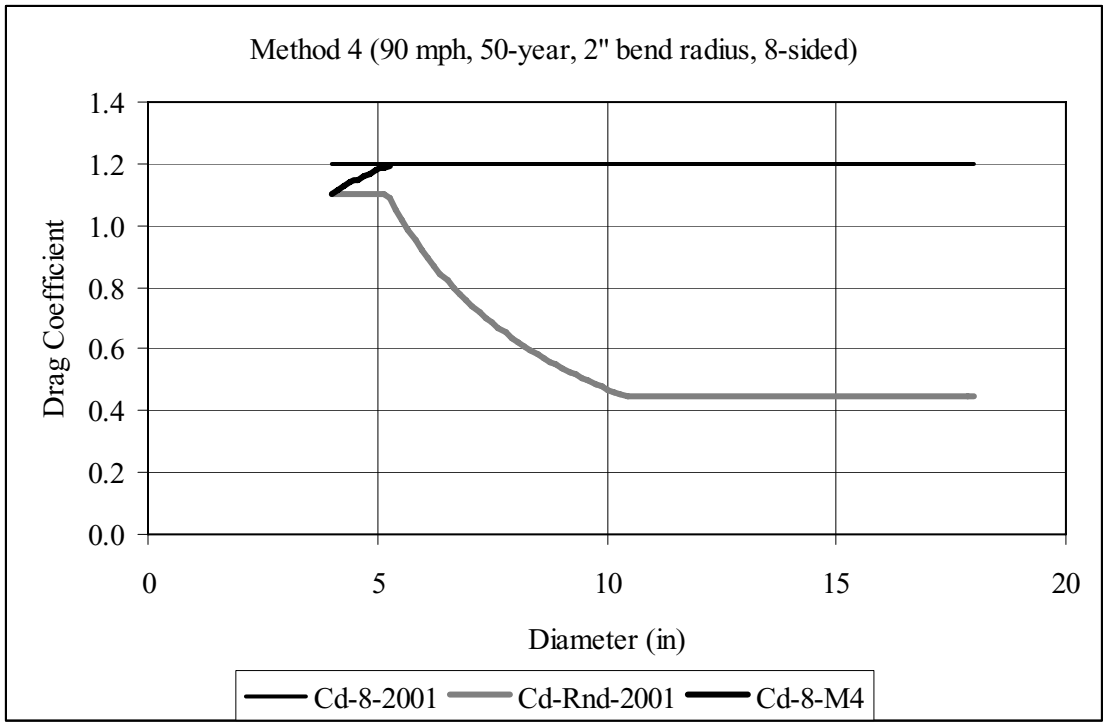

Figure D–95. Drag Coefficient Comparison: Method No. 4, 50-year MRI, 90 mph, 2” bend radius, 8-sided

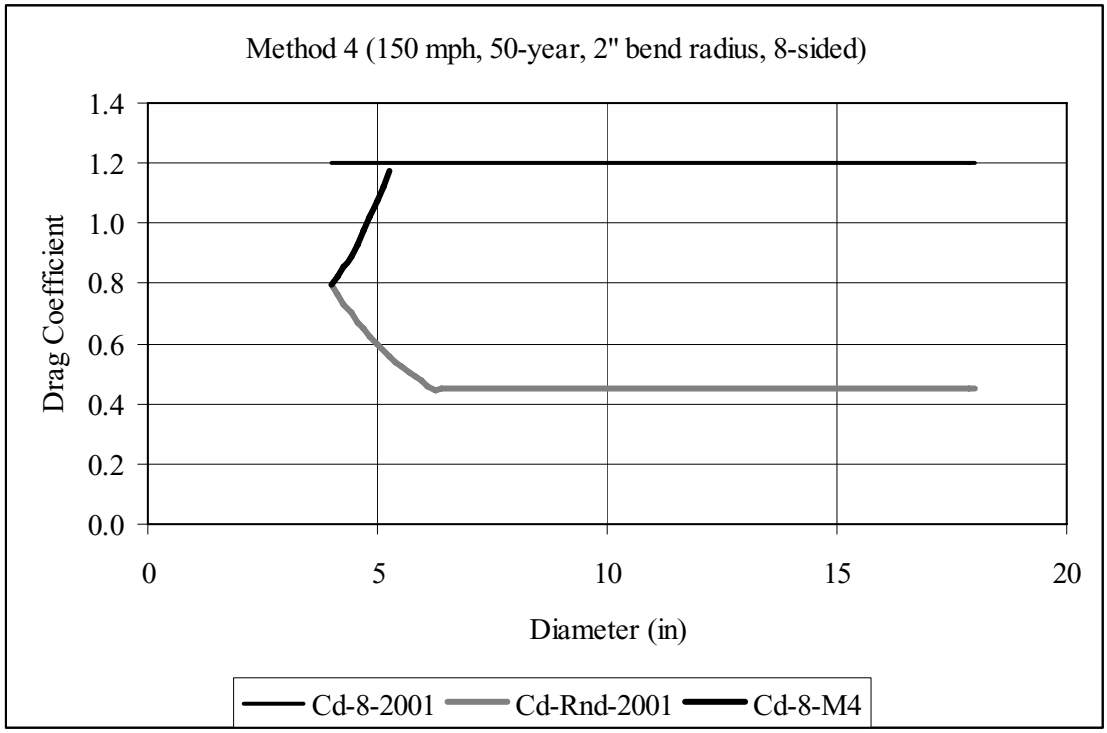

Figure D–96. Drag Coefficient Comparison: Method No. 4, 50-year MRI, 150 mph, 2” bend radius, 8-sided

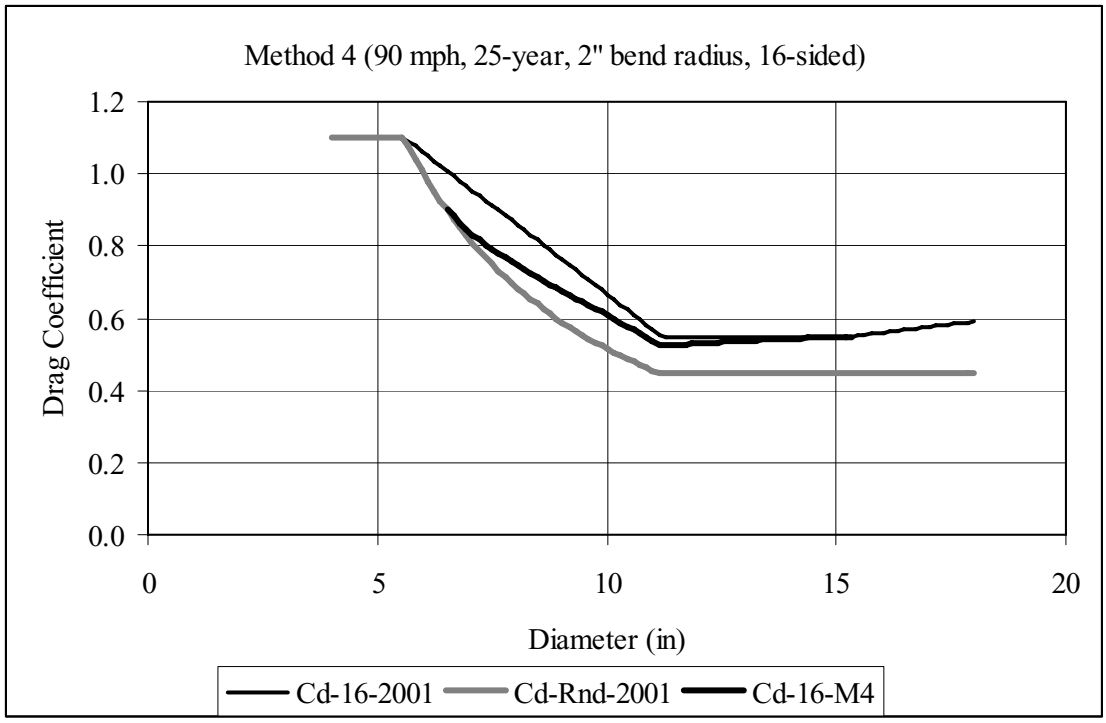

Figure D–97. Drag Coefficient Comparison: Method No. 4, 25-year MRI, 90 mph, 2" bend radius, 16-sided

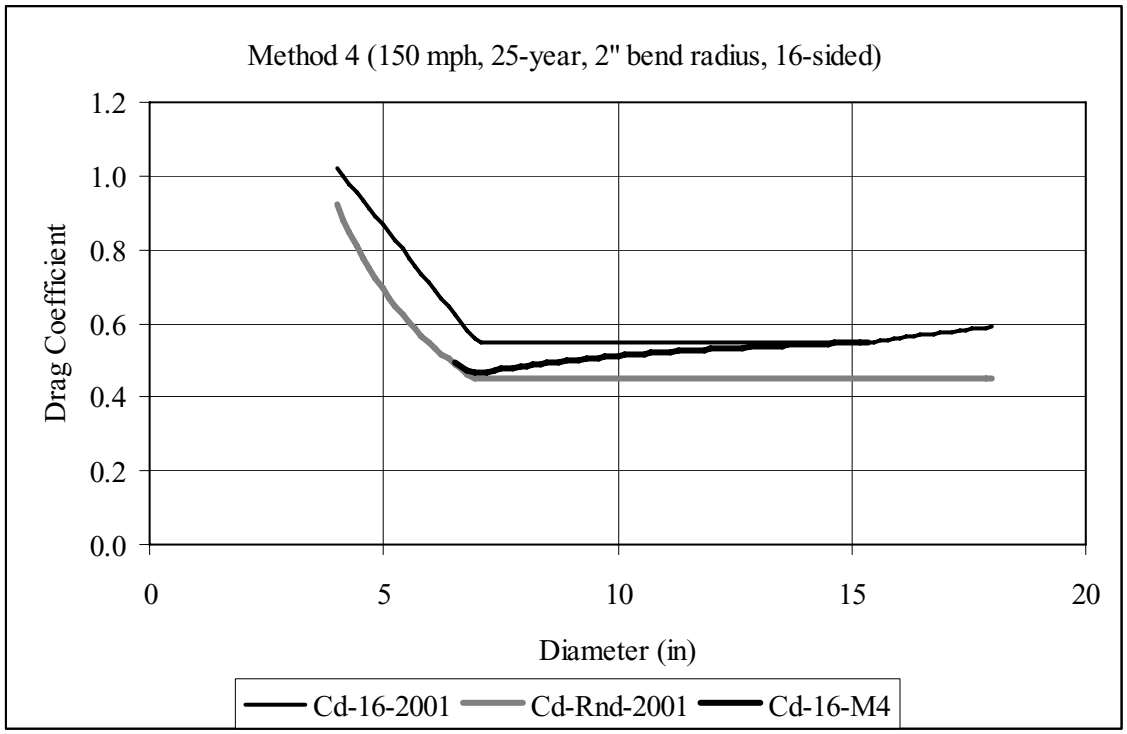

Figure D–98. Drag Coefficient Comparison: Method No. 4, 25-year MRI, 150 mph, 2" bend radius, 16-sided

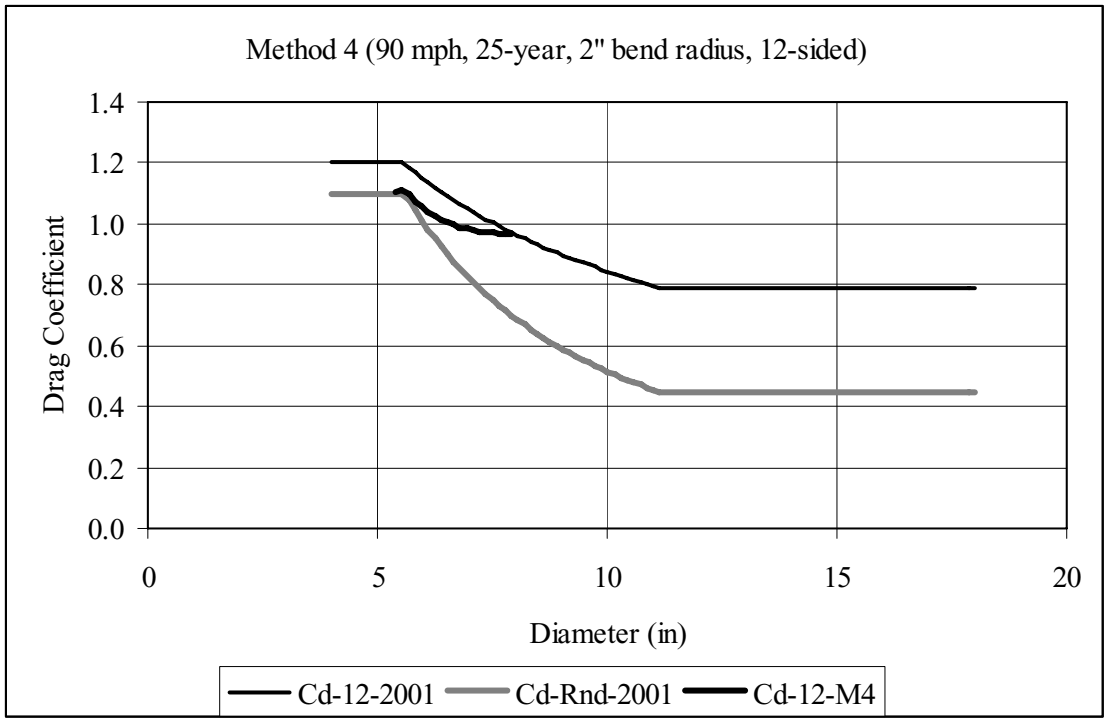

Figure D–99. Drag Coefficient Comparison: Method No. 4, 25-year MRI, 90 mph, 2" bend radius, 12-sided

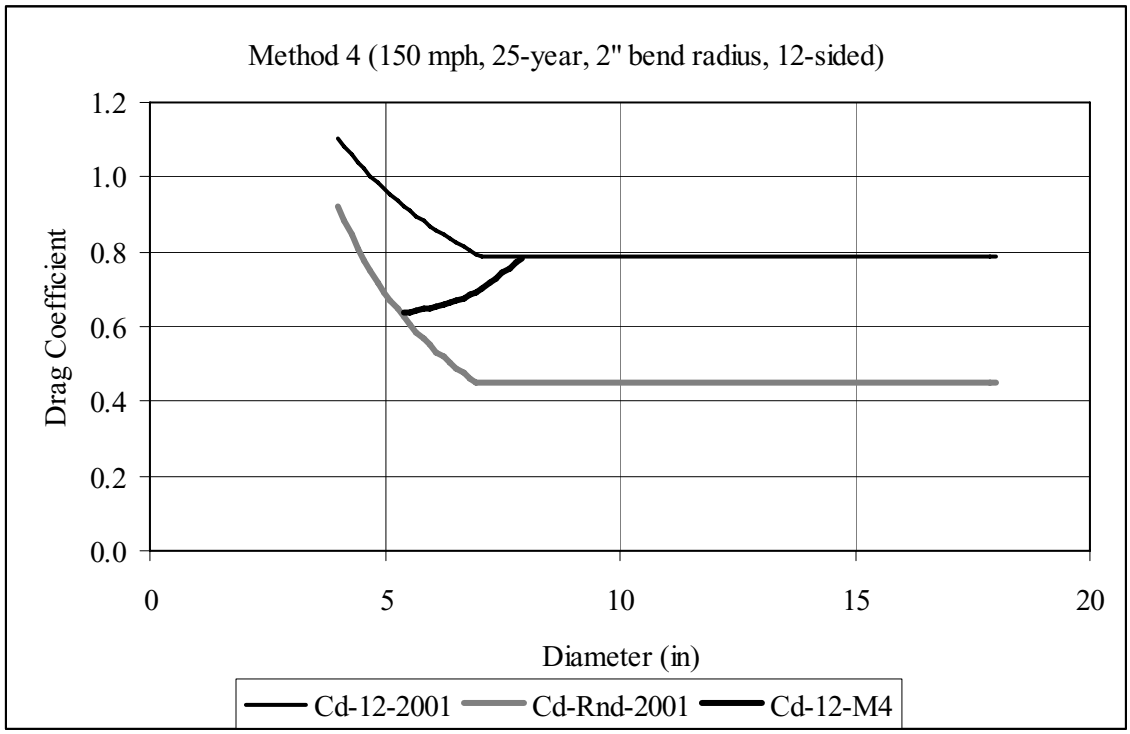

Figure D–100. Drag Coefficient Comparison: Method No. 4, 25-year MRI, 150 mph, 2" bend radius, 12-sided

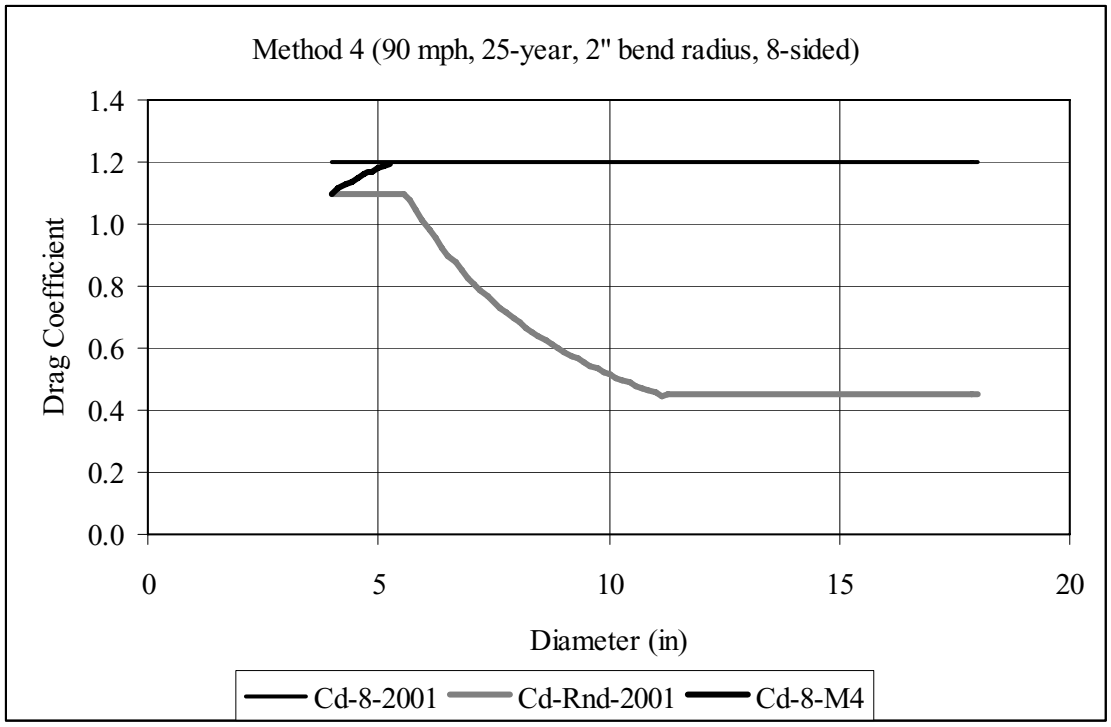

Figure D–101. Drag Coefficient Comparison: Method No. 4, 25-year MRI, 90 mph, 2" bend radius, 8-sided

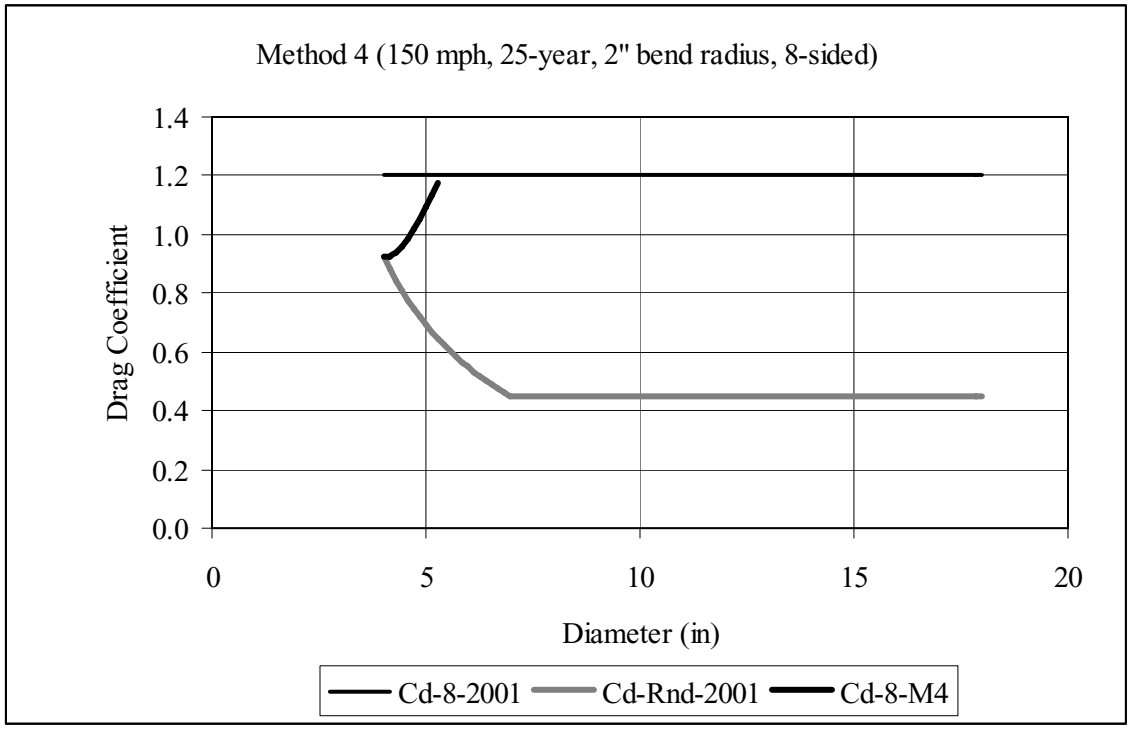

Figure D–102. Drag Coefficient Comparison: Method No. 4, 25-year MRI, 150 mph, 2" bend radius, 8-sided

Appendix E

Proposed Combined Stress Ratio Equation for Square and Rectangular Tubes Bent About a Diagonal Axis

Table of Contents

List of Tables

List of Figures

Proposed Combined Stress Ratio Equation for Square and Rectangular Tubes Bent About a Diagonal Axis

E.1 Preliminary Comments

In the design of cantilever support structures for lighting and similar applications, bending about the diagonal of square and rectangular steel tubes invariably controls the design. This is because the section modulus about the diagonal axis of the tube is smaller than the geometric-axis section modulus. Using the notation shown in Figure E-1, the section modulus about the x-axis (geometric axis) is $S_x = \frac{I_x}{c}$, where $I_x = \int_A y^2 dA$. For a square tube, $S_x = \frac{b^4 - b_i^4}{6b}$. The section modulus about the x'-axis (diagonal axis) is $S_{x'} = \frac{I_{x'}}{c'}$, where $I_{x'} = I_x \cos^2 \phi + I_y \sin^2 \phi$. For a square tube, $I_{x'} = I_x = I_y$, so $S_{x'} = \frac{S_x}{\sqrt{2}}$. This shows that the section modulus about the principal axes of a square tube is 41 percent larger than the section modulus about the diagonal axis.

Preliminary tests (Ref. E-1) have shown that the strength of square tubes bent about the diagonal axis is greater than what is predicted by the current calculation procedures. The current approach is limited in that it can only predict the theoretical point at which the first yield in the cross section occurs. For compact sections, the moment which causes failure in the tube is predicted more accurately using the plastic modulus. The plastic modulus of a square tube bent about the x-axis is $Z_x = \frac{b^3 - b_i^3}{4}$. The plastic modulus about the x'-axis is $Z_{x'} = \frac{b^3 - b_i^3}{3\sqrt{2}}$. The plastic modulus about the principal axes of a square tube is only 6 percent larger than the plastic modulus about the diagonal axis.

The inherent safety factor N for bending about the principal axis and for bending about the diagonal can be calculated for a square tube by assuming a compact cross section and an allowable stress $F_b = 0.6F_y$.

For bending about the principal axes,

$$N_p = \frac{Z_x / S_x}{0.6} = \frac{1.13}{0.6} = 1.88 .$$

For bending about the diagonal axis,

$$N_d = \frac{Z_{x'} / S_{x'}}{0.6} = \frac{1.5}{0.6} = 2.50 .$$

The safety factor for bending about the diagonal axis is approximately 33 percent higher than the safety factor for bending about the principal axes.

For design of square and rectangular tubes bent about a skewed axis, it is recommended that the moment be broken down into components that coincide with the geometric axes of the tube. The moments about the geometric axis can be used with interaction equations that take into account the post-yield strength of the member.

Local buckling of the tube walls is a failure mode that must be taken into account. The buckling capacity is affected by material and geometric properties that vary depending on the manufacturer of the tube. Theoretical plate buckling formulas cannot be used without modification because of the influence that the imperfections have on the buckling load.

Figure E-2 shows the stress distribution for a tube bent in the elastic range. Bending about the geometric axis is shown in Figure E-2a. The stress distribution is rectangular on the critical wall. Figure E-2b shows a triangular stress distribution for a tube bent about a diagonal axis. The theoretical plate buckling formulas can be compared for the two loading conditions to show that tubes bent about the geometric axis are more susceptible to local buckling than tubes bent about the diagonal axis. For tubes that are stressed into the inelastic zone, the stress distribution changes but the strain distribution remains triangular, therefore, the local buckling strength will be greater for all tubes bent about the diagonal axis.

E.2 Experimental Results

Unpublished test data on bending about the diagonal were obtained from Valmont (Ref. E-1). The tests showed that the procedure specified in the current code is very conservative. The test data is shown in Annex A. The test results are compared to the proposed design method in Section E.7.

E.3 Literature Review

General behavior under plastic bending about the geometric axes was researched by Wilkinson (Ref. E-2). His work shows that compact cold-formed rectangular tubes have adequate rotation capacity to be designed using the plastic capacity of the section.

Information about the material and geometric properties of cold-formed tubes was discussed by Sherman (Ref. E-3, E-4). The residual stress around the perimeter of the tube is in a pattern that has a compressive stress of about 10% of the yield stress at the corners. The yield strength at the corners is about 10% higher than the yield strength at the walls. The tube thickness is greater in the corners than in the walls due to the forming process.

References E-5, E-6, and E-7 recommend an interaction equation for members under combined loading conditions. If only moments about the geometric axes are present, the equation reduces to

$$\left(\frac{M_x}{M_{xall}}\right)^{\alpha} + \left(\frac{M_y}{M_{yall}}\right)^{\alpha} \le 1.0 \qquad \text{(E-3.1)}$$

References E-5 and E-6 recommend using $\alpha = 1.6$ for wide flange shapes. Reference E-7 specifies $\alpha = 1.7$ for box-section members.

A theoretical study was conducted by Pillai (Ref. E-8) on the capacity of square and rectangular tubes subject to axial loading and biaxial bending. The theoretical equations were too complex for typical design office use. As a slightly conservative approximation for the load case of biaxial moments with no axial load, he recommended that Equation (E-3.1) be used with $\alpha = 1.6$. The research is applicable to compact sections only.

Wardenier (Ref. E-9) recommended using the following equations to predict the capacity of square and rectangular tubes subject to biaxial bending

$$\text{If } \frac{M_x}{M_{xall}} \le \frac{2}{3}: \ \frac{3}{4}\left(\frac{M_x}{M_{xall}}\right)^2 + \frac{M_y}{M_{yall}} \le 1.0 \qquad \text{(E-3.2a)}$$

$$\text{If } \frac{M_x}{M_{xall}} > \frac{2}{3}: \ \frac{3}{4}\left(\frac{M_y}{M_{yall}}\right)^2 + \frac{M_x}{M_{xall}} \le 1.0 \qquad \text{(E-3.2b)}$$

AISC (Ref. E-10) specifies wall slenderness limits for tube walls under combined flexure and axial compression. These equations can be modified to account for the stress distribution caused by biaxial loading with no axial load. The resulting limits are

$$\lambda_r = \frac{971}{\sqrt{F_y}}\left[1 - 0.75\left(\frac{\sin\theta}{\sin\theta + \cos\theta}\right)\right] \text{ for } 0^o \le \theta \le 90^o \qquad \text{(E-3.3)}$$

$$\lambda_p = \frac{640}{\sqrt{F_y}}\left[1 - 2.75\left(\frac{\sin\theta}{\sin\theta + \cos\theta}\right)\right] \text{ for } \theta \le 8^o \qquad \text{(E-3.4a)}$$

$$\lambda_p = \frac{190}{\sqrt{F_y}}\left[2.33 - \left(\frac{\sin\theta}{\sin\theta + \cos\theta}\right)\right] \text{ for } 8^o < \theta \le 90^o \qquad \text{(E-3.4b)}$$

θ is the angle between the bending axis and the geometric axis that is perpendicular to the wall in question. For angles other than 45 degrees, the slenderness limit for each wall will be different.

E.4 Comments on the Interaction Equation

The capacities calculated using Equations (E-3.2) are almost identical to the capacities calculated using equation (E-3.1) with $\alpha = 1.7$. Because equation (E-3.1) is easier to use, it is recommended for design use. The exponent $\alpha = 1.6$ is recommended because it is slightly more conservative than using $\alpha = 1.7$. The preceding recommendations are for cross sections with adequate rotation capacity to allow a plastic stress distribution.

For noncompact cross sections, linear interaction is recommended. This can be accomplished by using $\alpha = 1.0$ in equation (E-3.1). In effect, this is the procedure that is currently specified in Reference E-11 for compact and noncompact cross sections.

E.5 Comments on Local Buckling

For square tubes bent about the diagonal axis, $\theta = 45^o$ can be substituted into equations (E-3.3) and (E-3.4b) to find the slenderness limit. The equations are

$$\lambda_r = \frac{607}{\sqrt{F_y}} \tag{E-5.1}$$

$$\lambda_p = \frac{348}{\sqrt{F_y}} \tag{E-5.2}$$

The recommended procedure uses the values specified in Reference E-11 for the wall slenderness ratios and allowable stresses, however, all ratios below λ_r are assumed to be compact. This is because λ_r specified in Reference E-11 is $\frac{260}{\sqrt{F_y}}$ which is less than $\lambda_p = \frac{348}{\sqrt{F_y}}$ for tubes bent about the diagonal axis. The proposed reduction in allowable stress due to local buckling is plotted in Figure E-3.

E.6 Proposed Design Method

The design procedure in this section applies to square and rectangular tubes that are bent about a skewed axis. The tube must also be designed separately for the maximum moments about each geometric axes using the procedure in Reference E-11. The following interaction equation must be satisfied

$$\left(\frac{M_x}{M_{xall}}\right)^{\alpha} + \left(\frac{M_y}{M_{yall}}\right)^{\alpha} \le 1.0 \tag{E-6.1}$$

For tubes with $\lambda \le \lambda_r$:

$$\alpha = 1.6$$

$$M_{xall} = 0.6 S_x F_y \tag{E-6.2a}$$

$$M_{yall} = 0.6 S_y F_y \tag{E-6.2b}$$

For tubes with $\lambda_r < \lambda \le \lambda_{max}$:

$$\alpha = 1.0$$

$$M_{xall} = S_x F_b \tag{E-6.3a}$$

$$M_{yall} = S_y F_b \tag{E-6.3b}$$

where

$$F_b = 0.74 F_y \left(1 - \frac{0.194}{\sqrt{E/F_y}} \frac{b}{t} \right) \tag{E-6.4}$$

$$\lambda_r = \frac{260}{\sqrt{F_y}} \tag{E-6.5}$$

$$\lambda_{max} = \frac{365}{\sqrt{F_y}} \tag{E-6.6}$$

Equations (E-6.4), (E-6.5), and (E-6.6) are the same equations as in Reference E-11.

E.7 Comparison of Proposed Design Method to the Experimental Results

Table E-1 compares the experimental results (Ref. E-1) to the proposed design procedure. The experimental moments are shown in the fourth column. The eighth column lists the allowable moments calculated using the proposed design procedure. The last column shows the ratio of the experimental moment to the calculated moment. The details of the specimens for the experimental results are shown in Annex A.

Table E-1. Comparison of Experimental Moments to Design Equations

Specimen Number	Width to thickness ratio λ	Minimum Yield Strength (ksi)	M_E (ft-kips)	λ_r (Eqn. E-6.5)	λ_{max} (Eqn. E-6.6)	α	M_{all} (ft-kips)	M_E / M_{all}
1	18.60	68.90	19.53	31.32	43.97	1.6	9.34	2.09
2	20.93	67.50	33.53	31.65	44.43	1.6	17.18	1.95
3	31.80	47.50	76.42	37.72	52.96	1.6	38.02	2.01
4	37.01	55.00	53.61	35.06	49.22	1.0	18.80	2.85
5	41.36	50.00	46.98	36.77	51.62	1.0	20.01	2.35
6	42.68	52.50	5.92	35.88	50.37	1.0	2.35	2.52
7	43.75	52.00	6.26	36.05	50.62	1.0	2.25	2.78
8	44.30	53.20	6.32	35.65	50.04	1.0	2.24	2.82
9	52.21	67.20	21.39	31.72	44.52	1.0	9.36	2.28
10	55.63	64.40	26.72	32.40	45.48	1.0	10.43	2.56

The ratios of experimental moment to calculated moment show that the safety factor using the proposed design procedure ranged from 1.95 to 2.85. The required safety factor

against collapse is 1.925 (Ref. E-12). A plot of M_E versus $1.925 M_{all}$ is shown in Figure E-4. All data points are above the plotted line, therefore the proposed design procedure is conservative.

E.8 Design Examples

E.8.1 Example 1

A TS 10x10x1/4 is bent about its diagonal axis with a 60 ft-kip moment. The material is A500 Gr. B. Is the tube adequate?

$$F_y = 46 \text{ ksi} \qquad S_x = 30.1 \text{ in}^3 \qquad S_y = 30.1 \text{ in}^3$$

$$\lambda = \frac{b}{t} = \frac{10'' - (5)(0.25'')}{0.25''} = 35.0 \qquad \lambda_r = \frac{260}{\sqrt{46}} = 38.3$$

$\lambda < \lambda_r$; therefore Equation (E-6.1) will be used with $\alpha = 1.6$.

$$M_{xall} = 0.6 S_x F_y = 0.6(30.1 \text{ in}^3)(46 \text{ ksi}) = 830.8 \text{ in - kips}$$

$$M_{yall} = 0.6 S_y F_y = 0.6(30.1 \text{ in}^3)(46 \text{ ksi}) = 830.8 \text{ in - kips}$$

$$M_x = \frac{(60 \text{ ft - kips})\left(12 \frac{\text{in}}{\text{ft}}\right)}{\sqrt{2}} = 509.1 \text{ in - kips}$$

$$M_y = \frac{(60 \text{ ft - kips})\left(12 \frac{\text{in}}{\text{ft}}\right)}{\sqrt{2}} = 509.1 \text{ in - kips}$$

$$\left(\frac{509.1 \text{ in - kips}}{830.8 \text{ in - kips}}\right)^{1.6} + \left(\frac{509.1 \text{ in - kips}}{830.8 \text{ in - kips}}\right)^{1.6} = 0.91 < 1.0 ;$$

therefore, the TS 10x10x1/4 is adequate.

Using the design method in the current AASHTO Code (Ref. E-11), the tube is overstressed by 35%. According to the proposed design procedure, the allowable bending capacity is 48% greater than the current code allows.

E.8.2 Example 2

A TS 10x10x3/16 is bent about its diagonal axis with a 25 ft-kip moment. The material is A500 Gr. B. Is the tube adequate?

$$F_y = 46 \text{ ksi} \qquad S_x = 23.2 \text{ in}^3 \qquad S_y = 23.2 \text{ in}^3$$

$$\lambda = \frac{b}{t} = \frac{10" - (5)(0.1875")}{0.1875"} = 48.3 \qquad \lambda_r = \frac{260}{\sqrt{46}} = 38.3 \qquad \lambda_{\max} = \frac{365}{\sqrt{46}} = 53.8$$

$\lambda_r < \lambda < \lambda_{\max}$; therefore Equation (E-6.1) will be used with $\alpha = 1.0$.

$$F_b = 0.74(46 \text{ ksi})\left(1 - \frac{0.194}{\sqrt{\frac{29{,}000 \text{ ksi}}{46 \text{ ksi}}}}(48.3)\right) = 21.3 \text{ ksi}$$

$$M_{xall} = S_x F_b = (23.2 \text{ in}^3)(21.3 \text{ ksi}) = 494.2 \text{ in - kips}$$

$$M_{yall} = S_y F_b = (23.2 \text{ in}^3)(21.3 \text{ ksi}) = 494.2 \text{ in - kips}$$

$$M_x = \frac{(25 \text{ ft - kips})\left(12 \frac{\text{in}}{\text{ft}}\right)}{\sqrt{2}} = 212.1 \text{ in - kips}$$

$$M_y = \frac{(25 \text{ ft - kips})\left(12 \frac{\text{in}}{\text{ft}}\right)}{\sqrt{2}} = 212.1 \text{ in - kips}$$

$$\left(\frac{212.1 \text{ in - kips}}{494.2 \text{ in - kips}}\right)^{1.0} + \left(\frac{212.1 \text{ in - kips}}{494.2 \text{ in - kips}}\right)^{1.0} = 0.86 < 1.0;$$

therefore, the TS 10x10x3/16 is adequate.

The proposed design procedure produces the same results as the current AASHTO Code (Ref. E-11) for tubes with $\lambda_r < \lambda \le \lambda_{max}$.

E.9 Conclusion

A design method was developed to determine the allowable bending capacity of square and rectangular tubes bent about the diagonal axis. Compared to the allowable moment in the current AASHTO Code (Ref. E-11), the design procedure was shown to greatly increase the allowable moment for tubes with $\lambda \le \lambda_r$.

E.10 Notation

B	Overall tube width for short side.
D	Overall tube width for long side.

F_b	Allowable bending stress reduced for the effect of local buckling.
F_y	Yield stress of the tube.
M_{all}	Allowable moment about the diagonal axis.
M_E	Ultimate test moment.
M_x	Applied moment about the *x* axis.
M_y	Applied moment about the *y* axis.
M_{xall}	Allowable moment about the *x* axis.
M_{yall}	Allowable moment about the *y* axis.
S_x	Section modulus about the *x* axis.
S_y	Section modulus about the *y* axis.
b	Flat width of the tube wall in question.
t	Tube wall thickness.
α	Exponent for interaction equation.
λ	Width-to-thickness ratio of the wall in question.
λ_r	Width-to-thickness ratio at the compact limit.
λ_p	Width-to-thickness ratio at the noncompact limit.
λ_{max}	Maximum width-to-thickness ratio allowed.
θ	Angle between the bending axis and the geometric axis that is perpendicular to the wall in question.

References

E-1. Unpublished test results, Valmont.

E-2. Wilkinson, T., *The Plastic Behavior of Cold-Formed Rectangular Hollow Sections*. Thesis Presented for the Degree of Doctor of Philosophy. Department of Civil Engineering, The University of Sydney, Sydney, Australia, 1999.

E-3. Sherman, D. R., "Tubular Members." *Constructional Steel Design, An International Guide*, Elsevier Science Publishers, LTD, Essex, England, 1992.

E-4. Sherman, D. R., "Designing With Structural Tubing." *Modern Steel Construction*, AISC, Chicago, IL, February, 1997, pp 36-45.

E-5. Tebedge, N., and Chen, W. F., "Design Criteria for H-Columns Under Biaxial Loading." *Journal of the Structural Division*, ASCE, Vol. 100, No. ST3, March, 1974, pp. 579-598.

E-6. *Guide to Stability Design Criteria for Metal Structures.* Structural Stability Research Council, Fifth Edition, T. V. Galambos, ed., John Wiley and Sons, New York, 1998.

E-7. *Load and Resistance Design Specification for Structural Steel Buildings*, American Institute of Steel Construction, Chicago, IL, December 1, 1993.

E-8. Pallai, S. Unnikrishna, "Design of Rectangular Hollow Structural Section Beam-Columns." *Stability of Structures Under Static and Dynamic Loads*, American Society of Civil Engineers, New York, 1977, pp 392-406.

E-9. Wardenier, J., *Hollow Section Joints*, Delft University Press, The Netherlands, 1982.

E-10. *Specification for the Design of Steel Hollow Structural Sections*. American Institute of Steel Construction, Chicago, IL, April 15, 1997.

E-11. AASHTO, *Standard Specifications for Structural Supports for Highway Signs, Luminaires and Traffic Signals*. Fourth Edition, American Association of State Highway and Transportation Officials, Washington, D.C., 2001.

E-12. Fouad, F. H.; Calvert, E. A.; and Nunez, E., "Structural Supports for Highway Signs, Luminaries, and Traffic Signals." *NCHRP Report 411*, Transportation Research Board, National Research Council, Washington, D. C., 1998.

Annex A: Valmont Test Results

Note: The failure mode for specimen 2 was yielding. The failure mode for the remaining specimens was local buckling.

Valmont Test Data for Square Tubes Bent about the Diagonal Axis								
Specimen Number	Actual Width (in)	Actual Wall Thickness (in)	Outside Corner Radius (in)	Flat Width (in)	Width to thickness ratio λ	Minimum Yield Strength (ksi)	Ultimate Test Moment (ft-kips)	S_x and S_y
1	4.00	0.168	0.438	3.12	18.60	68.90	19.53	2.96
2	5.00	0.197	0.438	4.12	20.93	67.50	33.53	5.55
3	8.00	0.228	0.375	7.25	31.80	47.50	76.42	17.46
4	7.25	0.179	0.313	6.62	37.01	55.00	53.61	11.40
5	8.03	0.176	0.375	7.28	41.36	50.00	46.98	13.82
6	4.00	0.082	0.250	3.50	42.68	52.50	5.92	1.59
7	4.00	0.080	0.250	3.50	43.75	52.00	6.26	1.55
8	4.00	0.079	0.250	3.50	44.30	53.20	6.32	1.53
9	6.63	0.115	0.313	6.00	52.21	67.20	21.39	6.23
10	7.19	0.118	0.313	6.56	55.63	64.40	26.72	7.56

Annex B: Figures

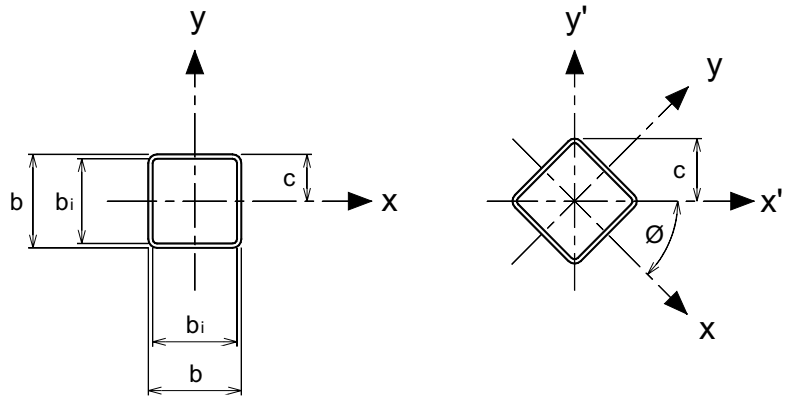

Figure E-1. Notation for Bending About the Diagonal of a Square Steel Tube

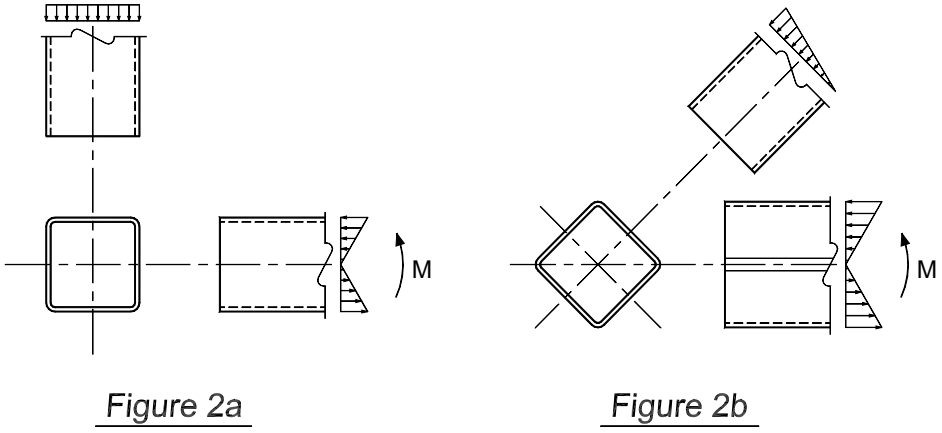

Figure E-2. Stress Distribution for a Square Tube Bend in the Elastic Range

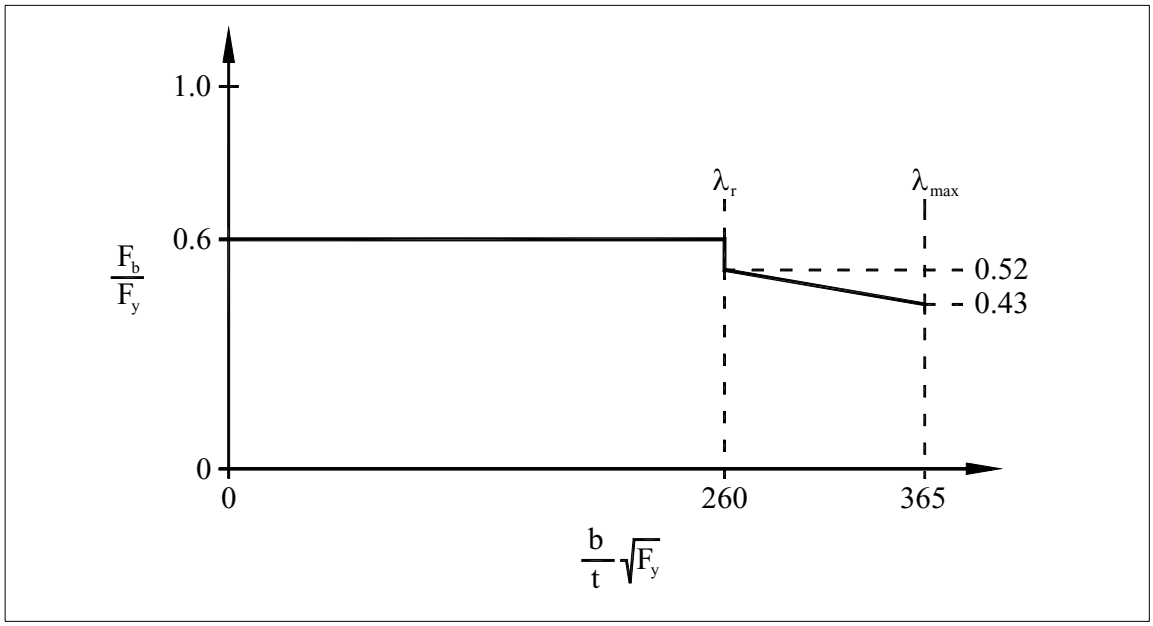

Figure E-3. Proposed Combined Stress Ratio Equation for Square and Rectangular Tubes Bent About a Diagonal Axis

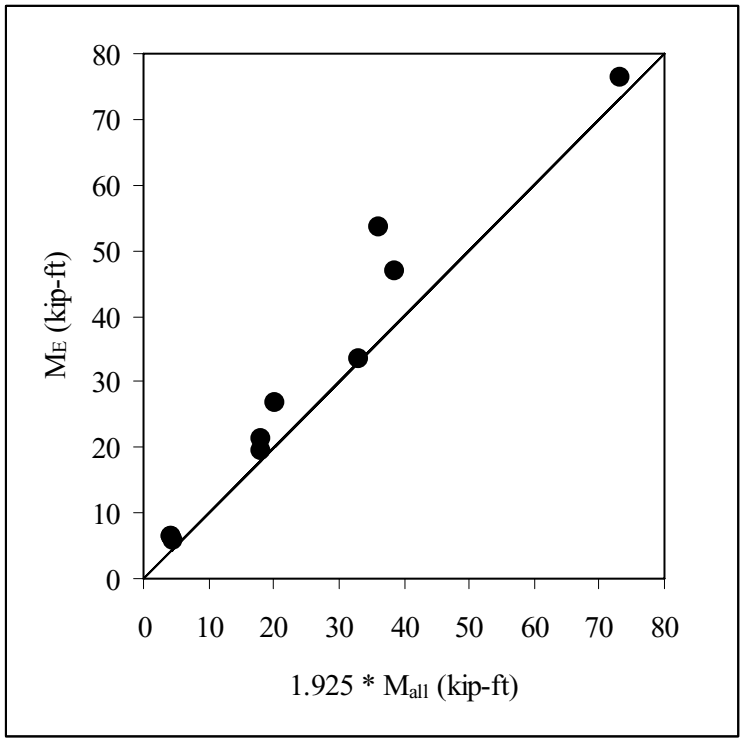

Figure E-4. *M_E* Versus *1.925 M_{all}*

Appendix F

Proposed Performance Specification for FRP Poles

This appendix presents the proposed performance specification on fiber-reinforced composite poles. It follows the format and nomenclature of Section 8 of the 2001 AASHTO *Standard Specifications for Structural Supports for Highway Signs, Luminaires and Traffic Signals*.

Performance Specification of Fiber-Reinforced Composite Poles

Appendix F – Performance Specification for Fiber-Reinforced Composite Poles

SPECIFICATION

COMMENTARY

F.1 SCOPE

This specification provides physical requirements and performance characteristics of lighting poles manufactured from fiberglass reinforced plastic (FRP).

Applications of fiber-reinforced composites are expanding as the experience in using these materials increase. This specification provides guidelines for the design of lighting poles manufactured from fiberglass reinforced plastic (FRP).

F.2 REFERENCED STANDARDS AND SPECIFICATIONS

This specification is intended to be used in conjunction with the following standards and specifications.

AASHTO LTS-4, *Standard Specifications for Structural Supports for Highway Signs, Luminaires and Traffic Signals*

ASTM D4923-01, "Standard Specification for Reinforced Thermosetting Plastic Poles"

ANSI C136.20-1996, "Fiber-Reinforced Plastic (FRP) Lighting Poles"

ASTM D635-98, "Standard Test Method for Rate of Burning and/or Extent and Time of Burning of Plastics in a Horizontal Position"

ASTM G154-00a, "Standard Practice for Operating Fluorescent Light Apparatus for UV Exposure of Non-Metallic Materials"

F.3 DEFINITIONS

Fiber-reinforced composite (FRC) -- a composite material in which the polymer resin matrix is reinforced with high-strength fibers.

Fiberglass reinforced plastic (FRP) -- a composite material in which the polymer resin matrix is reinforced with glass fibers.

Surface veil -- a surfacing mat used in the outer surrounding layer of an FRP pole to produce a smooth surface and to protect the underlying material from weathering degradation.

UV -- ultraviolet light originating from solar radiation

Weathering resistance -- a property of the FRP material that resists degradation due to environmental factors such as outdoor sunlight and wind-borne particulates. Degradation is evidenced by exposed fibers, cracks, crazes, or checks in the pole surface.

F.4 NOTATION

h = pole height above ground (m, ft)

M_{max} = maximum bending moment induced by the wind on pole, arm, and luminaire computed according to the AASHTO *Standard Specifications for Structural Supports for Highway Signs, Luminaires and Traffic Signals* (N-m, lb-ft). For the fatigue test described in Article F.8.3, M_{max} shall be computed for a wind pressure of 110 Pa (2.3 psf)

M_{tor} = maximum torsional moment induced by the wind on the arm and luminaire computed according to

SPECIFICATION COMMENTARY

the AASHTO *Standard Specifications for Structural Supports for Highway Signs, Luminaires and Traffic Signals* (N-m, lb-ft). For the fatigue test described in Article F.8.3, M_{tor} shall be computed for a wind pressure of 110 Pa (2.3 psf)

P_{eb} = load to produce a moment at ground line equal to the design moment resultant (N, lb)

P_{et} = load to produce a torsional moment equal to the design torsional moment resultant (N, lb)

x_a = Distance from center of the pole cross section at the arm connection to the centroid of arm-luminaire combination (m, ft)

F.5 GENERAL

FRP lighting poles shall be manufactured from class "E" or higher grade glass and a polymer, which is typically a polyester resin, and shall be suitable for direct-burial or base-mounted installation.

FRP lighting poles shall be either direct-burial or base-mounted type.

This specification covers primarily fiberglass reinforced plastic (FRP) composites, which are the most widely used composites for lighting poles.

F.6 PHYSICAL CHARACTERISTICS

FRP lighting poles shall be manufactured by filament winding, pultrusion, or centrifugal casting.

FRP lighting poles shall be round, hollow, electrically nonconductive and chemically inert.

The wall thickness of the cross section shall be uniform, and the manufacturing process shall insure a dense, void-free wall with a smooth exterior surface.

Filament winding is the oldest and most common method of producing FRP poles. A filament winding machine is used where glass fibers strands are impregnated with polymer resin matrix and continuously wound onto a tapered mandrel. The number of windings and the angle at which the glass fiber strands are wound on the mandrel are controlled and set according to design. The laminate is then cured, sometimes with the assistance of an external heat source, and upon completion, the mandrel is removed.

Pultrusion is a continuous molding process where selected reinforcements are fed continuously in predetermined amounts and pre-planned layering from multiple creels through a resin bath. The resin impregnated reinforcement is pulled through a die that determines the sectional geometry of the product and controls reinforcement and resin content. Resin cure is initiated in the heated section of the die. The product is drawn through the die by a puller mechanism and is cut to the desired length. Pultrusion is appropriate for any shape that may be extruded, but it is limited to prismatic FRP lighting poles.

Centrifugal casting is a method most suited for cylindrical shapes such as pipes, poles, and tubing. In this process, glass fabric in predetermined amount and configuration is placed in a hollow steel mold. The mold is rotated (spun) at high speeds during which resin is injected and distributed uniformly throughout the reinforcement. Centrifugal forces distribute and compact the resin and reinforcement against the wall of

SPECIFICATION

COMMENTARY

the rotating mold. Curing of the product is accelerated through the application of an external heat source.

F.7 STRUCTURAL PERFORMANCE

F.7.1 Design Loads

FRP lighting poles shall be designed to withstand the gravitational and environmental loads prescribed by the AASHTO *Standard Specifications for Structural Supports for Highway Signs, Luminaires and Traffic Signals* for the geographic location where the poles are to be installed. FRP lighting poles shall also be designed to withstand the gravitational and environmental loads resulting from the attachments connected to them, such as luminaries, arms, and wires.

Gravitational loads include dead and live loads from the structure and attachments. Environmental loads include loads induced by wind, snow, and ice.

F.7.2 Maximum Loads

FRP lighting poles shall be capable of sustaining a maximum of two times the design loads before failure. When a hand hole is specified, the poles shall withstand the maximum load with the hand hole in compression and with the hand hole cover removed.

F.7.3 Deflection Limits

FRP lighting poles subjected to design loads shall exhibit a lateral deflection at the top of no more than 15 percent of the height above ground (maximum deflection limit).

The lateral deflection is measured from the deflected top end of the pole along a line perpendicular to the longitudinal axis of the undeflected pole.

For FRP lighting poles with mast arms, the slope at the top of the pole resulting from the dead load moment of the arm and attachments shall not exceed 30 mm per meter (0.35 in per foot) (maximum slope limit).

The maximum deflection limit and the maximum slope limit are consistent with the deflection limits requirements of the AASHTO *Standard Specifications for Structural Supports for Highway Signs, Luminaires and Traffic Signals* for pole-type structural supports.

The top of FRP lighting poles shall not deflect more than 5 percent of the height above ground when subjected to a 890 N (200 lb) lateral top load (stiffness deflection limit).

The stiffness deflection limit is intended to ensure that the pole does not deflect excessively when maintenance workers use ladders to access attachments at the top of the pole.

F.8 PERFORMANCE VERIFICATION BY TESTING

The performance of FRP lighting poles for bending, torsion, fatigue, and UV exposure shall be verified by testing following the procedures outlined in F.8.1, F.8.2, F.8.3, F.8.4, and F.8.5, with the load

The owner may request testing of a pole specimen per a certain number of poles purchased. For purchase orders of 100 poles or more, it is common practice to request at least two tests per purchase. For

SPECIFICATION

COMMENTARY

provisions of Chapter 3 in the AASHTO *Standard Specifications for Structural Supports for Highway Signs, Luminaires and Traffic Signals*. The owner shall specify the number of tests required per batch of poles.

purchase orders of less than 100 poles, it is common practice to request at least one test per purchase order. This information is provided as a guide, but the final decision on the number of tests required is to be agreed upon between the owner and the manufacturer.

F.8.1 Bending Strength of FRP Poles

The bending strength of FRP poles shall be determined in accordance to ASTM D4923 procedure, except for the following requirements:

a) The pole shall be capable of sustaining an equivalent point load P_{eb} applied 0.3 m (1 ft) from the top with a maximum deflection at the top no greater than 15 percent of the pole height above ground. The equivalent point load shall be computed as

$$P_{eb} = \frac{M_{max}}{(h - 0.30)} \text{ (N)} \qquad \text{Eq. F-1}$$

$$P_{eb} = \frac{M_{max}}{(h - 1.0)} \text{ (lb)}$$

b) The pole permanent deflection shall not exceed 2 percent of the maximum deflection obtained by the application of the equivalent point load P_{eb}. The equivalent point load P_{eb} shall be applied for 5 minutes and the permanent deflection shall be measured 5 minutes after unloading.

c) The pole shall be capable of sustaining a maximum point load of *two times* P_{eb} applied 0.3 m (1 ft) from the top before failure.

d) When a hand hole is specified, the pole shall be tested with the hand hole in compression and the hand hole cover removed.

e) The pole shall not deflect more than 5 percent of the height above ground when subjected to a 890 N (200 lb) lateral top load.

f) For poles with mast arms, the slope at the top of the pole resulting from the dead load moment of the arm and luminaire shall not exceed 30 mm per meter (0.35 in per foot).

g) During the test, the load shall be applied at 223 N (50 lb) increments, and deflections shall be recorded at each load increment.

The AASHTO *Standard Specifications for Structural Supports for Highway Signs, Luminaires and Traffic Signals* specifies a different safety factor for bending than ASTM D4923 in order to account for the variability in mechanical properties of FRP lighting poles.

The bending test described herein is intended to establish the performance of the FRP poles under service and ultimate strength conditions. Therefore, the FRP pole should be tested for serviceability conditions such as the maximum deflection under design service load and the permanent deflection after unloading, and then the FRP pole should be tested for ultimate strength.

A safety factor of 2.0 against failure in bending is specified for the test. The safety factor is greater than the 1.5 value specified by ASTM D4923 standard in order to account for the variability in mechanical properties of FRP.

SPECIFICATION

COMMENTARY

F.8.2 Torsion Strength of FRP Poles

The torsion strength of FRP poles shall be determined in accordance to ASTM D4923 procedure, except for the following requirement:

a) The pole shall be capable of sustaining a maximum point load of *two times* P_{et} applied at the centroid of the arm and luminaire projected area. The equivalent point load P_{et} shall be computed as

$$P_{et} = \frac{M_{tor}}{x_a} \qquad \text{Eq. F-2}$$

b) During the test, the load shall be applied at 223 N (50 lb) increments, and deflections shall be recorded at each load increment.

A safety factor of 2.0 against failure in torsion is specified for the test. The safety factor is greater than the 1.5 value specified by ASTM D4923 standard in order to account for material variability.

F.8.3 Fatigue Strength of FRP Poles

The fatigue strength of FRP poles shall be determined in accordance to ASTM D4923 procedure, except for the following requirements:

a) The pole shall be tested for a fatigue load P_{eb} or P_{et} computed according to Article F.8.1 or Article F.8.2, whichever is appropriate, for an equivalent wind pressure of 110 Pa (2.3 psf).

b) The fatigue load P_{eb} or P_{et} shall be applied for 10^6 cycles at a rate not exceeding 200 cycles per minute. At the end of the test there shall be no delamination or surface crazing on the pole.

c) After application of the cyclic fatigue load, the pole shall satisfy the requirements for bending or torsion strength of Article F.8.1 or Article F.8.2, whichever is appropriate.

The fatigue test described herein may be conducted prior to the bending or torsion strength tests described in Article F.8.1 or Article F.8.2.

The equivalent wind pressure of 110 Pa (2.3 psf) corresponds to a wind speed of 48.3 km/h (30 mph) without a gust factor, computed according to the *1994 AASHTO Standard Specification for Structural Supports for Highway Signs, Luminaires and Traffic Signals*, as specified by ASTM D4923.

F.8.4 Weathering Resistance

The finished surface of the pole shall be capable of withstanding a minimum of 2500 hours of accelerated weathering when tested according to ASTM G154. Test lamps shall be UV-B type with 313 nm wavelength. The testing cycle shall be 4 hours of UV exposure at 60^0 Celsius and 4 hours of condensation at 50^0 Celsius.

After testing, the finished surface shall not exhibit fading, fiber exposure, chalking, cracking, or crazing.

UV-B 313 lamps produce the shortest wavelengths found in sunlight in the surface of the earth. This particular type of sunlight is known to be responsible for considerable polymer damage capable of affecting the mechanical performance of FRP poles.

The owner and manufacturer may agree upon using different testing lamps and testing cycles depending on the solar radiation conditions of the location where the FRP pole will be installed.

SPECIFICATION

COMMENTARY

F.8.5 Flame Resistance

FRP poles shall be flame resistant in accordance with ASTM D635. FRP specimens shall cease to burn before the gage mark of 100 mm (3.9 inches) is reached.

Flame resistance is required in order to prevent propagation of fires initiated by short circuits or fuel spills.

F.8.6 Other Tests

The following additional test shall be performed, if required by the owner:

a) adhesion of coatings
b) color change from UV exposure
c) fatigue strength of connections

F.9 CONSTRUCTION

F.9.1 Surface Protection and Finish

FRP lighting poles shall be protected from UV radiation to avoid degradation of the structural properties of the member. FRP lighting poles as fabricated shall not show evidence of exposed fibers, cracks, crazes, or checks on the member surface.

UV protection of FRP lighting poles shall be provided by using one or more of the following methods:

a) surface veil
b) urethane coating
c) UV stabilizers

Other UV protection methods may be used if proven effective and agreed upon between owner and the manufacturer.

The pole finish shall be uniform and consistent over its entire length and shall be either of textured, wood grain, smooth or brushed aluminum appearance. The coating shall be formulated to match the color requested by the owner.

Ultraviolet rays and heat from solar radiation degrade the natural molecular structure of FRP. Other weathering elements, such as industrial pollutants or salt-spray, can accelerate the degradation due to UV radiation. The results of exposing FRP to any of these conditions can be discoloration, loss of mechanical strength, embrittlement, and loss of electrical insulation and resistance properties. Chemical stabilizers, fillers, and weather resistant paints or coatings should be used to provide the necessary protection. The service life of coatings is dependent on the coating's quality, adhesion, and thickness.

F.9.2 Holes, Wiring Access, and Caps

Pole tops shall be prepared for attaching side-mounted luminaires or tenon-mounted luminaires or side-mounted mast arms with holes drilled as required and with pole wall reinforcing provided at bolt holes, hand holes, and similar pole wall penetrations.

SPECIFICATION

COMMENTARY

FRP poles shall permit complete internal wiring from an underground source.

For direct-burial FRP poles, two wire entry holes shall be provided. The wire entry holes shall be located between 457 mm (18 in) and 762 mm (30 in) below the ground line, or as specified by the owner.

When specified by the owner, FRP poles shall have a hand hole of adequate size to provide access to wiring. The hand hole shall not reduce the strength of the pole below design values. The centerline of the hand hole shall be located between 475 mm (18 in) and 1220 mm (48 in) above the ground line, or otherwise as specified by owner.

Fiberglass poles shall be reinforced at wire holes, hand holes, and bolt holes.

Wire holes shall be bushed, lined, fitted with grommets or otherwise protected to allow for normal use of electric conductors.

The hand hole shall have a removable cover of noncorrosive material capable of withstanding the same environmental exposure requirements as the FRP pole.

A top cap shall be securely mounted to each pole top if no top-mounted fixture is present. The cap shall be capable of withstanding the same environmental exposure requirements as the FRP lighting pole.

F.9.3 Special Provisions for Direct-Burial FRP Poles

The burial depth of a direct-burial FRP pole shall be determined by proper consideration of loading and soil conditions.

Direct-burial FRP poles shall also be provided with mechanisms to prevent rotation of the pole induced by torsion. Acceptable anti-rotation mechanisms include squared ends, asymmetric flared bases, wing flanges, or pipe extensions. Any such mechanism shall not extent over 100 mm (4 in) from the face of the pole.

Burial depths may be determined analytically by following the procedures outlined in “Section 13: Foundations Design” of the AASHTO *Standard Specifications for Structural Supports for Highway Signs, Luminaires and Traffic Signals*. Table F-1 shows suggested standard burial depths according to ANSI C136.20.

Anti-rotation mechanisms should be provided to control the torsion induced rotation of direct burial FRP poles when acted by lateral wind loads.

Table F-1. Suggested Values for Burial Depth

Total Length of Pole m (ft)	Burial Depth m (ft)
0-5.48 (0-18)	0.91 (3)
5.49-7.62 (18.1-25)	1.22 (4)
7.63-12.19 (25.1-40)	1.52 (5)
12.20-15.24 (40.1-50)	1.83 (6)

F.9.4 Special Provisions for Base-Mounted FRP Poles

Base-mounted FRP poles shall have a galvanized steel base mount whose shaft is factory arc-welded to a steel base plate. The anchor base mount shall be bonded to the pole with a high-strength epoxy adhesive and coated with color matching urethane finish.

Table F-2 shows suggested standard values for bolt circle according to ANSI C136.20.

Table F-2. Suggested Values for Bolt Circle

Total Length of Pole m (ft)	Range of Bolt Circle mm (in)
0-6.4 (0-21)	200-305 (8-12)
6.41-9.45 (21.1-31)	215-355 (8.5-14)
9.46-13.7 (31.1-45)	355-432 (14-17)

F.9.5 Packaging and Labeling

Poles shall be wrapped in their entirety with a weatherproof wrap by the manufacturer after fabrication and prior to shipment for protection during shipping and storage.

The owner and manufacturer may agree upon different packaging methods depending on pole size, number of poles being delivered, and storage location.

Each pole shall have a permanent identification plate attached to the shaft at no more than 3 ft (0.9 m) above the ground line. The identification plate shall include the manufacturer name or trademark, the catalog number of the pole, the date, month, and year of fabrication, and the moment capacity of the pole.

F.10 QUALITY CONTROL

Prior to fabrication, the manufacturer shall

Because the structural properties of FRP

SPECIFICATION

submit for approval the following items

a) Detailed shop drawings for FRP lighting poles, foundations and connections
b) Manufacturer's catalog data or quality control manual showing dimensions, design tables, materials of construction, and test data on performance.
c) Manufactured FRP samples of proposed product including resin, fibers and UV coatings.

FRP lighting poles shall be produced from new materials of the best quality and shall be free from defects and imperfections that might affect the structural performance and reliability of the finished product. Materials used in the production of FRP lighting poles shall be of the kind and quality specified, and if the quality is not specified, the manufacturer shall provide adequate supporting information to prove that the proposed material is suitable for the purpose intended.

FRP lighting poles shall have smooth surfaces true to form. After manufacturing and prior to erection, FRP lighting poles shall be stored and shipped in a manner to prevent cracking, twisting, bending, breaking, chipping or damage of any king to the structural member.

After fabrication and erection, FRP lighting poles shall be protected to prevent intrusion of moisture by sealing cut ends, holes, and abrasions with a compatible resin coating.

COMMENTARY

lighting poles may vary widely depending on the manufacturing process and the kind and quality of materials used, it is required that the manufacturer provides supporting information regarding the proposed product. The supporting information should be used in determining whether a particular product is fit for structural use.

Manufactured samples are small pieces of FRP produced with the same materials and the same manufacturing procedure as the proposed structural FRP lighting poles.

F.11 REFERENCES

City of Seattle Standard Specification 8-32: Poles, Pedestals and Foundations, Seattle, WA, 2001.

Evaluation of Deflection and Bending Characteristics of Fiber-Reinforced Plastic Lighting Standards, Caltrans Study # F92TL12, California Department of Transportation, Sacramento, California, November 1995.

Fiberglass Lighting Pole Specifications, SES-PD-087, The Southern Company, Atlanta, GA, June 1994.

Guidelines and Recommended Practices for Fiberglass Reinforced Plastic Architectural Products, Composites Fabricators Association Architectural Committee, 1992.

Group Specification GS-32 for Fiberglass Post, Carolina Power and Light Company, Raleigh, NC, February 1993.

Material Specifications for Fiberglass Street Lighting Poles, Illinois Power Company, Decatur, IL, 1988.

PNM Specification SL2 Revision 3: Aluminum/Fiberglass Lighting Poles, Public Service Company of New Mexico, Albuquerque, New Mexico, August 1997.

Shakespeare Composite Utility Pole Specifications, The Shakespeare Company, Newberry, SC, 2001.

Special Provisions, Specifications, Proposal and Contract for Furnishing and Delivering Street Light and Traffic Signal Poles, Arms, Bases, Luminaires and Cable, Project HWY-C-06-98, Hawaii Department of Transportation, Honolulu, Hawaii, 1998.

Fiberglass Reinforced Plastic Street Lighting Electroliers, Specification MS32-1995, Southern California Edison Company, Rosemead, CA, 1995.

Specification for Fiberglass Reinforced Composite Poles, Newmark International, Birmingham, AL, 1998.

Specification for Non-Wood Distribution Poles, PG&E Specification No. 60, Pacific Gas and Electric Company, San Francisco, California, January, 1995.

Standard Specifications for Structural Supports for Highway Signs, Luminaires and Traffic Signals, 4th Edition, American Association of State Highway and Transportation Officials, Washington, D.C., 2001.

"Design of Lighting Columns," *Design Manual for Roads and Bridges*, British Standard BD 26/94, British Standards Institute, London, United Kingdom, September 1994.

ANSI C136.20, *Fiber-Reinforced Plastic (FRP) Lighting Poles*, American National Standards Institute, Washington D.C., 1996.

ASTM D4923-01, "Standard Specification for Reinforced Thermosetting Plastic Poles," *Annual Book of ASTM Standards,* American Society for Testing and Materials, West Conshohocken, PA, 2001.

ASTM D635-98, "Standard Test Method for Rate of Burning and/or Extent and Time of Burning of Plastics in Horizontal Position," *Annual Book of ASTM Standards,* American Society for Testing and Materials, West Conshohocken, PA, 2001.

ASTM G154-00a, "Standard Practice for Operating Fluorescent Light Apparatus for UV Exposure of Non-Metallic Materials," *Annual Book of ASTM Standards,* American Society for Testing and Materials, West Conshohocken, PA, 2001.

"Fiberglass Lighting Standards," Caltrans Standard Special Provision 86.08.5, California Department of Transportation, Sacramento, CA, 1995.

Castiglioni, C., and Imbimbo, M., "Experimental Results on Centrifugated GFRP Poles for Electric Lifelines," *Journal of Composites for Construction*, Vol. 3, No. 3, August 1999.

Clarke, J. L., Editor, *Structural Design of Polymer Composites – Eurocomp Design Code and Handbook*, E&F Spon, London, 1996.

Fouad, F. H.; Calvert, E. A.; and Nunez, E.; "Structural Supports for Highway Signs, Luminaires and Traffic Signals," *NCHRP Report 411*, Transportation Research Board, Washington, D.C., 1998.

Polyzois, D.; Ibrahim, S.; and Raftoyiannis, G.; "Performance of Fiber-Reinforced Plastic Tapered Poles under Lateral Loading," *Journal of Composite Materials*, Vol. 33, No. 10, 1999.

Appendix G

Retrofitting and Rehabilitating Fatigue-Damaged Support Structures

TABLE OF CONTENTS

LIST OF FIGURES

LIST OF TABLES

CHAPTER 1. INTRODUCTION

1.1 General

Although few catastrophic fatigue-related failures have been reported, results from the survey conducted during NCHRP Project 17-10(2) revealed that 52% of the states that responded have attributed failure of support structures to fatigue-related causes. Information provided by states indicates a wide range of problems including weld failures at various locations and anchor bolt failures. Furthermore, these problems have been attributed to truck induced vibrations as well as vibrations induced by natural wind.

In order to circumvent fatigue problems, many states have recently adopted sign support inspection programs. The inspection frequency and types of structures inspected widely vary from one state DOT to another. Some DOTs conduct only intermittent inspections while others have adopted a regular inspection program. Also, some states conduct their own inspections while others contract their inspections.

After inspection procedures have indicated problems with the support structure, the owner must decide what action to take. Fatigue repair and retrofitting of existing support structures is one option of mitigating risk. However, the goals and economics of retrofitting may differ from those of new construction. The option of doing nothing and thus accepting the risk of failure, and the option of replacing the structure, may also be considered. This requires that both the importance and degree of vulnerability of the structure be evaluated. Important structures with high vulnerability should be given first priority for retrofitting. Furthermore, because of the difficulty and cost involved in strengthening an existing structure to meet the new design standards and its provisions regarding fatigue, it is usually not economically justifiable to do so unless failure is imminent. For this reason, the goal of retrofitting is often limited to preventing unacceptable failure.

Methods of repair include re-welding, replacing damaged components, and replacing the entire structure. The repair method chosen typically depends on the structure and connection type, as well as the availability of appropriate skill needed to do the repair.

Some states have installed vibration mitigation devices to help dampen excessive vibration. The survey performed under NCHRP Project 17-10(2) indicated that twenty states out of the forty-eight that responded have used or investigated some kind of vibration mitigation devices. Some DOTs use standard dampers or plates. The type of device used is dependent upon the structure type, i.e., lighting poles, cantilevered support structures, aluminum structures, etc.

1.2 Objectives

Because states have encountered problems with sign support structures, and because there is a large variation in inspection, repair, and mitigation practices among states, NCHRP decided that it was necessary to identify characteristics of fatigue-related problems and provide guidance for reducing the risk of failure. This report, therefore, summarizes current inspection, repair, and mitigation practices and provides guidance. The objective of Task 11 of NCHRP Project 17-10(2) was to:

> *"Prepare a manual for retrofitting and rehabilitating fatigue-damaged support structures. It is anticipated that this manual can be developed based on the experience of the states and fabricators. Guidance on repair/replacement decisions shall also be provided."*

1.3 Methodology, Scope, and Applicability

To accomplish the objectives of Task 11, the investigators first collected as much published and publicly available literature as possible regarding the inspection, repair, rehabilitation, and retrofit of sign support structures. Second, states that indicated that they have adopted procedures for inspection, repair, rehabilitation, and retrofit of sign support structures were contacted for additional information. Third, researchers conducting NCHRP Project 10-38(2), "Fatigue-Resistant Design of Cantilevered Signal, Sign, and Light Supports," were visited. Finally, support structure manufacturers were surveyed and representative manufacturers were visited. All relevant information was synthesized in this report.

Unfortunately, the states provided very limited information that could be integrated into a manual. Michigan is one exception. The Michigan DOT provided a set of guidelines and other relevant information that is integrated into this report. Materials obtained from contacts with other state DOTs are also included. NCHRP Report 206 "Detection and Repair of Fatigue Damage in Welded Highway Bridges" and a report by Tubby (1989) from the British Department of Energy entitled "Fatigue Performance of Repaired Tubular Joints" also provided useful information. The original work plan for Task 11 also planned to include relevant finding of NCHRP Project 10-38(2); however, the final report for NCHRP Project 10-38(2) was not available at the time of this writing. Preliminary results provided by the NCHRP Project 10-38(2) researchers were reviewed. As a consequence, the guidelines contained in this report may need to be updated to represent more complete evaluation of fatigue cases and the methods to mitigate fatigue-induced effects and to integrate the final results of NCHRP Project 10-38(2).

1.4 Report Organization

This report is essentially broken into a section on "Inspection," a section on "Repair and Rehabilitation," and a section on "Mitigation." The chapters summarize relevant information

while specific procedures acquired from sources such as the Michigan DOT are provided in the Annex.

CHAPTER 2, "BACKGROUND," presents results of DOT and support manufacturer surveys, summarizes input from contacts, and presents fatigue cases.

CHAPTER 3, "INSPECTION," provides a general inspection and screening procedure for sign and luminaire support structures and summarizes methods for weld inspection.

CHAPTER 4, "REPAIR AND REHABILITATION PROCEDURES," summarizes techniques to extend fatigue life and procedures for repair and rehabilitation of support structures.

CHAPTER 5, "VIBRATION MITIGATION MEASURES," summarizes mitigation methods and discusses the effectiveness of various devices that can be used to reduce vibration.

CHAPTER 6, "SUMMARY, CONCLUSIONS AND RECOMMENDATIONS," summarizes the results and conclusions, and makes recommendations for related additional work.

2. BACKGROUND

2.1. DOT Survey Results

A survey was conducted at the beginning of NCHRP Project 17-10(2) that included questions regarding fatigue related problems and inspection, rehabilitation, and retrofit procedures. Of the forty-eight state DOTs that replied to the survey, twenty-five states reported fatigue-related failure of support structures. Thirty-two DOTs responded that they performed inspection of sign support structures. The inspection frequency and types of structures inspected varies from one DOT to another. Some DOTs conduct only intermittent inspections while others have adopted a regular inspection program. Inspections of fatigue sensitive structures such as cantilevered sign and signal structures, are conducted on one to five year intervals.

The survey was designed to collect information about the actual performance of various types of support structures, fatigue problems encountered by these structures, actions that have been taken, and the use of vibration mitigation devices.

The following two questions were asked regarding the performance of support structures:

QUESTION 1. Has your agency observed any wind damage failures of structural supports designed using current guidelines? To what type of loading or event (wind, truck vibration, etc.) was the failure attributed?

Yes ____ No ____

Loading type:
Wind less than 50 mph_____ Wind more than 50 mph_____
Truck vibration _____ Vehicle impact _____ Other (please specify):

QUESTION 2. Has your agency observed any fatigue-related failures of structural supports designed using 1994 or earlier guidelines? If so, what types of structures?

Yes ____ No ____
Structure type: Overhead cantilever ____ Overhead bridge ____ Roadside sign ____
Street lighting poles ____ High-level lighting poles____Traffic sign supports ____ Span wire supports ____
Other (please specify):

The purpose of question 1 was to identify the reasons for failure and whether it can be attributed to fatigue. The following causes of failure associated with wind could be selected: low-speed wind (less than 50 mph), high-speed wind (more than 50 mph), and truck induced vibration. Twenty-eight out of forty eight replies indicated that failures have been encountered. Eleven replies indicated failures attributed to low-speed wind while five indicated truck induced vibration.

Question 2 was intended to identify susceptibility to fatigue failures of various types of structures. The replies indicated that twenty-five states have had failures that were considered to be fatigue-related. Among these twenty-five replies, twelve were for overhead cantilevered structures, eight for overhead bridge, four for street lighting poles, four for high-level lighting poles and traffic sign supports, and one for span wire supports.

Inspection frequency for various types of support structures were collected from the answers to Question 3 and the following table:

> *QUESTION 3. For the typical support structures listed in the table below, please check those that your agency inspects and the frequency of inspection.*

Structure Type	Not Inspected	Inspected Semi Annually	Inspected Annually	Other (Specify)
Overhead cantilever				
Overhead bridge				
Roadside sign				
Street lighting poles				
High-level lighting poles				
Traffic signal supports				
Span wire supports				

The replies indicated that twenty-nine states perform inspection for overhead cantilever support structures, twenty-eight for overhead bridge, six for roadside signs, five for street lighting poles, twenty-one for high level lighting pole, and seven for both traffic signal supports and span wire supports. Inspection frequency varies significantly from bi-yearly to every five years.

The following two questions were regarding the effort of state DOTs towards repair and retrofitting. Most of the DOTs that replied to these two questions were contacted to obtain additional information.

QUESTION 4. Do you repair fatigue-damaged structures? If so, what methods do you typically use?

Yes ____ No ____
Methods:

QUESTION 5. Have you developed a maintenance plan, set of procedures, or manual for the retrofit and rehabilitation of fatigue-damaged structures? If so, please send a copy to the address on the last page of the survey.

Yes ____ No ____

Thirteen DOTs replied that they repair fatigue-damaged support structures. Some replies indicated that cantilevered VMS structures failed during construction and that they were replaced with overhead structures. Replies also indicated that most of the problems are caused by inappropriate or incorrect fit-up at time of fabrication or improper construction practice. Other replies indicated that rehabilitation processes depend on the structure type. Common actions include drilling holes to halt crack progression, retrofitting to upgrade capacity, and attaching dampers.

Replies regarding repair procedures were general. The methods of repair included re-welding, replacing damaged components, and replacing entire structures. Some DOTs mentioned that the method depends on the structure type and availability of appropriate level of skill. They also mentioned that they have had mixed results from repair. Only the Michigan Department of Transportation provided documentation and details on repair processes. In general, these processes emphasize drilling holes at crack tips and tapering the gusset plate.

QUESTION 6. Has your agency investigated or used any vibration mitigation measures (devices or practices) for support structures? Please send information about any devices used to the address on the last page of the survey.

Yes ____ No ____

Survey results revealed that twenty out of the forty-eight state DOTs used or investigated vibration mitigation devices. The responses indicated that some DOTs use standard dampers or plates. The type of device used is dependent upon the structure material and type, i.e., lighting poles, cantilevered support structures, aluminum structures, etc. The replies were too general to provide good indication about the use and effectiveness of these dampers.

2.2. Manufacturers' Survey Results

Also, a survey was sent to seven leading sign and luminaire support manufacturers that included questions regarding repair, rehabilitation, and retrofit.

Questions:

1. *Have you been involved in the repair of fatigue-damaged structures? If so, what methods do you typically use?*

   Yes ____ No ____ N/A ____
   Methods:

2. *Have you developed a maintenance plan, set of procedures, or manual for the retrofit and rehabilitation of fatigue-damaged structures? If so, please send a copy to the address on the last page of the survey.*

   Yes ____ No ____ N/A ____

3. *If there is a person or persons in your company who can provide additional information on retrofit and rehabilitation of fatigue-damaged support structures, please provide contact information at the end of the survey.*

4. *Have you investigated or used any vibration mitigation measures (devices or practices) for support structures? Please send information about any devices used to the address on the last page of the survey.*

   Yes ____ No ____ N/A ____

None of the manufacturers indicated that they have encountered fatigue problems. Only Union Metal Corporation mentioned they have repaired fatigue-damaged structures. None of the manufacturers indicated that they have a repair plan or procedure. Union Metal and Walpar indicated that they use commercial dampers such as those produced by Alcoa. They also described the use of loads to change the frequency and hence reduce vibrations.

2.3. Contacts Made

Numerous contacts were made to help gather additional information. This includes phone calls to the maintenance engineers of state DOTs, visits with engineers of support manufacturers, contacts with industry involved in inspection and repair, and meetings with other researchers involved in support research.

State DOT's that reported problems attributed to fatigue were contacted. Although significant time and effort was consumed in trying to collect information from state DOTs regarding fatigue cases and repair, very little usable information was found. While states do have procedures to inspect and repair damaged structures, it is not often written in a formalized procedure specific to sign support structures. Also a comprehensive Web search of all state DOT websites was conducted to identify additional contacts regarding sign support structure inspection and maintenance.

Michigan is one exception. The Michigan DOT provided a set of guidelines and other relevant information that is integrated into this report. This includes memorandums, reports to the management about fatigue problems, and procedures for inspection and repair of sign support structures and luminaires. A complete list of the material provided by Michigan is listed in the reference section.

Engineers of the Georgia DOT were contacted for information on fatigue-damaged structures and inspection methods. To the knowledge of the persons contacted, no sign support problems attributed to fatigue have been encountered. The GDOT typically replaces rather than repairs damaged support structures. Structure age and condition plays a role in determining if a given structure is reset or replaced. GDOT also mentioned that problems continue to exist with the inspection of overhead sign structures. A survey of existing cantilevered structures in Georgia revealed a distressing number of anchor bolt deficiencies in particular, such as missing nuts, lock washers, and flat washers, loose nuts, and bolts with less than full thread exposed. These deficiencies could lead to anchor bolt fatigue, cracking, and ultimate failure.

Walpar, Inc., in Birmingham, Alabama was visited to review their fabrication and inspection processes and requirements and to discuss whether any fatigue cases were encountered. The need for inspection after galvanizing was emphasized. One case was described where problems with the weld of small diagonals to chords had occurred. It was emphasized that aluminum structures must have signs installed immediately after construction to prevent damaging vibration. Weld inspection methods varies depending on the standards of the state for which the structure is being produced. Ultrasonic and magnetic methods are used for inspection. Some failure cases were described to be erection or maintenance problems. Walpar provides dampers upon the request of the owner.

The researchers also met with Dr. Raymond G. Thompson from the UAB Department of Materials and Mechanical Engineering to discuss weld inspection methods and repair of fatigue cracks. Dr. Thompson mentioned that the most difficult aspect of weld inspection is locating the end of the crack. He recommended careful and thorough grinding of the crack

before retrofitting. Also, he suggested using dye penetrant after retrofitting to ensure that the crack has been eliminated.

Collins Engineers, Inc. was contacted. Collins has conducted inspections for several states and has written inspection manuals that are used by several states. Investigators of this project requested any relevant information that Collins would be willing to share, but no such information was received at the time of this writing.

The NCHRP Project 10-38(2) investigators met with those of Project 17-10(2) at University of Alabama at Birmingham in July of 2000 to discuss and share relevant activities and findings. The meeting was very productive. Methods to mitigate fatigue-induced effects and inspection and maintenance of support structures as well as VMS design were points of detailed discussion. The damper devices used or developed by the Florida DOT, Wyoming DOT, and Texas DOT, along with their effectiveness in reducing the vibration for galloping and vortex shedding were reviewed. The final results from Project 10-38(2) were not available at the time of this writing.

2.4. Review of Fatigue Cases

The following sections describe specific fatigue cases that were studied.

2.4.1 Michigan DOT Cantilever Sign Structures

Cook *et al.*, (2000) studied the fatigue cracks at the end of the horizontal gussets that were detected in 1996 in Michigan. In September 1996, the Michigan Department of Transportation visually detected fatigue cracks at the end of horizontal gusset plates on cantilever sign structures as shown in Figure 2.1. The ends of the horizontal gusset plate at the vertical pole connection of approximately 1100 cantilevers sign structures were visually examined for signs of fatigue cracking between April 1997 and July 1998. It was found that, of approximately 1100 cantilever structures inspected, 76 were found to have visual cracks in the galvanizing at one or more of the four horizontal gusset plate connections. After visual examination, 209 ends of horizontally gusset plate connections were ultrasonically inspected to determine fatigue crack severity. In 1998, several cantilever sign structures were removed from service as a result of fatigue cracks at the end of horizontal gusset plate to vertical pole connection confirmed by ultrasonic testing.

Visual inspections were performed on 108 cantilevers held at the maintenance yard for storage and future disposal. Eight of the 108 cantilevers inspected had visual cracks in the galvanizing at the end of the horizontal gusset plate. Fourteen horizontal gusset plate connections were removed and analyzed for fatigue cracks. Nine of the fourteen horizontal gusset plate connections revealed signs of fatigue striations below the galvanizing coating into the 10 mm (3/8-inch) thick pipe wall. Cracks varied from hairline to complete fatigue fracture through the 10 mm (3/8-inch) pipe wall. A typical fatigue crack is shown in Figure 2.2 where the pipe wall at the end of the horizontal gusset plate is broken to expose the

fatigue crack. The end of horizontal gusset plate is at the top of the figure. Note the upper and lower are mating surfaces.

Cantilevers that predominantly show signs of fatigue cracking at the horizontal gusset plate connections have an upper and lower chord forming a truss arm for sign mounting. There are four possible locations where fatigue cracks initiate, one at each of four horizontal gusset plate terminations where the arm attaches to the vertical pole. The length of these arms from the centerline of the vertical pole to the end of the sign panel is either 10.7 or 14 m (35 or 46 feet), depending on the type of sign structure. The vertical pole centerline coincides with the end of the horizontal gusset plate connection.

2.4.2 Michigan DOT Sign Support Trusses on the Zilwaukee Bridge

A description of fatigue cases was found in an office memorandum dated October 1996 that investigate cracking of sign support trusses on the Zilwaukee bridge. Five aluminum trusses with a span length between 73 and 76 feet exhibited cracked members. The personnel who performed the inspection stated that the vertical members sustained the most cracking, followed by wind bracing between front and back trusses, the diagonals, and the chords. There were few cracks in the chord members. Many of the cracks occurred at intersecting/overlapping welds. Cracking generally appeared on the side of the member toward the interior of the truss box section. More cracking occurs in the members away from the sign panel compared with near the sign panel.

2.4.3 Cracks Due to Galvanizing

During a visit to Walpar, Inc., in Birmingham, Alabama, Walpar engineers stressed the need for a careful inspection after galvanizing. The engineers demonstrated that cracks sometimes formed after galvanizing, especially when there is a big difference between member sizes such as where small web members are attached to large chord members.

Figures 2.3 and 2.4 show examples of these cracks. As the structure is galvanized, the members are exposed to very high temperature. During cooling, the members will contract at varying rates. This encourages the formation of cracks at points of high stress concentration such as at the tip of the weld of the angle to chord (Figure 2.3) and where the web pulls the chord out (Figure 2.4).

2.4.4 Wyoming DOT Traffic Signal Structures

Due to the collapse of two traffic signals in Wyoming, the University of Wyoming conducted research on the fatigue and vibration problems associated with traffic signals structures (Puckett *et al.* 2001). The failures are believed to be due to fatigue, as the failures did not take place during high-wind event. The cause of the collapse was described as a fracture between the cantilever signal light support arm and the pole. This was confirmed by the

Wyoming Department of Transportation. A test pole, which was originally located in Cheyenne, WY, was supplied by WYDOT. The pole was removed from service and reassembled by WYDOT personnel at the maintenance yard located in Laramie, WY, for further study. Figure 2.5 shows a fatigue crack along the side of the post. The fatigue crack initiated at the weld of the side plate to the post due to the excessive vibration of the arm. The crack caused the failure of the structure at the arm/post connection in Wyoming (Puckett *et. al.* 2001).

2.4.5 Wisconsin DOT Support Structures

In a paper presented in Structural Materials Technology IV NDT Conference, Fish (2000) of the Wisconsin DOT described failures on support structures. Fish described three types of support structures that have had problems.

1. In 1990, anchor bolt failure occurred on 150-foot high mast light poles. The anchor bolt failures were found before the poles tipped over. All anchor bolts on high mast light poles, overhead sign bridges, and cantilever sign structures are inspected visually and with ultrasonic inspection every four years.

2. Serious cracking was discovered in some overhead sign structures in 1994. The structures were welded aluminum and steel truss type structures. The cracks found were fatigue type cracks in critical locations on main load carrying members and cracks in vertical members that filled with water and frozen in winter months. These structures were inspected with the primary inspection procedure of visual inspection, supported by nondestructive evaluation of cracks. Nondestructive methods included ultrasound, magnetic particle, dye penetrant, and acoustic emission. This inspection program found several structures with critical member failure resulting in immediate removal from service. Other conditions found by the inspection include: cracked welds at truss diagonal connections to main chords, incorrectly assembled truss sections, truss splice connection bolts missing or failed.

3. In 1998, three failures of 50-foot high light poles occurred in the Milwaukee metropolitan area at a time of high winds. More than 700 similar poles were inspected as a result. The inspection procedure was nondestructive testing with a testing gauge to measure for section loss, supported by visual inspection. Several poles were removed under emergency procedures that had cracks exceeding 50% of the circumference.

2.5. Other Relevant Literature

Tubby (1989) obtained fatigue data for tubular T-connections that are similar to sign support structure details. These connections were tested in out-of-plane bending after they had been repaired for fatigue precracking. A number of repair methods were investigated including repair welding and crack retardation by hole drilling and cold expansion and removal of part-wall cracks by grinding without subsequent rewelding. They concluded that the last two

methods could be effective especially if they avoid the expense and difficulty of making weld repair.

NCHRP Report 206 “Detection and Repair of Fatigue Damage in Welded Highway Bridges” was studied. Techniques to increase the fatigue life of welding and the inspection methods that were used to detect fatigue cracks were reviewed. Other relevant references such as the AWS handbook “Fundamentals of the Welding Process,” ASM Vol. 17 “Nondestructive Testing” and the “Structural Welding Code” (1994) were reviewed.

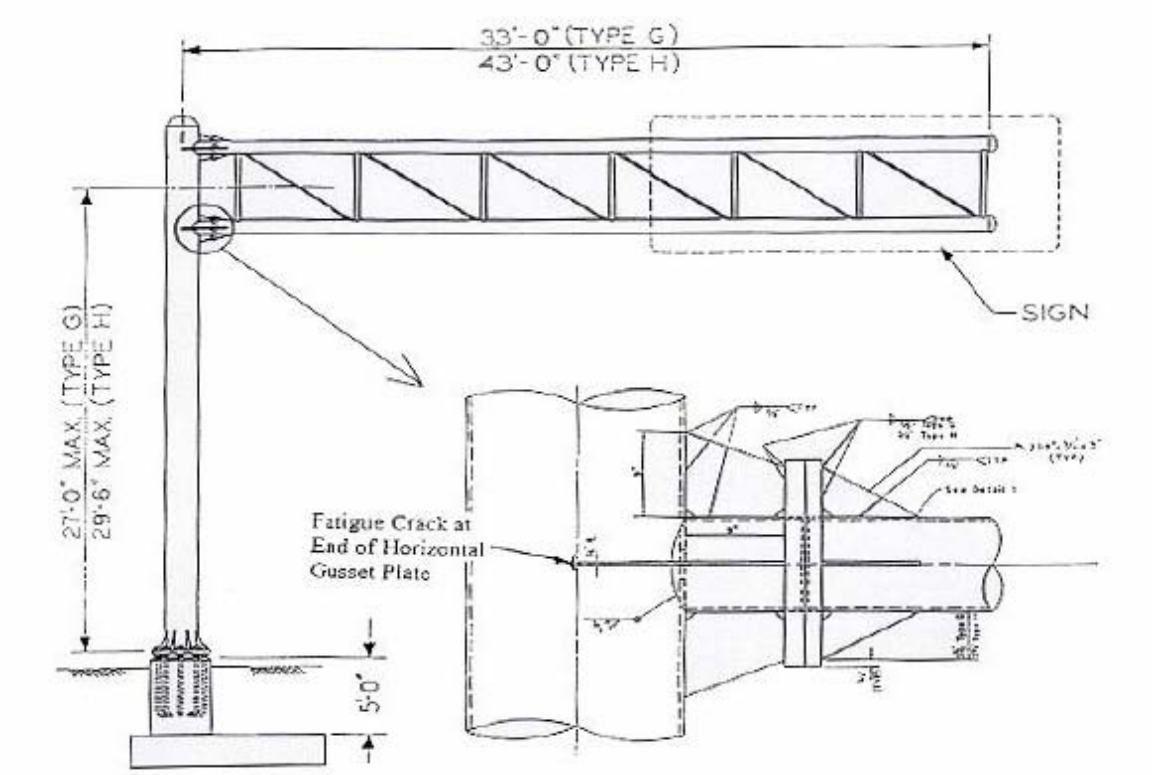

Figure 2.1. Details of Horizontal Gusset Plate to Vertical Pole Connection of Cantilever Sign Structure and Crack Location
Cook *et al.* (2000)

Figure 2.2. Fatigue Crack at End of Horizontal Gusset Plate Connection.
Cook *et al.* (2000)

Figure 2.3. Crack Formed at the End of the Weld of an Angle to the Chord Member During Galvanizing

Figure 2.4. Crack Formed at the Connection of Small Diagonal Members to a Big Chord Member During Galvanizing

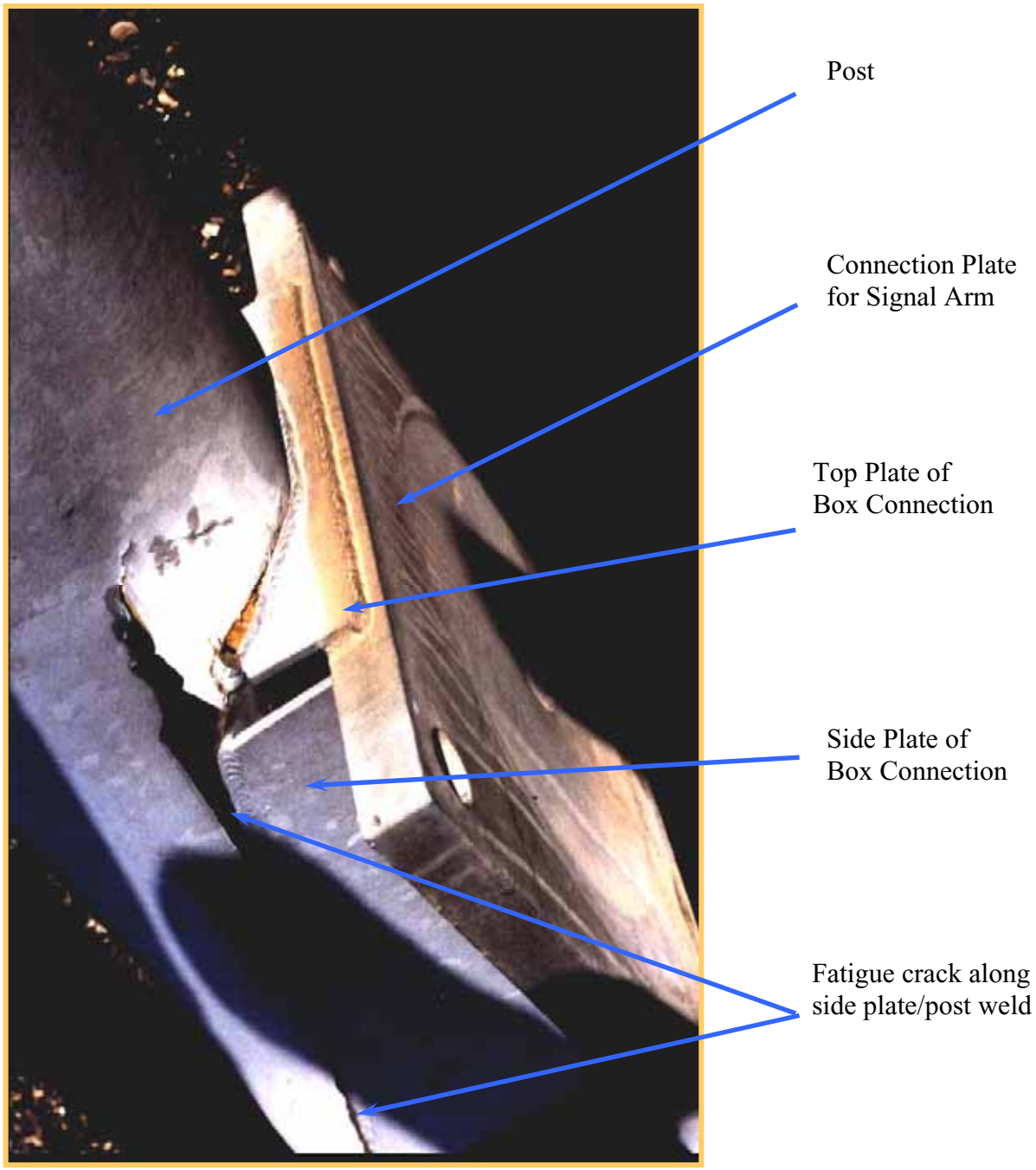

Figure 2.5. Fatigue Crack Along Side Plate/Post Weld of Traffic Signal Support Structure (Puckett, 2001)

3. INSPECTION

This chapter summarizes inspection procedures for high mast luminaires and sign support structures. The standards and procedures for the inspection of sign and luminaire support structures currently being used by state DOTs vary greatly. Because of the lack of written information available from state DOTs, this information is largely based upon procedures adopted by the Michigan Department of Transportation. This chapter provides an overview of methods, while detailed procedures are provided in the annex. This information can also serve as a start for the development of inspection procedures by state DOTs.

3.1. Inspection of High Mast Luminaires

High mast luminaires (HML) are 24.4 to 61 meter (80 to 200 ft) tall lighting structures assembled by telescoping and welding three or more individual sections. The cross-section of the poles is typically circular or 12-sided. Each HML pole is topped with a fixture ring containing a group of four to eight individual lighting heads. High mast luminaires are illustrated in Figure 3.1.

The Michigan DOT conducted an investigation (Isola *et al.,* 1996) after reviewing reports from Maryland, Indiana, and Illinois DOTs regarding fatigue of HMLs. Major areas of problems were identified. This section provides a general description of the fatigue-related problems. Annex A provides an example of a procedure obtained from Michigan DOT that can be used in inspection of HMLs. The annex also provides a sample procedure for tightening the anchor bolt nuts.

3.1.1 Cracks in the Longitudinal Weld

Michigan found that 27% of their high mast luminaires had developed longitudinal cracks. These cracks usually occur at the telescoping joints with a length that varies between 24 mm and 432 mm (1 and 12 inches). One crack was found in the longitudinal weld away from the telescoping end. The crack, shown in Figure 3.2, was 430 mm (17 in) long.

3.1.2 Partial Penetration Weld in the Telescoping Joint

Partial penetration welds in the telescoping joint area were found by the Michigan DOT for numerous HML Poles. Cracks in partial penetration welds can be detected by ultrasonic testing. Partial penetration welding can contribute to an increasing probability of cracking.

3.1.3 Corrosion

The Michigan DOT found that potentially corrosive situations exist on nearly all HML Poles, particularly near the base. Ultrasonic thickness measurements were taken to verify the remaining metal thickness at the base of each structure. Corrosion can take place from the inside or outside of the pole.

Site conditions can promote external corrosion. The two most extreme conditions noted were: (1) HML Poles located adjacent to the roadway and exposed to salt spray (see Figure 3.3) and (2) HML Poles located in low-lying areas, such as ditch lines and median depressions, which are typically covered with soil and gravel (see Figure 3.4).

Bases, when completely sealed, allow water buildup on the inside of the structure. This situation initiates corrosion from the inside of the pole due to moisture that condenses and collects at the base. Significant levels of corrosion may develop from inadequate air circulation needed to keep the bases dry.

3.1.4 Anchor Bolt Nuts

High mast luminaires typically have a four or six anchor bolt pattern on a 381.0 to 736.6 mm (15 to 29 inch) bolt circle. Inspection includes sounding the nuts for tightness as well as ultrasonic testing to determine if the anchor bolt is flawed. Tack-welded anchor bolt nuts, for the purpose of locking the nut to the anchor rod and base, are often found on HML (see Figure 3.5). Tack welds create high stress concentrations between the anchor nut and base and eventually break loose. Therefore, according to the Michigan DOT, tack welds should not be used.

3.1.5 Bending

The Michigan DOT indicated that nearly all HML inspected exhibited minor bending due to out-of-vertical alignment. This out of alignment is typically 0.3 to 0.61 meters (1 to 2 feet) at the top of the pole. Four HML were found by Michigan DOT to have bending in excess of 1.22 meters (4 feet) (see Figure 3.6). The problem structures were installed by Michigan DOT and have a significantly smaller cross section at the top of the structure than the remaining HML population. These HML may be susceptible to weld cracks due to high tensile stress in the telescoping joint areas and must be closely monitored.

3.2. Inspection of Sign Structures

Sign support structures can be classified into cantilevered sign support structures and bridge support structure. As a result of two cantilever sign base failures, a plan was devised to ensure a high level of confidence in the safety of sign structures (Culp, Witteveen, and Wong (Michigan DOT) 1990). Soon after these two failures, an inspection program was

implemented to identify other structures at risk. The 1990 report mentioned that Michigan DOT will participate in a program to determine the national extent of the problem and the need to change the design code to consider fatigue regarding cantilevered sign support structures.

This section provides a general description of the fatigue-related problems associated with sign structures. Annex B provides an example of a procedure obtained from Michigan DOT that can be used in inspection of these structures. Also, Annex B provides a sample procedure for tightening the anchor bolt nuts.

The following major problem areas were identified for cantilevered support structures:

1. Anchor bolt cracking due to improper construction practices, severe corrosion, and fatigue of the rods caused by loose anchor nuts; and

2. Fatigue cracking of horizontal gusset plates at arm-to-pole connection of cantilever sign structures.

The following problem areas were identified for noncantilevered (bridge-type) support structures:

1. Bottom chord cracks found in the middle half of the truss box span.
2. Cracks in the chord flange connection plate welds.
3. Cracks in the fillet weld at the bottom chord greater than or equal to 25mm (1 inch) long or perpendicular to the chord.
4. Cracks originating in a web member, parallel to the web member, and extending into the fillet weld at the bottom chord.
5. Cracks or blowouts in the web members in the middle half of the truss box span.
6. Web member cracks or blowouts in the end quarter of the truss box span that are parallel to the web member.
7. Cracks in the fillet weld at the web member-bottom chord intersection when its length is less than 25 mm (1 inch) and parallel to the chord.
8. Cracks or blowouts in wind bracing that do not extend into the wind bracing-bottom chord weld inspection.

3.3. Weld Inspection Methods

A variety of inspection methods can be used to inspect the support structure welds. The weld inspector should be Level II ASTM certified. This section describes the types of weld faults that can be found by visual inspection. It then introduces other methods used for inspection such as ultrasonic testing, Eddy current, magnetic particles, and dye penetrants. The information provided in this section was obtained from several contacts and collected from

the websites of agencies such as Georgia DOT (Fry, 2000), FHWA (Lamtenzan *et al.*, 1997), and the NCHRP Project 10-38(2) research team (Puckett *et. al* 2001).

3.3.1 Visual Inspection

The Georgia DOT Testing Bureau provided information related to the inspection of support structures and the inspection of fatigue cracks. The material provided in this section was obtained from the Georgia DOT web site.

Visual examination can be an invaluable tool when properly applied to locate surface flaws and imperfections. Cracks form in the weld and base metal when localized stresses exceed the ultimate strength of the material. Cracking may occur at elevated temperatures during weld metal solidification, or may occur after solidification after the weldment has equalized in temperature. Cracking is generally associated with stress amplification near discontinuities in welds and base metal or near notches associated with the weld joint design. High residual stresses are generally present, and hydrogen embrittlement is often a contributor to crack formation. Welding-related cracks are generally brittle in nature, exhibiting little plastic deformation at the crack boundaries. There are various types and locations of weld zone cracks, some of which will not be visible during visual examination of the weld surface.
Cracks can be classified as either hot cracks or cold cracks. Hot cracks develop at elevated temperatures. They form on solidification of the metal at temperatures near the melting point. Cold cracks develop after solidification is complete. Cracking associated with hydrogen embrittlement, commonly referred to as "delayed cracking," is a form of cold cracking. Hot cracks propagate along grain boundaries. Cold cracks propagate both along grain boundaries and through grains. Figure 3.7 plus the following definitions illustrate types of weld cracks and discontinuities. Figure 3.7 plus the definitions were obtained from a presentation of the basics of visual inspection for welded structures that was found on the web page of the Georgia DOT bridge division.

Throat Cracks - Throat cracks are longitudinal cracks in the weld face in the direction of the weld axis. They are generally, but not always, hot cracks.

Root Cracks - Root cracks are longitudinal cracks in the weld root. They are generally hot cracks.

Crater Cracks - Crater cracks occur in the weld crater and are formed by improper termination of the welding arc. A nonstandard term for crater cracks is star crack though they may have other shapes. Crater cracks are shallow hot cracks usually forming a multi-pointed star-like cluster.

Toe Cracks - Toe cracks are generally cold cracks. They initiate and propagate from the weld toe where restraint stresses are highest. Abrupt profile changes at the toe caused by excessive convexity or weld reinforcement can amplify stresses, making the weld toe a more likely area for cracking to occur.

Toe cracks initiate approximately normal to the base metal surface. These cracks are generally the result of thermal shrinkage stresses acting on a weld heat affected zone. Some toe cracks occur because the transverse tensile properties of the heat affected zone cannot accommodate the shrinkage stresses that are imposed by welding.

Heat Affected Zone Cracks - Underbead and heat affected zone cracks are generally cold cracks that form in the heat-affected zone of the base metal. Underbead and heat affected zone cracks can be either longitudinal or transverse. They are found at regular intervals under the weld and also outline boundaries of the weld where residual stresses are highest. Underbead cracks can become a serious problem.

Incomplete Fusion - Incomplete fusion is termed as fusion that does not occur over the entire base metal surfaces intended for welding and between adjoining weld beads. It can result from insufficient heat input or the improper manipulation of the welding electrode. While it is a discontinuity more commonly associated with weld technique, it could also be caused by the presence of contaminants on the surface being welded.

Undercut - Undercut creates a transition that should be evaluated for a reduction in cross section, and for stress concentrations or notch effect which fatigue is a consideration. Undercut, controlled within the limits of the specification, is not usually considered a weld defect. Undercut is generally associated with improper welding techniques or weld parameters, excessive welding currents or voltages, or both.

Overlap - Overlap is the protrusion of weld metal beyond the weld toe. It can occur as a result of poor control of the welding process, improper selection of the welding materials, or improper preparation of materials prior to welding.

Incomplete Joint Penetration - Incomplete joint penetration is defined as penetration by weld metal that does not extend for the full thickness of the base metal in a joint with a groove weld. The condition shown for the single V-groove weld will only be evident using visual examination if there is access to the weld root side. The condition shown on the double bevel T-joint will not be evident on the completed weld, except at the starts and stops.
Incomplete joint penetration may result from insufficient welding heat or improper lateral control of the welding arc. Many designs call for back gouging the weld root with subsequent welding on that same side to ensure that there are no areas of incomplete joint penetration or incomplete fusion.

Spatter - Spatter consists of metal particles expelled during fusion welding that do not form a part of the weld. Those particles that are actually attached to the base metal adjacent to the weld are the most disconcerting form of spatter. Particles that are thrown away from the weld and base metal are, by definition, spatter. In total, spatter is particles of metal that comprise the difference between the amount of filler metal melted and the amount of filler metal actually deposited in the weld joint. Normally, spatter is not considered to be a serious flaw unless its presence interferes with subsequent operations, especially nondestructive testing.

Arc Strikes - An arc strike is a discontinuity consisting of any localized remelted metal, heat-affected metal, or change in the surface profile of any part of a weld or base metal resulting from an arc. Arc strikes result when the arc is initiated on the base metal surface away from the weld joint, either intentionally or accidentally. When this occurs, there is a localized area of the base metal surface that is melted and then rapidly cooled due to the massive heat sink created by the surrounding base metal. Arc strikes are not desirable and often not acceptable, as they could lead to cracking during the cooling process or under fatigue conditions.

Slag Inclusion - Slag inclusions are nonmetallic solid material entrapped in weld metal or between weld metal and base metal. Slag inclusions are regions within the weld cross-section or at the weld surface where the once-molten flux used to protect the molten metal is mechanically trapped within the solidified metal. This solidified slag represents a portion of the weld's cross-section where the metal is not fused to itself. This can result in a weakened condition that could impair the serviceability of the component. Inclusions may also appear at the weld surface. Like incomplete fusion, slag inclusions can occur between the weld and base metal or between individual weld passes. In fact, slag inclusions are often associated with incomplete fusion.

3.3.2 Ultrasonic and Sonic

Striking a specimen and listening for the characteristics "ring" has been used as a means of detecting flaws. The ringing note emitted by a steel specimen containing a crack is dull and harsh compared with the note emitted by identical "good" specimen. This "ringing" technique will detect only gross defects. The wavelength of audible sound waves is generally large in comparison of the size of the defect, and the sound travels around the defect.

With the development of reliable methods for generating and detecting ultrasonic waves, small defects can now be found. This is due to the fact that the wavelength of the ultrasonic waves is approximately equal to the size of the defects to be found. Fortunately, most metals readily transmit ultrasonic vibrations because of their good elastic properties. If discontinuities exist, a measurable scattering or reflection will occur because the acoustic mismatch. Figures 3.8 and 3.9 show the transducers used for ultrasonic testing during research conducted by University of Wyoming.

3.3.3 Magnetic Particles

Inhomogeneities such as cracks and inclusions in a magnetic material produce a distortion in an induced magnetic field. The path of the magnetic flux is distorted because the inhomogeneities have different magnetic properties than the surrounding material.

Basically, magnetic particles testing is comprised of two steps - magnetization of the material and application of magnetic particles. The finely divided magnetic particles or powder can be either dry or suspended in liquid. The surface must be clean, dry and free of slag or rust. Wire brushing or sand blasting will usually clean the surface sufficiently.

Surface defects usually produce powder patterns that are sharp and tightly held with a heavy build-up of powder pattern. Subsurface defects usually give less sharply defined powder pattern since the powder is less tightly held. Figure 3.10 shows the application if magnetic particles method for detecting cracks.

3.3.4 Eddy Current Method

The information presented here was obtained from a FHWA technical report by Lamtenzan *et al.* (2000). Eddy Current (EC) is a noncontact method that provides instantaneous test results. Its small, portable components are available at low cost. These characteristics make the EC method appropriate for field-testing. Lamtenzan concluded that the EC method effectively detects cracks in weld metals that have irregular surfaces and magnetic properties that vary spatially. They also concluded that the EC method penetrates paint coating.

Eddy currents are induced when an energized probe coil is placed near the surface of a conductive material. The currents are proportional to the electrical conductivity of the material itself. Figure 3.11 illustrates the current induced in a metal surface oscillate in a circular pattern, flowing in a direction opposite to the current in the coil. Eddy currents induced at the surface of a test material are of a certain magnitude and phase and vary with time. Discontinuities, such as cracks disturb the trajectories of the eddy current and thus affect the magnitude and the induced current. The probe senses the magnetic field induced by currents that produce a complex voltage in the coil. The probe consists of two circular coils with axes parallel to the surfaces and perpendicular to each other. A sketch of the probe configuration is shown in Figure 3.12.

In the event that both coils are simultaneously affected by the same material conditions, there will be no signal, meaning the bridge is balanced. Any electromagnetic condition that is not common to the areas of specimen being tested will produce an imbalance in the system and will be detected. The maximum probe response is observed when the crack is perpendicular to the direction of either winding coil. The minimum probe response occurs when the crack is at 45 angle from the direction of either winding coil. The probe frequency range is 100 to 800 kHz.

Four scans were performed on the crack surface to attenuate the noises observed with the variations in magnetic permeability. The data set collected were arranged to overlap the maximum points of the four scan signal inclusions. Cracks profiles were then estimated by calculating the mean of the data samples. Figure 3.13 shows crack profiles for specimens. The percent change in inductive resistance signal increases along with the depth of the defect.

3.3.5 Penetrants

Penetrant inspection is a nondestructive testing method that can be used for the detection of surface discontinuities or flaws that extend to the surface. The use of penetrants can be considered as an extension to the visual inspection. Penetrants make the inspection much less dependent on the human element, and thus increase the reliability and speed of inspection. The primary limitation and disadvantage of penetrant inspection is that only surface defects that are open to the surface are revealed. All defects found by use of penetrants give only an approximate indication of the depth and size of the flaw. The defects must behave as capillaries to draw in the penetrant and retain it after the excess material has been removed.

The simplest and oldest penetrant test is the oil and whitening test. Penetration oil such as kerosene is applied to the surface to be inspected. After allowing enough oil sufficient time to penetrate any surface defects, the excess oil is completely removed and the surface thoroughly dried. A thin coating of whiting (calcium carbonate) either as dry powder or mixed with alcohol is applied to the surface. When dry, the whiting has nearly the same refractive index as the oil. After a period of time, the oil seeps out of the defects into the whiting causing an appreciable reduction in whiting. A hammer can be used to help force the oil out of the minute cracks.

The basic steps in penetrant inspection are

1. Cleaning the surface

It is essential that the specimen surface to be free of dirt, lint, wax, paint, grease, scale, or any other material which will fill or clog the surface openings. Penetrant held by dirt or any other material on the surface can give false indication. Liquid solvents, vapor blasting, vapor degreasing, and acid etching can be used to prepare the surface properly. Sand blasting is not recommended for cleaning the surface, since it has a tendency to close up small surfaces. Scale is best removed by vapor blasting, which will not cover or close up existing defects. Any operation that tends to bridge over the flaws should not be performed.

2. Applying the penetrant

The penetrant is applied to the surface of the test object by immersion, brushing, or spraying. Spraying gives a more uniform coat of material. Because of low surface tension, penetrant is

rapidly drawn into small surface openings by capillary action. If the surface of the specimen object is warm when the penetrant is applied, better results will be obtained because the surface openings will be slightly expanded and therefore more easily penetrated.

Specimens are sometimes heated and then immersed in cooler penetrant. The drop in temperature causes a low pressure area in the defect. This pressure differential may aid in drawing penetrants into the defects. The penetrant is allowed to remain on the surface for a period of time that depends on material, type and size of defects, and type of penetrant used.

3. Removing the excess penetrant

All traces of penetrant must be removed from the surface of the specimen, using tap water or a solvent recommended by the manufacturer. Removing excess penetrant is a critical operation. Too much washing may remove the penetrant from the flaws and insufficient washing will leave penetrant on the surface. The specimen is then dried by a hot-air dryer, by blasting clean dry air, or simply by standing in the air.

4. Applying the developer

Developer is applied to the dried surface. The developer usually consists of finely divided powder such as talc. The purpose of the developer is to draw the penetrant from the defect by blotting action and spread it on the surface of the test object for a small area around the defect. The rate of seepage out of the defect may be improved by heating the part. Striking or vibrating the specimen aids in forcing the penetrant out of the defects.

Two kinds of developer are used, a dry developer and a wet developer. Dry developer may be applied with a spray bulb or powder gun, or by digging small parts in the powder. It has a tendency to build up in any complex contours of the specimen. Wet developer consists of a powder suspended in a volatile or quick-drying liquid. Wet developer may be applied by dipping or spraying. Care must be used in applying wet developer, too sparingly will not cover the entire surface - too liberally will wash out the penetrant. Hot air is recommended for drying the wet developer.

5. Inspection and Interpretation

This is the most important operation in the entire procedure. The type and thickness of the developer coating determines the minimum size that is detectable. A thick coat will not reveal small defects. Dry developer will enable detecting the minimum defect sizes. The interpretation of the characteristic patterns indicating the types of flaws is of extreme importance. A crack or a cold shot will be indicated by a line of penetrant. Dots of penetrant indicate pits or porosity. A series of dots indicates a tight crack, cold shot, or partially welded lap. A rough estimate of the opening may be estimated by the width of the indication or spreading of the penetrant on the developer.

Figure 3.1. High Mast Luminaire Structure

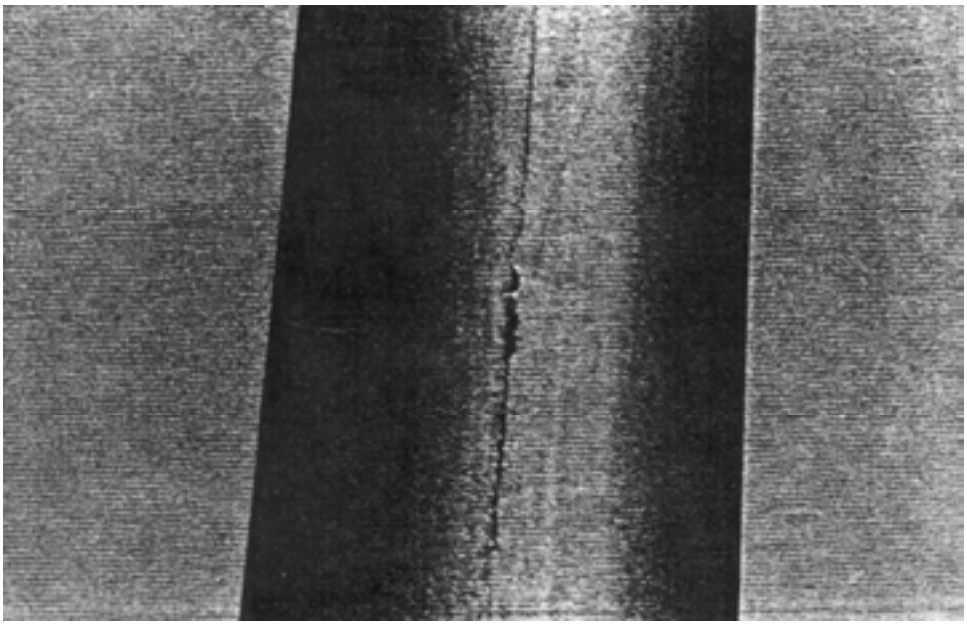

Figure 3.2. Crack Along the Longitudinal Weld of an A-588 Weathering Steel Pole Isola *et al.* (1996)

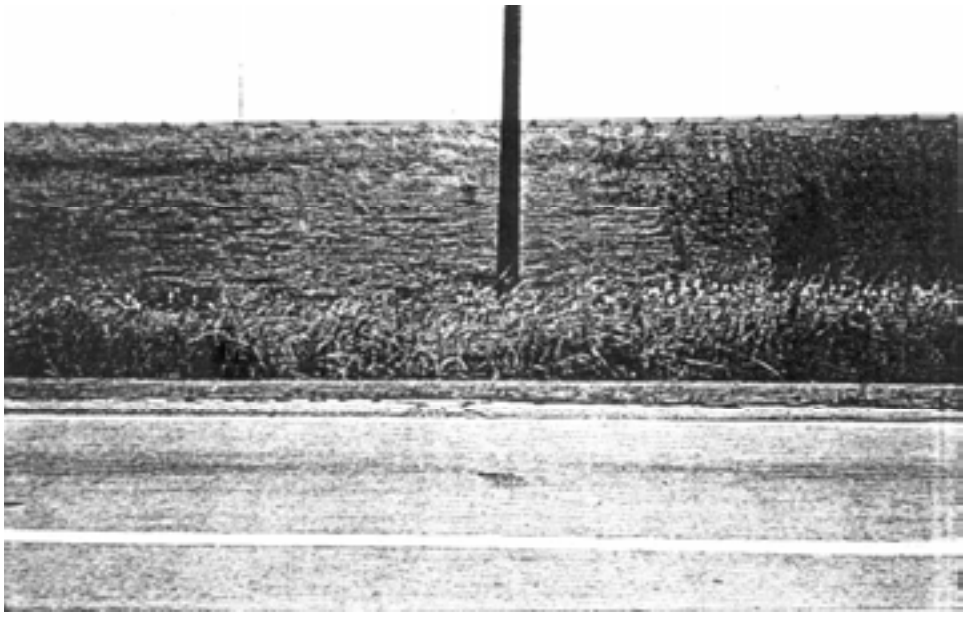

Figure 3.3. HML Located Adjacent to Roadway and in Ditch Line
Isola *et al.* (1996)

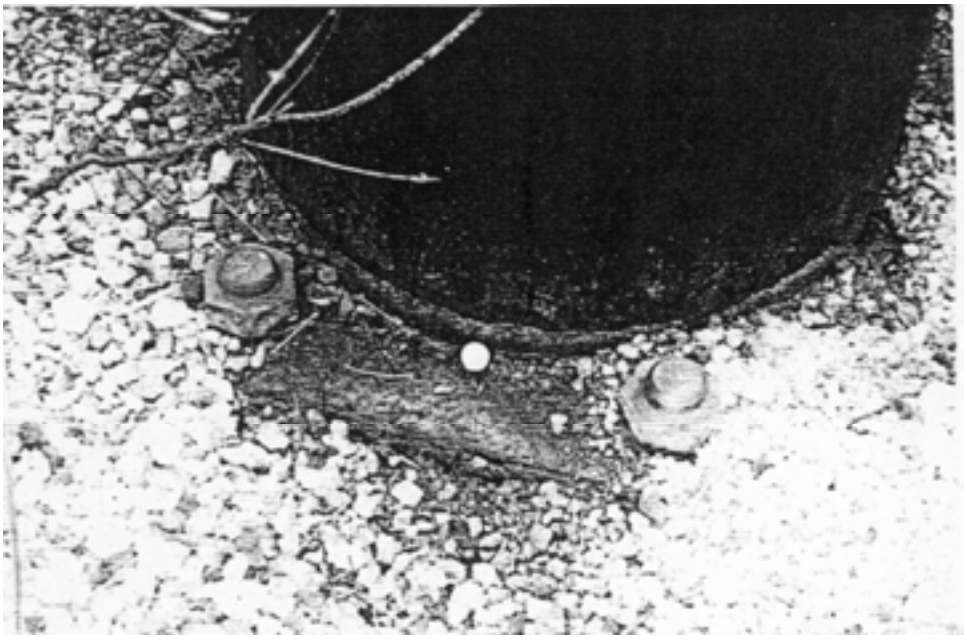

Figure 3.4. HML Located in Ditch Line Covered with Soil and Gravel
Isola *et al.* (1996)

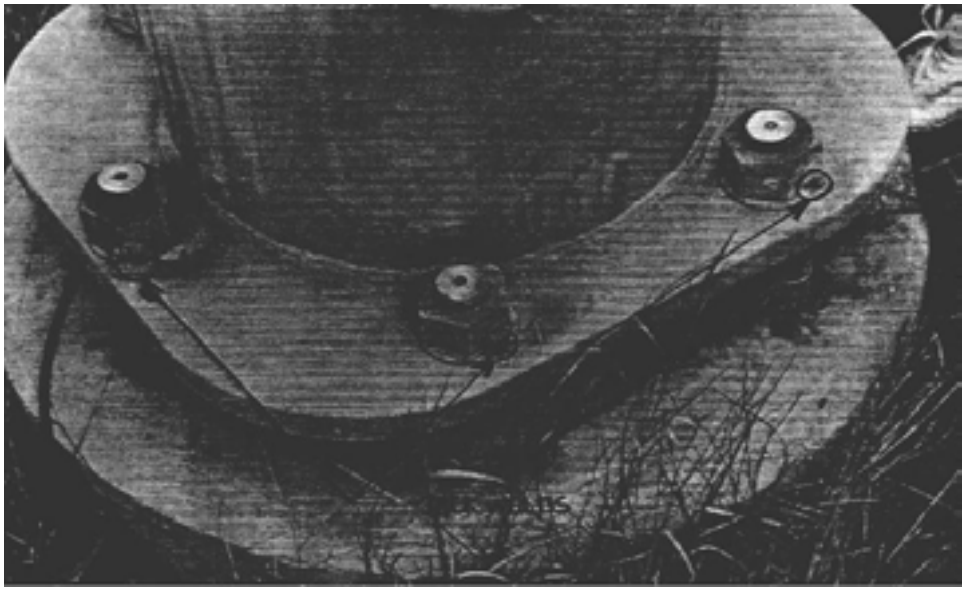

Figure 3.5. Tack Weld on Anchor Bolt Nut
Isola *et al.* (1996)

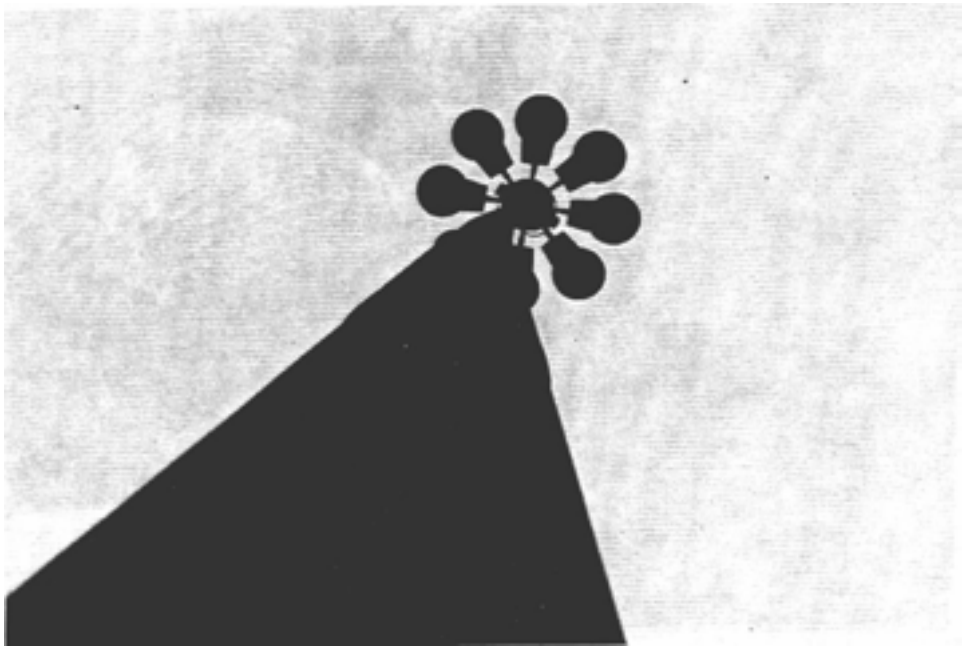

Figure 3.6. Severe Bending at Top of HML Pole
Isola *et al.* (1996)

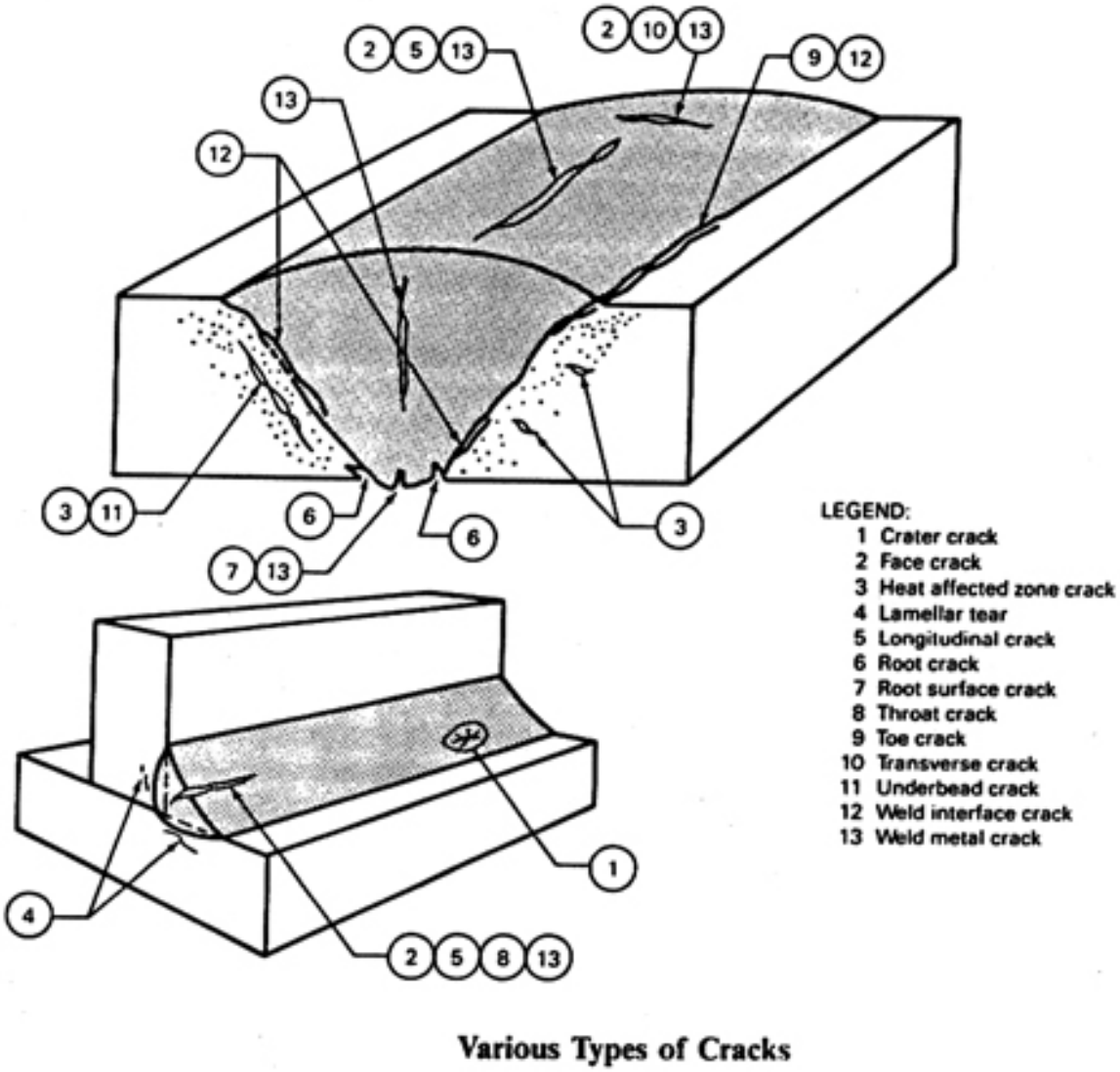

Figure 3.7. Types of Weld Cracks and Discontinuities (Georgia DOT 2000)

Figure 3.8. Ultrasonic Testing
Puckett *et al.* (2001)

Figure 3.9. Acoustic Emission
Puckett *et al.* (2001)

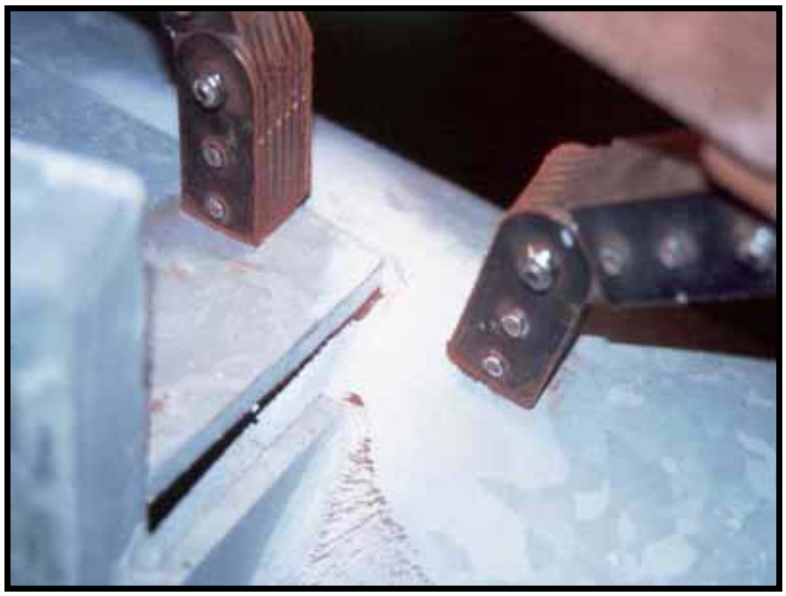

Figure 3.10. Magnetic Particles Testing
Puckett *et al.* (2001)

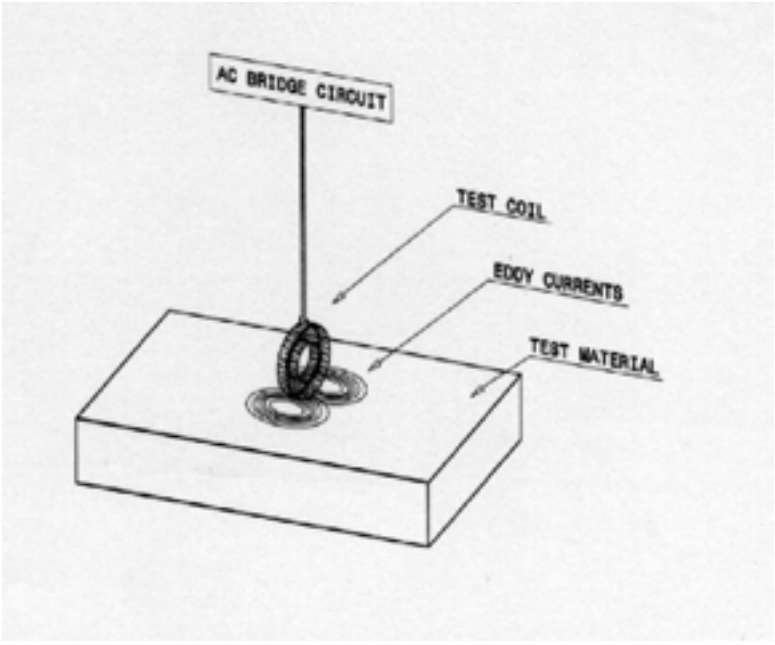

Figure 3.11. Induced Eddy Currents for a Coil with an Axis Parallel to the Surface
Lamtenzan *et al.* (1997)

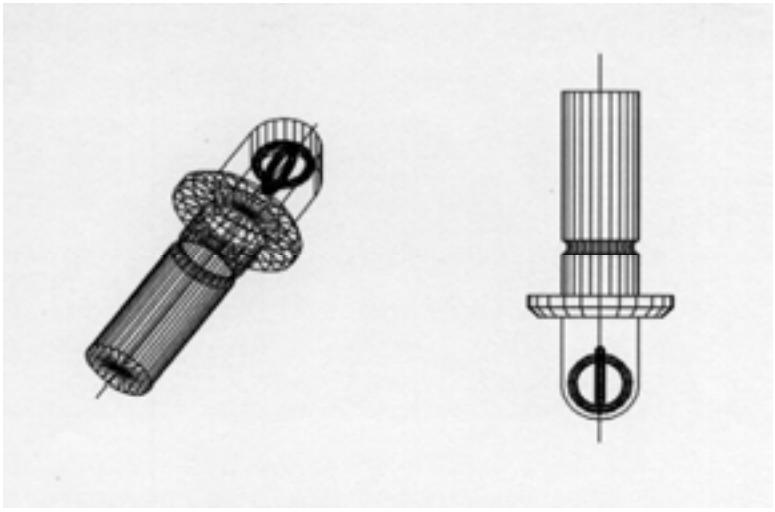

Figure 3.12. Plus-Point Probe Arrangement
Lamtenzan *et al.* (1997)

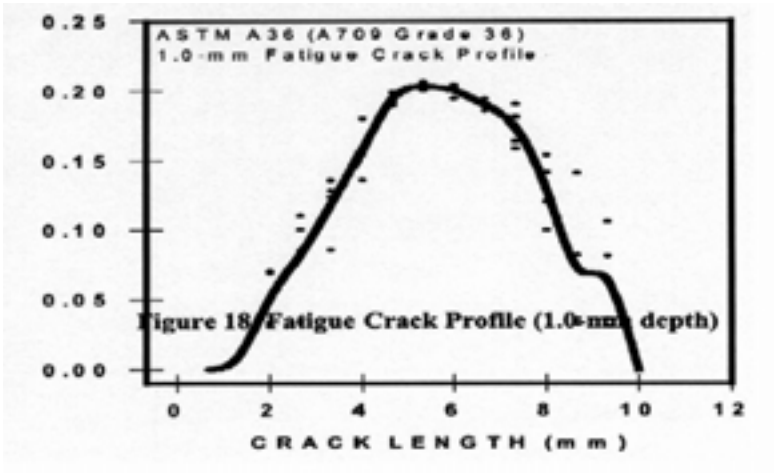

Figure 3.13. Fatigue Crack Profile
Lamtenzan *et al.* (1997)

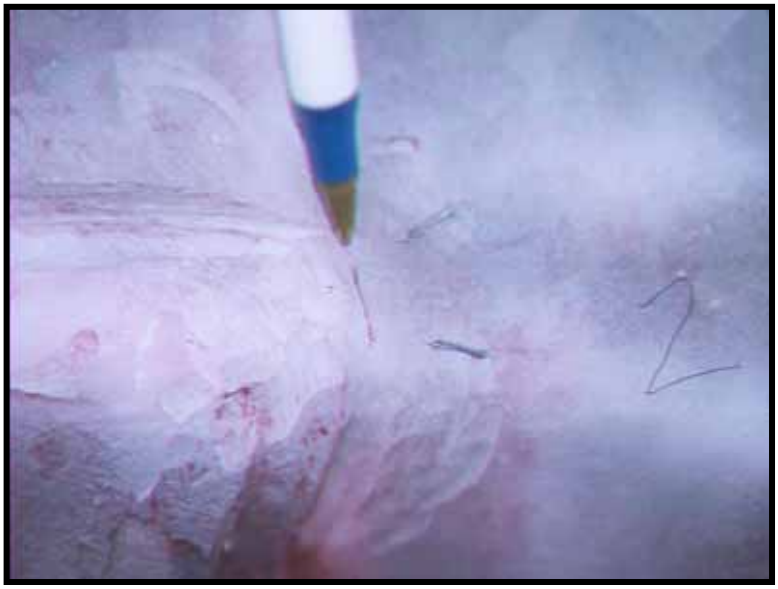

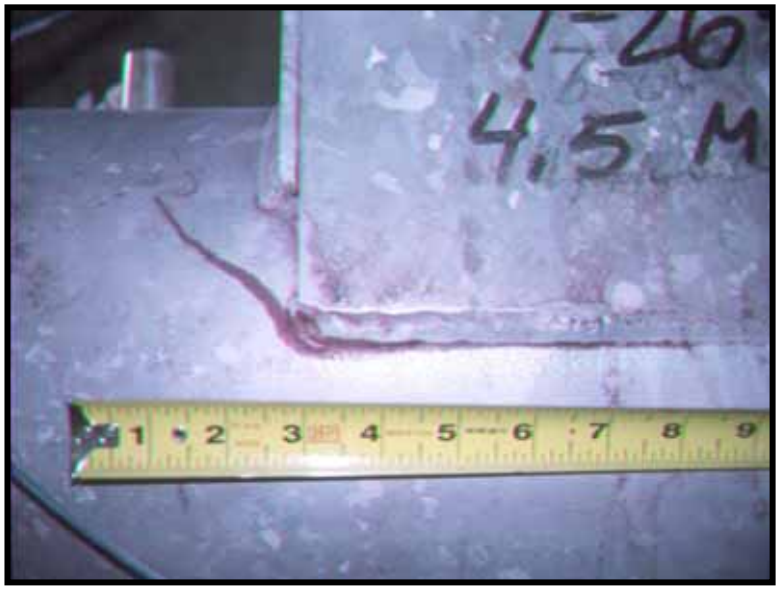

Figure 3.14. Dye Penetrant Testing
Puckett *et al.* (2001)

4. REPAIR AND REHABILITATION PROCEDURES

The methods and techniques that are used to increase fatigue strength and extend fatigue life are described in this chapter. Also, repair of specific fatigue cases that were described in Chapter 3 are provided.

4.1. Techniques to Extend Fatigue Life

Techniques generally used to extend fatigue life include grinding the weld, air hammering the weld toe (peening), melting the weld toe, and drilling holes. The following describes these procedures. This information essentially comes from techniques used for the rehabilitation of bridge structures that is presented in NCHRP Report 206 (Fisher *et al.* 1979).

1. Grinding the weld to remove the slag intrusions and reduce the stress concentration

   Grinding the weld to remove the slag intrusions and reduce the stress concentration is a method that has been successfully used to reduce stress concentrations and increase the fatigue life of welded details. Studies have shown (Watkinson *et al.* 1971 and Gurney 1968) that grinding provides an increase in fatigue life by increasing the time required for crack initiation. This is accomplished by reducing the stress concentration at the weld toe and by removing the tiny intrusions or undercut that exists at the weld periphery. Grinding is confined to the toe of the fillet weld. The depth of the grinding at the weld toe is typically between 0.8 mm (0.031 in.) and 1.6 mm (0.063 in). Grinding should be continued until the weld toe is smooth and free of visible defects. Figure 4.1 shows a grinding tool. For pre-cracked details, grinding should be applied until the crack is no longer visible. As the weld-toe region is ground, the crack appears as a fine line. When this line is no longer visible (without magnification), the grinding operation should be stopped. Care should be taken not to leave grind marks perpendicular to the direction of the applied load in order to avoid introducing new crack initiation sites.

2. Air-hammering the weld toe to introduce compression residual stresses (Peening)

   The weld toe can be mechanically air-hammer peened until plastically deformed. Thus, compressive residual stresses are introduced. This stress condition prevents the full stress area in the vicinity of the weld toe from being effective. This influences both the crack initiation and crack growth.

Peening should be continued until the weld toe becomes smooth. When a crack is visually apparent, peening should be continued until the crack is no longer visible. These variable criteria are necessary because of the variation in the weld bead shape and crack depth. Welds may have cracks that become visible after a light peening. The peening should be continued until the crack disappears.

3. Remelting the weld toe using the Gas Tungsten Arc process (GTA), referred to as Tungsten Inert Gas process (TIG).

This process involves melting metal at the weld toe. The tungsten electrode can be manually moved along the weld toe at a constant rate to melt a volume of the fillet weld and base metal. This process removes nonmetallic intrusions present along the weld toe and reduces the stress concentration condition. When a crack is present, a sufficient volume of metal surrounding the crack can be melted to incorporate the crack so that the crack is eliminated.

A typical welding apparatus is a 300-amp d-c power source with dropping V-I characteristics. A Linde HW-18 water-cooled torch with a 4-mm (0.156-in.) diameter, 2 percent thoriated tungsten electrode can be used. The depth of the remelted zone is critical to the success of this procedure because insufficient penetration would leave a crack buried below the surface and would result in premature failure. Argon can be used successfully for shielding throughout the TA tests.

For a set of tests that involve pre-cracked beams, Fisher *et al*. (1979) found the depth of penetration to be insufficient. Earlier studies (Sherman et. al 1964) show that penetration would increase with the proper selection of shielding gas and electrode cone angle. An experimental program was undertaken by the Michigan DOT to determine the most effective combination of these two variables. The results led to the use of a mixture of argon-helium shielding gas and an electrode cone angle of 60 degrees. With this combination, there was a 42 percent increase in penetration for the same current.

The area near the transverse fillet welds of all specimens should be sand blasted to remove all mill scale. Undercutting can result when scale is not removed. The welds should be started at the longitudinal weld about 19 mm (0.75 in.) from the transverse fillet weld, and continued along the toe of the transverse fillet weld to avoid weld craters in the critical toe region. It may become necessary to terminate a weld along the transverse weld. Care should be taken to stop the weld along the face of the fillet weld and not along the toe.

Experience in the laboratory and in the field has demonstrated that a few hours of training are required before support personnel could achieve the desired retrofit condition. An adequate depth of penetration must be obtained, which must be verified by metallographic examination of test plates.

4. Drilled holes

The typical size of the drilled holes used for retrofitting fatigue cracks formed at the end of vertical stiffeners in the web between the stiffener and the flange used in "Detection and Repair of Fatigue Damage in Welded Highway Bridges" NCHRP Report 206 (1979) was 13 mm (0.5 in) diameter. All holes were drilled using a magnetic base drill. To arrest and retrofit the web inserts, 19 mm (0.75 in.) holes were used. Different sizes can be used.

4.2. Fatigue Performance of Repaired Tubular Joints

Tubby (1989) studied the fatigue performance of repaired tubular joints. These joints, however, are similar to the joints used with support structures. The principal objective of this study was to establish a ranking for the repair method in terms of residual fatigue performance and to establish whether it is necessary to repair the entire joint, or only the cracked region. The repair methods investigated were as follows:

1. Repair welding - Cracks were removed by grinding, and the resulting groove filled by manual metal arc welding.
2. Repair welding and burr grinding - Repair welds made as described above were fully burr ground to remove the repair weld toe and to achieve a smooth finish on the repair weld face.
3. Hole drilling and cold expansion - The fatigue crack tips were removed by drilling through-thickness holes, which were then cold-expanded to include compressive residual stress in the hole circumference.
4. Grinding alone - Part wall cracks were removed by burr grinding and the resulting excavations left unrepaired.

The principal findings are summarized as follows:

1. Expressed in terms of the hot spot stress range, the fatigue strength of as-welded repair welds is marginally lower than that of un-repaired joints. However, this is compensated by the fact that in making the repair, the overall weld leg length is increased, which leads to a reduction in the stress range at the repair of the weld toe. As a result, if the applied loading is of the same magnitude after repair as before, the fatigue endurance for through-thickness cracking after repair is on average similar to, or marginally greater than, that before repair.

2. Burr grinding the repair weld may considerably improve the fatigue strength, although a smooth surface finish must be achieved to avoid premature crack initiation on the weld face. Where the applied loading continues unchanged after repair, the fatigue life for the through-thickness cracking may be in excess of five times that before repair.

3. Through-thickness and part-wall weld repairs behave similarly. Under the mode of loading investigated, relatively large lack of penetration defects can be tolerated at the root in through-thickness repairs.

4. Cold expanded holes at the crack tips were not effective as a means of delaying crack propagation.

5. Removal of part-wall flaws by grinding is an effective repair method giving endurance after repair equal to or up to four times greater than the mean of the unrepaired joints.

6. It is necessary to burr the un-repaired weld toes on both the chord and the brace to avoid premature failure.

7. The crack growth rates in hyperbaric repair welds would be expected to be similar to the one-atmosphere repairs.

4.3. Retrofit of High Mast Luminaire Poles

As a result of weld cracks found in Union Metal HML at the telescoping joint area, a repair procedure was developed by the Michigan DOT. The decision was made to repair the defective Union Metal HML based on cost estimates of replacement, as well as their remaining service life (approximately 10 to 15 years). If these structures had not been repaired, the replacement of a defective HML with a new A-572 galvanized steel HML would have cost approximately $35,000 per pole for a total cost of $595,000 for 17 cracks. The initial repair of each defective Union Metal HML consisted of the following steps:

1. The area around the crack region was ground to remove A-588 steel "pitting" and create a smooth surface. Surface preparation is essential to make accurate ultrasonic test results (see Figure 4.3).

2. The crack extension in the weld area was found by ultrasonic inspection (see Figure 4.4).

3. A 38.1 mm (1½ inch) diameter hole was drilled at the crack tip as determined by the ultrasonic inspection. The hole relieved the residual tensile stresses that were present at the crack tip and precluded further extension of the crack (see Figure 4.5).

4. A dye penetrant test was performed to confirm that the crack did not extend beyond the upper end of the hole (see Figure 4.6).

5. The hole area and weld area around the hole were painted with a zinc-based paint to prevent further corrosion of the HML. Finally, the hole was plugged with a rubber stopper (see Figure 4.7).

The cores that were removed from the hole in the cracked region were further examined in the laboratory (see Figure 4.8). After the discs were polished and etched, it was found that all cracks were contained in the weld itself or in the adjacent heat affected zone.

4.3.1 Fracture Mechanics Analysis And Retrofit Methodology

The cracking of HML pole is apparently the result of major defects in the longitudinal welds combined with high residual stress field that allows stress corrosion cracking (SCC) to occur. Such cracking is not normally a problem for weathering steels since the stress necessary for initiation does not normally occur. Stress studies performed by the Illinois Department of Transportation indicate that the material used in making some of their HML poles was cold worked to the point that higher than normal residual stresses remained adjacent to the weld area. This allows smaller defects than would otherwise have been the case to create the effectively greater stress intensity factors necessary for SCC.

The stress intensity factor necessary for SCC is roughly the same magnitude as that necessary for unstable crack growth in weathering steel sections that are most susceptible to fracture (i.e., thicker sections with higher constraint, more dynamic loading rates, etc). Understandably there was some concern about the potential for unstable fracture of the Michigan structures.

Michigan DOT decided to provide clamps to go around the poles at the cracked areas to compensate for the material lost. This action would also reduce the stress in the *blunted* crack tip area since the tensile force applied with the clamps imposes a compensating compressive field in the underlying pole material. The stress reduction will reduce the stress intensity at the repaired crack tip and, therefore, the likelihood of future cracking. The clamps also effectively reduce the seriousness of any reoccurrence of cracking by effectively changing the existing edge cracks to a configuration more like a center or through-thickness crack. A center crack requires roughly twice the crack extension, at the same stress level, to achieve the same stress intensity factor as an edge crack. This means that any reoccurrence of cracking must progress almost twice as far before possessing the same possible danger (from a fracture mechanics viewpoint) as the original cracks. Fracture mechanics and existing field experience suggest that a crack on a repaired lap joint might grow up as much as 305 mm (12 inches) beyond the repair clamps before becoming a potential fracture risk.

Michigan DOT designed a 100 mm (4 inch) wide by 6 mm (0.25 inch) thick collar that wrapped around the area of the crack to replace lost cross section, as well as, reduce the stress intensity in the area of the blunted crack. The collar was constructed of A-588 weathering steel to maintain compatibility with the existing structure and help eliminate the need for further maintenance. The collar's 25 mm (1 inch) diameter A325 Type 3 bolts and high-strength connection lugs allowed us to tighten the bolts to 133 KN (30,000 pounds), thus applying a circumferential or hoop stress of approximately 207 MPa (30 ksi) into the pole. This load was chosen because it provides a desired amount of compressive stress across the crack, minimizes the further corrosion between the collar and HML, and still allows reserve capacity for any wind loads. The A325 Type 3 bolts used were first strength

tested in a 10-degree and 20-degree wedge test according to ASTM F606 then additional bolts were calibrated in a skidmore for the desired tension. The bolts were positioned perpendicular to the crack surface as near as possible. All eighteen of the defective Union Metal HML were repaired. Tension in bolts of several initial installations were checked and found to be sustaining the desired load.

4.3.2 Conclusions

Because of the problems encountered by the Michigan DOT and resulting repairs, an inspection program has been developed to ensure the integrity of both the repaired and unrepaired HML for their remaining service life. An inspection procedure was developed and is shown in Annex A. the procedure details the necessary steps that must be taken to prevent or recognize future problems with the HML population.

4.3.3 Recommendations

Based on the inspection of the Michigan HML poles, Michigan DOT recommended the following:

1. Maintenance Division

    A. Inspect all HML statewide every two years using the inspection procedure published by the Materials and Technology Division in Michigan DOT (Included in Annex A).

    B. Remove grout that is located under the base plate of HML so that adequate air circulation can be provided to the inside of the pole.

2. Design Division

    A. Adhere to the following recommendations regarding the design and placement of high mast luminaire structures:

        1. Do not use tack welds on anchor bolt nuts.

        2. Do not use grout under the base plate of HML.

        3. Take the necessary steps in the geometric design of a roadway to avoid placing HML in a ditch line. High mast luminaires should be placed at least 10 m (33 ft) from the roadway to minimize the amount of salt spray reaching the pole. This should not be a problem since the required clear zone is usually equal to or greater than this distance.

3. Traffic and Safety Division:

   A. Take the necessary steps in the geometric design of a roadway to avoid placing HML in a ditch line. High mast luminaires should be placed at least 10 m (33 ft) from the roadway to minimize the amount of salt spray reaching the pole. This should not be a problem since the required clear zone is equal to or greater than this distance.

4.4. Aluminum Overhead Sign Truss and Foundation Reuse Guide

4.4.1 General

The following sections regarding the reuse of existing aluminum overhead sign truss structures and foundations is intended to be used in determining whether the truss and/or foundation will remain in service or will be replaced with a new truss and/or foundation. It was obtained from an office correspondence from the structural research unit of Michigan DOT to the Design Division. Aluminum truss boxes longer than 25.90 m (85 feet) have been found to be susceptible to blowouts in the web members and to cracking at various locations.

A truss as used in this guide is defined as the truss box and end supports. Each end support rests on a separate foundation. A truss box section is defined as that section of a box bolted chord flanges that consists of 2 vertical plane trusses, wind bracing and horizontal chord member in the vertical plane of the truss box.

Wind bracing is defined as secondary members that are between each vertical plane truss. A main chord member is defined as a horizontal member along the length of the truss box. An end support contains two column and bracing.

The length of time a truss has been in service must be considered when determining its reuse. Expected service life of these trusses based on the effects of a corrosive environment and fatigue is about 30 years. Any truss that will be reused must have been inspected within the previous 6 months. When a truss is to be removed for repairs, traffic costs incurred and the remaining service life of a truss must be considered. Replacement of 20-30 year old end supports should usually be included when it is necessary to replace the truss box. These factors can be significant in determining whether to repair or replace a truss when considering long-term benefits. Costs to remove and re-erect an existing truss box are estimated to be 15 percent of the truss replacement costs (excluding traffic costs).

4.4.2 Truss Evaluation

<u>Critical cracks</u>

Repair of critical cracks will not be permitted and would be cause for replacement of the damaged box section. The following define critical cracks:

1. Bottom chord cracks found in the middle half of the truss box span.
2. Cracks in the chord flange connection plate welds.
3. Cracks in the fillet weld at the bottom chord greater than or equal to 25 mm (1 inch) long or perpendicular to the chord.
4. Cracks originating in a web member, parallel to the web member, and extending into the fillet weld at the bottom chord.

Non-critical cracks or blowouts

The non-critical cracks or blowouts would be as follows:

1. Cracks or blowouts in the web members in the middle half of the truss box span.
2. Web member cracks or blowouts in the end quarter of the truss box span that are parallel to the web member.
3. Cracks in the fillet weld at the web member bottom chord intersection when its length is less than 25 mm (1 inch) and parallel to the chord.
4. Cracks or blowouts in wind bracing that do not extend into the wind bracing-bottom chord weld inspection.

Replace Truss and/or truss box sections:

1. Replacement of the truss is necessary when it is approximately 20 years in age or older. Repairs require removal of the truss box.
2. Replacement of the truss is necessary when it is less than 20 years in age and more than half of the truss box sections require replacement. More than 15 non-critical cracks or blowouts in a truss box section would be cause for replacement of that section.

Repair Existing Truss

1. Repair of a truss can be done when it is approximately 20-30 years in age and the truss box or end supports require only minor repairs such as bolt tightening, drilling holes to repair cracks, or base plate shoe repairs that can be performed in-place.

   Minor repairs include:

   a. Replace aluminum bolts with stainless steel bolts. (Base connection bolts, chord connection bolts, truss u-bolts.)

b. Tighten anchor bolts. Loose anchor bolts that cannot be tightened-remove the nut with an auto-splitter. Clean anchor bolts with a wire brush, galvanize and place new nut and washer then tighten.

c. A truss box with less than 3 non-critical cracks or blowouts. Repair on-site by drilling 6.25 mm (¼ inch) diameter holes in the crack tips if the cracks are unlikely to propagate in a member that would affect the capacity of the structure or reclassify the crack as critical.

Maintaining traffic costs must also be minimal for minor repairs.

2. Repair of truss can be done when it is less than 20 years in age and more than half of the truss section have less than 15 non-critical cracks or blowouts each. Welding will be required to do the repair. All structural welding shall be performed in shop-controlled conditions according to AWS Specifications for Structural Welding Code. Aluminum D 1.2 or shall be approved by Materials and Technology Division. Overlapping and intersecting welds shall not be permitted.

4.4.3 Foundation Evaluation

1. Replacement of the foundation may be necessary when the foundation is found to be tilted, moved, etc, or have large structural concrete cracks.

2. Replacement of the foundation is necessary when one of the following occurs:

   a. When the truss requires replacement.

   b. When two or more of the foundation anchor bolts are damaged. Determine by ultrasonic testing.

   c. When the engagement of the top nut onto the anchor bolt is 3 or more threads short on two foundation anchor bolts, and if the end support cannot be lowered by tightening all the leveling nuts down to the top of the concrete.

   d. When the foundation anchor bolts are in a diamond pattern. This pattern was used in truss foundation prior to approximately 1963 and is referred to as a Type VII.

   e. When end supports are buried in a median barrier. A new median barrier foundation shall be constructed adjacent to the existing standards plans and new foundation on the shoulder. If the truss can be reused according to the repair guidelines and is less than 27.43 m (90 feet), build new end supports and reuse the truss box, otherwise replace the truss.

4.5. The Replacement and Repair Decision

The following was obtained from an office memorandum from the structural research unit of Michigan DOT to the design division. Replacement or reuse of a truss box is based on the estimated remaining life, the location and orientation of the cracks, the cost of repair and the cost of replacement. To remove and replace a cantilevered with four cracks at each horizontal gusset plate connection costs about $33,000 per location. The following alternatives might be studied in light of the previously stated factors:

1. Remove the truss box sections from their support and repair the cracked welds in a fabrication shop. It is likely that any repair welds done in the shop would re-crack based on the experience with previous repair welds and this bridge special case study.
2. Replace the truss box sections in kind using the existing end supports at their current locations.
3. Replace aluminum sign support structures with a steel support structure. The fatigue stress limit for steel is about 2.5 times that of aluminum, and the secondary members for steel truss are bolted to gusset plates, which are welded to the chord members. The bolted connection provides greater damping. A two-inch radius at the corner where the gusset plate is attached to the chord is recommended to allow better stress flow through the members. Use of gusset plates welded to the chord member eliminates intersecting/overlapping welds that commonly occur in aluminum trusses.
4. Relocate the sign support structures.
5. Add dampers to the sign supports.

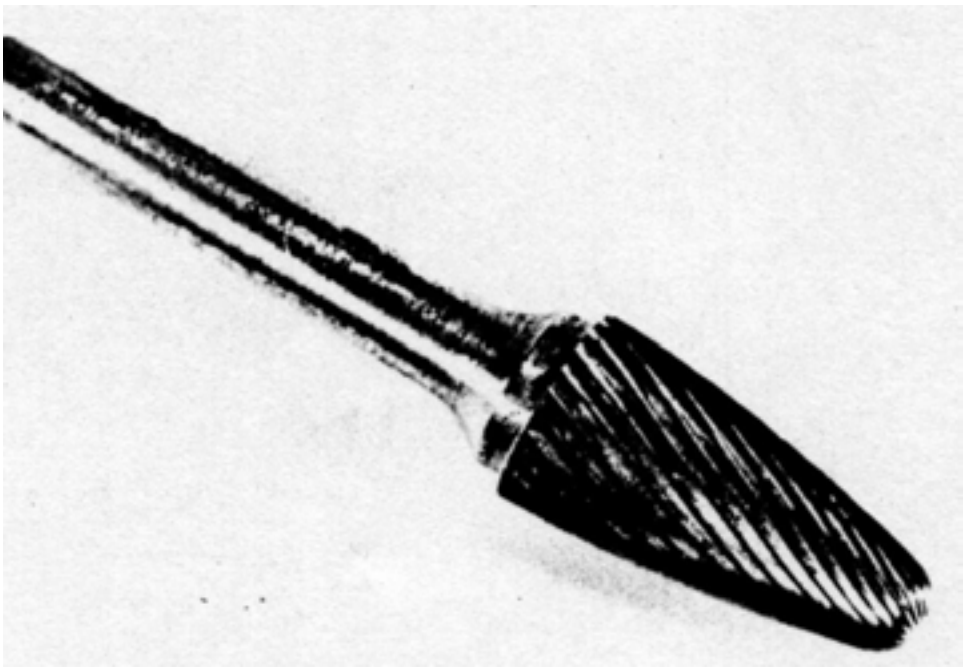

Figure 4.1. Tree-Shape Burring Bit for Grinding Tool
Fisher *et al.* (1979)

Figure 4.2. Peening Tool
Fisher *et al.* (1979)

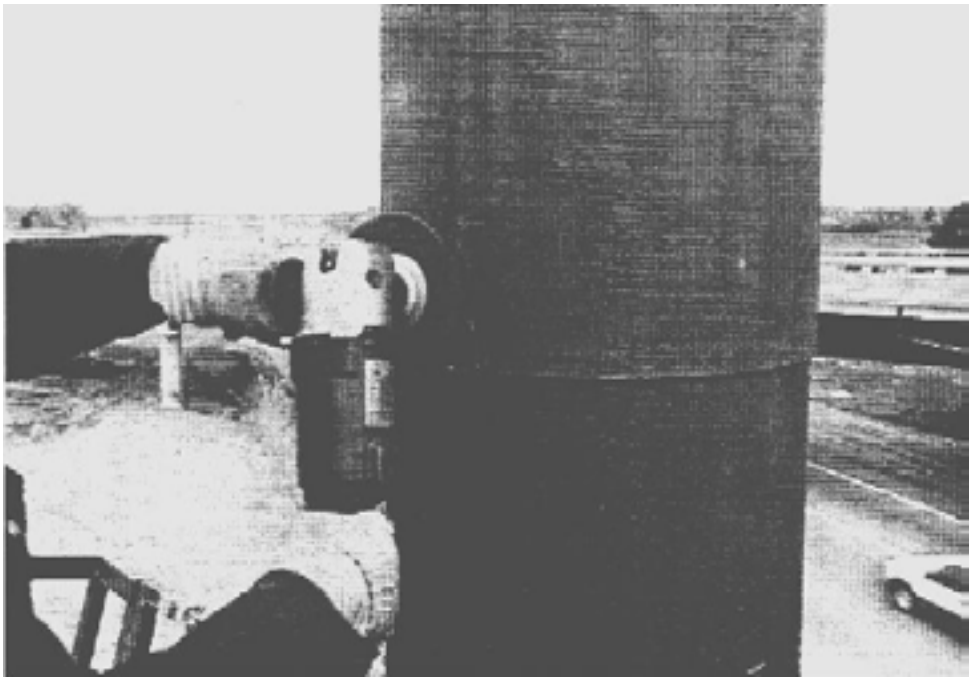

Figure 4.3. Preparation of Surface for Ultrasonic Testing
Isola *et al.* (1996)

Figure 4.4. Ultrasonic Testing of Crack Area to Determine How High the Crack Propagates Above the Crack Region
Fisher *et al.* (1979)

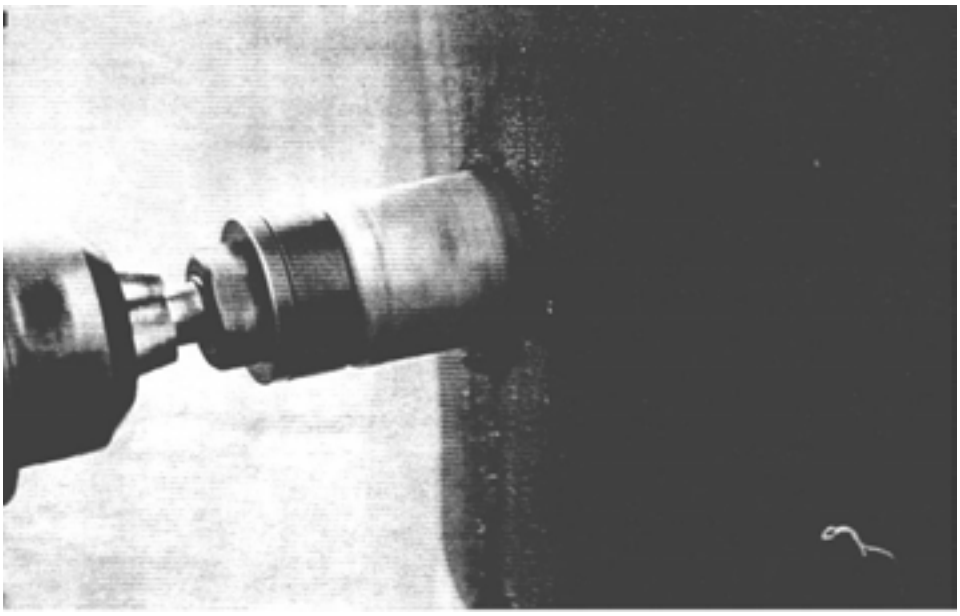

Figure 4.5. Hole Being Cut at the Tip of the Crack to Relieve the Residual Tensile Stresses
Fisher *et al.* (1979)

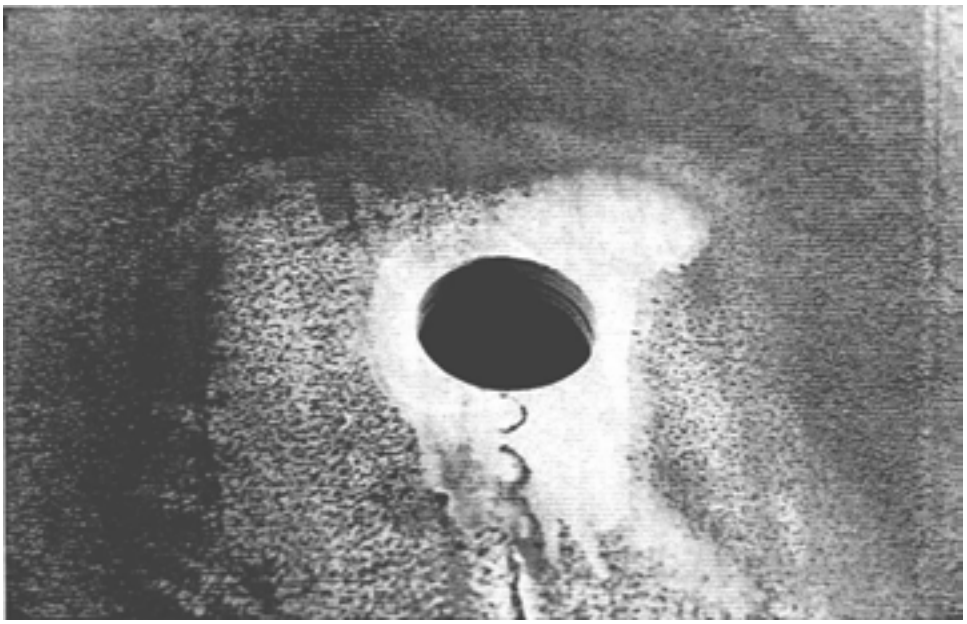

Figure 4.6. A Dye Penetrant Being Performed to Confirm That the Crack Did Not Extend Beyond the Upper End of the Hole
Fisher *et al.* (1979)

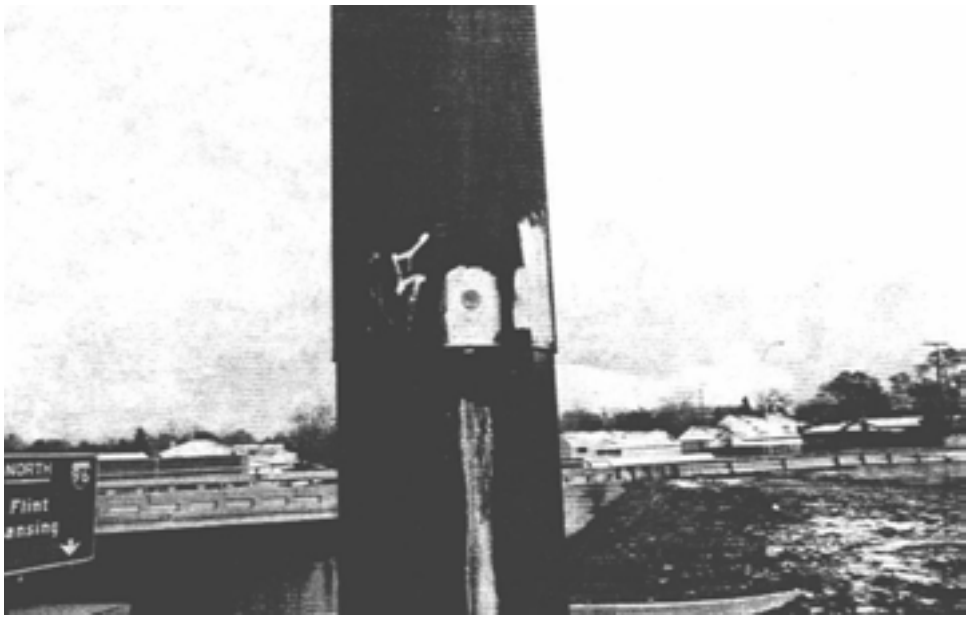

Figure 4.7. Rubber Stopper Inserted in Core Area and Zinc-Based Paint Used to Prevent Corrosion
Fisher *et al.* (1979)

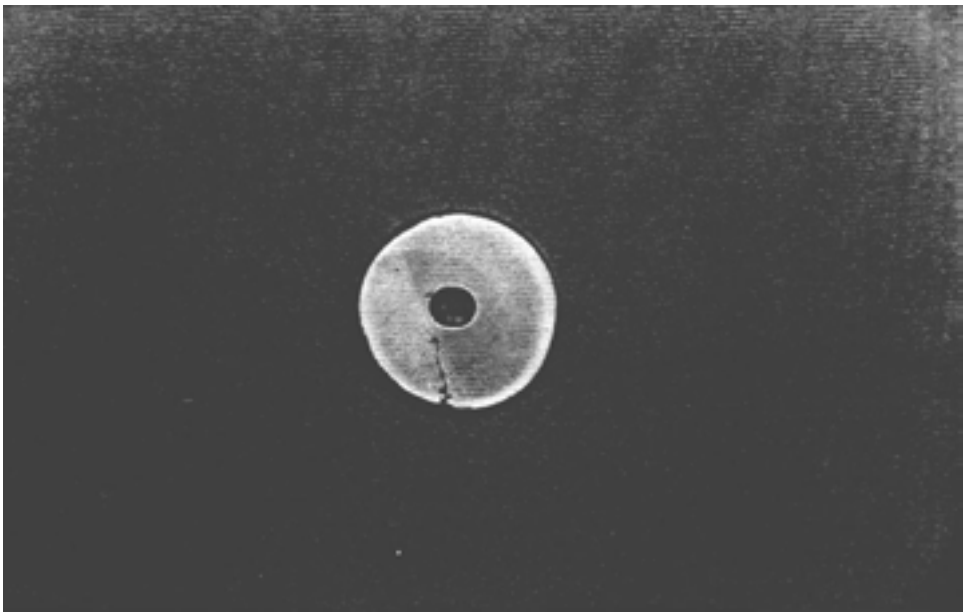

Figure 4.8. Polished and Etched Disc Removed from Crack Region
Fisher *et al.* (1979)

5. VIBRATION MITIGATION METHODS

5.1. General

Support structures and luminaires are flexible structures that are primarily subjected to wind loads. The specification resulting from NCHRP Project 17-10 adopted fatigue calculations to ensure that connections will incur stresses below the fatigue resistance associated with the appropriate connection detail type. However, upgrading the detail or applying these fatigue loads might result in uneconomical member sizes. In such cases, vibration mitigation devices can be used to reduce the loads that could cause fatigue. Also for the structures in service that exhibit excessive vibrations, these devices can be used to mitigate these vibrations and therefore increase the life of the structure.

5.2. Mitigation Methods

Each of the main four wind loading types – galloping, vortex shedding, natural wind gust, truck induced gust - has its own characteristics. Hence, different types of mitigation measures are required. Kaczinski *et al*. (1996) suggested the following measures for cantilevered support structures:

A. Galloping

1. Change the dynamic characteristics of the structure (mass - stiffness - damping) such that the magnitude of the onset wind velocity is greater than the wind velocity for which steady-state flows are typically maintained.
2. The aerodynamic nature of the attachments could be changed such that the structure will experience positive aerodynamic damping when subjected to periodically varying angle of attack of the wind flow.

B. Vortex shedding

1. Alter the dynamic properties of structure (mass -stiffness -damping).
2. Alter the aerodynamic characteristics of the structure. Altering the cross section of the element such that the formation of a coherent pattern of vortices from members with circular cross section, helical strakes, shrouds, and the rectangular plate installed at intervals along the members has proven to be an effective method by which to mitigate vibrations in structures such as stacks and chimneys.

C. Natural wind

1. Alter the damping of the structure to lower dynamic amplification factor. Tune-mass and impact dampers have been proposed for galloping and vortex shedding, however, mixed results have been obtained. Stiffening the structure will not mitigate natural wind vibration significantly since the loading is not aerodynamic.

D. Truck-Induced Gust vibration

1. Increase the vertical clearance of the sign panel above the tops of the trucks. Sometimes this action is limited by roadway geometric constraints and sight distance. The values presented in Table 5.1 can be used as a guideline to reduce the pressure. These values were obtained by rounding the values recommended by Dexter *et al.* (1999).
2. Perforated panels and open grating can be used to reduce the effective horizontal projected area.

Table 5-1 Recommended values to reduce truck induced gust (Johns and Dexter, 1999)

Elevation Above Road Surface		Percentage of the Pressure values
(m)	(ft)	%
(1)	(2)	(3)
6 or less	20 or less	100
6.1 to 7	20.1 to 23.33	85
7.1 to 8	23.66 to 26.67	65
8.1 to 9	27 to 30	40
9.1 to 10	30.33 to 33.33	20
10.1 and above	33.67 and above	0

5.3. Vibration Mitigation Devices

There are several types of mitigation devices that have been proven to reduce vibration of sign support structures. The research behind showing the effectiveness of these devices is summarized in the Task 4 report of NCHRP Project 17-10(2). The following describes each of these structures and their potential application for mitigation vibration of sign and luminaire support structures.

5.3.1. Work Done by Cook et al. (Florida)

Cook et *al.* (2000) tested the following damping devices:

1. Damping at arm-pole connection (disc springs and neoprene pads)
2. Stock bridge damper
3. Liquid tuned damper
4. Tuned mass damper
5. Spring/mass friction damper
6. Spring/mass tapered friction damper

The device that was chosen to be the most suitable in damping the vibrations of the arm was the tapered impact device shown in Figure 5.1. The device is composed of 102 mm (4 in) steel galvanized pipe, 686 mm (27.5 in) total length, a spring of 0.025 kg/mm (1.415 lb/in) and a mass of 6.8 kg (15 lb). This device was chosen because it provided a significant reduction in amplitude and number of cycles associated with the vibration of typical mast arm traffic signals. The device produced 3.6% critical damping on an 11.0 m (36.7 ft) mast arm (0.7 Hz) and 2.8 critical damping on a 24.1 m (80.3 ft), mast arm (1.4 Hz) as compared to 0.2% and 0.6 % critical damping respectively without the devices.

5.3.2 Work Done by Hamilton et al. (Wyoming)

Hamilton *et al.* (January 2001) reassembled cantilevered fatigue-damaged structure with a 15.2 m (50 ft) mast arm and tested the several types of damping devices described below. The device descriptions and dimensions presented here are identical to those provided in the draft NCHRP Project 10-38(2) report. Other device configurations may be available upon the completion of NCHRP Project 10-38(2). However these devices represent the general ideas and trends to mitigate vibrations.

1. Elastomeric Pad

An elastomeric pad was placed between the mast arm base plate and the base plate of the box connection. The elastomeric pad was 13 mm (½ in.) thick and was fabricated by Fabreeka International. The durometer hardness of the elastomeric pad was 80 Shore “A” Durometer average.

2. Strut

A strut with a shock absorber attached to the end was placed in the plane of the structure between the pole and mast arm. The strut was secured with steel collars and was approximately 7 m (24 ft) long. The shock absorber was a Rancho adjustable automobile

shock absorber (Model RS 9000) with 5 settings: setting 1 being the softest position and setting 5 being the firmest position (most damping).

3. Hapco Impact Damper

Hapco manufactures an impact damper that is successfully used on luminaires to suppress high frequency modes caused by vortex shedding. The damper is constructed from a 51- mm (2-in) diameter aluminum pipe with a rod/teflon ring placed loosely inside. As the pipe vibrates laterally, the Teflon ring impacts the inside of the aluminum pipe.

4. Flat bar impact damper

An impact damper consisting of a flat steel bar and a 4.5 kg (10 lb) steel weight was secured to the mast arm. When the mast arm oscillates in plane, the weight oscillates and impacts a steel bar mounted to the mast arm. This impact dissipates energy and provides a damping effect.

5. Strand impact damper

The flat bar impact damper showed that the impact concept could provide increased damping. However, the low strength combined with the low stiffness necessary to provide a damper with the same natural frequency as the pole resulted in yielding at the support. An increase in yield strength was needed without an associated increase in stiffness. A new impact device was designed that utilizes a 13 mm (½ in) diameter high-strength 1860 MPa (270 ksi) seven-wire strand (ASTM A416) as the support for the weights. The span of the impact damper could be raised or lowered to control the damper's natural period. The weights were wrapped with neoprene to reduce the noise produced at impact.

6. Shot-put impact damper

An impact damper consisting of a steel pipe and a 9-kg (20-lb) steel shot-put was attached to the mast arm. The shot-put was confined within the pipe by steel plates. The total gap distance between the shot-put and steel plates was adjustable, allowing the damper to be tested at different gap widths. As with the Hapco damper, this damper relied on the impact to dissipate energy. The shot-put traveled the pipe's length, impacting the steel end plates. The impact damper's configuration could be changed by rotating the damper at 45-deg intervals allowing the device to be multi-directional and dampen the mast arm's motion for both the in- and out-of-plane direction.

7. Alcoa dumbbell damper

Alcoa Fujikura, Ltd. manufactures a “bus damper” that is used for tubular busses in electrical substations. The damper had a multi-wire cable with two 3.1 kg (6.9 lbs) weights suspended from the each end of the cable. As the weights oscillate at the end of the cable, friction between the wires dissipates energy. The period of the dumbbell damper was measured to be approximately 0.8 sec.

The configuration of some of these devices is shown in Figures 5.2 through Figure 5.6. Their results can be summarized as the following:

In-plane:

- Structure with no damper had a damping of 0.15% period 1.17 sec (0.85 Hz);
- The best damping device was the strut which provided 6% damping;
- The order of effectiveness is Strut, Strand, Hapco impact, dumbbell, and pads.

Out of plane:

- Structure with no damper had a damping of 0.47 sec period 1.2 sec (0.83Hz);
- The best damping device was the pad at base which provided 2.8% damping;
- The order of effectiveness is pads, strand, shot put, Hapco impact, dumbbell, and struts;
- It was concluded that each retrofit increased damping, some significantly, but refinement and in service validation are necessary. To provide effective damping in both directions, a combination of two damping systems may be considered.

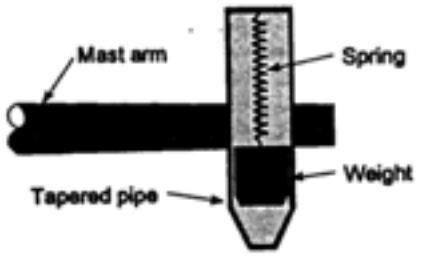

Figure 5.1. Tapered Impact Damping Device
(Puckett *et al.* 2001)

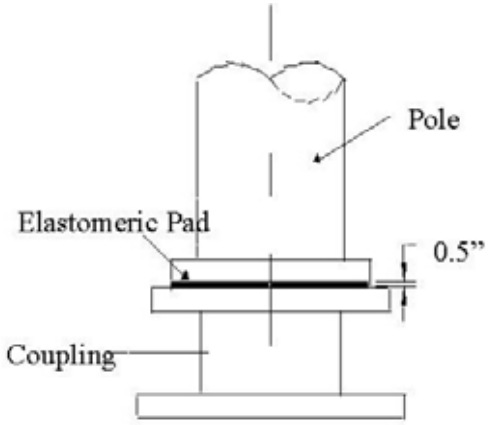

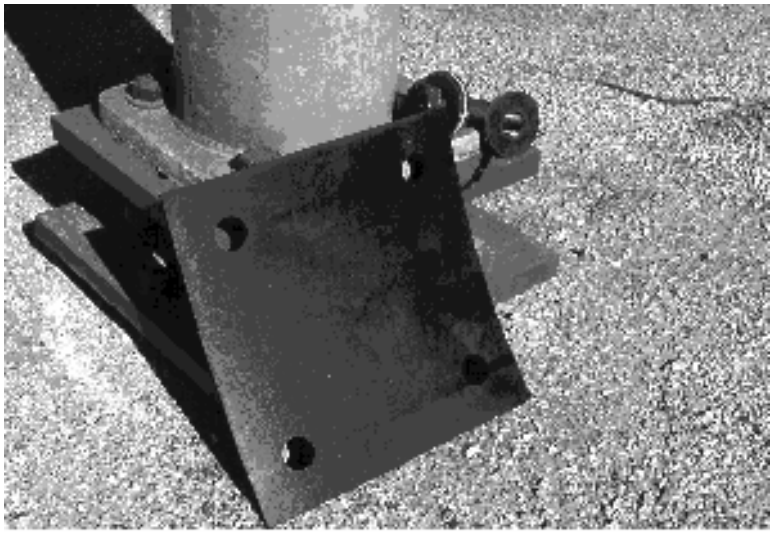

Figure 5.2. Pad at Base
(Puckett *et al.* 2001)

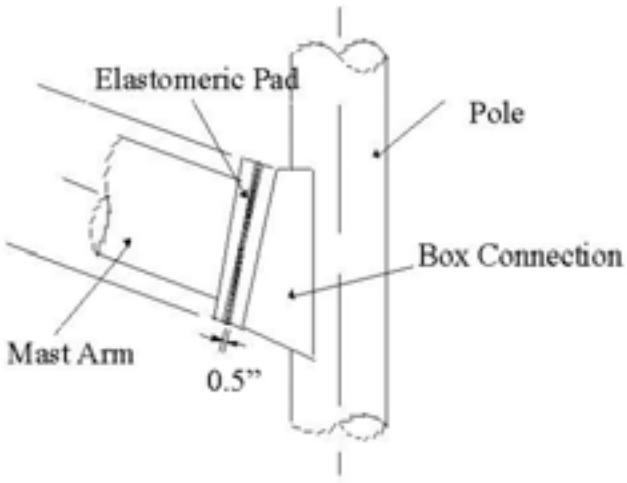

Figure 5.3. Pad at Mast Arm
(Puckett *et al.* 2001)

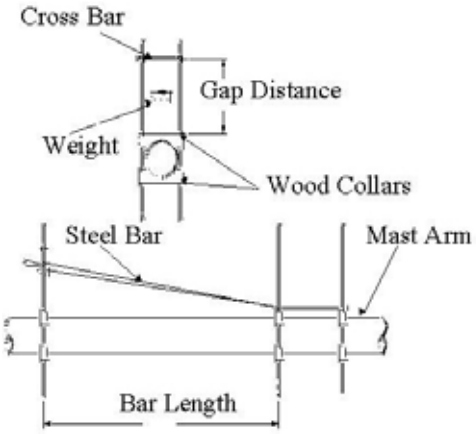

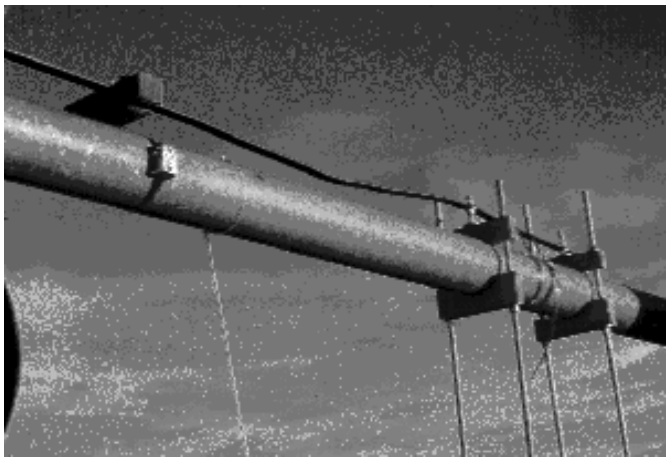

Figure 5.4. Flat Steel Bar
(Puckett *et al.* 2001)

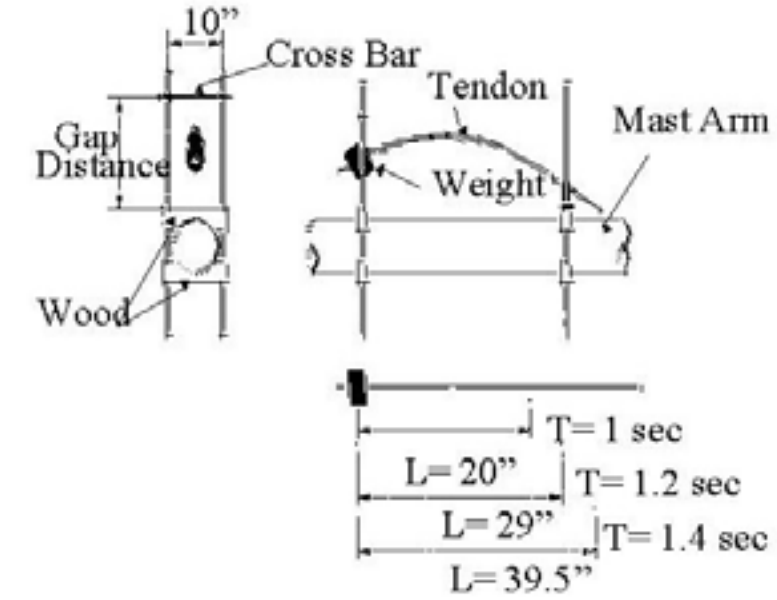

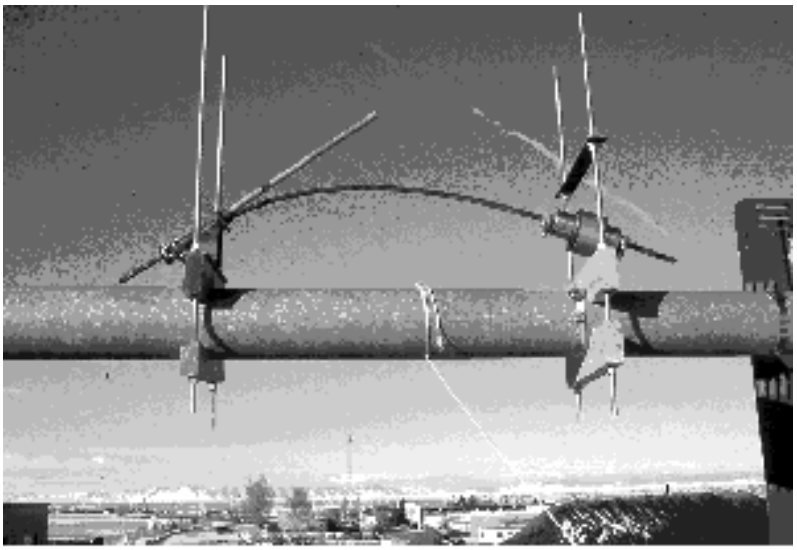

Figure 5.5. Strand Impact Damper
(Puckett *et al.* 2001)

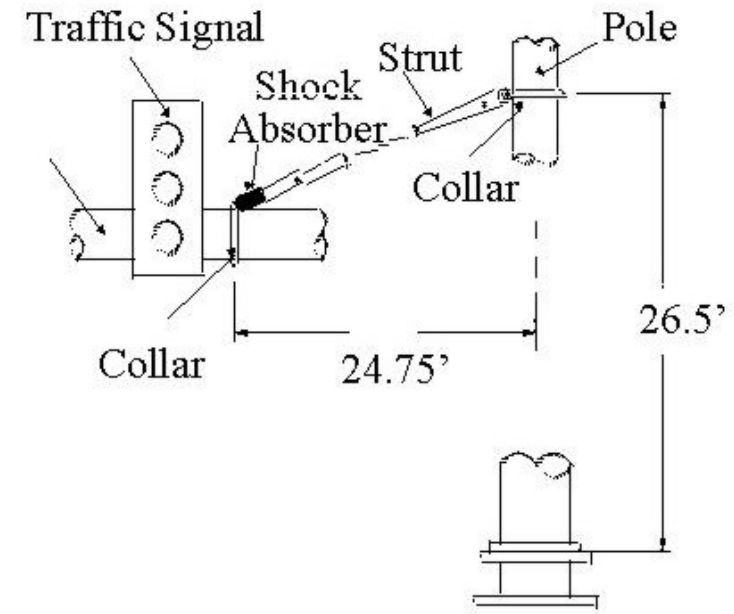

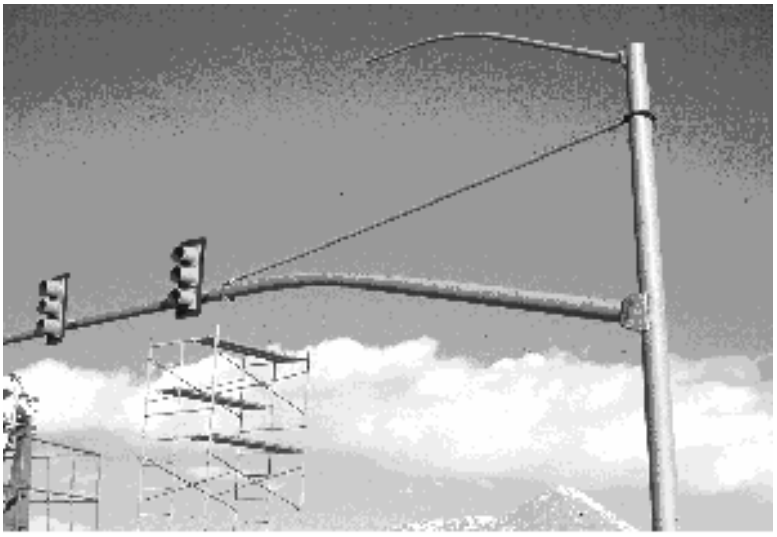

Figure 5.6. Strut and Shock Absorber Damper (Puckett *et al.* 2001)

6. SUMMARY, CONCLUSIONS AND RECOMMENDATIONS

6.1. Summary

Due to an increasing number of support structure failures resulting from fatigue, fatigue load cases have been included in the 1999 support specifications that resulted from NCHRP Project 17-10. However, there are many structures currently in service that may not be appropriately designed for fatigue. The objective of NCHRP Project 17-10(2) Task 11 was to prepare a manual for retrofitting and rehabilitating fatigue-damaged support structures.

First, a survey was sent to state DOTs and sign support manufacturers to determine the frequency of inspection of different types of structures and whether these agencies have repair procedures or plans. The survey also helped to establish contacts with the persons responsible for repair. The survey response shows that nearly two thirds of the states conduct regular inspections, with inspection frequencies varying from yearly to every five years. Thirteen responses out of forty-eight indicated that they repair fatigue-damaged structures. However, only the Michigan DOT indicated that they have maintenance plans and procedures and provided substantive information.

The materials for this manual were collected from many resources. Other related literature such as NCHRP reports regarding bridge inspection and repair and FHWA publications were also reviewed. Furthermore, reported fatigue cases for sign support structures were investigated.

This report presents procedures for the general inspection of luminaires and sign support structures. Inspection methods such as visual inspection, ultrasonic, magnetic particles, eddy currents and dye penetrant are discussed. The report also presents general techniques to improve fatigue resistance and extend fatigue life, and it provides procedures for the retrofit of various sign support structures and luminaires.

6.2. Conclusions

General conclusions from this research can be summarized as follows:

- There is a lack of information regarding repair of support structures for fatigue. The state DOT's responses indicated that the most common decision was (actions were generally) to replace the entire structure or damaged part.

- Periodic inspection is important to evaluate the overall structure conditions and identify any problems. The inspection period may vary depending on the available qualified personnel to do the inspection.

- A detailed evaluation of the structure for fatigue is necessary when the structure exhibits fatigue problems.

- Different alternatives regarding retrofitting of the structures by drilling holes to stop further cracking or providing mitigation devices, replacement of part of the structure, or replacing the whole structures should be studied considering all the factors such as cost and age of structure.

6.3. Recommendations

General conclusions from this research can be summarized as follows:

- Each state should develop an assessment plan;

- This plan should begin with a survey of all support structures and luminaires to define problems;

- Next step should be a detailed inspection of the structures that have problems;

- Problems should be prioritized;

- This report can be used as a start to a guide to solving some of the anticipated problems;

6.4. Suggested Research

The following items are recommended for future research:

1. The recommendations for vibration mitigation were based on Project 10-38(2) project to measure the effectiveness of different systems of dampers. Limited information was available for the effectiveness of dampers used by DOT. Evaluations the effect of the types used already in field would be valuable.

2. The final report of NCHRP 10-38(2) could not be obtained at the time of preparing this report. The information regarding vibration mitigation obtained from this project will be necessary to incorporate to any future work with the retrofit of sign support structures.

3. The procedures and methods used for retrofitting used in this report were based on experience. No experimental research work was done on the repair some of the fatigue problems like “fatigue crack of horizontal gusset plate.”

4. One of the main problems anticipated with preparing this report was the lack of documented information regarding fatigue cases and the repair methods used. It would be very valuable for future update of this report if there will be a system to

collect information about the general behavior and the fatigue problems anticipated with support structures.

REFERENCES

AWS Structural Welding Committee *Structural Welding Code* American Welding Society, FL, 1994.

ASM International Handbook Committee "Metal Handbook vol. 17 Nondestructive Evaluation and Quality Control" ASM International, OH, 1989.

"Cantilevered anchor bolt tightening procedure," Construction and Technology Division, Michigan Department of Transportation, internal document, undated.

Clup, J. D. (Material and Technology Division), Witteveen, M. (Maintenance Division), and Wong H. (Design Division), "Action plan for cantilevered sign problem - report to management ", Michigan Department of Transportation, April 1990.

Cook, S. J., Till, R. D., Pearson, L., "Fatigue cracking of horizontal gusset plates at arm-to-pole connection of cantilevered sign structures" Proceedings, Structural Materials Technology IV and NDT Conference, pp. 419-427, Technomic Publishing Company, NJ, 2000.

Fish P. "Inspection of Ancillary Structures, A Public Safety Responsibility" Proceedings, Structural Materials Technology IV and NDT Conference, pp. 38-43, Technomic Publishing Company, NJ, 2000.

Fisher, J. W., Hausmann, H., Sullivan, M. D., and Pense, A.W., "Detection and repair of fatigue damage in welded highway bridges." *National Cooperative Highway Research Program, Rep. No. 206*, Transportation Research Board, Washington, D.C., 1979

Fry, R., "Fundamentals of Visual Inspection" http://www.dot.state.ga.us/homeoffs/fpmr.www/testing/vis_inspect/index.htm, accessed August 2000.

Gurney, T. R., "Fatigue of Welded Structures" Cambridge University Press, 1968.

Isola, M.C., and McCrum, R. L., "Inspection and repair of high mast luminaires (HML)," Research and Technology Section, Material and Technology Division, Michigan Department of Transportation, Research Project 91 TI-1594, Research Report No. R-1342 August 1996.

Lamtenzan, D., Washer G. and Lozev, M., (1997) "Detection and Sizing of Cracks in Structural Steel Using the Eddy Current Methods" http://www.tfhrc.gov/hnr20/pubs/0018.pdf, accessed April 2001.

McGonnagle, W. J., "Nondestructive Testing," Gordon and Breach, New York, NY, 1966.

"Michigan DOT 1996 Standard Specifications for Construction" Michigan Department of Transportation, 1996.

"Procedure for inspection of sign structures," Construction and Technology Division, Michigan Department of Transportation, internal document, undated.

"Procedure for inspection of high mast luminaires," Material and Technology Division, Michigan Department of Transportation, internal document, undated.

Puckett, J. A., Hamilton, H. R., Collins, B. P., and Huck, P., "Traffic Signal Pole Fatigue in Wyoming – A Research Overview" http://wwweng.uwyo.edu/civil/Kester-Lab/Traffic_Signal_Poles.htm, accessed Jan 2001.

Puckett, J. A. and Hamilton, H. R. "Traffic Signal Structure Damping" http://wwweng.uwyo.edu/civil/Kester-Lab/SignalPole/signalpole.htm, accessed Jan 2001.

"Repair procedure for cantilevered sign support gusset plate weld," Construction and Technology Division, Michigan Department of Transportation, internal document, undated.

Sherman, D. R., and Stallmyer, J. E., "Cover Plate Welded and Fatigue Strength of Fillet Welded Joints" IIW Document No. XIII-340-64, Department of Civil Engineering, University of Illinois, 1964.

Till, R.D., and Lefke, N.A. "The relationship between torque, tension, and nut rotation of large diameter anchor bolts," Research and Technology Section, Materials and Technology Division, Michigan Department of Transportation, Research Project 91 TI-1556, Research Report No. R-1330, 1994.

Till, R. D., and Ness, B. W., "Cantilevered sign support inspection," Testing Laboratory Section, Material and Technology Division, M&T Report No. R-1319, August 1992.

Till, R. D., "Sign Support Trusses on the Zilwaukee Bridge B03 of 73112", office memorandum from R.D. Till, Supervisor Engineer Structural Research unit to S.R. Kullarni, Design Division, Michigan Department of Transportation, October 1, 1996.

Watkinson, F., Bodger, P.H., and Harrison, J.D., "The Fatigue strength of welded joints and Methods for its Improvement." Proceedings, Conference on fatigue of Welded Structures, The Welding Institute, 1971, pp. 97-113.

ANNEX A: Inspection Procedures for High Mast Luminaires

Establishing Structure Location: Location information should include district number, DOT structure inventory number, county number, route number, control section, and description of structure location using visible reference (ramps, overpasses, intersections, buildings) to facilitate future inspections. Also, reference to stationing or mile markers should be used if available. Structures must be stenciled with inventory number for future reference.

General Structure Inspection: Record the condition of galvanized coating on the structure. Many structures are A588 without coating. In all cases, note the general condition (heavy corrosive areas, bleed rust, etc.) of the structure. Inspect the condition of any visible welds (base plate to upright, hand hole, longitudinal seam welds, etc.). Count the number of sections that makeup the high mast luminaire and visually examine the longitudinal welded splice and/or transverse welds with binoculars. Most of high mast arm luminaires are 18.3 to 30.5 m (60 to 100 feet) and have at least one lap splice. Record any tilt or lean the high mast luminaire may have (north, south, east or west and approximate horizontal distance of tilt from center of concrete foundation).

All of the above information must be recorded on the inspection form with any additional comments noted.

Inspection of Base: Determine the bolt pattern for the anchor base. With a plastic tie, attach a plastic tag to the number one bolt (this can be any bolt if not already tagged). This tag should be placed between the base plate and the concrete foundation tied to the anchor bolt. Using a permanent marker mark the corresponding bolt numbers on the vertical support in a clockwise pattern from the number one or tagged anchor bolt for future reference. Measure and record the anchor bolt diameter. Look for missing or damaged anchor bolts or nuts (gouges, corrosion, etc.). Note any bolt ends that have been bent to align with the holes in the base plate or anchor bolts that are not plumb. Note any bolt ends that are lower than the top nut. If the bolt is lower than one or two threads, measure the depth and mark it on the inspection from in the box corresponding to the bolt number. Note any nuts that are tack welded to the base plate. Visually inspect any welds in the base (gusset, vertical support to base plate connection) looking for cracks or unusual welds. Also, note any damage (corrosion, cracks, gouges, dents) to the base, gussets, and vertical support.

Inspect the condition of the concrete foundation. Note spalling, cracks, and general deterioration.

Using a 24-ounce ball-peen hammer, hit the side of the top and leveling nuts and hit the top of the bolts. This is done to check for loose nuts (leveling and top) and/or cracked or broken bolts. If the nuts are tight, there is a sharp ringing sound; if the nuts are loose, there is a dull sound. A loose leveling nut can also be the cause of the dull sound; so do not immediately tighten the top nut. Inspection of leveling nut and washer may require the removal of a rodent screen between the base plate and the foundation. Rodent screens are steel mesh wrapped around the base plate with the ends wire tied together. After removing the rodent

screen, visually check for any gaps between the leveling nut and the base plate. Physically grasp the washer and try to remove it to determine the leveling nut tightness. If the leveling nut is loose, tighten it after tightening the corresponding top nut. If the leveling nut appears to be tight, proceed to tighten the top nut. After all leveling nuts and washers have been inspected, tag the number one bolt, as stated above, and reinstall the rodent screen tying the ends together with new galvanized tie wire. Be sure the rodent screen is securely in place and tightly tied at the ends. Because some bases have a grout between the vertical support base and the concrete foundation, inspection of the leveling nut is not always possible. If this is the case try to tighten the top nut. If the top nut cannot be tightened further, note this on the inspection form and proceed. Some grout may need to be removed at one bolt to attach the plastic tag to the bolt.

Tightening either of the anchor bolt nuts (leveling or top) can be done using an appropriately sized spud wrench, spanner wrench or socket wrench. A 0.9 to 1.2 m (3-foot to 4-foot) (maximum of 4-foot length) pipe is added to the wrench to increase leverage. The nut is tightened until no further movement takes place. Any broken rods should be easily identified as both the nut and the bolt will continue to twist with little applied torque. If only the nut rotates under the applied torque, complete the tightening and resound the side of the nut and the bolt with the hammer. Note all the nuts that require tightening on the inspection form.

Ultrasonic Inspection: The individual performing the ultrasonic testing (UT) must be certified at ASNT Level II, on recommended practice No. SNT-TC-1A.

Grind all anchor bolt ends flat (perpendicular to the shank of the bolt) being sure to remove all galvanizing, paint, dirt, and debris. Because deep 4.2 mm (1/6 inch or greater) surface imperfections (gouges, cuts) can affect the UT results, make the ground surface as smooth as possible. Some bolts been marked with an "X" for use as benchmarks. It is not necessary to grind the bolt until the indentations are completely removed, as these are usually shallow and should not affect the UT inspection. Only grind the bolt a sufficient amount to remove any painted smooth the surface. There are some bolt ends that have some extreme slant and cannot be ground to a flat, perpendicular surface. Note any bolts that have this problem on the inspection form. At some future date, these bolts should be corrected with a flat, perpendicular surface to allow for inspection.

Calibrate the ultrasonic unit for straight beam probe method using a 10-inch diameter beam probe. The probe is placed on a 25mm (1-in) thick calibration block and the indications on the screen are adjusted so that a reflection is positioned at each inch mark. Place the probe on a 0.228 m (9-inch) long test bar that has a 3.2mm (1/8 inch) deep saw cut at a set distance 75 to 100 mm (3 inches to 4 inches from the end) in the threaded portion of the rod. Peak the back reflection from the 1/8-inch deep saw cut until the indication is at 60% or 80% of screen height. Record the dB reading to establish a "REFERENCE LEVEL." Set the "SCANNING LEVEL" is set by adding 14 to 30 dB over the reference level. Check the calibration at each location before inspecting any bolts

Check the calibration at each location before inspecting any bolts. Apply couplant (glycerin) to the ends of the bolts. Ultrasonically test the anchor bolts using a circular motion

inspection pattern and record the results. When scanning the anchor bolts, there should be no indication on the CRT screen between the Main Bang (zero depth) and the end of the screen (10 inch depth). Any indication that is displayed after the Main Bang is a possible flow. Record the depth of the discontinuity observed and the amount of dB required to bring the indication to the "REFERENCE LEVEL" on the screen. This is recorded as "INDICATION LEVEL."

After the inspection is complete, wipe off all the couplant (glycerin) and spray the bolts ends with cold galvanizing or zinc-rich paint.

Reporting Procedure: All written reports shall be legible, accurate and detailed. These documents will be used as evidence of work performed (pay item). Payment for work will not be made if data gathered is illegible or undecipherable. Any unusual or potentially dangerous findings shall be reported immediately to the department of transportation.

Safety: High mast luminaire inspections and related work (hammering, grinding) shall follow appropriate safety standards (use of safety apparel and equipment safety guards). Safety apparel and equipment (hard hats, leather gloves, safety glasses, safety shoes, safety vest) shall be worn by all workers.

Equipment/Tool List:

- Complete ultrasonic unit with straight beam probe
- Portable generator to operate ultrasonic unit and grinder
- 100-foot electrical power cord
- 24-ounce ball-peen hammer
- 4-ft level
- Container of couplant (glycerin)
- Box of rags for cleaning
- Cans of cold galvanizing or zinc-rich paint
- L-head grinder with grinding disks
- 5- gallon gas can, must be safety type
- 12-foot tape measure
- Round point shovel
- Wrenches (spud, spanner or socket) and 4-foot pipe extension
- Report forms
- Binoculars
- Stencil pad with numbers and letters
- Black and white spray paint

Michigan Department of Transportation
1018 (N1/94)

HIGH MASK LUMINAIRE INSPECTION

REPORT NO.	INSPECTED BY	DATE
DISTRICT	COUNTY	ROUTE
CONTROL SECTION	JOB NO.	
LOCATION		

MANUFACTURER	HEIGHT OF LUMINAIRE	# OF SECTIONS
SECTION TYPE	DATE INSTALLED	STEEL TYPE

	1	2	3	4	5	6	7	8
HAMMER TEST FOR ANCHOR BOLT/NUT SOUNDING								
	1	2	3	4	5	6	7	8
ANCHOR BOLT UT								

ANCHOR BOLT/NUT COMMENTS (Thread Condition, Plumbness, Corrosion, etc.):

	1	2	3	4	5	6	7	8
PROJECTION OF BOLT BEYOND TOP NUT								

BASE WELD CONDITION:

	1	2	3	4	5
LAP JOINT WELD VISUAL INSPECTION					

LAP JOINT WELD UT

UPRIGHT CONDITION:

BASE ELEVATED ☐ YES ☐ NO	HANDHOLE COVER ☐ YES ☐ NO	IF POLE FALLS, WILL IT REACH ROADWAY? ☐ YES ☐ NO

ADDITIONAL COMMENTS:

ANNEX B: Inspection Procedures for Sign Support Structures

B.1. General Inspection Procedure

Description: This procedure describes the requirements for inspecting cantilever, truss, and bridge mounted sign structures.

Establishing Structure Location: Location information should include district number, DOT structure inventory number, county number, route number, control section, and description of structure location using visible reference (ramps, overpasses, intersections, buildings) to facilitate future inspections. Also, reference to stationing or mile markers should be used if available.

General Sign Structure Inspection: If the structure information is not in the inspection form, the following should be noted. Record cantilever or truss type, material type (steel or aluminum for trusses), coating material (galvanized or painted), and upright diameter. Measure and record as much additional sign data as possible (upright height, upright diameter, etc.). An eight-meter collapsible survey rod aids in obtaining many of the dimensions. A set of Sign Structure Standards should be used to determine the dimensions that cannot be measured.

Visually inspect the condition of the support components. This may require the use of binoculars or other visual aids. The inspection shall include the horizontal to vertical support connection for cantilevers and a walk-through inspection of the truss box for sign truss bridges. Note any unusual gaps between the bolt flanges, loose or missing bolts, missing hardware or caps, cracked welds, cracks at the end of the gusset plates, sagging of the horizontal support, and any broken or missing cross braces. Inspect the condition of the sign or signs noting any missing hardware or damage. Record the sign legend in the appropriate box. Visually inspect the U-bolts (where located, what connection, noting stainless or galvanized steel) and record any that are missing or damaged. Inspect the bottom of the signs for direct bolting through the vertical "I" beams (which prevent signs from slipping down on the "I" beams). Also, note any non-highway signs mounted on the sign structure. Estimate size, material types, and mounting locations of these signs.

Inspect gusset plates at arm to upright connection of cantilever sign supports, visual inspection at arm length. Note gusset and crack locations according to designation on UT form referenced in Section III.

Check the vertical support for plumbness using a one-meter level. Record any tilt as millimeters per length of level (i.e. 38 mm in 1 meter), either towards the roadway or away from the roadway. Also, measure and record any longitudinal tilt (i.e. upright tilts 50 mm in 1 meter north or south).

Inspection of Base: Determine the bolt pattern for the anchor base using the examples on the back of the attached Inspection form and, using a permanent marker mark the corresponding bolt numbers on the vertical support for future reference. Measure and record the anchor bolt

diameter. Look for missing or damaged anchor bolts or nuts (gouges, corrosion, etc.). Note any bolt ends that have been bent to align with the holes in the base. Note any bolt ends that are lower than the top nut. If the bolt is lower, measure the depth and mark it on the inspection from in the box corresponding to the bolt number. Visually inspect any welds in the base (gusset, vertical support to base plate connection) looking for cracks or unusual welds. Also, note any damage (corrosion, cracks, gouges, dents) to the base, gussets, and vertical support.

Inspect the condition of the concrete foundation, noting any spalling, cracks, and general deterioration.

Using a 680 g ball-peen hammer, hit the side of the top and leveling nuts and hit the top of the bolts. This is done to check for loose nuts (leveling and top) and/or cracked or broken bolts. If the nuts are tight, there is a sharp ringing sound; if the nuts are loose, there is a dull sound. A loose leveling nut can also be the cause of the dull sound, so do not immediately tighten the top nut. Visually check for any gaps between the leveling nuts and base plate. Tap one side of each washer placing one hand on the washer opposite the side being tapped. If the washer moves, the nut is not properly tightened. Physically grasp the washer and try to move it to determine the leveling nut tightness. If the leveling nut appears to be tight, proceed to tighten the top nut. Because some bases have a grout between the vertical support base and the concrete foundation, inspection of the leveling nut is not always possible. If this is the case try to tighten the top nut. If the top nut cannot be tightened further, note this on the inspection form and proceed.

Tightening either of the anchor bolt nuts (leveling or top) can be done using an appropriately sized spud wrench, spanner wrench or socket wrench. A 3-foot to 4-foot (maximum of 4-foot length) pipe is added to the wrench to increase leverage. The nut is tightened until no further movement takes place. Any broken rods should be easily identified as both the nut and the bolt will continue to twist with little applied torque. If only the nut rotates under the applied torque, complete the tightening and resound the side of the nut and the bolt with the hammer. Note all the nuts that require tightening on the inspection form.

Ultrasonic Inspection: The individual performing the ultrasonic testing (UT) must be certified at ASNT Level II, on recommended practice No. SNT-TC-1A.

Grind all anchor bolt ends flat (perpendicular to the shank of the bolt) being sure to remove all galvanizing, paint, dirt, and debris. Because deep (1.6 mm or greater) surface imperfections (gouges, cuts) can affect the UT results, make the ground surface as smooth as possible. Some bolts been marked with an "X" for use as benchmarks. It is not necessary to grind the bolt until the indentations are completely removed, as these are usually shallow and should not affect the UT inspection. Only grind the bolt a sufficient amount to remove any painted smooth the surface. There are some bolts ends that have some extreme slant and cannot be ground to a flat, perpendicular surface. Note any bolts that have this problem on the inspection form. At some future date, these bolts should be corrected with a flat, perpendicular surface to allow for inspection.

Calibrate the ultrasonic unit for straight beam probe method using a 250 mm screen with a 25 mm diameter straight beam probe. The probe is placed on a 25 mm thick calibration block and the indications on the screen are adjusted so that a reflection is positioned at each inch mark. Place the probe on a 230 mm long test bar that has a 3 mm deep saw cut at a set distance (75 mm from the end) in the threaded portion of the rod. Peak the back reflection from the 3 mm deep saw cut until the indication is at 60% or 80% of screen height. Record the dB reading to establish a "REFERENCE LEVEL." Set the "SCANNING LEVEL" is set by adding 14 to 30 dB over the reference level. Check the calibration at each location before inspecting any bolts. Check the calibration at each location before inspecting any bolts.

Apply couplant (glycerin) to the ends of the bolts. Ultrasonically test the anchor bolts using a circular motion inspection pattern and record the results. When scanning the anchor bolts, there should be no indication on the CRT screen between the Main Bang (zero depth) and the end of the screen (250 mm depth). Any indication that is displayed after the Main Bang is a possible flow. Record the depth of the discontinuity observed and the amount of dB required to bring the indication to the "REFERENCE LEVEL" on the screen. This is recorded as "INDICATION LEVEL"

After the inspection is complete, wipe off all the couplant (glycerin) and spray the bolts ends with cold galvanizing or zinc-rich paint.

B.2. Inspection of High-Strength Bolts At Arm to Upright Connection for Cantilevered Sign Structures

Description: This section of the inspection procedure describes the requirements for inspecting the 25.4 mm diameter bolts connecting the cantilever arm to the pipe upright. This connection is a double arm connection (top arm and bottom arm) with four or twelve bolts per arm connection depending on the type of cantilever. Each arm connection is a double flange connection with the pipe welded all around to each flange.

Specification Tightening: During new support installations, each bolt is required to be tightened according to Subsection 707.03 D.9.c of the 1996 Standard Specification for Construction. This requires each bolt to be tightened using the turn-of-nut method. This tightening method requires the nut to be snugged up and then turned beyond the snug tight an additional ½ turn. After this tightening is complete each flange plate should be drawn tight together with no visible gap between the plates.

Field Inspection: Visually exam the contact area between the flange plates and measure and record any gap. Visually exam each bolt that connects each arm to the pole upright. Verify that the bolt diameter is 25.4 mm, if not, record the bolt diameter. Check the bolt head to confirm that the bolt is ASTM A325. The bolt head should have three radial lines coming out from the center of the bolt head. If these lines are not present on the bolt head, record which bolt lacks these markings. As a minimum, each bolt end should be at least flush with the nut. If there is not at least a flush condition between the bolt end and the nut, record this in the inspection report. Each bolt should have a flat washer on the bolt head and a flat

washer and lock washer on the nut end. Record any parts that are missing or not in their proper location. All bolts, nuts and washers should have galvanizing on them. Record any signs of rust.

Placing a 360 to 480 mm long wrench on each nut, try to move each nut by using one hand on the wrench and pulling firmly using your body weight as leverage. With the wrench on the nut and pulling firmly, check for loose nuts or nuts you can turn either by loosening or tightening. If a nut can be removed, remove it and lubricate the bolt threads and nut bearing face with beeswax or equivalent (not oil or grease). Make sure that the flat washer and lock washer are present, if not, place one of each on the bolt before installing the nut (the flat washer should be installed before the lock washer). Reinstall the nut and tighten it with both hands on the end of the wrench turning the nut with full effort until the nut stops turning (you may need more than one wrench to prevent the bolt from turning initial tightening). Remove only one nut a one time. Repeat this operation, as necessary, until all the nuts have been tightened for a given flange connection. Taking the nut off is only necessary when it can be removed as described above. For documentation purposes, describe each bolt as located in the top or bottom arm and numbered clockwise on each flange connection while standing looking at the cantilever upright from the roadway with the number one bolt being on top just right of vertical. Note which nuts were removed and reinstalled and any other non-compliant items within the connection.

B.3. Ultrasonic Testing of Gusset Plates on Cantilever Sign Supports

Description: This section of the inspection procedure is used when performing ultrasonic testing at the end of horizontal gusset plates on cantilever sign supports only when cracks are found through visual examination. Ultrasonically examine each crack found visually and document the results.

B.4. Report Writing, Safety and Equipment

Reporting Procedure: All written reports shall be legible, accurate and detailed. These documents will be used as evidence of work performed (pay item). Payment for work will not be made if data gathered is illegible or undecipherable. Any unusual or potentially dangerous findings shall be reported immediately to the department of transportation.

Safety: All cantilever, bridge mounts and truss sign support inspections and related work (hammering, grinding) shall follow MIOSHA safety standards (use of safety apparel and equipment safety guards). Safety apparel and equipment (hard hats, leather gloves, safety glasses, safety shoes, safety vest) shall be worn by all workers.

Equipment/Tool List:

- Bucket truck
- Complete ultrasonic unit with straight and angle beam probe 70-5 MHZ miniature transducer, (6.35 mm x 6.35 mm element)

- DSC (Distance and sensitivity calibration) block
- Portable generator to operate ultrasonic unit and grinder
- 100-foot electrical power cord
- 24-ounce ball-peen hammer
- 4-ft level
- Container of couplant (glycerin)
- Box of rags for cleaning
- Cans of cold galvanizing or zinc-rich paint
- L-head grinder with grinding disks
- 50 – 80 Grit Sanding Disks for grinder (used to grind off zinc on cantilevered pipe wall)
- 5- gallon gas can, must be safety type
- 12-foot tape measure
- Round point shovel
- Wrenches (spud, spanner or socket) and 4-foot pipe extension
- Two 350 mm long wrenches
- Binoculars
- 8 meter Collapsible Survey rod
- Beeswax, Toilet Ring wax or equivalent (not oil or grease)
- Hot Dip Galvanized flat and lock washers
- Report forms
- Traffic Signs
- Safety Equipment for walk through truss sign support box – harness, lanyards, hooks, etc.

ANNEX C: Repair Procedure for Cantilevered Sign Support Horizontal Gusset Plate Weld

C.1 Equipment

- 9/16 -inch annular cutter
- portable magnetic drill
- cutting oil
- ratchet tie down straps
- 100' electric rod
- 7-inch right angle electric grinders
- 7-inch grinding wheels (50-80 grit)
- ¼-hp rotary grinder
- grinding tips
- dye penetrant kit
- rubber plug with stainless steel bolt, washers, and nut
- portable generator
- portable band saw
- saw blades for band saw
- zinc rich spray paint

C.2 Evaluation Procedure

All visual cracks must be confirmed ultrasonically before any repair may be done

The following are the criteria for determination of repair work

1 crack – no repairs, monitor the crack
2 cracks – drill holes at crack tips and taper all four-gusset plates
3 cracks – drill holes at crack tips and taper all four-gusset plates
4 cracks – remove the cantilever.

C.3 Repair Procedure

Find crack tips either by ultrasonic inspection or using dye penetrant

The maximum distance from outside edge of one hole to the outside edge of the second hole shall not exceed 2.6 inches. If the distance will be greater than 2.6 inches, please contact

____. Before continuing repairs, center the 9/16-inch annular cutter over the crack tip and proceed to drill through the mast at the crack tip.

After completion of the drilling, reexamine the wall of the hole using dye penetrant to determine to determine if the crack continues beyond the hole.

If the crack continues beyond the hole, remove the crack using a rotary grinder.

Repeat the procedure for each crack tip.

After removing the crack tips, draw a line on the gusset plate from a point 3.5 inch back from the gusset to a point 1/8 inch from the mast at the end of the gusset plate. Using a portable band saw or reciprocating saw, cut along the line drawn previously as close as practical.

After cutting, use the 7-inch right angle grinder to smooth the surface just cut. Continue to grind the weld until there is a smooth transaction between the weld at the end of the gusset plate and the mast.

Repeat steps 2.6 and 2.7 for all four-gusset plates.

After all work has been completed, clean the entire repair area using rubbing alcohol and a clean rag. Once the area has been cleaned, spray the zinc rich paint on to the exposed surfaces.

Plug drilled holes with a rubber plug with metal washers at each end. The plug is held in place by tightening stainless steel bolt that is concentric with washered plug